AD-A100 632 PURDUE RESEARCH FOUNDATION LAFAYETTE IND F/G 20/4
WORKSHOP ON COHERENT STRUCTURE OF TURBULENT BOUNDARY LAYERS,(U)
NOV 78 D E ABBOTT, C R SMITH AFOSR-76-3015
UNCLASSIFIED AFOSR-TR-78-1533 NL

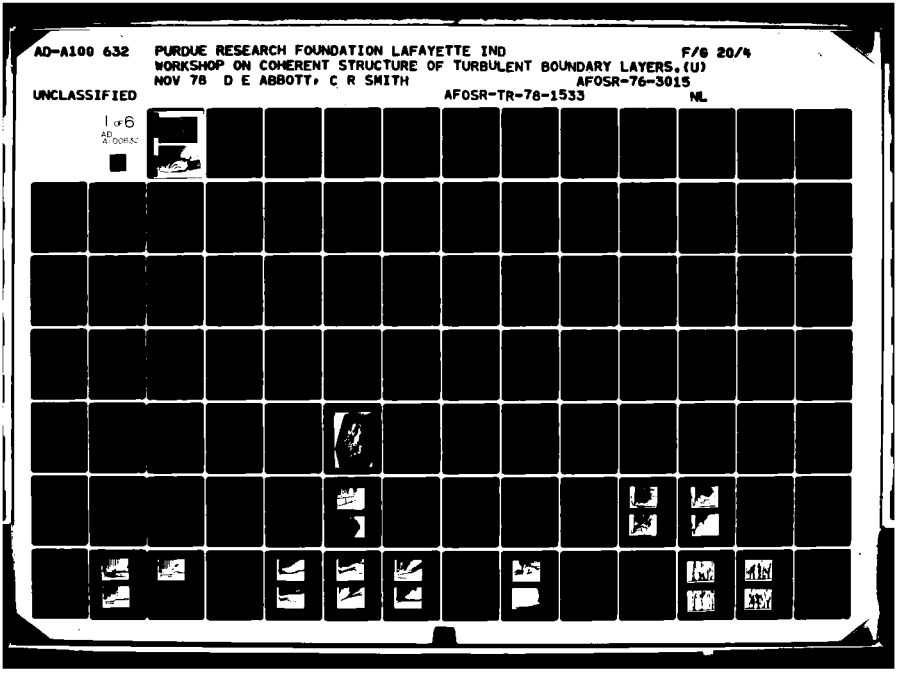

An AFOSR/Lehigh University Workshop

AFOSR-TR-78-1533

LEVEL II

AD A100632

COHERENT STRUCTURE OF TURBULENT BOUNDARY LAYERS

Approved for public release;
distribution unlimited.

DTIC FILE COPY

JUN 26 1981

EDITORS and CHAIRMEN
C. R. Smith and D. E. Abbott

UNCLASSIFIED

SECURITY CLASSIFICATION OF THIS PAGE *(When Data Entered)*

REPORT DOCUMENTATION PAGE	READ INSTRUCTIONS BEFORE COMPLETING FORM
1. REPORT NUMBER: AFOSR-TR-78-1533 / 2. GOVT ACCESSION NO.: AD-A100632	3. RECIPIENT'S CATALOG NUMBER:
4. TITLE *(and Subtitle)*: WORKSHOP ON COHERENT STRUCTURE OF TURBULENT BOUNDARY LAYERS.	5. TYPE OF REPORT & PERIOD COVERED: FINAL, 1 Jun – 30 Sep 78
	6. PERFORMING ORG. REPORT NUMBER:
7. AUTHOR(s): D.E. ABBOTT, C.R. SMITH	8. CONTRACT OR GRANT NUMBER(s): AFOSR-76-3015
9. PERFORMING ORGANIZATION NAME AND ADDRESS: PURDUE RESEARCH FOUNDATION, CHAFFEE HALL, WEST LAFAYETTE, INDIANA 47907	10. PROGRAM ELEMENT, PROJECT, TASK AREA & WORK UNIT NUMBERS: 2307/A2, 61102F
11. CONTROLLING OFFICE NAME AND ADDRESS: AIR FORCE OFFICE OF SCIENTIFIC RESEARCH/NA, BLDG 410, BOLLING AFB, DC 20332	12. REPORT DATE: 1978
	13. NUMBER OF PAGES: 544
14. MONITORING AGENCY NAME & ADDRESS *(if different from Controlling Office)*	15. SECURITY CLASS. *(of this report)*: UNCLASSIFIED
	15a. DECLASSIFICATION/DOWNGRADING SCHEDULE

16. DISTRIBUTION STATEMENT *(of this Report)*

APPROVED FOR PUBLIC RELEASE; DISTRIBUTION UNLIMITED

17. DISTRIBUTION STATEMENT *(of the abstract entered in Block 20, if different from Report)*

18. SUPPLEMENTARY NOTES

19 KEY WORDS *(Continue on reverse side if necessary and identify by block number)*

TURBULENT BOUNDARY LAYER

20 ABSTRACT *(Continue on reverse side if necessary and identify by block number)*

A discussion of the role of visual and probe measurements in turbulent structure research is given, stressing the constraining limitations of each and the interrelationships of the two methods. A selective history of the use of visual results is discussed in terms of the constraining limitations of the visual methods. Retrospective remarks are presented concerning the Stanford visual data on the inner portions of turbulent boundary layer structure. The final section discusses some general features of what is currently known about the structure of turbulent boundary layers, draws conclusions from (cont.

DD FORM 1 JAN 73 1473 / EDITION OF 1 NOV 65 IS OBSOLETE

UNCLASSIFIED 21600

SECURITY CLASSIFICATION OF THIS PAGE *(When Data Entered)*

81 6 25 023

20. this general knowledge, and poses questions that seem currently important in gaining further understanding . The paper stresses overall aspects of the structure problem at the expense of details in an attempt to gain perspective.

AFOSR-TR-78-1533

(1)

WORKSHOP
ON
COHERENT STRUCTURE
OF
TURBULENT BOUNDARY LAYERS

Edited by

C.R. SMITH
and
D.E. ABBOTT

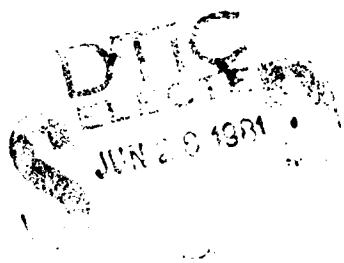

November, 1978

Approved for public release;
distribution unlimited.

Sponsored by
Air Force Office of Scientific Research

Department of Mechanical Engineering and Mechanics
Lehigh University
Bethlehem, Pennsylvania

AIR FORCE OFFICE OF SCIENTIFIC RESEARCH (AFSC)
NOTICE OF TRANSMITTAL TO DDC
This technical report has been reviewed and is
approved for public release IAW AFR 190-12 (7b).
Distribution is unlimited.
A. D. BLOSE
Technical Information Officer

81 6 25 025

A Workshop sponsored by the Air Force Office of Scientific Research, Air Force Systems Command, USAF, under Grant No. AFOSR-76-3015. The United States Government is authorized to reproduce and distribute reprints for Governmental purposes notwithstanding and copyright notation hereon.

ACKNOWLEDGMENTS

The Editors would first like to express their appreciation to the Air Force Office of Scientific Research for its financial support of the workshop. Particular thanks go to Lt. Col. Robert Smith and Lt. Col. Lowell Ormand whose continuing support helped make this workshop a reality. In addition, the Editors are appreciative of the efforts of Mr. Roger Smith, Division of Sponsored Programs at Purdue University, for his coordination of a transfer of workshop funding from Purdue to Lehigh University.

Special thanks are also due to the Organizing Committee of S.J. Kline, L.S.G. Kovasznay, W.C. Reynolds, and M.V. Morkovin for their help in program selection, chairing of the sessions, and editing of the discussion.

The task of physically running the workshop was greatly facilitated through the help of several Purdue University students and Lehigh University students, faculty, and staff who served as session aides, recorders, guides, etc. and helped to make the workshop a successful experience. Particular thanks are due to Mr. Fred Wehden for equipment and space coordination, Mr. Tim Nixon for assistance with electronic equipment, Mr. Traver Schadler for audio assistance, and Professor Donald Rockwell for coordination of the student aides.

Finally, a special accolade must go to Ms. Joan Decker for her tape transcription and, with Ms. Donna Reiss, the final typing of the Proceedings. Ms. Decker was also responsible for handling many of the procedural details before, during, and after the workshop, and it was her efforts, as much as anyone elses, that made the workshop a success.

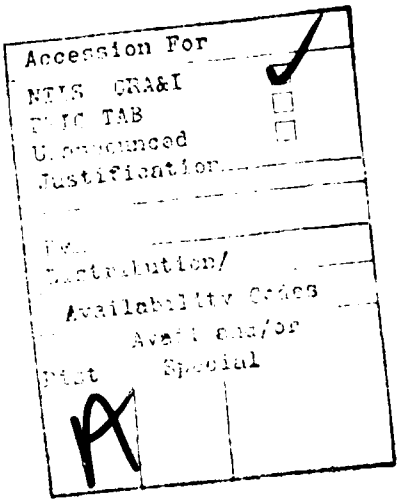

PREFACE

The recognition of coherent structure within turbulent boundary layers is not a recent discovery and its origins are clearly evident in early flow visualization studies by Prandtl and his students in the late 1920's using cameras moving with the flow; see Steve Kline's excellent review in this volume. It is interesting, however, that since the "discoverer" of turbulence, Osborn Reynolds, described the phenomena in 1883 as fluctuations, random in nature, there have evolved strong proponents of coherent structure versus purely random behavior and visa versa. There has been an unproductive waste of intellectual energy spent by these two groups arguing their respective points of view. If there is a single theme of this Workshop it is for a more open-minded and constructive focus on the phenomena of turbulence itself. As Kovasznay has put it, "advancements in the fields of turbulence require close collaboration of the experimentalist, analyst, and the predictor, and a mutual understanding of the strengths and needs of each by the other." Certainly Prandtl's group recognized the importance of this scientific interaction, and it is unfortunate that this complex and seemingly perverse subject of turbulence has not led to more testing of ideas than wills.

The central objective of this Workshop was to discuss and study the role of coherent structure as objectively and openly, as possible. Specifically, we wanted to establish what can be learned from coherent structure regarding phenomenological understanding, fundamental analysis of the turbulence process, and the development of better prediction methods. Perhaps Morris Rubesin in his paper in this volume has put his finger on the timeliness of this aprticular Workshop. He argues that in the past, many important experimental observations were ignored by analysts and predictors simply because they revealed details of turbulence that were beyond available mathematical tools. Thus, it is perhaps significant that in our present era, two major tools of analysis have matured to the point of having direct impact on our field; namely, the large scale digital computer and the method of multi-scale, rational analysis (i.e., the method of matched asymptotic expansions). It will become apparent from reading this volume that rather formidable attacks on some of the more complicated details of turbulence have been initiated using these techniques. Don Coles in his comments in the panel discussion of this volume agrees that "what is happening in the turbulence business how is the first significant advance in the development of ideas since roughly 1935,...." He goes on to close with the timely perspective that he really hopes that young people are coming along who don't pay quite so much attention to the oldtimers. "Crises are created by the established people because the old methods aren't good enough, but they are solved by new people."

One rather surprising failure emerged over the three days of the meeting when it became apparent that it would not be possible 1) to provide the reader with a very significant summary of what was known or not known regarding the mechanistic details of turbulence structure and 2) to agree on a consistent terminology. Early in the meeting a committee was formed to produce such a list. [See Committee Report 4 in this volume.] Not only did this committee find it could not produce any broadly based consensus of agreement, but that many research teams were using different meanings for now popular terms such as "burst", "sweep", "streak", and so forth. It is most encouraging, then, that this committee decided to meet again in July, 1978, at Stanford University and an interim report on their progress is included in this volume.

Turning now to procedural details of the present Workshop, let us review how the meeting was organized. The three main technical sessions (I. Flow Visualization, II: Sensors & Correlation, and III: Analysis & Prediction) began with a keynote speaker chosen for his ability to put his topic into some historical perspective, identify the leading issues (where possible), and set the stage for three subsequent speakers who presented fairly detailed papers on specific aspects of each topic. Where competing view existed, an attempt was made to have all sides fairly represented, although time allowed for only the three papers. Regarding the discussion for each session, the Session Chairman chose several participants in advance from the audience to serve as session secretaries and their collective wisdom was used in deciding which discussion to include from the transcriptions and which to exclude. It had been decided in advance that in order to publish this volume as quickly as possible, the tape transcriptions would not be sent to the individual discussors for editing. The tapes were transcribed and sent to the Session Chairman for preliminary editing. The final decision on the inclusion and wording of discussion was made by the Editors. In that sense, the discussion should be read as a paraphrase of actual comments. Every effort was made to be fair and accurate with this paraphrasing, but the Editors apologize in advance, and accept personal responsibility if anyone was accidentally misquoted.

Session IV, Short Presentations, includes twelve papers screened in advance by a local paper's committee. Ten of these were presented at the Workshop and include appropriate discussion, while two (by Coles and Falco) were received after the Workshop and are printed without benefit of discussion.

Session V consisted of Committee Reports and a Panel Discussion. Four Committee Reports were given on topics which arose during the course of the Workshop. The edited transcripts of three of these with discussion, are printed in this volume. Report 4 has already been discussed; since the transcription of this report indicated that considerable further work was needed, that transcription does not appear. In its place is an interim report of the follow-on discussions at Stanford of turbulent

structure mechanisms, written by Steve Kline. The Panel Discussion was presented by five authorities representing university research, industry designers, governmental laboratories and government funding agencies. The panel members spoke to the topic of the direction of future research on coherent structure in terms of both basic understanding and the needs of the design engineer. The panel presentations were recorded, transcribed and are included along with several of the visual aids employed. The reader should find these presentations particularly interesting because they are very reflective discussions of the utility of the present study of turbulent boundary-layer structure and where the emphasis for future work in this area should be placed.

In conclusion, the three-day Workshop provided an opportunity to focus a considerable amount of effort toward the development of a consensus of what is known, and not known, regarding coherent structure of turbulent boundary layers. It came as some surprise to the participants to find that it was not possible to develop a significant list of agreement on either turbulence mechanisms, or parts of mechanisms, or even the terminology that has evolved over the past few years. However, this recognition did lead to open and quite objective discussions that it is hoped will continue on a fairly regular basis. It is our feeling that the Workshop will have been a success if the cooperation and understanding which was fostered at the meeting can be sustained and extended to the turbulence community as a whole.

D.E. Abbott C.R. Smith

Lehigh University
November, 1978

TABLE OF CONTENTS

	Page
Acknowledgements	i
Preface	ii
Table of Contents	v
Participants	ix
Welcoming Remarks Hans Mark, Undersecretary of the Air Force	xi
S E S S I O N I **F L O W V I S U A L I Z A T I O N** Chairman: S.J. Kline	
Keynote: *The Role of Visualization in the Study of the Structure of the Turbulent Boundary Layer* S.J. Kline	1
Flow Visualization and Simultaneous Anemometry Studies of Turbulent Shear Flows R.S. Brodkey	28
Visualization of Turbulent Boundary-Layer Structure Using a Moving Hydrogen Bubble-Wire Probe C.R. Smith	48
Combined Flow Visualization and Hot-Wire Measurements in Turbulent Boundary Layers M.R. Head and P. Bandyopadhyay	98
S E S S I O N II **S E N S O R S A N D C O R R E L A T I O N S** Chairman: L.S.G. Kovasznay	
Keynote: *Survey of Multiple Sensor Measurements and Correlations in Boundary Layers* W.W. Willmarth	130

Page

On the Possible Relationship Between the Transition Process and the Large Coherent Structures in Turbulent Boundary Layers..... 168
I Wygnanski

The Structure of Turbulence in the Near Wall Region.. 195
H. Eckelmann

The Bursting Process in Turbulent Boundary Layers.... 211
R.F. Blackwelder

S E S S I O N III

A N A L Y S I S A N D P R E D I C T I O N

Chairman: W.C. Reynolds

Keynote: *The Role of Coherent Structure in Turbulent Boundary Layer Analysis*..... 228
M.W. Rubesin

Model of Burst Formation in Turbulent Boundary Layers. 258
S.A. Orszag

Shear Layer Breakdown Due to Vortex Motion..... 288
T.L. Doligalski and J.D.A. Walker

Modeling of Coherent Structure in Boundary Layer Turbulence..... 340
M.T. Landahl

S E S S I O N IV

S H O R T P R E S E N T A T I O N S

Chairman: D.E. Abbott

Application of a Smoke-Wire Visualization Technique to Turbulent Boundary Layers..... 372
H.M. Nagib, Y. Guezennec, and T.C. Corke

On the Period of the Coherent Structure in Boundary Layers at Large Reynolds Numbers..... 380
M.A.B. Narayanan and J.G. Marvin

Page

Coherent Structure of Turbulence at High Subsonic Speeds..... 387
V. Zakkay, V. Barra, and C.R. Wang

Effects of Heated Coherent Structures on Measurements by Laser Doppler Anemometry..... 396
J.A. Stabile and D.M. Mc Eligot

Experimental Investigation of Large Scale Structures in Turbulent Jet Mixing Layers..... 402
O. Leuchter and K. Dang

Universal Laws of Vortex Merger in the Two-Dimensional Mixing Layer..... 410
R. Takaki

Structural Information Obtained from Analysis Using Conditional Vector Events: A Potential Tool for the Study of Coherent Structures..... 416
R.J. Adrian

Reynolds Averaging and Large Eddy Structure..... 422
S.F. Birch

On the Feasibility of a Vortex Model of the Turbulent Boundary Layer Burst Phenomena..... 429
J.E. Danberg

The Interpretation of the Viscous Wall Region as a Driven Flow..... 438
D.T. Hatziavramidis and T.J. Hanratty

The Role of Outer Flow Coherent Motions in the Production of Turbulence Near a Wall..... 448
R.E. Falco

A Model for Flow in the Viscous Sublayer..... 462
D. Coles

Page

SESSION V(a)

COMMITTEE REPORTS

Chairman: D.E. Abbott

1) *"Which Equations of Motion are Suitable for Prediction of Coherent Structures?"*..... 476
reported by E. Reshotko

2) *"What is Universally Understood Regarding Turbulent Spots?"*..... 477
reported by C.W. Van Atta

3) *"What is the Relationship Between Vortical Structures in the Inner and Outer Layers?"*..... 482
reported by J.M. Wallace

4) *"What are the Main Distinguishing Features Between Different Breakdown Models and to What Extent are These Features Measureable?"*..... 485
reported by S.J. Kline

SESSION V(b)

PANEL DISCUSSION

Chairman: M.V. Morkovin

PRESENTATIONS:

1) *Dr. Brian Quinn, AFOSR*..... 489

2) *Prof. Donald Coles, Cal. Tech*..... 501

3) *Prof. Peter Bradshaw, Imperial College*..... 504

4) *Dr. Dennis Bushnell, NASA Langley*..... 507

5) *Dr. AMO Smith, Dynamics Tehcnology, Inc*.... 523

FLOOR DISCUSSION 526

LIST OF PARTICIPANTS

AFOSR/LEHIGH WORKSHOP
ON
COHERENT STRUCTURE OF TURBULENT BOUNDARY LAYERS

1. Prof. Douglas Abbott, Lehigh University
2. Prof. Ronald Adrian, University of Illinois
3. Dr. P. Bandyopadhyay, Cambridge University, England
4. Dr. Vincent Barra, New York University
5. Dr. Paul Bevilaqua, Rockwell International, Columbus
6. Dr. Stanley Birch, Boeing Commercial Airplane Company
7. Dr. Ronald Blackwelder, University of Southern California
8. Dr. Peter Bradshaw, Imperial College, England
9. Prof. Robert Brodkey, Ohio State University
10. Dr. Dennis Bushnell, NASA-Langley
11. Prof. John Chambers, Stanford University
12. Dr. Frank Champagne, University of California, San Diego
13. Prof. Donald Coles, California Institute of Technology
14. Prof. James Danberg, University of Delaware
15. Dr. Coleman Donaldson, Aeronautical Research Associates of Princeton, Inc.
16. Dr. Helmut Eckelmann, Max-Plank Institute fur Stromungsforschung
17. Prof. Robert Falco, Michigan State University
18. Dr. W. Fallar, NASA
19. Dr. Mohamed Gad-el-Hak, Flow Research Co., Seattle
20. Dr. Thomas Gatski, NASA-Langley
21. Dr. William George, SUNY-Buffalo
22. Dr. Fredrick Gessner, University of Washington
23. Dr. Giselher Gust, M.I.T.
24. Prof. Francis Hama, Princeton, New Jersey
25. Dr. Thomas Hanratty, University of Illinois
26. Dr. Gary Hanus, The Trane Company
27. Dr. Kenneth Helland, University of California, San Diego
28. Prof. Chih-Ming Ho, University of Southern California
29. Dr. Gilbert Hoffman, Pennsylvania State University
30. Dr. Fazle Hussain, University of Houston
31. Prof. Stephen Kline, Stanford University
32. Dr. Doyle Knight, Rutgers University
33. Dr. Leslie Kovasznay, Johns Hopkins University
34. Dr. Isoroku Kubo, Pennsylvania State University
35. Prof. Marten Landahl, M.I.T.
36. Dr. R. Vaglio Laurin, N.Y.U.
37. Dr. Otto Leuchter, ONERA
38. Dr. T. C. Liu, Brown University
39. Dr. Albert Loeffler, Jr., Grumman Aerospace Corp.
40. Dr. Hans Mark, Undersecretary of the Air Force
41. Dr. Donald Mc Eligot, University of Arizona
42. Prof. James Miller, Naval Postgraduate School, Monterey
43. Prof. Mark Morkovin, Illinois Institute of Technology
44. Prof. Hal Moses, Virginia Polytechnic Institute
45. Dr. Hassan Nagib, Illinois Institute of Technology

46. Dr. Badri Narayanan, NASA-Ames Research Center
47. Lt. Col. Lowell Ormand, AFOSR/NA
48. Dr. Steven Orszag, M.I.T.
49. Prof. Gary Patterson, University of Missouri-Rolla
50. Dr. Brian Quinn, AFOSR/NA
51. Dr. Eli Reshotko, Case Western Reserve University
52. Dr. J. Reynolds, Knolls Atomic Power Laboratory
53. Dr. William Reynolds, Stanford University
54. Dr. Basil Robbins, Pennsylvania State University
55. Mr. Morris Rubesin, NASA-Ames Research Center
56. Dr. John Russell, M.I.T.
57. Prof. Willy Sadeh, Colorado State University
58. Dr. R. Sathyakumar, Thermo-Systems, Inc.
59. Prof. John Shea, AFIT/ENY, Ohio
60. Mr. Amo Smith, Dynamic Technology, Inc.
61. Prof. Charles Smith, Lehigh University
62. Dr. J. Smith, A.R.A.P.
63. Lt. Col. Robert Smith, AFOSR/NA
64. Dr. Gino Sovran, General Motors Research Labs
65. Dr. K. Sreenivasan, John Hopkins University
66. Dr. Ryuji Takaki, Tokyo University of Agriculture and Tech.
67. Dr. Andrew Thomas, Lockheed-Georgia Company
68. Dr. Charles Van Atta, Univ. of California, San Diego
69. Dr. James Waletzko, Thermo-Systems, Inc.
70. Prof. David Walker, Lehigh University
71. Prof. James Wallace, University of Maryland
72. Dr. Wassman, Naval Surface Weapons Center
73. Dr. William Willmarth, University of Michigan
74. Dr. Israel Wygnanski, University of Tel-Aviv
75. Mr. Victor Zakkay, New York University

PARTICIPATING LEHIGH FACULTY

76. Prof. Philip Blythe
77. Prof. Forbes Brown
78. Dr. Frank Chen
79. Prof. Raymond Emrich
80. Prof. Edward Levy
81. Dr. Sudakar Neti
82. Prof. Donald Rockwell
83. Dr. Andreas Schachenmann

STUDENT AIDES

G. Abdelnour, Lehigh University
T. Cerra, Lehigh University
T. Conlisk, Purdue University
T. Doligalski, Purdue University
C. Knisely, Lehigh University
D. Kuzo, Lehigh University
R. Linney, Lehigh University
S. Nijhawan, Lehigh University
A. Tabatabaie-Raissi, Lehigh University
G. Weigand, Purdue University
S. Ziada, Lehigh University

WELCOMING REMARKS

HANS MARK

Undersecretary of the Air Force
Washington, D.C.

Ladies and Gentlemen. I am delighted to be here and to have the opportunity to open this very important conference. What is most surprising to me is that I still have sufficient standing among you, my scientific colleagues, to be invited here at all and for this I am grateful. So even though I am now just another one of the Washington bureaucrats, I hope that I can still count on you to give me at least a somewhat friendly reception on such an occasion.

A few days ago I was having lunch with two of my friends at the Pentagon, both senior Air Force officers and both former fighter pilots. I asked them why the Air Force should be interested in the field of fluid mechanics and why the Air Force should consider sponsoring a conference such as this. One of them immediately siad that all you have to do is to live through one good compressor stall in a fighter plane and you'll know why. I had a feeling that this comment was really completely unanswerable and that it explains in a nut-shell why we must continue to maintain a commanding position in the physics of fluids and in gas dynamics. We then continued to talk about engines and the huge investment that the Air Force has made in experimental engine test facilities. As you know, we have recently started the construction of the new large engine test facility at the Arnold Engineering Development Center. This facility is the largest single military construction item that has ever been funded by the government. When completed, the total cost of the facility will be just under 500 million dollars.

This is truly a mindboggling sum for a research and test facility. The existence of this project clearly illustrates the interest of the Air Force in the field, but what is more important, it highlights the necessity for much better understanding of the basic science. Only if our basic knowledge improves will this investment eventually pay for itself. The facility will be used for scientific work as well as testing and I want to return to this point in a few minutes. At some point during the discussion I mentioned earlier, the other officer said that, "We ought to be better than we are at the business." I thought that was an extremely interesting comment because it was made almost instinctively. I asked him why he thought this was so and his first reaction was that we'd been at it for a very long time. We have indeed been at the business of fluid mechanics for a long time. It is remarkable that

the development of the basic equations of viscous flow was started by C.L.M.H. Navier in 1822 and completed by Sir George Stokes in a famous series of papers written between 1845 and 1850. The fundamental relationships have been known for a century and a half. It is an example of the extraordinary difficulty that we face in understanding the subtleties of fluid flow to recognize that we are still struggling with the proper form for the solution of these equations. Personally, I believe that the full understanding of turbulent flow in fluids is the most difficult problem in modern theoretical physics. You all know that the great Werner Heisenberg did his Ph.D. thesis on turbulence in liquids and after receiving his degree went on to something much easier - he invented quantum mechanics! It is interesting that we have done very well at particle physics and we have done well at statistical mechanics. What we have not done well as yet is to gain an understanding of phenomena that are somewhere in between these two extremes. While statistical methods in turbulence have been useful, they do not match the precision that we have gained in conventional statistical mechanics.

There is also still, in my own mind anyway, at least the sneaking suspicion that the Navier-Stokes equations, as important as they are, do not contain all the physics necessary to describe a fully developed turbulent flow. As you know, the Navier-Stokes equations can be derived from the general Boltzmann transport equation and they constitute a rather simple approximation of that equation. The approximation is one in which the collision integral is approximated by a single constant - the viscosity of the fluid. Many attempts have been made to get other approximations of the Boltzmann equation for various purposes. Unfortunately, for the nonlinear case that we are considering here, none of these attempts have been very successful. The problem is that the physical interpretation of the constants introduced by the approximation process have proved to be very elusive indeed. Thus, it is not clear whether my suspicion is right and whether anything is to be gained by looking for a new set of equations that may be more fundamental than those developed by Navier and Stokes so many years ago. Nevertheless, I will still put it before you as a proposition that we should keep working on new formulations of the transport equation for fluids. It is very probable that any new formulation of this kind will not replace the Navier-Stokes equations in terms of practical importance just as the theory of relativity did not displace Newtonian mechanics. What I hope might happen is that a new and basic look at the physical foundations of the Navier-Stokes equations may lead to the necessary insight to explain the quasi-statistical behavior that seems to characterize turbulent flow. Perhaps something will come of it, especially as new experimental methods develop.

All of which finally brings me to the topic of this conference. We have made great progress in the field of computational fluid mechanics in the past ten years by exploiting computer methods for solving at least some simplified approximations of the Navier-Stokes equations. While this has resulted in some extremely important practical advances in the calculation of various practical aerodynamic configurations, it is not at all clear how much our fundamental understanding of the basic phenomena has been enhanced. This is why this conference is so important. I am convinced that there are new instruments and techniques, which when applied to experimentation and fluid flow, will be more fruitful in the next decade than computational fluid mechanics has proved to be in the past. I am thinking here specifically of coherent optical techniques which have been greatly improved from the classical Schlieren methods by the use of modern lasers. Correlation measurements on fluctuating quantities have become somewhat easier because of the availability of better computers that can be used interactively with an experiment. Thus, it may be possible to define new parameters that characterize turbulent flow experimentally and so, hopefully, broaden our theoretical horizon as well. There may be other things as well that are on the experimental horizons. The really astounding advances in solid state electronics and in our understanding of surface phenomena may lead to new kinds of electronic transducers that could give us a much clearer picture of the wall effects in turbulent flows. Finally, I should return for a moment to talk about large facilities. The means for creating interesting and unique flow fields are as important as the diagnostic equipment used for observing them. In this sense, I would like to invite you think seriously about how best to employ for basic research the high volume, high quality flow fields that will be produced by large facilities such as the one now being constructed at the Arnold Engineering Development Center. I believe that there is much promise in all of this and that it is most important to pursue these developments as vigorously as possible.

There is no doubt in my mind that this a most significant conference. In fact, I believe that it will be another landmark as the Stanford Conference on the same subject was a decade ago. Good luck, best wishes, and thank you.

SESSION I

FLOW VISUALIZATION

Session Chairman:

Stephen J. Kline

THE ROLE OF VISUALIZATION IN THE STUDY OF THE STRUCTURE OF THE TURBULENT BOUNDARY LAYER

S. J. Kline

Department of Mechanical Engineering

Stanford University, Stanford, California 94305

ABSTRACT

A discussion of the role of visual and probe measurements in turbulent structure research is given, stressing the constraining limitations of each and the interrelationships of the two methods. A selective history of the use of visual results is discussed in terms of the constraining limitations of the visual methods. Retrospective remarks are presented concerning the Stanford visual data on the inner portions of turbulent boundary layer structure. The final section discusses some general features of what is currently known about the structure of turbulent boundary layers, draws conclusions from this general knowledge, and poses questions that seem currently important in gaining further understanding. The paper stresses overall aspects of the structure problem at the expense of details in an attempt to gain perspective.

INTRODUCTION

This paper was originally intended to cover only the topic of the title, but as the writing evolved it became evident that, for good reasons, the visual data have become so closely entwined with probe data that it is necessary to discuss both. For reasons of length, I have limited myself primarily to the experimental evidence, for the most part, leaving to others the relationships to theory.

The intent of this paper is to focus certain issues of methodology, of substance, and of communications process that seem to me important at this time. In order to provide this focus, I have been selective, rather than exhaustive, in the evidence cited. This is done in an attempt to obtain a very broad overview as free as possible from the distorting noise of excessive detail. The details will surely have to be filled in, but

what seemed more important to me as a beginning point for this conference was to try to formulate a clearer framework that might help the process of clarifying the current questions about turbulence structure in boundary layers.

The paper has four parts:

I. A brief reminder of the comparative advantages and disadvantages of visual and probe methods.

II. A selective history of the role of visual studies in the turbulence structure problem.

III. Some retrospective remarks on the Stanford visual data on wall-layer structure and the relationship to later data.

IV. The structure problem -- critical questions and attitudes towards them.

I. VISUALIZATION AND PROBE METHODS

There are several recent summaries of visual techniques, and the purposes of visualization are discussed at length in the motion picture, "Flow Visualization," NCFMF (1964). Even if this were not so, telling this audience about basic techniques and purposes of flow visualization would be entirely redundant. It may be useful, however, to remind ourselves of the advantages and disadvantages of visual and probe methods in summary form and to recapitulate the particular difficulties encountered by each in turbulent structure studies.

Table I

Some Advantages/Disadvantages of Visual and Probe Methods

Visualization Methods	Probe Methods
• Give global picture.	• Give point-by-point data.
• Allow relatively easy survey of an entire flow field.	• Survey of an entire flow field very costly, time-consuming.
• Provide phase relations over time and space for motions of particles or structures.	• Provide phase relations for limited number of points but not for motion of particles; difficult to track structures.
• Can be used very close to surfaces and in separated zones.	• Difficult and of high uncertainty very near surfaces and in separated zones.
• Relatively high uncertainty in numerical values.	• Can be relatively accurate.
• Subjective to the extent that the human eyeball is involved with its considerable limitations in frequency and reliability. (cont.)	• Can be objectified if the "noise" can be removed from the signal for the structure. (cont.)

• No need to average over either time or space.	• Spatial resolution usually a difficulty in at least one dimension. Averaging needed for many types of data to remove "noise."
• Technique dependent particularly with regard to location of marking and reference frame of viewing.	• Technique dependent particularly with respect to data-reduction procedures.

It is evident from the table that the characteristics of typical probes and of visual methods complement each other to a remarkable degree. This complementarity implies several things.

(i) Both methods are needed and should be used syncretically and to check each other. Results cross-checked in this way are much less apt to yield misinterpretations than results of either visual or probe methods alone.

(ii) The simultaneous use of both visual methods and probes in some cases may be more illuminating than iterative application, for example in the work of Offen (1974) and several recent papers by Falco and others in Mac Head's group (we shall have the most recent by Bandyopadhay later in this session).

There is an even more powerful but subtler reason for simultaneous or iterative use of both methods than is explicit in Table I. Zilberman et al. (1977) have recently made this point well.

> "Part of the difficulty stems from the fact that we are concerned with a quasi-cyclic process of repeatable events which occur randomly in space and time imbedded in an environment of finer scales. We cannot unambiguously define the signature of an eddy without a priori knowledge of its shape and its location relative to the observation station, and cannot map such an eddy because we do not have a proper criterion for pattern recognition."

This statement implies that in some instances it will be literally impossible to extract desired results from probe measurements alone. In this context it may be helpful to recapitulate in a more detailed way the critical limiting difficulties of each type of technique, since these aspects tend to substantiate the remark of Zilberman et al. and suggest an even stronger interdependence of the methods than indicated by Table I. The remarks may also help interpret better the selective history that follows.

The critical difficulties in visual methods do not center on the high uncertainty of the data, but rather on the fact that one observes streaklines rather than pathlines or mean streamlines in unsteady flows. Streaklines are not well-adapted to the formation of mathematical models in accessible modes of analysis, and as a result one tries to relate the visual results subjectively, via heuristic mental processes, to the physical modules and then in turn to mathematical models. These subjective inferences need to be checked by probe methods for final empirical

verification. The truly considerable problem raised by this subjective examination of streaklines has been most forcibly illustrated by Hama (1962). One of his figures is reproduced, with his permission, as Fig. 1 of the present paper. Fig. 1 shows how an oscillatory motion superposed on shear-layer motion might be misinterpreted as vortices by subjective visual pattern study. The example is extreme but not inappropriate. Since a great deal of the data on turbulence structure in boundary layers is visual, it is not surprising that the current scientific controversies include many points that concern interpretation rather than the data per se. Much of this difficulty is eliminated by use of combined-time-streak markers (see Schraub et al. (1964). Moreover, if one marks a particle at a given location, A, and then at a later time sees the marker at location B, it is prima facie evidence that some trajectory connects locations A and B.

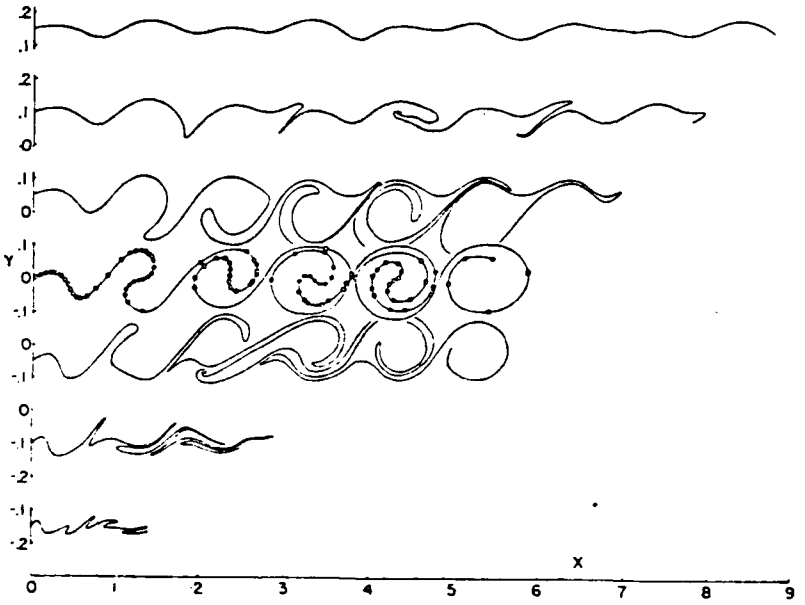

Fig. 1. Apparent vortices shown by streaklines for a shear layer with a superposed sinusoidal oscillation of amplitude 0.05 $\bar{u}$. From Hama (1962).

The most critical difficulty with probes comes from two sources and is again not related to the sometimes considerable basic uncertainty in data, but rather to questions of averaging and to the extraction of signals from relatively high noise backgrounds. The critical difficulties thus focus not to much on interpretation as on omission -- the danger is that important phenomena will be missed. This is not hypothetical; it has occurred in a number of instances. For concreteness I shall mention two here. There were probe measurements of at least the outer portion of the viscous sublayer prior to the 1950's, but there was no indication in these measurements of the alternating array of transverse high-speed and low-speed streaks that is the dominating feature of the structure of that layer. This omission was probably due to the fact that the transverse

length of the typical probes (hot-wires) is many times the length of a streak in low-speed air flows of conventional research, and hence the structure is simply averaged out. The difficulty may have been compounded by the fact that the streaks are not stationary in location over time, but the spatial averaging alone would probably have been enough to have caused investigators using only probes to miss the phenomenon. Another instance that is at least as striking occurred in free-shear layers. The clever and extensive studies of Browand and Mollo-Christensen (as well as those of many other workers) in the near region of jets failed to reveal the now familiar "pairing" process uncovered in visual studies by Brown and Roshko (1974) and also by Winant and Browand (1974). Mollo-Christensen and Browand did find subharmonics, but the effect of averaging hid from them the nature of the underlying structural feature (pairing) that created the subharmonics, and their interpretation was limited to discussions of nonlinear interactions which fall short of providing a clear structural picture. I choose this example precisely because the difficulties lie with the basic problem of probe techniques and not in any lack of ability of these very able investigators. Browand's recollection on the matter in a letter to the author is attached as Appendix I. Fred Browand's letter also makes another point: pictures in themselves are not sufficient, either. The critical thing is appropriate interpretation of the pictures to select centrally important structure features. This point will recur.

I also want to show a very short film clip of pairing taken recently by Gene Bouchard, a current doctoral student of Bill Reynolds' at Stanford. Bouchard's work shows some interesting effects of modulation on pairing, but that is not the purpose of showing it here; it is rather so that we can see in vivo the very real difficulties of interpretation. Imagine you are an investigator who is trying to deduce flow structure from one probe standing in the critical region where pairing vortices pass the probe, but without the benefit of associated or prior visual study. If you were to use several probes, but did not know of pairing, the likelihood of a placement that would reveal the structure is vanishingly small.

Notice also that a single hot-wire registers the magnitude of the vector normal to the wire, so there is a good probability that large v components of velocity will be read as changes in u if the picture is not known.

Nor is visual study alone enough. As Browand notes, there is the further difficult task of focusing attention on those few details, among the myriad present in any turbulent flow, that are important to the physical process and are not just noise. In this connection, Ø. Oseberg and I (1971) failed to observe pairing in a different but related experiment, even with visualization. When I look back now at Oseberg's films, the pairing is clearly there. Moreover, the pairing seems obviously important -- now that I know to look for it as a result of the attention focused on this flow module by Brown and Roshko (1974), Winant and Browand (1974), and others.

This short recap of the critical difficulties in visualization and probe methods is perhaps enough to remind us of the need for cooperative effort between those of us who emphasize visual and those who tend to rely more on probe methods. It also makes very clear the need for iterative or simultaneous use of the two methods. We need the visual (recognition) methods plus good insight to survey total flow fields, disclose phenomena, and suggest hypotheses. We need the probe (dissection) methods to improve the accuracy, extend knowledge of details, and check hypotheses. Without the foreknowledge thus far usually provided by visual studies, probe methods are in a very real sense blind and may fail to disclose important phenomena. Without the greater accuracy and dissective power of probe measurement, visual results often leave unchecked critical questions of interpretation. We shall see the same lessons repeated in the next section on the history of visualization in the structure problem.

II. A SELECTIVE HISTORY OF THE ROLE OF VISUAL STUDIES

As we all know, the discovery of the phenomena of turbulence by O. Reynolds (1883) in pipe flow was visual. And in this first instance, the interpretation of the visual results led to some later difficulties. If I can take the liberty of oversimplifying Reynolds' remarks, he concludes that turbulence is more or less "a random fluctuation on the basic meanflow." He then proceeds to analyze turbulent motions, as we well know, in terms of a two-part decomposition: the meanflow and the fluctuations. This view leads to the formation of mixing length models that imply (although do not require) that Reynolds stresses are more or less continuous as a result of random fluctuations in a transverse velocity gradient. The mixing length models have gradually been found to lack universality, so that they are today usually seen as "postdictive" empirical fits rather than as explanatory in the sense of a basic flow module. The view proposed by Reynolds also led to the early statistical measurements that emphasized homogeneous fields and have not been very productive in terms of applications, at least for shear flows. The probability is very high that if the problem of turbulence were really characterizable as "random fluctuations on the meanflow," the statistical methods would have solved at least many important problems long ago; the well-developed methods of statistical mechanics are too powerful to believe otherwise. A central difficulty with the early statistical measurements is that they are based on the idea that long-time averages will by themselves educe the underlying structure. As we now know, this is sometimes untrue; it is to this point that the quotation above from Zilberman et al. speaks. The discussions in the Proceedings of the 1968 AFOSR-IFP-Stanford Conference on Computation of Turbulent Boundary Layers (Eds. Kline et al., 1968) show there was still strong disagreement on this point at that time.

There is clear evidence in the literature that all is not right with at least part of the view implied by Reynolds in relatively early times. The Prandtl-Ahlborn pictures, taken in the late 1920's[†] with a traversing camera, show clear evidence of quasi-coherent structure in turbulent flow

[†]These films are undated, but Sydney Goldstein, who participated in the filming, indicated to the NCFMF that they were taken in the late 1920's. Copies of movies available as 'loops' from the Encyclopedia Britannica Films.

(see for example the pictures in Prandtl-Tietjens (1934)). The views of the wall layers by Fage and Townend (1932), using particles and an ultramicroscope, also show that the near wall layers are decidedly unsteady -- not merely slightly perturbed -- and hence that something is wrong with the view of the viscous sublayer as a "laminar film." Why is it, then, that the view implied by Reynolds remains the central paradigm, the central conceptual belief system, in the turbulent research community until well after 1950? It seems to be a case of the theorem of T. Kuhn (1962) in his famous work on scientific revolutions. Kuhn concludes from study of many historical examples that such central paradigms are never overthrown until someone advances another that seems to fit the data better. The mere fact of contrary data seldom overthrows a central paradigm; indeed, since we are always dealing with approximate representations of nature in our scientific concepts, models, theories and 'laws', some contrary data nearly always exist.

What happened after 1950, then, to begin to change the view of turbulence as a meanflow plus random fluctuations? First, there seems to have been a growing realization that we were not increasing our understanding or predictive ability concerning turbulence proportional to the amounts of sophisticated research efforts devoted to the problem. Second, the seminal work of Townsend (1956) on the Structure of Turbulent Shear Flow was published. In this work Townsend takes a fundamentally different view, namely, that large, relatively coherent structures play a dominant role in maintaining shear-flow turbulence. From the experimental side, a number of investigators, four sets to my knowledge, uncovered data that were flatly contradictory to existing ideas about the flow modules in the wall layers, and all these arose because markers were used in the wall layers. These four groups included: Beatty, Ferrell and Richardson (see Corrsin (1957)); Francis Hama (1957); Howard Emmons and Mort Mitchner (unreported in the literature circa 1951); and the group at Stanford beginning in 1956. The work of Beatty et al. seems to have influenced chemical engineers, particularly, to develop a body of theory concerning "replacement theories" of the wall layers that have played an important role in mass transfer theory, although I have not traced that literature in detail. Hama did not follow up on his observations on the discussion of Corrsin's paper with further publication. In his discussion, Hama does point to the difference between laminar and turbulent near-wall layers as seen with dye markers, but focuses on the strong similarity between the wall-layers in the turbulent layer and in the natural transition at the Klebanoff-Tidstrom streak and initial spot formation stages. In a private conversation, Prof. Emmons has told me that he and M. Mitchner observed sublayer streaks in their famous work that first disclosed turbulent spots in laminar-turbulent transition on a plate, but that they thought the streaks were due to spurious experimental technique, and did not follow up. In the Stanford group we began observing the anomalous wall-layer behavior in studies on diffuser flows, and hence in adverse pressure gradients. In such flows the flow modules very near the wall are even more anomalous than for a flat plate, when compared to the older view of the viscous sublayer as a uniform sheet of laminar flow. We came rather quickly to hypothesize that this anomaly played a significant role in turbulence production in boundary layers, and hence instigated a series of studies to check this idea.

The difference between the work at Stanford and the other wall-layer work seems to have been that we did move beyond recording the anomalous data to extract what we thought were central structural features, to hypothesize what these features might mean, and to formulate experiments to check the hypotheses. This is the point that Fred Browand makes in his letter to me about the discovery of pairing, and that I have extracted and underlined above: Observation does not seem to be enough -- we need to move to the extraction of critical structural events and their interpretation. These two ideas -- the need for interpretation, for identification of central events, and the need for checks on the interpretation by other forms of data -- have perhaps not been made sufficiently explicit in earlier discussions of the role of visual methods in turbulent structure studies, and hence I stress them here.

There are now enough data cross-checked between visual and probe methods to make it quite clear not only that the Reynolds stress is highly intermittent but also that it is associated with certain more or less identifiable events. Indeed, this conference is largely concerned with further clarification of the characteristics and repeatability of such events.

With this in view, it may be helpful to ask what it was that led Reynolds to interpret his visual results as a meanflow plus more or less steady "random fluctuations"? One can never be certain about someone else's thinking process, but the ideas in the first section do suggest some possible reasons. As noted, the results are strongly dependent on the location of marking and the reference frame of viewing. In Reynolds' experiment, he injected dye in the center of his pipe (and not in the wall layers), and he viewed the markers from the reference frame of laboratory coordinates. Such a marking location and view do give an appearance of relatively steady random fluctuations superposed on a meanflow -- probably nearly everyone in this conference has seen the experiment done and knows this picture from student days, texts, or NCFMF movies. Osborne Reynolds' conclusions were consistent with the marking method and reference frame he employed. Hence the review here does not detract from Rdynolds' landmark contribution; it merely emphasizes the cautionary note concerning the constraining uncertainty of visual methods discussed in Section I above.

Independently, based on probe measurements, Corrsin and Kistler (1955) showed that the outer portion of the layer is intermittent and hence also does not conform to the idea of simple meanflow plus random perturbations; large eddies of some sort are present. This seems to be one of the few incidents where a major structure feature has been initially revealed by probe measurements. Without meaning to detract from this important contribution, it may be useful to note that it is possible to observe intermittency in the outer layers with minimal conditioning of data. Since there is a low noise background in the non-turbulent portions of the flow, detection is thereby considerably simplified, and probe measurements alone are less likely to be misleading.

After the 1950's, there have been many other significant visual studies of boundary layers, particularly those of: Brodkey and colleagues at Ohio State and Göttingen; of Falco, Mac Head, and others at Cambridge; and more recently of Coles and others at Cal Tech.

I shall postpone further remarks on these more recent studies until after a brief recapitulation of the main results of the Stanford studies in the following section, in order to clarify certain matters of nomenclature and interpretation beforehand.

III. RETROSPECTIVE REMARKS ON THE STANFORD VISUAL STUDIES OF BOUNDARY LAYERS

The visual studies of the wall layers at Stanford between 1957 and 1974 include primarily studies of the turbulent layer on smooth surfaces with zero or small pressure gradient: Kline and Runstadler (1959); Runstadler and Kline (1963); Kline et al. (1967); Kim et al. (1971); Offen and Kline (1974); and Kline and Offen (1974). However, one dissertation was done on flows with positive and negative pressure gradients (Schraub, 1965), one on rough surfaces (Liu, 1966), one on transition comparing structures in the later stages with those of the turbulent layer (Meyer, 1961), and two on effects of system rotation (Coreolis force) in channel flows (Halleen & Johnston, 1967, Lezius and Johnston, 1971). Some smaller works were also done on the zone of incipient separation (Kline, 1957, and Sandborn and Kline, 1961) and on laminar-turbulent transition 'bubbles', i.e., quite thin, three-dimensional separations with transition occurring in the free-shear layer prior to reattachment. The range of phenomena studied is mentioned here for two reasons: first, to give an idea of the generality of the phenomena observed; second, to suggest that the flat plate, both transition and fully turbulent, has now been studied in some detail by many observers, but that almost all the other phenomena still could profit from more detailed visual as well as combined visual-probe and probe studies. See, for example, the survey by Kline in the volume edited by Sovran (1967). This seems to me particularly true of the zones of separation and reattachment, and of pressure-gradient flows where we have yet a great deal to learn about structure. An additional case of great importance not covered in the earlier surveys also needing study is wall curvature which extends via mathematical analogy to many cases of body forces. Moreover, for slow separations, for reattachments of shear layers, and for adverse pressure gradients, the data available suggest that the wall layer structure is probably even more important to understanding the flow physics than for the flat plate.

What all these studies showed as a uniform feature, with no observed exceptions in thousands of individual observations in the Stanford laboratory and also at times in other laboratories, is summarized in Fig. 2. which shows a plan view and a side view of flow marked with a transverse line of dye or bubbles. I shall run a movie of several views of these phenomena shortly. Since the early studies at Stanford used marking in the wall layers, we saw only the outgoing motions (see further comment in final section). We were aware of this, and cognizant that return flows had to exist by virtue of continuity, but initially were not sure why we saw mainly outward motions. Nevertheless, the results of the early studies, prior to 1965, established several points. Please see Fig. 2 for nomenclature.

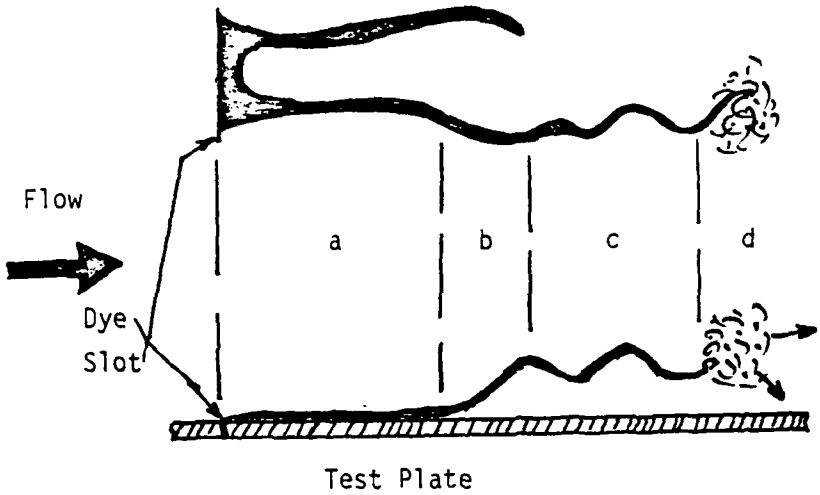

Fig. 2a. Plan view.
a = Wall migration
b = Streak lifting
c = Oscillation
d = Breakup

Fig. 2b. Side view.

Figs. 2a,b. Schematic of wall-layer bursting as seen by dye injection through wall.

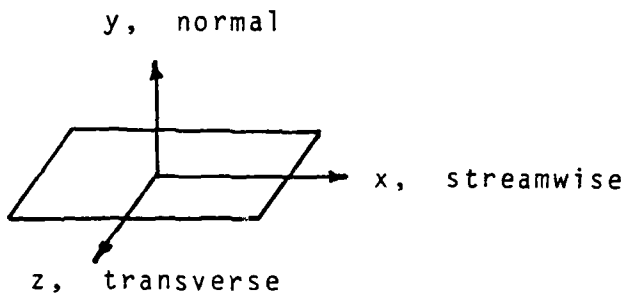

	Marker Line Direction	Views (Camera Sight Lines)
x	Not used	Streamwise
y	Normal	Plan
z	Transverse	Side

Fig. 2c. Coordinates and Nomenclature

1. Structure of Sublayer and Buffer Layer

The primary structure of the viscous sublayer is an alternating array of low-speed and high-speed streaks. The array has a well-defined and repeatable mean spacing, but a very large standard deviation of spacing about the mean*. The mean spacing for all pressure gradients on smooth surfaces is 100 wall-layer units. The low-speed streaks are wider near the surface; the high-speed streaks are wider farther out. Clear evidence of the streak structure is seen to $y^+ = 40$ for the flat plate, but it is well defined and dominant only for $y^+ \leq 10$ at moderate R_θ.

2. Intermittency

The viscous sublayer is distinctly intermittent in the sense that markers introduced into the sublayer do not stay there as the fluid moves downstream. Fluid marked very near the surface of a flat plate (we estimate at $y^+ < 0.1$ for some observations and well below $y^+ = 1$ in many) moves very slowly outward, but after some distance was always seen, in our observations, well out into the buffer or log zone before the markers diffused and could no longer be followed. Following the argument made in the first section of this paper, the result is unequivocal; fluid does physically interchange intermittently between the layers closest to the wall and the zones farther from the surface. Nothing is implied at this stage about interpretation or significance; it is simply a uniformly observed fact that interchange of fluid occurs between the fluid closest to the wall and the buffer and log regions. We did not at first see the return flows; so far as I know these were first documented by Brodkey and co-workers (1969) using different marking techniques and viewing frames.

3. The outgoing motions described in part in the preceding paragraph comprise a definite repeatable quasi-cycle of events. This quasi-cycle has a definable and repeatable period; however, the period also has a very high standard deviation. Questions existed, and to some extent still exist, about how best to define the mean period and on what parameters to correlate it (see next section), but the central fact is that it exists.

---

*Perhaps the most surprising things about this streak structure are its strength and universality. It is present in every observation from the turbulent spot stage downstream, whenever the flow is turbulent. We have yet to see a single exception. In fact, I now consider the presence of wall-layer streaks as a critical diagnostic for whether a given zone or patch of the layer is turbulent. In many instances we tried to see how long it would take to establish the streaks when markers were inserted uniformly; we used several dye and bubble techniques striving to increase uniformity of marking transversely. In no case were we able to make visible a delay period where the markers were uniform for some distance from their insertion, and then gathered into streaks. They always appear to move into streaky patterns without visible delay. One might say the structure enforces itself very strongly on the markers.

4. The features described in the preceding paragraphs 1, 2, 3 have time-sequences or phase relations that can be described in four parts:

a. Wall migration. Markers inserted within the sublayer always go into the low-speed streaks -- not the high-speed. These marked low-speed streaks migrate very slowly outward. The closer the low-speed streaks are to the wall when marked, the longer the average distance of this slow outward motion. This migration may involve many boundary layer thicknesses.

b. Streak-lifting. At some point, when the markers reach near to the edge of the viscous sublayer, the low-speed streak 'lifts', that is, it turns sharply outward and in a relatively short distance, typically less than a boundary layer thickness, it is seen to be in the buffer or inner portion of the log layer.

c. Oscillation. The lifted low-speed streak appears to oscillate violently, but only for a few cycles, typically two or three. The oscillation is seen in both plan and side views, and hence is three-dimensional.

d. Breakup. The streak is observed to "break up" into much finer grain, smaller scale, and more chaotic motion. At this point the visibility of markers is quickly destroyed, and we were unable to track the motion farther as a coherent structure using this type of technique in a laboratory reference frame.

Relatively early in the work (see Kline and Runstadler, 1959), we hypothesized that this set of specific events played a role in turbulence production. The study of Kim et al. (1971), which was the first to use the combined-time-streak marker method (developed for this purpose and for the teaching movies of the NCFMF), established the validity of this hypothesis at least for relatively low Reynolds number layers on a flat plate. In particular, H. T. Kim showed that approximately 70% of the total turbulence production in the boundary layer occurs during the events in the quasi-cycle called 'bursting', (d) above (see also Section IV).

At a later time, the results of Brodkey and Corino (1969) led us to employ visual methods that overlapped the earlier studies but also made visible inward motions -- "sweeps". These results, Offen and Kline (1974), and also those of Brodkey et al. at roughly the same time, show that the sequence of events (a), (b), (c), (d) above become involved in larger-scale motions that propagate disturbances which observably, about half the time, appear to set off a new sequence of low-speed-streak lifting, oscillation, and breakup*. Thus the complete process appears to be quasi-cyclic over time and space. Since I am summarizing the Stanford studies, it seems a good place to attempt to clarify some misconceptions

*In Offen and Kline (1974) we also suggest some possible interpretations regarding interaction of inner and outer layers, but I leave this to discussion in the conference for reasons that appear below.

about those studies that have appeared in the literature or have repeatedly formed the basis for questions.

First, do the low-speed sublayer streaks move upstream? In our observations, the answer is quite clear, but it must be given in two parts. For zero and favorable pressure gradients we have never observed an upstream motion in laboratory coordinates. For the flat plate case, the velocity excursion of the high- and low-speed streaks is 50% up and down from the long-term mean speed at a given y^+. Thus the excursions are surprisingly large, but do not extend to flow reversal for favorable or zero-pressure-gradient cases. For adverse pressure-gradient cases, flow reversals of the low-speed streaks are observed (see Kline, 1957, and Sandborn and Kline, 1961). At first we called this "small transitory stall," but I now believe that "incipient separation" is more accurate and descriptive. I think this phenomenon is well worth further study; our studies were not extensive, and the phenomenon is, I believe, critically important in all turbulent layers that are near or slowly approaching complete separation. Only two further detailed studies have been done to my knowledge, by Simpson and colleagues (see Strickland and Simpson, 1970). The same remark is true concerning reattachment of shear layers; no really enlightening study of structure has yet occurred; see J. Kim and Kline (1978) on reattaching flow for an example of why structure is important. I understand Dr. Bandyopradhay will also speak about reattaching flow later in the session. Some current further research at Stanford also concerns reattachment.

Second is a matter of nomenclature that has become confusing. We called the total three-part sequence described in (b), (c), (d) above 'bursting'. That is, bursting as we used the word included: streak-lifting, oscillation, and breakup. In view of later results, it might have been better to have called (d) alone 'breakup' by the name 'bursting', but we did not. A number of measurements by others identified bursts in various ways, usually by monitoring the Reynolds stress or some derivative of it. Since the high Reynolds stress and turbulence production occur in what we called 'breakup', this is the identification I believe should be made, and not to what we called 'bursting'. However, as Offen and Kline (1973) showed, the various techniques were not in good correspondence; they agreed much better than chance, when directly compared, but at that time none of the available methods for picking out bursts correlated well enough to be sure we were getting sufficient overlap of the samples of the events involved in the periods of high Reynolds stress. It may well be that the more recent and sophisticated correlation methods such as that of Zilberman et al. (1977) will show better agreement, but that remains to be checked at this time.

Third, we have sometimes been quoted as suggesting that the sublayer is unstable. Our data do not support this remark, and, so far as I know, we did not make it. We did suggest that the lifted-low-speed streaks appeared to become unstable, but this occurs in the buffer- or lower log-layer after the low-speed-streak has 'lifted' away from the wall, and that is qualitatively different from saying the sublayer is inherently unstable. See also remarks below, and in the final section, on this point.

Fourth, did we observe upstream extending trajectories of lifted streaks, that is, of outgoing motions? The answer for the flat plate is unequivocably No! For adverse pressure gradients, incipient separation, one sees short upstream motions, but these quickly reverse into outward and downstream trajectories so long as the flow is not fully separated.

Fifth, there has been some discussion of G. I. Taylor's suggestion that separation might play a role in transition and, by extension, in low-speed-streak lifting. Separation in the sense of recirculating flow in a laboratory frame of reference can play a role, but it need not and does not in our observations of the zero and favorable pressure-gradient cases. The remark of Offen and Kline concerning flow separation is restricted to a moving reference frame and cannot be detached from that frame without doing violence to the concept and the observations.

I would like at this point to introduce a plea for clarity on certain points that seem to me an object lesson of the preceding paragraphs on questions about our work and the remarks on the central difficulties of visualization in Section I. At least in this conference it would seem very helpful, I would like to say imperative, that we be clear on certain points if we are to understand each other accurately. In particular, I hope we can regularly identify three things: (i) reference of coordinates; (ii) locations of markers; (iii) lines of sight, views, camera angles. It is very helpful to use different words for (ii) and (iii), as in Fig. 2. Even more important, given the fact that we are talking about a complex series of events apparently occurring in a quasi-cyclic way over time and space, when we speak of an event or a flow module, such as an instability, I hope we can say clearly: (i) where it is in space, the y^+ for example; and (ii) its relation in time to other events. Finally, if we use the word "burst", I hope we can agree to give the criterion (or concept) used to identify it.

What is given to this point in the present section is a report on observables; up to the limits of technique and uncertainty, it seems safe to take them as facts. However, I need to move now into a qualitatively different kind of realm -- that of interpretation -- and I want to mark the transition clearly. In the realm of interpretation, much doubt and considerable difference even of qualitative explanation still exist. And in recent years these differences seem to have grown rather than shrunk. I hope that one function of this meeting, restricted as it is to research workers active on problems of boundary layer structure, will be to begin to sort out agreements, questions, and differences and assist in planning strategies for clarifying questions and differences. I shall return to this point in the final section.

I cannot in a reasonable length treat all the problems of interpretation, but I should like to discuss three I see as currently important to get them on the floor for continuing discussion in this meeting: (i) the relative importance of the inner and outer layers in producing and maintaining turbulence, and the relationship, if any, between those layers; (ii) the relative importance of large- and small-scale motions in producing Reynolds stress; (iii) the flow module or cause, if you insist, of the intense intermittent periods of high Reynolds stress.

In regard to the inner and outer layers, I want to employ the method of logic I call negative inference*. I have done this before, but not for publication. In this method one delineates a complete set of hypotheses, covering all possible cases, and then eliminates some of them by counter-example. Unlike the method of positive (inductive) inference, negative inference closes and can give clear-cut results. Let me form a complete set of three hypotheses with regard to the roles of inner and outer layers: (a) outer-layer-dominated; (b) inner-layer-dominated; (c) interactive. (a) implies that the important events occur in the outer layers and the inner layers are in a sense merely "dragged along for the ride" by Reynolds stresses; this is at least the implicit view of most of the older literature on boundary layers. (b) implies that something, usually an instability, occurs in the inner sublayer that drives the outer flow. Three theories based on this kind of idea have been published: Einstein and Li (1957), Hanratty (1956), and Black (1966). (c) implies that both the inner and outer layers are important and that the two layers interact with each other, either rapidly or slowly, in some significant way. It is not difficult, given the evidence now available to eliminate (a) and (b) by negative inference. I shall not cite all the data, since only one counter-example is logically required, but I shall give several in each case to supply redundant arguments.

To eliminate hypothesis (a), outer-layer-dominated, consider the data data on drag-reducing polymers and on rough walls. We know that if polymers are present in the outer (but not the inner) layers of the flow, little if any effect on turbulence levels and turbulence production occurs. On the other hand, introducing polymers into the wall layers (but not the outer layers) causes an almost immediate and often large (up to 80% in some data) reduction in turbulence production and dissipation. See for example Oldaker and Tiederman (1977) and underlying references. Consider the flow over a plate with a smooth surface for some distance, followed by an abrupt jump to a rough surface. After the jump in roughness, the smooth-surface-type equilibrium layer established on the early part of the plate will be gradually "eroded" by the rough-surface-type layer, since a rough layer grows faster; thus, sufficiently far downstream, the entire layer will have the characteristics of an equilibrium rough layer, consistent with the new value of wall shear. For data see Tani in the volume edited by Kline et al. (1968). Further, see the remarks in the final section regarding many different kinds of effects that 'stabilize' or 'destabilize' the wall layers. These two effects, roughness and polymers at the wall, thus show beyond doubt that what happens at the wall or very near it is important through the whole layer on the most significant physical quantities, and this directly contradicts an outer-layer-dominated view.

With regard to hypothesis (b), inner-layer-dominated, consider the data of Brodkey and colleagues and of Offen and Kline. In both these studies the "breakup" is seen to cause disturbances that in some cases (observably about half the time) appear to start the next cycle of low-speed-streak lifting, oscillation, and burst farther downstream. Also, many sets of data show unequivocally that wall-pressure fluctuations

*Called "strong inference" by some; see for example Platt (1966).

scale on outer-flow frequencies, not wall layer variables, as a function of Reynolds number; see for example Willmarth (1977) and underlying references.

Also, the very clear "tracks" of inward-moving "sweeps" that begin sublayer streaks presented by Oldaker and Tiederman (1977) show that the outer flow does strongly impress itself on the wall layers. Finally, the recent papers by Falco (1977) and underlying references indicate that important, Reynolds-stress-bearing events in the outer layer are characterized by length scales of inner variables*.

In sum, the only tenable hypothesis, in view of much present data, is hypothesis (c) -- the inner and outer layers interact. Both inner and outer layers are important in understanding the physics of turbulent boundary layers, and the actual interaction process is very probably also important to that understanding.

Looking at them retrospectively, the results of the Stanford visual studies appear consistent with an interaction model. Observe, in particular, that the oscillation and breakup stages, in our nomenclature, involve a strong interaction of the lifted streak with the surrounding flow. This is evident from the fact that the lifted streak typically begins with a characteristic cross-section dimension of roughly 20 wall-layer units, and the oscillation and breakup appear to have characteristic overall dimensions an order of magnitude larger. The lifted-low-speed streak has become involved with other fluid, apparently owing to either an instability of the shear-layer formed by the lifted-streak or of some other kind of interaction process. We suggested the possibility of instability at this point because the instantaneous $U(y)$ profiles in such flow modules reported by H. T. Kim et al. were characteristically strongly inflexional. But our data do not rule out the possibility that the breakup stage arises from an interaction with the outer flow; indeed, as I have just suggested, the data imply an interaction in some sense -- it is the 'sense' that still seems to me to be in question. Moreover, there is nothing in the data that suggests that the sublayer-streak structure cannot be the result of 'footprints' of the outer flow; indeed, the totality of data and theory now suggest that they are such 'footprints'. This is also in some sense an interaction, and again it is the 'sense' that seems to me still undetermined at present.

It has been the common wisdom for some time that the large eddies carry the Reynolds stresses. However, recent data raise doubts concerning this view. The data of Falco (1977) and underlying papers suggest that the high Reynolds stresses occur in eddies that scale on inner variables and are much smaller (the order of the microscale) than the largest identifiable eddies in the boundary layer. Willmarth and Bogar (1977) reach similar conclusions, on a tentative basis, from measurements with exceptionally small hot-wire probes. The data of H. T. Kim et al. (1971) and

*The mean time between such events is still subject to very large uncertainty owing to problems of recognition (conditioning). As Laufer (1972) notes, the uncertainty is the order of a factor of 5, conclusions that rest on discrimination of this mean period to tighter levels seem to me still questionable.

of Offen and Kline (1974) also create some doubt on this issue. In particular, Offen and Kline did not observe high Reynolds stress in the oscillation stage, as we expected beforehand from the common wisdom about scale; instead we observed the high Reynolds stresses in the breakup stage where the characteristic scale is much smaller. Moreover, conditionally sampled spectra taken by Offen to include only 'breakup' times showed increased energy in the minus-one range of the spectra, but an even larger increase in the dissipation range -- that is, at small scales. (As an aside, it may be well to note with regard to difficulties mentioned in Section I above that the long-time averages from the same flow showed no bulges in the spectra at all; the critical phenomena are missed.) I do not want to comment further on this point here; I want only to get these data and the question of the contribution of small-scale and large-scale motions to Reynolds stresses before the meeting as a potentially important question for discussion.

In recent years the flow modules and theoretical concepts advanced as potential explanations for turbulence production have proliferated. Landahl (1977) has continued his work that conceives of the production as a wave-guide phenomenon dependent on subtle phase relations. Coles and Cantwell (1977) and also Brown and Thomas (1977) view the production of turbulence as arising from the passage of large-scale structures arising in the later stages of transition and sweeping downstream. These authors also suggest that the sublayer-streak structure arises from Taylor-Görtler instabilities, owing to the passage of these larger structures over the wall layers. Falco (1977) suggests that the turbulence production arises in the outer flow from characteristic eddies occurring on the back, the upstream face, of the largest eddies (bulges). Zilberman et al. (1977) describe the characteristic eddy as an arch underneath which faster-moving fluid is observed at one stage, and suggest this faster-moving fluid may be 'sweeps' that interact with the wall layers. Kim et al. (1971) suggested that production might arise from an instability owing to the sharp shear layers created by low-speed-streak lifting.

All this looks pretty confusing; it might seem as if we have 'too much' evidence. I don't think this is so, however, for several reasons that I take up in the final section. I need not dwell on the fact that this conference needs to try to assess these views as competing bases; that will naturally occur. But I do want to suggest that we give equal attention to the questions: "To what extent are these competing concepts merely different views of the same thing?" "In what ways are they consistent with each other when we take acount of the different ways in which they are framed?" I discuss these and related questions in the final section of this paper.

IV. THE STRUCTURE PROBLEM: SOME CRITICAL QUESTIONS AND ATTITUDES TOWARD THEM

In this section, I shall revert to talking about the characteristic turbulence structure as a herd of elephants -- as this research community has done before -- by analogy to the story of the three blind men and the elephant. What do we know in 1978 about this herd of beasts? What does

the selective summary of the preceding section tell us? Taking again an overview to avoid confusion from too many details, it is clear that we do know some general things quite clearly. I shall enumerate some and then discuss them.

1. The herd and each individual elephant are very complex. It is hard to see how they could be much more complex. Unlike most physical phenomena, turbulence is not simple, and thus far does not seem amenable to extraction into simple elements and models.

2. The elephants are intermittent in their appearance at a given location, and they are set in a background of high noise.

3. All the observable features of each elephant have high standard deviations of the central properties about mean values extracted by appropriate conditioning of data.

4. The passage of an elephant appears to include a quasi-cyclic set of at least several events occurring over time and space. (However, it is not clear at present how long an individual elephant lives. Does he die and then become reincarnated by later events? Does she go on forever, presumably by extracting energy from the mean flow? Or does the elephant change her spots, so to speak, become, say, a leopard for a short time at some stage like 'bursting', and then retransform to an elephant at the next stage in the quasi-cycle farther downstream?)

5. The inner and outer layers have distinct and different characteristic lengths and times. Both layers are physically important. The two layers interact with each other, but usually approach "equilibrium" relatively slowly. Nevertheless, the interaction appears important to the physics.

6. We have a number of views of a single elephant taken with different techniques and from different reference frames.

7. The nature of the elephant is such that the effective shear forces (and more generally all the important properties of the layer) are significantly altered by a wide variety of parameters that for the most part do not affect laminar layers in the same way. These include:

   (1) streamwise pressure gradient
   (2) centrifugal force (with or without density gradient)
   (3) Coriolis forces
   (4) wall curvature
   (5) wall roughness
   (6) compliant walls
   (7) energy release, chemical reactions
   (8) density stratification in gravity (or other force) field
   (9) additives (e.g., polymers)
   (10) compressibility, at least at hypersonic speeds
   (11) two-phase flow
   (12) EHD forces
   (13) MHD forces
   (14) oscillations of mainstream

Each of these effects is capable of changing levels of turbulent shear and turbulent production up and/or down by an order of magnitude. Hence the elephant is functionally as well as structurally complex. Adequate understanding of turbulent shear layers must include at least an explanation for these phenomena, since any explanation that does not is incomplete. Moreover, these data for boundary layers uniformly follow the qualitative idea that when the wall-layers are stabilized*, the level of turbulent shear, production and dissipation in the layer drop. Conversely, when the wall-layers are destabilized, turbulent shear, production and dissipation rise, but in some cases only to an upper limit. We are not able to put numbers on many of these effects, at present, but the qualitative trends are known. This fact, the effect of wall-layer stabilization (or destabilization) beyond a laminar effect, provides another strong contradiction to the idea of outer-layer dominance of the boundary layer in the sense discussed in the previous section. It also indicates that turbulence is not a single state or condition, but a spectrum of states over more than one dimension. This in turn also helps understand why correlations (such as mixing length) taken from one flow do not extrapolate well to flows with different structure.

What can we get from this list of very general statements that are quite lacking in specificity?

As a first item, it is evident that we can rule out conceptual bases that imply anything too simple -- for example, a basis that implies complete dominance by either inner or outer layer or that cannot at least in principle explain the list of phenomena that raise or lower production in item 7 above.

Item 4 in the list warns us against talking easily about causation. In a cycle, a looped process, cause and effect blend as one goes around the loop. What one sees as either cause or effect becomes at bottom merely phase relations. We might say A leads to B, but we need to be cautious about saying, "A causes the whole structure or sequence of events."

The long list of events in the quasi-cycle warns us of the very real danger of mistaking a view of one piece of the elephant for the whole beast, or the whole herd. This difficulty is compounded by the "views" of specific measuring techniques discussed in Section I.

What else can we get from this seemingly discouraging list? If we assume nature is not playing tricks on us, and no evidence in science elsewhere suggests that nature is that nasty, then there is only one elephant, and one herd. How, then, can we have views as different as those summarized at the end of the previous section? The answer is supplied at least in part by item 6, when viewed with the other items, and

*Stabilized here implies that the layer is stabilized if the forces on the flow are such that either (a) a slow-moving particle perturbed by a motion away from the wall tends to be 'pushed' back and/or (b) the velocity differential between transverse streaks is diminished.

also with the central difficulties of interpreting visual and probe data summarized in Section I above. What we have, for the most part, is not flat contradictions. Rather, we have different views of parts of the elephant taken in ways that emphasize different properties and, if we are not careful, lead us to extrapolate to different shapes for a whole beast or for the herd. Both the discussion of how different techniques give different views and the history of scientific controversy suggest the likelihood that each of the views we have contains a part of the whole truth. Each is probably a truth in some sense, but only a partial truth*. If that is so, then a currently pressing task is to seek ways to synthesize a better image of the whole truth from the various views now available.

Let me be more specific with regard to the nature of some of these views, in order to point out how the available views may go together. I shall not here attempt a synthesis; I shall merely point a possible direction. Suppose we assume, for understanding, that the elephants face downstream and walk along the surface. Then the Stanford visual data give a view that emphasizes a cut through the underside of the elephant, mostly in plan and side views. Bob Falco has a view that emphasizes the top of the elephant and tends to show more of the skin than the inside, at least visually; he also has slices that run down the middle axially and at various sections transversely. Coles has views that show more clearly the edges of one or a few elephants than the middle, also usually in plan view. Brodkey and Corino have a slice of the elephant that is usually very thin. All these views stand and watch elephants tramp by. Nychas and Brodkey have a view from a howdah on the back of an adjacent elephant, and Chuck Smith has views from a jeep moving along at various speeds which we shall see later this morning. There are, of course, others.

The picture from this simple analogy helps us see why we are disagreeing on some points. Schematically, we do not even have anything as simple as a jig-saw puzzle. In a jig-saw puzzle, there is a principle of conservation of total surface; in the data available on turbulent boundary layers, we have some bits that overlap and we are probably still missing some pieces.

Can we see where some overlaps must occur? I believe we can. If Falco's data and those of H. T. Kim et al. are to be believed, then there must be some relation between Falco's characteristic eddies and the 'breakup' flow module in the Stanford data, at least in the inner layers, since otherwise we shall account for more than 100% of the turbulence production in that part of the layer. Both these views should then also be related to the faster-moving fluid observed under the arch by Zilberman et al. (1977), if their suggestion is correct. In this mode of thought, when we attempt to look for overlaps and similarities rather than differences, we also see that there is not a fundamental contradiction between the view of some kind of 'structure' (or 'operator') passing overhead, through the outer layers, and the quasi-cyclic events near the wall summarized via the Stanford data above. If we accept the idea of the previous sentence and also accept that the interaction between the

*As some anonymous cynic has remarked, "Science tells the truth, nothing but the truth, but never the whole truth."

inner and outer layers is important, then we see the possibility that this interaction could occur between lifted low-speed-streaks and structures passing overhead. The passage could both trigger the interaction and be maintained by it via the production of high Reynolds stress, and this part of the sequence of events might account for the transformation of elephants to leopards, and back again, if that is the way we ultimately choose to conceptualize this part of the processes. These kinds of questions seem to me peculiarly timely to the present state of knowledge and to this conference. However, the suggestions here are intended to be provocative -- not definitive -- so that the details are left open for discussions involving the originators of the various views -- that is, to the work of the conference.

One aspect of what is suggested in the preceding paragraph seems anomalous and therefore worth focusing on. The low-speed-lifted streak generates a deficiency of velocity and momentum. Yet the incoming sweeps that arise after breakup and appear to trigger more streak-lifting farther downstream have excess velocity and momentum. Since both these effects seem to be associated with one event, the processes appear unclear to me. They seem to need some kind of strong mixing or overturning, or some explicit three-dimensional effect we have not seen. Comments on this point might be useful.

Throughout this paper, I have tried to focus on some issues and thereby raise what seem to me timely questions. The questions I see as most important currently have been recapitulated on a separate sheet. Don Coles and some others have also tried to prepare a list of questions that they see as currently important. Those lists have been consolidated. I should like at this time to invite any member of the meeting who wants to read the list and possibly add to it to do so during the breaks this morning or at the end of this morning's session. We have already made arrangements to reproduce the results of the complete list and circulate them to you shortly thereafter in order to aid the ongoing discussions of the conference.

Finally, in closing, I should like to discuss attitudes toward the structure problem as they are suggested by the material in this paper. If it is true that we are studying a very complicated herd of elephants and also that we now have a variety of overlapping but probably less than complete views of the individual beast and of the herd, then it follows that we shall get on more rapidly at this point in time with the task of understanding and providing a basis for improved mathematical modeling if we operate in a more cooperative and less competitive mode than is historically normal in Western science. In particular, we need to pay careful attention to the views of the elephant obtained by others with regard to how these other views add to, reinforce, and suggest modifications of what is seen from the views we have found individually. This is particularly true of the interpretations of the data. We must make such interpetations, since, as Fred Brownd says about quantitative measurements, "They don't mean much if you don't understand the underlying physics." And, so far, the best tool we have on the average for understanding the physics in this sense is an insightful interpretation of appropriate visual data. However, the examples of this paper show

that such interpretations are not only inductive inferences, but are strongly affected by marking location and viewing frame. Hence, they must be checked against other views and other forms of data. Moreover, similar remarks apply to interpretations of probe data, for different reasons, as the examples above show.

It is at this point that the competitive mode gets in our way. It is very hard for most of us even to consider modifying interpretations that seriously involve our own work and our own thinking. But that is what we need to do if we are to honestly seek an integration of the variety of current views of the herd of elephants we call turbulent boundary layer structure, and this integration seems to me the currently critical task if we are to form a clear and consistent picture based on the maximum information input. As a personal offering toward increased community cooperation, let me mention four points on which past interpretations we have made from the Stanford data may or do need modification.

1. In the work of H. T. Kim et al. (1971), we remarked that essentially all the production occurs during bursting times. That statement needs modification. As Willmarth (1975) and Brodkey, Wallace and Eckelmann (1974) have shown, only about 70% of the total production occurs during such times. We made the interpretation mentioned because at that time only long-time average measurements of production were available; hence no one was aware that for every 140 units of total production about 40 are balanced out by negative production. Kim's data show that essentially all the net production occurs during bursting times -- not the total -- and this is approximately 70% of the total. This does not modify the conclusion that bursting times are significant events.

2. Because we had a view that emphasizes the underside of the elephant in lab coordinates, and because other views of comparable detail were at that time lacking, we probably overemphasized the importance of wall layers, or at least sounded as if we were doing so. This may have contributed to the misunderstanding that some readers obtained concerning "sublayer instability" mentioned above. My present views on this question are contained in the discussion of Section III above and will not be repeated here.

3. In the results of H. T. Kim et al. (1971), we correlate mean time between bursts by normalizing on wall variables. Within the range of Reynolds number available to us at that time, and the uncertainty in the data, it was not possible to tell whether inner or outer variables provided the better collapse of the data. Nor was there a theory to guide us. Later data at other Reynolds numbers suggest, on balance, that outer variables do correlate mean bursting time better; see particularly Laufer and Badri-Narayanan (1971). However, the data are such that this question is not entirely settled at present.

4. In the work of Offen and Kline (1975) we speculated that perhaps pairing of the bursts created the larger eddies in the outer flow. In view of the recent work of Brown and Thomas (1977), this suggestion may be wrong. It needs more study.

I hope that this list of matters that do or may need modifying in our interpretations will encourage individuals to consider what modifications of their own interpretations are suggested by the 'views' of others, in order that in this conference we can make common cause toward increased understanding of the problem of turbulent boundary layer structure.

Acknowledgments

I want to express sincere appreciation to the Air Force Office of Scientific Research for long-standing support of the structure work described in Section III above, under several contracts. The work was also supported, for a time, by the Mechanics Division of the National Science Foundation. Thanks are also due to Prof. J. P. Johnston for important comments on an earlier draft of the manuscript.

References

Black, T. J. (1966), Proc. Heat Transfer & Fluid Mechs. Inst., pp. 366 ff, Stanford Univ. Press.

Brodkey, R. S., J. M. Wallace, and H. Eckelmann (1974), J. Fluid Mechs., 63, 1209 ff.

Brown, G. L., and A. Roshko (1974), J. Fluid Mech., 64, 775-816.

Brown, G. L., and A. S. W. Thomas (1977), Physics of Fluids, 20, 10, Part 11, S243-252.

Cantwell, B., D. Coles, and P. Dimotakis (1977), Physics of Fluids, 20, 10, Part 11.

Corrsin, S., and A. L. Kistler (1955), NACA Rept. 1244.

Corrsin, S. (1957), Naval Hydrodynamics Bull. 515, Natl. Acad. Sci.; Natl. Res. Council.

Einstein, H. A., and H. Li (1956), ASCE Proc. 82.

Fage, A., and H. C. H. Townend (1932), Proc. Royal Soc. 135a, p. 656 ff.

Falco, R. E. (1977), Physics of Fluids Suppl. on Structure of Turbulence and Drag Reduction, 10, 11, 5124-32.

Hama, F. R. (1957). See Corrsin (1957) and discussion by Hama therein.

Hama, F. R. (1962), Physics of Fluids, 5, 6, 644-50.

Hanratty, T. J. (1956), J. Am. Inst. Chem. Engrs., 2, 3, p. 359 ff.

Kline, S. J. (1957), J. Aero. Sci. 24, 6, 469-70.

Kline, S. J., and P. W. Runstadler (1959), J. Appl. Mechs., June, 1959.

Kline, S. J., W. C. Reynolds, F. A. Schraub, and P. W. Runstadler (1967), J. Fluid Mechs., 30, p. 741 ff.

Kline, S. J., M. V. Morkovin, G. Sovran, and D. J. Cockrell (eds) (1968), "Computation of Turbulent Boundary Layers -- 1968 AFOSR-IFP-Stanford Conference. Publisher: Thermosciences Div., Dept. Mech. Engrg., Stanford Univ., Stanford CA. 94305.

Kim, H. T., S. J. Kline, and W. C. Reynolds (1971), J. Fluid Mechs., 50, p. 133.

Kim, J., and S. J. Kline (1978), Rept. MD-37, Dept. of Mech. Engrg., Stanford University.

Kuhn, T.S., (1962), "The Structure of Scientific Revolutions,"Univ of Chicago Press.

Landahl, M.T. (1977), J. Physics of Fluids, 20, 10, Part 11, p. 525 ff.

Laufer, J., and M.A. Badri-Narayanan (1971), J. Physics of Fluids, 14,

Laufer, J., (1975), Annual Review of Fluid Mechanics, 2, p. 95.

Liu, C.K., J.P. Johnston, and S.J. Kline (1966), Rept. MD-15, Dept. of Mech. Engrg., Stanford Univ., Stanford, CA. 94305.

Meyer, K.A., and S.J. Kline (1961), Rept. MD-7, Dept. of Mech. Engrg., Stanford Univ., Stanford CA. 94305

NCFMF (1964), motion picture, "Flow Visualization", available from Encyclopedia Britannica Films, principal S.J. Kline.

Nychas, S.G., H.C. Hershey, and R.S. Brodkey (1973), J. Fluid Mechs., 61, p. 513 ff.

Offen, G.R., and S.J. Kline (1975), J. Fluid Mechs., 70, 2, 209-228.

Offen, G.R., and S.J. Kline (1974), J. Fluid Mechs., 62, 2, p. 223 ff.

Offen, G.R., and S.J. Kline (1973), Proc. 3rd Biennial Symposium on Turbulence in Liquids, Dept. Chem. Engrg., Univ of Mo., Rolla, 289 ff.

Oldaker, D.K., and W.G. Tiederman (1977), J. Physics of Fluids, 20, 10, Part 11, S133 ff.

Oseberg, Ø., and S.J. Kline (1971) Rept. MD-28, Dept. of Mech. Engrg., Stanford Univ., Stanford, CA. 94305.

Platt, J.R. (1966), "The Step to Man," John Wiley & Sons, Inc., N.Y.

Prandtl, L., and O.G. Tietjens (1934), "Applied Hydro- and Aeromechanics," McGraw-Hill Book Co., p. 294. (Note: these are derived from earlier lectures, presumably in the 1920's.)

Reynolds, O. (1883), Trans. Royal Socl. (London), 174.

Runstadler, P.W., S.J. Kline, and W.C. Reynolds (1963), Rept. MD-8, Dept. of Mech. Engrg., Stanford Univ., Stanfrod, CA. 94305.

Sandborn, V.A., and S.J. Kline (1961), TASME 83, D,3.

Schraub, F.A., S.J. Kline, J. Henry, P.W. Runstadler, and A. Littell,Jr. (1965), J. Basic Engrg., TASME, Ser. D., 87, p. 429 ff.

Schraub, F.A., and S.J. Kline (1965), Rept. MD-12, Dept. of Mech. Engrg., Stanford Univ., Stanford, CA. 94305

Sovran, G., ed. (1967),"Fluid Mech. of Internal Flow," Elsevier Press.

Townsend, A. A. (1956), "Structure of Turbulent Shear Flow," Cambridge Press.

Willmarth, W. W. (1975), "Advances in Fluid Mechanics," (Acad. N.Y. 1975) 15, p. 158 ff.

Willmarth, W. W., and Bogar, T. J. (1977), Physics of Fluids, 20, 10, Part II, S9-S21.

Winant, C. D., and F. K. Browand, J. Fluid Mechs., 20, 417 ff.

Zilberman, M., I. Wygnanski, and R. R. Kaplan (1977), Physics of Fluids, 20, 10, Part 11, S258-271.

Appendix I

RECOLLECTIONS OF SHEAR LAYER EXPERIMENTS

F. K. Browand
Department of Aerospace Engineering
University of Southern California
Los Angeles, California 90007

My original experiments in the mixing layer (1964-65) were confined to the first 4 or 5 wave lengths of the most unstable wave. The maximum Reynolds number was $\Delta Ux/\nu = 4 \times 10^4$. The results were primarily u' velocity fluctuation measurements with hot wires. I did do some visualization with smoke in the initial stages of the experiemnt, but the significance of the pairing vortices completely escaped me. My interpretation of the hot wire measurements in the non-linear transition region was essentially spectral. I looked at filtered hot wire outputs to determine the amplitude contribution of the various components in the spectrum. (There were perhaps 6 discrete components.) I remember having the feeling at the time that very little new information could be learned from visualization, and I wanted to be as quantitative as possible.

In the intervening years I have, or course, changed my opinion considerably. There are probably several reasons. First, I was very impressed with the work you did about that time in the boundary layer. (I first saw this work after I had finished my thesis.) You were taking a fresh, unprejudiced look at the boundary layer and learning startling new physics. Second, I guess I was less impressed with quantitative measurements -- they don't mean much if you don't understand the underlying physics. Third, we started visualizing the mixing layer in our water channel with a density difference between the two layers. Here was a new and different problem, and we could clearly learn a great deal by using visualization. Clint Winant's thesis topic was originally to be the stratified mixing layer. As a start, he looked first at the homogeneous mixing layer. Because we introduced dye initially into the region with vorticity, the downstream vortex lumps showed up very clearly. When we first observed the repeated pairing interactions, our feeling was -- what an interesting sequence of events taking place in the mixing layer! Gradually, it dawned upon us that these events were not taking place in the mixing layer, but rather these pairing interactions were the mixing layer in a very essential way. I think this was our contribution -- to postulate that these relatively deterministic vortex-pairing interactions are the mechanism by which the fully turbulent mixing layer grows and sustains itself.

FLOW VISUALIZATION AND SIMULTANEOUS ANEMOMETRY STUDIES OF TURBULENT SHEAR FLOWS

Robert S. Brodkey

Department of Chemical Engineering

The Ohio State University, Columbus, Ohio 43210 USA

ABSTRACT

The present paper is an attempt to summarize and interpret the results of visual studies at The Ohio State University in terms of the coherent structure approach to the understanding of turbulent shear flows. Research involving simultaneous anemometry and stereoscopic flow visualization is outlined. However, no attempt has been made to summarize the extensive anemometry work and analysis done in Germany with which the author has been associated. Nevertheless, it should be clear that it is impossible to remove from the author's mind all the influences from that work as well as all that seen in the literature; thus, in a true sense the integration of ideas presented here is a product of not only our work in Columbus, but also the extensive cooperative work in Germany as well as that by others from all around the world.

1. INTRODUCTION

In order to place the visual studies carried out at The Ohio State University in context with studies on coherent structures in general, a review is provided in Figure 1. The early visual and anemometry studies can, in retrospect, be considered the beginning of the concept of coherent structures. The efforts of Ferrell, Richardson, and Beatty (1); Hama (2); and of Kline and Runstadler (3) are noteworthy in that they uncovered the streaky nature of the flow in the wall region. More recent visual and anemometry studies of the last ten years or so have concentrated on using a wide variety of methods in order to elucidate the coherent structures that exist in turbulent shear flows. Most of these efforts are being continued today as well as newer efforts at making simultaneous anemometry measurements and flow visualization studies. This latter should allow a better understanding of the specific signal signatures of the coherent structures. Certainly, all of this work is

EARLY VISUAL (Wall Streaky Structure)

North Carolina State
University of Maryland
Stanford University

EARLY ANEMOMETRY (Zone Avenue)

Johns Hopkins University
University of Southern California

MORE RECENT VISUAL

Stanford University
The Ohio State University
California Institute of Technology
Cambridge University

MORE RECENT ANEMOMETRY

Johns Hopkins University
University of Southern California
University of Michigan
Max-Planck-Institut für Strömungsforschung
The Ohio State University
University of Maryland
California Institute of Technology
France, Australia, India and many others around the world.

SIMULTANEOUS MEASUREMENTS

Cambridge University
The Ohio State University
Max-Planck-Institut für Strömungsforschung
Michigan State University

THE MECHANISM AND MODELING

Figure 1. Coherent Structures Studies

only a preliminary to establishing the best possible concept of the mechanism of the flow and hopefully to model such a flow in a relatively simple manner for practical engineering applications.

The work at Columbus has been only a small part of the total effort put forward around the world. In many cases there has been very close cooperation between various investigators. For example, I have been fortunate to have been closely associated with the work on extensive anemometry measurements that has been accomplished in Germany. I have also been fortunate to have had close interactions with researchers from other places including the University of Michigan, University of Southern California, Cambridge University, and Michigan State University. There are joint publications involving various institutions and individuals and it would be difficult if not impossible to tell one person's contributions from another and probably undesirable to do so. Although closely associated with much of this work, it will not be discussed here, but as noted in the abstract it seems impossible for its influence not to be felt.

Before embarking upon a summary, some details, and an interpretation of our visual results, it would be well to present a brief overview of visual techniques in general with an effort to try to indicate some of the advantages and implications.

2. VISUAL TECHNIQUES FOR FLOW VISUALIZATION

The approaches available to the experimenter for the visualization of turbulent flows are extensive and are in part reviewed in Figure 2.

MARKING LIMITED AREAS OF THE FLOW

- Dye Wash-Out
- Dye Injection
- Hydrogen Bubbles From a Fine Wire
- Smoke Particles From A Heated Wire
- Helium-Soap Bubbles in Air
- Pulsed Laser Blue Print Reaction
- Smoke or Dye at Leading Edge to Mark the Boundary Layer
- Schlieren Methods
- Combinations

INJECTION OR GENERATION METHODS

- Continuous Streaks, Pulse Lines, Streak Lines, and Other Variations

MARKING THE ENTIRE FLOW

FLOW MARKERS UNIFORMLY DISPERSED IN THE FLOW FIELD

- Scale to be Marked
  - Small Particles, Large Particles,
  - Neutrally Buoyant Particles,
  - Heavy Particles, and Combinations

COMBINATIONS

Figure 2. Visual Techniques for Flow Visualization

In general most experimental techniques involve marking limited areas of the flow and have involved dye and other marker techniques as noted in the figure. Such methods involve injection or generation of the marker in the form of continuous or pulsed streak or sheet lines, and various variations of these. In direct contrast are techniques that use flow markers uniformly dispersed in the field in order to mark the entire

flow. With this technique, there is the possibility of marking the fluid with small particles in order to mark the entire flow or using larger particles that will only mark the larger scales of the flow. In all such cases, one should use neutrally buoyant particles. There are processes, however, that involve the motions of heavy particles that do not follow the flow. Such problems would involve the use of markers that are not neutrally buoyant and would act more like the solid phase in the process of concern. Some important chemical engineering applications of such a situation would be in crystalization, heterogeneous chemical reaction in a mixer, and certain types of combustion processes where solid fuels are involved. In addition, one need not rule out the use of combinations of markers, some marking the flow and others marking the solid particle paths of interest.

In all cases, further combinations can be used. One specific case comes to mind that we have used in our visual boundary layer studies; the fluid motions were marked by small neutrally buoyant particles while simultaneously we injected a dye at the leading edge in front of the trips on our flat plate so as to mark the edge of the boundary layer.

There are, of course, limitations involved with all flow visualization techniques. The object is to minimize these. For example, with the use of injection techniques there is a need to carefully consider flow disturbances. The injected or generated material marks all structures equally at one instance in time rather than marking just one specific structure. The injected or generated material can only be followed a relatively limited distance downstream. Finally, there is difficulty in the interpretation of streak lines when the flow field is unsteady as it is in turbulent flow. When marking the entire flow field and using light scattered from the particles at right angles, there is a great deal of difficulty in obtaining enough light and proper exposure. Sometimes it is nearly impossible to find the perfect flow marker. But once the flow visualization technique is perfected, it is normally possible to obtain a reasonable interpretation of the flow field, even in an unsteady flow situation.

There are variations in techniques of viewing the flow which are summarized in Figure 3. There are three views one can take: looking into the flow (y, z) is the most difficult. How to do the viewing is another variable. Most studies have been two-dimensional views obtained as a result of a narrow depth of field and/or a narrow beam of light. One can use pseudo three-dimensional viewing which uses two cameras, mirror arrangements, or color band filters to light the third dimension. Pseudo three-dimensional viewing of a flow has advantages over two-dimensional views, but there are difficulties in analyzing such views for one must reconstruct the three-dimensional view in one's mind. The mind as a computer is good, but it has not been programmed (prewired) to do this task efficiently in real time. True three-dimensional viewing of the flow as is done with our eyes would be the best. Two methods for this are available, holographic and stereoscopic visualization. Unfortunately, holographic techniques are only beginning to be investigated and the critical requirements of stability (as well as high cost) have limited the application of the method. Fortunately, however, these limitations

Longitudinal (xy)
Lateral (yz)
Parallel (xz)

Two-Dimensional
  Narrow Light Beam
Pseudo Three-Dimensional
  Two Cameras
  Mirrors
  Color Band Filters
True Three-Dimensional
  Holographic
  Stereoscopic

Non-Convected (effects at a position)
Convected (development with time)

Figure 3. Viewing the flow

do not exist for stereoscopic viewing of the flow which involves taking two simultaneous pictures which correspond to the two views one would see with one's eyes. With this technique we are in luck, since the mind has been programmed to take the two views and reconstruct a true three-dimensional picture in real time. Indeed this is what we do all the time, although about 5% of the population are stereo-blind. The stereoscopic visualization technique for a boundary layer flow has been described in some detail by Praturi et al. (4). Another aspect of viewing the flow is the frame of reference, that is, in a non-convected or convected view. In the former, one views the flow at a specific position and is concerned with the development of the flow at this location in time. A good example would be the development of the vortex flow behind a cylinder in a flow started up from rest. In the convected view, one can follow a specific flow element or structure in time. An example would be the development of a vortex in the flow behind a sphere as it moves downstream or the development of coherent structures in a turbulent boundary layer as they are convected downstream.

In any visual technique, there are difficulties: stereoscopic viewing is simple when one has a point of reference or perspective. In this case, the size and flow directions are easily distinguished. If the object being viewed is large enough, one will have a three-dimensional feel of the flow as a result of perspective even without stereoscopic viewing. For example, if you had only one eye and were out in the road, it would not take long for you to recognize if a car were coming at or away from you, due to its size change. Unfortunately in many fluid flow problems, perspective is not available and it is difficult to distinguish the flow direction. Marked particles under scattered lighting do not change the viewed size appreciably, thus one cannot use the size to indicate the direction of flow. For this the mind must use the change in angle as a particle moves. Although difficult, the mind is an extremely efficient

computer that allows us to integrate the two views instantaneously and give us a true three-dimensional visualization of the flow, with certain limitations. When we are watching an unfamiliar view of particles, it may take longer than what is necessary for real time to allow the mind to function. The program in the mind is just a bit inefficient for this application. However, we have found that by making relatively short film loops and looking at these loops for extended periods of time, the three-dimensional aspect can be recovered. In effect, we are providing the additional time necessary for the mind to handle this new type of data.

One direction of current research into coherent structures is an effort to tie down more closely the actual anemometry signal signatures of specific coherent motions and structures. There are several ways one can approach this; one "insane" method would be to try to extract extensive information directly from visual studies. It is difficult, tedious, inhumane, and just not nice to do to graduate students although we have tried it on a limited scale. It might be possible to recognize certain structures or signals by various conditional sampling or pattern recognition techniques as will be discussed by others. There is also the possibility of measuring and viewing the flow simultaneously. Thus, one would combine many of the preceding visualization techniques with simultaneous anemometry measurements.

The anemometry technique must be selected so as not to drastically interfere with the flow. Hot-wire or hot-film anemometry can be used in an unconvected view or in a view convected with the flow as long as the convection velocity is less than any velocity that will be found in the flow. In effect, the probe must be convected at a velocity so that the flow is always over the probe. Better, but more difficult, would be to use a laser doppler anemometer which would not interfere with the flow. This latter has not been tried due to the stability requirements which are similar to those of holographic methods. Newer integrated commercial units may now be rugged enough so as to be useful for this application, which does require the use of a back-scattering mode. A more detailed review of visual studies in complex turbulent shear flow has been given by Brodkey (5).

3. VISUAL STUDIES AT OHIO STATE

The visual studies at Ohio State started with the work of Corino which culminated in his Ph.D. dissertation in 1965 and with the article by Corino and Brodkey (6) in 1969. The work by Corino was on the wall region of a pipe flow and not in a boundary layer. However, this region has exactly the same characteristics in both flows. From a visual standpoint, the work of Corino involved marking the entire flow with small particles and photographing these in a convected view with a narrow beam of light and a small depth of field so that the view was effectively two-dimensional. The convected view allowed one to follow the development of flow structures.

To summarize the results, one can quote from our earlier works:
"The wall area showed a distinct pattern characterized by a deterministic sequence of events occurring randomly in space and time. This

pattern was a function of the distance from the wall. The area $0 \leq y^+ \leq 5$ (sublayer region) was found not to be laminar; it was characterized by velocity fluctuations of small magnitude and disturbed by fluid elements coming from the adjacent region. The area $0 \leq y^+ \leq 30$ was characterized by ejections of fluid elements away from the wall. These ejections were found to occur intermittently and randomly in both space and time; they were part of a sequence of events. The first event of this sequence was a deceleration of the axial velocity characterized by the essential disappearance of the velocity gradient and by a velocity defect as great as 50% of the local mean velocity. The second event was an acceleration; i.e. a mass of fluid coming from upstream and entering at a y^+ of about 15 was directed towards the wall at angles of 0-15° and interacted with the fluid in the decelerated region. The third event was an ejection; i.e. an abrupt outward motion of fluid originating in the decelerated region. The fourth major event was the entry from upstream of a mass of fluid moving almost parallel to the wall, the sweep event. This latter higher speed fluid was often a part of the same mass of fluid as gave rise to the acceleration stage. The above cycle was repeated randomly in space and time."

The motions described and the resulting fluctuations were the most important features of the wall region, and were believed to be a factor in the generation and maintenance of turbulence.

Nychas (7) in 1972 completed a similar visual study of the entire boundary layer, which resulted in the paper by Nychas *et al.* (8) in 1973. Again to quote from our earlier work:

"The single most important event observed in the outer region was fluid motions which in the convected view of the traveling camera appeared as a transverse vortex. This was a large-scale motion transported downstream almost parallel to the wall with an average velocity slightly smaller than the local mean. It appeared to be the result of an instability interaction between accelerated and decelerated fluid, and it is believed to be closely associated with the wall-region ejections. The transverse vortex was part of a deterministic sequence of events, although these events occurred randomly in space and time. The first of these events was a decelerated flow exhibiting velocities considerably smaller than the local mean. It was immediately followed by an accelerated flow. Both these events extended from near the wall to the far outer region. Their interaction resulted in the formation of one or more transverse vortices. While the transverse vortex was transported downstream, small-scale fluid elements, originating in the wall area of the decelerated flow, were ejected outwards (ejection event). After traveling some distance outwards the ejected elements interacted with the oncoming accelerated fluid in the wall region and were subsequently swept downstream (sweep event). The sequence of events closed with two large-scale motions."

"Estimated positive and negative contributions to the instantaneous Reynolds stress during the events were many times higher than the local mean values."

Our most recent effort was by Praturi (9) who used a stereoscopic view of the same flow field as observed by Nychas. Besides the difference in the viewing manner, Praturi also injected dye in some experiments at the leading edge of the flat plate to help delineate the outer edge of the boundary layer. The stereoscopic technique allowed the three-dimensional aspects of the flow to be studied in some detail, and in particular allowed axial vortex motions in the wall region to be identified. To quote from Praturi and Brodkey (10):

"The flow was found to exhibit three characteristic regions which can be roughly divided into the wall and outer regions of the boundary layer and into an irrotational region, unmarked by dye, outside the instantaneous edge of the boundary layer. Briefly, the outer region of the boundary layer was dominated by transverse vortex motions that formed as a result of an interaction between low and high (sweep) speed fluid elements in that region. The present results clearly show that bulges in the edge of the boundary layer are associated with transverse vortex motions. In addition, the transverse vortex motions appear to induce massive inflows of fluid from the irrotational region deep into the outer region of the boundary layer. The outer edge of the boundary layer thus becomes further contorted contributing to the intermittency of the region. Furthermore, the outer region motions give rise to the conditions necessary for the dominant wall region activity of ejections and axial vortex motions. It is not the energetic wall region ejections that move to the outer region and give rise to the contorted edge of the boundary layer as has been suggested by others."

"The wall region axial vortex motions were intense and lasted for a short time when compared to the lifetime of outer region transverse vortex motions. The present results strongly suggest that wall region vortex motions are a result of the interaction between the incoming higher speed fluid of the outer region of the boundary layer and the outflowing low speed wall region fluid. This is in direct contrast to all models that suggest that axial vortex wall motion pairs are the causative factor that gives rise to the outflow of low speed fluid trapped between."

"Although all the elements necessary to make up a horseshoe vortex structure riding along the wall were present, such a composite was not observed. However, this could be visualized as a possible model to represent the ensembled average of the flow."

"Finally, the massive inflows from the irrotational region were observed to precede the appearance of low and high speed fluid elements in the boundary layer, thus completing the deterministic cycle of individual coherent events."

The current work now in progress by B. Ghorashi is the extension of the stereoscopic effort by Praturi to the simultaneous measurements necessary to define the signal signatures of the structures of the

outer region. Initially an x-film probe is being used and the results are being compared to the pattern recognized signals reported by Wallace et al. (11). Later the five-film probe reported by Eckelmann et al. (12) will be used and the results obtained for vorticity and turbulence production will be compared to those reported, again by pattern-recognization, in that reference (12). Hopefully the pattern-recognized results can be firmly associated with specific structures in the flow.

4. A COMPOSITE MECHANISTIC PICTURE OF THE FLOW

The present mechanistic picture of the flow is based on all of our previous work and has been presented in part by Praturi and Brodkey (10), Eckelmann et al. (12), and Kastrinakis et al. (13). Figure 4 from reference 10 is a sketch in the xy plane of the development of the sequence of events observed. The frame of reference used in the description is that of the camera moving with the flow (convected flow). The following is from Praturi and Brodkey:

> "The appearance of a high speed front is chosen as the starting point of the model. Downstream of the front, fluid in the low speed element moves slower than fluid in the high speed element. The low speed fluid is characterized by a quiescent laminar-like flow and the flow in the high speed fluid is primarily axial with a small angle towards the wall. The presence of the high shear zone on the front between the high and low speed fluid elements leads to a Helmholtz type instability and culminates in the formation of a transverse vortex in the outer region of the boundary layer as sketched in part A of Figure 4. In this and subsequent parts, the location of the instantaneous boundary layer edge is also sketched."

> "During the second stage of the cycle, the transverse vortex is convected in the flow and the wall region becomes active as characterized by ejections and vortical motions. Ejections appear to be a direct result of the activity associated with the high speed front and appear to be a consequence of low speed fluid being trapped between fingers of high speed fluid, thus being forced (continuity) in and away from the wall. The ejections started in the region of

> $5 < y^+ < 30$ and traveled to the region of a y^+ of 100 or so where

> they interacted with the high speed front. The stronger ejections penetrated the shear zone, entered the high speed fluid, and were carried away. In rare cases, strong ejections were observed to travel out as far as to a y^+ of 300 or so. However, weaker ejections, especially those with an injection angle of about 90° in the convected view became a part of the vortical motions at the high speed front in the wall region. The streamwise and transverse vortical motions in the wall region appear to be the result of the shear zone at the front between the wallward moving high speed fluid and trapped, but outflowing, low speed fluid moving around the fingers of high speed fluid. This stage is shown as part B of Figure 4."

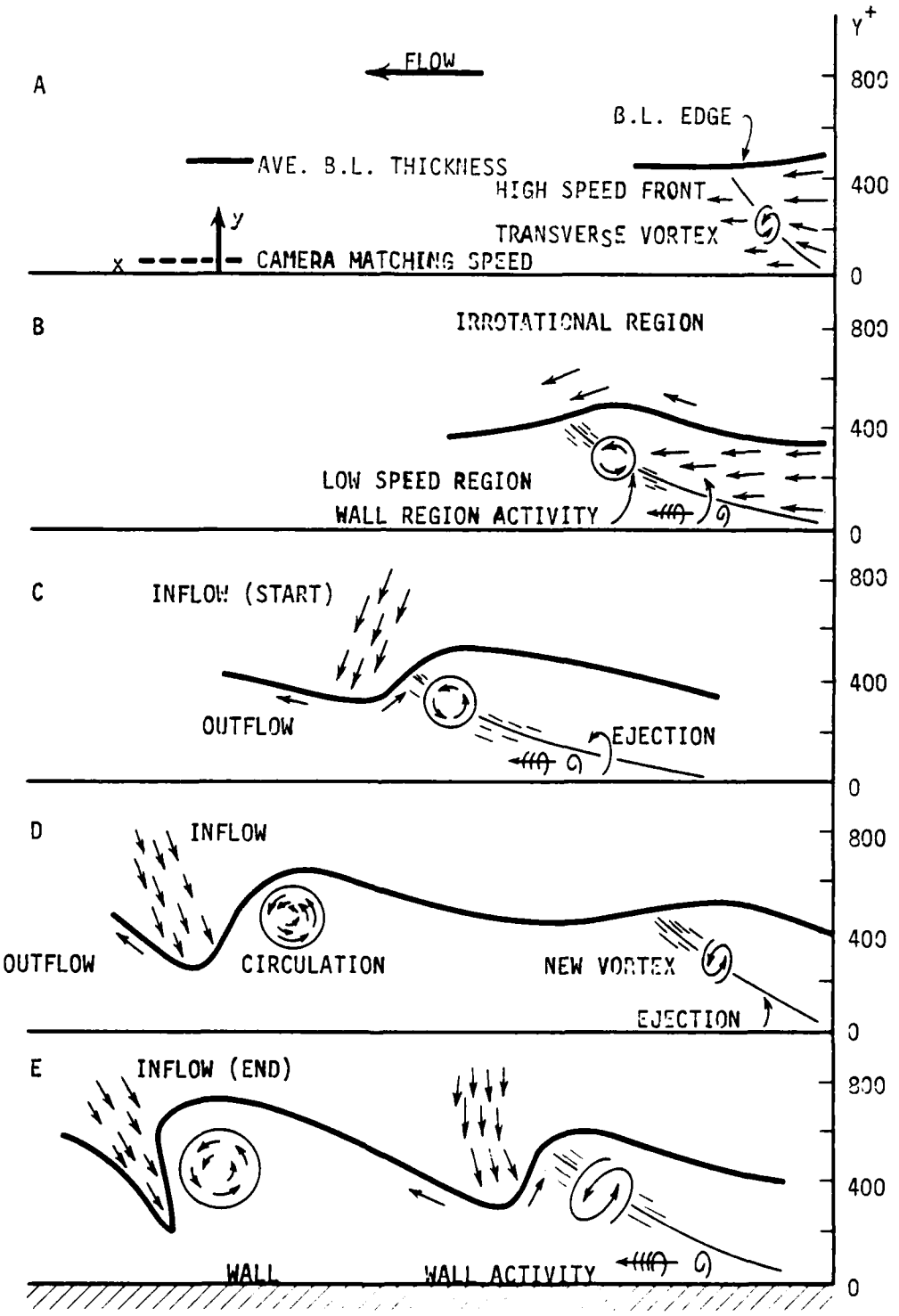

Figure 4. Sketch of the progression of the flow (ref. 10)

"The third stage of the cycle is characterized by the decay of the transverse vortex and the cessation of activity in the wall region. The transverse vortex, as it travels downstream, becomes bigger in diameter and less intense, ultimately manifesting into a gentle circulation as shown in parts C and D of Figure 4. The transverse vortex usually moves slightly away from the wall. At the same time, the high and low speed fluid elements disappear and become a region characterized by a more uniform flow. The shear zone is consumed by the transverse vortex as it is convected downstream. The gentle circulation, moving slightly away from the wall, then appears as a bulge in the turbulent-nonturbulent interface. This circulation induces an inflow of fluid from the irrotational region. At this point in the cycle, the flow in the boundary layer is slower than that in the irrotational region. The relatively higher momentum of the fluid from the irrotational region reinforces the inflow as it moves toward the wall in the shape of a jet. Due to the overall velocity gradient, the wallward part of the inflow slows down to a much slower speed than the part away from the wall. The inflow appears to deflect backwards in the convected view of the camera. The initiation and convection of the inflow are pictorally shown in parts C to E of Figure 4. The outflow (parts C and D of Figure 4) comes from the boundary layer fluid and appears to be a reaction (maybe due to continuity) to the inflow."

"Events do follow each other rapidly and a second sequence is illustrated following the first. At higher Reynolds numbers, the events would be closer together and the outflow might well become part of the circulation motion. Fluid in the inflow event is eventually swept away by the oncoming high speed fluid and probably entrained into the boundary layer by engulfment."

A single high speed front or sweeping motion can be seen in more detail in Figure 5 taken from reference 12. This figure is based on both visual and anemometry studies, especially a series of measurements made with a five-film probe that measured, among other things, the gradients of the axial velocity in the y-direction. In reference 12, Figure 5 is discussed in detail in terms of pattern recognized signals, and this will not be repeated here.

Figure 6 from reference 13 is still another view of the flow with emphasis on the streaky structure and the associated axial vortex motions. This figure is also based on visual and anemometry studies, especially a series of measurements made with axial vorticity probes. In reference 13, Figure 6 is discussed in detail in terms of pattern recognized signals, and this also will not be repeated here.

"The pictures of Figures 4 through 6 are two-dimensional cuts through a three-dimensional structure. The high speed front is not uniform across the flow in the lateral direction. The front would seem to be more like fingers with the low speed fluid below and trapped between the fingers as sketched in Figure 7. These fingers are very long and correspond to the high-low speed streaks of the wall region. In this shear region, axial vortices that are small lie along these fingers. Note that in this model, the axial vortex

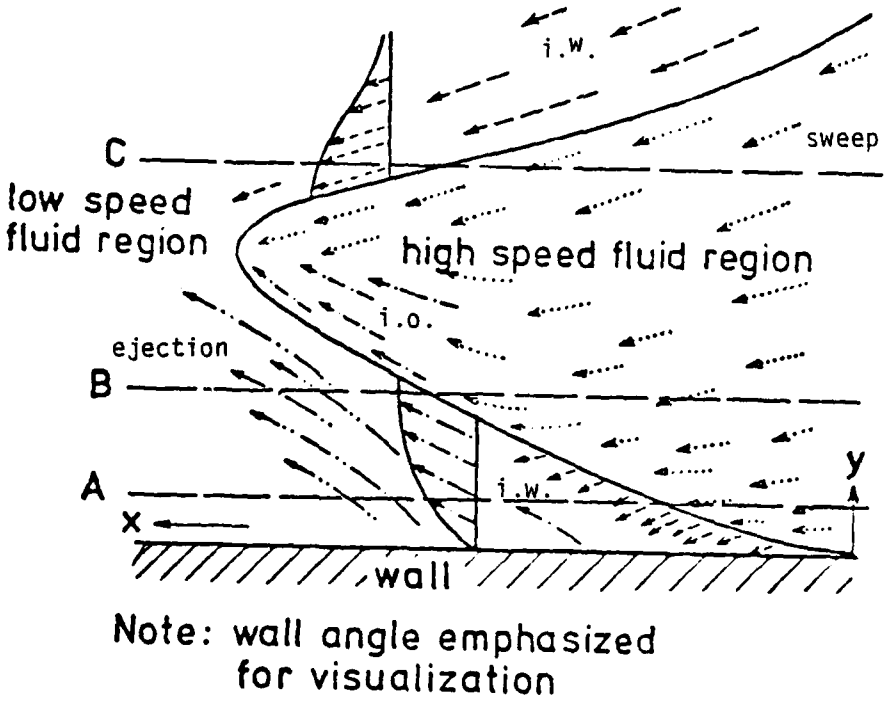

Figure 5. Side View of Flow Field (ref. 12)

motion is caused by the fingering effect rather than the other way around as in some models that suggest that the low-high speed streaks are caused by extended axial vortex pairs. Actually, the same general vortex pattern would be observed in both cases, but in the present model, the vortices are many and small and the pattern would be weaker as it is a consequence rather than a causative factor."

In the view of Praturi and Brodkey (10), the high speed front was pictured as the main causative step in the formation of the transverse vortices and the short lived axial vortices that were observed in the wall region.

5. SIMULTANEOUS ANEMOMETRY AND VISUAL STUDIES

Our current effort is directed towards obtaining simultaneous anemometry and stereoscopic visual studies in order to identify specific signal signatures for the various structures known to exist. As a first effort u, v, and uv measurements with an x-probe are being made along with the visual studies and these results will be used to establish the exact structures that correspond to the pattern recognized signals presented by Wallace et al. (11). Later the five-film probe will be used

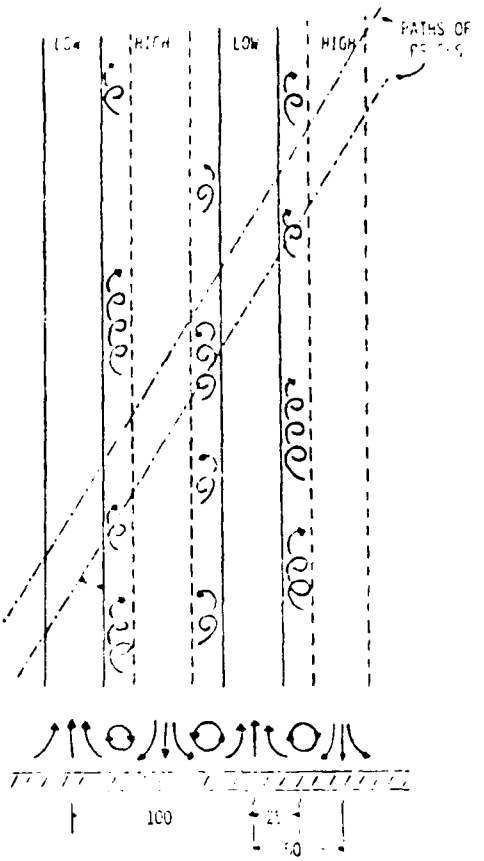

Figure 6. Probes are aligned with the mean flow and the structures cross the probes at small angles (ref. 13)

and these results compared to those presented for the pattern recognized signals by Eckelmann et al. (12).

A skematic drawing of the anemometry system for the studies is given in Figure 8. The anemometry signals are filtered, amplified, and conditioned (necessary sums, differences, and products) by a TR-20 analog computer. Of unique design is a multiplexer that provides a series of vertical bouncing dots on the oscilloscope screen that can be photographed at the same time the stereoscopic films are being taken. The design utilizes Intersil 16 channel analog multiplexer chips (IH5060). The analog computer outputs are multiplexed into the single vertical scale of the scope. As the multiplexer steps through the analog signals, a second segment of the multiplexer puts out a step voltage for the horizontal scale of the scope. The step increases in a fixed increment with each step of the vertical signal. The net result is that the analog signals appear as vertical moving dots, each displaced a fixed amount along the horizontal.

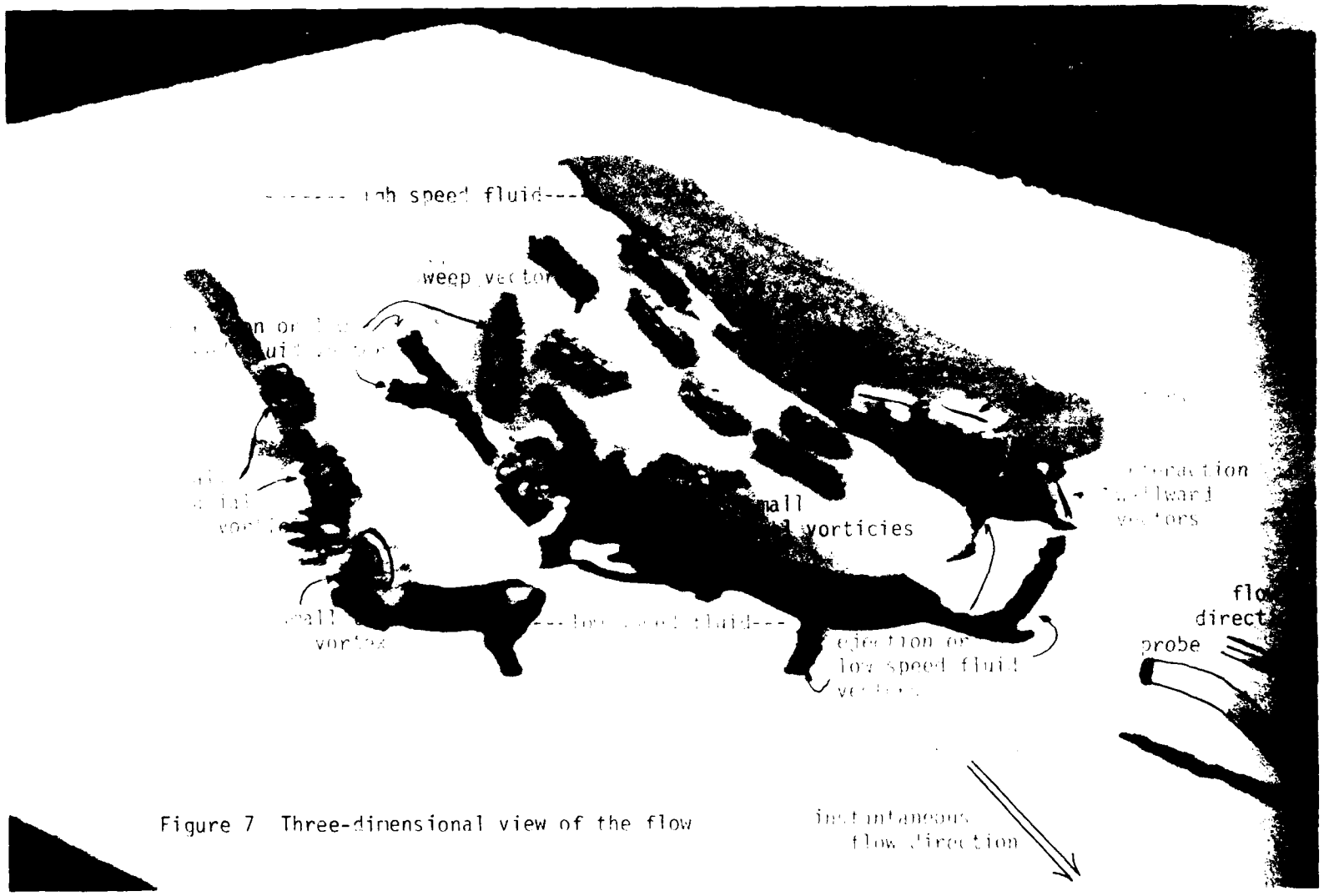

Figure 7 Three-dimensional view of the flow

Some preliminary results have been obtained, but these are not detailed or complete enough at the time of writing to allow us to define the signal signatures of specific structures; however, some sample movies will be shown.

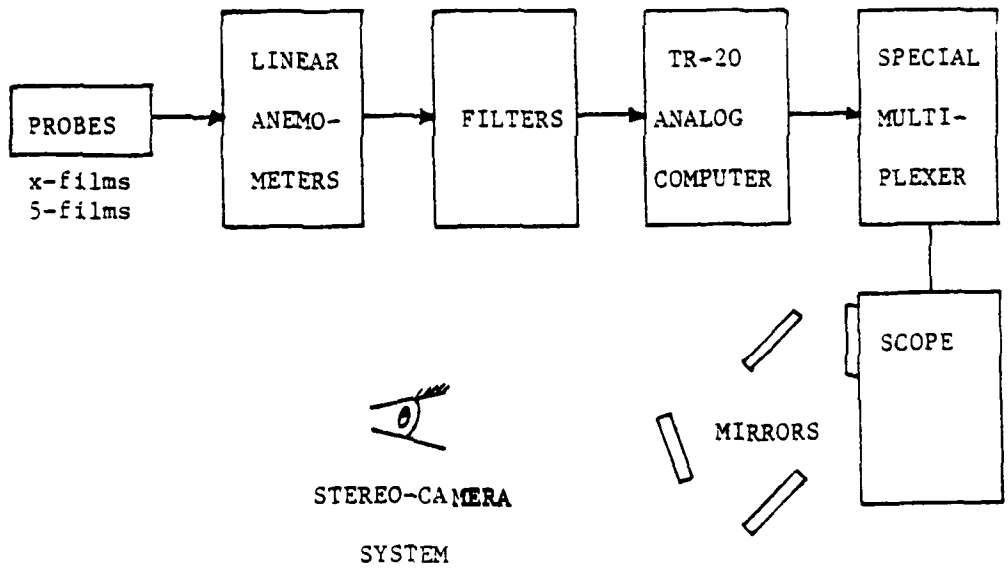

Figure 8. Set-up for simultaneous anemometry and stereoscopic flow visualization

1. Ferrell, J.K., F.M. Richardson, and K.O. Beatty, Jr. (1955), Ind. Eng. Chem., 47, 29. See reference 2 for photograph.

2. Hama, F.R. (1957), in article by S. Corrsin, Symp. on Naval Hydrodynamics, Pub. 515, NAS-NRC 373.

3. Kline, S.J. and P.W. Runstadler (1959), J. Appl. Mech., 26, 166.

4. Praturi, A.K., H.C. Hershey, and R.S. Brodkey (1977), Turbulence in Liquids, Proc. of the 4th Symposium, page 345, Science Press, Princeton, N.J.

5. Brodkey, R.S. (1977), The International Symposium on Flow Visualization, Tokyo, page 75.

6. Corino, E.R., and R.S. Brodkey (1969), J. Fluid Mech., 37, 1.

7. Nychas, S.G. (1972), Ph.D. Dissertation, The Ohio State University.

8. Nychas, S.G., H.C. Hershey, and R.S. Brodkey (1973), J. Fluid Mech., 61, 513.

9. Praturi, A.K. (1975), Ph.D. Dissertation, The Ohio State University.

10. Praturi, A.K., and R.S. Brodkey (1978), J. Fluid Mech. (in press).

11. Wallace, J.M., R.S. Brodkey, and H. Eckelmann (1977), J. Fluid Mech., 83, 673.

12. Eckelmann, H., S.G. Nychas, R.S. Brodkey, and J.M. Wallace (1977), Phys. Fluids, 10, S 225.

13. Kastrinakis, E., J.M. Wallace, W.W. Willmarth, B. Ghorashi, and R.S. Brodkey (1978), Lecture Notes in Physics, Springer-Verlag (in press).

DISCUSSION

Morkovin:

With respect to the circulation, that is elements with w_z present, you said it grows from around $y^+ = 100$ ...

Brodkey:

There are two distinct scales and structures. The main vortices are transverse, contain w_z ; they are in the outer part of the layer, from say y^+ of 250 or 400 to the outer edge. The structures seen in the cut look like a large transverse vortex. In actuality some are transverse, but at times we also see parts that are tilted in the flow direction. These various parts look like they are from a horseshoe vortex coming back. However, we never see complete horseshoe vortices. Now the other -- the smaller scale vortices look like they are essentially axial, and they are always very close to the wall. In these movies we can only say they were closer than a y^+ of 25 to 100. We reported this in Berlin after Jim Wallace and I looked at the Corino movies. There is clearly a vortex structure illustrated within a y^+ of about 5 to 15. (Editor's comment. The spoken version on tape is not clear here. We take Prof. Brodkey's meaning to be that the smaller, axially-oriented vortices center on a y^+ location of 5 to 15, but can be seen now and then as far out as y^+ 25 to 100. This is consistent with Prof. Kline's comment in the Wednesday morning session stating that the modal location of such vortices is just outside the sublayer, but that a distribution exists with a very long tail in the outward, plus y, direction. Since Prof. Brodkey agreed with that comment, we have taken that to be his meaning here. Editor).

Morkovin:

I would like you to give similar numbers for the w_z structure. Where do you see it first? How does it grow outward? What is the spanwise extent of the structure? Etc.? I'm talking here of w_z oriented vortical structures.

Brodkey:

In Nychas' work the outer structure, w_z , is the transverse vortex. In the two-dimensional cut a diameter of $d^+ = 150$ to say 100 is seen first going up to maybe 250 non-dimensional diameter units. This is no closer to the wall than 150 and normally 200 to 250 units from the wall. It moves, mostly, slightly away from the wall as it is convected downstream.

Bradshaw:

When we talk about these inner-layer structures, I think we have to be careful to decide whether or not our models agree with the ordinary inner-layer scaling. I'm talking now about flow at say y^+ greater than 30. Where the local

arguments, in which half of us believe and the other half half-believe, imply that the length scales of the shear-stress producing motion should all be proportional to y. But somehow these structures have got either to expand or to redistribute themselves over space so as to give you an effective scale which is proportional to y. And quite a lot of the models that have been proposed, and again I'm not talking about anyone in particular, don't seem to scale properly. I'd be glad of your comments on that thought.

Brodkey:

Our pictures suggest they will reach this scale as a result of the interaction between the high-speed fluid coming in and the low-speed fluid being forced out. We're looking at it at a y^+ of about 25 to 100; that's about all we can see in there. We find those axial vortices are about a crude diameter average of 50 and a length of 100. This is -- I would think -- about the right magnitude. The ejections themselves -- it's a little hard to say what their size is, but they go out until generally they hit that high speed front where they begin to be carried downstream and interact and that is a very violent interaction and certainly a turbulence producing area. That can be almost anywhere from fairly close to the wall, meaning 30 or so, I would make a rough guess, out to one extreme we saw these things go out as far as 300 y^+ units.

Bradshaw:

Look, the point that I'm making, Bob, is that the scales that you measure of y^+ 50 ought to be half the length-scales that you measure or would measure at a y^+ of 100.

Brodkey:

If you have a structure, that's what you're really talking about, a structure that sort of sits in there. I mean the structure may set at about 75 and cover from 50 to 100. This vortex-type motion is just about the same size.

Bradshaw:

Sure -- but if it's set at 37.5 instead of 75, it ought to have half the scale.

Brodkey:

I think this is true. When Jim and I went back and tried to dig these out of Corino's movies, which are an expanded view of that wall region, (we looked at one movie and reported it in Berlin), there was a y^+ of 90, I believe. Correct Jim? About 90. It was much smaller, but it was still about the same L over D ratio, but it was much smaller because it was closer to the wall -- I really didn't think of it in terms of scales though.

Kline:

Can I get in this act just a second? It seems to me that if I am understanding Peter(Bradshaw) correctly -- what he's saying is that the characteristic

structure, whatever that is, has to scale linearly with the distance from the wall in that zone. So this is a check on the characteristic structure and a rejection criteria. Have you checked that specifically? Is that your question, Peter?

Bradshaw:

Yes -- I'm not suggesting that Bob could check it very easily from his qualitative flow bed, but I'm suggesting that any qualitative model or at least the first approximation could be integrated within the layer scale.

Brodkey:

Well, I can check it qualitatively in that the one vortex we looked at -- the one or two in the wall region were considerably smaller and were of the order of about 10 to 25. I think near the wall it was only about 15 units in diameter.

Kline:

I think Jim Wallace wants to comment on this also.

Wallace:

I'd just like to comment on what I think I've seen in Bob Brodkey's movies -- in respect to Peter Bradshaw's question. The vortices that we've observed that were of small scale -- that is about a non-dimensional diameter size of about 50 in the wall region at about that y^+, so they scale with the y^+. The w_z vortices that Bob and Starvos Nychas have observed -- they are much larger in scale, lie much further out at y^+ locations that scale with the size of the vortex.

Kline:

So what you're saying, if I understand you, is that you do observe this kind of linear scaling. Okay. Thank you.

Brodkey:

One of the types of vortices that I mentioned, the axial vortices, was centered on about 15 and extended from 10 to 25. This also seems to follow the scaling idea. (This comment has also been edited to conform with the ideas expressed above concerning axial vortices near the wall. Editor)

Kline:

I think that clarifies the point about which Peter Bradshaw was asking.

VISUALIZATION OF TURBULENT BOUNDARY-LAYER STRUCTURE USING A MOVING HYDROGEN BUBBLE-WIRE PROBE.

C. R. Smith

Department of Mechanical Engineering and Mechanics

Lehigh University, Bethlehem, PA. 18018

ABSTRACT

Water channel flow visualization studies of turbulent boundary layer structure are described. An overview of the flow visualization system, which employs moving hydrogen bubble-wire probes and a video viewing system, is presented and visual results obtained for both side and plan views are discussed. The results are consistent with previous visualization and sensor results, and provide further insight into 1) the role of outer region structure in the "bursting" process and 2) the characteristics and dynamics of inner wall-region structure and the relation of this structure to low-speed streak behavior.

1. INTRODUCTION

The last fifteen years have witnessed a substantial increase in available information regarding turbulent boundary layer structure. Although some structure is apparent in early photographs taken by Prandtl and his students [1], until recently it was generally believed that turbulent boundary layers were essentially random phenomena. Beginning in 1959, however, extensive studies using both flow visualization [2-7] and probe measurements [8-10] revealed a number of discernable structures and deterministic "events" occurring both in space and time.

The two basic structures which are observed are low-speed wall "streaks" and convected transverse vortex-like structures moving in the outer regions of the boundary layer. The "streak" is a finger-like region of low-speed fluid which extends in a longitudinal direction near the wall. These streaks migrate back and forth transversely across the wall, often coalescing with each other. It has also been found that a statistically determinant length scale can be defined based on the spacing between the streaks. The transverse vortex structures have normally

been represented as larger-scale, vortex-like structure which are convected downstream in the outer regions of the boundary layer. The sizes and vorticity of these vortices can vary widely, but it has been found that their convective velocity is approximately 80 percent of the free-stream velocity.

These structures, and perhaps others, interact in a number of distinct events. The most important of these events is termed a "burst" [2,3,9]. A definite burst sequence has been observed which involves first the appearance of a streak, which then grows and eventually lifts up away from the wall. During the "lift-up" phase, fluid motion is amplified in an oscillatory fashion,often forming what appears to be a transverse vortex. Finally, in the burst itself the lifted-up streak breaks up into apparently non-coherent motion, and fluid is ejected away from the wall. Another event observed in previous investigations is the "sweep" [5,6,7]. This involves a region of comparatively quiescent fluid which "sweeps" from the outer regions of the boundary layer into a region where a burst occurred. After the sweep occurs the region is relatively devoid of any large-scale disturbances or area s of decelerated flow. The burst and sweep are parts of what appears to be a regenerative, cyclical process.

The length and time scales of these boundary layer structures have been investigated in a number of studies. Falco [11] studied the dimensions of a "typical eddy" and found them to scale on inner region variables such that:

$$\frac{c_x u^*}{\nu} \simeq 200$$

$$\frac{c_y u^*}{\nu} \simeq 100$$

where c_x and c_y are the longitudinal and vertical dimensions of the eddy, respectively. These eddies have been observed [12] to decay after having travelled a distance approximately equal to five times their longitudinal extent. The mean streak spacing λ has been found [3] to scale with the inner variables, so that

$$\frac{\lambda u_*}{\nu} \simeq 100$$

Finally, the average burst period $\overline{T}$ has been measured and found to scale with the outer variables U_∞ and δ or δ^* [3,3]. An approximate relation is

$$\frac{\overline{T} U_\infty}{\delta^*} \simeq 32$$

Using these relations, it is therefore possible to estimate the sizes and life spans of the structures.

However, many questions remain to be answered. In particularly, the source, geometric characteristics, and time scale of the structures in the outer layer are unclear, and the mechanism of interaction between these outer structures and those of the inner layer is subject to much debate. One fundamental reason for the failure of past research to answer these questions is that the structures are convected downstream at varying speeds, while most of the observations and measurements have been done in a fixed reference frame. Thus, the structures are observed for only a short duration during their lifetimes, which strongly limits the time available for observation or detection of structural characteristics and time history. Thus it would appear desirable to employ a method of moving flow visualization and velocity measurement devices along with the structures.

The concept of observing turbulent boundary layer structure from a moving reference frame is not new; Prandtl and his students [1] obtained photographs and movies from a moving reference frame, using aluminum powder sprinkled on the free surface of a water channel as the visualization medium. In Prandtl's study a vortex-type motion was observed, the appearance of which changed markedly as the camera velocity was varied. More recently, Corino and Brodkey [6], Nychas, Hershey, and Brodkey [7], Falco [11] and Eckelmann [13] have all performed experiments using a convected frame of reference.

Corino and Brodkey [6] used a high-speed movie camera mounted on a lathe bed to study the wall region in turbulent pipe flow. In their study, tiny particles of aluminum oxide in suspension in the working fluid (trichlorethylene) were employed as tracers. A mercury arc lamp traveling with the camera illiminated a thin plane of the fluid perpendicular to the viewing direction, allowing observation of these tracers. The camera and lamp were mounted on a carriage which was driven along the lathe bed by a hydraulic piston at pre-selected speeds of up to 0.3 m/s. This investigation revealed that the bursts were somehow related to the interaction of a region of decelerated flow with a large-scale disturbance in the outer flow field. This study was also to point out the existence of the sweep events.

A system similar to that of Corino and Brodkey was used by Nychas, Hershey, and Brodkey [7] to study turbulent flow structure in a boundary layer over a flat plate. The same basic visualization techniques were employed; however, the flat plate was mounted in a water channel with pliolite particles used as the flow tracers. This study showed that the large-scale structure in the outer regions of the boundary layer had the characteristics of a vortex with 1) its axis of rotation in the transverse direction and 2) an average axial velocity approximately 0.8 times the local mean velocity. Based on his observations, Nychas speculated that this transverse vortex-like structure resulted from an interaction between accelerated and decelerated regions of fluid and that it was somehow associated with the bursts.

Falco [11] performed some limited flow visualization studies using a convected frame of reference. In his experiments, Falco employed a low velocity (0.3 - 1.5 m/s) smoke tunnel which could produce turbulent boundary layers with Reynolds numbers (based on momentum thickness) of

around 500-1000. The top and side walls of the tunnel were constructed of clear plexiglas to allow observation of a smoke-filled boundary layer which was produced by introducing a dense "smoke" of fine oil droplets near the entrance of the tunnel. The smoke was illuminated by a 6 mm thick light plane which could be rotated to provide either streamwise or spanwise views of the structure. A motion picture camera was employed which could be traversed along the entire test section. The same visualization techniques were employed for a fixed reference frame to examine large scale motions in the outer region of a turbulent boundary layer at a $Re_\theta \simeq 4000$. The effect or Reynolds number on the length scales of "typical eddies" was studied, and the non-dimensional relationship mentioned previously was developed.

The various studies described above, although excellent pieces of research, do have several limitations. The use of particles suspended to the flow, as used in references [6,7], relies on a thin slit of light to define the viewing plane. This procedure severely limits the types of motion which can be observed. For example, the regions of slow-moving fluid described by Corino may or may not have been streaks; but even if they were his method would not have allowed him to see the whole streak. In addition, motion of the particles perpendicular to the viewing plane could not be detected. It is also somewhat difficult to interpret the results of visualization studies using tracers because the pictures obtained do not directly reveal such recognizable patterns as streamlines, time lines, etc. It is possible to derive these flow lines from a series of photographs, but this is a very time consuming process. Finally, the pictures of suspended-particle motion are often rather ill-defined, making it difficult to perceive any recognizable structure.

The use of an oil fog (smoke) by Falco [11], does allow a much clearer qualitiative visualization of flow structure. However, this technique does not supply a means for quantitative evaluation of local velocity behavior from the pictorial data, and will often visualize "inactive" structures as well as "active" structures. In addition, so much smoke is present that normally only structures which occur near the outer interface of the smoke are observable (often referred to as observing the "skin" of the structure).

The present study extends the use of flow visualization in a moving reference frame to the use of the hydrogen bubble-wire technique. The use of hydrogen bubble-wires for visualization of turbulent boundary layer structure has become relatively standard [2,3,4,5], however, they have never been employed in a moving frame of reference in order to "follow" flow structures. The benefits of such a system are that 1) a plane of instantaneous, active behavior can be clearly defined, 2) the frequency of the bubble line generation can be controlled to optimize the visualization of structures moving at differing speeds, and 3) quantitative information is directly derivable from the visualization pictures.

Thus, the objectives of the present work were 1) to develop a moving hydrogen bubble-wire system which allows the visualization of boundary layer structure from a moving reference frame, and 2) to employ this system to determine the characteristics, history, and interaction of the different types of structure within a turbulent boundary layer. To facilitate the acquisition of the flow visualization data, a closed-

circuit video monitoring and recording system was employed which allows both on-line viewing, recording, and frame-by-frame playback of flow visualization experiments.

2. EXPERIMENTAL FACILITY

A. Water Channel

A schematic of the water channel flow system and the moving reference platform is shown in Figure 1. The working section of the water channel (pictured in Figure 2) is 5.2 meters long with a bed 0.9 meters wide by 0.30 meters deep. For boundary layer studies, flat plate test sections of up to 4 meters in length can be accommodated in the working section. The maximum volumetric flowrate for the channel is 1.25 m^3/min. with an overall system capacity of 4.20 m^3 of filtered water. Special care has been taken in the design and fabrication of the inlet and outlet sections of the test channel. The inlet flow initially enters a large inlet tank through a specially designed distribution manifold and a 5 cm thick plastic settling sponge. From the inlet tank, the flow passes into the channel through a 2.5:1 inlet contraction, a honeycomb flow straightener, and two 20-mesh turbulence damping screens. The resulting inlet flow is uniform to within ± 0.5% across the center 90% of the channel. With false side walls in place, inlet velocities of up to 30 cm/s and Reynolds numbers of up to $Re_L \approx 10^6$ (based on plate length) and $Re_\theta \tilde{=} 2300$ (based on momentum thickness) can be attained.

Three different test sections were used in this study. Two were flat plate test sections 2.5 meter and 3.7 meters in length with eliptical leading edges. The shorter plate was used for lower Reynolds number studies ($Re_\theta < 1000$), the longer plate (which employed false sidewalls to increase the freestream velocity) was used for higher Reynolds number studies ($Re_\theta > 1000$). Each plate was elevated 6 cm to prevent interference by the channel floor boundary layer. The channel floor itself was employed directly as the third test surface, which provided a low velocity development length of up to 4.4 meters. To assure the developing boundary layer was turbulent, a boundary layer trip consisting of 1-1/2 mm thick triangular elements was located 5 cm back from the leading edge of each test plate and 15 cm downstream from the last damping screen for the channel floor studies.

B. Moving Reference Platform

The moving frame reference platform utilized in this research is a 1.0 meter x 0.6 meter rectangular frame constructed of 5 cm x 5 cm square aluminum tubing with a series of interior stainless steel support shafts for equipment and probe support. The platform rides on a pair of 3.8 cm diameter hardened steel shafts mounted directly to the water channel frame. The platform is guided on one shaft by two linear motion bearings which provide both vertical and lateral support; the opposite side of the platform is supported on two precision ball bearing cam followers which have only rolling contact with the top of the shaft. The drive motor is a one-horsepower variable speed DC motor with reversing and dynamic braking. The motor, coupled to a 3.7 meter lead screw, can drive the reference platform over a velocity range from 0-50 cm/s.

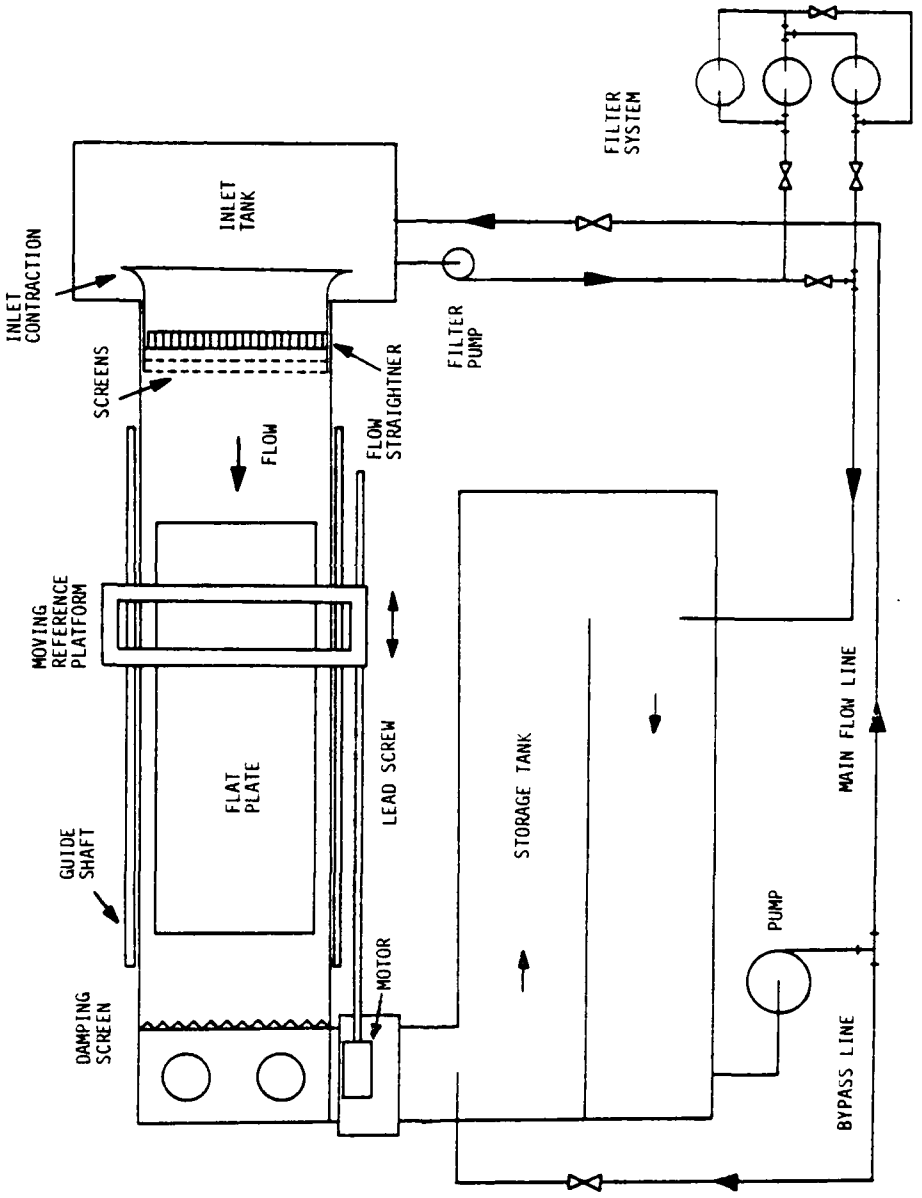

(a) Plan View

Fig. 1. Water Channel Schematic

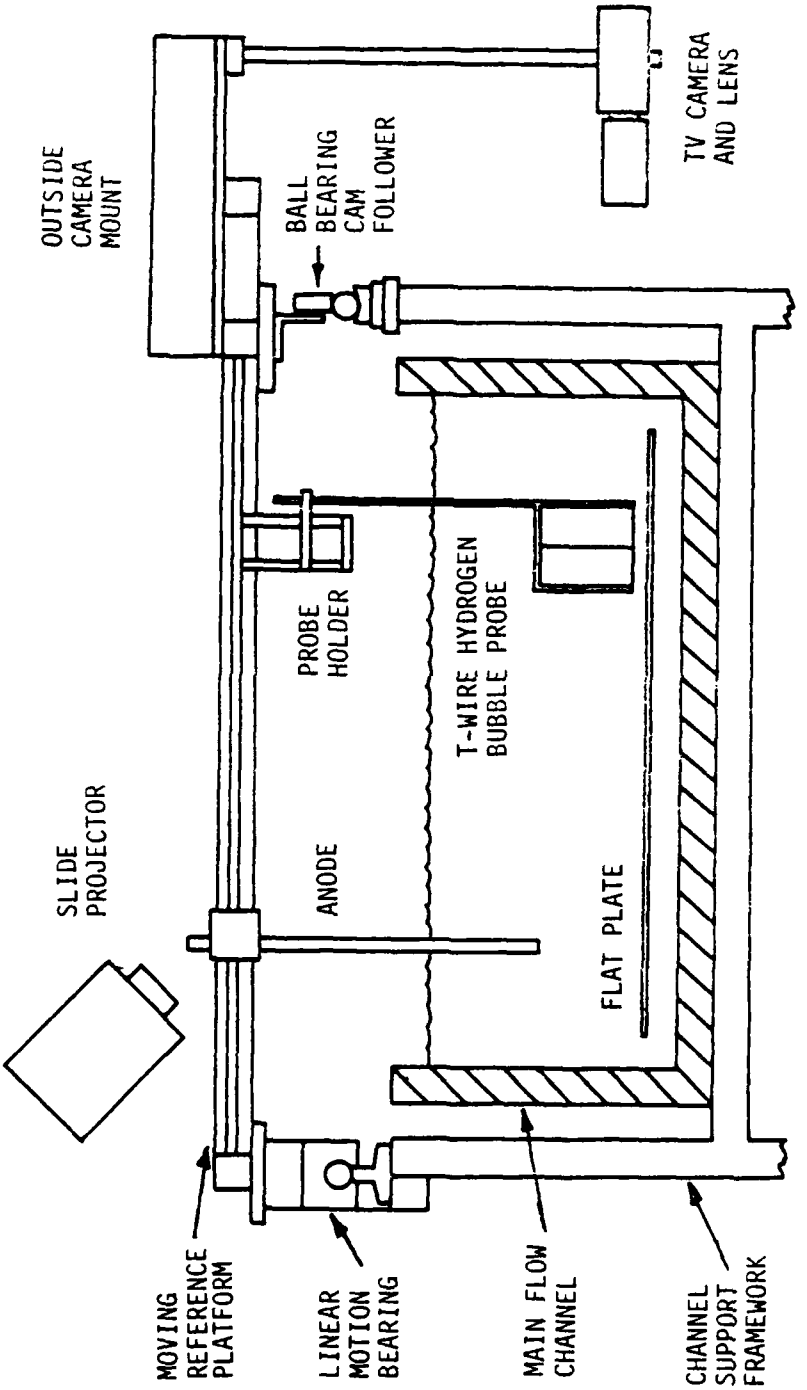

(b) End View

Fig. 1., cont.

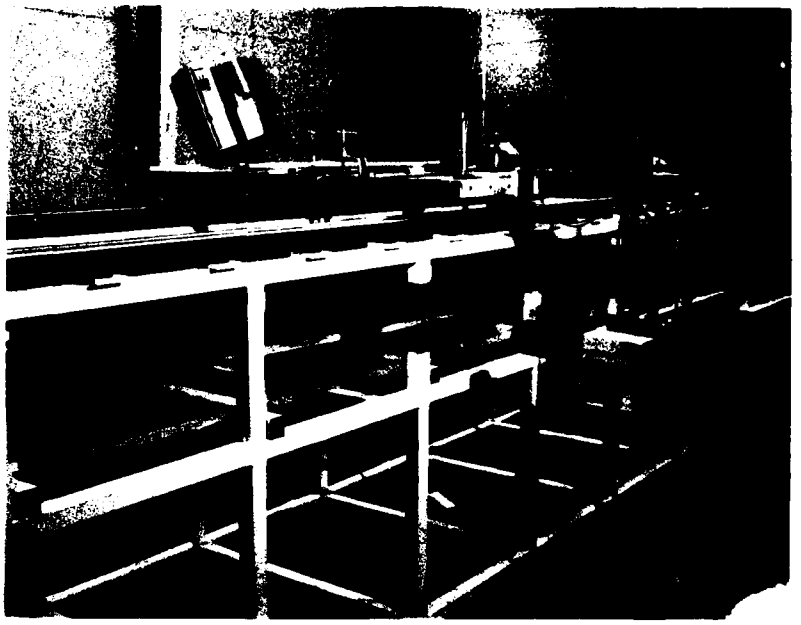

Figure 2. Working Section of Water Channel, Moving Reference Platform, and TV Camera

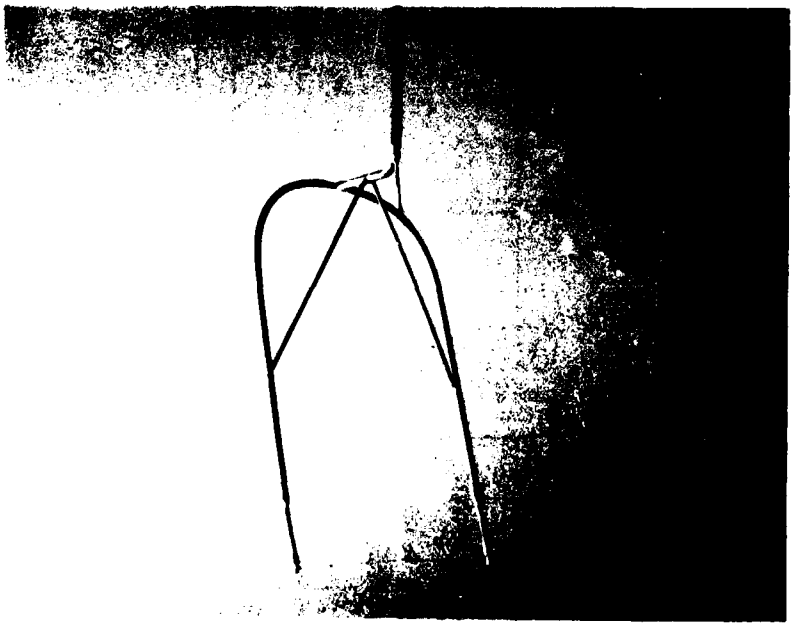

Figure 3. U-Shape Bubble Wire Probe Support (with vertical wire in place)

C. Flow Visualization System

The hydrogen bubble technique as employed previously by Runstadler et al. [3], Kim et al. [4], and Offen and Kline [5] was the primary method of flow visualization used in the present study. Some dye injection was employed but only as a back-up technique and for establishment of probe interference effects. The flow visualization system consisted of a power pulse generator, specially designed bubble-wires, and illumination source. The power pulse generator was a specially built DC power supply which provides controlled square-wave voltage pulses at frequencies up to 225 Hz.

In previous flow visualization studies, only fixed reference bubble wires have been used. The objective of the present study was to visualize turbulent boundary layer structure from a moving reference frame, thus a probe support which allowed movement of the bubble-wire with the flow needed to be developed. A picture of the final probe design is shown in figure 3. This probe is constructed in the shape of an inverted U from 3 mm and 1.5 mm brass tubing. The span between the projecting support legs was approximately 20 cm. To prevent the generation of spurious bubbles, the probe was insulated using thin-wall shrink fit tubing. Using this basic probe support, bubble-wire probes with either a vertical or horizontal hydrogen bubble-wire could be fabricated. Vertical-wire probes were first constructed by soft soldering an insulated constantan thermocouple wire of 0.17 mm total diameter horizontally between the tips of the probe legs. A 2 mm center section of this horizontal support wire was then carefully scraped and one end of a 0.05 mm platinum wire was spot welded to the exposed constantan wire and soft soldered to the upper arm of the probe support. 5 mm of the platinum bubble-wire was left extending below the hotizontal support wire, which allowed the tip of the vertical bubble wire to be located right down to the wall. A horizontal bubble-wire probe was constructed by simply soft soldering a 0.05 mm platinum wire between the tips of the probe legs. Note that in the final support probe design, the legs are angled about 20° to vertical to allow for minimal visual obstruction of the bubble-wire by the probe support legs.

In order to establish the degree of probe interference which results from the streamwise movement of the probe, a series of visualizations were done of a laminar flat plate boundary layer using a vertical wire probe. The probe was observed to have minimal effect on the flow profile and stability as long as relative probe motion was initiated such that the probe reached a constant velocity at least 0.3 m prior to passing on to the flat plate test section. Comparison of laminar velocity profiles obtained at the same streamwise location showed essentially no difference between profiles obtained with the probe stationary and with the probe moving at relative velocities as high as U_∞. For the highest plate Reynolds number attainable with the water channel ($Re_L \approx 10^6$), the location of natural transition ($Re_x \approx 6 \times 10^5$) was found to decrease about 10% for a relative probe velocity of $0.5\, U_\infty$. Higher and lower probe velocities appeared to have a lesser effect on transition. The conclusion is that the bubble-wire probe does slightly interfere with the flow, but that the effect of this interference in a fully turbulent boundary layer should affect neither the basic flow structure nor its behavior.

Although the bubble-wire probe design should hypothetically allow moving reference frame visualizations to be done essentially right down to the surface of a test plate, in practice this was not attainable due to limitations in leveling of the test plate. The best that was achieved in leveling the plate was $\pm$ 0.8 mm over a plate length of 3.7 m. This limited to approximately 1 mm the minimal distance the tip of a vertical wire could be located off the plate (if the wire touched the plate during its movement, the extended tail would be bent severely or broken off).

Bubble illumination was done using a conventional 500 watt slide projector mounted directly on the moving reference platform. Due to the low light sensitivity of the television camera, no higher intensity light source was required.

D. Closed Circuit Television System

It was recognized early in the research that one of the major limitations in most flow visualization experiments is the inability to have instant access to the visual data for immediate playback and analysis. Film is both expensive and requires a development delay of several days before the results of an experimental run can be observed. And more often than not, one finds that either the camera position, focus, or light setting was incorrect, necessitating refilming of an experimental run. A closed-circuit television system with a video tape recorder eliminates all of the uncertainties of camera position, focus, and light setting since a scene is viewed just as it will be recorded. Television does have several limitations, such as a maximum framing rate of 60 pps and reduced resolution of individual still frames. However, it has the advantages of much lower lighting requirements, less sensitivity to background, simultaneous display of multiple views, and a direct analog output for picture digitizing. And from a cost point of view, a 1 hour reel of video tape costs the same as 100 feet of developed 16 mm film (4 minutes worth) and is reusable.

The closed-circuit television system used in this research consists of a TV camera. lens, monitor, and video tape recorded (VTR). The TV camera is a compact surveillance camera with low light sensitivity which is mounted on the reference platform either from above or cantilevered from the side (as shown in Figure 2). The camera lens is a remote control zoom lens with various degrees of close-up capability. The zoom, focus, and iris adjustments are remotely controlled from a central console (which also houses the TV monitor, the reference platform speed control, and the bubble-wire power pulse control). The output from the camera can be viewed on-line with the high-resolution TV monitor and simultaneously recorded on a time-lapse VTR. This recorder has the capability of taping events in real-time and playing them back in either real-time or at several different time delayed speeds ranging from 1/9 real-time to single frame (stop-action).

3. RESULTS AND DISCUSSION

A series of visual studies were conducted using both vertically and horizontally oriented hydrogen bubble-wires. Both fixed reference sequences and moving reference sequences have been recorded and examined in detail for

several flow conditions, viewing locations, and fields of view. In all, over six hours of information were recorded; the essence of the structural characteristics observed in this six hours of information is condensed and described in this section.

As can be imagined, the analysis of this amount of data, even qualitatively, is extremely time consuming and tedious. And when one is dealing with both side-view and plan-view observations for several different reference frame velocities and distances from the wall, the task of extracting and understanding even qualitative aspects of the flow structure of a turbulent boundary layer becomes incredibly painstaking and difficult. Thus, the results presented here consist of general, qualitative descriptions of observed behavior augmented with quantitative information (such as relative length scales, time scales and convection velocities). Extensive use is made of pictures (individual and sequences) taken directly from the video screen, as well as simple sketches. The results will be presented and discussed in two parts:

1) side-view visualizations of a turbulent boundary layer employing a bubble-wire normal to the flow

2) plan-view visualizations of a turbulent boundary layer utilizing a horizontally transverse bubble wire.

The observed flow events, as evidenced in these results, and their relationship to and consistency with existing flow structure models will then be discussed.

Note that discussion of length scales is done in terms of non-dimensional distances x^+, y^+, and z^+ (streamwise, normal, and spanwise distances). Distances relative to boundary layer thickness are generally avoided because all the flows so far examined were for $800 < Re_\theta < 2300$, below what is generally considered necessary for "fully developed" conditions. In addition, the boundary layer was continually growing as the camera and probe convected with the flow (much more so than the viscous length ν/u^*). However, it is not felt that the low $Re\theta$ at which these studies were done significantly biases the qualitative results since the velocity profiles over the last half of each test section were shown to be in substantial agreement with accepted "law of the wall" correlations. In addition, the range of Re_θ examined is essentially the same or greater than the ranges examined in the visual studies of Runstadler et al. [3], Kim et al. [4], Offen and Kline, [5], Nychas et al. [7], and is of the order of the low Reynolds number studies of Falco [11].

Values of δ, θ, and u^* were determined at several locations along the test plate for the U_∞ = 12 cm/s flow cases using mean velocity profiles obtained by averaging bubble-wire time-lines over a period of 40 seconds. This method of time-averaging, used previously by Kim et al. [4], was corrected for bubble defect effects using the results of Shraub et al. [14]. u^* was determined from the time-averaged velocity profiles using the modified Clauser Fit technique employed by Runstadler et al. [3]. For all the U_∞ = 12 cm/s data, δ, θ, u^* were all found to fall within $\pm$ 4% (the order of the uncertainty of the data) of the correspond-

ing values one would predict using standard empirical relationships for zero pressure gradient flow over a flat plate with the boundary layer turbulent from the leading edge onwards. Thus, for the U_∞ = 27 cm/s flow, δ, θ, and u* were estimated using standard empirical relationships.

As pointed out in Section 2, although a video recording system is extremely versatile, it can present some problems in terms of picture clarity and resolution. Due to the effective shutter speed of 0.0167s for a standard video camera, blurring will occur when there is large relative motion of the time-lines within the field of view (this is particularly troublesome when extreme close-up views are taken). Thus, almost all photographs presented in this section are from the lower velocity studies since these gave the clearest photographic reproduction. The problem of shutter speed is being resolved by the acquisition of a video unit which employs a synchronized strobe light to achieve effective shutter speeds of 10^{-4}s. This faster camera should allow future studies to be done at flows of up to 1 m/s with good picture clarity and resolution.

A. Side-View Visualization

Figure 4a is a typical side-view bubble-wire visualization of a turbulent boundary layer of Re_θ = 1200. In this figure, as in almost all of the side-view pictures in this section, the vertical bubble-wire is located on the far left of the picture where the bubble-lines originate. The blurred, elongated object projecting from the left boundary of the picture down near the wall is one of the vertical probe supports, which is located 10 cm out of the plane of the bubble-lines, or a non-dimensional z+ distance of $\approx$ 450. Note that the bubble-lines appear a bit blurred due to the video shutter speed problem mentioned above; however, several characteristic aspects of coherent structure are observable in this picture. First, is the large scale motion or LSM (indicated by the brackets on the upper edge of the figure) noted by Falco [16]. This structure also appears to be essentially the same type of structure observed by Offen and Kline [5], which they indicated was associated with the occurrence of a burst-sweep sequence. As can be observed in Figure 4a, the passage of this large structure does appear to result in the formation of a burst as evidenced by the wavy wall region structures (indicated by the coordinates b-b). After viewing many, many sequences of this type it was observed that almost every burst sequence could be related to the passage of a large-scale motion with a clockwise transverse rotation, which is consistent with the observations of Offen and Kline. The outermost extent of these large-scale motions (LSM) for the present studies ranged from $100 \leq y^+ \leq 400$ depending on the degree of boundary layer development. Normally, the higher the Re_θ, the larger the LSM (in ν/u^* units) which appeared to initiate a burst. It is to be pointed out that these LSMs are not a single, large vortex, but generally consist of an agglomeration of smaller scale vortical structures of varying sizes, strengths, orientations, and coherency. Although it was clear that the passage of a LSM correlated with the occurrence of a burst, whether it was the overall LSM or one of the substructures of the LSM which initiated the burst was unclear.

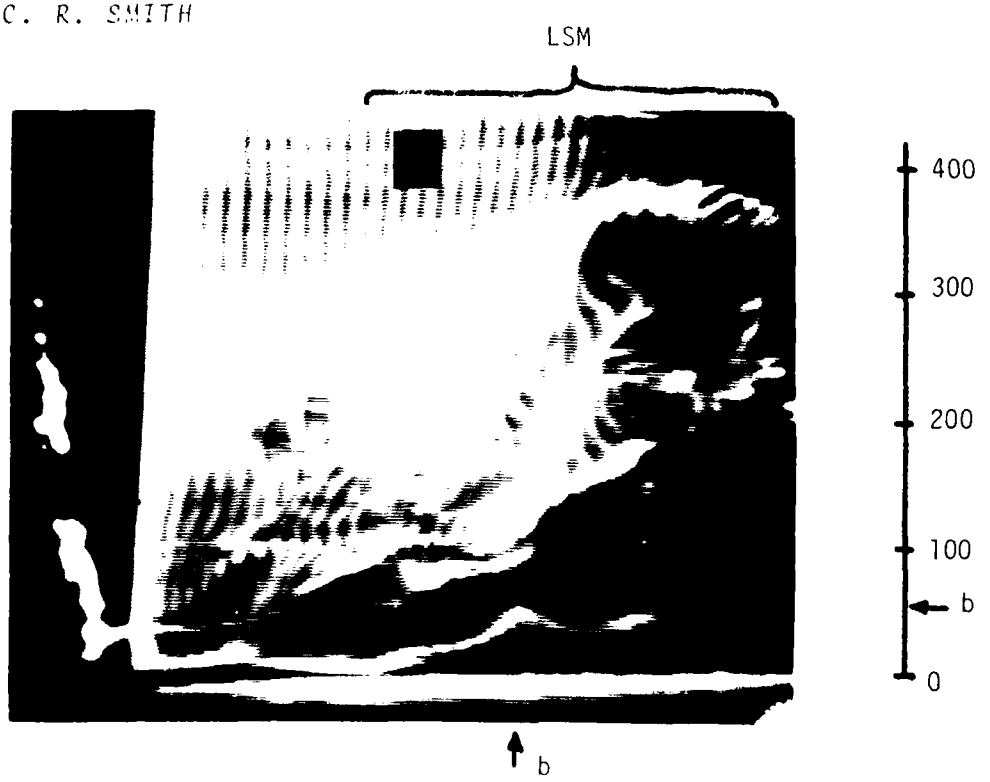

Figure 4a. Side View, Stationary Reference.

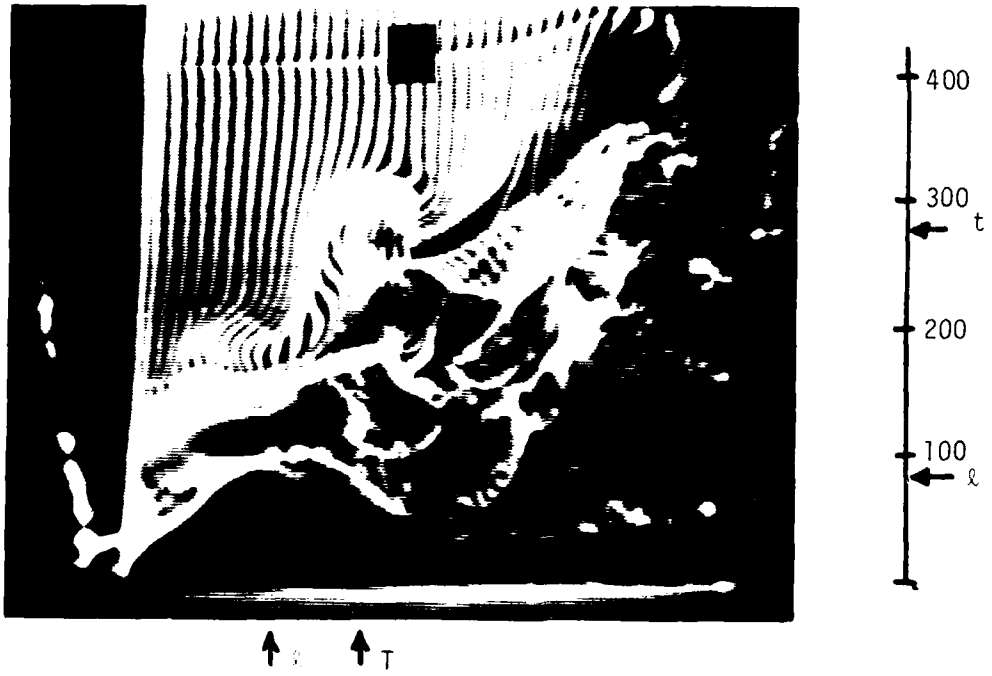

Figure 4b. Side View, $V_{ref} = 0.48\ U_{\infty}$

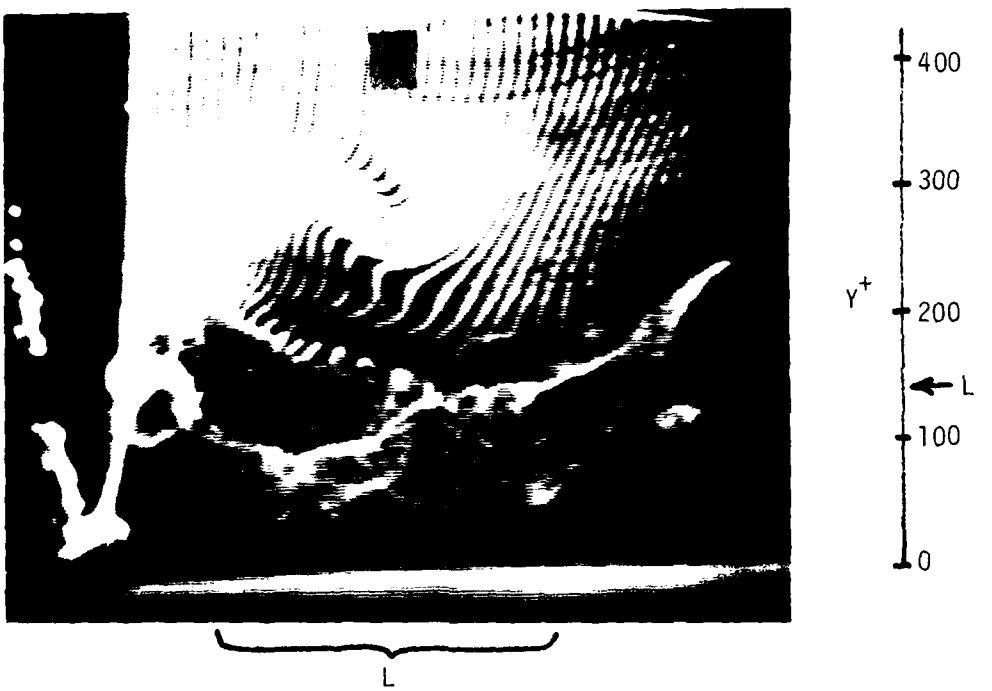

Figure 4c. Side View, V_{ref} = 0.71 U_∞

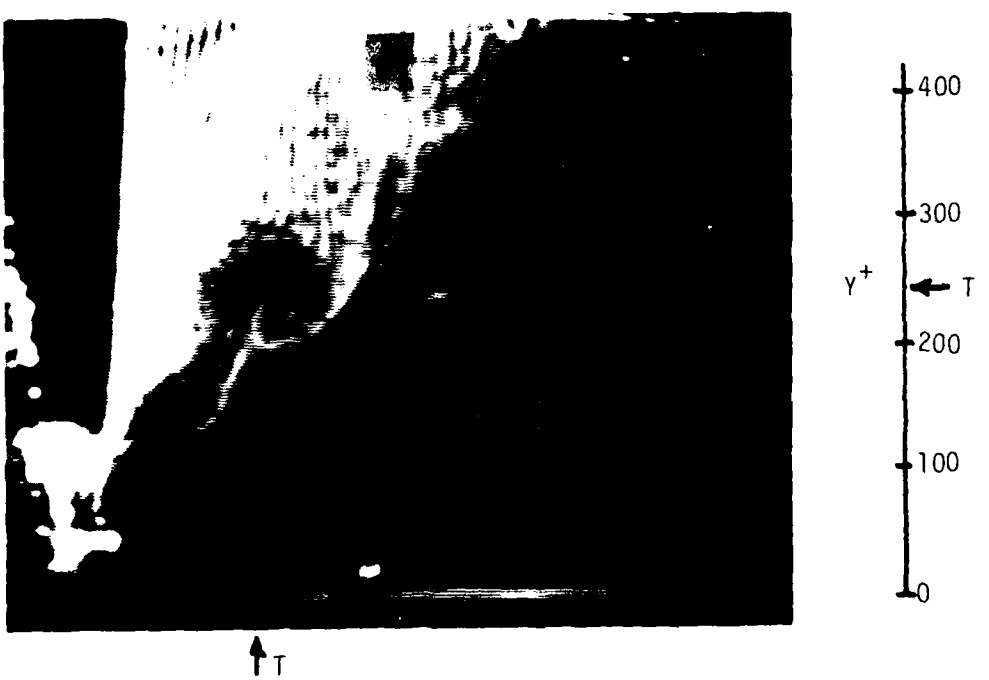

Figure 4d. Side View, V_{ref} = 0.86 U_∞

Figure 4b, obtained at the same relative location and Re_θ as Figure 4a, but at a relative reference frame velocity of 0.48 U_∞, shows more clearly the scales and intertwined appearance of a LSM. Note the very coherent transverse vortex indicated in the figure at the coordinates T-T is of essentially the same scale (~ 100 y^+ units) as the "typical" eddies observed by Falco [16]. Note also the large, almost triangular region devoid of bubbles located near the wall at the location ℓ - ℓ. This appeared to be a very large upwelling from the wall region which was initiated by the passage of the LSM and fed with fluid both from upstream and from the wall region on either side of the plane of the bubbles. As this upwelling region formed, it was observed to interact quite strongly with a thick, longitudinal vortex which looped and penetrated up from the wall into the LSM to $y^+ \approx 300$. The upper termination of this longitudinal structure was not obvious, but it appeared to be connected with a large, transverse vortex located in the upper region of the LSM.

As pointed out above, the LSMs observed appeared to have an overall transverse rotation (as a ball rolling along the wall in the flow direction). This is consistent with the composite velocity distribution in the outer region of the boundary layer as educed by Kovasznay et al. [8] from correlation measurements, and the proposed outer region flow model of Thomas and Brown [17]. Although the velocities of the different structures within the LSM were anywhere from 0.7 U_∞ to 0.95 U_∞, the center of rotation of most LSM's observed appeared to move between 0.8 U_∞ and 0.85 U_∞. From the convected visualization studies, this rotation appeared to be the result of a multiple coalescence of many smaller vortical structures of like rotation, both with each other and with the LSM. An additional observation was that the structures which appear on the upstream interface of the LSM appear to interact with the irrotational, non-turbulent outer flow resulting in outer flow entrainment into the LSM. The result of this process is to "energize" and to make more coherent these outer eddies and most likely to provide a source of higher energy fluid to sustain the LSM motion.

The constant overturning of the LSM was observed to result in a continual transfer of fluid from the outer region to the wall near the downstream portion of the LSM. This transfer of fluid to the wall can be seen in Figures 4b and 4c as blotches of fluid (as characterized by indistinct bubble patterns) near the front of the LSM and near the wall. As fluid was returned to the wall, it appeared to decelerate and spread rearward (as viewed in the moving reference frame). Both high and low momentum fluid were observed to be transferred to the wall. Obviously, the source of the higher momentum fluid must have been the irrotational outer flow, although no clear path from this outer region to the wall could be followed. The source of the low momentum fluid could frequently be traced to what appeared to be the residue of a recent upstream burst. And in several sequences, two smaller vortices formed from upstream burst events were observed to rotate about one another, returning one of the vortices to the wall where it was rapidly stretched and deformed by viscous action. This tendency of some of the fluid from a prior burst to return to the wall downstream of the burst has been noted previously by Offen and Kline [5].

As the reference frame speed is increased, only those flow structures which are moving at speeds either equal to or greater than the reference speed will be visualized. This must be kept in mind or one will be prone to misinterpret the moving reference frame visualization pictures since all low speed flow structure (generally that near the wall) is "left behind" as the reference moves relative to the wall. Figure 4c, obtained at a reference velocity of 0.71 U_∞, illustrates this point since only larger, outer region structures moving in excess of 0.71 U_∞ are visualized. Note how the region near the wall is somewhat devoid of bubbles (except for blotches of fluid returned to the wall) since all the flow below $y^+ \cong 60$ will be moving more slowly than the reference velocity (on the average) and therefore, bubbles generated in this lower region will never move into the field of view.

A large, transverse vortical structure moving faster ($\sim 0.8\ U_\infty$) than the reference velocity is clearly shown in the upper left of Figure 4c. This structure again has dimensions on the order of the typical eddy of Falco [16]. Note that at the location L-L, a long longitudinal vortex is observed which extends from the transverse structure forward to a previous transverse vortical structure (which is just leaving the field of view on the right at $y^+ \approx 200$). Although not typical, such a "connecting" longitudinal vortex was often noted far out from the plate, implying that individual outer region structures may be only part of a more involved vortex loop or warped sheet of vorticity.

If one examines the time lines near the leading edge of the large transverse vortex shown in Figure 4c, a downward movement of irrotational outer region flow toward the wall is observed. This appears to be part of the outer region entrainment process which feeds energy into the LSMs and is probably an example of laminar, nonturbulent fluid moving negatively (wallward) in the intermittent region, as measured previously by Kovasznay et al. [7]. If one studies closely the time-lines in this region of entrainment, it is noted that the inflow 1) decelerates upstream, moving back toward and rotating around the large transverse vortex, and 2) accelerates downstream, moving toward (and down around the sides) of the previous vortex structure. The entrainment process appears to be both 1) feeding energy into the large outer structure, and 2) feeding a source of higher momentum fluid toward the inner region. This higher momentum fluid may be a source of the inner region "sweeps" which were originally observed by Corino and Brodkey [6], and which will be pointed out later in this paper to be associated with the passage of a "back" of a transverse vortex. It is of significance also to note the magnitude of the decelerating effect that the entrained fluid experiences near the large transverse vortex of Figure 4c. This deceleration effect when translated to the wall would appear as the wall layer deceleration observed by Corino and Brodkey [6] prior to the occurrence of a burst, and would be felt as the temporary adverse pressure gradient which is speculated by Offen and Kline [5] to initiate the lift-up of a low-speed wall streak.

Figure 4d, which was obtained at a reference speed of 0.86 U_∞, shows essentially only a single large transverse vortex in the outer region of the boundary layer. The vortex is moving at about 0.9 U_∞, and is again on the scale of the Falco typical eddy. The blurring of the bubble lines

in the photograph is due to a buoyancy coalescence of the bubbles, a problem that can occur when a very low relative velocity between the flow and the reference frame occurs. Although this coalescence does impair the accuracy of the visualization technique, the qualitative behavior of the flow can still be observed. Note that entrainment of the outer flow is observed to occur over the front of the vortex and wrap inwards toward the vortex center. In addition, fluid from below the vortex is observed to be drawn upward into the vortex. This latter motion is indicated by the thin line of bubbles projecting upward into the vortex from the wall region. This spiraling inward of both bubbles and injected dye was a relatively common observation when the large transverse vortical structures of the outer region were followed at or near their convection velocities.

In order to examine the more detailed characteristics of the bursting process, a series of studies was done with a substantially reduced field of view. The outer extent of this viewing field was $y^+ \cong 70$, which is essentially the upper extent of what Corino and Brodkey [6] term the "generation region". Figure 5 (taken from a stationary reference) illustrates the beginning of a typical burst lift-up as described by Kim et al. [4] and Offen and Kline [5]. Figure 5a is a picture of a relatively quiescent period in which the wall layer region (approximately outlined by the thick bright line near the wall) is growing by diffusion. Note that the somewhat distorted appearance of the bubble lines at $y^+ \approx 20$ is due to the wake of the 0.17 mm support wire to which the vertical bubble wire is anchored. In Figure 5b, which is taken $t^+ = tu_*^2/\nu \cong 5$ later, a vortical disturbance (which appears as a series of inflectional time-lines), has come into the field of view and appears to be interacting with the wall layer, causing it to lift from the wall. Figure 5c, taken at $t^+ \cong 10$, shows that the wall layer has lifted off the wall and moved well up toward the vortex. Note also the appearance of a sweep effect that appears to propagate along the back of the vortex (inflectional time-lines), pushing the lift-up before it. The appearance of a sweep as an almost concentrated region right behind an interacting vortex-like structure was a quite common observance in both stationary and convected reference frame visualizations of the bursting process.

Note that the region over which the lift-up in Figure 5 occurs is about $10 < y^+ < 25$, which is the general region of low speed lift-up as established by Corino and Brodkey [6], and the lift-up moves about $x^+ = 100$ at an average velocity of $\sim 0.37\ U_\infty$. The outer disturbance which appears to be associated with the lift-up moves at velocity of $\sim 0.68\ U_\infty$ during the same time period. This lower convection velocity is consistent with the observations of Corino and Brodkey that low speed parcels (as they termed them) often moved at velocities as much as 50% less than the local mean velocity (which was about $0.55\ U_\infty$ at $y^+ = 15$ for our flow). In addition, Emmerling [18] has noted very small scale regions (less than 100 ν/u^* units in extent) of wall pressure convecting at speeds as low as $0.39\ U_\infty$. One is then led to conjecture that the wall lift-up and burst of these low-speed regions could be the source of these small traveling pressure regions.

Figure 5a. Side View, Stationary Reference
$t^+ = 0$

Figure 5b. Side View, Stationary Reference
$t^+ = 5$

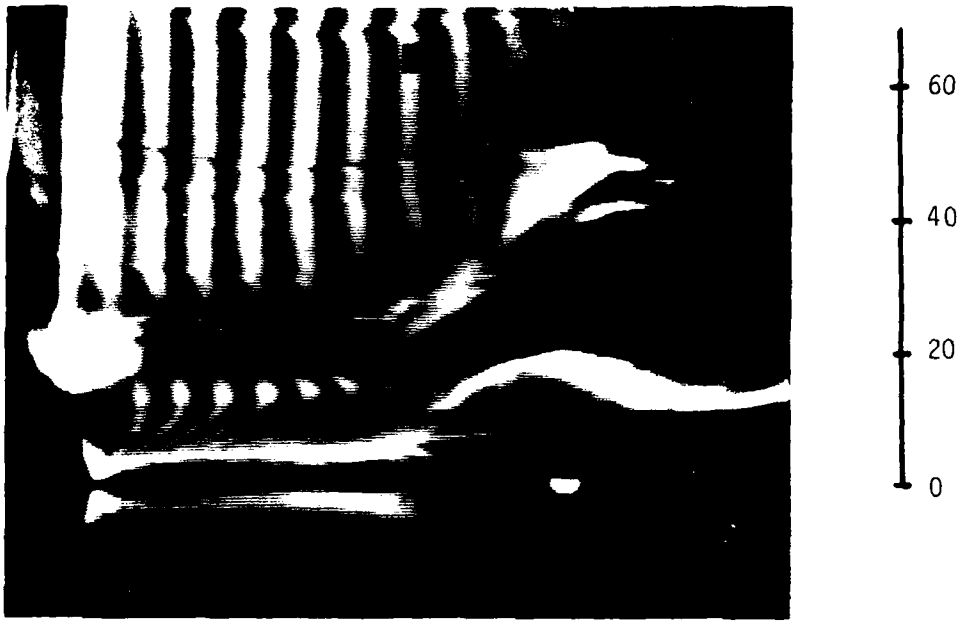

Figure 5c. Side View, Stationary Reference
$t^+ = 10$

It is to be pointed out that while the lift-up shown in Figure 5 was typical of the scale and convection speed of other lift-ups observed, the size and convection velocity of the vortical disturbances associated with the initiation of a lift-up was not at all consistent in size or flow characteristics. Frequently, only a portion of the outer disturbance could be observed, and thus size and rotational characteristics were difficult to determine with the reduced field of view. Frequently only an obvious flow deceleration followed by a flow acceleration (sweep) was observed during the initiation of the lift-up. However, the relative convection velocities could be estimated, and were almost always (as best as one could tell for the restricted field of view of Figure 5) greater than 0.65 U_∞. Thus, although the vortical structure in Figure 5 is untypical of the general size of the structure which appears to initiate the lift-up stage of bursting, Figure 5 is shown to accentuate the fact that a vortical disturbance in the outer region does, as implied by Offen and Kline [5], play a direct role in producing a burst.

Figure 6 is second sequence with a field of view of $y^+ \approx 70$, but taken with the reference frame moving at 0.23 U_∞. Since the reference frame moves with the flow, a burst can be followed further through its development process. The location and Re_θ for this sequence is essentially the same as in Figure 5, with Figure 6a at $t^+ = 0$ illustrating the slowly diffusing quiescent period which occurs prior to the burst sequence (essentially the same initial flow condition as was shown in Figure 5). The region ℓ - ℓ indicated on the figure shows evidence of a residual longitudinal vortex at a location $y^+ \approx 20$ off the wall. In Figure 6b at $t^+ = 10$, a sharp inflection point has appeared at location I-I ($y^+ \cong 50$). This inflection is accompanied by a strong deceleration near the plate which retards the wall-layer region, causing a low speed region of fluid to build-up on the wall. This low speed region, which appears at the dark "hump" outlined by a bright concentration of bubbles, appears to have its origin from wall layer fluid ahead of the inflection point which is decelerated and overtaken by the oncoming flow. The extent of the influx of fluid from lateral regions in the flow could not be ascertained from the video tapes, but inflow from lateral regions is speculated to contribute to the formation of the hump" as well (particularly in view of the results of plan view studies to be discussed later in this paper). This sharp deceleration of fluid near the wall is essentially the effect of a temporary, convected adverse pressure caused by the passage of an outer region structure as described by Offen and Kline [5]. In Figure 6c at $t^+ = 20$ the decelerated fluid region has grown outward to $y^+ \cong 30$ and is moving at a convection velocity of $\sim 0.47\ U_\infty$. Notice the strong upward deflection of the outer flow over the back of the decelerated region and the movement of the maximum inflection point downstream and outward to $y^+ \cong 60$. Figure 6d at $t^+ = 27$ shows a sweep of accelerated fluid impinging down upon the decelerated fluid. The beginning of the sweep appears as a very bright region of bubble concentration lying just above the bright outline of the decelerated region and indicated by the dark arrow on the photograph. Note that the impingement of the oncoming sweep in conjunction with the upstream deceleration effect has caused the decelerated wall region fluid to lift further from the wall to a $y^+ \cong 40$. The convection of the leading edge of the decelerated fluid

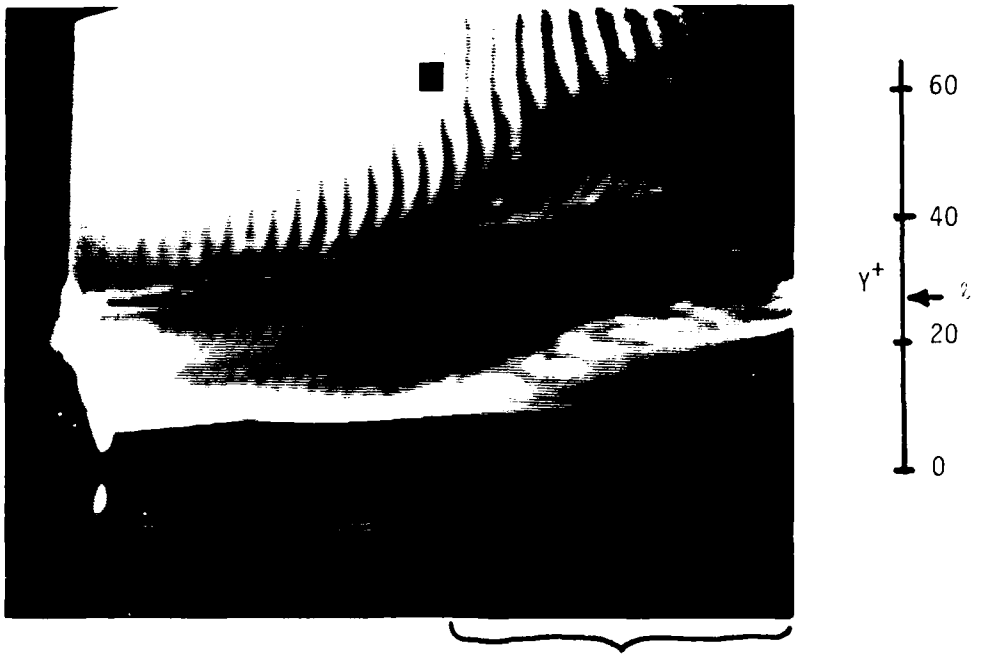

Figure 6a. Side View, V_{ref} = 0.23 U_∞
t^+ = 0

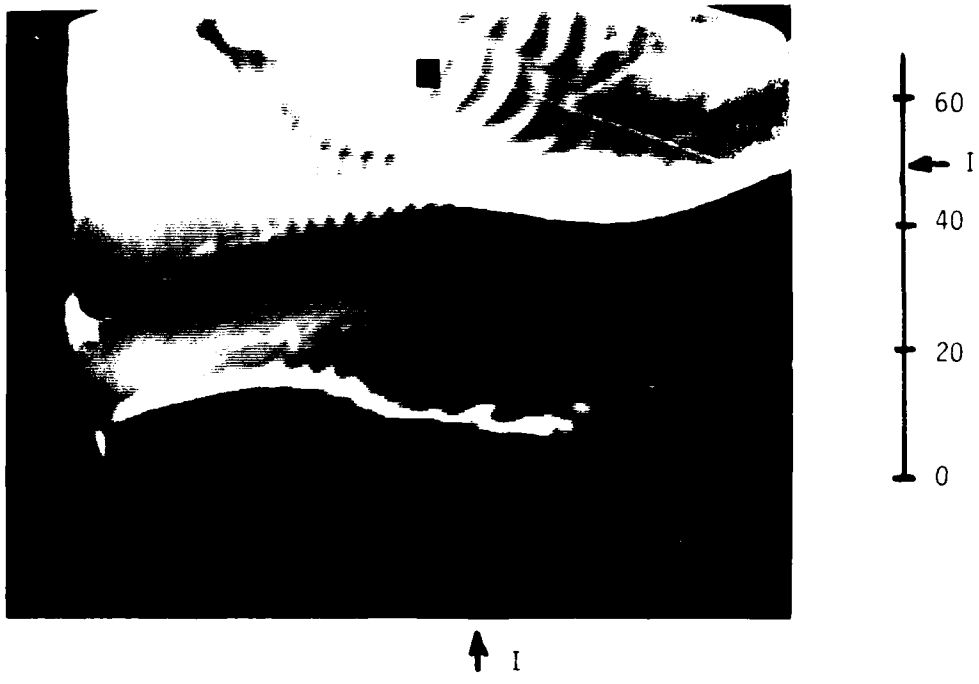

Figure 6b. Side View, V_{ref} = 0.23 U_∞
t^+ = 10

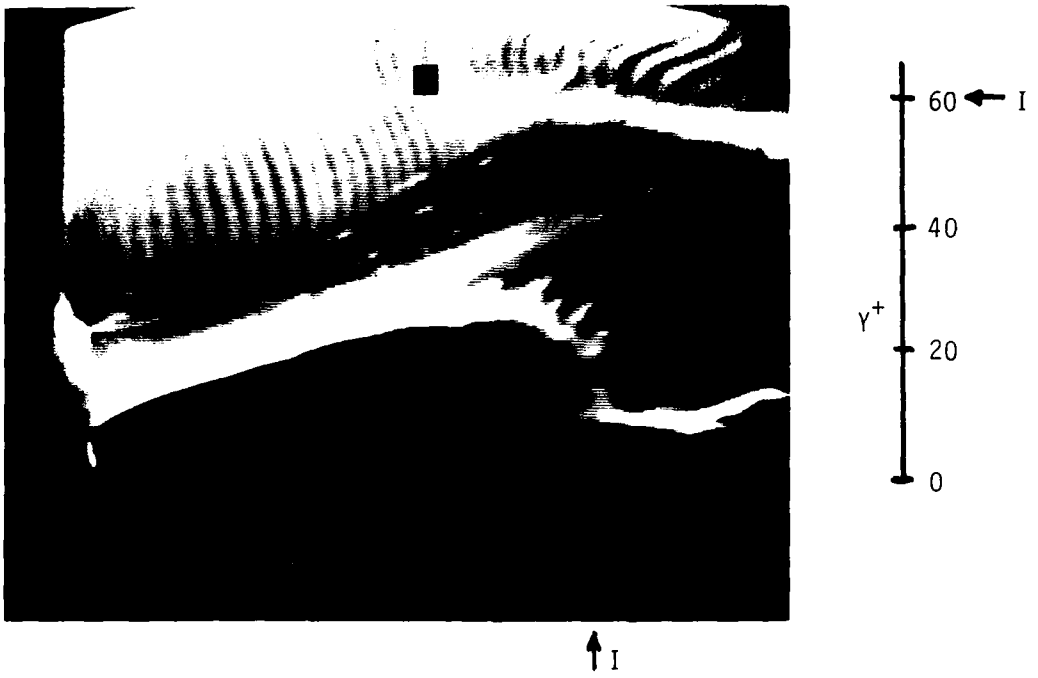

Figure 6c. Side View, $V_{ref} = 0.23\ U_\infty$
$t^+ = 20$

Figure 6d. Side View, $V_{ref} = 0.23\ U_\infty$
$t^+ = 27$

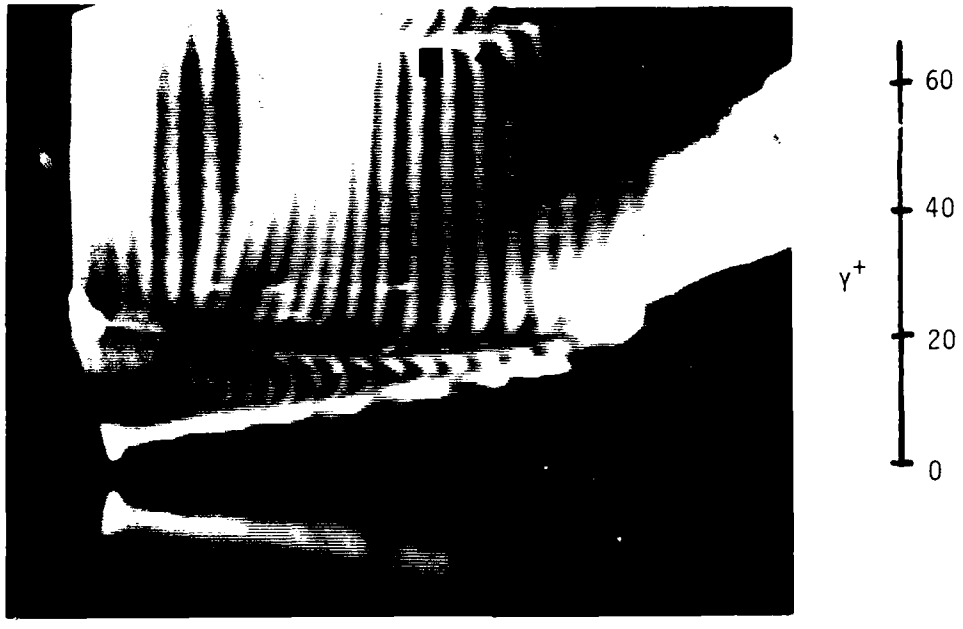

Figure 6e. Side View, $V_{ref} = 0.23\ U_\infty$
$t^+ = 38$

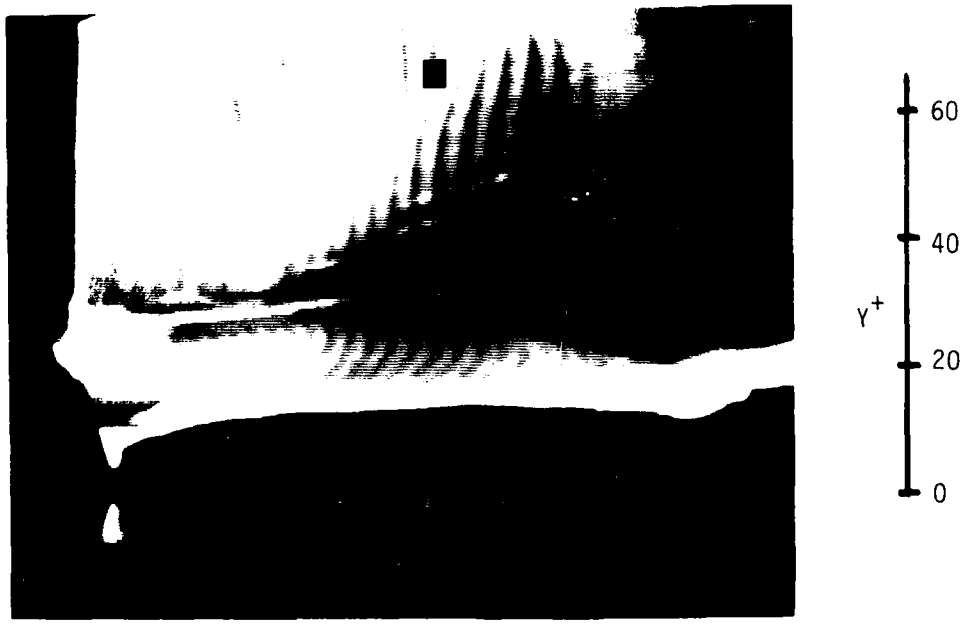

Figure 6f. Side View, $V_{ref} = 0.23\ U_\infty$
$t^+ = 48$

is still ~ 0.47 U_∞. Also, the deflection of the impinging flow is even more substantial.

As the sweep passes through the field of view, the decelerated "hump" is forced forward and away from the wall by the sweep, resulting in its movement away from the wall. Figure 6e at $t^+ = 38$ shows the sweep pushing the tail of the decelerated region out of the field of view. The bright region of bubbles indicated again by the dark arrow marks the leading edge of the sweep. Note that this very sharply defined interface between slower moving fluid and the higher speed fluid is consistent with the observations of both Corino and Brodkey [6] and Nychas et al. [7]. The accelerated flow behind the sweep interface is clearly evidenced by the noticeably wider spacing between the bubble time-lines. In this particular burst sequence, the velocity at $y^+ \cong 40$ varies from about 0.60 U_∞ just prior to the sweep (Figure 6c) to 0.79 U_∞ after the passage of the sweep interface (Figure 6e). These changes in velocity seem consistent with the changes observed during a burst sweep sequence by Nychas et al. [7] and Corino and Brodkey [6]. Figure 6f taken at time $t^+ = 48$ shows the wall layer returning to a somewhat quiescent state, as the higher speed fluid of the sweep has "cleansed" the wall of the slow, decelerated fluid region.

With regard to bursting times, a sequence of video tape of the $y^+ \cong 70$ field of view was examined for the boundary layer region shown in Figures 5 and 6. The sequence was found to contain 77 burst events passing the field of view. The average burst period was $T_b = 4.4$ seconds which yields non-dimensional values of $T_b u^{*2}/\nu \cong 97$ and $TU_\infty/\delta^* \cong 39$, which compare well with previous values measured by Kim et al [4] ($T_b u^{*2}/\nu \cong 94$) using visual techniques and by Rao et al. [19] ($T_b U_\infty/\delta^* \cong 32$) using hot wire anemometer measurements.

One of the difficulties in following a burst from the initial lift-up to ejection into the outer flow is that the burst fluid is continually accelerating during the process. Thus, at a fixed reference speed it is essentially impossible to follow a burst through its entire history unless one resorts to a rather large field of view (y^+ ~ 400 to 500) in which resolution is sacrificed. With a field of view on the order of y^+ ~ 70, one must be content to "capture" as well as possible the different parts of the burst cycle by judicious selection of reference frame velocities. These parts of the cycle can then be used to reconstruct a model of the overall burst process. One of the parts that the present study has been able to observe with some effectiveness is the interaction of the decelerated wall layer fluid with the outer flow.

Figure 7 illustrates one type of motion involving the interaction of wall region fluid with the outer flow. In this figure, the bubble wire is located as indicated, and the reference velocity is 0.54 U_∞ At this reference velocity, bubbles generated by the bubble wire move downstream (right) in the upper part of the figure where the velocity is > 0.54 U_∞ and rearward (left) in the lower portion of the figure where velocities are < 0.54 U_∞. Thus, in this figure activity in both the higher speed outer flow and in the low speed wall region is visualized. The visualized flow pattern indicates that the interaction process creates free-shear layer type vortical structures similar to those

Figure 7. Side View, $V_{ref} = 0.54\ U_\infty$
$Re_\theta \cong 1200$

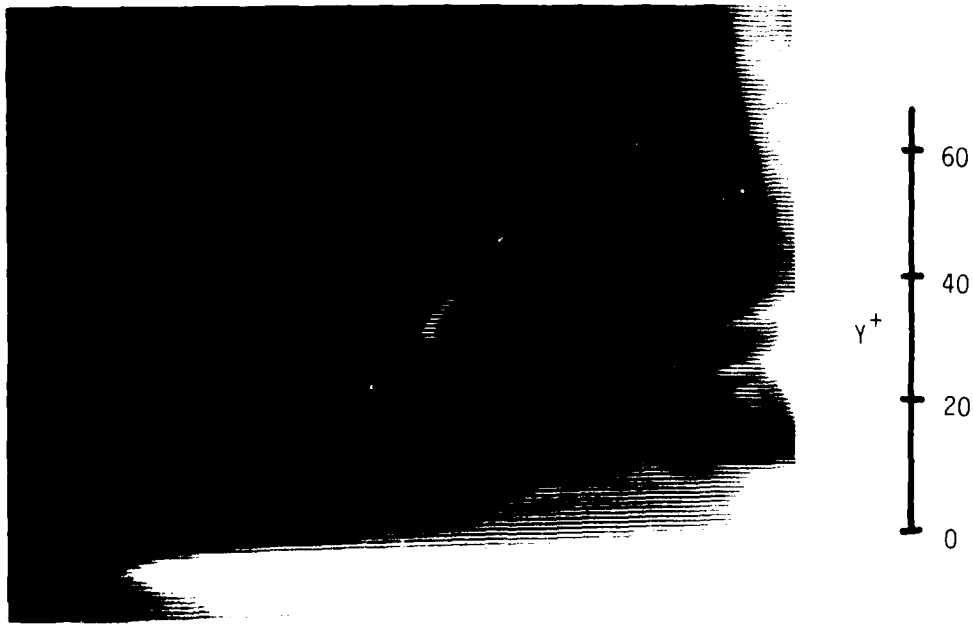

Figure 8. Side View, $V_{ref} = 0.52\ U_\infty$
$Re_\theta \cong 2100$

observed in mixing layers by Brown and Roshko [20], and Winant and Browand [21]. These structures were observed to form as a consequence of the interaction of the lifted, decelerated wall fluid and the accelerated sweep fluid. The appearance of these wave-like, mixing layer structures occurred very rapidly, and once formed, they moved quickly away from the wall and into the sweep fluid where they were quickly stretched and distorted. The basic configuration and behavior of these structures depended on several parameters, such as the size of the decelerated flow region, the relative velocity differences between the decelerated flow and the sweep, and the magnitude of the outer region structure which initiated the burst. Sometimes only one vortical structure would be observed; more frequently, multiple structures would be observed to form (as in Figure 7). There were also a number of times that lifted fluid would appear to pass out of the field of view without forming a structure. Whether this latter behavior eventually resulted in the formation of a vortical structure outside the field of view was unclear.

Figure 8 shows the formation of a wave-like vortical structure very similar to those in Figure 7. This figure is from the higher velocity studies with U_∞ = 27 cm/s and an $Re_\theta \cong 2100$. The bubble wire is located just out of the field of view to the right and the reference velocity is 0.52 U_∞. Under these conditions bubbles appear only in the low velocity wall region which is at a velocity < 0.52 U_∞. The ghostly quality of the figure is a consequence of the higher velocity flow and a very diffuse bubble concentration. Note that the character of this structure is essentially the same as the vortical structures shown in Figure 7 and that it forms at the same approximate y^+ location. Again, after initial formation this vortical structure accelerated away from the wall, and out of the field of view.

In general, all wall region, wave-like vortical structures such as appear in Figure 7 and 8, were observed to form above $y^+ \cong 10$, and generally below $y^+ \cong 40$. This is essentially the region termed the region of generation by Corino and Brodkey [6] in which they observed the maximum interaction to occur between fluid ejections and the outer region fluid. In addition, the amplitude of these wave-like structures ($y^+ \cong 15$ to 20) is of the same approximate size as the finger-like ejections observed by Corino and Brodkey. In contrast to their description of the ejection process, however, it does appear from the present studies that the wave-like formations are the result of a strong interaction at the interface between the decelerated wall region fluid and the high speed sweep fluid.

It would appear that the formation of these wave-like structures is a key mechanism in the entrainment process of the low speed, wall region fluid into the higher speed sweep fluid, and thus is a source of the high Reynolds stress production in the wall region during the bursting process. It is to be clarified that formation of the wave-like structure only occurred after a deceleration and lift-up of wall region fluid had occurred and only when the decelerated region interacted with an outer region sweep. It was necessary for both of these events to occur before the wave-like structures appeared. It is significant that a prescribed sequence of events must take place before the formation of low speed ejections of fluid can take place, because it implies that an interaction

between an outer region structure and the inner wall-region must begin the initial lift-up process leading to the burst, and that the burst does not occur spontaneously.

A particularly significant analytical study showing that an outer region structure can induce a wall region lift-up has been done by Doligalski and Walker [22]. This study shows that the sudden introduction of a convected vortex near a surface will result in the creation of a lifted region of decelerated fluid. The analysis has not been extended to examine the effects of a following sweep on the lifted region, but one can surmise that the result should be similar to the type of vortex roll-ups observed in free-shear flows [20], [21]. Such a roll-up would approximate the wave-like structures observed in the present studies.

In order to examine Doligalski's analysis, a preliminary flow visualization study was done which attempted to introduce a single vortical structure into an otherwise laminar, flat-plate flow. After much trial and error, a reasonably clean, two-dimensional vortex was successfully generated upstream of a flat-plate test section, such that the subsequent interaction with the developing laminar boundary layer could be observed as the vortex was convected over the plate. Although the coordination between the generation of the vortex and the movement of the reference frame to establish optimum visualization of the resultant interaction was very difficult, it was observed that the convected vortex did indeed cause a lift-up type behavior to occur in the wall region upstream of the vortex center. And although the visualization technique employed was not optimum, on several occasions wave-like structures reminiscent of those in Figures 7 and 8 were observed to form. More sophisticated studies of the interaction of a single vortical structure with an otherwise laminar flow are presently being conducted and will be reported in a future paper.

B Plan-View Visualization

A series of plan-view studies of the flow behavior in and near the wall region were done using a horizontal bubble wire 20 cm in length oriented transverse to the flow. The bubble wire was mounted between the supports of the inverted U-shape traversing probe, which allowed the bubble-wire to be traversed relative to the flow at distances as close as 1 mm to the wall. The objective of this study was to examine the behavior of the low-speed streaks which occur adjacent to the wall and their relationship to the flow structures which were observed in the side-view visualizations. Both stationary and convected reference frame studies for $8 < y^+ < 50$ were carried out for $Re_\theta \cong 1200$ and $Re_\theta \cong 2100$. Only pictures at $Re_\theta \cong 1200$ are presented in this paper.

Figure 9 is a typical plan-view sequence in a stationary reference frame showing wall-region behavior at $y^+ = 8$. In all figures the flow is left to right, as is all relative reference frame motion. Although slightly blurred due to relative motion effects, the characteristic low-speed streaks as observed and studied by Runstadler et al. [3] are clearly evident. The streak spacing determined by visual counting and averaging of streaks was determined as $\lambda^+ = \lambda u^*/\nu = 107$, slightly higher

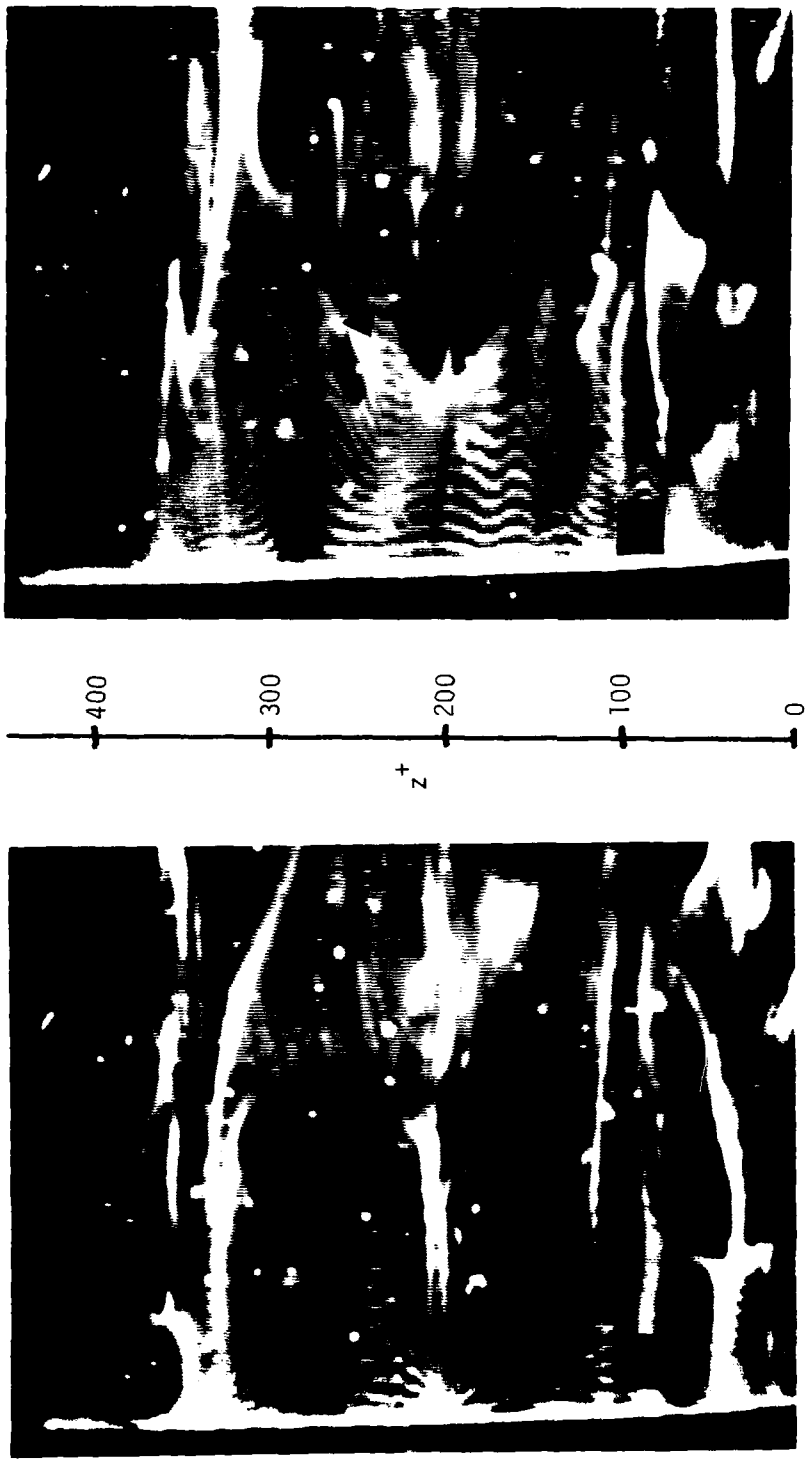

Figure 9a. Plan View, Stationary Reference
$y^+ = 8$ $t^+ = 0$

Figure 9b. Plan View, Stationary Reference
$y^+ = 8$ $t^+ = 10$

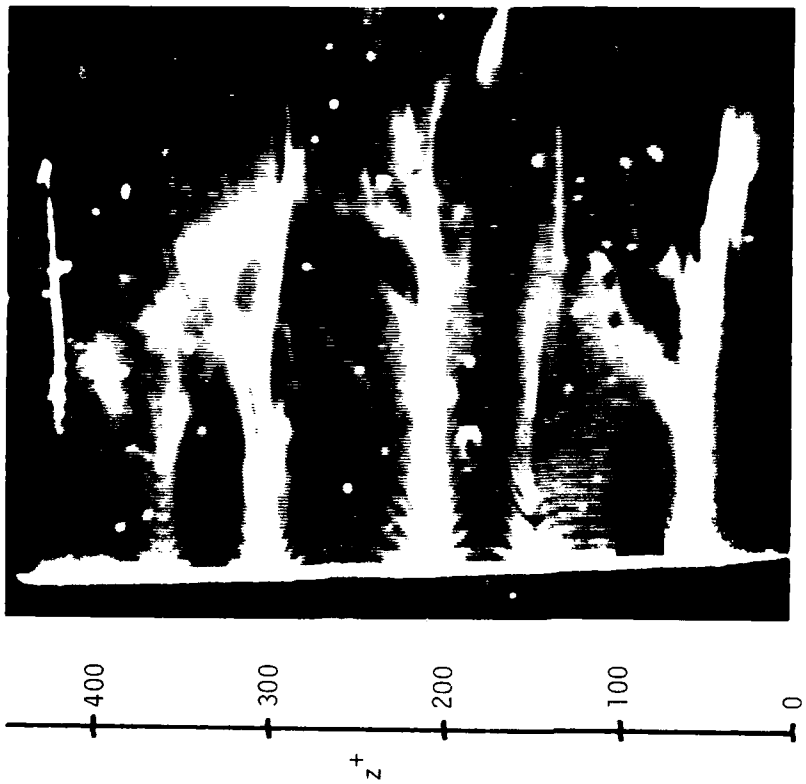

Figure 9c. Plan View, Stationary Reference
$y^+ = 8$ $t^+ = 20$

Figure 9d. Plan View, Stationary Reference
$y^+ = 8$ $t^+ = 30$

than the generally accepted $\lambda^+ \cong 100$. Note that the field of view in these studies ($z^+ \approx 400$) was kept small relative to the streak spacing in order that close study could be done of the origin and termination of individual streak structures. It was hoped that by this more detailed study of individual streaks a better understanding could be gained of 1) the counter-rotating, longitudinal vortices which cause the streak formation and 2) the role one streak structure plays in the formation of subsequent streaks.

The important feature to notice in figure 9 is the low-speed streak located at $z^+ \approx 200$ (indicated by the arrow on the photograph) in figure 9a and the subsequent process of streak termination and re-formation illustrated sequentially in Figures 9b, 9c, and 9d. Figure 9a shows the streak just prior to termination. Notice that the tail of the streak (nearest to the wire) has taken on a less concentrated appearance than the remainder of the streak. This was generally noted as a precursor to streak lift-up. In Figure 9b, the lift-up of the streak has resulted in the formation of a concave forward "front" of bubbles (indicated by the arrow) which appears to sweep across the streak and eliminate it. This sweeping motion always appeared as a sharply defined high-speed front which was usually preceded by a clear, bubble-free region. The formation of this clear region was observed visually to be the result of an influx of outer region fluid toward the wall. A second point to note are the slightly kinked regions that appear to trail back upstream from either side of the front. As the front passed through and eliminated the initial streak, these kinked regions were observed to concentrate the bubbles and to move laterally together. Repeated observations indicated that these kinked regions were the result of longitudinal vortices trailing back from the front. These vortices are observed to rotate counter to each other as indicated below.

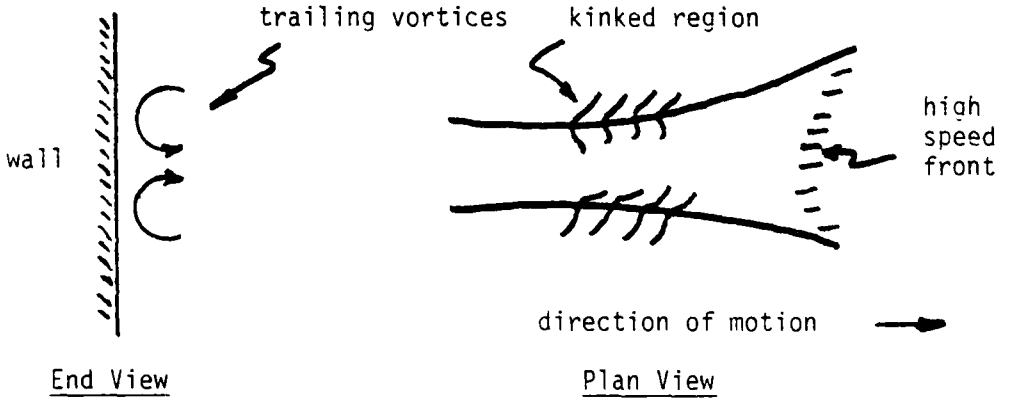

Note that these counter-rotating longitudinal vortices are essentially the "legs" of the lifted vortex-loop model of a burst proposed by Offen and Kline [5]. However, the legs of the vortex are not nearly as laterally separated as indicated by Offen. Due to their counter-rotation, these longitudinal vortices move together, concentrating low speed fluid between themselves into the observed streak. This presence of longitudinal, counter-rotating vortices has been established [illegible]

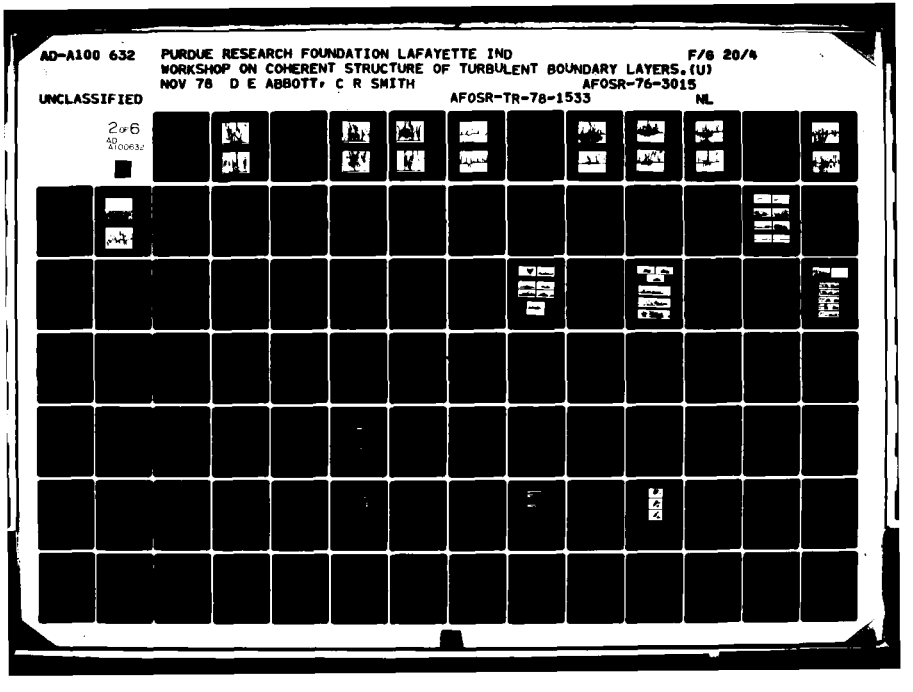
AD-A100 632
PURDUE RESEARCH FOUNDATION LAFAYETTE IND
F/G 20/4
WORKSHOP ON COHERENT STRUCTURE OF TURBULENT BOUNDARY LAYERS.(U)
NOV 78 D E ABBOTT, C R SMITH
AFOSR-76-3015
UNCLASSIFIED
AFOSR-TR-78-1533
NL
2 of 6
AD
A100632

contours of pressure and spanwise velocity by Tu and Willmarth [23], their measurements indicating that these vortices form a critical part of general sweptback disturbance patterns near the wall. Willmarth [24] also points out that mutual induction effects should cause these counter-rotating vortices to move both together and out away from the wall. He speculates that this mutual induction, in conjunction with stretching effects due to the strong velocity gradients near the wall may strongly contribute to the bursting phenomena.

The beginning of a new streak due to this lateral convergence of the counter-rotating vortices is apparent in Figures 9c and 9d. Figure 9c shows a wide, low-speed streak which has formed in essentially the same transverse location as the original streak (indicated again by the arrow). If one looks closely near the head of the forming streak (to the right), the clear region associated with the high-speed front can be seen. Spread out laterally from this clear region are two thin, bright regions of bubble concentrations which appear to be a spreading of the longitudinal vortices near the high-speed front (the ends of these bright regions appear at $z^+ \sim 180$ and 250). Figure 9d shows that the streak has subsequently become more concentrated, which is speculated to be the result of stretching and intensification of the longitudinal vortices, causing them to draw closer together.

The question arises as to what is the high-speed front which precipitates the termination of a streak? If one calculates the convection velocity of these fronts at $y^+ \tilde{=} 8$, the fronts are found to move at velocities from 0.37 U_∞ to 0.44 U_∞. This is essentially comparable to the convection velocities of the decelerated fluid lift-up shown in side view in Figure 6. Thus, the front observed in plan view would appear to be related to the decelerated fluid lift-up. Note that bright, concentrated high speed fronts are also observed further out from the wall, often up to $y^+ \simeq 50$. Figures 10 and 11 illustrate the appearance of high-speed fronts as they appear at $y^+ = 19$ and $y^+ = 35$. Although varying in shape from convex to concave downstream, these fronts were almost always observed as the terminating structure of a low-speed streak. Note that the further the bubble-sheet is from the wall, the faster the high-speed fronts are observed to move. In addition, the fronts are observed to continually accelerate, regardless of the distance of the bubble-sheet from the wall. As an example, the front in Figure 10 accelerated from 0.56 U_∞ to 0.75 U_∞ over a $\Delta x^+ \tilde{=} 180$, and the front in Figure 11 accelerated from 0.70 U_∞ to 0.91 U_∞ over a $\Delta x^+ \tilde{=} 280$.

A striking similarity exists between the present high speed fronts and the warped wave fronts observed in transition studies by Hama and Nutant [25]. Hama and Nutant, using fixed bubble-wires oriented both vertically and horizontally transverse, established that the appearance of a front-like region of bubble concentration in plan-view was coincident with the formation of a strong inflectional profile and subsequent breakdown into discrete vortices in side-view. The implication is that the high-speed fronts observed in the plan-view pictures of the present study most probably represent the formation of the inflectional profiles and subsequent transverse vortical motions as observed in the side-view visualizations of the present study. Hama and Nutant went on to show that their transition wave fronts warped into horseshoe-shaped vortices

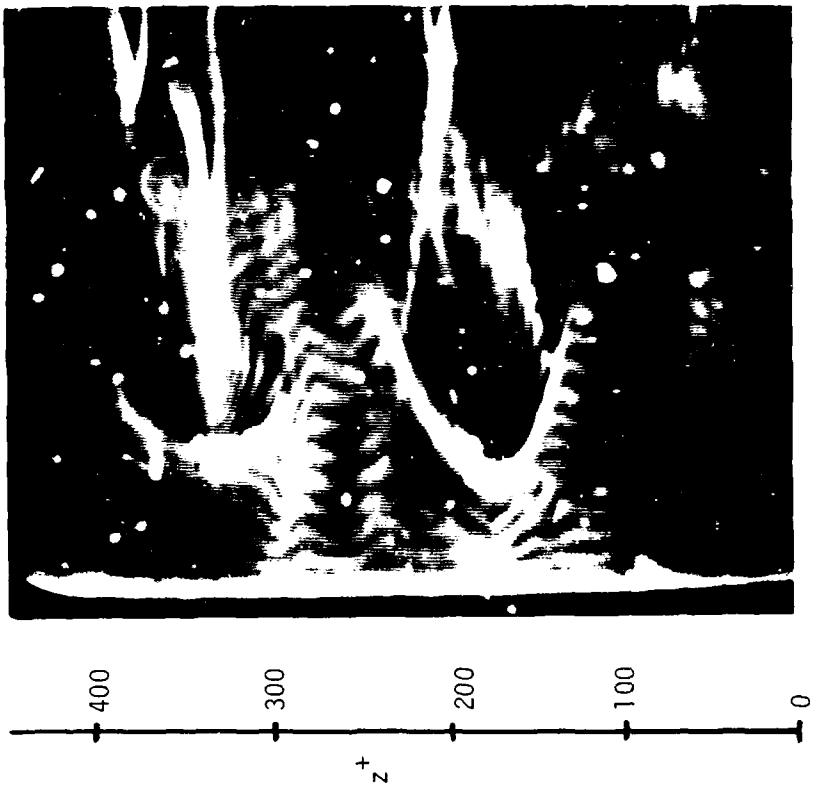

Figure 11. Plan View, Stationary Reference $y^+ = 35$

Figure 10. Plan View, Stationary Reference $y^+ = 19$

similar to the lifted vortex-loop model of Runstadler et al. And similar to the Runstadler model, Hama and Nutant observed the leading edge of this horseshoe vortex to be "snatched" up from the surface, migrating into the higher velocity region of the boundary layer. In difference with the lifted loop-vortex model, Hama observed the legs of his warped wave-front vortex to move together laterally in a "necking" fashion, which appears consistent with the behavior of the counter-rotating longitudinal vortices observed in the present study. That the rapid lifting of the leading edge of the vortex loop and the necking of the trailing legs can be a consequence of the dynamics of a stretched vortex-loop has been shown theoretically by Hama, and more recently by Danberg [26].

It would appear that the high-speed fronts observed in this study are the result of the breakdown of a lifted low-speed streak into a horseshoe-shaped vortical structure whose leading edge (which appears transverse) lifts away from the wall and whose legs appear to trail behind in the low speed wall region, causing the formation of a subsequent low-speed streak. If the concept of an ejected vortex loop is valid, the effects of the presence of the counter rotating legs should be observable as they are stretched up away from the wall. Figure 12 is a stationary sequence of four pictures at $y^+ = 35$ which shows the termination and re-establishment of a low-speed streak further from the wall. The original streak is indicated at $z^+ \cong 100$ in Figure 12a by the dark arrow on the picture. In figure 12b a high speed front has entered the flow field, terminating the previous streak and creating the typical concave region of unmarked fluid. The legs of the loop (the head of which is assumed to be the high-speed front) appear as the kinked regions to the sides of the front. Just as the front passes out of the field of view, the longitudinally rotating legs appear as the two converging elongated regions at the bottom of Figure 12c. In this picture the lateral "necking" of the legs to form a subsequent streak is clear. Finally, the resulting streak formed as a consequence of the longitudinal legs appears at a $z^+ \cong 80$, or very close to the z^+ location of the previous streak.

One of the difficulties in ascertaining the presence of a lifted vortex-loop with counter-rotating legs is that vorticity can only be visualized indirectly. And the presence of a vortex loop of weak or moderate vorticity may only appear as a small disturbance or flow irregularity when convected in a strong mean flow and viewed from a laboratory reference frame. Thus, the removal of the mean flow effects by relative movement of both the visualization medium and the observation reference will accentuate the presence of convected vorticity effects.

Figure 13 is a plan-view sequence taken with the bubble-wire at $y^+ = 26$ and a relative reference velocity of $0.58\ U_\infty$. Note the strongly retarded region indicated by the arrow in Figure 13a. This is a low-speed region of essentially clear fluid indicating that it most likely originated either from below or in front of the bubble wire. Upon close examination two axially rotating strands of bubbles can be seen to either side of the retarded area, which would appear to be evidence of a streamwise vortex pair. In the subsequent Figure 13b, the axis of rotation of this vortex pair has been shifted from streamwise to a direction almost normal to the wall, thus appearing as double Cochela type vortex-pair

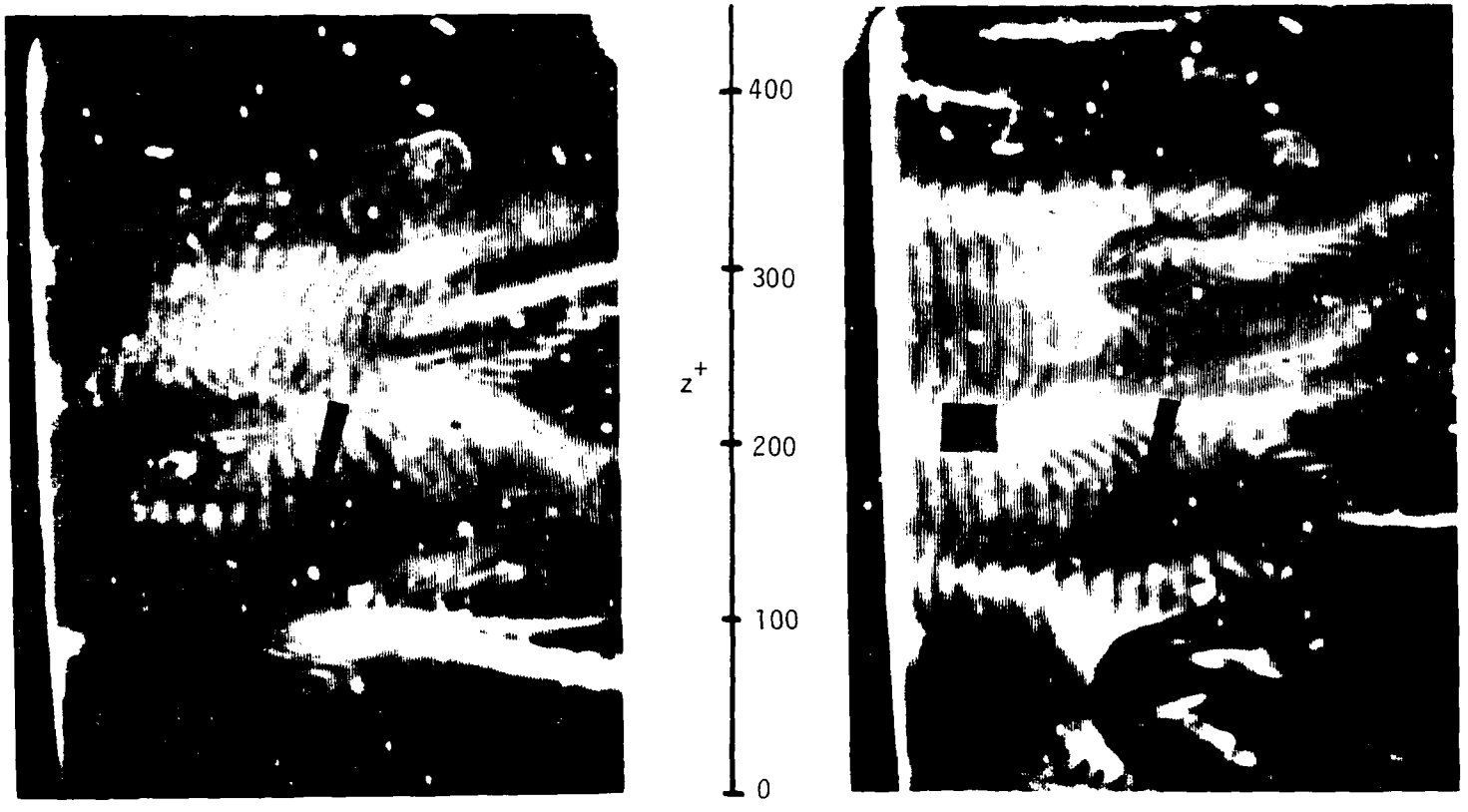

Figure 12a. Plan View, Stationary Reference
$y^+ = 35$ $t^+ = 0$

Figure 12b. Plan View, Stationary Reference
$y^+ = 35$ $t^+ = 10$

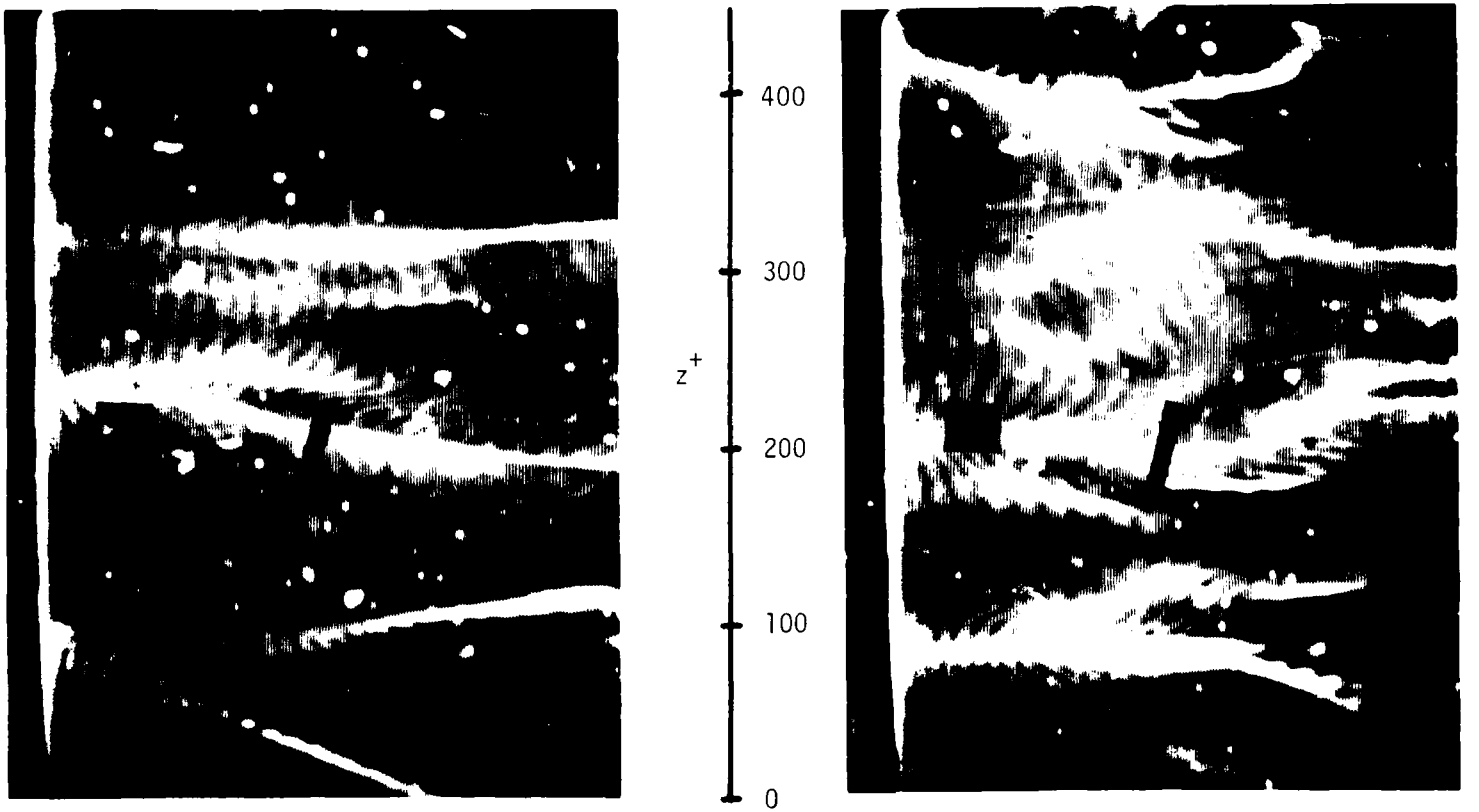

Figure 12c. Plan View, Stationary Reference
$y^+ = 35$ $t^+ = 20$

Figure 12d. Plan View, Stationary Reference
$y^+ = 35$ $t^+ = 30$

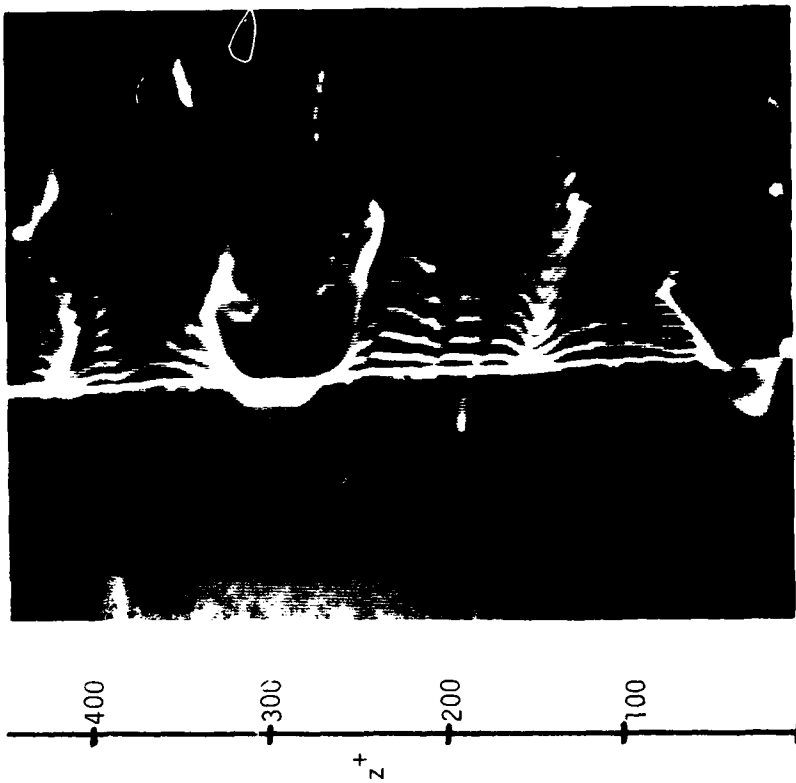

Figure 13b. Plan View, $V_{ref} = 0.58\ U_\infty$
$y^+ = 26$ $t^+ = 15$

Figure 13a. Plan View, $V_{ref} = 0.58\ U_\infty$
$y^+ = 26$ $t^+ = 0$

reminiscent of Falco's mushroom-shape typical eddies. The reason for the dramatic shift in axes is probably a result of the lifting of the leading edge of a loop vortex away from the wall region, thus re-orienting a portion of the counter-rotating legs into an axis more normal to the wall (and the bubble sheet). A simple sketch of this process is shown below.

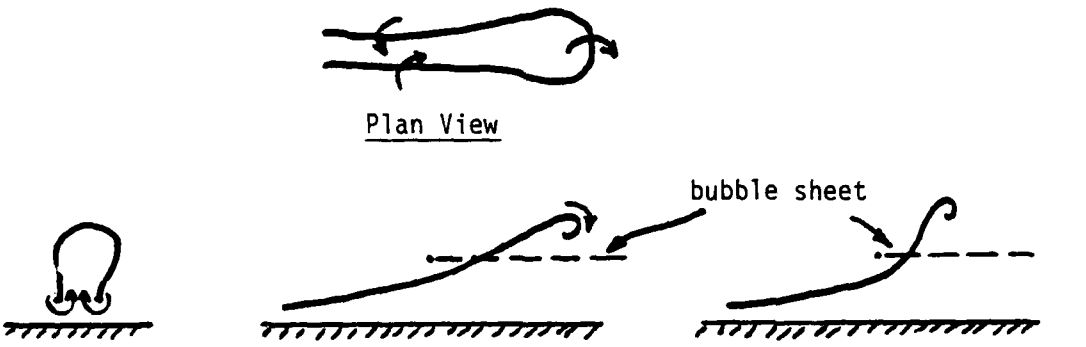

Figures 14 and 15 show further evidence of the presence of paired counter-rotating vortices out to a $y^+ = 47$. These pictures, which were again obtained at a relative velocity of 0.58 U_∞, illustrate both the *double Cochlea configuration* (Figure 14) and streamwise counter-rotating pairs (Figure 15). The double Cochlea configuration is less distinct than Figure 13b, first as a result of a decreased velocity gradient (and thus reduced local vortex stretching), and secondly because the relative reference velocity was less than the convection velocity of the vortex pair, which tends to degrade the visualization of vorticity effects. Figure 15 clearly illustrates what appear to be several longitudinal pairs of counter-rotating vortices. Although a lack of depth perception makes it difficult to discern the sense of rotation of the vortices (the video tapes show that the sense is consistent with the counter-rotations illustrated in the previous sketch above), it appears that the longitudinal structures are vortex pairs of large diameter and relatively slow rotation. The reason for the larger diameters and slower rotations than are encountered near the wall is again due to a reduced local velocity gradient and thus reduced vortex stretching.

The use of relative reference frame motion can be employed to accentuate other physical characteristics of low-speed streak behavior. Figure 16 is a sequence of four stages of a streak development with the bubble-wire at $y^+ = 11$ and reference frame velocity of 0.36 U_∞. Figure 16a shows a high-speed front passing through the field of view at a $z^+ \approx 275$. Note that as a result of the relative reference frame motion the trailing vortices are much more apparent, their effect being to concentrate the bubbles into two bright strands with a spacing of $\Delta z^+ \approx 50$. In Figure 16b, the legs trailing the front have moved closer together, to a $\Delta z^+ \approx 25$, and in Figure 16c at $t^+ = 50$ the legs appear to have merged yielding a total spanwise width of $\Delta z^+ \approx 20$. At this point, the combined vortex pair begins to move upward out of the plane of the bubble sheet, and in the process slower momentum fluid is concentrated

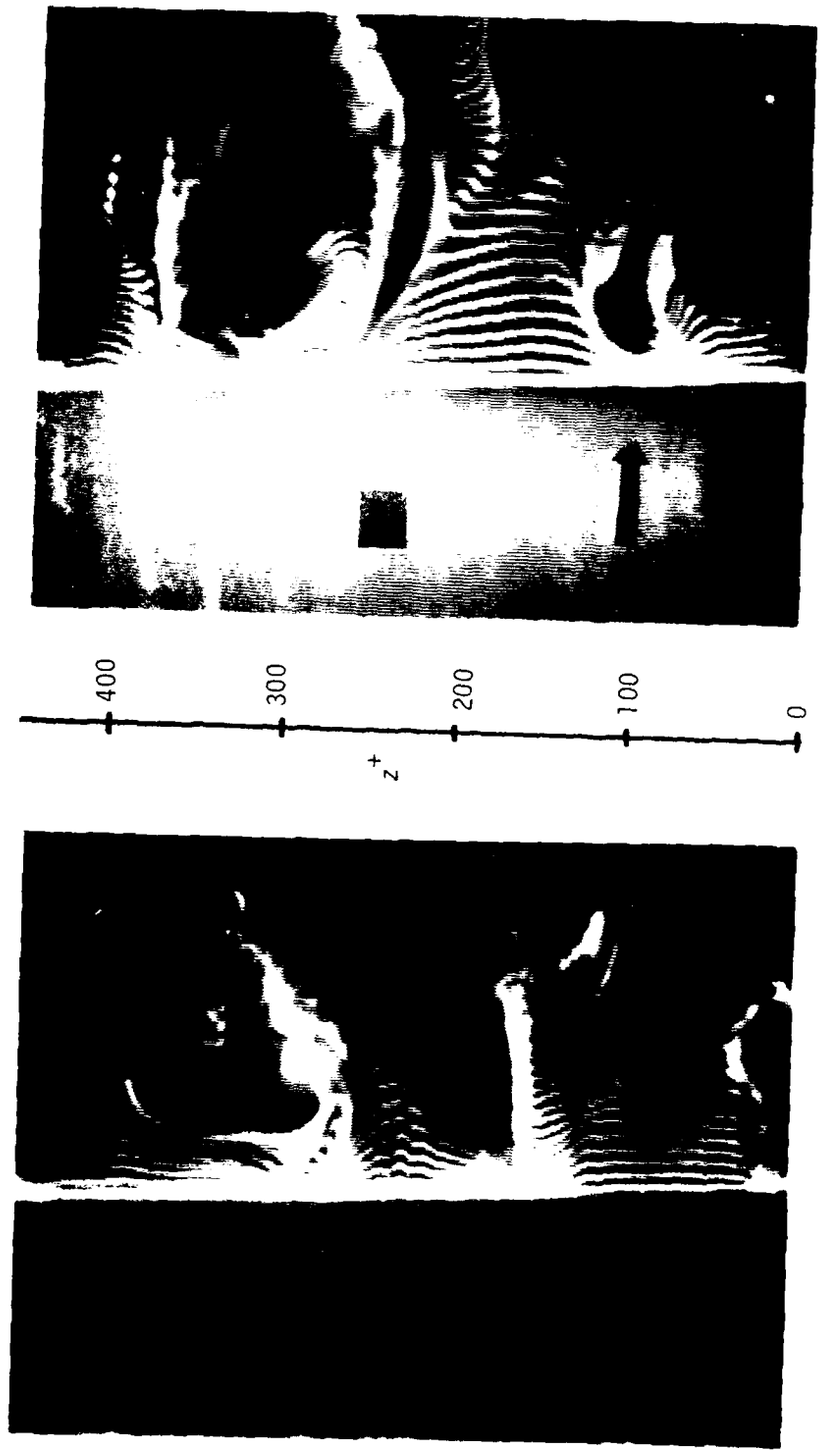

Figure 14. Plan View, $V_{ref} = 0.58\ U_\infty$
$y^+ = 47$

Figure 15. Plan View, $V_{ref} = 0.58\ U_\infty$
$y^+ = 47$

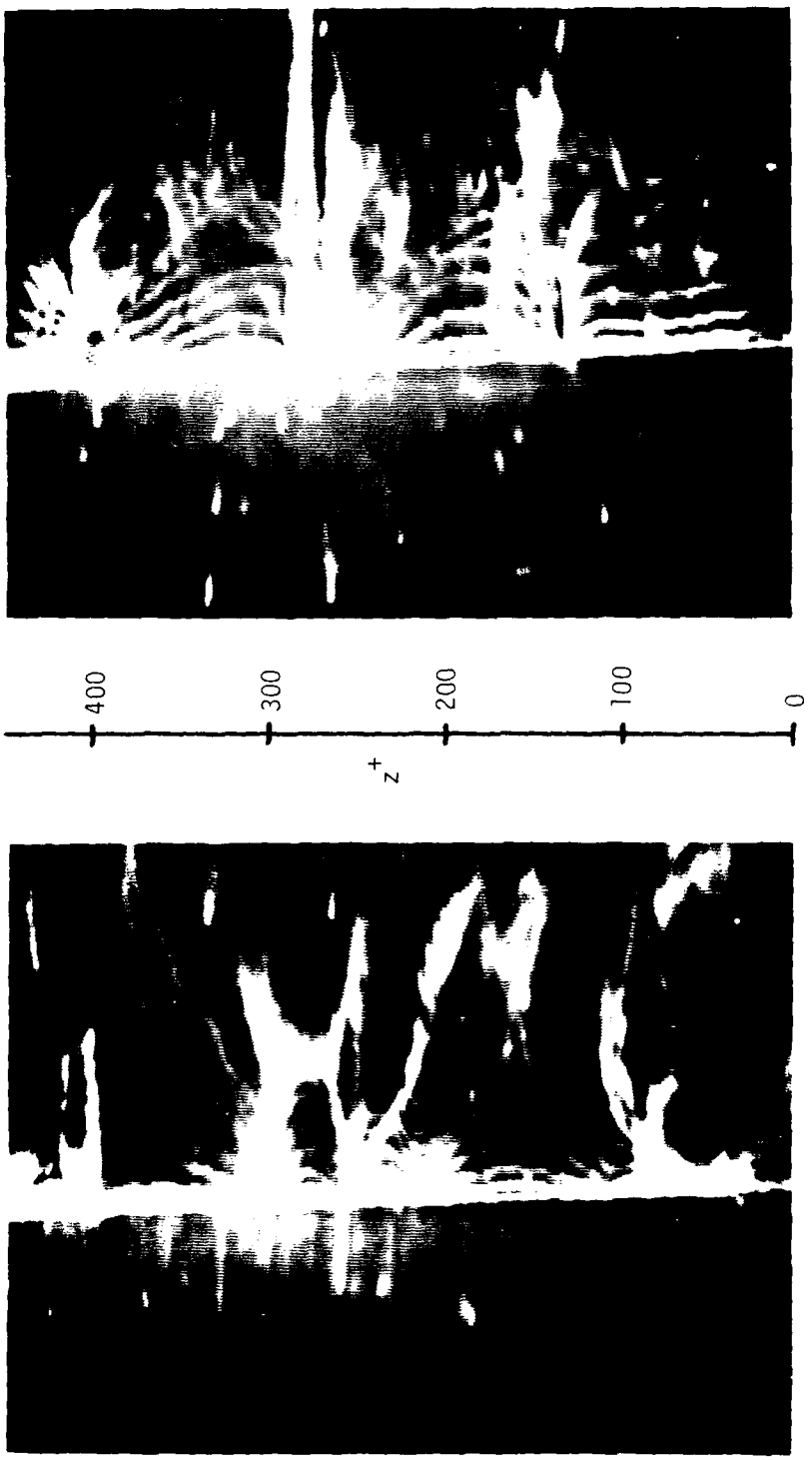

Figure 16b. Plan View, $V_{ref} = 0.36\ U_\infty$
$y^+ = 11$ $t^+ = 30$

Figure 16a. Plan View, $V_{ref} = 0.36\ U_\infty$
$y^+ = 11$ $t^+ = 0$

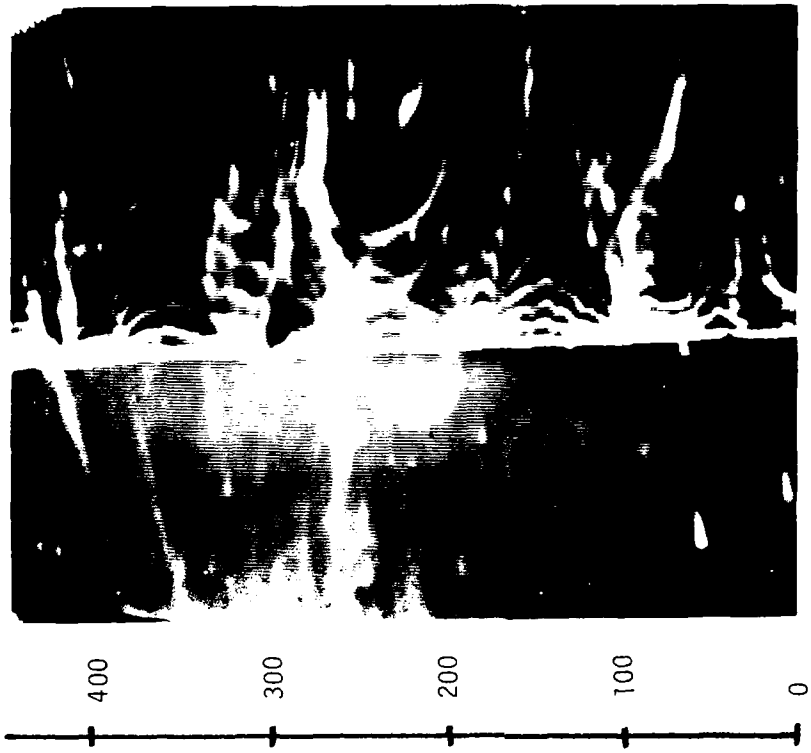

Figure 16d. Plan View, $V_{ref.} = 0.36\ U_\infty$
$y^+ = 11$ $t^+ = 70$

Figure 16c. Plan View, $V_{ref.} = 0.36\ U_\infty$
$t^+ = 11$ $t^+ = 50$

beneath it. The presence of this lower momentum fluid can be seen in 16d as a thin "tail" trailing behind (left) of the bubble wire. This tail consists of very low velocity fluid ($\sim 0.10\ U_\infty$) which has moved downward from the bubble sheet and been concentrated almost on the wall by the counter-rotating vortex pair. Note that due to lifting effects, the streak which was so apparent in Figure 16c has moved up away from the surface, interacted with the outer region, and another high-speed front has begun to form just ahead of the bubble-wire.

The trailing "tails" of lower velocity fluid appear to be the product of the concentrating effects of the counter-rotating vortex pair, and are observed any time the bubble wire convects faster than the local velocity. One must be careful in interpreting the behavior of these tails because the vertical lifting motion of the streaks becomes a dominant characteristic when the reference velocity is at or near that of the local mean flow. Thus, strong distortions of the streak behavior in the 2-D plan-view can be the result of movement of the streaks out of the plane of the bubble-sheet. Figures 17 and 18, obtained for a reference frame velocity of $0.46\ U_\infty$ at $y^+ \approx 11$, illustrate the above situation. In Figure 17, two relatively bright "tails" appear at $z^+ \simeq 100$ and 275. These both represent regions of low speed fluid which have grown outward from the wall and are penetrating beyond $y^+ \approx 11$. Note that the growth of this fluid has a rather pronounced streamwise extent, as evidenced by the elongated dark region directly in front of the bubble wire at $z^+ \approx 100$. These tails will, however, suddenly stop their rearward movement, stagnate and suddenly move forward, which is a result of the lifting and interaction of the streak with the outer flow. This lifting of the bright "tails" is illustrated in Figure 18 for two streaks at a $z^+ \approx 60$ and 200. A second less obvious "tail" which appears in these two figures is diffuse and much longer, normally appearing below the brighter tails. Two of these diffuse tails appear at $z^+ \approx 325$ and 400 in Figure 18. These tails are regions of very low speed momentum which occur right down on the wall. The bubbles which visualize these tails are fed down to the wall by the counter-rotating vortices which initially form the low-speed streak. This process of "tail" formation is sketched below.

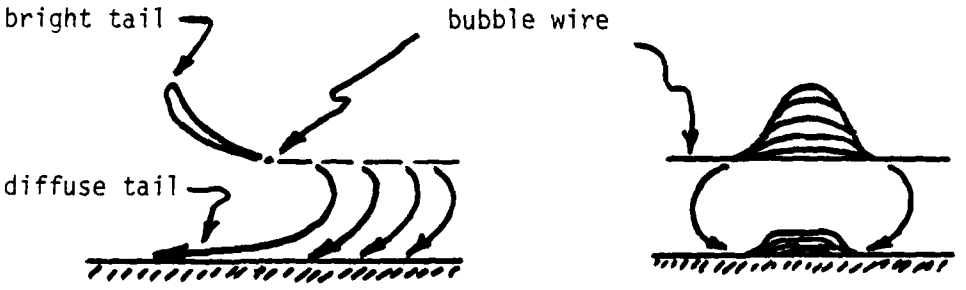

Side View End View

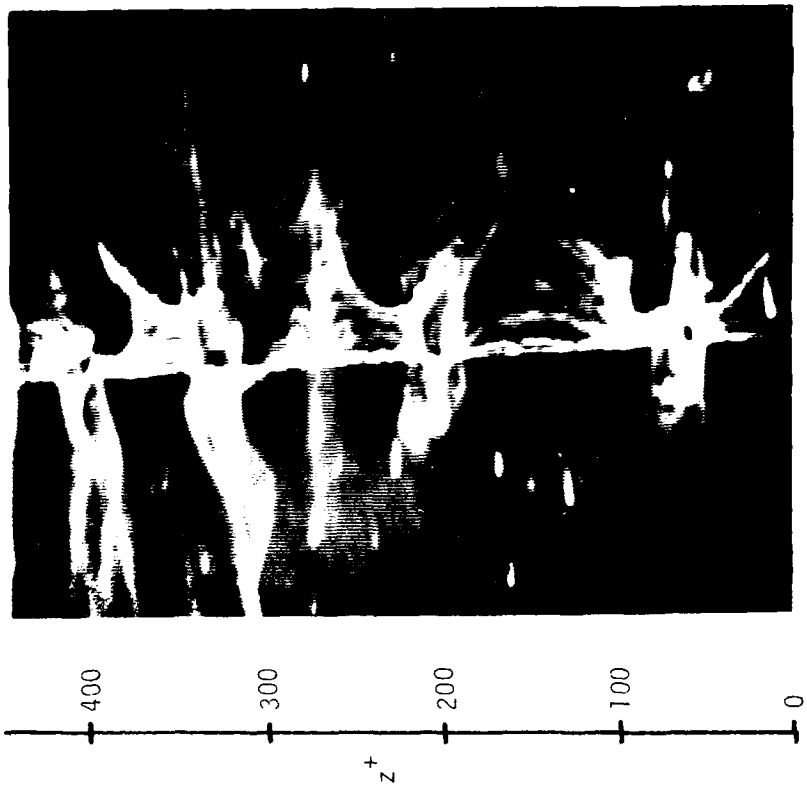

Figure 17. Plan View, $V_{ref} = 0.46\ U_{\infty}$
$y^+ = 11$

Figure 18. Plan View, $V_{ref} = 0.46\ U_{\infty}$
$y^+ = 11$

The final two plan-view figures, 19 and 20, illustrate the appearance of the wall region at $y^+ = 11$ for reference velocities of 0.57 U_∞ and 0.77 U_∞ respectively. In figure 19, the almost regular spanwise spacing of low-speed and high-speed velocity regions is quite apparent. At this reference speed the wire was moving slightly faster than the local mean velocity at $y^+ = 11$, which allowed one to observe spanwise changes in streamwise velocity. What is observed on the video tape is a strong lateral shifting and merging of the high-speed/low-speed pattern, accompanied by periodic breakdown and re-formation of the low-speed regions. A definite low-speed/high-speed pattern was always in evidence near the wall, but these regions were observed to move back and forth laterally, creating a sort of slow waving motion within the velocity pattern, similar to the "wavy " motion of streaks reported by Runstadler et al. [3]. In addition, low-speed regions were observed to frequently move together and apparently merge into a larger low-speed region. During this merging process, the high-speed region caught between the two merging low-speed regions was observed to diminish steadily and disappear as merging took place. After a low-speed region had grown to a substantial width, with or without merging, it was observed to accelerate rapidly in the downstream direction and "wash-out" of the field of view. When this wash-out occurred, an acceleration and growth of the high-speed regions in the vicinity of the wash-out would often take place and a low-speed region would reform near the location of the previous low-speed region. It appeared that either the residual of the previous low-speed region formed the nucleus for development of a subsequent low-speed region, or the established spanwise distribution of longitudinal vorticity may induce the re-formation of a low-speed region.

Figure 20 illustrates the appearance of the streak behavior with the reference moving faster than even the high-speed regions of the flow. Note that a spanwise streak pattern is clearly visible, but at this reference speed the streaks observed are high-speed streaks. The explanation for these high-speed streaks must be that they are formed by the concentration of high-speed fluid by two adjacent pairs of counter-rotating vortices as shown in the sketch below.

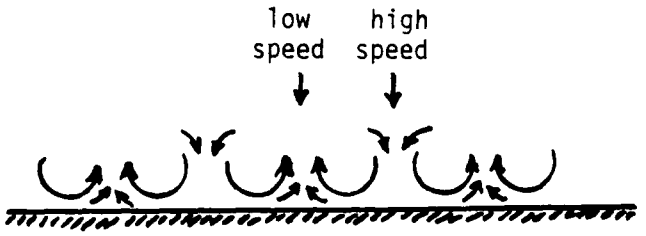

Thus, the inducement of flow toward the wall by the adjacent legs of two counter-rotating vortex pairs would appear as the high-speed streaks illustrated in Figure 20.

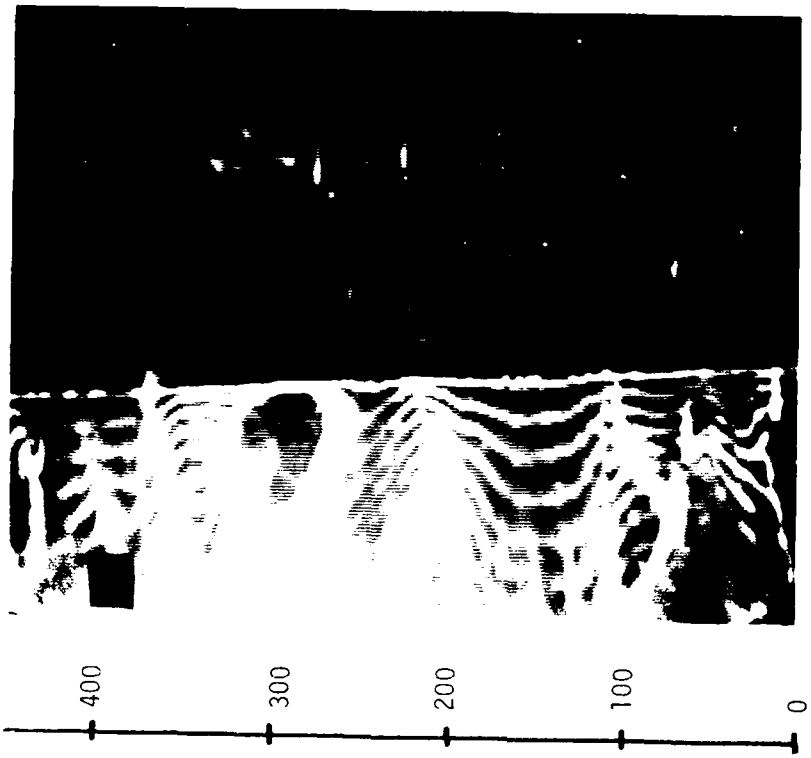

Figure 20. Plan View, $V_{ref} = 0.77\ U_\infty$
$y^+ = 11$

Figure 19. Plan View, $V_{ref} = 0.57\ U_\infty$
$y^+ = 11$

SUMMARY

The present moving reference frame flow visualization system has been shown to be useful in examining both the physical and temporal characteristics of turbulent boundary layer structure. The present results have shown essential consistency with previous flow visualization and sensor studies,as well as extending the understanding of certain aspects of turbulent structure.

The present studies have confirmed the presence of a large scale motion which tends to dominate the appearance of the outer region of the boundary layer. This LSM has been observed to be an agglomeration of numerous smaller scale structures, many vortical in appearance, which are in various stages of coalescence, interaction and decay. The interaction of the LSM with irrotational outer region fluid has been observed to be intimately connected with the formation of Falco's typical eddy structures, which appear to be a consequence of the entrainment process.

Detailed observation of the inner wall-region indicates that outer region structure plays a significant part in causing low-speed fluid lift-up, thus initiating the first phase of the "bursting" sequence. This lifted, low-speed fluid is observed to interact quite strongly, with higher speed "sweep" fluid which results in the formation of a vortical roll-up quite similar to that observed in free-shear layer studies. One result of this interaction appears to be the formation near the wall of a small loop-type vortex very elongated in the flow direction. The visual data suggests that the formation of this loop vortex supplies the mechanism for concentration of low momentum fluid near the wall, thus initiating the formation (or re-formation) of a subsequent low-speed streak.

Note that the present paper has presented initial observations and interpretations of those observations; these should not be misconstrued as a "model" of turbulent boundary layer structure. More detailed studies are necessary, both visualization and sensor studies, in order to confirm and clarify the observed structural characteristics before an overall model of the turbulent structure can be firmly established.

ACKNOWLEDGMENTS

I gratefully acknowledge the assistance of Stuart Huston, Jeffrey Brown, Mark Rothrock, and Daniel Oren, who contributed to both the overall construction of the experimental system and to the acquisition of the video data.

I am also deeply appreciative of the support of this research by the Air Force Office of Scientific Research under contract number F4460-76-C-0099.

REFERENCES

1. Tollmien, W., Turbulente Strömungen. Handbuch der Experimentalphysik, Vol. 4, Pt. I, 1931, p. 291.

2. Schraub, F. A., and S.J. Kline, "Study of the Structure of the Turbulent Boundary Layer with and without Longitudinal Pressure Gradients", Report MD-12, Thermosciences Div., Mech. Engrg. Dept., Stanford University, 1965.

3. Runstadler, P.W., S.J. Kline, and W.C. Reynolds, "An Experimental Investigation of the Flow Structure of the Turbulent Boundary Layer", Report MD-8, Thermosciences Div., Mech, Engrg. Dept., Stanford University, 1963.

4. Kim, H.T., Kline, S.J., and Reynolds, W.C., "The Production of Turbulence Near a Smooth Wall in a Turbulent Boundary Layer", Journal of Fluid Mechanics, Vol. 50, 1973.

5. Offen, G.R., and S.J. Kline, "Experiments on the Velocity Characteristics of 'Bursts' and on the Interactions between the Inner and Outer Regions of a Turbulent Boundary Layer", Report MD-31, Thermosciences Div., Mech. Engrg. Dept., Stanford University, 1973.

6. Corino, E.R., and R.S. Brodkey, "A Visual Investigation of the Wall Region in Turbulent Flow", Journal of Fluid Mechanics, Vol. 37, 1969.

7. Nychas, S.G., H.C. Hershey, and R.S. Brodkey, "A Visual Study of Turbulent Shear Flow", Journal of Fluid Mechanics, Vol. 61, 1973.

8. Kovasznay, L.S.G., V. Kibbens, and R.F.Blackwelder, "Large Scale Motion in the Intermittent Region of a Turbulent Boundary Layer", Journal of Fluid Mechanics, Vol. 41, 1970.

9. Willmarth, W.W., and C.E. Wooldridge, "Measurements of the Fluctuating Pressure at the Wall Beneath a Thick Turbulent Boundary Layer", Journal of Fluid Mechanics, Vol. 14, 1962.

10. Blackwelder, R.F., and L.S.G. Kovasznay, "Time Scales and Correlations in a Turbulent Boundary Layer", Physics of Fluids, Vol. 15, No. 9, 1972.

11. Falco, R.E., "Some Comments on Turbulent Boundary Layer Structure Inferred From the Motions of a Passive Contaminant", A.I.A.A. Paper No. 74-99, 1974 (12th A.I.A.A. Aerospace Conf.).

12. Willmarth, W.W., "Structure of Turbulent Boundary Layers," Advances in Applied Mechanics, Vol. 15, C.S.Yih, ed. Academic Press, 1975.

13. Eckelmann, H., "The Structure of the Viscous Sublayer and the Adjacent Wall Region in a Turbulent Channel Flow", Journal of Fluid Mechanics, Vol. 65, 1974.

14. Schraub, F.A., S.J.Kline, J.Henry, P.W. Runstadler, and A. Litell, "Use of Hydrogen Bubbles for Quantitative Determination of Time Dependent Velocity Fields in Low Speed Water Flows", Report MD-10, Thermosciences Div., Mech. Engrg. Dept., Stanford University, 1964.

15. White, F.M., Viscous Fluid Flow, McGraw-Hill, 1974.

16. Falco, R.E., "Coherent Motions in the Outer Region of Turbulent Boundary Layers", The Physics of Fluids, Vol. 20, No. 10, Pt. II, Oct. 1977.

17. Thomas, A.S.W., and Brown, G.L., "Large Structure in a Turbulent Boundary Layer", Proceedings of the 6th Australasian Hydraulics and Fluid Mechanics Conference, Adelaide, Australia, December 1977.

18. Emmerling, P., Meier, G.E., and Dinkelacker, A., "The Instantaneous Structure of the Wall Pressure Under a Turbulent Boundary Layer Flow", AGARD Conf. Noise Mech., Preprint No. 131, 1973.

19. Rao, K.N., Narisimha, R., and Badri Narayanan, M.A.,"The Bursting Phenomenon in a Turbulent Boundary Layer," Journal of Fluid Mechanics, Vol. 48, 1971.

20. Brown, G.L. and Roshko, A., "On Density Effects and Large Scale Structure in Turbulent Mixing Layers", Journal of Fluid Mechanics, Vol. 64, 1971.

21. Winant, C.D. and Browand, F.K., "Vortex Pairing: The Mechanism of Turbulent Mixing Layer Growth at Moderate Reynolds Number", Journal of Fluid Mechanics, Vol. 63, 1974.

22. Doligalski, T.L. and Walker, J.D.A., "Shear Layer Breakdown Due to Vortex Motion", Proc. Workshop on Coherent Structure in Turbulent Boundary Layers", C.R.Smith and D.E.Abbott, ed., Lehigh University, May, 1978.

23. Willmarth, W.W. and Tu, B.J., "Structure of Turbulence in the Boundary Layer Near the Wall", Physics of Fluids, Supplement to Vol. 10, 1967.

24. Willmarth, W.W., "Structure of Turbulent Boundary Layers", Advances in Applied Mechanics, Vol. 15, C.S.Yih, et., Academic Press, 1975.

25. Hama, F.R. and Nutant, J., "Detailed Flow Field Observations in the Transition Process in a Thick Boundary Layer", Proc. 1963 Heat Transfer and Fluid Mechanics Institute, Vol. 77, Stanford University Press, 1963.

26. Danberg, J.E., "On the Feasibility of a Vortex Model of the Turbulent Boundary Layer Burst Phenomena", Proc. Workshop on Coherent Structure in Turbulent Boundary Layers", C.R.Smith & D.E.Abbott, ed., Lehigh University, May 1978.

DISCUSSION

Abbott:

I would like to make a point of clarification about this new method. Please remember what Chuck (Smith) is doing by moving with the flow in this technique. He is able to get the wire into the legs of some of these structures. As they go by they are visualized in a plane; he can then track them as they move out of that plane. In fact in the last view Chuck showed, you could see the ends of these structures as they tilted upwards. The legs which were shown were in quite a different plane then where the bubble wire was located. If you're using a fixed bubble wire you will usually not get it into the right place. If there is vorticity, you may not get the bubbles into the vortex. But when he's moving through vortices, they do pick up bubbles, and then the picture persists a great while.

(Editor's comment. An unclear discussion occurred here between Smith, Wallace, Brodkey and others about the nature of the interaction between inner and outer layers. This discussion led to the formation of a committee headed by Jim Wallace to discuss the issues more fully and report back at the plenary session on Wednesday morning. Please see report of committee 3 under committee reports).

Kline:

I would like to comment in the spirit of what I said in my talk -- there do seem to be connections between some of these events. I hope this committee will not only look for what connections exist in the various views at the present time, but also what kinds of experiments we might now do to clarify these connections. These connections certainly seem to affect the inner and outer interaction that seem to be concerning everybody.

Reynolds:

Chuck (Smith), it seems to me that these visualization methods really show most clearly that there is vorticity perpendicular to the plane of the bubbles. For this reason I would like to suggest you try creating a bubble sheet across the flow spanwise and see if you can pick up the legs of the vortices by passing through them in both directions.

Kline:

Can you say that again please.

Reynolds:

Run a bubble wire across the flow, and take a picture looking up endwise and see if you can pick-out the legs.

Smith:

That is one of the things that we plan to do. As a matter of fact, we're setting up a system where we will have two video cameras which can

record simultaneously. Then we can look at two simultaneous views and try to determine a bit more about the three-dimensionality. Also, we should be able to look at small scale events and the corresponding large scale behavior simultaneously to determine if there is a cause-and-effect. And, if so, how the cause-and-effect takes place.

Kline:

We have such views, you saw some this morning looking upstream -- not too many. Those were in the sublayer. There are also views in the channel flow taken by Lezius and by Halleen. Particularly in the report by Lezius and Johnston with and without coriolis forces. They do show the axial vorticity quite clearly -- I agree with Bill Reynolds completely on that.

Hussain:

I would like to ask you for a clarification Chuck -- you were suggesting the lift up from the sub-layer as a possible pairing mechanism, typically the pairing-event Steve Kline showed. Results from the two vortices with same vorticity or helicity -- whichever way you want to say it. It seems to me, adjacent to the wall the logitudinal structure have alternate vorticity in adjacent legs. So therefore I do not quite see the possibility of two adjacent, longitudinal streaks pairing to form a single vortex and ejecting away from the wall.

Smith:

That's not what I meant to imply. What the two counter-rotating, logitudinal vortices do is concentrate low momentum fluid between themselves near the wall. This low momentum fluid builds up until a structure passes over -- let's speculate that its a large eddy -- whatever large means is not quite clear at this point ... which interacts with that low momentum region near the wall, causing it to lift. We thus get a low-speed fluid region lifted from the wall, which then interacts with a higher speed region of incoming fluid forming that thing -- that ejection or roll-up that I illustrated.

If you can wait for a day, Dave Walker is going to discuss an analytical technique which indicates that this kind of characteristic inner-outer interaction behavior can occur. That is, that a passing structure can cause a lifting of low-speed fluid away from the wall. What happens then -- I'm speculating -- is that a roll-up interaction occurs similar to that seen by Brown and Roshko.

Kline:

Can I say one thing about Hussain's question. A number of people have shown this model. There is also some theory. Chuck was reconfirming it. Motions toward the wall crowd low-speed fluid in the sublayer, concentrate it and move it up, away from the wall. You saw this in the old, combined-time-streak marker movies I ran during my talk. Now suppose you have two 'lifted' pieces of fluid like this such that each has

the same sign of vorticity at the head. If the later one gets over the other, having say originated a bit farther upstream, then they could 'pair' or almagamate. This is what Offen reported seeing now and then. You get a picture of two eddies like the sketch.

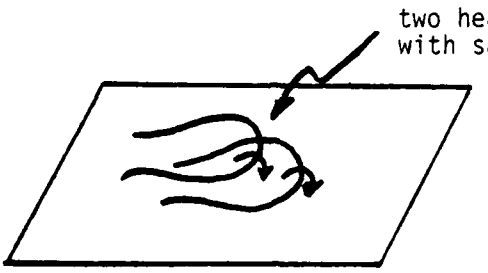

COMBINED FLOW VISUALIZATION AND HOT-WIRE MEASUREMENTS IN TURBULENT BOUNDARY LAYERS

M.R. Head & P. Bandyopadhyay

Department of Engineering

Cambridge University, England

ABSTRACT

Cine films have been made of illuminated longitudinal sections of the smoke-filled boundary layer at values of Re_θ of approximately 1000, 2000 and 7000. Simultaneous measurements of u-fluctuations have been made using a staggered array of three hot wires and synchronised with the visual records. The results confirm earlier observations that, over significant patches of the flow, strong correlations in u-fluctuations occur along lines at approximately 40^o to the surface. It is inferred that these represent arrays of hairpin vortices, and visual evidence supports this conclusion. Large-scale motions are seen as random agglomerations of such hairpin vortices, with some evidence of more systematic structures at high Reynolds numbers.

1. INTRODUCTION

This report is largely an extension of an earlier paper presented at the Berlin Symposium on Turbulence (Bandyopadhyay, 1977). Further results have been obtained which confirm earlier interpretations and suggest a rather different picture of the turbulent boundary layer from that which is generally accepted.

Although several aspects of this picture require further clarification, it emerges quite clearly, both from the cine films and the hot-wire records, that the horseshoe (or hairpin) vortices postulated by Theodorsen (1952) and others (notably Black, 1968) are the most significant feature of the boundary layer, at least for values of Re_θ in the range 1000 - 7000 . Over this range, large-scale features appear to consist almost solely of random agglomerations of such vortices. The only exception is the very occasional appearance, at $Re_\theta \simeq 7000$, of rather more ordered structures of characteristic form. Whether or not

these become a dominant feature of the boundary layer at really high Reynolds numbers is a matter for conjecture.

Certainly, although the structures we have described as random agglomerations of horseshoe vortices must possess certain well-defined long-term statistical properties, there is no evidence from the cine films of any obvious length scale, periodicity or overall form associated with them that can be readily discerned. Whether they should therefore be categorised as coherent structures, or whether this term should be reserved for the more regular and infrequent features observed only at $Re_\theta \approx 7000$, it is left to participants in the Workshop to decide.

2. PRELIMINARY DISCUSSION

In this section we shall briefly review the results presented in the earlier paper (Bandyopadhyay, 1977). The finding of greatest interest was the occurrence of highly correlated patches of u-fluctuations, about 2δ long, with the correlations extending along lines at approximately 40^o to the surface. Two hot wires were used, staggered at this angle, so that the highly correlated patches were distinguished by virtually identical signals from the two wires, without any phase shift. At that stage the possibility could not be dismissed that the observed correspondence of the signals from the two wires was simply due to random coincidence. The first task, then, was to demonstrate that the results were, in fact, significant.

Again, the results had been obtained from the analysis of only one film, at $Re_\theta \approx 2000$, and it seemed worthwhile to obtain further records, particularly at higher Reynolds numbers. A cine film had been made at $Re_\theta \approx 7000$ but without complementary hot-wire recordings.

It also seemed worthwhile to analyse the hot-wire records with a computer program to show up patches of high correlation, which had hitherto been established only by visual inspection.

Finally, it was felt that some attempt should be made to relate the observation of these rather rare patches of high correlation to the more commonly observed features of the turbulent boundary layer, such as bursts or sweeps, if that were possible.

It may be said here that not all of these objectives have been satisfactorily achieved, and that the experiments were terminated in October 1977 when the loan of the 4W laser used for illumination expired. However a considerable amount of data had been accumulated by then, and the techniques of recording and analysis had been firmly established.

3. EXPERIMENTS

3.1 General description of technique The basic technique, which is described in rather more detail in the earlier paper (Bandyopadhyay,

1977) may be summarised as follows.

(i) The boundary layer develops on the floor of a wind tunnel with smoke admitted close to entry across the full width of the tunnel. A serrated strip is normally used to trip the boundary layer just downstream of the point where smoke is admitted. The smoke is actually a fog of condensed oil vapour, and at exit from the tunnel the flow is ducted out of the building so that the laboratory remains clear of smoke.

(ii) The smoke-filled boundary layer is continuously illuminated by a plane of light from above the tunnel using either a 1000W quartz-halogen light source and a suitable optical system (Fiedler & Head, 1966), or a 4W water-cooled laser with a glass rod used to fan-out the beam. The latter system is by far the better and was used for all the experiments described here. A cine-camera outside the tunnel is used to photograph the illuminated section of the smoke-filled boundary layer, which may be either longitudinal or transverse. A high-speed camera has been used throughout, with framing rates up to 900 per sec.

(iii) Two or more hot wires are positioned in the boundary layer just off the plane of illumination and in the field of view of the camera. The signals from the hot wires are displayed on a storage oscilloscope which is also within the field of view of the camera. A suitable sweep time is chosen and the oscilloscope is triggered manually several times while the camera is running.

(iv) As well as being displayed on the oscilloscope, the signals from the hot wires are recorded on magnetic tape, along with a timing signal (either sine-wave or square-wave) which is used to synchronise the taped record with the cine film. The timing signal is given a transient-free start just after the tape recorder has been switched on and the camera run up to speed. As well as being recorded on the tape, the timing signal operates a counter which is within the field of view of the camera.

(v) The hot-wire signals and the timing signal recorded on the tape are digitised in the Department's 'Alpha' computer and stored on floppy disc. In digitised form the signals are then passed to the 'Sigma 6' computer for processing, including counting the number of waves in the timing signal. The output is then (normally) 'Calcomp' plotted on a continuous paper roll on which the timing signal counts are indicated.

(vi) A check on the synchronisation procedure, and indeed of the whole taping digitising and plotting process, is provided by comparing the 'Calcomp' plotted signals with the oscilloscope display for the same timing-signal counts. A typical comparison showing very satisfactory agreement, is given in Bandyopadhyay (1977).

3.2 Wind tunnels Over the past 20 years various wind tunnels in the Department have been used for boundary-layer flow visualisation. First attempts were made using titanium tetrachloride painted on to the surface of models in a small smoke tunnel. One typical result, comparing

laminar and turbulent flow over a kinked plate, was given by Bandyopadhyay (1977). A similar result for flow over a curved plate is given here in Photos 1(a) and (b).

Later experiments were carried out in a larger blower tunnel with the set-up described by Fiedler & Head (1966). A cine film was made showing the turbulent boundary layer in favourable, zero and adverse pressure gradient conditions. This was presented at the 1967 Canadian Congress of Applied Mechanics (Head et al, 1967). Photos 2(a) and (b) compare longitudinal sections at high and low Reynolds numbers and Photos 3(a) and (b) show the boundary layer in highly favourable and adverse pressure gradients respectively.

A much larger blower tunnel was then constructed with a working section approximately 12 m long and 0.9 m square (40 ft x 3 ft sq). In its original form shown in Figure 1(a) it was used to make a cine film showing inter alia the growth of turbulent spots and the interaction of the turbulent boundary layer with the free stream. This film was shown at the Boeing Symposium on Turbulence in 1969, and enlarged frames from it are shown in Photos 4(a) and (b) and 5(a) and (b).

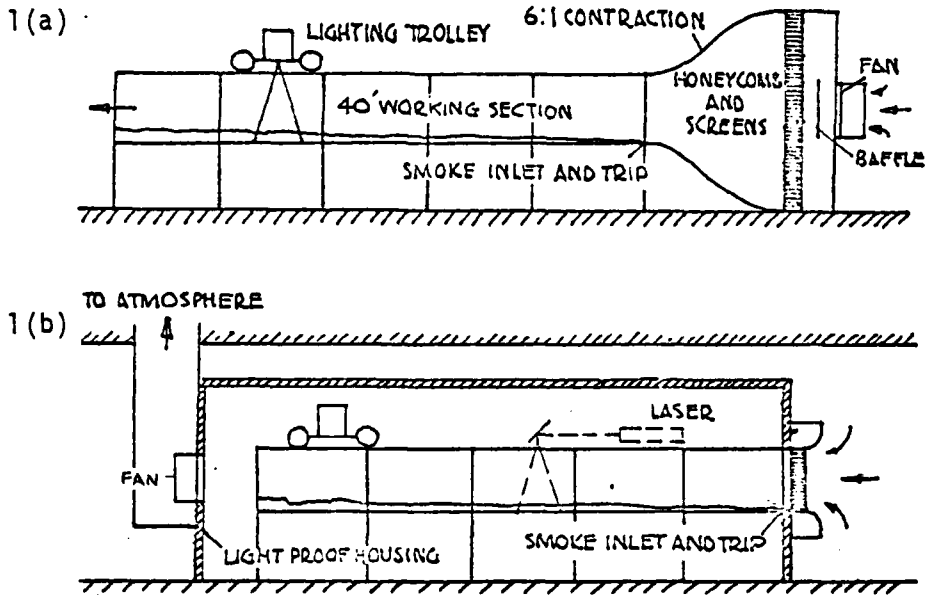

Figure 1. Smoke tunnel in original and final forms

In the modified form shown in Figure 1(b) the tunnel was used by Falco (1977) with the lighting system unaltered and still substantially the same as that used earlier by Fiedler & Head (1966).

For the combined experiments described here and in the paper by Bandyopadhyay (1977) conditions were modified only to the extent that a 4W laser was used as light source, as indicated in Figure 1(b).

(a) laminar separation (b) turbulent separation

Photo 1 Low Reynolds number flow over curved plate

(a) low Reynolds number (b) high Reynolds number

Photo 2 Turbulent boundary layer different at Reynolds numbers

(a) favourable pressure gradient (b) adverse pressure gradient

Photo 3 Effect of pressure gradient

(a) smoke in free stream only (b) smoke in b.l. and free stream

Photo 4 Interaction between boundary layer and free stream

Because the speeds in the smoke tunnel were very low, with a maximum in the region of 3m/s , it was decided to perform at least a limited number of experiments in one of the straight-through tunnels in the laboratory, modified as shown in Figure 2 by fitting an extension to the working section and directing the exit flow through an adjacent window.

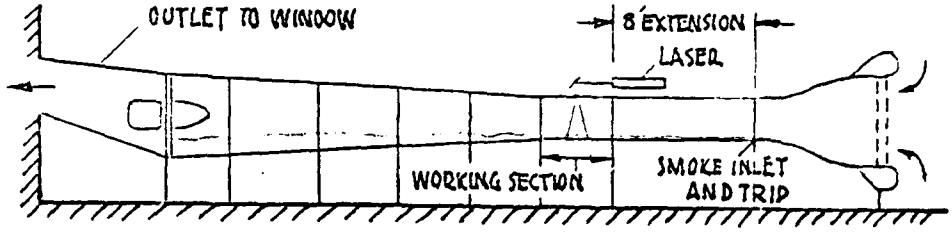

Figure 2. Modified straight-through tunnel.

Experiments with Re_θ in region of 2000 or less were performed in the large smoke tunnel, while for $Re_\theta \approx 7000$, the modified straight-through tunnel was used.

4. RECORDS OBTAINED

The records were normally in the form of 16mm cine film, plus the corresponding 'Calcomp' plotting output of the hot-wire and timing signals. Alternatively, or in addition, the output might take the form of a printout of the hot-wire data processed to indicate regions of high correlation (see below). A particular set of records is referred to by the number allocated to the cine film (e.g. Cine 22B). A complete list of records and the conditions in which they were obtained is available but will not be presented here, where we confine ourselves to giving a brief outline of the course of the experiments. These include some which were performed in turbulent spots and in the attaching flow behind a circular rod on the surface, where horseshoe (or hairpin) vortices were known to occur.

Initial experiments were performed in the large smoke tunnel at values of Re_θ in the region of 1200 , using a single crossed-wire at different levels in the boundary layer. These experiments were mainly concerned with developing the 'combined' technique, the objective at this stage being the accumulation of more extensive and accurate shear-stress data that would enable ensemble-averaged Reynolds stress distribution to be obtained, following basically the procedure described by Falco (1977). In the event, this objective was abandoned in favour of what seemed a more promising line. The major difficulty in these early trials was that of obtaining a transient-free start to the timing signal, so that recourse had to be made to the oscilloscope trace for synchronisation. In using the crossed wire, values of uv could be obtained either from the analogue uv output or by multiplying together in the computer the individual u and v analogue signals. The records of uv and $u \times v$ were found to agree very closely.

When the difficulty of obtaining a transient-free start to the timing signal was overcome no further difficulties were encountered in synchronisation, the frequency of the timing signal being adjusted roughly to the framing speed of the camera.

Cines 22 and 23 represented the first useful efforts in the present series. Here a single hot wire was positioned at a y^+ of about 4 , with a crossed wire directly above it in the outer part of the layer. The objective here was to see whether correlations could be discerned between the signals from the hot wire close to the surface, which would be a measure of the skin friction, and the uv signals in the outer part of the layer during the passage of a large-scale motion. In Cines 24 and 25 conditions were similar, but the wires were staggered at an angle of about 50^o to the surface. Cines 22, 23 and 24 were recorded at an Re_θ of 1170 and Cine 25 was virtually a re-run of Cine 24 but at approximately double the Reynolds number.

Cine 31 was the first of the combined records obtained at a high Reynolds number ($Re_\theta \simeq 7000$). Here again a single wire very close to the wall served as a measure of skin friction, but the outer crossed-wire was replaced by a single wire.

Up to this stage, the results suggested that there was some correlation between skin-friction activity and the passage of a large-scale motion, and between skin friction and the shear stress in the outer part of the layer on the upstream side of large-scale motions, but the signatures did not show any obvious correlation over extended periods of time. In addition it was not at all easy to distinguish from the films what should be categorised as large-scale motions. The only really distinctive feature of the layer, which appeared again and again, was a general inclination of smoke-free fissures or smoke-filled filaments at a characteristic angle to the wall, which appeared to be in the region of 40^o . The visual evidence suggested that this angle was characteristic of the flow in the outer part of the layer and it seemed reasonable to expect that it should not extend into the sublayer and buffer region. The single wire closest to the wall was therefore moved out of the sublayer to a y^+ of about 40 (for $Re_\theta \simeq 2000$), and the second hot wire was staggered behind it so that the line joining the two wires made an angle of 40^o to the surface; the outer wire was at rather less than half the boundary layer thickness.

Cine 32 was made in the large smoke tunnel with the hot-wire configuration just described and $Re_\theta \simeq 2000$. It was this film and the corresponding 'Calcomp' plotted hot-wire records that provided most of the material for the paper by Bandyopadhyay (1977). Visual inspection of the signals from the two hot wires showed quite extended regions (in the region of 2δ long) where the two signals were virtually identical, leading to the speculation that arrays of hairpin vortices, inclined at an angle of about 40^o to the surface, were being convected past the wires. Subsequent experiments have been directed towards testing this hypothesis.

Cine 33B was basically a repeat of Cine 32, but with a third single wire inserted between the other two, at the same stagger angle.

Cines 34A and B were made using the same hot-wire configuration in the straight-through wind tunnel at $Re_\theta \approx 7000$.

The remaining experiments were performed in circumstances where hairpin vortices developed in substantially turbulence-free surroundings. Cines 35, 36 and 38 were made in the reattaching flow behind a circular rod placed across the floor of the large smoke tunnel, in a laminar smoke-filled boundary layer, and Cine 37B was made in the plane of symmetry of developing turbulent spots.

Measured mean velocity profiles representative of the three Reynolds numbers at which experiments were commonly performed are shown in Figure 3 below.

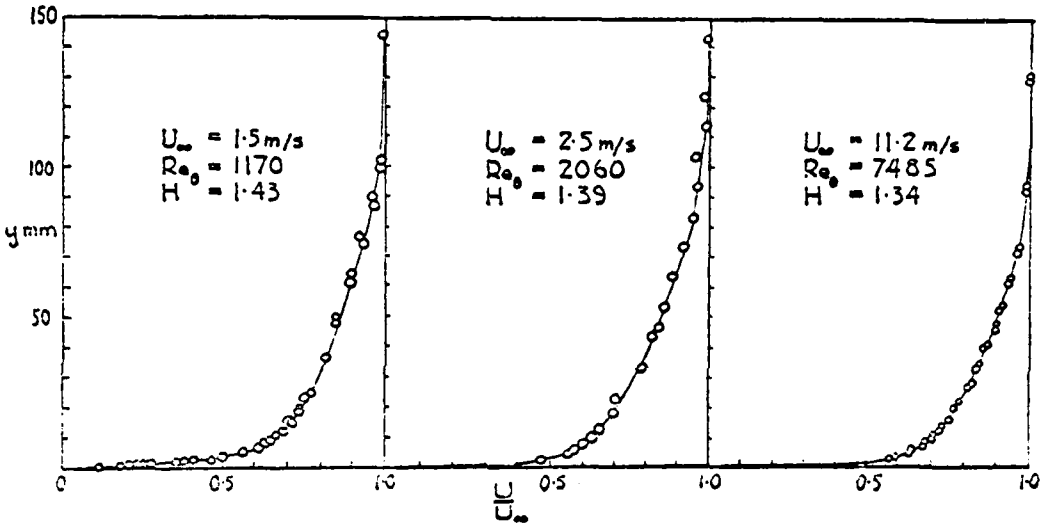

Figure 3. Measured mean velocity profiles.

5. COMPUTER RECOGNITION OF SIMILAR PATCHES

In the earlier paper (Bandyopadhyay, 1977) the correspondence of signals from the two wires used in Cine 32 was established by visual inspection. In fact this procedure left little doubt that patches of very high correlation existed, but no figures could be attached to the correlations, and it could be objected that the procedure was somewhat subjective. It therefore seemed worthwhile to program the computer to distinguish regions (in terms of timing-signal counts) where the mean correlation over a certain fixed time interval, traversed along the sample, exceeded some stipulated value. The way in which this was done is indicated in Figure 4 on the next page.

Effectively, what we are doing is determining a running average, over a fixed time interval corresponding to roughly 2δ , of the correlation between the two signals. This mean correlation could have been 'Calcomp' plotted over the full length of the sample, as indicated in the lower part of the figure, but in fact a printout was made of the counts defining regions where the chosen criterion was exceeded, and of

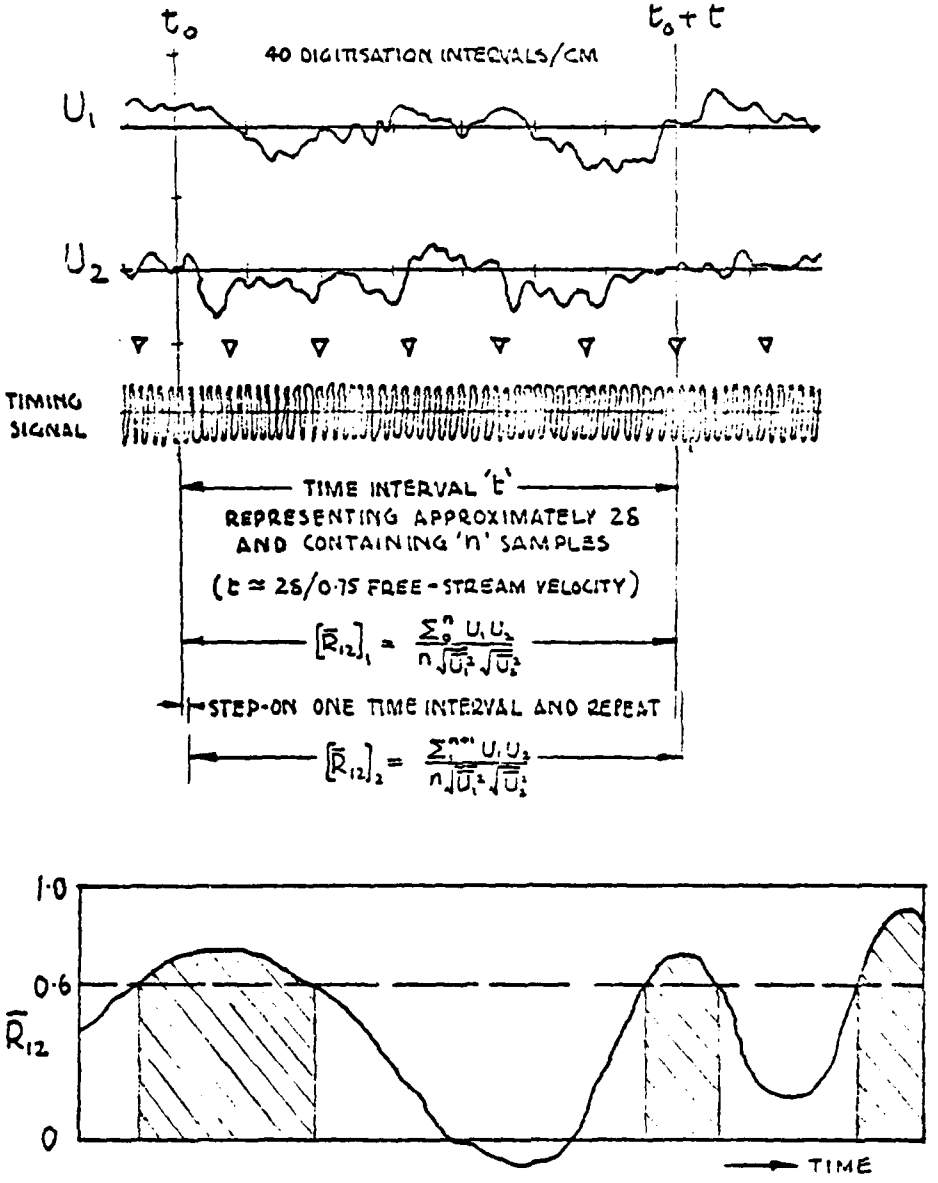

$\Sigma \bar{R}_{12}$ OVER COMPLETE SAMPLE LENGTH TAKEN AS SUM OF HATCHED AREAS, REPRESENTED BY SUM $\Sigma \bar{R}_{12}$ FOR $\bar{R}_{12}$ > SPECIFIED CRITERION (0·6 SAY) (MULTIPLIED BY SAMPLING INTERVAL, $\Sigma \bar{R}_{12}$ WILL REPRESENT TIME FOR WHICH CRITERION EXCEEDED)

Figure 4. Computer recognition of similar patches.

both the sum of the hatched areas indicated on the figure and the total number of occasions on which the prescribed criterion was exceeded.

Time intervals corresponding to 2δ, δ or $\delta/2$ were chosen for different runs through the computer, and on each run results could be obtained for different values of the criterion (say 0.6, 0.7 and 0.8) and with different leads or lags applied to the signal from the top wire.

When this procedure was applied, two things became apparent. First, a few regions were found where the correlation was extremely high (up to 0.88 over a patch length 2δ) and the effects of lead or lag corresponding to changes in effective stagger angle of $\pm 20^{0}$ were in some cases very small, indicating a lack of correspondence of small-scale features in the signals despite a high level of correlation. The second observation was that occasional patches where the eye would have judged the signals to be substantially similar remained undetected.

The answer to both these observations lay in the fact that very high correlations could be achieved, without detailed similarity of the signals, if u_1 and u_2 had substantial mean components (over the time interval considered) which were different from the long-term means. This led to our selecting too high a correlation coefficient as a criterion for similarity, which led in turn to visually similar patches remaining undetected, while at the same time detailed similarity of the signals was by no means assured.

The program was therefore modified so that the mean values of u_1 and u_2 over each interval were subtracted from the instantaneous values. This had the effect of focussing attention on features of small extent in the streamwise direction (say of order $\delta/10$) but of relatively large extent along lines where the correlation remained high. At the same time, of course, we were discarding information which might be valuable in defining true large-scale motions, and it might be worth re-examining the records to see whether the relatively sustained departure from long-term mean velocities form a coherent pattern.

The modified program proved satisfactory and it appeared that, where the correlation coefficient exceeded 0.6 the signals would be judged by eye to be very similar. Two examples are shown in Figure 5 below.

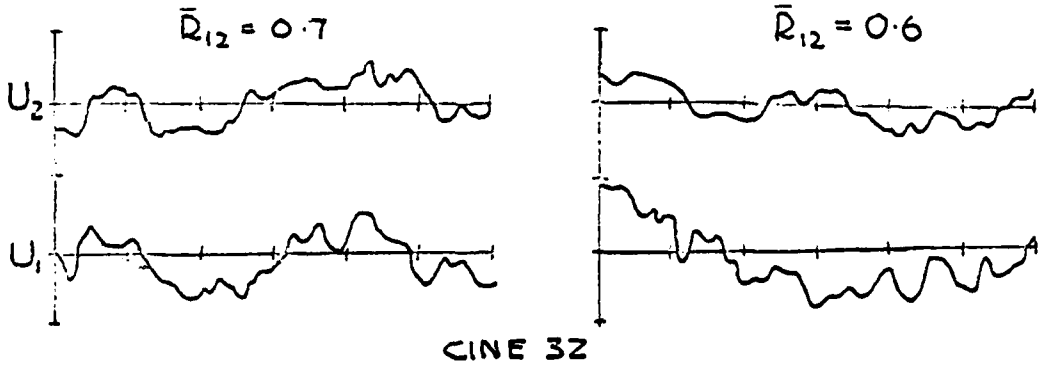

Figure 5. Examples of similar patches identified by computer.

6. OVERALL CORRELATIONS

With the digitised hot-wire records available, it seemed worthwhile to determine the long-term correlation between hot-wire signals, with different values of lead and lag applied to one of them. The results would at least tell us whether the 40^{0} stagger angle chosen showed the highest correlation.

Cines 33B and 34A with 3-wire staggered arrays were treated in this way. The results for Cine 33B are shown in Figure 6 below. The results for the other film are quite similar.

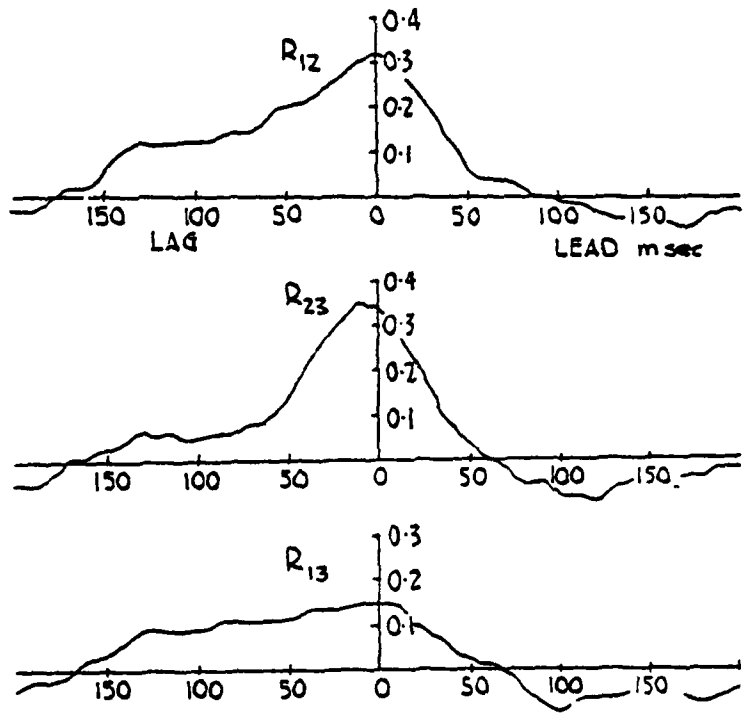

Figure 6. Effect of lead or lag on overall correlations.

As would be expected, with 2 the intermediate wire, the correlations between 1 and 2, and between 2 and 3 are much higher than those between 1 and 3. For 1 and 2, and 2 and 3, the peak correlation of approximately 0.3 occurs with zero lead or lag, indicating that the choice of stagger angle for the wires was correct. The correlation falls off rapidly with increasing lead (i.e. higher angles to the surface) but shows a rather extended plateau-like region with increasing lag, indicating some appreciable correlation at smaller angles to the surface. These features are also evident in the results of Favre et al. (1957).

7. HIGHLY CORRELATED PATCHES

7.1 Possibility of random coincidence In the earlier paper it was stated that the possibility could not be dismissed that the patches where signals from the two wires showed a marked similarity was simply

due to the fortuitous coincidence of signals that covered much the same frequency range. It seemed that the simplest way of eliminating this possibility was to fit a third wire between the original two.

Typical results obtained from Cine 33B are shown in Figure 7.

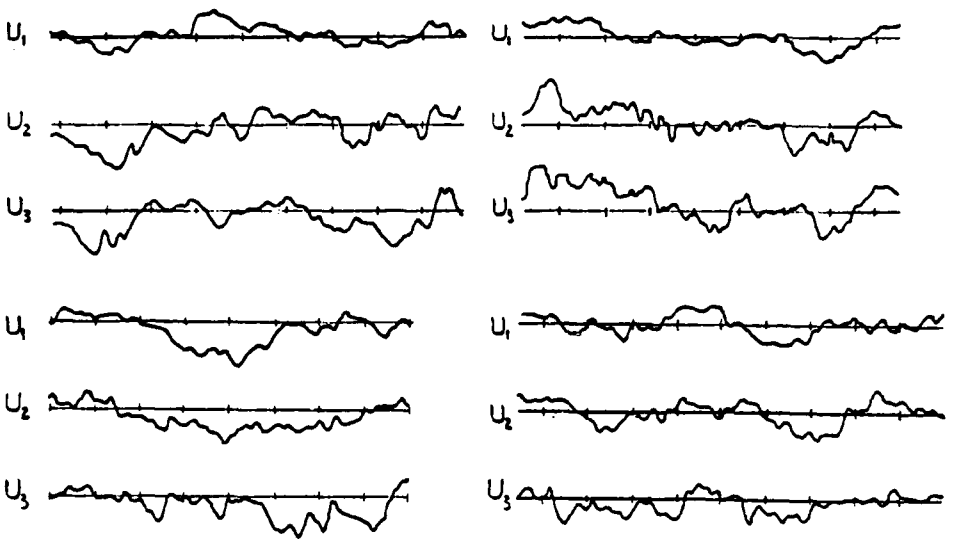

Figure 7. Similar patches for 3-wire arrays.

From this and a large number of similar examples it appears that the possibility of explaining the similarity of signals by random coincidence can, in fact, reasonably be dismissed. If we number the wires, 1, 2, 3 in order of their distance from the surface, as in the previous section, then similarity of the signals from 1 and 2, and from 2 and 3 are more often observed than similarity of the signals from 1 and 3, but, more important, whenever such similarity is observed between the signals from 1 and 3, it also exists between those from 1 and 2, and 2 and 3. Similar results were obtained at $Re_\theta \approx 7000$, but patches of high correlation between wires 1 and 3 were less frequent at this higher Reynolds number.

The results obtained by computer processing the signals from two wires with varying lead and lag could also be used to demonstrate that the similar patches were not due to random coincidence. If similar patches appeared much more rarely with arbitrarily large lead or lag applied to one of the signals, this would effectively demonstrate the point. The computer program for recognizing similar patches was applied to the digitised data from Cines 32, 33B and 34A over different sample lengths with different leads and lags, and using different values of the criterion. The results for 34A, shown in Figure 8, are quite typical.

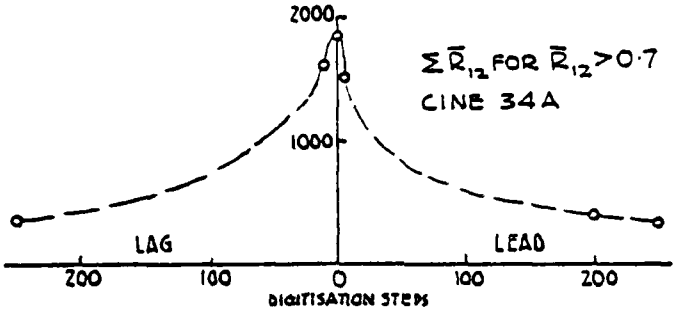

Figure 8. Effect of large lead or lag on occurrence of similar patches.

At this stage the computer program had not been modified to eliminate sustained departures from the long-term means, but it is believed the results would be only quantitatively affected, and that the very large reduction in correlation for large lead or lag would still be quite evident.

The general conclusion, then, must be that the observed highly correlated patches are not due to random coincidence.

7.2 Effect of small lead or lag The modified procedure for computer recognition of highly correlated patches 2δ long was applied to the results of Cine 32 with different amounts of lead or lag applied to the signal from the upper wire. Results averaged over several sample lengths are shown in Figure 9.

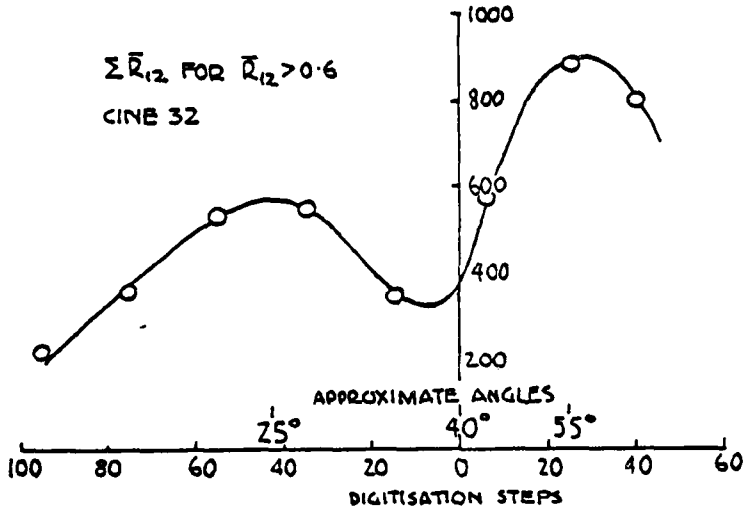

Figure 9. Effect of small lead or lag on correlation.

Very long sample lengths would have been required to obtain completely consistent results and computer time was limited. In fact, a considerable time saving could have been effected, without any

appreciable loss of accuracy, if the 2δ "window" had been shifted-on each time by (say) 20 digitisation intervals rather than the single interval specified in the program, but this possibility was recognised too late to be of service.

From the results shown in Figure 8 it will be seen that the chosen stagger angle of 40^{o} lies somewhat unexpectedly in the trough between two peaks which occur at approximately 25^{o} and 55^{o} to the surface. (It should be noted that, while the lead or lag can be specified accurately in terms of digitisation intervals, the specification of angles can only be approximate and depends on defining an appropriate convection velocity, which in this case was arbitrarily taken as $0.75U_{\infty}$). The existence of two peaks might signify either that we are dealing with two different types of structure, or that individual small features are inclined at either of these angles (and of course a range of others besides) in any patch with high correlation. The answer is almost certainly to be found in the recorded data but has not yet been extracted. This point requires further investigation.

Comparing the results in Figure 9 with the long-term correlations shown in Figure 6, we see that the two become compatible only if the correlations observed in the 2δ patches of high correlation are supplemented by a sufficient number of 40^{o} correlations outside these patches.

7.3 Results of film scrutiny The hot-wire records demonstrate conclusively that, over significant patches of the flow, u-fluctuations occur which are closely correlated over a substantial part of the boundary layer thickness. The streamwise extent of the fluctuations is small compared with the distance of the outer hot wire from the wall, and the inference must be that groups of highly elongated structures exist, inclined at an angle of something like 40^{o} to the wall. Arrays of horseshoe (or hairpin) vortices would seem to provide the most likely physical explanation and all the films that had been made were carefully examined to see whether visual evidence existed for such arrays.

In the outer part of the layer individual vortices abounded, at all Reynolds numbers, but it was very difficult to distinguish from the illuminated longitudinal sections whether they were more or less isolated structures, or the visible traces of much more extensive features originating at the wall. The difficulty here was that the boundary layer was, in most cases, more or less uniformly filled with smoke, so that features extending to the wall could be clearly seen to do so only when fortuitously surrounded by smoke-free fluid. However, with just the right smoke concentration and lighting it was sometimes possible to follow density gradients in the smoke down through the layer.

Photos 6(a) to (d) show cases where more or less straight inclined features, which can be most readily interpreted as hairpin vortices, are quite evident. Photo 7 shows a very definite array of such features, which can be associated with the corresponding hot-wire traces shown in Figure 10 below.

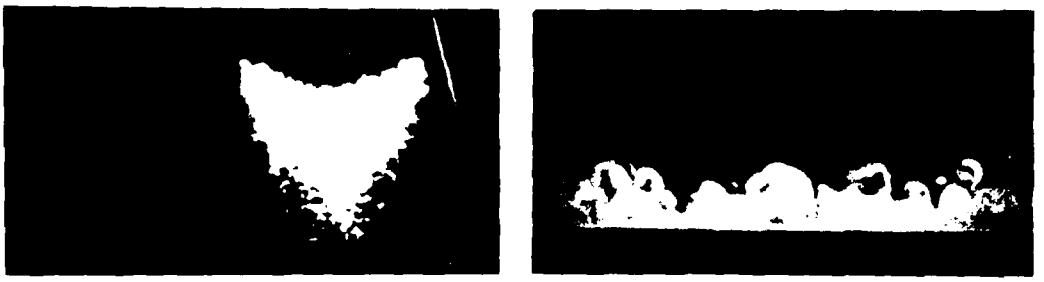

(a) turbulent spot (b) cross-stream view at $Re_\theta = 700$

Photo 5 Developed spot and boundary layer cross section

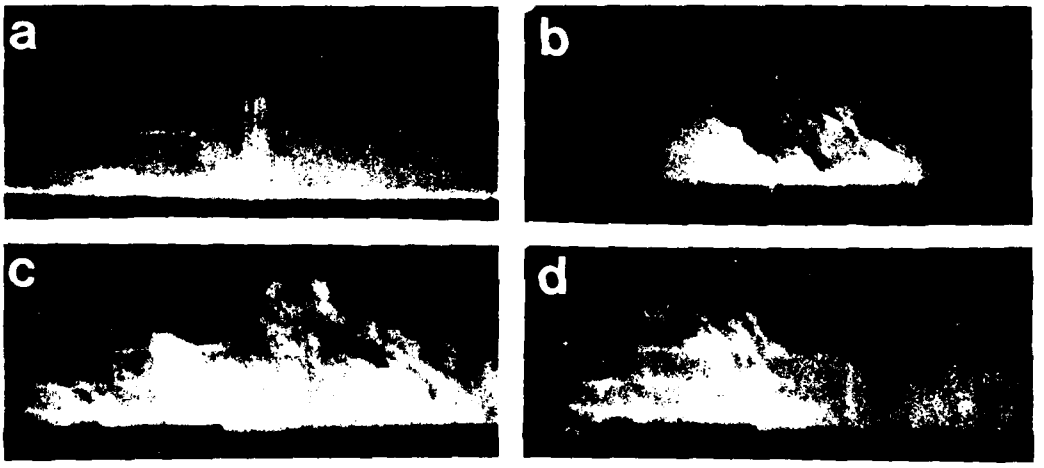

Photo 6 Evidence of straight inclined features

Photo 7 Cine frame corresponding to signals shown in Figure 10

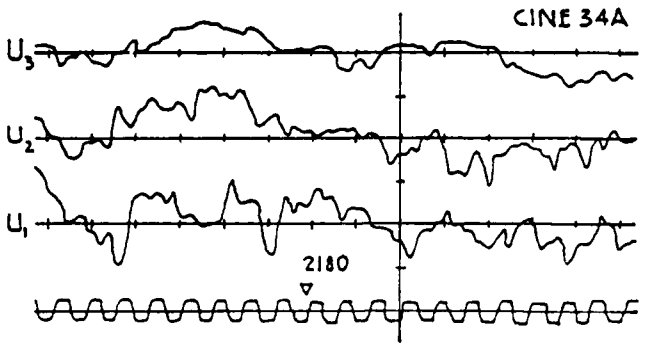

Figure 10. Hot-wire signals corresponding to visually identified array.

Photos 8(a) to (c) show examples of the rather regular features occasionally observed at $Re_\theta \approx 7000$.

Once the widespread existence of hairpin vortices in the boundary layer has been accepted, the cine films take on a rather different aspect, and the boundary layer itself, with both large and small-scale featutes, can be seen as no more than an assemblage of such vortices, in some cases extending right through the layer, more or less straight and inclined at a more or less constant characteristic angle to the surface.

Earlier authors, notably Theodorsen (1952) and Black (1968) have emphasized the importance of horseshoe vortices, and the latter has developed a quite detailed theory, but it may be doubted whether even these authors could have envisaged the highly elongated and in some cases very regular forms that such features may take. However, Black (1968) goes so far as to state "The theory asserts that the turbulent transfer of mass, heat, momentum and energy within the boundary layer are essentially effected within discrete, horseshoe-vortex structures which are generated and maintained by powerful, localised non-linear instabilities within the sublayer and which move downstream over the wall in a characteristic, quasi-frozen, spatial array." This statement would seem to be in excellent accord with the results we have obtained.

8. TURBULENT SPOTS

Black (1968) suggests that the initial instability which produces a turbulent spot in the laminar boundary layer, persists into the fully-developed turbulent layer, continuing to govern the process of turbulence production and momentum transfer. It had been observed in the smoke tunnel that the first evidence of the appearance of a spot was the production of one or more hairpin vortices, and, with the evidence from the hot-wire signals of regular arrays of such vortices in the fully-developed turbulent boundary layer, this provided substantial support for Black's hypothesis.

However, the present brief investigation of turbulent spots was undertaken simply with the objective of finding out something about

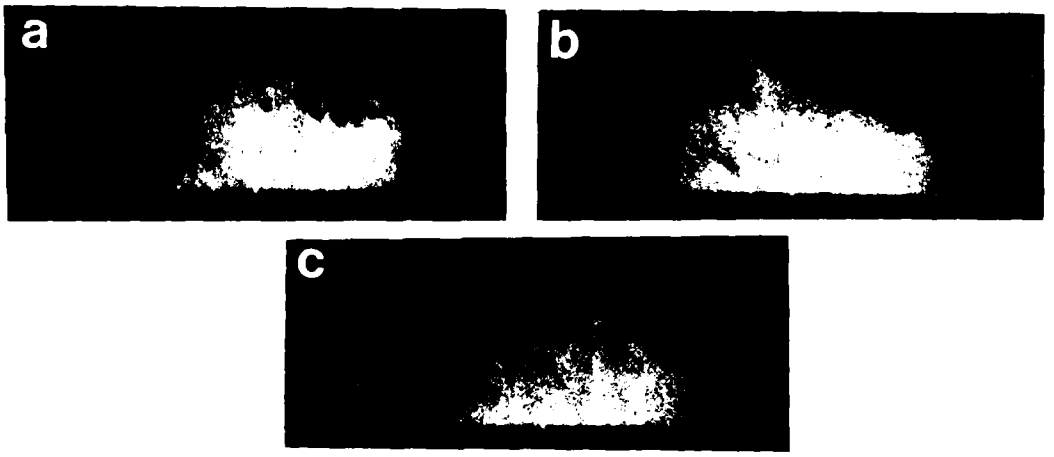

Photo 8 Regular features observed at $Re_\theta = 7000$

Photo 9 Upstream edge of spot

Photo 10 Slowly overturning large eddies

Photo 11 Downstream region of spot

hairpin vortices and the way in which they evolve into turbulent motions. Photo 5(a) referred to earlier shows a typical spot, grown to large dimensions. Those investigated here were generally at much earlier stages of development.

A staggered array of three hot wires was used, with a longitudinal plane of illumination on the tunnel centreline. Spots were induced to form on or close to the centreline by suitably adjusting the tunnel speed with a small obstruction over the honeycomb at entry to the tunnel producing a localised wake. (The low-speed smoke tunnel was used for these experiments.)

Visual observations, both of the flow itself and of film Cine 37B lead to the following descriptions of the main features of a developing turbulent spot.

(i) At the upstream side of the spot there is a general outward motion consisting of an array of features growing out from the wall, as may be seen in Photo 9.

(ii) As these features grow sufficiently large and numerous, they amalgamate to form slowly-overturning large eddies (Photo 10).

(iii) As the spot grows, the number of such eddies formed increases and, towards the downstream side of the spot, the flow comes to resemble a low Reynolds number turbulent boundary layer (Photo 11).

Examination of the hot-wire traces revealed a substantial number of patches where the signatures were very similar. Figure 11 below shows the signals corresponding to the passage of a single hairpin past the wires.

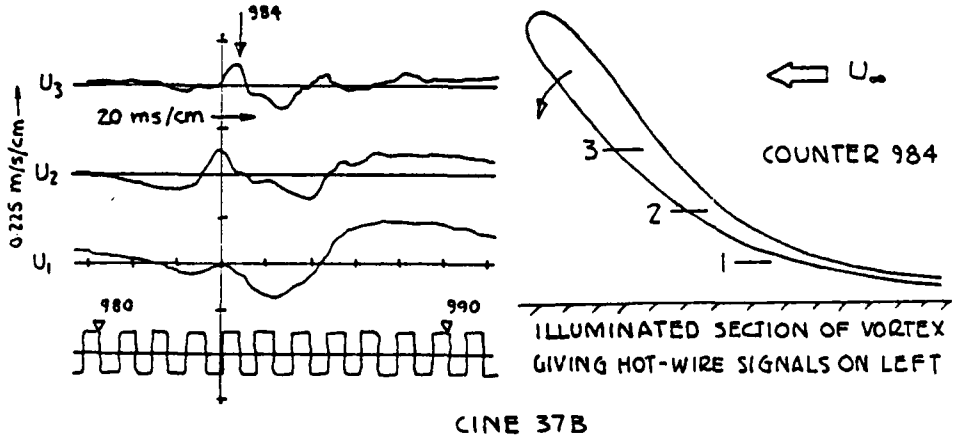

Figure 11. Hot-wire traces due to passage of observed hairpin vortex.

The spot experiment provided general support for the hairpin hypothesis as applied to fully turbulent boundary layers and showed how,

at low Reynolds numbers, hairpin vortices may evolve into coherent large-scale motions, which appear as a train of slowly overturning eddies.

9. FLOW BEHIND A CIRCULAR ROD

Photos 12(a) and (b) are from a film made by Head & Graham in 1969 and show hairpin (or horseshoe) vortices behind a circular rod. From the film these are seen to form in a regular periodic fashion as the reattachment position moves back and forth.

In the present experiment the three-wire rake was again used, at distances 7.5, 11 and 17 diameters downstream of the rod. The rod itself was about $1\frac{1}{2}$ cm in diameter and close to entry where the boundary layer was laminar and filled with smoke.

Visual observation of the flow and cine-films 35, 36 and 38 which were taken with a longitudinal light plane indicated that, shortly after separation the free shear layer rolls up into discrete vortices. Very often vortex pairing occurred in the region of reattachment. The precise position where this occurred relative to reattachment was not easy to discern, because both the layer itself and the cavity beneath were filled with smoke. Photos 13(a) to (e) show a sequence of frames where vortices 1 and 2 first combine to form a pair which rapidly disintegrates into a turbulent lump containing many small-scale features, and with fissures of smoke-free fluid extending almost to the wall.

Because of the relatively large scales of the horseshoes or hairpin vortices compared with the thickness of the light plane, they might appear in several different forms. If sufficiently twisted, the entire vortex might show up as a closed loop, while if it were untwisted it might appear in stages, starting with a small island of rotational fluid which grows and moves outwards until finally a filament appears from the side and joins it to the wall. Or, in some cases the process might be reversed. Quite similar observations are of course very common in the outer part of turbulent boundary layers, although it is not usually possible in that case to trace the motion ultimately back to the wall.

As in the case of the spot, the hairpins as they moved downstream rapidly formed discrete coherent turbulent structures which were, in this case, initially quite widely separated.

The hot-wire signals appear in no way to contradict the visual observations, and the only significant feature we remark upon here is the characteristic W type of signature apparently associated with the passage of a vortex pair.

10. EFFECTS OF REYNOLDS NUMBER AND TRIPPING DEVICE

In view of the present observations of fully developed turbulent boundary layers to be seen on cine film, it is not at all obvious how the idea of characteristic large-scale coherent motions in the turbulent boundary layer has come to be generally accepted. It may be that flow

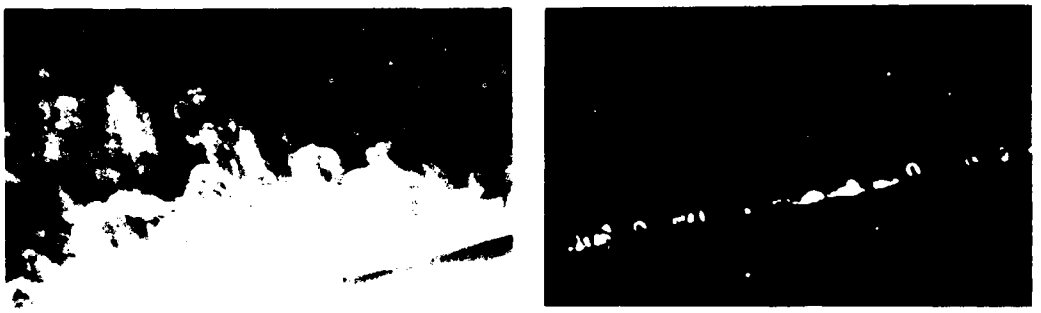

(a) general lighting; (b) vertical light plane

Photo 12 Formation of vortices behind circular rod

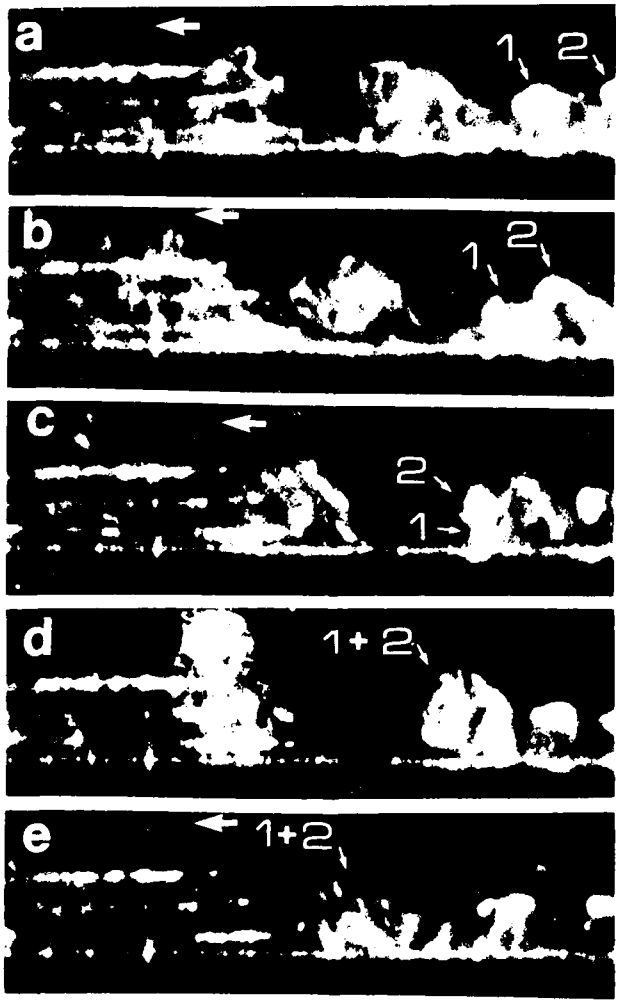

Photo 13 Sequence showing vortex pairing and subsequent break-up of turbulent lump

visualisation experiments tend to have been carried out at low Reynolds numbers, where, as we see below, coherent structures seem more likely to form, while hot-wire experiments have in general been performed at comparatively high Reynolds numbers, where the results are wholly statistical, thus tending to obscure any wide variations in large-scale flow structure that might actually be present.

Let us consider first the probable effect of Reynolds number on the vortex structure. It seems likely that the spacing of the legs of the hairpin vortices in both longitudinal and cross-stream directions should scale with the wall variables U_τ and ν, but it appears also that their length, at least up to $Re_\theta \approx 7000$, is limited only by the thickness of the layer. (It seems quite possible, incidentally, that the typical eddies, or small-scale motions, measured by Falco & Newman (see Falco, 1977), which evidently do scale on wall variables, represent no more than the tips of the hairpins.)

Now, if the foregoing is true, it is to be expected that there will be quite substantial Reynolds number effects on boundary layer structure as the ratio of length to breadth of the vortices changes. At the lowest Reynolds numbers (say $Re_\theta \approx 500$) they may appear as rather wide loops; at rather higher values of Re_θ (say 1000-2000) as somewhat elongated horseshoes, and at high values of Re_θ (say 7000) as greatly elongated hairpins. (See Figure 12 below.)

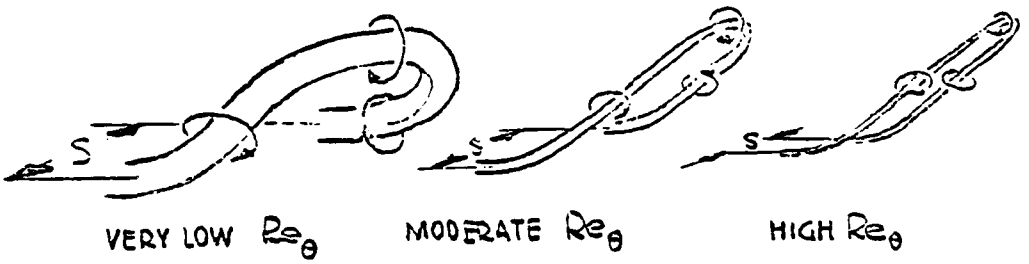

Figure 12. Sketch of horseshoe vortices at different Reynolds numbers.

At very low Reynolds numbers it seems quite likely that all scales of the vortex motion should be quite comparable with the boundary layer thickness, so that it might take only one, two or three of these vortices to produce a coherent large-scale motion. Thus, such motions may be relatively common at low values of Re_θ.

At higher Reynolds numbers, where there are comparatively very many more hairpins, the variety of possible combinations becomes large and at $Re_\theta \approx 2000$ (say) the structure might tend to appear relatively chaotic, as indeed appears to be the case. At very high Re_θ again ($Re_\theta > 5000$, say) there may be a return to the production of large-scale structures of a more or less typical form and there is some evidence of this in the films made at $Re_\theta \approx 7000$, as Photos 8(a) to (c) show. Even here, however, it takes no great effort of the imagination to see these apparently regular features as arrays of outgrowing vortices which take on a

rather orderly pattern.

Turning now to the possible effects of tripping devices, we have noted that the flow over a rod produces large, discrete turbulent lumps at some distance downstream, and a similar effect was noted in the flow of a turbulent boundary layer over a rearward facing step (Bandyopadhyay, 1977). From isolated observations made in the smoke tunnel, it appears that the effects of a trip in organising the motion may extend as far downstream as at least 150 trip heights, and at sufficiently low Reynolds numbers this may have a substantial effect in producing a more or less regular train of large-scale features.

11. SPECULATIONS CONCERNING LARGE-SCALE STRUCTURES

Up to now the suggestions that have been made have not been entirely free of conjecture, but we now pass to the realm of pure speculation in an effort to provide some sort of overall explanation for the observations. In fact we present two hypotheses, the first of which has certain attractive features but has now been discarded in favour of the second, which begins to look remarkably similar to the picture presented by Black (1968), although we have reached it by a very different route.

11.1 Initial hypothesis The following outlines the steps in an argument which explains the evolution of large-scale motions from the observed vortex arrays.

(i) Figure 13 shows a somewhat idealised picture of the boundary layer which would seem to accord with accepted ideas.

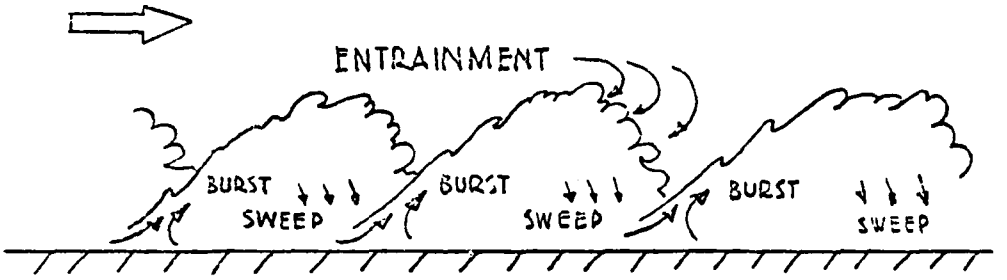

Figure 13. Train of coherent motions (idealised).

The sketch shows large-scale features of typical form being swept downstream, with high smoke concentrations originating from the sublayer on their upstream sides (positive v and negative u) and lower smoke concentrations on their downstream sides (negative v and positive u). The real picture is, of course, likely to be very much less regular than the sketch would suggest; moreover it gives no indication as to how the large-scale features originate.

(ii) Corrsin (1957) has remarked that the Reynolds numbers of fully turbulent wakes and jets, based on eddy viscosity, are constant

and very similar to the corresponding critical Reynolds numbers for their laminar counterparts, and Townsend (1970) has suggested the mechanism by which ν_T in such flows is maintained at the appropriate value. He suggests that, in fact, ν_T first decays, creating an instability that results in an abrupt increase in entrainment, which increases ν_T, which then decays, and so on. Essentially it would seem that he is postulating a quasi-periodic breakdown of the flow as the means by which ν_T is maintained (in the mean) at the appropriate value.

(iii) For the turbulent flat-plate boundary layer, it is well known that $U\delta^*/\nu_T$ maintains a constant value (1/0.016), and it can be simply shown that this corresponds to a value of $U_\tau\delta/\nu_T$ equal to 15 (very closely). Now this is very near the value of $U_\tau\delta_s/\nu$ (where δ_s is the sublayer thickness), which may be regarded as the critical Reynolds number for highly disturbed laminar flow. There is thus some reason for placing the flat-plate turbulent boundary layer in a similar category to jets and wakes, and it would then seem appropriate to postulate a generally similar mechanism by which ν_T is maintained at an appropriate value, i.e. by a quasi-periodic breakdown of the turbulent flow, in this case causing a disruption of the viscous sublayer as well as an increased interaction with the outer flow.

(iv) It would not seem necessary to postulate such an intermittent breakdown, since the boundary layer is continually being energised by the entrainment of free-stream fluid, and the viscous sublayer could remain in a state of quasi-equilibrium by either breaking down regularly at a time-scale proportional to ν/U_τ^2, or perhaps at a time-scale controlled by the passage of large-scale structures, or perhaps both. Nevertheless, it is clear that large-scale structures arise, persist for an appreciable period and then decay or amalgamate with other structures, and the highly correlated patches that we have interpreted as arrays of hairpin vortices may represent the initial stages of the type of breakdown we have been discussing.

Figure 14 below suggests how the regular arrays of hairpin vortices that we have inferred from the measurements may collapse to form large-scale structures of a more general form.

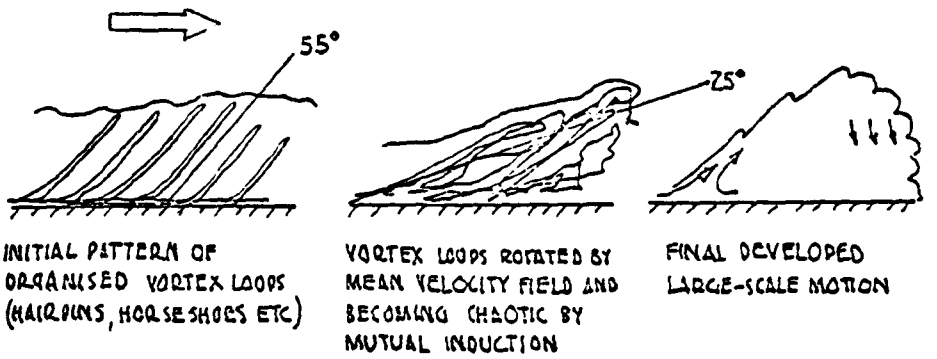

Figure 14. Change of vortex array to large-scale motion.

Once formed, it seems possible that the fully developed large-scale motion should remain in a state of quasi-equilibrium for some considerable time.

The only major difficulty with the foregoing would seem to be that the large-scale structures we assume as the end product, with a typical form and internal circulation, just do not seem to appear, except possibly very infrequently, in the cine films. Even when we do see structures that seem to have something like the appropriate features, as appears to happen occasionally at $Re_\theta \approx 7000$ (see Photos 8(a) to (c)), they can also be interpreted, as we have already remarked, as having a small-scale structure that consists of arrays of individual vortices at a steeper angle to the surface than the upstream interface of the structure as a whole. It therefore seems appropriate to consider the alternative hypothesis outlined below.

11.2 Alternative hypothesis This is developed as follows.

(i) In earlier sections it appears to have been established that the patches of high correlation between widely separated wires were unlikely to have arisen solely by the chance coincidence of random signals.

(ii) However, this by no means precludes the possibility that the boundary layer should at all times be composed of random arrays of hairpins, very often in a highly disorganised form, but occasionally, and perhaps quite by chance, conforming to the exacting standard of orderliness required if they are to generate the extended patches of similar signals observed.

(iii) In this case it does not seem necessary that similar patches should have any special signficance in the generation of large-scale motions, and large-scale structures are now simply seen as random agglomerations of hairpin vortices which maintain some measure of orderliness in their spacing and their angles to the wall.

(iv) This hypothesis seems to give a good account of the observations and in no way contradicts the known constancy of the Reynolds number $U\delta^*/\nu_T$ mentioned in para (iii) of section 11.1 above. It only suggests that Townsend (1970) was correct in placing the boundary layer in a different category from jets and wakes in not being subject to recurrent breakdown.

(v) The possibility of hairpins extending in many cases right through the boundary layer, albeit in a distorted form, explains the appearance of small-scale structures at the turbulent non-turbulent interface, and indeed the isolated islands that sometimes appear beyond it, and makes unnecessary the consideration of any localised instability at the interface. Falco's typical eddies and these isolated islands are seen as no more than illuminated slices through the tips of hairpin vortices. The cross-stream views shown by Falco are also not incompatible with vertical slices through inclined vortex pairs (or hairpins).

(vi) If we assume, as does Black (1968), the existence of an instability of the viscous sublayer moving upstream with respect to the

outer flow (though downstream in absolute terms), then the tips of successive vortices produced by the instability will lie along a line which is inclined at a much smaller angle to the surface than the individual vortices which give rise to it, as indicated in Figure 15 below.

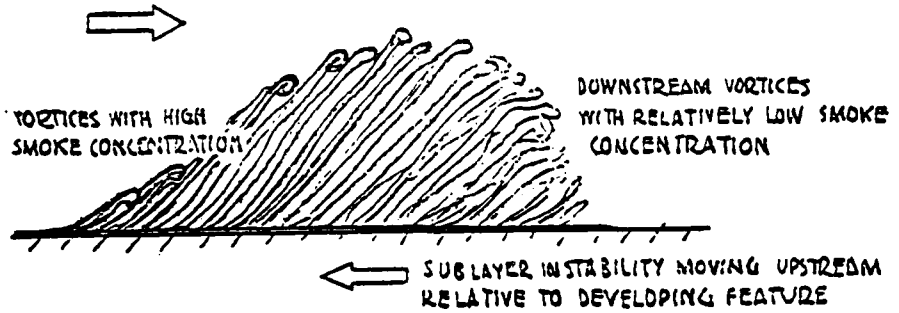

Figure 15. Array of hairpin vortices formed by advancing sublayer instability.

This would explain (a) the existence of small-scale vortices on the upstream face of the large-scale structures (b) the existence of high smoke concentrations along the upstream face close to the wall and (c) the comparatively disorderly nature of the downstream region and the weak smoke concentration there, due partly to vortex stretching and partly to entrainment.

(vii) If the lifetime of the sublayer instability is limited, and in some way related to δ/U, then a mechanism exists for the repetitive formation of characteristic features of the type shown in Photos 8(a) to (c). At the present stage it is by no means clear why or if this should occur only at high Reynolds numbers.

The two hypotheses may not be altogether incompatible, and it seems intuitively likely that regular arrays of hairpin vortices must at some stage of their development give way to much less coherent and orderly flow. The true picture, then, may contain features of both hypotheses, as well as (very possibly) additional features we have overlooked.

So far as the practical application of the present results is concerned, the considerations outlined in an earlier paper by the first author (Head, 1976) would seem to be entirely relevant. In that paper, the hypothesis was made that the boundary layer could be viewed as an assemblage of vortex elements which, in the mean, were arrayed at some substantial angle to the wall. This hypothesis now seems to be quite firmly based, and the tentative explanations arrived at for observed variations in eddy viscosity must take on an altogether higher degree of credibility.

12. CONCLUSIONS

The present investigation leads to the following conclusions.

(i) The patches of strong correlation in u-fluctuations observed earlier, using wires staggered at 40^{o} to the surface, are not due to random coincidence.

(ii) There is now a great deal of evidence to support the original suggestion that these patches represent regular arrays of hairpin vortices convected past the wires.

(iii) In turbulent spots the upstream region consists of arrays of hairpin vortices while the downstream region closely resembles a low Reynolds number turbulent boundary layer. The change from hairpin vortices to clumps of turbulent fluid takes place with great rapidity.

(iv) In the reattaching flow behind a circular rod in a laminar boundary layer, vortex loops or hairpins again appear and occasional vortex pairing is seen to occur in the reattachment region. The vortex loops again change rapidly into discrete clumps of turbulent fluid.

(v) The more or less regular appearance of coherent motions with streamwise dimensions comparable to the boundary layer thickness is believed to be characteristic of low Reynolds number flows ($Re_{\theta} < 1000$), either because of the organising effect of the trip (see (iv) above) or because of low Reynolds number effects per se.

(vi) For values of Re_{θ} in the range 1000 - 7000 the most characteristic feature of the boundary layer is not the existence of large-scale coherent motions but of structures formed by the random amalgamation of features that are small in the streamwise direction but highly elongated along lines at about 40^{o} to the surface. It is inferred that these substructures represent hairpin vortices.

(vii) At the highest Reynolds number ($Re_{\theta} \simeq 7000$) there occur a few examples of more regular large-scale structures of characteristic form. These also appear to be composed of arrays of hairpin vortices.

(viii) The final picture that emerges is one in which hairpin vortices originating in the viscous sublayer play a dominant role. Although still speculative, it explains many earlier observations. In particular, the emergence of the tips of the vortices at the turbulent : non-turbulent interface explains the appearance there of small-scale features that it would otherwise be necessary to ascribe to some form of local instability. The picture may also explain the discrepancy between the relatively small (upstream-interface ?) angles determined by Brown & Thomas (1977) and the much larger angles that we have found to produce the highest correlations.

(ix) The present picture exhibits so many features in common with that proposed by Black (1968) that it may almost be taken as an experimental verification of many of his basic ideas. His theory is evidently worthy of much more detailed study than we have so far been able to

give it.

(x) A general conclusion of the present research is that Reynolds number effects on the detailed boundary layer structure are likely to be important. Experiments at values of $Re_\theta < 1000$ (say) may give results that are quite unrepresentative of those at really high Reynolds numbers, which are likely to be of greatest practical significance.

ACKNOWLEDGMENTS

The authors are grateful to the sponsors of this workshop for providing the incentive for writing this paper and the opportunity to present it. They also apologise to the many authors whose publications, for want of a proper literature survey, have not been referenced.

REFERENCES

Bandyopadhyay, P — Combined smoke-flow visualisation and hot-wire anemometry in turbulent boundary layers
Berlin Symposium on Turbulence, 1977

Theodorsen, T — Mechanism of turbulence
Proc. 2nd Midwestern Conf. Fluid Mechanics,
Ohio State University, 1952

Black, T J — An analytical study of the measured wall pressure field under supersonic turbulent boundary layers
NASA Contractor Report CR 888, 1968

Fiedler, H E and Head, M R — Intermittency measurements in a turbulent boundary layer
J Fluid Mech 25, pp 719-735, 1966

Head, M R Fiedler, H E and Rogers, B E — Flow visualisation in the turbulent boundary layer
Canadian Congress of Applied Mechanics, 1967

Falco, R E — Coherent motions in the outer region of turbulent boundary layers
Physics of Fluids 20 pp S124-S132, 1977

Favre, A J Gaviglio, J J and Dumas, R — Space-time double correlations and spectra in a turbulent boundary layer
J Fluid Mech 2, pp 313-342, 1957

Corrsin, S — Some current problems in turbulent shear flows
Naval Hydrodynamics, Publication 515, 1957

Townsend, A A — Entrainment and the structure of turbulent flow
J Fluid Mech 41 pp 13-46, 1970

Head, M R — Eddy viscosity in the turbulent boundary layer
Aero Quart XXVII pp 270-275, 1976

Brown, G L
and Thomas, A S W — Large structures in a turbulent boundary layer
Physics of Fluids 20 pp S243-S252, 1976

DISCUSSION

Willmarth:

I'm not sure I understood exactly what you said with regard to to your smoke visualization, but the thing that interests me most was your picture with the hairpin going way across. Now, I'm only asking do you actually see those with your smoke? I mean it was not clear, but I think that's terribly significant.

Bandopadhyay:

Only in some cases is it possible to follow the hairpins and their growth away from the wall -- if you're fortunate that it's not surrounded by other smoke regions. But we have some examples where you can see them slowly coming out, and we see them normally on the upstream side of an interface.

Willmarth:

Do you see a lot of them?

Bandopadhyay:

Yes, we do see quite a lot of them.

Kline:

Before we recognize someone else -- can we continue this point? I don't see many "pins" in your pictures and I guess that's what Bill (Willmarth) is asking. I see some, but there is a critical difference between some and most of the time, or the average eddy, or the dominating feature. As I commented before on your method, which is also used by Falco, you see mostly the skin. You do not see inside the smoke-filled layer very much, hence, I don't understand how you get this picture of all these eddies coming out -- can you explain that for us?

Bandopadhyay:

At low Reynolds number, it's very difficult to see the legs of the "pins" within the smoke-filled region. But at very high Reynolds number, especially at the order of 7,000, within the smoke-filled-region, i.e. the large-scale-motion, we do see smoke concentration regions which suggest that the features are inclined at this sort of characteristic angle, and we have seen those "pins" which are twisted in the plane of illumination. I have the frame numbers marked which I can show and we can see how the hairpins appear.

Kline:

Thank you. Let's see...Marten Landahl.

Landahl:

I think one should be very careful in trying to describe flows with the aid of vorticity; after all, vorticity is nothing more than the curl of the velocity field. Whether you describe the velocity directly or by its curl could be significant, but then there may not necessarily be a substantial difference between the two. If you have two regions of different velocity, you can either say there is a velocity-discontinuity or you could say there is a vorticity-sheet. Of course, one thing you have to be aware of is that by describing the flow by vorticity, you do not catch all of the motion. You only catch the vortical motion, but not the irrotational part; it's not a complete description. Also, I think that one should view the description by hairpin vortices and so forth as a kinematical model and not as an explanation of anything. I think that the only thing that Theodorsen did that had dynamics in it was that he suggested that vortex stretching was a mechanism whereby you produced additional vorticity in the turbulent flow. Possibly it's the spanwise vortex stretching rather than logitudinal one that's significant here...but I think that's where the only dynamics come in.

Kline:

I'd like to say one thing. I don't understand how you induce from the pictures you showed us the idea that there is a sub-layer instability. Now if you're using the word sub-layer in the sense of the viscous sub-layer, $y^+ < 10$, I don't think we saw any pictures of this in your smoke visualization at all. There are other difficulties I have with some of the ideas you presented, but that one in particular I would like to ask you to clarify what you mean by the word sub-layer in this sense because I don't understand -- I can't follow you on that at all.

Bandopadhyay:

I don't think in the smoke visualizaiton you see very much what is going on in the sub-layer.

Kline:

In that case, how can you come to the conclusion that there is an instability in the sub-layer from these data? I don't follow the argument.

Bandopadhyay:

Well, we gave some evidence which suggests that there is an area of hairpin vortices, and then in the last pahse of the talk I presented a purely speculative hypothesis which proposes that

Bandopadhyay: (cont'd)

these pins possibly appear from the instability in the sub-layer.

Kline:

Okay, but would you agree that there are other possible explanations for the source of hairpin vortices than sub-layer instability? Would you agree or disagree with that?

Bandopadhyay:

Well, it's again a speculation and we want to say that this model seems to suggest and again we may be wrong, that it's not really necessary to postulate another type of instability on the upstream side of the interface. One would like to take a hypothesis which has least number of assumptions.

Kline:

We better stop at this point -- let me recognize Ron Blackwelder.

Blackwelder:

In addition to these other problems, I have one comment on this type of measurement. You can see from your films that these things come about in the outer region. Your flow being in this direction, I think you're probably getting your major correlation from back here -- you mentioned it's from the back. (Points at the back or upstream face of a large outer region bulge.)

Bandopadhyay:

Opposite interface -- yes!

Blackwelder:

But this interface slope obviously changes as you go downstream, and you have your probe set at a very fixed angle. This tends to tell me that you're going to be picking out a certain sub-set of these events from which you are getting most of your measurements. That sub-set would change I would presume if you change the sweepback angle between your probes. Also, I think what you are measuring probably is one of the structures at a given age in its lifetime. It starts out and you can see some of these in your film, maybe something like that -- and it bends over with the top moving relatively downstream, and then it gets even flatter. There's also possibly a Reynolds number effect involved. Eckelmann's data from his oil channel was different,

Blackwelder: (cont'd)

I don't know what their maximum angle was, but it was probably small compared to what you have. Brown and Thomas, which I believe is at even a higher Ryenolds number, have still another angle. So I think there's a little confusion -- we're mixing too many things together involving too many variables.

Bandopadhyay:

Well Brown and Thomas, I think they are talking about the opposite interface, but we are not talking about that, the envelope of the individual features...

Blackwelder:

I guess I disagree with that because looking at your film it seemed to me that when you had the largest correlation of events was when the upstream face of a bulge crossed your probe, and you could actually see a black area without any smoke.

SESSION II

SENSORS AND CORRELATION

Session Chairman:

L. S. G. Kovasznay

SURVEY OF MULTIPLE SENSOR MEASUREMENTS AND CORRELATIONS IN BOUNDARY LAYERS

William W. Willmarth

Department of Aerospace Engineering

The University of Michigan, Ann Arbor, MI 48109

ABSTRACT

The paper is a survey of space-time correlation and a few conditionally sampled measurements of turbulent structure in boundary layers using various sensors. The measurements discussed show that while much has been learned during the past few decades the structure of the turbulence in boundary layers near the wall is still an open question. One of these questions that must be examined is the nature of the flow field at very small scales since the available evidence indicates that very few sensor measurements were made with sensors that properly resolve the small scale fluctuations. Measurements with a small X array hot wire probe are described. The measurements were not valid below $y^+ < 400$ because the probe was too large to resolve turbulent fluctuations whose smallest scale was of the order of one viscous length, ν/u_τ. This result indicates a need for better instrumentation to advance our knowledge of the energetic small scale turbulent structure near the wall. Such knowledge should lead to better understanding of the phenomenon of drag reduction and the development of better prediction methods for turbulent flows.

I. INTRODUCTION

The subject of this paper is sensor measurements and correlations in turbulent boundary layers. It is intended that the paper should be a survey of the field which will provide a frame of reference for further discussion and set the stage for the three invited papers which follow.

One of the principal goals of turbulence research is knowledge of correlations among flow variables. For example, as a result of research on turbulent shear flow we would like to understand the flow structure that produces the correlation, $\overline{uv}$, between the velocity fluctuations parallel and normal to the wall. This would allow prediction of the Reynolds stress, $-\rho\overline{uv}$ (i.e. the average rate of turbulent momentum transfer). In other problems we may need to know the correlation between normal velocity and mass or temperature fluctuations in order to understand turbulent transfer of mass or heat. We will confine our discussion to flow structures important for streamwise momentum transfer in incompressible turbulent boundary layers.

Approximately 25 years ago numerous results from measurements of velocity fluctuations at a point using hot wires had been published. The measurements were used to determine the intensity and spectra of the velocity fluctuations and the magnitude of terms in the turbulent energy balance equation. According to Perry and Abell (1975) the experimental results from these and other studies of the fully developed flow in a tube show considerable inconsistencies with differences in the reported rms turbulence level as large as 25%. Perry and Abell (1975) attributed the differences to a number of factors primarily associated with ill-conditioned hot wire-anemometer calibration methods and inaccurate knowledge of the hot wire filament position. Perry and Abell made new measurements of the streamwise velocity fluctuations in fully developed pipe flow. They used dynamically calibrated hot wire anemometers and carefully observed the actual position of the heated hot wire filament. Their new measurements were accurate enough to reveal the scaling laws for streamwise velocity fluctuations.

It is well known that in the wall region the mean velocity depends upon, y, the distance from the wall and scales with the friction velocity, u_τ, where $u_\tau = \sqrt{\tau_w/\rho}$. The distance from the wall scales with the viscous length, ν/u_τ, so that the scaling law for mean velocity in the wall region is

$$\overline{U}/u_\tau = f(yu_\tau/\nu) \tag{1}$$

In the outer or wake region the mean velocity defect, $U_\infty - \overline{u}$, scales with u_τ and the length scale is the pipe radius, R. The scaling law is

$$(U_\infty - \overline{U})/u_\tau = g(y/\delta) \tag{2}$$

The measurements of Perry and Abell (1975) showed for the first time the same scaling for the streamwise velocity fluctuations.

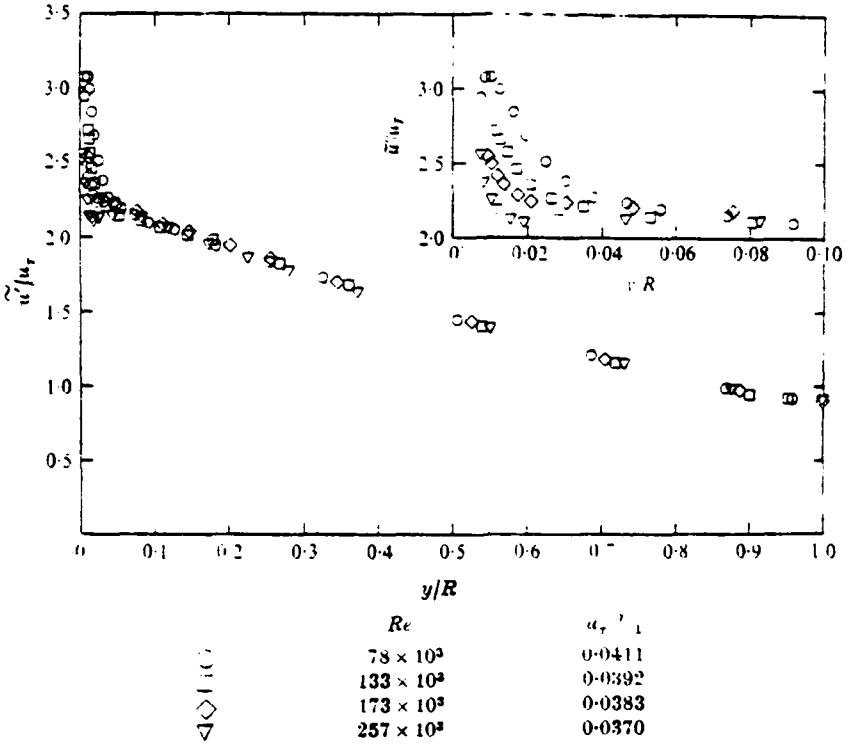

Figure 1 RMS Longitudinal turbulent velocity outer flow scaling: from Perry and Abell (1975)

In Fig. 1 are shown their measured rms velocity fluctuations scaled with outer flow variables. The inset in Fig. 1 shows that for $y/R < 0.1$ the data do not scale with outer variables. In this region close to the wall the data scale with the wall variables. Perry and Abell (1975) plotted the data as shown in Fig. 2. The consequence of the two plots is that a region of constant $\tilde{u}'/u_\tau$ appears for $y/R < 0.1$ and $yu_\tau/\nu > 100$. This is the region of overlap between the law of the wall and the outer variable scaling. In this overlap region the rms velocity fluctuations, $\tilde{u}'$, should scale with either inner (wall) or outer (wake) variables.

Figure 3 from Perry and Abell (1975) is a plot of the quantity Ψ versus frequency, ω, in the region of overlap where $\tilde{u}'/u_\tau$ is constant. In Fig. 3 the quantity

$$\Psi = \omega\Phi \, . \tag{3}$$

Φ is the power spectrum given by

$$\int_0^\infty \Phi(\omega, x_1, x_2, x_3)\, d\omega = (\tilde{u}'/u_\tau)^2 . \tag{4}$$

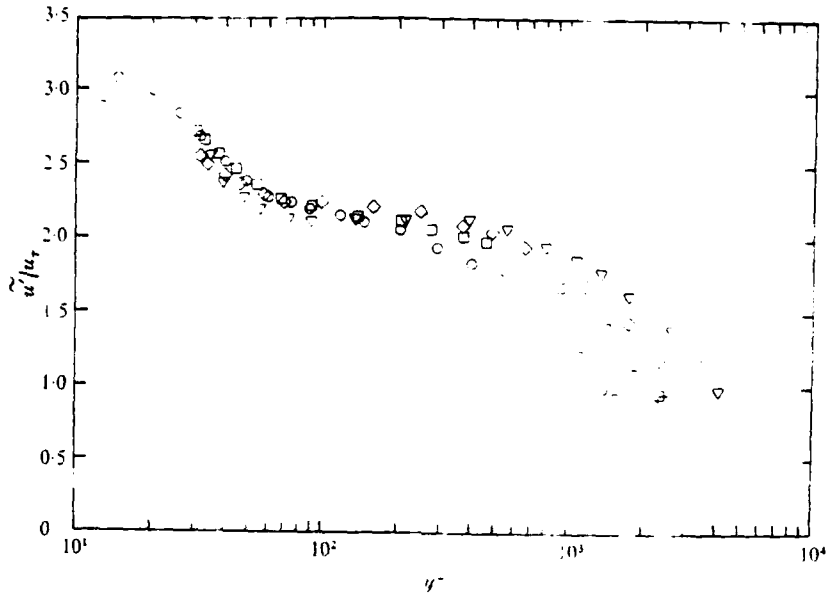

Figure 2 RMS Longitudinal turbulent velocity inner scaling symbols as for figure 1: from Perry and Abell (1975)

The data of Fig. 3 at 4 different Reynolds numbers and at various values of y/R show that in the region of overlap, $y/R < 0.1$ and $yu_\tau/\nu > 100$, the power spectra in the energy containing range scale with the characteristic frequency U/y. Perry and Abell conjectured that in the region of overlap a more precise universality of the power spectrum would occur if wave number/phase-velocity concepts were used.*

The results of Perry and Abell (1975) for the complete scaling of streamwise velocity fluctuations with wall and outer variables could not be extended to the velocity components normal to the wall and transverse to the wall. Their measurements with X hot wire-anemometers were not sufficiently accurate to give results without errors of the order of ±5%. It was possible to observe approximate scaling of the normal rms velocity fluctuations, $\tilde{v}'$, with outer variables. Perry and Abell concluded that scaling of $\tilde{v}'$, with outer variables was plausible. The errors in the measurements which prevented the verification of the scaling with inner variables is caused by the sensitivity of transverse velocity measurements to slight probe misalignment and/or bowing of the heated hot wire filaments. If bowing occurs and cannot be observed Perry and Abell are of the opinion that dynamic calibration of the probe is no more reliable than conventional static calibration methods.

The above results are very significant because they are the first measurements known to this author showing consistent scaling laws for any of the fluctuating turbulent flow variables. The mean flow velocity scaling, which is produced by the turbulent mixing caused by fluctuating velocities has been known for a long time. It is certain that the fluctuating flow must therefore obey similar scaling laws but the accurate measurement of fluctuating quantities is much more difficult than measurement of mean quantities.

*See their latest paper, Perry and Abell (1977), for further information.

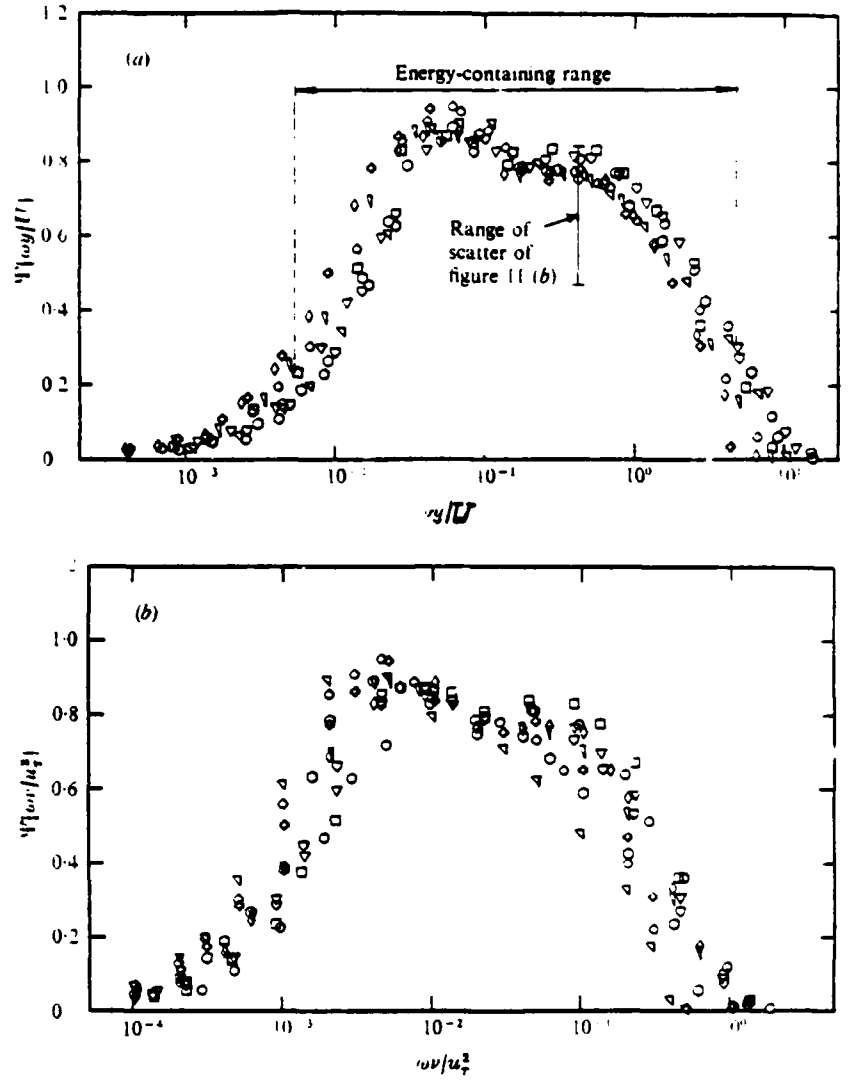

Figure 3 Power spectra of longitudinal turbulent velocity within region of constant $\tilde{u}/u_\tau$: from Perry and Abell (1975)

	$Re \times 10^{-3}$	y^+	y/R	U/u_τ
△	80	150	0·0934	17·6
◇	120	100	0·043	16.6
+	120	150	0·064	17.59
◁	120	200	0·086	18·3
▷	180	104	0·03	16·6
□	180	138	0·04	17·31
▽	180	275	0·08	19·2
○	260	148	0·03	17·6
○	260	246	0·05	18·8
○	260	444	0·09	20·4

The measurement of fluctuating quantities in turbulent boundary layers is more difficult than measurements in fully developed pipe flow. In boundary layers one must contend with the effects of free stream disturbances, spanwise flow nonuniformity and variations in the mode (natural or tripping) of the transition to turbulence, in addition to the difficult instrumentation and calibration problems addressed by Perry and Abell. The hot wire anemometer measurements to be discussed in the remainder of this paper were not made with the dynamic calibration methods that Perry and Abell have shown are necessary for accurate results. Consequently, only general conclusions involving relatively large changes in measured quantities will be reliable. Differences between turbulence measurements of less than 25% obtained with different sensors or in different experimental environments, see Perry and Abell's (1975) discussion, may be caused by effects unknown to or beyond the control of the investigator.

II. SPACE-TIME CORRELATION MEASUREMENTS

The first two point, space-time correlation measurements in turbulent flows were made by Favre. A summary of the measurements is reported in Favre, Gaviglio and Dumas (1957) and (1958). The flow sensors used in the measurements were single hot wires sensitive to streamwise velocity fluctuations. Assuming that the velocity fluctuations are statistically stationary in time, the correlation coefficient

$$R(\vec{x}',\vec{x},\tau) = \overline{u(\vec{x}',t)\, u(\vec{x},t+\tau)} \Big/ \left[\overline{u^2(\vec{x}',t)}\ \overline{u^2(\vec{x},t+\tau)}\right]^{1/2} \qquad (5)$$

is a function only of the time delay, τ, between the two velocity signals. In boundary layers the flow field is very nearly statistically homogeneous in planes parallel to the wall. The correlation coefficient is then a function of the distance of one wire from the wall and of the separation vector between the two wires.

$$R(\vec{x}',\vec{x},\tau) = R(y',\vec{x}' - \vec{x},\tau) \qquad (6)$$

The measurements of Favre et al. (1957), (1958), were an important advance because they gave evidence for the evolution and structure of the turbulent velocity field. In general their results showed that the large scale streamwise velocity fluctuations are convected with the local mean speed. They concluded that Taylor's hypothesis may be applied to the larger scale features at distances from the wall greater than 3% of the boundary layer thickness. Favre et al. also measured the time delay required for the maximum correlation between two probes at the same streamwise and spanwise station but at different distances from the wall. Their measurements showed that the convected turbulent structure was inclined to the wall. A positive time delay of the signal from the probe nearest the wall was required for a maximum of the correlation coefficient. The time delay required for maximum correlation was greater as the distance between the probes increased.

The three-dimensional nature of the turbulent structure was also examined. Figures 4 and 5 from Favre et al. (1958) show two-point

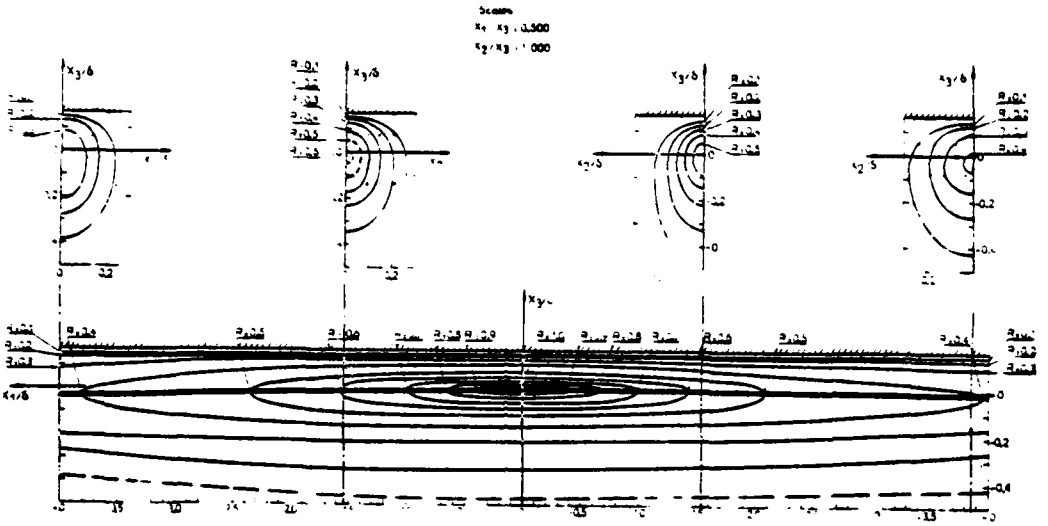

Figure 4 Space-time isocorrelation contours with optimum delay δ = 22 mm, R_δ = 27900 y'/δ = 0.15: from Favre et al (1958)

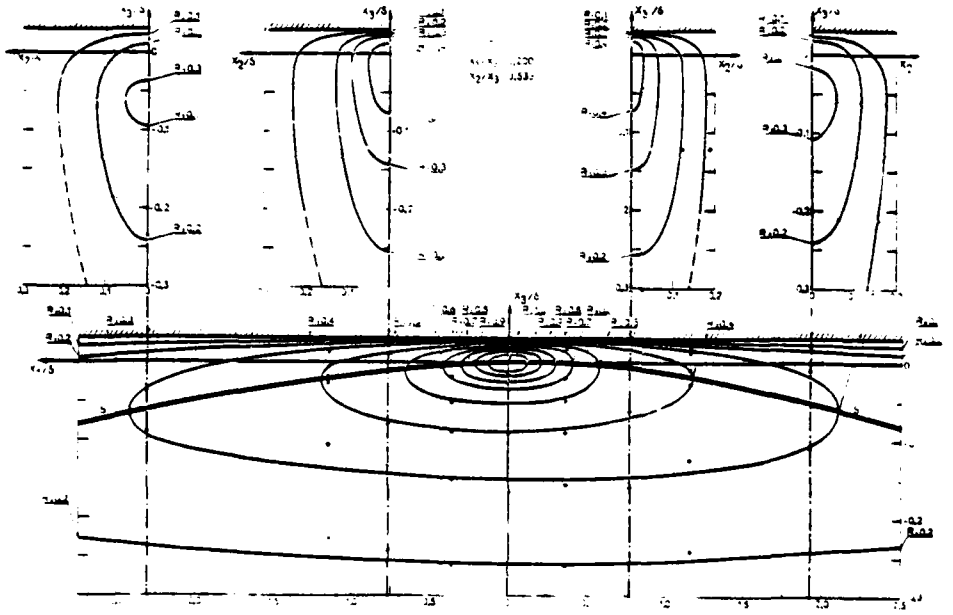

Figure 5 Same as figure 4 except y'/δ = 0.03: from Favre et al (1958) isocorrelation contours in the boundary layer when one velocity sensor is moved about relative to the other fixed sensor and the time delay is that required for maximum correlation. Favre et al. call this time delay the optimum time delay. In Fig. 4 the fixed sensor is located at y'/δ = 0.15 and in Fig. 5 it is very near the wall at y'/δ = 0.3. The isocorrelation surfaces are sausage like and are greatly elongated in the streamwise direction and more inclined to the wall when the fixed probe is near the wall. Figures 4 and 5 are, however, rather misleading because the optimum time delay varies a great deal and actually changes sign when the probe farthest from the wall is moved from an upstream to a downstream position.

Recently, Blackwelder and Kovasznay (1972) have published results using space-time correlation measurements that show more clearly the actual average shape of the convected turbulent structure. Figure 6 is a plot of two-point space-time isocorrelation contours measured with probes separated only by a variable distance normal to the wall. Since the structure is convected a negative time delay is analogous to a downstream separation distance between the probes. The average shape of the convected evolving turbulent structures is clearly evident. The dashed line is the locus of greatest downstream extent of a given value of the correlation coefficient and is located approximately along the trajectory of eddies ejected from the wall region, see Kline et al.

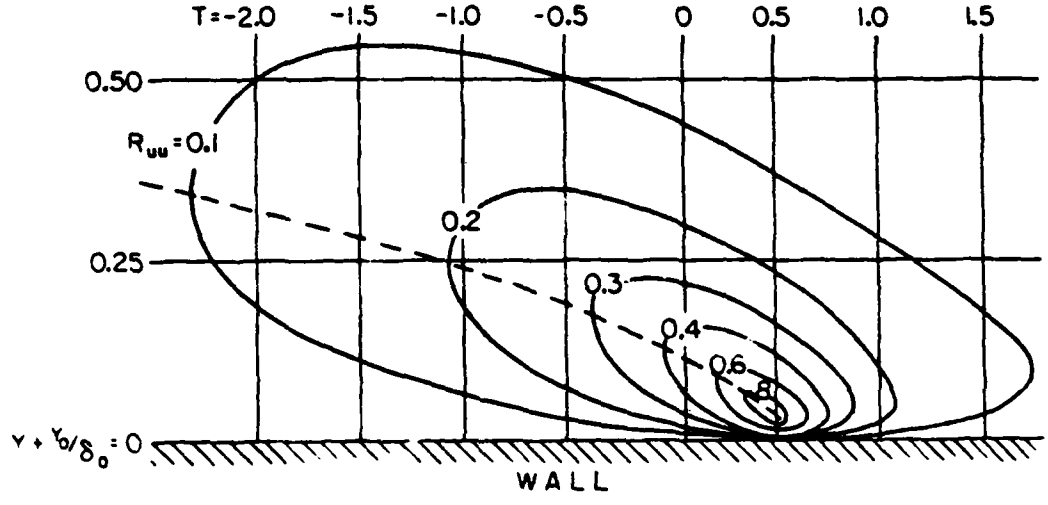

Figure 6 Space-time correlation map of u deep in the boundary layer. Fixed probe at y/δ = 0.03 (y^+=24): from Blackwelder and Kovasznay (1972)

(1967). Note that Favre et al. (1951),(1958), obtained similar data but did not plot it in this form.

Figure 7 shows the results of similar measurements of the space-time correlation of velocity fluctuations normal to the wall also published by Blackwelder and Kovasznay (1972). Note that in this case the

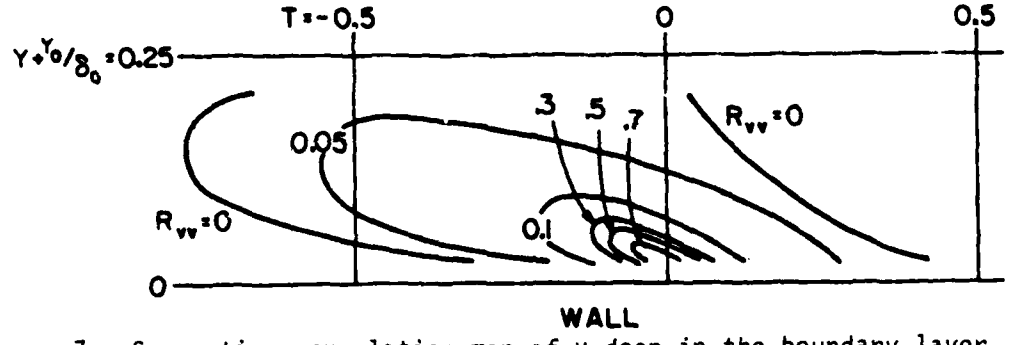

Figure 7 Space-time correlation map of v deep in the boundary layer. Fixed probe at y/δ = 0.03 (y^+=24): from Blackwelder and Kovasznay (1972)

reduced size of the isocorrelation contours in directions normal and parallel to the wall. It appears that the spatial extent of coherent vertical velocity fluctuations is much less than the scale of longitudinal velocity fluctuations.

In both Figs. 6 and 7 the fixed probe is very near the wall at $y'/\delta = 0.03$. Blackwelder and Kovasznay (1972) point out that the correlation patterns indicate that ejected bursts from the wall region must effect the outer intermittent flow field since the correlation coefficient is still 0.1 at $y'/\delta > 0.5$ which is well within the intermittent region.

These results obtained from space-time correlations are very interesting and suggest that there is a relationship between the flow in the wall region and the outer flow. It is very difficult to extract more specific information from long time average correlation measurements. In this regard Mollo-Christensen has pointed out that averages may hide rather than reveal the physics of a process. He gave the following absurd example to serve as an illustration, Mollo-Christensen (1971);

> "Say that a blind man using a road bed sensor attempted to find out what motor vehicles looked like. Happening to use a road only traveled by airport limousines and motorcycles, he concludes that the average vehicle is a compact car with 2.4 wheels. He might later attempt to construct a theoretical model of the mechanics of such a vehicle, and may attain fame for a tentative model that looks like a motorcycle with a sidecar whose wheel is only in contact with the ground forty percent of the time."

In the boundary layer the concept of conditionally sampled and/or averaged measurements of the flow field was used by Kovasznay et al. (1970) in an attempt to remove some of the ambiguity introduced by long time averages. Conditionally sampled measurements have been quite successful in revealing new facts about the turbulent structure. However, in the interest of a brevity only a very few results of conditionally sampled measurements will be cited.

III. CONDITIONALLY SAMPLED MEASUREMENTS OF VELOCITY AND TEMPERATURE

There is not time to properly discuss the difficult problems associated with conditionally sampled measurements. These problems include the detection of the desired phenomenon to be used for conditional sampling and the removal of random spatial or temporal variation from sampled sensor signals.

Conditionally sampled measurements were made by Chen (1975), under Blackwelders direction, of the temperature contaminated flow field in a boundary layer developed on a slightly heated wall. Chen employed an array of hot wire sensors to detect the ejection of heated fluid from the wall region. Figure 8 is a reproduction from Chen's thesis of the simultaneous temperature traces from an array of ten hot wire sensors operated at very low heating current. The sensors were placed one

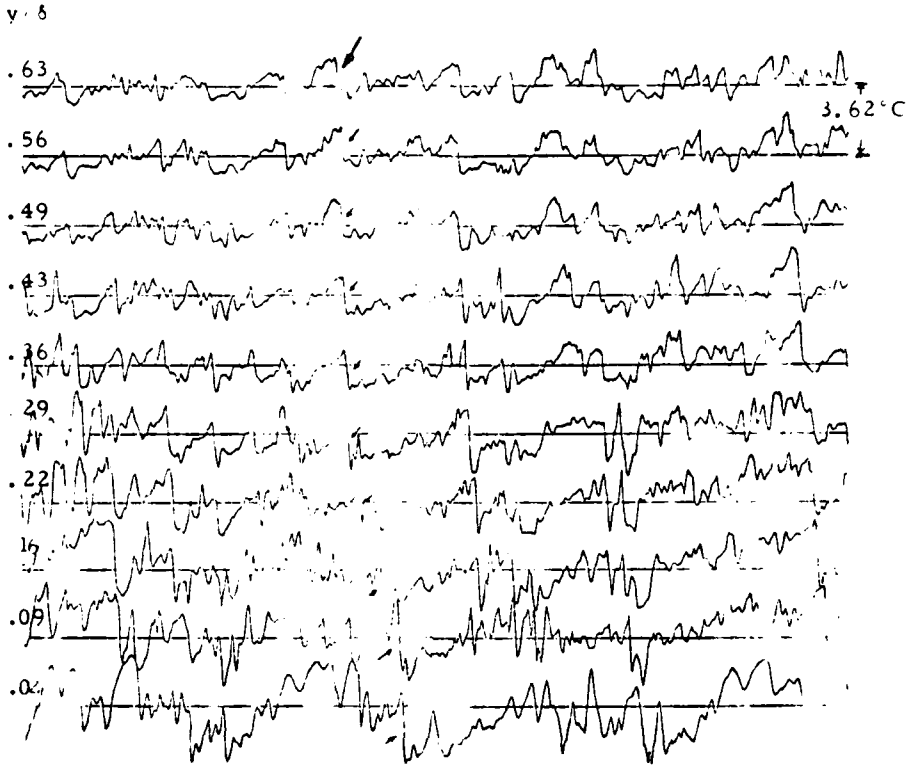

Figure 8 Simultaneous temperature traces from ten wire rake. Horizontal time span 18.7 δ/U_∞ : from Chen (1975)

above the other across the boundary layer. There are, on occasion, similar and clearly identifiable changes in temperature on each temperature trace in Fig. 8. One such temperature change is identified by the arrows in the middle of the figure. These identifiable temperature changes indicate the occurrence of "internal fronts" of ejected parcels of slightly heated fluid from the region near the wall out to the intermittent region. Chen (1975) studied this phenomenon in great detail and made conditionally averaged measurements of the u and v velocity fluctuations as well as the temperature fluctuations.

The conclusion that he reached was that the internal fronts display a strong spatial coherence and exist at all locations across the boundary layer. The velocity measurements associated with the internal fronts revealed that downstream of the front heated fluid with a streamwise momentum defect was moving upward. Upstream of the front colder fluid with a streamwise momentum excess was moving downward towards the wall. Figure 9 is a composite picture of the velocity field associated with the internal front. Far from the wall the internal front was associated with the back of a turbulent bulge in the intermittent region, see Kovasznay et al. (1970). Near the wall the internal front was associated with the "bursting phenomenon," see Willmarth (1975) or Blackwelder and Kaplan (1976), which is responsible for a large fraction of the Reynolds stress in the wall region.

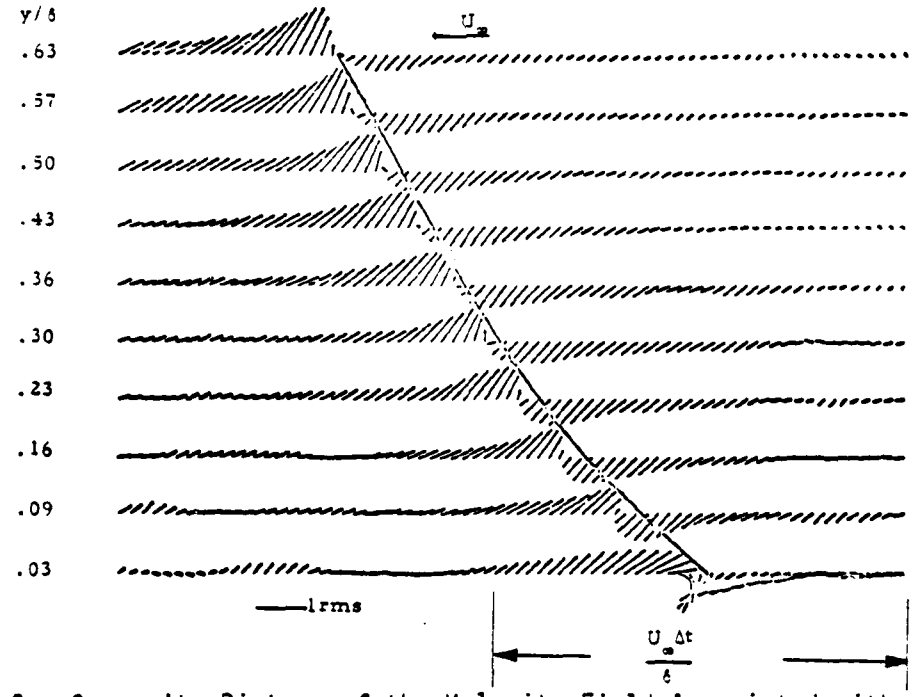

Figure 9 Composite Picture of the Velocity Field Associated with the Internal Front. Each Velocity Component is Normalized with its Local Fluctuation Level: from Chen (1975)

IV. SPACE-TIME CORRELATION MEASUREMENTS OF PRESSURE, VELOCITY & VORTICITY

Let us now return to correlation measurements of other flow variables. In 1954 I began work, under Hans Liepmann's direction, on measurements of pressure fluctuations in turbulent boundary layers. The work was initially oriented towards the study of aerodynamic sound generated by turbulent boundary layers. The radiated sound is small at subsonic Mach numbers. In practical problems the turbulent pressure fluctuations at the wall produce a motion of the wall which then radiates sound. At Liepmann's suggestion, space-time correlation measurements of the wall pressure fluctuations were made using a recently developed space-time correlator, Skinner (1956). Convection of the wall pressure fluctuations was discovered using two transducers; one downstream of the other. The research was continued at The University of Michigan in a thick turbulent boundary layer, Willmarth and Wooldridge (1962). Figure 10 shows a summary of the results of these space-time correlation measurements which were made with the aid of a tape recorder with variable playback head spacing to provide time delay. The convection of the wall pressure fluctuations is revealed by the occurrence of a ridge of positive $R_{pp}(x,\tau)$ above the x,τ plane. Here,

$$R_{pp}(x,\tau) = \overline{p(x_1,o,o,t)\ p(x_1 + x,o,o,t+\tau)} \Big/ \left[\overline{p^2(x_1,o,o,t)}\ \overline{p^2(x_1 + x,o,o,t + \tau)}\right]^{1/2} \qquad (7)$$

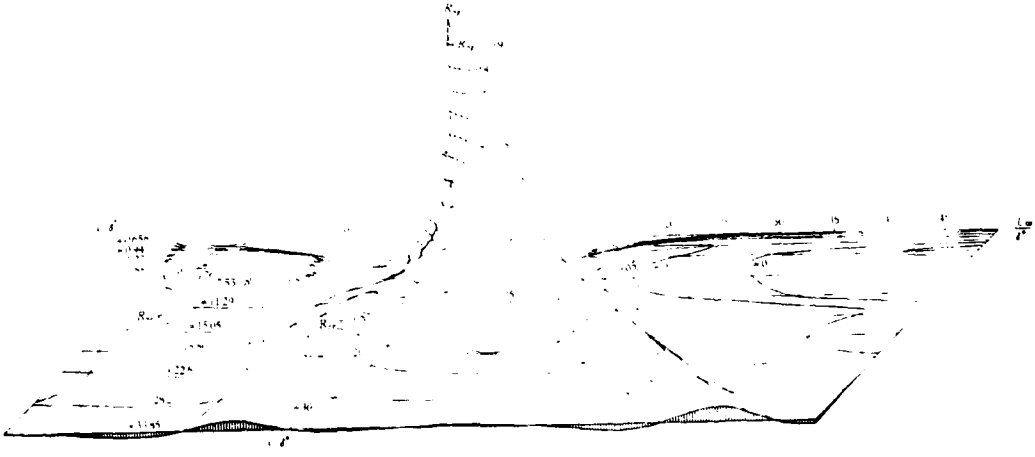

Figure 10 Longitudinal space-time correlation of the wall pressure: from Willmarth and Wooldridge (1962)

is the wall pressure correlation coefficient. In Eq. (7) the downstream growth of the boundary layer has been ignored. Thus, R_{pp} is a function of x and τ only because the wall pressure is assumed to be statistically homogeneous in space (the plane of the wall) and stationary in time. The slope of the trajectory of the ridge of positive R_{pp} in the x,τ plane is in some sense indicative of the convection speed of the turbulent eddies which produce the wall pressure fluctuations. The trajectory is somewhat curved in such a way that the slope is greater as x or τ increases. This indicates that when x and τ are large R_{pp} is small and only the larger longer lasting eddies are still correlated, along the ridge, and move at higher convection speeds. The convection speed is higher for the large eddies because they extend to a greater distance from the wall where the mean speed is higher.

After the space-time-correlation measurements of the wall pressure had been obtained we set out to determine more about the wall pressure field and the velocity field associated with the wall pressure fluctuations, see Willmarth and Wooldridge (1963). It was found that the spanwise extent of the instantaneous wall pressure correlation, measured in a reference frame moving at the convection speed, was somewhat greater than the streamwise extent of the same correlation. Measurements were made of the space-time correlation between the wall pressure and the three orthogonal velocity components u, v and w. The velocity components were measured with an "X" hot wire probe that could be moved about in the boundary layer. A strong convection of the space-time correlation between the wall pressure and any of the three velocity components was measured. Figures 11 and 12 show the result of correlation measurements R_{pu} and R_{pv}. Here the typical correlation coefficient between wall pressure and a velocity component (u for example) is defined as,

$$R_{pu}(x_1,x_2,x_3,\tau) = \overline{p(o,o,o,t)\ u(x_1,x_2,x_3,t+\tau)} \Big/ \left[\overline{p^2(o,o,o,t)}\ \ \overline{u^2(x_1,x_2,x_3,t+\tau)}\right]^{1/2} \qquad (8)$$

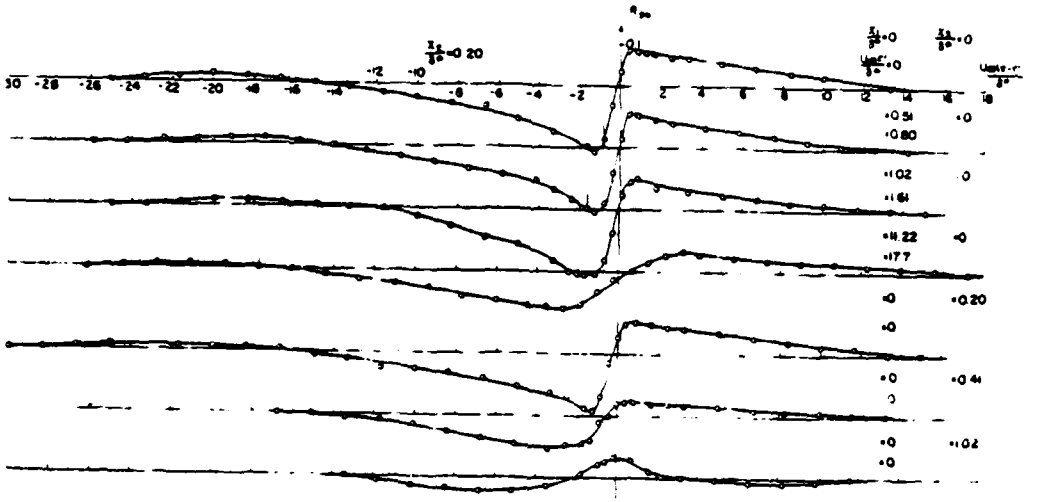

Figure 11 Measured values of the space-time correlation of fluctuating longitudinal velocity with fluctuating wall pressure: from *Willmarth and Wooldridge* (1963)

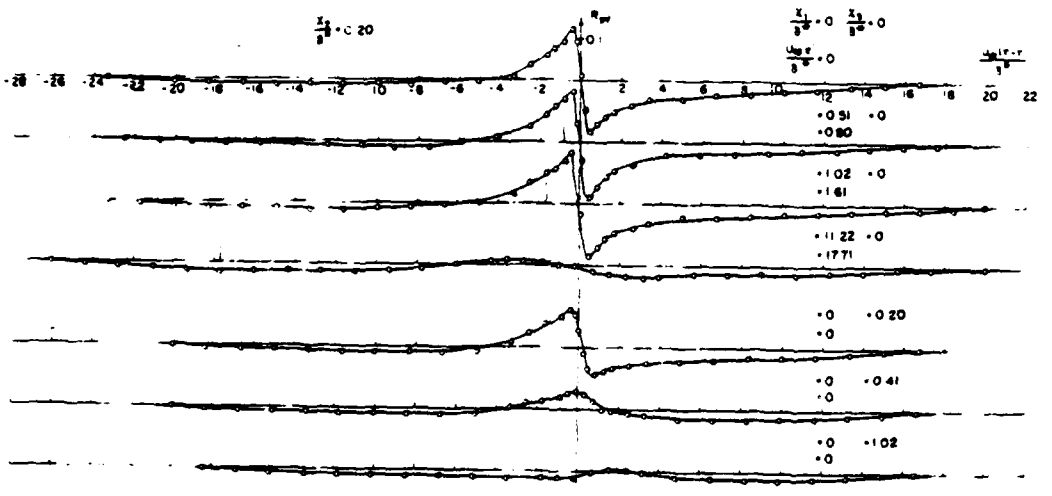

Figure 12 Measured values of the space-time correlation of fluctuating normal velocity with fluctuating wall pressure: from Willmarth and Wooldridge (1963)

In Figs. 11 and 12 one should note that the correlations measured with the hot wire probe in a streamwise plane normal to the wall and containing the pressure transducer indicate a strong convection effect. The short vertical bars on the second, third and fourth abscissa indicate the zero time delay location. It should also be noted that the correlations R_{pu} and R_{pv} are antisymmetric about the location of the velocity disturbance correlated with the wall pressure disturbance. The assymetry is quite remarkable and led us to propose a crude model for the pressure-velocity correlation in which a two-dimensional vortex moves past a wall-pressure transducer and a hot wire above the wall. A correlation coefficient was then defined as in Eq. (8) (with u replaced by v) and with an arbitrary displacement x of the hot wire probe (measuring v) with respect to the pressure probe. F.W. Roos (unpublished) computed the correlation by integrating the contributions of the wall pressure and v to the correlation during passage of the vortex (with solid-body core) past the hot wire and wall-pressure transducer, holding x = constant. The result of the computation is shown in Fig. 13 along with an actual measurement of R_{pv} from Willmarth and Wooldridge (1963). This crude

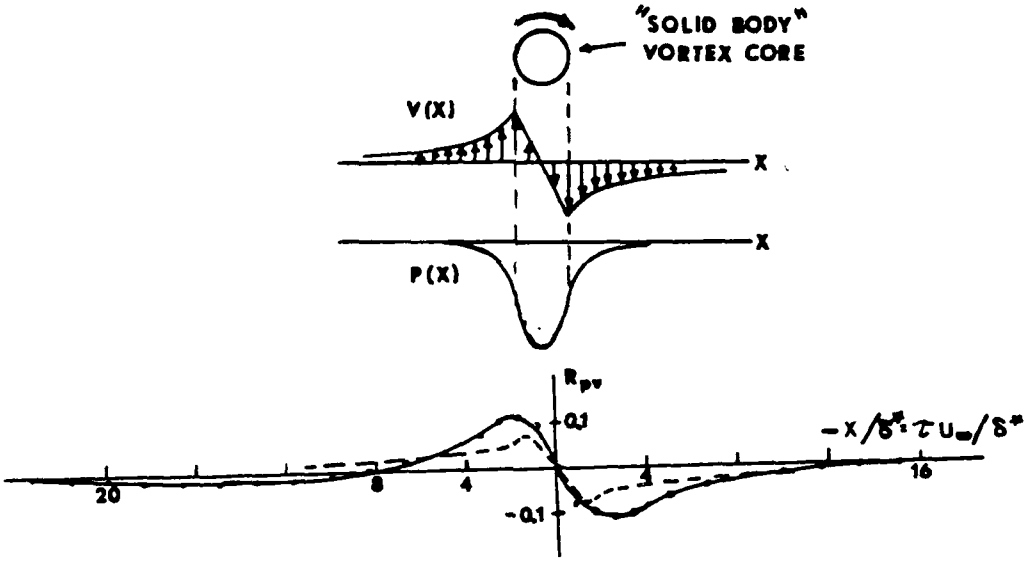

Figure 13 Qualitative model of the correlation R_{pv} computed by F.W. Roos and compared with a measurement by Willmarth and Woodridge (1963): - - - - model; —— measurement: from Willmarth (1975)

two-dimensional model produces correlations which are qualitatively comparable to the actual measurements.

We, Willmarth and Wooldridge (1963), also devised a scheme called the "vector field of correlations" in which the asymmetry of the R_{pu} and R_{pv} correlations leads to an interesting two-dimensional pattern shown in Fig. 14. In Fig. 14 one may visualize the average velocity field as a summation over an ensemble of flow disturbances. The direction of the average flow disturbance has been chosen assuming that a negative pressure perturbation is produced on the wall. One should note that this

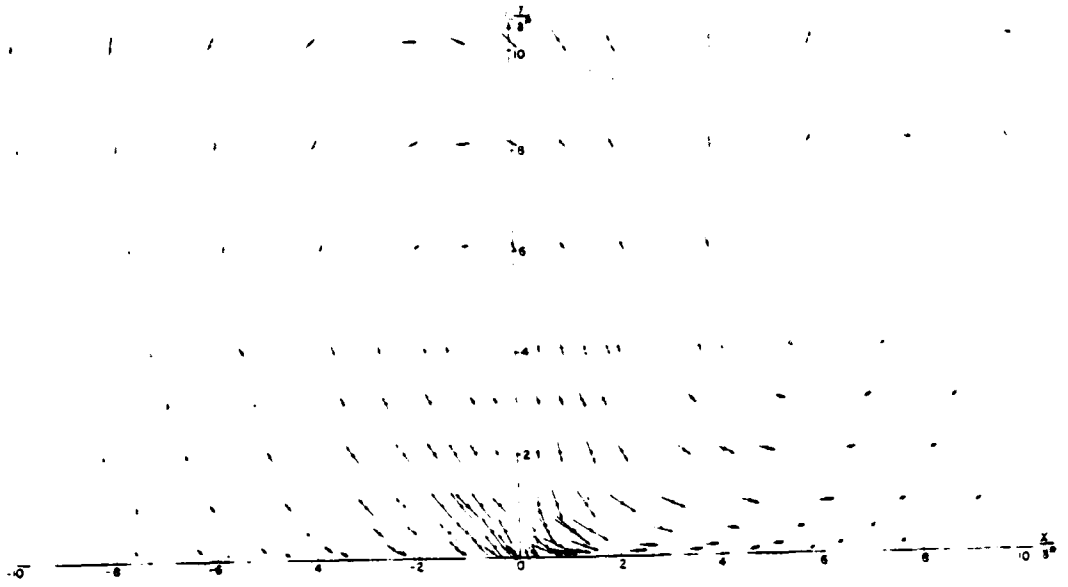

Figure 14 Vector field of correlation. Magnitude of the vector at any point is $\sqrt{(R_{pu}^2 + R_{pv}^2)}$. Direction of the vector at any point as measured from the positive x_1 axis is given by $\tan.^{-1} \frac{R_{pv}}{R_{pu}}$: from Willmarth and Woodridge (1963)

average flow disturbance is opposite to that associated with the internal fronts of heated air moving upward that were measured by Chen (1975), see Fig. 9. The relationship between flow disturbances responsible for ejections of fluid from the wall region and the flow disturbances associated with the wall pressure is not yet understood.

Willmarth and Wooldridge (1963) also considered the spanwise extent of the velocity field that is correlated with the wall pressure perturbations. It was found that far from the wall the surfaces of constant correlation of the wall pressure and the streamwise, u, or the normal velocity, v, fluctuations were elongated in the stream direction and roughly circular in planes normal to the wall and stream. However, when the hot wire probe was very near the wall the lines of constant correlation of R_{pv} at zero time delay became oblique to the stream in planes parallel to the wall. Figure 15 is an example showing the obliquity of the field of normal velocity perturbations which are correlated with the wall pressure perturbations. There is clearly a predominant obliquity of the vertical velocity field near the wall.

In an attempt to learn more about the oblique velocity field near the wall an extensive series of space-time correlation measurements was undertaken by Tu and Willmarth (1966). The measurements of the correlation between the wall pressure and the spanwise, w, velocity fluctuations were especially interesting. Figure 16 is a summary of these measurements. It can be inferred from these results that an oblique disturbance inclined to both the wall and the stream direction is associated with the

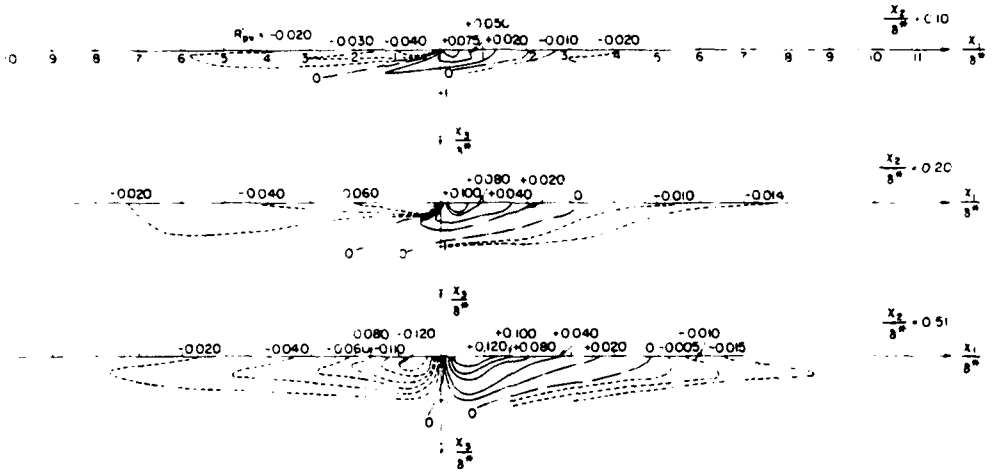

Figure 15 Correlation contours of R_{pv} in the x_1 - x_3 plane. Correlation normalized on the value of the velocity fluctuation at $x_2/\delta^* = 0.51$. Origin of coordinate system at pressure transducer: from Willmarth and Wooldridge (1963)

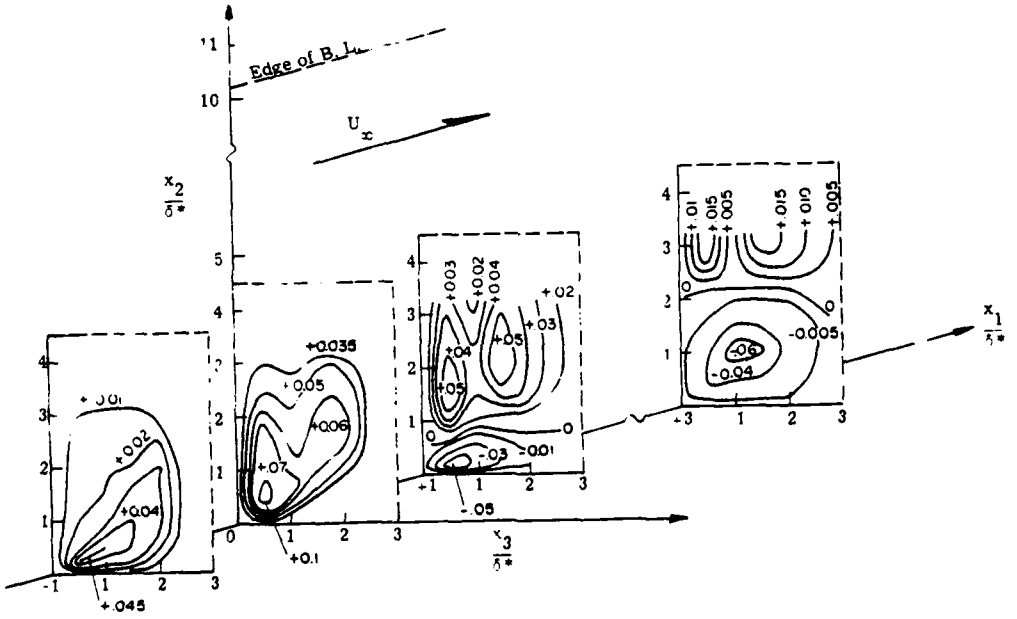

Figure 16 Three-dimensional diagram of contours of R_{pw} = constant: from Tu and Willmarth (1966)

wall pressure fluctuations. The disturbance clearly "lifts up" away from the wall in the downstream direction. The lifted up disturbance appears to be associated with a change in sign of the spanwise velocity fluctuation, w. This suggests that the lifted disturbance contains streamwise vorticity.

In order to investigate this flow field two probes each consisting of an array of four hot wires to measure streamwise vorticity were constructed by Bo Jang Tu, see Willmarth (1975), according to a scheme devised by Kovasznay (1954). The probes were placed side by side and as close together and as near the wall as possible. Space-time correlation measurements of the two probe signals were made but the correlation coefficient near the wall was zero for all time delays. This result indicates that the probes were too large to allow them to be placed close enough to measure the correlation produced by the streamwise vorticity near the wall. The vorticity probe dimensions were of the order of 150 viscous lengths (150 ν/u_τ). This means that the spacing between the probes was greater than 150 ν/u_τ and that the centers of the probes were more than 75 ν/u_τ from the wall.

Wyngaard (1969) has analyzed the spatial resolution of a streamwise vorticity probe exposed to isotropic turbulence. The analysis showed that the measurement errors are considerable unless the probe dimensions are of the order of the smallest turbulent scales (the Kohlmogorov microscale for isotropic turbulence). In the turbulent flow near the wall the smallest length scale in the newly generated turbulence must be of the order of the viscous length scale. The vorticity probe is much too large and is furthermore not within the sublayer. It is known, Kline et al. (1967), that the streaky, sublayer structure has a spanwise length scale of 100 viscous lengths. The vorticity probe could not resolve the streamwise vorticity presumably associated with the streaks.

Despite the poor spatial resolution a significant correlation between wall shear stress and streamwise vorticity was measured. Figure 17 shows the results of measurements of the instantaneous correlation, R, between the streamwise velocity very near the wall at the edge of the sublayer and the streamwise vorticity at an oblique angle downstream and slightly above and to the side of the point where the velocity was measured.

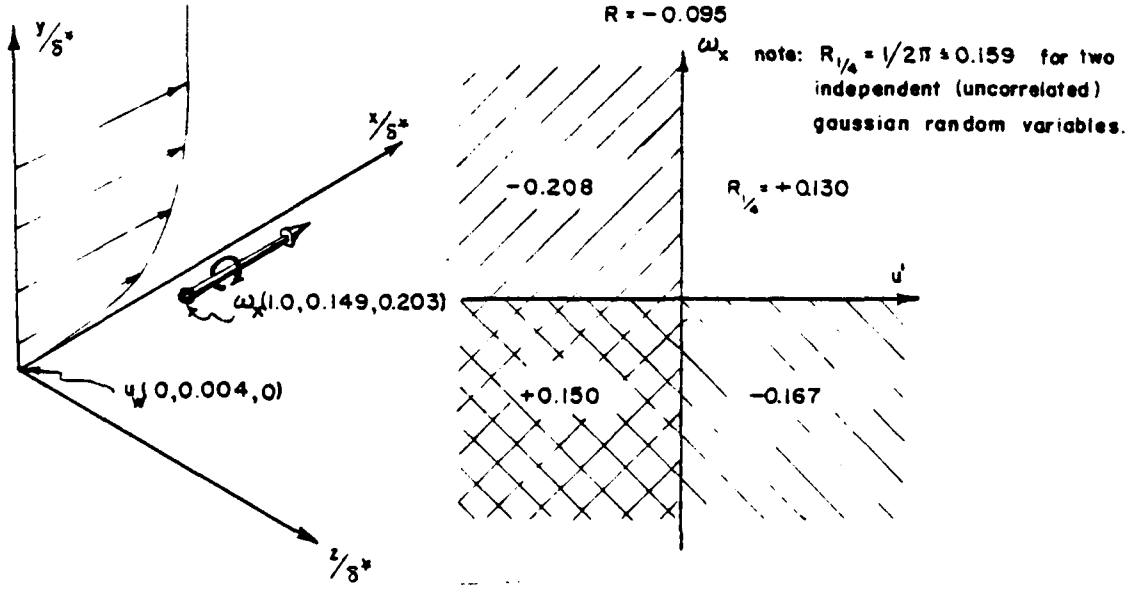

Figure 17 Contributions to Correlation Between Streamwise Vorticity and Velocity in the Sublayer from Four Quadrants in the u,ω_x Plane U_∞ = 204 ft./sec.: from Willmarth (1975)

The correlation, R, is defined as

$$R = \overline{u\omega_x} / \sqrt{\overline{u^2}\ \overline{\omega_x^2}} \qquad (9)$$

The velocity, u, very near the wall is proportional to the wall shear stress so that the correlation between the vorticity and velocity in Fig. 17 indicates a relationship between the flow structure and wall shear stress. At the position of the vorticity probe relative to the hot wire location near the wall the magnitude of the correlation between, u, and ω_x was a maximum. This indicates that oblique streamwise vorticity is associated with Reynolds stress which in turn is the cause of the wall shear stress. It is of interest to examine the most important contributions to the negative value of the correlation, R = - 0.095. If one selectively removes either the positive or the negative portions of both the u and ω_x signals one can determine the correlation in each quadrant of the u, ω_x plane. In Fig. 17 the result of the quadrant correlation measurements of R are displayed. It was found that the majority of contributions to the total correlation, R = - 0.095, occur in the second quadrant where u is negative and ω_x is positive.

Other results of the correlation measurements reported by Tu and Willmarth (1966) included measurements of the correlation between various velocity components measured at different points in the flow. As one example we found that the instantaneous correlation between vertical velocity components measured at two side by side points was positive far from the wall but became negative when the two probes were positioned very close to the wall. Figure 18 displays these results.

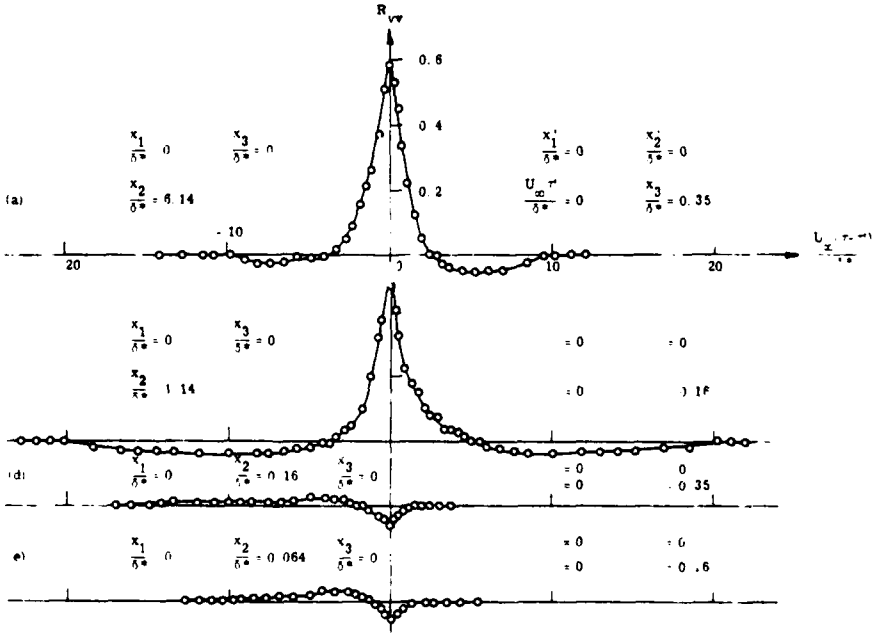

Figure 18 Measured values of the space-time correlation of v-v at various distances from the wall: from Tu and Willmarth (1966)

V. MODEL FOR TURBULENT STRUCTURE DURING BURSTING

Tu and Willmarth (1966) studied correlations between spanwise and normal velocity fluctuations at different points near the wall. From these measurements a model for the average structure of the flow fluctuations near the wall was devised. The model is consistent with the gross features of the flow but it was not intended to be accurate enough to provide quantitative information. Figure 19 is a sketch of the flow model which consists of hairpin shaped vortices produced by the lifting and stretching of initially spanwise vorticity. In this model a predominant

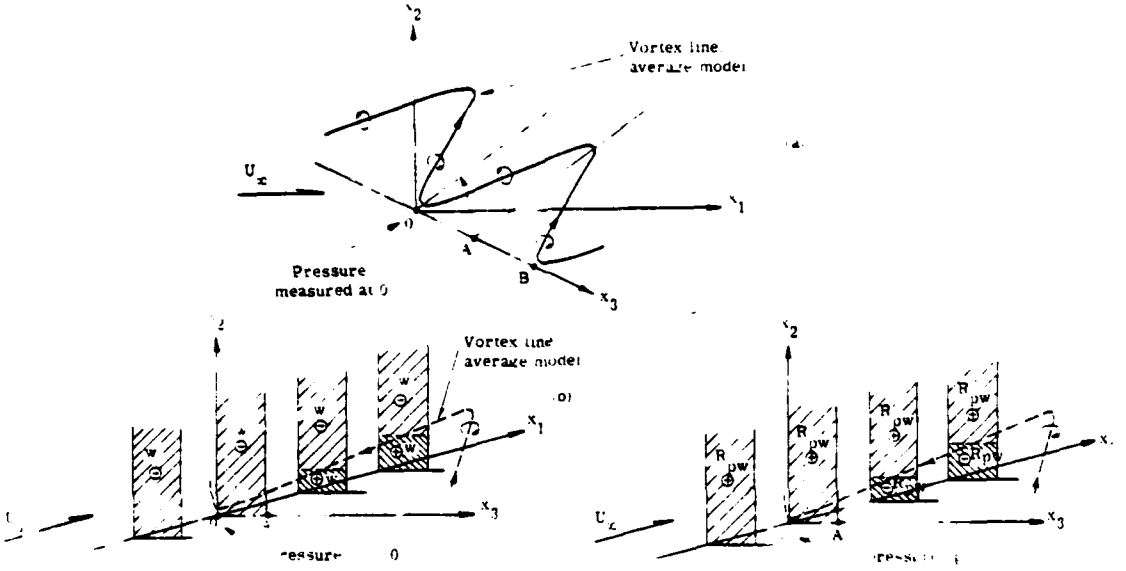

Figure 19 Structure of a random vortex line near the wall and the explanation of measurements of contours of constant R_{pw} at different x_2-x_3 planes: from Tu and Willmarth (1966)

feature is the occurrence of a pair of oblique vortices of opposite sign. We have proposed, Willmarth (1975), that if such closely spaced pairs of vortices occur there will be a strong mutual induction which will cause the vortices to move rapidly outward. The effect is shown schematically in Fig. 20.

If the vortices are very near the wall they will tend to move together as a result of the induction of the "image" vorticity beneath the wall. When the vortices are close together the outward motion will become more rapid and violent. This is however a matter of speculation because the occurrence of pairs of streamwise vorticies has not been experimentally verified.

There have been a number of other investigators who have proposed models for the turbulent flow structure responsible for erruptions of low speed fluid from the wall region which,as Lu and Willmarth (1973) have shown, produce large contributions to the Reynolds stress. These models all contain oblique vortices in one form or another. Theodorsen (1952) was the first to propose that hairpin shaped vortices were important. Other models were proposed by Bakewell and Lumley (1967), Kline et al. (1967) and Townsend (1970). At present there is not enough

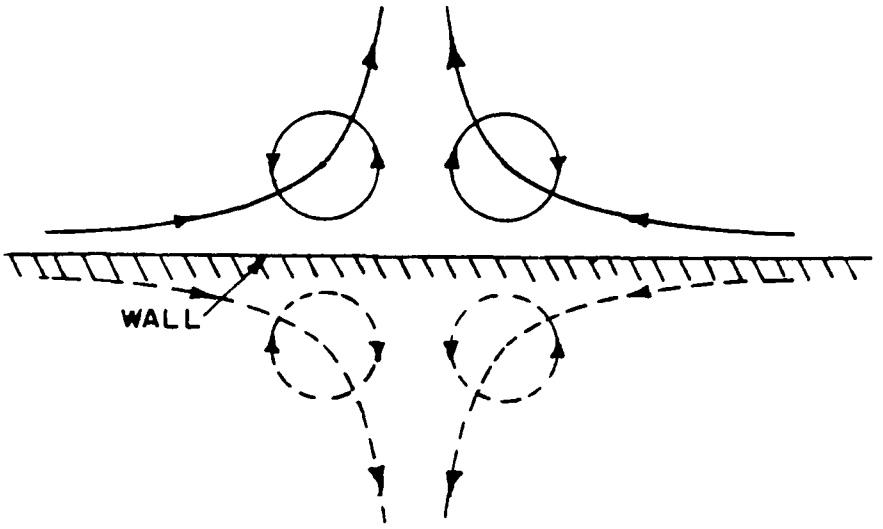

Figure 20 Sketch of vortex pair near the wall. Image of pair below the wall. Dashed lines are trajectories of vortex centers: from Willmarth (1975)

accurate information available from experimental measurements to determine the correct flow model.

VI. EVIDENCE FOR SMALL SCALE FLOW STRUCTURE NEAR THE WALL

To determine the important features of the flow during bursting so that a flow model can be constructed one must somehow extract coherent flow information from the random background turbulent flow. In addition, it has only recently become apparent that a very significant component of the flow structure near the wall is of extremely small scale and is very difficult to measure. There are a number of existing results from previous investigations that suggest that an energetic small scale turbulent flow structure occurs very near the wall.

Evidence for the existence of small scale turbulence near the wall has been obtained from pressure fluctuation measurements. Emmerling et al. (1973) performed an experiment in which a section of the wall of an acoustically quiet and vibration free wind tunnel was used as one of the mirrors of a Michelson interferometer. The pressure fluctuations within the boundary layer deflected the mirror surface, which was a thin reflecting membrane that covered an array of closely spaced holes drilled in the wall. Motion pictures of the fringe shift patterns on the membrane were analyzed to obtain instantaneous patterns of the wall pressure fluctuations. Figure 21 is an example of a sequence of four frames in which an intense small scale increase in pressure is observed to form and move downstream.

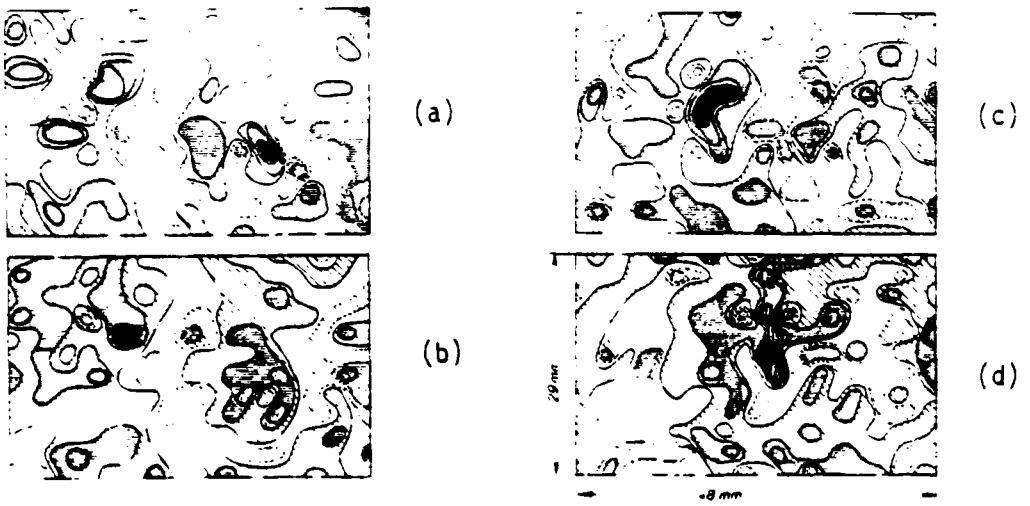

Figure 21 Contours of instantaneous pressure fluctuations. The darker shading indicates large pressure changes. Positive fluctuations are outlined with solid lines and negative fluctuations with dashed lines. Stream velocity is from left to right, time increases from (a) to (d): first frame (a) time = 17.57 msec, (b) time = 18 msec; (c) time = 19.14 msec; (d) time = 20.85 msec: from Emmerling et al (1973)

The smallest scale of the pressure fluctuations observable in these measurements was limited by the diameter (55 viscous lengths) of the holes drilled in the wall. On some occasions large reversals in the pressure fluctuations could be observed on the membrane surface over a single hole (during pressure reversals the fringes became "S" shaped). This indicates that the transverse scale of the pressure fluctuations is less than half the membrane diameter.

Further evidence supporting the existence of intense small scale pressure fluctuations was obtained from the results of measurements by a number of investigators of wall pressure fluctuations using small "pinhole" microphones. Figure 22 shows the results of these measurements as summarized by Bull and Thomas (1976). Notice that for pinhole diameters less than 100 viscous lengths there is a dramatic increase in the root-mean-square wall pressure. Bull and Thomas (1976) have shown that part of this increase is produced by the discontinuity in the surface caused by the pinhole. The open symbols in Fig. 22 show that the

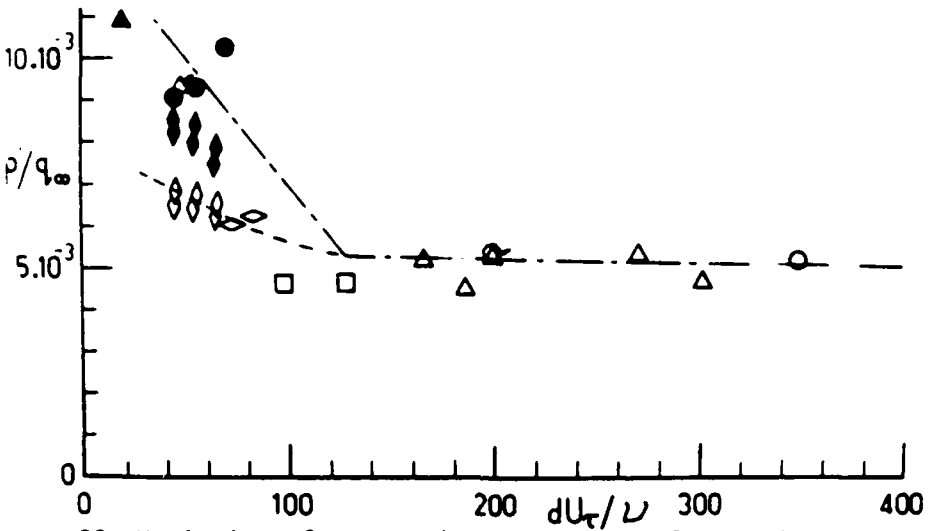

Figure 22 Variation of measured rms pressure fluctuation with transducer size and type. Pinhole data: ● Blake ; ▲ Emmerling ; solid diamond, present data. Flush-mounted capacitor microphone data: ⊿-Emmerling. Flush-mounted-piezoelectric data: ◇ Lim ; ○ Willmarth and Roos ; △ Bull ; □ Schloemer ; ◊ present data: from Bull and Thomas (1976)

smaller, correct, values measured by very small flush transducers are of the order of 50% higher than the value at $d^+ \simeq 100$. This indicates that the smaller scale wall pressure fluctuations (with scales less than 100 viscous lengths) are of comparable intensity to those of larger scales. (The addition of two uncorrelated random signals of equal strength will result in an increase in the root-mean-square of their sum by a factor of $\sqrt{2}$.)

Evidence for the existence of very small scale turbulent structure near the wall was obtained by Corino and Brodkey (1969) in their visual observations of the wall region. Figure 23 is a sketch based upon their visual observations of the wall region using high speed movies of the motion of small particles suspended in a liquid. The photographic field of view was highly magnified. For this reason the depth of field was small, of the order of 20 viscous lengths. On occasion, two layers of fluid could be observed moving in different directions at the same location within the field of view. This is direct evidence for highly sheared turbulent motions near the wall. The scale of these motions must be less than the depth of field, i.e. less than 20 viscous lengths.

VII. MEASUREMENTS WITH A SMALL HOT WIRE PROBE

The existence of small scale motions near the wall which appear to be very energetic induced us to attempt to develop an extremely small hot wire array. We have constructed an "X" hot wire array, for measurements of the u and v velocities and the Reynolds stress, that has typical dimensions (wire length and spacing) of 100μ (approximately 2.5 viscous lengths), see Willmarth and Bogar (1977). Figure 24 is a photograph of the probe and Fig. 25 is a drawing of the probe showing it positioned near the wall.

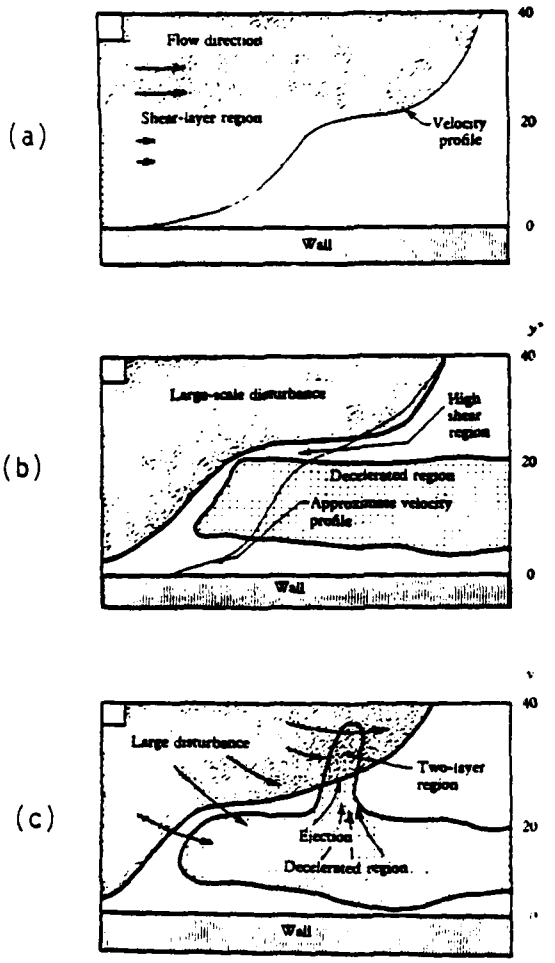

Figure 23 Sketch of a cross-sectional view of the flow during bursting: (a) formation of low speed region near wall, (b) entrance of large-scale disturbance, (c) ejection and two-layer velocity region: from Corrino and Brodkey (1969)

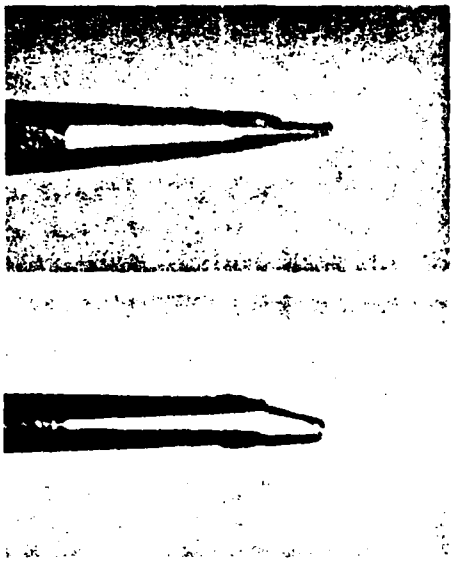

Figure 24 Small X probe. Photographs of top and side view: from Willmarth and Bogar (1977)

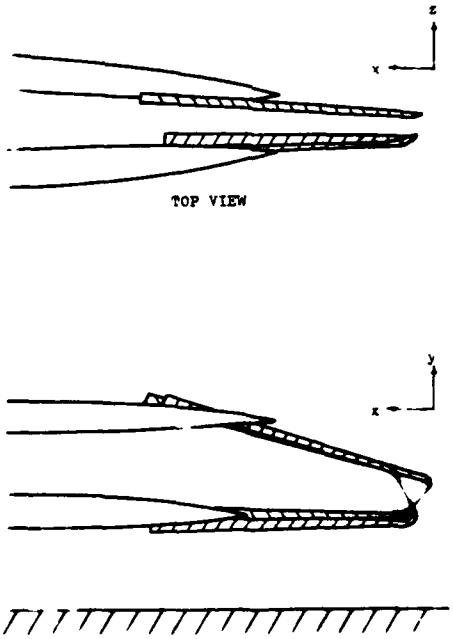

Figure 25 Small X probe. Drawing of sensitive region; top and side view: from Willmarth and Bogar (1977)

The X array was so small that it could not be made with a precisely aligned and oriented arrangement of the hot wires. To compensate for the lack of precision of the X array geometry a unique calibration scheme was developed to interpret the two electrical signals produced by the hot wire array. The method required that the X array be calibrated by exposure to every possible flow velocity vector. This was accomplished by placing the probe in a uniform flow and pitching it through a large angle, $\pm$ 75°, while slowly varying the flow speed. The instantaneous flow speed, U, pitch angle, Θ, and the two hot wire output signals, EL, and EU, were digitized and stored with the aid of a digital computer. Figure 26 is a sketch of the notation. From the stored calibration data a calibration "table" was set up so that for every pair of hot wire voltages, EL, and EU, there existed a unique pair of orthogonal velocity components, u, and v, relative to the probe axis.

The calibrated probe was then placed in the boundary layer and the two signals EL and EU were digitized and stored with the aid of the computer. A computer program was then used to "look up" in the calibration table the appropriate values of u and v for each of the voltage pairs EL and EU. The result of this measurement procedure was that far from the wall ($y^+ > 400$) the data for the root-mean-square values of the velocities u and v and the value of the Reynolds stress, $-\overline{uv}$, were in agreement with classical measurements. However, nearer the wall the measured pairs of EL and EU voltages would on occasion not correspond to any voltage pairs measured during calibration. As the probe was moved closer to the wall the occurrence of voltage pairs for which calibration data had not been obtained became more and more frequent.

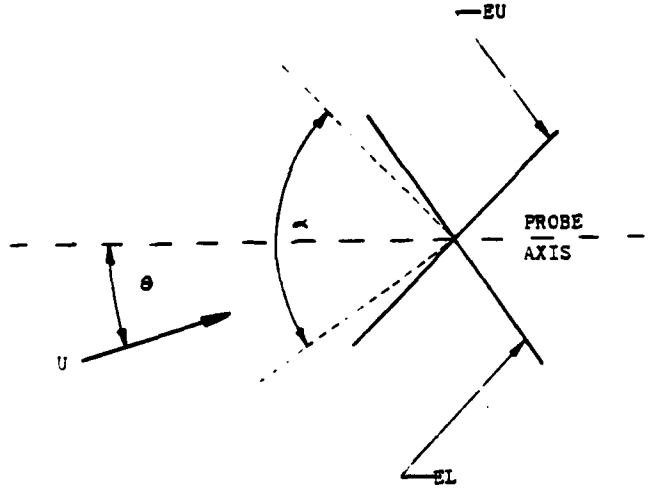

Figure 26 Geometrical arrangement and symbol definitions for X probe: from Willmarth and Bogar (1977)

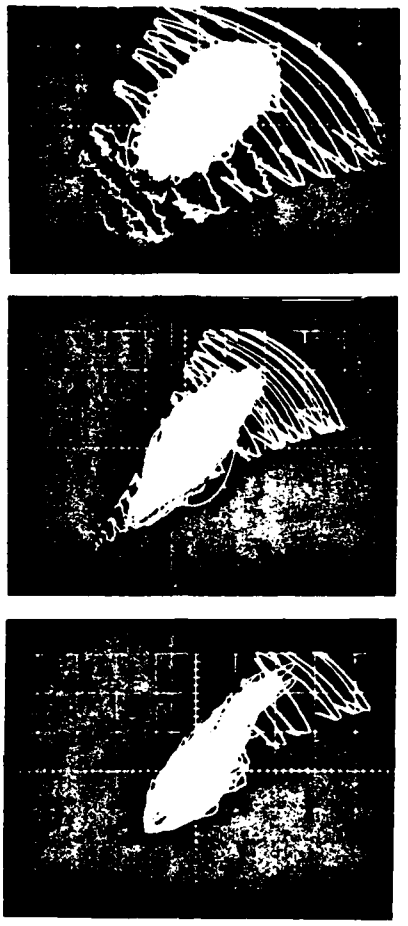

Figure 27 Photographs of EL and EU voltages during turbulence measurements and calibrations displayed on screen of storage oscilloscope. (a) $y^+ = 670$; (b) $y^+ = 65$; (c) $y^+ = 3$: from Willmarth and Bogar (1977)

Figure 27 is a series of three photographs of storage oscilloscope traces which were made to display this phenomenon. In each photo the triangular region covered by curved traces represents the area covered by the two hot wire signals EL vs EU during calibration of the probe. We will refer to this region as the calibration grid. In Fig. 27a the trace of the EL vs EU signals produced when the probe was a distance of $y^+ = 670$ from the wall occupies an elliptically shaped region that is well within the triangular calibration grid. However, in Fig. 27b and 27c, with the X probe a distance of $y^+ = 65$ and $y^+ = 3$ from the wall, the EL vs EU traces do not lie entirely within the calibration grid. In fact, in Fig. 27c approximately 40% of the time the EL vs EU trace at $y^+ = 3$ is outside the calibration grid. When the EL vs EU trace is outside the calibration grid the velocity pairs u and v are unknown. In other words the calibration scheme is clearly invalid.

We have carefully analyzed and examined the entire experimental procedure to determine why the EL, EU data does not always lie within the calibration grid, see Willmarth and Bogar (1977). The conclusion that we reached was that the flow in the region of the X probe hot wires was not uniform. Figure 28 is a sketch of the situation. Note that a small scale highly sheared region can cause vastly different cooling effects on the two hot wires. It should be noted that even though the EL, EU signals may lie within the calibration grid this does not guarantee that a highly sheared region of flow is not present at the X wires.

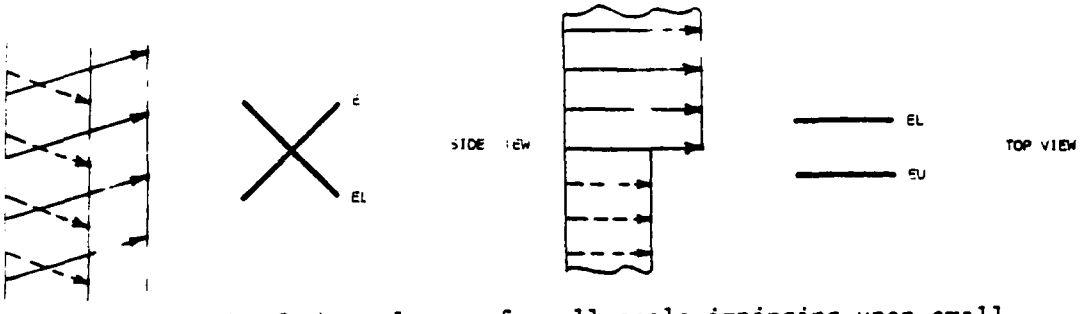

Figure 28 Sketch of shear layer of small scale impinging upon small X probe.

Data obtained with the X probe far from the wall, $y^+ > 400$, have been reduced using the calibration data. The results agree with classical measurements. Figure 29 is a plot of Reynolds stress versus distance from the wall obtained in this way. Nearer the wall, $y^+ < 400$, in Fig. 29 when the EL, EU data pairs made an excursion outside the calibration grid

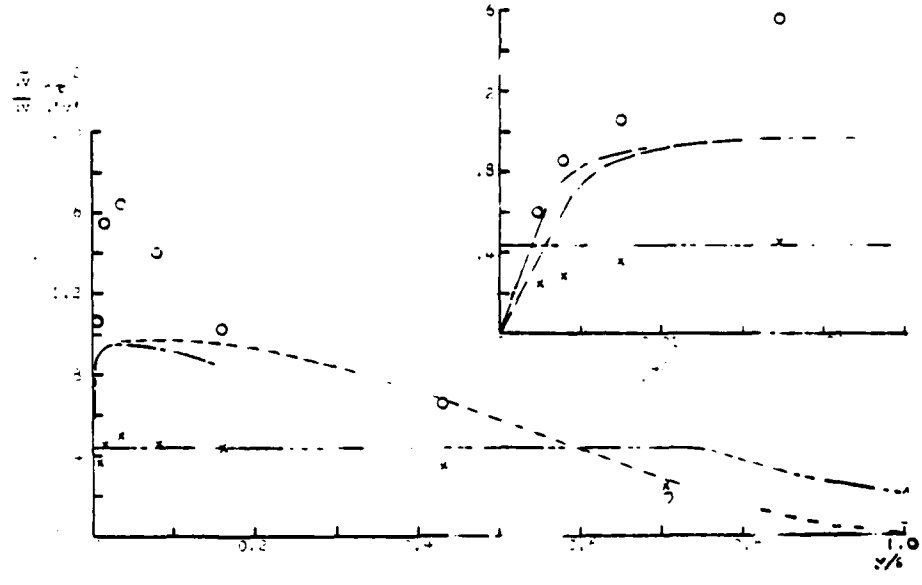

Figure 29 Profiles of Reynolds stress normalized with rms velocities and wall shear stress. o, $\overline{uv}/\overline{u^2}$, x, $\overline{uv}/u'v'$; ----, data of Klebanoff ; ——, data of Schubauer; —·—, data of Lu and Willmarth; — - —, profile calculated from mean profile: from Willmarth and Bogar (1977)

we obtained the u and v velocity components by using the last u,v pair that was within the calibration grid for every point outside the calibration grid during the excursion. In this way incorrect data was obtained. This arbitrary procedure is not correct and the data within the calibration grid is also incorrect when small scale highly sheared flow regions encounter the X probe. Therefore, the data in Fig. 29 for $y^+ < 400$ cannot be used and are not valid. There is no way to correct this data because it is not known when the presence of a thin shear layer at the X probe causes nonuniform flow at the point of measurement.

To summarize our results we conclude that the small X probe can be used if the flow over the sensitive region of the probe is uniform. If the flow is nonuniform and the nonuniformity of the flow is oriented in such a way that the EL, EU signal pair is not within the calibration region then the probe simply detects the presence of the nonuniform flow. However, it is also possible that the flow is nonuniform over the sensitive region of the probe and the nonuniformity is oriented in such a way that the EL, EU signal pair falls within the calibration region. In this case one cannot detect the presence of the nonuniform flow region. The u and v velocities obtained from the calibration data are erroneous in this case but there is no way to determine that the u,v data are incorrect.

We have also made measurements using the same calibration scheme with a larger X array hot wire probe. We purchased a Thermosystems Inc. Model 1248T1.5 X array and calibrated it in a uniform flow as described above. The wire length, ℓ, was 1200μ ($\ell^+ = 30$) and the spacing between the wires, s, was 500μ ($s^+ = 12.5$). When placed in the boundary layer near the wall, the EL, EU traces were almost always on the grid. However, near the wall with the center of the X array at a distance $y = 800\mu$ ($y^+ = 20$) from the wall occasional excursions off the calibration grid were observed. At $y^+ = 20$, only 0.05% of the data pairs EL and EU were off the grid. Furthermore, the excursions were smaller than those measured with the small X array. Although the excursions of the grid were suppressed, the root-mean-square values of the velocity components u and v determined from the calibration grid were 15 to 20% higher than the classical values and the Reynolds stress $\overline{uv}$ was between 50% to 100% higher than the mean shear at the wall for $20 < y^+ < 600$.

These results indicate that severe excursions from the calibration grid were suppressed by the spatial averaging of the small scale structure along the length of the larger X array hot wires and by the greater spacing between the wires. They also demonstrate that measurements with conventional X wire arrays are inaccurate when small scale structure is present. Serious measurement errors can occur even if there are no excursions from the calibration grid. This is consistent with the results of measurements of the wall pressure using small transducers, see the results of Bull and Thomas (1976) in Fig. 22.

VIII. SUMMARY AND CONCLUSIONS

During the past two decades long time average correlation or space-time correlation measurements using various sensors in the boundary layer have been used to infer the existence of an orderly, coherent structure embedded in the random turbulent flow field. In general correlation

measurements give useful information particularly for an engineer who desires to use the measured flow properties in the design of engineering systems. However, for the purpose of gaining a better understanding of the structure of turbulent flow it has been realized for some time that the correlation measurements must be supplemented with other types of measurement techniques. For example, visual observations or measurements of the flow field and/or selectively sampled measurements can and do provide further information about the flow structure, see the survey papers of Kovasznay (1970, 1972), Laufer (1972), Mollo-Christensen (1971), and Willmarth (1975).

It should be emphasized that all the measurements of turbulent flow structure are extremely difficult, time consuming and costly. The problem with visual methods is that one usually observes too much to allow comprehension or data reduction in a useful form. Sensor measurements can provide explicit information at a few isolated points (provided that the probes do not disturb the flow). The problem with sensor measurements is that one would like more information about the flow field associated with quantitative measurements at a few isolated points.

Steps to provide this additional information are underway. Chen (1975) used a number of sensors to find internal fronts of heated fluid carried outward from the wall, see the discussion in Section III. Head and Bandyopadhyay (1978) in this symposium as well as Falco (1975), who developed the method using the same facility at an earlier date, have reported combined flow visualization and sensor measurements which show promise for solving the problem of identifying flow structures in turbulence. In another recent development Favre and his colleagues have made space-time correlation measurements with three probes, see Dumas et al. (1973). They have also recently reported conditional correlation measurements, Dumas et al. (1977). There is not space or time to describe these new results and provide a coherent interpretation that would serve a useful purpose in this keynote paper.

As a final contribution I wish to emphasize that sensor measurements near the wall may be subject to serious errors caused by poor spatial resolution. (This is in addition to the curious probe interference anomalies to be described by Eckelmann (1978) in this symposium.) The spatial resolution problem as described in Section VII appears to me to be extremely difficult to solve. Most turbulent boundary layers of interest in engineering have extremely thin viscous sublayers. For example the boundary layer on an aircraft surface may be 10 cm thick at flight speeds of 60 m/s. However, the sublayer is of the order of 50μ thick. We have demonstrated, see Section VII, that the turbulent structure is of this scale or less near the wall. In this case, a relatively high Reynolds number flow, the viscous length scale is $\nu/u_\tau = 8.3\mu$. In the wall region proper resolution of the turbulent fluctuations of this scale will be necessary if the flow structure is to be measured. The small scale flow near the wall is very energetic relative to the local mean speed, see Section VI and VII. It will thus be necessary to properly measure the flow variables at scales comparable to the viscous length.

One may try to do this by increasing the viscous length scale, ν/u_τ either by reducing, u, by lowering the free stream speed or by increasing, ν, as Eckelmann (1974) has done in his oil channel measurements. Both these methods reduce the Reynolds number of the flow and make the wall region very thick compared to the boundary layer thickness. This means there is very little outer wake region in such low Reynolds number boundary layers. There is no guarantee that the flow structure in the wall region will remain the same at higher Reynolds numbers. Certainly the flow variables near the wall will still scale with wall variables ν and u_τ, but the boundary conditions on the wall region imposed by the wake region will surely be a function of Reynolds number of the outer flow.

We suggest the better sensors and/or measurement methods for small scale turbulent flow fields must be developed. When the small scale turbulent field near the wall can be measured we should then be able to better understand the mechanism of drag reduction using additives. It is also possible that knowledge of the turbulent structure will lead to better prediction measurements for turbulent flows.

REFERENCES

Bakewell, H.P. and Lumley, J.L. (1967). Viscous sublayer and adjacent wall region in turbulent pipe flow. Phys. Fluids 10, 1880.

Blackwelder, R.F. and Kaplan, R.E. (1976). On the bursting phenomenon near the wall in bounded turbulent shear flows. J. Fluid Mech. Vol. 76, pp 89.

Blackwelder, R.F. and Kovasznay, L.S.G. (1972). Time scales and correlations in a turbulent boundary layer. Phys. Fluids 15, 1545.

Bull, M.K. and Thomas, A.S.W. (1976). High frequency wall-pressure fluctuations in turbulent boundary layers. Phys. Fluids 19, 597.

Chen, C.H.P. (1975). The large scale motion in a turbulent boundary layer: A study using temperature contamination. Doctoral dissertation, Aerospace Engineering, University of Southern California, Los Angeles, California.

Corino, E.R. and Brodkey, R.S. (1969). A visual investigation of the wall region in turbulent flow. J. Fluid Mech. 37, 1.

Dumas, R., Arzoumanian, E., and Favre, A. (1973). Correlations spatio-temporelles triples dans une couche limite turbulente. C.R. Acad. Sci., Ser. A 277, 759.

Dumas, R., Arzoumanian, E., and Fulachier, L. (1977). Probabilites Conditionnelles Spatiotemporelles des Fluctuations de Temperature dans une Couche Limite Turbulent. C.R. Acad. Sci., Paris, Vol. 284, 487.

Eckelmann, H. (1974). The structure of the viscous sublayer and the adjacent wall region in a turbulent channel flow. J. Fluid Mech. 65, 439.

Eckelmann, H. (1978). The structure of turbulence in the near wall region. Proceedings of AFOSR-Lehigh Univ. Workshop on Coherent Structure of Turbulent Boundary Layers.

Emmerling, P., Meier, G.E.A., and Dinkelacker, A. (1973). AGARD Conf. Noise Mech. Prepr. No. 131.

Falco, R.E. (1975). Large scale motions in the inner region of the turbulent boundary layer. Am. Phys. Soc., Div. of Fluid Dynamics, Bulletin of Am. Phys. Soc., Vo.. 20, No. 11, pp 1430.

Favre, A., Gaviglio, J., and Dumas, R. (1957). Space-time double correlations and spectra in a turbulent boundary layer. J. Fluid Mech. 2, 313.

Favre, A., Gaviglio, J., and Dumas, R. (1958). Further space-time correlations of velocity in a turbulent boundary layer. J. Fluid Mech. 3, 344.

Head, M.E. and Bandyopadhyah (1978). "Combined Flow Visualization and Hot-Wire Measurements in Turbulent Boundary Layers", Proceedings AFOSR-Lehigh Univ. Workshop on Coherent Structure of Turbulent Boundary Layers.

Kline, S.J., Reynolds, W.C., Schraub, F.A., and Runstadler, P.W. (1967). The structure of turbulent boundary layers. J. Fluid Mech. 30, 741.

Kovasznay, L.S.G. (1954) "Hot Wire Method", Article F,2 Physical Measurements in Gas Dynamics and Combustion Volume IX High Speed Aerodynamics and Jet Propulsion; Princeton Univ. Press, Princeton, N.J.

Kovasznay, L.S.G. (1970), The turbulent boundary layer. Annu. Rev. Fluid Mech. 2, 95-112.

Kovasznay, L.S.G. (1972). Turbulent shear flow. Ist. Naz. Alta Mat., Symp. Math. 9.

Kovasznay, L.S.G., Kibens, V., and Blackwelder, R.F. (1970). Large-scale motion in the intermittent region of a turbulent boundary layer. J. Fluid Mech. 41, 283.

Laufer, J. (1972). Recent developments in turbulent boundary layer research. Ist. Naz. Alta Mat., Symp. Math. 9.

Lu, S.S., and Willmarth, W.W. (1973). Measurements of the structure of the Reynolds stress in a turbulent boundary layer. J. Fluid Mech. 60, 481.

Mollo-Christensen, E. (1971). Physics of turbulent flow. AIAA J. 9, 1217.

Perry, A.E. and Abell, C.J. (1975). "Scaling Laws for Pipe-Flow Turbulence". J. Fluid Mech. 67, 257.

Perry, A.E. and Abell, C.J. (1977) "Asymptotic Similarity of Turbulence Structures in Smooth-and Rough-Walled Pipes". J. Fluid Mech., 79, 785.

Theodorsen, T. (1952). Mechanism of turbulence. Proc. Midwestern Conf. Fluid Mech. 2nd Ohio State Univ. Columbus Ohio. 1952.

Townsend, A.A. (1970). "Entrainment and the Structure of Turbulent Flow". J. Fluid Mech. 41, 31-46.

Tu, B.J., and Willmarth, W.W. (1966). "An Experimental Study of Turbulence Near the Wall Through Correlation Measurements in a Thick Turbulent Boundary Layer," Tech. Rep. No. 02920-3-T. Dept. Aerosp. Eng., Univ. of Michigan, Ann Arbor (for a short summary, see Willmarth and Tu, 1967.

Willmarth, W.W., and Wooldridge, C.E. (1962). Measurements of the fluctuating pressure at the wall beneath a thick turbulent boundary layer, J. Fluid Mech. 14, 187.

Willmarth, W.W., and Wooldridge, C.E. (1963). Measurements of the correlation between the fluctuating velocities and the fluctuating wall pressure in a thick turbulent boundary layer. AGARD Rep. 456.

Willmarth W.W. (1975). "Structure of Turbulence in Boundary Layers" Advances in Applied Mechanics Vol 15 (edited by S.C. Yih) Academic Press, Inc. N.Y.

Willmarth, W.W. and Bogar, T.J. (1977). "Survey and New Measurements of Turbulent Structure Near the Wall". Physics of Fluids Vol 20, No. 10., 59-521.

Wyngaard, J.C. (1969). Spatial resolution of the vorticity meter and other hot-wire array. J. Scientific Instruments (J. of Physics E) Series 2, Vol. 2, 983.

DISCUSSION

Landahl:

I wonder a little bit about the interpretation of the long time averages. Couldn't it be that what one sees are really thin inclined shear layers that at one time face this way and the other time face that way -- and when you superimpose them you do get something that looks like an eddy?

Willmarth:

I don't believe so, because if you examine the flow visualization studies such as Bob Brodky's movies or the video tapes we saw this morning in Chuck Smith's presentation, you see these unidentified flying objects. We were watching his background bubbles, but every once in a while there would be a particle move quickly across the flow. I don't see how a shear layer could cause that. I can see how a couple of vortices could produce a small scale pressure fluctuation and resulting in an induced flow that would carry those things across the boundary layer.

Landahl:

It's not a question of vortex causing the flow. The vortex is a description of the flow. If you have velocities which are different in neighboring regions, that's vorticity.

Willmarth:

If I still smoked I could make a smoke ring and you would see it move across the room.

Landahl:

Yes, because you puff it away.

Kovasznay:

I will pose a question to Bill, as the Chairman's perrogative. Did you ever place two vorticity meters side-by-side and measure the transverse z-y correlation of the longitudinal vorticity and examine whether you obtain a negative peak showing a coherent pair of vortices?

Willmarth:

The only measurement I did was a correlation of the two y-component (v) velocities with Tu. I put the v-probes very close

Willmarth: (Cont'd)

together and as we approached very close to the wall, there was an opposite sign to the v-velocity. We also tried correlation and we got nothing. I believe this was because the vorticity probes were too large for the scale of our experiment.

Hussain:

If you look at the flow visualization near the wall and Emmerlings data, do you feel they're consistent? In other words, the Emmerling data suggests extremely small structures independent of the flow direction. Whereas, the sublayer structure definitely show elongated streak structure. Are they of the same scale to start with?

Willmarth:

Well, if you look at a lot of Emmerling's data you can often see footprints, pressure fluctuation patterns, that are actually a little longer spanwise than streamwise.

Hussain:

Yes, if at all. It's just in contradiction with the sublayer structure.

Kovasznay:

I would like to make a comment here. The longitudinal streaks, observed are really streak lines and therefore they can be accumulated in time. There is no evidence that there is correlation with something in the lengthwise direction. So I don't find sufficient evidence what there is really a correlation between two points separated in the streamwise direction, even when you actually see streaks.

Hussain:

Would that be then at least consistent with the watermelon structure of Kovasznay, et al?

Kovasznay:

The watermelon structure does not reach into low enough y^+. We were not so curious about the underside of the elephant.

Wallace:

I'd like to describe an experiment that I worked on this summer with Bob Brodky and Bill Willmarth, which I think speaks to the present question. Consider a model with alternate counter-rotating vortices in an idealized sense, which lie on

Wallace: (Cont'd)

the wall and rotate in such a way that they cause flow to move alternately up from the wall and down toward the wall. We placed two Kovasznay-type vorticity meters in the flow and identified regions where the velocity was low. We checked what the vorticity and the velocity were for the second probe separated in the z direction. If we set a z-separation of $25z^+$ dimensions, which is a quarter of the low speed streak spacing, we found the velocity was low with a strong axial vorticity of positive sign. If, however, we set our probe $25z^+$ units to the other side of the main probe, we obtained a very strong axial vorticity of negative sign. If we located the second probe 50 of these units laterally, we found the vorticity was virtually zero when the velocity was low.

Smith:

I want to make several comments...First, regarding what Jim Wallace just described. In our flow visualization studies, we find a consistency with the axial vortex model that Wallace just showed. When counter-rotating vortices are visualized, there is a spacing of about $25z^+$ between the vortices. Secondly, regarding Emmerling's measurements. In the video tape I showed this morning, the ejections which occurred near the wall move at essentially the same convected speed as Emmerling's small scale disturbances, on the order of $.3U_\infty$ to $.4U_\infty$. And I feel that these small scale ejections I observed in plain view are the same phenomena that Bob Falco has observed as pocket flow modules, and which I called instabilities. Falco's pocket flow modules move at the same convection velocities and most probably accelerate as they move outward. On the other hand, the convection velocity of the larger-scale structure which we observe, appears consistent with the velocity of Emmerling's large scale pressure fluctuations, on the order of $.8U_\infty$ to $.9U_\infty$. It would appear that there may be pressure effects on a surface resulting from both the large scale structure and the small scale structure. I believe that what is causing the small scale pressure fluctuations is the leading edge of a small loop-type vortex structure which we observe in our visualizations as small clear regions near the surface.

Kovasznay:

I want to make another comment on the channel experiment. I think this is going back to the Emmerling measurement, and is in answer to Hussain's question. A longitudinal vortex structure moving along the stream line would not produce pressure fluctuations of the first order.

Abbott:

Let me just explain what those unidentified flying objects were in Chuck Smith's video tape. Bubbles tend to collect on the side of the probe holder which supports the bubble wire and when they grow to a large enough size, they release and rise rapidly to the surface. They have nothing to do with the structure.

Willmarth:

Are they way out of the flow field?

Abbott:

Way out of the flow field. They are spurious, they tend to collect just at the very ends of the probe supports.

Willmarth:

They weren't carried up by the turbulence?

Abbott:

No.

Kline:

We have always had trouble with spurious bubbles. It's very hard not to have some bubbles at the end of your probe due to electrolysis. The comment I really wanted to make was in regard to what Les Kovasznay said about the accumulation of a streak line. It's true that if you put dye marking in you get an accumulation of a streak line. On the other hand, if you go to the combined time-streak marker technique, you have full streak marking and time marking. And thus you can get relatively accurate velocity profiles. And from those, you do get the low speed and high speed streaks. I think that is quite unequivocal. This has been done again and again, and you see very clearly below $y^+ = 10$ both low speed and high speed streaks. I think Hussain's question about the relation to the pressure correlations has to be viewed as the relation between pressure correlations and velocity correlations, and that we really haven't measured. Also, I agree with what Chuck Smith just said -- the balck holes, or gopher pockets -- or whatever they are -- which burrow in, also show in our old pictures and they're the things which seem to terminate a long streak. They're not the same structure and if that's true, they could be shorter and there wouldn't be any contradiction then between what Emmerling is measuring and the streak structure.

Willmarth:

I just wanted to say that what Doug Abbott said about those flying objects is that that is what Bob (Brodkey) saw in his field of view. The bubbles moved outward quite rapidly compared to the flow. That doesn't mean those things Brodkey observed weren't happening. They were, but the bubble behavior I speculated on was apparently a different phenomena.

ON THE POSSIBLE RELATIONSHIP BETWEEN THE TRANSITION PROCESS AND THE LARGE COHERENT STRUCTURES IN TURBULENT BOUNDARY LAYERS

I. Wygnanski

School of Engineering

Tel-Aviv University

Ramat Aviv, Israel

ABSTRACT

A transitional spot, being artificially evoked in a laminar boundary layer, is shown to be related to the large scale motion in a turbulent boundary layer. The evoked spot has a universal structure which remains coherent in a turbulent boundary layer over extremely large distances. The interaction between adjacent spots in tandem has been studied and it appears that some important features of the turbulent boundary layer may be simulated this way. A possible regeneration mechanism of the transitional spot was identified, reinforcing the notion that a transitional spot is an orderly structure which may be considered as the basic module in the turbulent boundary layer.

1. INTRODUCTION

There is an abundance of evidence for the existence of coherent structures in turbulent shear flows. Although some characteristic behaviour of these structures was observed, the information available to date is mostly of a descriptive nature. Because a number of survey articles on the subject can be found in the literature (Laufer 1975, Willmarth 1975, Willmarth and Bogar 1977), the purpose of this paper is to outline an approach taken by one group of researchers (see acknowledgement) towards obtaining a quantitative description of the coherent structures, rather than present another review article.

There are many ambiguities in defining the signal used to identify a large eddy and determining its transport properties. Some difficulty is attributed to the fact that the large coherent structures do not

appear at a given location at regular intervals, nor do they look exactly alike whenever they are observed. Furthermore, these structures are imbedded in an environment containing a wide spectrum of finer scales. Consequently, we cannot define a signature of such an eddy without a priori knowledge of its shape and the location of its origin. Another difficulty stems from the fact that the large eddy occupies a volume of fluid at any instant in time while most of our measuring devices provide information at a point. For this reason major contributions towards the recognition of coherent structures were made by visual methods. Blackwelder and Kaplan (1972) were probably the first ones who used an array of sensors giving instantaneous information across the entire boundary layer; however, even this information is insufficient to describe the entire event quantitatively.

A possible solution of the dilemma could be provided by pulsing the flow at a point in a way which will evoke the generation of a large coherent structure, and watching the development of the evoked eddy. In this way one obtains both a time reference and a mean trajectory along which the structure travels. Moreover, because the event is repeatable, the smaller scales which are superimposed on it randomly can be averaged out. The difficulty of this approach, in comparison to the conventional "chasing" of the large eddy, is transferred from the detection of the structure to its production.

The onset of turbulence in a boundary layer does not occur along a continuous front but rather at isolated spots which grow - as they pass downstream, eventually coalescing with one another to form a fully developed turbulent boundary layer (Emmons, 1951). The spots occur randomly in time and space but they are easily initiated (at sufficiently large Reynolds number) by roughness elements, surface imperfections or any other disturbances.

Sometimes a continuous stream of rapidly growing turbulence spots, occurring near a small protuberance, merge to form a wedge of turbulent flow. Such wedges were observed many a time and almost invariably their apex angle was 20° corresponding also to the growth angle of the individual spot (Schubauer and Klebanoff, 1956). It is thus believed that the spot is not only a universal structure in a boundary layer undergoing transition, but also a basic module in the fully turbulent boundary layer. Moreover, because of its large size, it could be related in some way to the large coherent structure.

On this assumption we addressed ourselves to the following tasks:

1. To determine the universality of the transitional boundary layer spot and some of its properties.

2. To let an evoked spot "disappear" in a turbulent boundary layer and try to recover it from the background turbulence, thus determining the distance over which it survives in a turbulent boundary layer.

3. To explore the mechanism by which neighbouring spots interact, in order to simulate the entrainment process into a turbulent boundary layer, and study the interactions that occur among neighbouring structures.

4. To explore the existence of a possible regeneration process of the spot.

2. ON THE TRANSITIONAL SPOT

Electrical discharge initiated the transitional spots in a Blasius boundary layer at $Re = \frac{U_\infty \delta^*}{\nu} > 500$. ($\delta^*$ being the displacement thickness and U_∞ is the velocity of the free stream). The spots grew in all directions as they were swept downstream, but they attained a universal self-similar shape approximately two feet downstream of the disturbance (for U_∞ = 10 m/s).

A typical spot has an arrowhead shape in a plan view, and a blunt triangular shape in an elevation view (Fig. 1). It is, however, a rather flat structure which cannot be represented graphically without the vertical dimension being stretched. Once the spot is developed its trailing interface (the interface between the turbulent and non-turbulent fluid) moves at a constant speed $U_{TE} = 0.5\ U_\infty$, while the velocity of the leading interface is only constant across the boundary layer, but varies in the spanwise direction. On the plane of symmetry $U_{LE} = 0.9\ U_\infty$.

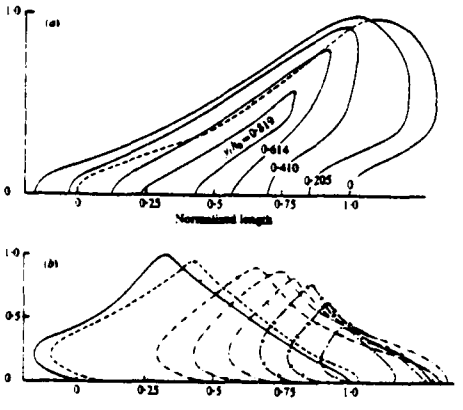

Figure 1. The shape of a typical spot: a) contour map at various relative elevations. b) Elevation view at various spanwise locations

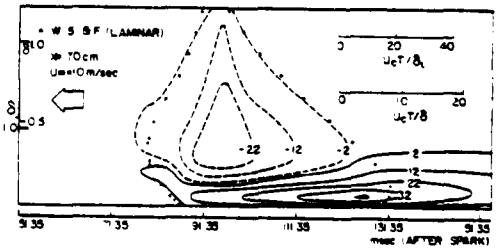

Figure 2. Contours of educed velocity difference of a transitional spot in a laminar boundary layer (numbers represent % U_∞). Vertical scale is the distance from the wall.

The spot grows in the direction of streaming by virtue of the difference between the convection velocities of both interfaces. The total wedge angle representing the growth of the spot in the spanwise direction is 20^{0}, irrespective of the location of the disturbance and the free stream velocity as long as the Re at the disturbance is large. The height of the spot follows approximately the height of a hypothetical boundary layer, originating at the disturbance with an initial thickness of the laminar boundary layer at that location. It is difficult to say whether the spot grows linearly with x_s (x_s is the distance from the disturbance) or as $x_s^{4/5}$, as may be implied from the growth of the turbulent boundary layer.

It was important to ascertain that the shape of the evoked spot depends on the laminar boundary layer and not on the disturbance which generated it. For this purpose both the geometry and the intensity of the disturbances were changed, but the resulting spot remained invariant. Furthermore, the shape of the spot measured in a wind tunnel agreed quite well with the shape of the spot measured by Coles and Barker (1975), in a water tunnel in spite of the different methods by which the spot boundaries were detected.

The flow-field associated with an isolated transitional spot was also measured because it is part of the flow field, rather than the interface, which could possibly remain identifiable in a fully turbulent flow. In fig. 2, contours of streamwise velocity perturbation relative to the laminar boundary layer are plotted against time and distance from the wall. The contours representing excess of velocity relative to the mean are shown as solid lines, while the contours showing a defect are marked by dashed lines. The borders of the spot, determined by detecting the interface are marked as dots. The spot may thus be represented by a closed loop of velocity defect extending outwards from $y/\delta_L = 0.3$ (δ_L being the laminar boundary layer thickness) riding above contours representing excess velocity which trail over a long distance behind the spot.

3. THE PERSEVERANCE OF THE TRANSITIONAL SPOT IN A TURBULENT BOUNDARY LAYER

For the purpose of this experiment the boundary layer was tripped by a row of spheres 1.5 mm in diameter 280 mm downstream of the leading edge (fig. 3). The Reynolds number based on the displacement thickness for the laminar boundary layer at this location and velocity was : $Re_{\delta^*} = 500$. Each sphere generated in its wake a wedge of turbulent flow, thus the spacing between the spheres determined the streamwise coordinate at which the boundary layer became completely turbulent. A spark source located 300 mm from the leading edge on the centerline of the plate evoked a transitional spot which merged into the turbulent layer. In a later version of the experiment (carried out at the University of Southern California), the spheres were moved upstream (to 150 mm from the leading edge) and an additional sand paper trip was added.

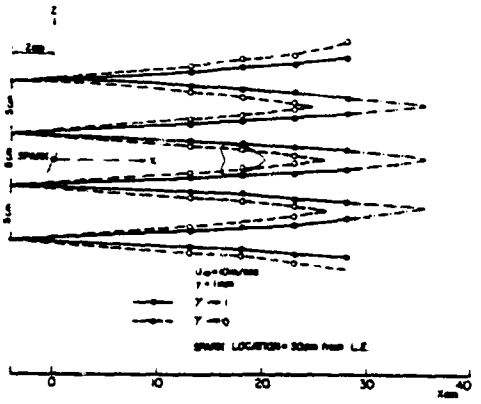

Figure 3. Plan view of the experimental configuration showing the location of the spark the tripping-spheres and contours of intermittency factor indicating the extent of turbulent flow.

The spark-signal triggered a clock which was used as a basic time reference. An acquisition program was activated by this trigger, and a time delay was programmed to allow the spot signature to reach the center of the data window. After this delay a velocity record covering a predetermined time-span was taken and stored on a digital tape. A typical experiment contained up to 1000 events. The data was ensemble-averaged for a fixed time reference relative to the spark and the educible average was written on a disc file. Subsequent processing involved a pattern recognition scheme whereupon the educed average, being regarded as zero iteration, was used as a pattern with which the individual realizations were cross-correlated. (Zilberman, Wygnanski and Kaplan 1977 - henceforth referred to as ZWK, Haritonidies, Kaplan and Wygnanski 1977). The time at which the correlation attained a maximum was noted and in the subsequent iterations, the average was recomputed using those time shifts. The reasoning for this procedure lies in the assumption that the events under consideration do not arrive at the measuring station precisely the same time. Therefore, all events detected within 10% of their nominal time of arrival were accepted as being evoked events. Time shifts exceeding this limit were disregarded. The new average obtained could serve again as a pattern for the entire process to be repeated. It was found empirically that the process converged, and the resultant averaged structure stopped changing, in most cases, after the second iteration.

Although the process is described in detail elsewhere (ZWK) an example is shown in Fig. 4, for the sake of completeness. The measure-

AD-A100 632 PURDUE RESEARCH FOUNDATION LAFAYETTE IND F/G 20/4
WORKSHOP ON COHERENT STRUCTURE OF TURBULENT BOUNDARY LAYERS.(U)
NOV 78 D E ABBOTT, C R SMITH AFOSR-76-3015

UNCLASSIFIED AFOSR-TR-78-1533 NL

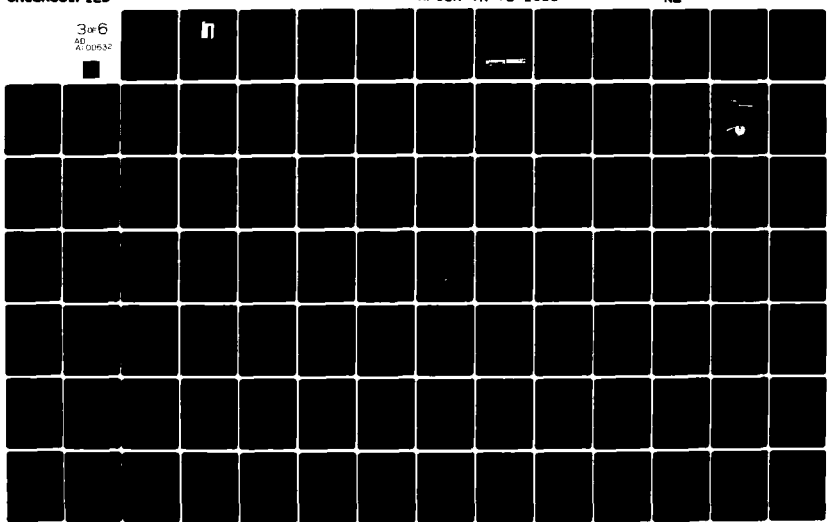

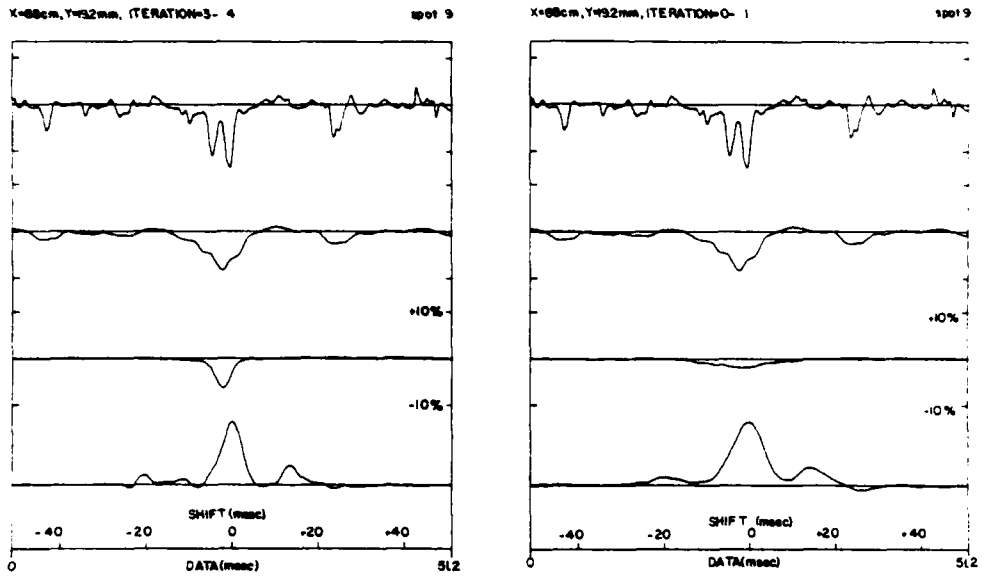

Figure 4. Illustration of the technique to align events in time upper trace - velocity history; second trace - smooth version of upper trace; third trace - test pattern for cross correlation; lowest trace - cross correlation of traces 2 and 3.

a) third trace is pattern from iteration 0 (time educed)

b) third trace is pattern from third iteration

ment station shown is located at the outer edge of the boundary layer so the evoked structure is easily identified by eye. In this figure the upper trace represents a streamwise velocity record, while the second trace is a filtered version of the signal. The third trace is the pattern used for the pattern-recognition scheme. In the zeroeth iteration the educed average is seldom representative of the individual events. The digital cross correlation is taken between the traces shown in lines 2 and 3 and is indicated at the bottom of the figure. One should also note that there is a factor of two in time for the bottom trace relative to the other three traces. The educed pattern after the third iteration (fig. 4b) is much sharper than the ensemble averaged velocity educed without time shifts (zeroeth iteration).

In the second version of the experiment (Haritonidis, Kaplan and

Wygnanski 1977) a rake of 10 hot wire probes was used (Fig. 5) giving a temporal record of velocity across the entire boundary layer. Two

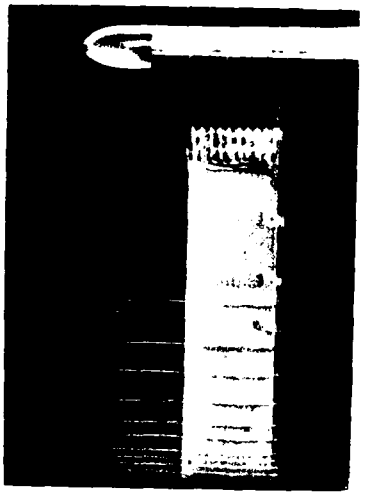

Figure 5. A rake of 10 hot-wires located at 1, 2, 3, 4, 6, 8, 11, 15, 19, 25 mm from surface. Wire diameter 2.5 μ and length 1.1 mm.

additional sensing probes were located at the outer part of the boundary layer at equidistant spanwise locations about the plane of symmetry. The purpose of these probes was to check if a spanwise alignment of the structure could also be realized.

A set of velocity histories measured 900 mm downstream of the disturbance is presented in Fig. 6. One can observe in this figure a number of large fluctuations in U which are quite coherent across the boundary layer. Embedded in this signal is an evoked pattern which becomes clearly visible when an average of 1,200 events was taken (Fig. 7a). The velocity scale in Fig. 7 is four times larger than in Fig. 6. Applying a pattern recognition technique to the wire located 15 mm from the surface (third trace from top) improved the coherence of the evoked structure in the vicinity of this wire (Fig. 7b). In particular, the velocity defect observed 15 mm from the surface almost doubled when compared with the unaligned pattern. The effect of alignment at y = 15 mm was not felt near the surface leaving the velocity history at y= 1 mm almost unaltered. When a hot wire located at y = 4 mm was used for alignment (Fig. 7c) the velocity perturbation near the surface became very much stronger. When each wire was treated separately the resulting velocity histories can be almost presented as a combination of Figs. 7b and 7c.

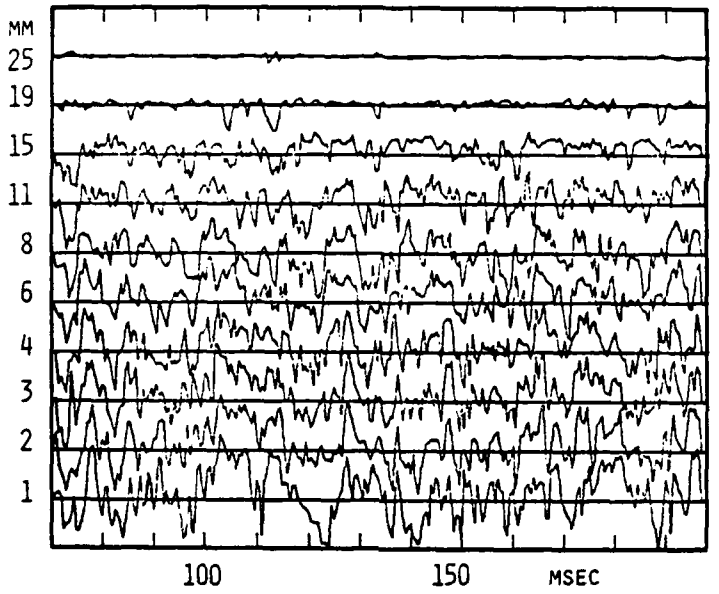

Figure 6. Velocity signals in a tripped turbulent boundary layer x_s = 900 mm. Each trace is displaced 20% U_∞.

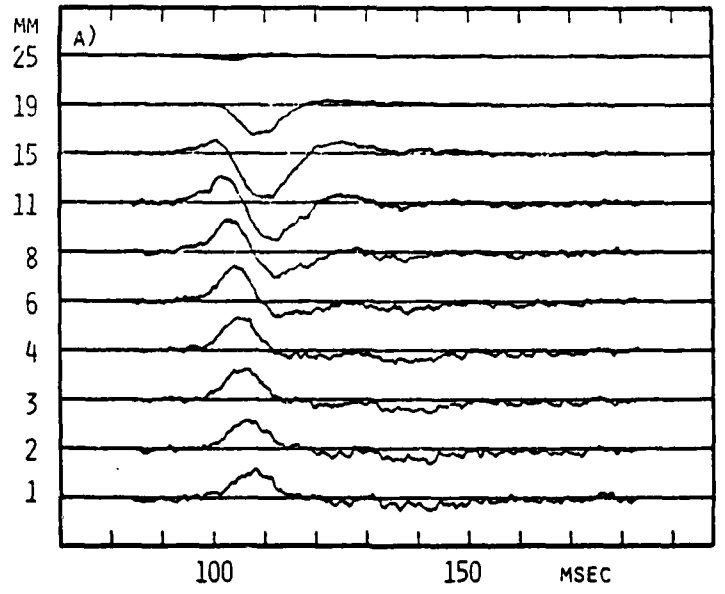

Figure 7. Ensemble averaged velocity histories at x_s = 900 mm. Each trace is displaced 5% U_∞.
a) No time alignment.

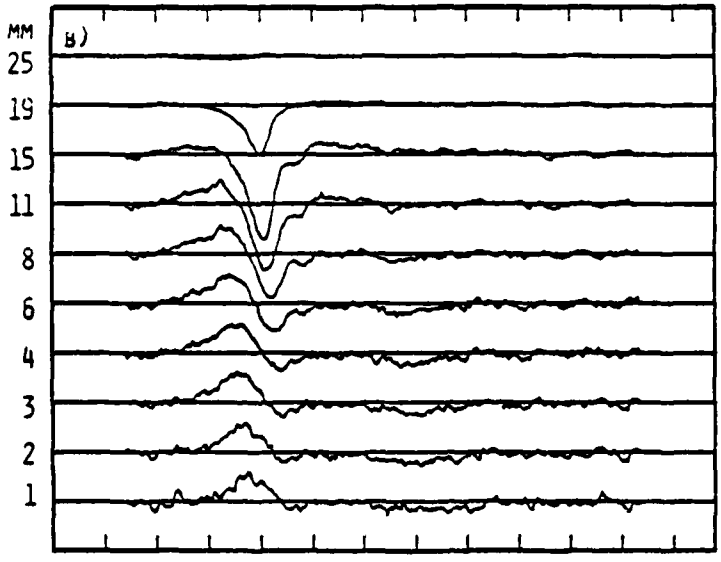

Figure 7. b) Educed and aligned with respect to wire 3 (15 mm)

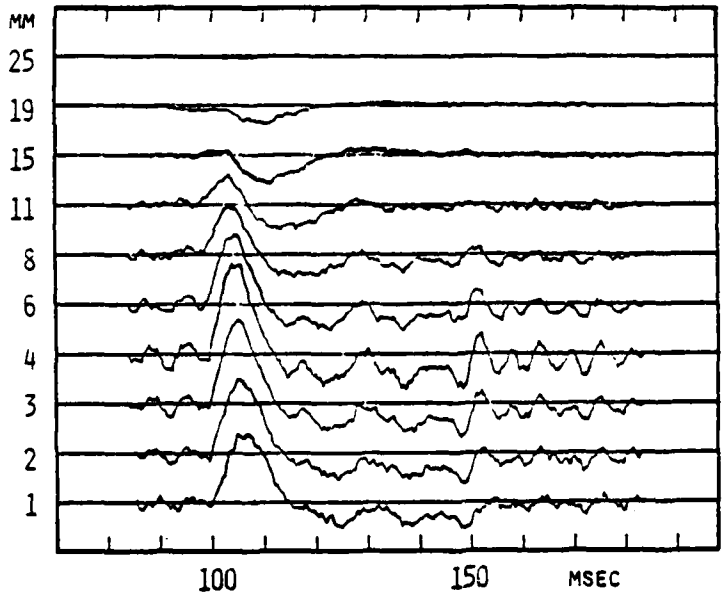

Figure 7. c) Educed and aligned with respect to wire 7 (4 mm)

Contours of constant perturbation velocity are generated by cross plotting and interpolating the results in Fig. 7. Fig. 8 a-c corresponds to Fig. 7 a-c showing contours at intervals of ± 1.5%. Negative perturbation contours are drawn in broken lines. The narrow rectangle above Fig. 8c is indicative of the distortion of the vertical scale calculated at a convection velocity characteristic of the structure. The contours shown in Fig. 9 a-b are obtained after each wire was realigned individually and are drawn at intervals of ±3%. The contours shown in Fig. 9a were measured 900 mm downstream of the disturbance while the contours in Fig. 9b were measured at the 1200 mm station. The perturbation did not weaken in the interval between x_s = 900 mm 1200 mm although the defect region shrank somewhat while the excess region grew in the streamwise (time) direction. In the direction normal to the surface the pattern scales approximately with the boundary layer thickness.

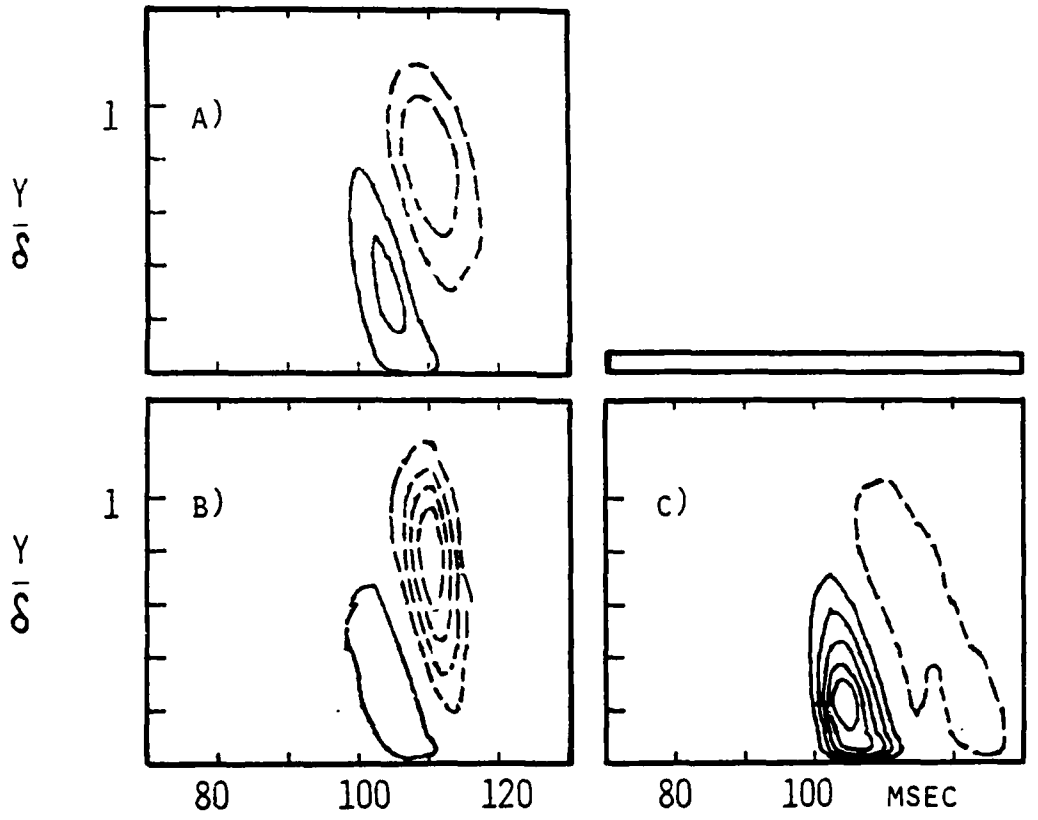

Figure 8. Velocity perturbation contours (every 1.5%U_∞) at x_s = 900 mm.
a) No alignment (corresponding to data in 7a)
b) Wire 3 aligned (15 mm)
c) Wire 7 aligned (4 mm)

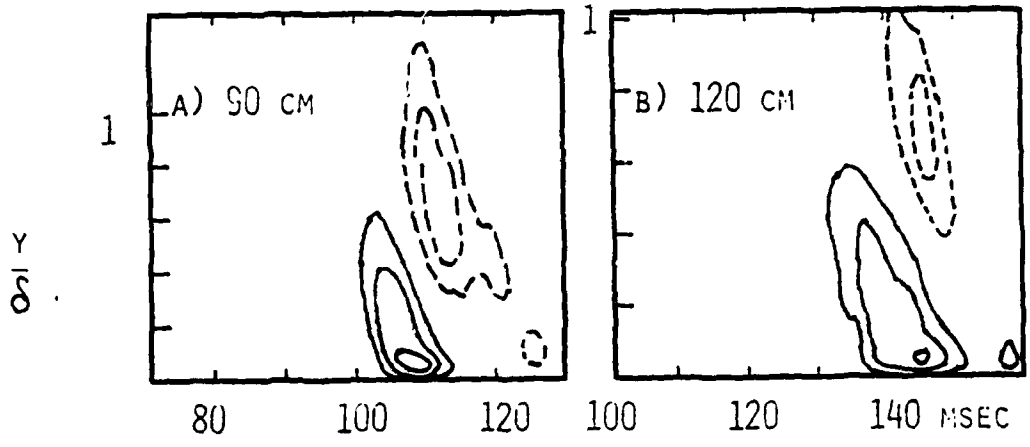

Figure 9. Velocity perturbation contours (every 3% U_∞)
at x_s = 900 mm and x_s = 1200 mm
Each wire is aligned separately.

The following conclusions were drawn from this experiment:

i) A transitional spot retains its coherence in a turbulent boundary layer over distances measured in hundreds of δ and perhaps further. To date, no deterioration of coherence with downstream distance was observed. (see Fig. 9).

ii) The structure is represented by an excess velocity perturbation near the surface and a defect in velocity which occurs at the outer edge of the boundary layer and slightly later in time. These perturbation contours could be caused by a slowly-rotating, large-eddy which transports high momentum fluid from the outer reaches of the boundary layer to the wall region. The fluid transported towards the surface causes a positive perturbation in velocity and vice versa. Preliminary measurements with an X-wire indicate that this indeed is the underlying mechanism of momentum transport.

iii) The scale of the structure is of the order of 10δ in the streamwise direction becoming $2\text{-}3\delta$ in the interface region. The outer part of the structure is convected downstream at 90% of the free stream velocity. The excess of velocity region near the wall is probably convected at slower speed, thus being slowly swept underneath the defect-region (see Fig. 9 and Fig. 14 of ZWK).

iv) Since the enhancement procedure shown in Fig. 7 is most effective on features near the reference probe, one must conclude that the motion of the structure is not a "solid body" translation, but is accompanied by rotation and internal distortion.

In this experiment the evoked structure was permitted to interact with other structures at random. The interaction may not be a simple one, and reflects the fact that the evoked structure is no longer self preserving. The variations from one occurrence to the next most probably depend on the number of interactions (and their form) which took place during the travel of the evoked structure. It thus seems that the turbulent boundary layer cannot be regarded as a superposition of transitional spots.

4. ON THE INTERACTION AMONG SUCCESSIVE SPOTS ORIGINATING FROM A SINGLE SOURCE

The large scale eddies occurring at high Reynolds numbers are seen quite clearly in the smoke pictures of Falco (1977). These eddies appear at regular intervals which suggest an interaction of successive spots which are in the process of merging into one another (Fig. 10). A controlled experiment was undertaken to simulate the interaction of successive transitional spots originating from a single point source. It is realized that only one mode of interaction is simulated this way. Other possible modes of interaction among spots of different origins, different sizes and at various relative locations to one another probably exist. Nevertheless, it is hoped that a simplified experiment would be helpful in explaining some of the complicated processes occurring in a turbulent boundary layer although it cannot simulate correctly all the characteristics of the flow. Some of the features that we seek to understand are:

1) The process which limits the growth of the evoked eddy in a turbulent boundary layer.

2) The mechanism of entrainment.

3) The mechanism responsible for the transfer of momentum towards the wall in a turbulent boundary layer.

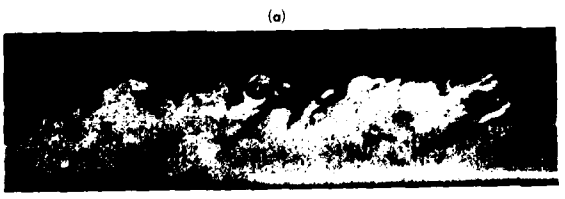

Figure 10a. The large eddies in a turbulent boundary layer (courtesy of Falco)

Figure 10b. The process of engulfment in a two dimensional mixing layer.

It will be recalled that the transitional spot grows linearly with downstream distance. In the streamwise direction this growth is expressed by the fact that the leading interface in the plane of symmetry has a celerity of 0.9 U_∞ while the trailing interface moves at 0.5 U_∞. By drawing pseudo streamlines relative to each interface Wygnanski, Sokolov and Friedman (1976) concluded that "no turbulent fluid escapes through an interface" and that most of the fluid is entrained through the slowly moving trailing interface (see Figs. 25 and 26 of their paper). In fact detailed breakdown of the entrainment shows that:

82% of the fluid is entrained through the rear interface although in the immediate vicinity of the solid surface this interface is inert.

10% of the fluid is entrained by the lower part of the leading interface (under the overhang) while an additional 6% is entrained by the leading interface above the overhang.

2% could not be accounted for from these figures.

Cantwell, Coles and Dimotakis (1977) (henceforth referred to as CCD), by assuming a conical similarity of the transitional spot, calculated the particle paths relative to the spot. They concluded that more than 80% of the entrainment occurs along the upper rear boundary, but find the upper leading front totally inert. This author doesn't think that the difference of 6% in the entrainment rate to the transitional spot is a crucial issue at the present state of our knowledge, although the calculation method presented by CCD is most valuable. It is however, important to establish how the flow is entrained. There are currently two qualitative descriptions of the entrainment process. According to one view, a relatively flat interface propagates slowly normal to itself and absorbs non-turbulent flow by viscous diffusion of vorticity. The process is sometimes referred to as "nibbling" because small scale eddies corrogate the interface and slowly eat their way into the non-turbulent fluid. Another process in which the non-turbulent fluid is "engulfed" by a turbulent interface may precede and facilitate the nibbling process. This process is clearly visible in the mixing layer (Fig. 10b) where two smoke filaments which are initially far apart are drawn together by an induced motion of a large eddy and are rolled together like a spiral. The contact area between the two layers of fluid in the spiral is large, either enhancing the nibbling process or leading perhaps to a violent instability, causing the core of the eddy to fill entirely with smoke. The process of entrainment into the spot cannot be classified in either category because the interface of the individual spot contains eddies which could be considered as being large (see Fig. 7, in the paper of CCD). Furthermore, interacting spots may entrain non-turbulent flow in a different manner than a single transitional spot does.

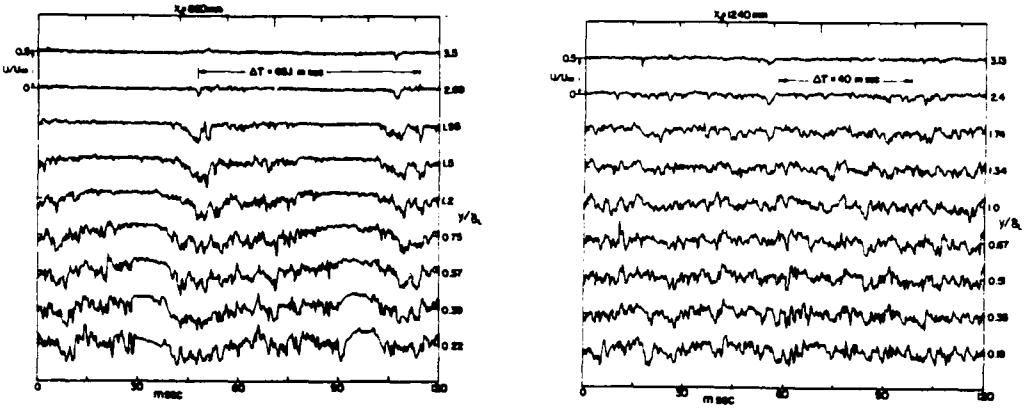

Figure 11. Velocity signals in interacting spots

a) x_s = 860 mm ΔT = 66 m sec.

b) x_s =1240 mm ΔT = 40 m sec.

An array of five to six consecutive spots originating from one point source at predetermined time intervals was monitored by a rake of hot wires located on the plane of symmetry at two distances downstream of the disturbance. The degree of interaction between adjacent spots could be varied by either changing the frequency of generation of the spots or changing the distance downstream at which the spots were monitored. Two sets of velocity histories are shown in Fig. 11 a-b. The individual spots are clearly recognizeable in Fig. 11a, where the time interval between adjacent spots was 66 m sec and the measurement was made 860 mm downstream of the disturbance (U_∞ = 10 m sec). However, when the time interval was decreased to 40 m sec at x_s = 1240 mm a continuously turbulent velocity signature is observed not only near the wall but over most of the boundary layer. This signal is quite similar to velocity histories measured in a fully turbulent boundary layer although some order is visible at large distances from the surface. A velocity profile obtained by ensemble-averaging over all the events and then averaging over time (excluding the calm region behind the last spot in an array)is shown in Fig. 12, for the various cases considered. Measurements made in the fully turbulent boundary layer at the same location on the plate are marked by diamonds on the figure. The interacting, successive spots give rise to a mean velocity profile which tends to the conventional profile as the interaction becomes stronger (c.f the result at x_s = 860 mm Δt = 66 m sec with the velocity at x_s = 1240 mm Δt=66m sec) In fact the two velocity profiles are almost identical as the time interval between adjacent spots is less than 40 m sec at x_s > 1000 mm.

Thus one may expect that an array of transitional spots will give rise to a logarithmic profile when $\Delta T U_\infty / x_s \leq 0.4$ where ΔT is the time interval between adjacent spots. This number is by no means definite

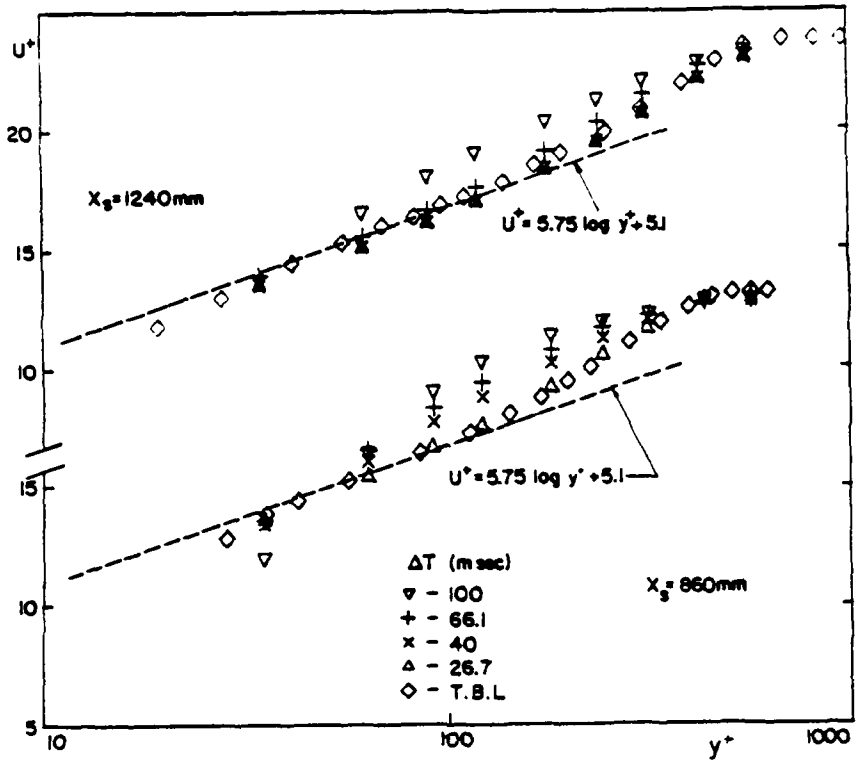

Figure 12. A comparison between the mean velocity in a turbulent boundary layer and the profile resulting from interacting spots.

and should be used as a guide only. The tendency of the time averaged profile towards a universal-logarithmic law is similar to the tendency observed by Patel and Head (1969), in channel and pipe flows which undergo transition.

When the velocity histories are ensemble averaged conditionally to the first spark the periodic behaviour introduced by the disturbance becomes apparent. Contours of constant velocity patterns are plotted in Figs. 13 a, b, c and 14 a, b, c, the contours representing excess of velocity relative to the mean are shown as solid lines, while the contours showing defect are marked by dashed lines. The pertubation contours in Fig. 13 refer to the laminar velocity profile existing at the measuring station in absence of any disturbance while the contours in Fig. 14 refer to the fully turbulent profile.

When the dimensionless interval between adjacent spots is $\Delta TU_\infty/x_s = 1.16$ the velocity pertubation contours (Fig. 13a) are very similar to those plotted for the isolated transitional spot (Fig. 2). The contours showing positive velocity perturbation which stretch over a long time period behind a single spot appear to join together in Fig. 13 b, where $\Delta TU_\infty/x_s=0.465$. This time interval is short enough to result in a continuously turbulent signal near the surface. The regions bounded by countours of large velocity pertubation (larger than 20% U_∞ say) shrink as the time interval between adjacent spots is decreased, implying that velocity gradients; $\frac{\partial u}{\partial t}$ in particular diminish when the degree of interaction increases (compare positive pertubation regions in Figs. 13 a to c). The general form of the negative pertubation contours is altered rather little by the interaction. The "calmed-region" which exists outside the turbulent interface in a single transitional spot disappears but the extent of the positive-velocity-pertubation region from the surface changes rather little when adjacent spots merge. Two velocity profiles are drawn to the same scale in the upper-left corner of Fig. 13c, one shows the laminar velocity profile while the other the turbulent velocity profile both existing at x_s = 1240 mm. The perturbation contours shown in the figure correspond approximately to the difference between the two profiles when the Blasius profile is taken as reference. The sequential interaction of transitional spots contains therefore, some of the most important elements of the turbulent boundary layer because we are trying to understand the mechanism leading to the generation of a turbulent velocity profile.

When the pertubation contours are plotted relative to the turbulent velocity profile, which would have existed at x_s = 1240 mm if the boundary layer were tripped, they do not necessarily resemble the single structure evoked in a turbulent boundary layer (Fig. 14 b,c). Comparing Figs. 13a, with 14a, reveals that the streamwise dimension of the defect region is approximately halved, also the perturbation level is reduced by a factor of two. The velocity defect region extends all the way to the wall, and is followed in time by an excess velocity region mostly away from the surface. For a short period of time the contours of +0.02 U_∞ reach the surface, indicating that the skin-friction under the rear portion of the spot may exceed the skin-friction in a fully turbulent boundary layer. In Fig. 14b the defect region moves away from the wall, a process which continues rather slowly as the structure moves downstream (Fig. 14c). The typical perturbation shown in Fig. 9 is not observed.

It now appears that the comparison relative to a fully turbulent velocity profile is not as significant physically as originally believed. The typical perturbation, (shown in Fig. 9) which is approximately self-sustained over the range of Re considered, was not observed in the present case whenever the interaction among successive spots was strong (Fig. 14c). In fact the sequence shown in Fig. 14, a,b,c indicates that the perturbation disappears with increasing interaction. The flow near the surface at $\Delta T\ U_\infty/x_s$ = 0.215 does not represent any perturbation relative to the turbulent velocity profile obtained by tripping the boundary alyer (Fig. 14c). One must deduce therefore, that a turbulent boundary layer (in the range of Re considered) consists mostly of spots

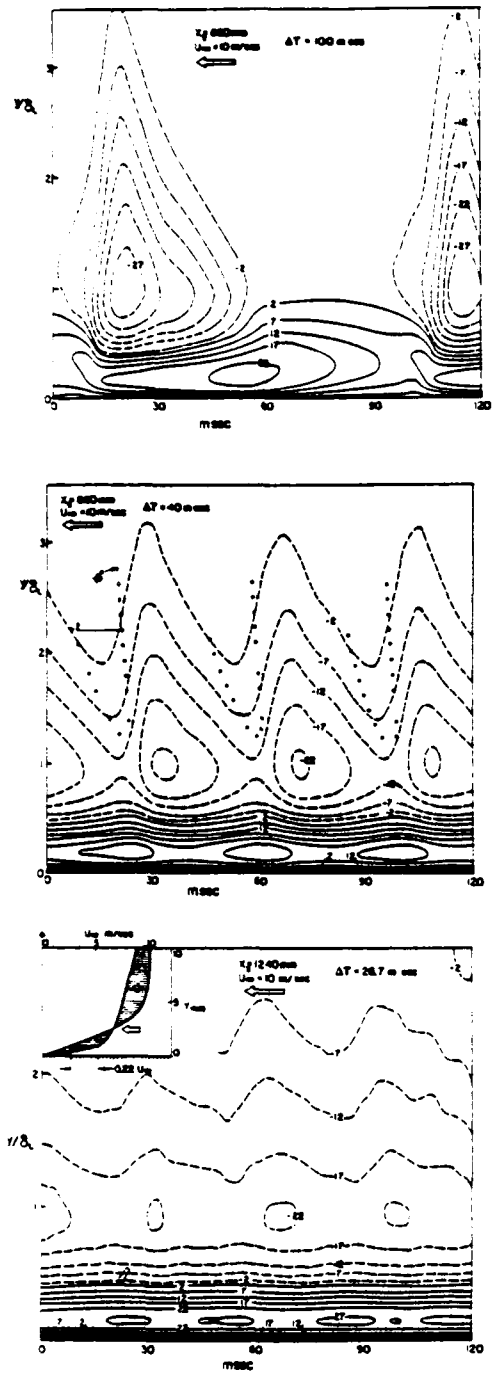

Figure 13. Perturbation contours relative to laminar boundary layer profile.

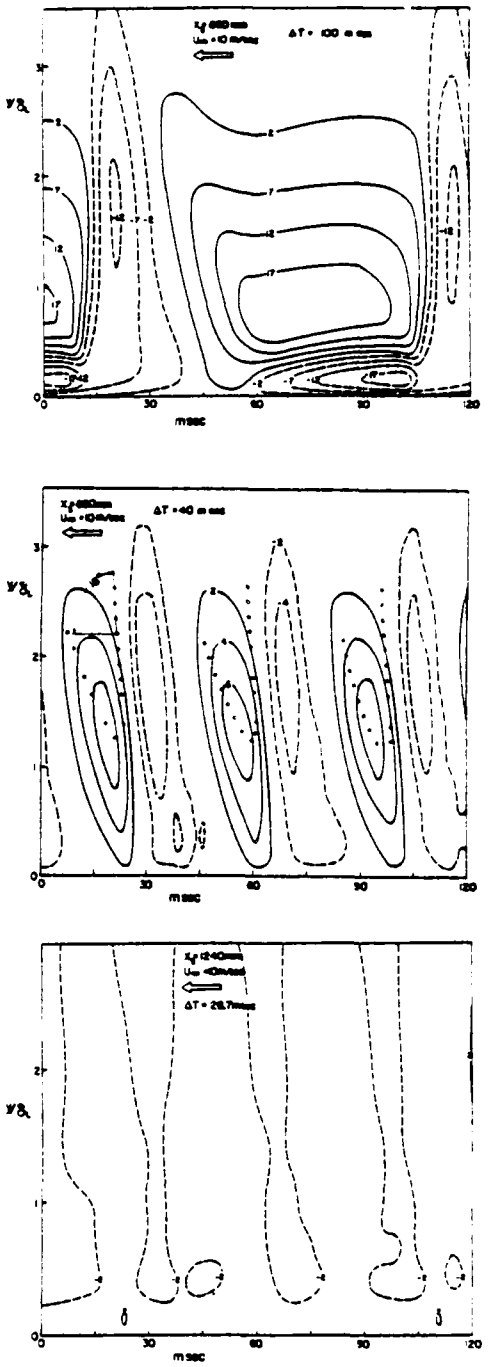

Figure 14. Perturbation contours relative to turbulent boundary layer profile.

a) x_s = 860 mm Δt = 100 msec
b) x_s = 860 mm Δt = 40 msec
c) x_s = 1240 mm Δt = 26.7 msec
(the numbers represent deviation in % U_∞).

interacting in sequence and that the interaction in the spanwise direction is of secondary importance. Furthermore, the fact that the evoked structure sustains itself in a turbulent boundary layer (Fig. 9) suggests that the degree of interaction occurring naturally (i.e. at random) between a single evoked structure and the turbulent background must be rather weak. This is not the case when a sequence of spots interact. Schubauer and Klebanoff (1956) observed that whenever a transitional spot penetrates a turbulent boundary layer the "calmed region" persists for a while "relaminarizing" the flow temporarily. The transitional spot therefore may influence its environment preventing a strong interaction in its vicinity.

In another experiment, described in the following section, it was observed that the generation of new spots occur only at the "wing-tips" of the evoked transitional spot. The "calmed region" thus prevents or delays the generation of new turbulence and perhaps weakens the interaction between adjacent turbulent regions. In the present experiment the spots were perhaps forced at higher frequency than would have occurred naturally, preventing the development of the calmed region, and increasing the interaction beyond the natural rate, this could cause the disappearance of the perturbation contours from Fig. 14c.

The average location of the interface is marked on Figs. 13b and 14b. The method used for determining the interface is described in the paper by Wygnanski, Sokolov and Friedman 1976, and will not be repeated here. By having two sets of measurements, one at x_s = 860 mm and one at x_s = 1240 mm, the celerity of the average interface was determined at the outer part of the boundary layer and tabulated:

ΔT (m sec. between sparks)	U_{LE}/U_∞	U_{TE}/U_∞	U_C/U_∞
100	0.85	0.55	0.76
66.1	0.84	0.59	0.77
40.0	?	0.70	0.76
26.7	0.88	0.76	0.775

The celerity of the leading interface U_{LE} remains fairly constant, independent of the degree of interaction between spots. The celerity of the trailing interface U_{TE} increases when the degree of interaction between adjacent spots increases, causing a reduction in the rate of entrainment of non-turbulent flow. The last column in the table was obtained by tracking the locus of minimum velocity at constant distance from the surface. It gives a measure of the celerity of the entire structure, though it fails to account for the growth of the structure occurring between the measuring stations (see Wygnanski, Sokolov and Friedman, 1976). The evoked array of coherent structures moves downstream with a celerity of 0.77 U_∞; this velocity agrees with the celerity measured by CCD for the single transitional spot using the same technique, but is in disagreement with a celerity deduced from correlation measurements.

Brown and Thomas (1977) correlated the shear stress at the wall with the velocity measured at various distances from the surface. They observed the existence of an organized structure which is inclined to the surface at 18°. The smoke picture of Falco (1977) also shows an oblique gap between two neighbouring large scale eddies at the same inclination angle. This angle is plotted on Fig. 14b (using $U_c = 0.84\ U_\infty$). It suggests that the average leading interface in an array of interacting spots is indeed inclined at 18° to the wall. This interface retains its inclination with downstream distance. The trailing interface which is initially inclined at a shallower angle to the surface slowly rotates and becomes steeper as the pattern proceeds downstream. The change of angle is brought about by the acceleration of this interface with downstream distance. The potential flow overtaking one spot may be engulfed into the gap between adjacent spots and entrained by the trailing interface of the spot ahead of it (further downstream in laboratory coordinates).

The velocity profiles associated with the passage of the spot are shown in Figs.15, 16. The educed velocity profiles occurring over a cycle (fig. 15) are compared with a turbulent profile which is marked

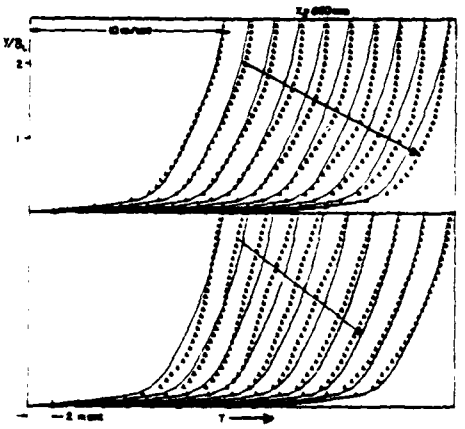

Figure 15. Ensemble averaged velocity profiles on the plane of symmetry of interacting spots

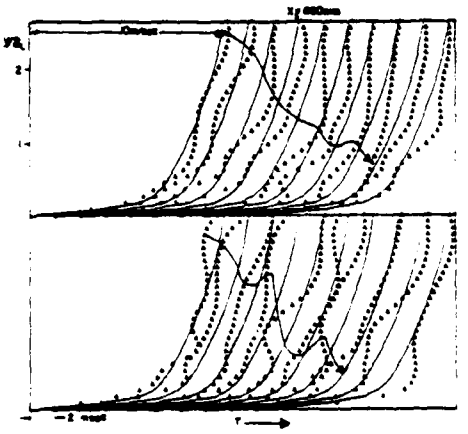

Figure 16. Instantaneous velocity profiles on the plane of symmetry of interacting spots

x_s = 860 mm ΔT = 40 m sec

by a solid curve. Time is increasing from left to right. Relative to the average turbulent profile both positive and negative average pertubations start far away from the surface and move towards the surface with increasing time. Similar trend, although much more irregular and

much more violent is seen in Fig. 16, where a single, filtered event is considered (see also Figs. 45-48 Aminis 1978 thesis). Comparison of Figs. 15 and 16 as well as flow visualization pictures (CCD, Falco 1977) suggest that the large coherent eddy carries with it a substructure which contains perhaps most of the turbulent energy. This substructure, which is fairly well ordered in the individual spot may be related to the breakdown process. Klebanoff, Tidstrom and Sargent (1962) while studying the breakdown of a T.S. wave train observed that the first "spike" which originates at the outer region of the layer makes itself felt across the entire layer. Amini (1978) studying the evolution of the spot from a single disturbance also observed that breakdown starts far away from the surface and proceeds towards it. However, a perturbation moving towards the wall should not be interpreted as a motion of fluid in the same direction.

5. ON THE POSSIBLE REGENERATION MECHANISM OF THE TURBULENT SPOT

It would be naive to assume that the entire structure of a turbulent boundary layer at large Reynolds Numbers is determined in the transition region. Thus if one were to accept a concept in which a transitional spot is a main building module of a turbulent boundary layer, one has to find a mechanism by which it reproduces. A plausible regeneration mechnism was identified by Wygnanski, Haritonidis and Kaplan,(1977)and is associated with a breakdown of a Tollmien-Schlichting wave packet which trails a turbulent spot. The wave packet can only be observed near the "wing-tips" of the spot as shown in Fig. 17. Two sets of measurements 2

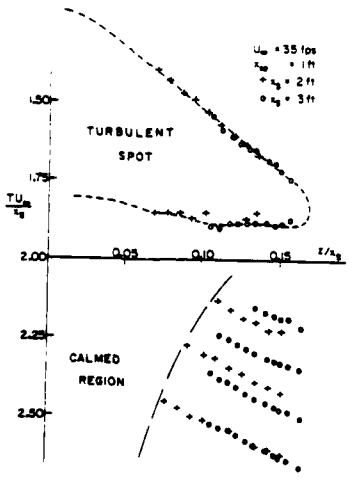

Figure 17. The geometry of a wave packet trailing a transitional spot.

and 3 ft downstream of the disturbance are shown in the figure, yet the boundaries of the spot collapse onto a single curve since the abscissa

and the ordinate in this figure were divided by the distance from the spark which is the similarity parameter for the transitional spot. The visible troughs of the waves in the packet are also shown. The waves may extend beyond the spot in the spanwise direction but they disappear in the "calmed" region where the laminar velocity profile is more convex, and thus more stable to small disturbances than the Blasius profile.

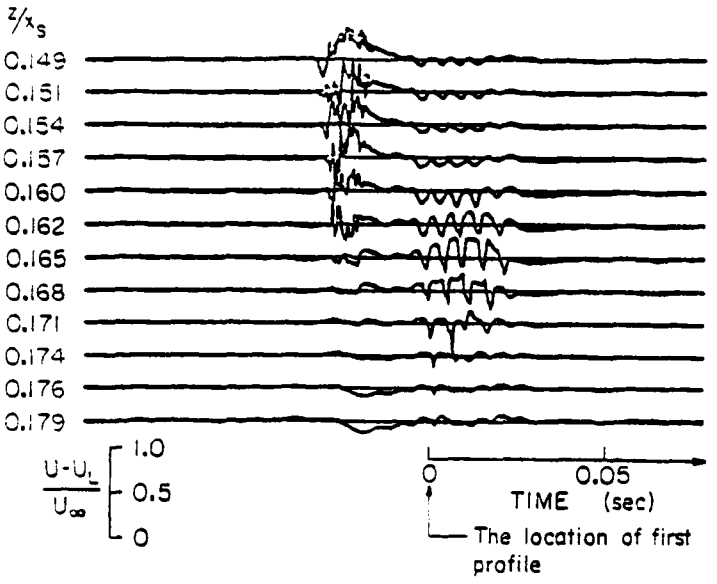

Figure 18. Velocity signals near the "wing-tips" of a spot x_s = 900 mm.

When the velocity is increased from 35 fps to 65 fps, the wave packet usually breaks down. In Fig. 18, the time history of an individual event is recorded. The measurements were made with a rake of hot wires, which were displaced in the z direction and are in a plane parallel to the surface (the spacing between adjacent wires is 2.5 mm). The turbulent signature in the top 7 velocity traces shows part of the evoked transitional spot, its "wing tip" is located near z/x_s = 0.165. To the rear of the spot (i.e. upstream of it in the laboratory coordinates) a wave packet is visible. It seems to ride on the unperturbed Blasius profile and is not visible in the immediate neighbourhood of the turbulent interface. The amplitude of the packet increases towards the "wing-tip" of the spot and in the case shown the packet is on the verge of breakdown at $0.160 < z/x_s < 0.175$. The amplitude of the "spikes" in the U component of velocity at the onset of breakdown is extremely large. The spike recorded by the wire located at z/x_s = 0.171 indicates the possibility that the flow is brought close to stagnation. Although one cannot rely on the response of the hot wire in this particular instance, the average amplitude of the spikes at breakdown is of the order of 0.4 U_∞. This is very consistent with the observations of Klebanoff et al.,(1962). Instantaneous velocity perturbation profiles in the z direction enable us to

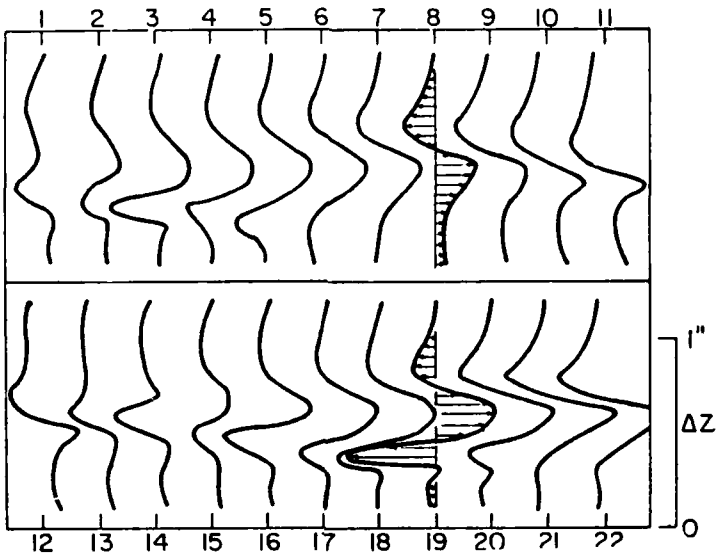

Figure 19. Spanwise variation of velocity at breakdown

have a glimpse into the breakdown process. Twenty-two profiles are shown in Fig. 19 at intervals equal to $\Delta T\ U_\infty = 0.312"$. The elocity scale is shown at the bottom of the figure with positive pertubation of velocity being to the right of the tick marks. Extremely concentrated shear layers appear in profile 19. The width of such shear layers is comparable to the spatial resolution of the wires in the rake (i.e. 2.5 mm) while the velocity jump across the layer is approximately $0.35\ U_\infty$.

Thus, at breakdown $\partial u/\partial z$ can become comparable to $\partial u/\partial y$ which is considered to be the dominant factor in boundary layer stability. Komoda (1967) observed that whenever there is a considerable spanwise variation in the boundary layer thickness, as is the case near the "wing-tip" of the turbulent spot, breakdown is preceded by a concentration of vorticity in a thin vertical layer; thus, the appearance of such shear layers in the present experiment should not be surprising. Typically those shear layers are very long in comparison to their lateral dimension and we conclude, albeit from a small sample of observations, that the dominant aspect ratio of these layers is:

$$.025 \leq z/tU_\infty \leq .05.$$

These numbers are in agreement with pictures visualizing sublayer streaks in a turbulent spot (CCD)

Instantaneous observations in the y-t plane were made with the 10 wire y-rake at various spanwise and streamwise locations. The most interesting observations are those showing the breakdown of the wave packet and the generation of a new spot. The uppermost trace in Fig. 20 shows a velocity record obtained from a single hot wire located on the plane of

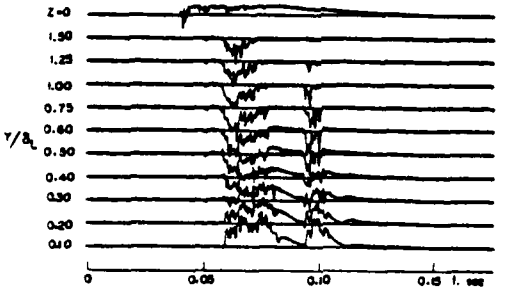

Figure 20. Velocity signatures showing the generation of a new spot. x_s = 900 mm z/x_s = 0.115 upper trace taken at z = 0.

symmetry. From this record alone, one would deduce a passage of a single spot. At the same time (all other velocity traces in Fig. 20) a rake located at z/x_s = 0.115 indicated that behind the parent spot a new transitional spot appears. This spot was generated by the breakdown of the wave packet and occurs outside the calmed region at z/x_s 0.1. At earlier stages of breakdown one could clearly recognize the transitional spikes in velocity which were observed many years ago by Klebanoff et al, (1962). In fact, when instantaneous velocity profiles were plotted in a plane normal to the surface, some of them showed inflection points and general characteristics which are very similar to those of Klebanoff.

The development of a single momentary perturbation into a transitional spot was examined by Amini (1978). Ensemble averaged velocity profiles measured by Amini indicate the possibility that the perturbation develops into a three dimensional wave packet which breaks down as it proceeds downstream. The wavy nature of the disturbance is most clear in the outer region of the layer (Fig. 21), thus having some similarity to the experiments of Gaster and Grant (1975). It is therefore believed that the generation of smaller scale eddies, streaks, and new tran-

sitional spots results from a breakdown of Tollmien Schlichting waves. The critical question is whether the regeneration mechanism occurs also in a turbulent environment.

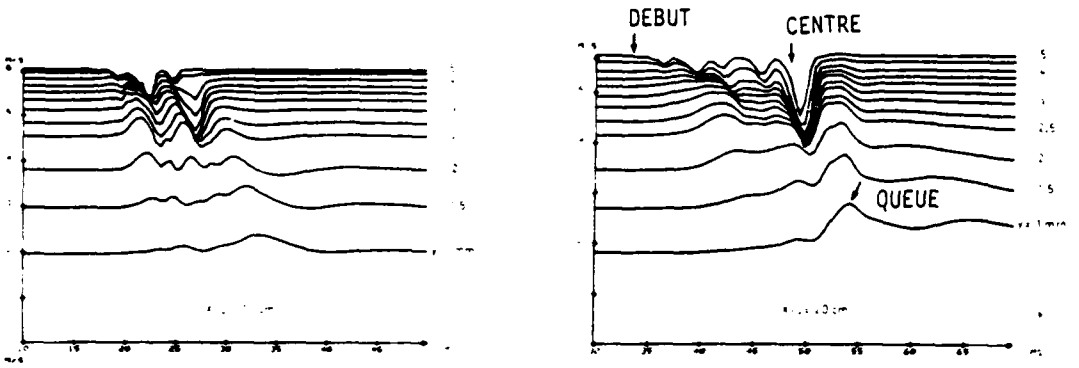

Figure 21. Ensemble averaged velocity in the incipient spot at various distances from the surface z=0 (courtesy of Amini)

a) x_s = 100 mm b) x_s = 200 mm

6. THE EFFECT OF TRANSITION ON THE LARGE COHERENT STRUCTURES IN OTHER TURBULENT SHEAR FLOWS

The velocity distribution in a turbulent pipe flow can be described by the same universal profile as boundary layer flows. This leads one to believe that the underlying processes are similar in both flows, although there is no entrainment of irrotational fluid in a pipe. Therefore, the large coherent eddies in a turbulent pipe flow should be related to the transitional structure existing at lower Reynolds numbers. There are however, two very different types of intermittently turbulent flows occurring naturally in a pipe: (i) slugs, which are caused by instability of the boundary layer to small disturbances in the inlet region of the pipe, and (ii) puffs which are generated by large disturbances at the inlet and occur at a lower Reynolds number. It was observed (Wygnanski and Champagne (1973)) that slugs are much larger and the structure of turbulence in their interior is identical to the structure of a fully developed pipe flow. To resolve the difficulty, a study was undertaken in which a fully developed Poisseille flow was momentarily disturbed at fairly low Reynolds numbers. The resulting transitional structures were again puffs and slugs with the former occurring at slightly lower Reynolds numbers. However, at some critical Re, puffs started to split, indicating the existence of a regeneration process. (See also Lindgren 1957 and Wygnanski, Sokolov and

Friedman, 1975). A further increase in Re results in a faster rate of splitting and almost instantaneous interaction between adjacent puffs leading to the creation of a larger structure - namely a slug. The puff has then the same role in turbulent pipe flow as the transitional spot in boundary layer flow. In fact, an experiment in which evoked puffs interact was recently finished and data is being processed.

One still has to reconcile the differences between the puff and the spot. This task was greatly facilitated by the recent observations of Amini on the incipient spot. In Fig. 22 two stream line patterns relative to the trailing interface are shown for the puff and for the incipient spot. The similarity between the two patterns cannot be dismissed as a mere coincidence in spite of the different geometry. The streamwise velocities as observed on oscilograms also exhibit a striking similarity between the two cases.

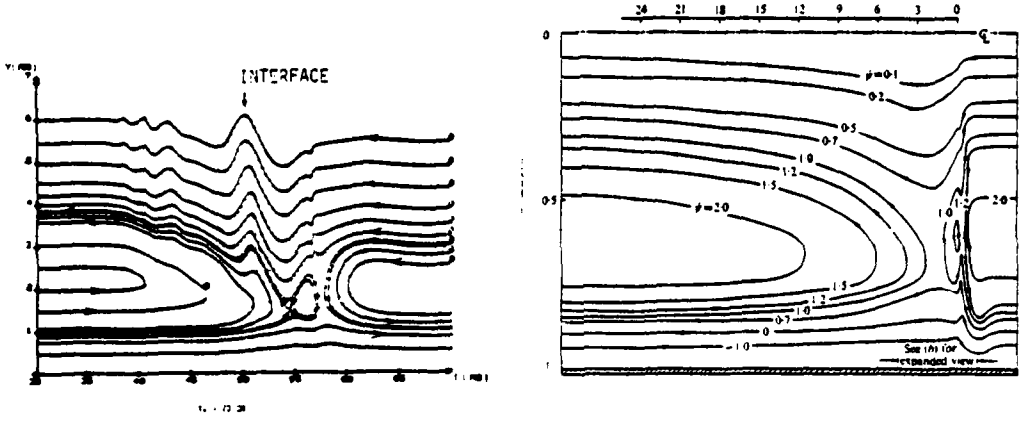

Figure 22. Stream line patterns in boundary layer and pipe flows

a) The incipient transitional spot b) A puff in a pipe flow (curtesy of Amini)

The large coherent eddies in a turbulent mixing layer at fairly high Re originate at the beginning of the mixing process before the flow becomes fully turbulent. In this case, as in the other two discussed, the basic charactertistics of the coherent structure is determined in the transition region and is remembered in the fully developed flow.

In conclusion, statements of the kind "....the conditions at the initiation of the flow are mostly irrelevant" or "...the structure of turbulence is determined to a great extent by local conditions" or "turbulent flow forgets...." which were often made, and the concepts which they represent should be carefully reexamined in view of the above mentioned results.

ACKNOWLEDGEMENT

The presentation of these results would not have been possible were it not for the help of: D. Friedman, J. Haritonidis, R.E. Kaplan, M. Sokolov and M. Zilberman, as well as the financial assistance of AFOSR under Grant No. 77-3275.

REFERENCES

1. Laufer, J. (1975). Annual Rev. Fluid Mech. 7, 307.
2. Willmarth, W.W. (1975). Adv. in Appl. Mech. 15,159.
3. Willmarth, W.W. and Bogar, T.J. (1977). Phys. of Fluids, 20, S9.
4. Blackwelder, R.F. and Kaplan, R.E. (1972). Proceedings 12th IUTAM Congress of Applied Mechanics, Moscow.
5. Emmons, H.W. (1951). J. Aero. Sc. 18, 490.
6. Schubauer, G.B. and Klebanoff, P.S. (1956). N.A.C.A. Report, No. 1289.
7. Coles, D. and Barker, S. (1975), in Turbulent Mixing in Non-Reactive and Reactive Flows, Plenum Press, New York.
8. Zilberman, M., Wygnanski, I. and Kaplan, R.E. (1977). Phys. of Fluids, 20, S258.
9. Haritonidis, J.H., Kaplan, R.E. and Wygnanski, I. (1977). Proceedings of Symposium on Turbulence, Berlin, Springer Verlag, Berlin.
10. Falco, R.E. (1977). Phys. of Fluids, 20, S124.
11. Wygnanski, I., Sokolov, M. and Friedman, D. (1976). Jour. of Fluid Mech. 18, 185.
12. Cantwell, B., Coles, D., Dimotakis, P. (1977). California Institute of Technology Report (To be published in JFM).
13. Patel, V.C. and Head, M.R. (1969). Jour. of Fluid Mech. 38, 181.
14. Brown, G.L. and Thomas, A.S.W. (1977). Phys. of Fluids, 20, S243.
15. Klebanoff, P.S., Tidstrom, K.D. and Sargent, L.M. (1962). Jour. of Fluid Mech. 12, 1.
16. Komoda, H. (1967). Phys. of Fluids, 10, S87.
17. Amini, J. (1978). Transition controlee en couche limite: Ph.D. thesis Universite Scientifique et Medicale de Grenoble.
18. Gaster, M. and Grant, I. (1975). Proc. Roy. Soc. London A, 347,235.
19. Wygnanski, I., Haritonidis, J.H. and Kaplan, R.E. (1977). University of Southern California. Interim report (to be published in Jour. of Fluid Mech.)
20. Wygnanski, I. and Champagne, F.H. (1973). Jour. of Fluid Mech. 59. 281.
21. Lindgren, E.R. (1957). Ark. Fys. 12, 1.
22. Wygnanski, I., Sokolov, M. and Friedman, D. (1975). Jour. of Fluid Mech. 69, 283.

DISCUSSION

Bradshaw:

Just a short comment and a warning. Since all these eddies are rather elephants they probably have a pretty long memory for almost any sort of perturbations and in fact, if you put a longitudinal vortex, even a very weak one, into a boundary layer it goes on and on and on. I think mentally we sometimes overestimate the amount of mixing and dispersing that the turbulent boundary layer can really do. This obviously isn't a criticism of your work, but is is perhaps an explanation of how the initially laminar spot can proceed still identifiably in a turbulent boundary layer, as long as it doesn't interact very strongly. The warning incidentally, is if you flow a jet through a boundary layer, the vertical velocity component is likely to be very large compared to that in the boundary layer itself, as Lowell Ormand just pointed out to me, and you may therefore blow part of the vorticity right out of the boundary layer so it sits in the free stream. We found this ourselves in flowing jet studies trying to produce turbulent spots.

Morkovin:

If what you have is a remnant of your perturbation which is related in some way to a turbulent eddy, does it have a connection with the Kovaszny, Kibens, Blackwelder, donut or watermelon? After all, that thing also arose by itself from some kind of a transition. Why is it not the way that you have it.

Wygnanski:

Its convection velocity is somewhere in the higher 80% to 90% of the free stream velocity. In the Z direction we could interpret the contours in a way which we're corresponding to the watermelon. If I were to take the positive and the negative contours which we measure at Z/δ away from the center, we would obtain something that looked very much like a positive correlation, with a negative correlation at the side. The distance between the center of these correlations would be approximately 1/2 to 2/3 Delta. That's very good agreement.

Kovaszney:

I have one more comment. If you compare it not with a double correlation, but with a triple correlation, the thing is not automatically symmetricized. Then, of course, these things are even more striking. That's what they should be compared with.

Falco:

Is it comparable in that sense.

Kovaszney:

It's comparable in size and orientation.

THE STRUCTURE OF TURBULENCE IN THE NEAR WALL REGION

Helmut Eckelmann

Lehrstuhl für Angewandte Mechanik und Strömungsphysik
am Max-Planck-Institut für Strömungsforschung
D 34 Göttingen, Federal Republic of Germany

ABSTRACT

In a fully developed turbulent channel flow the streamwise and spanwise velocity components, and the wall gradients of these components, were measured by using hot-film sensors and flush-mounted wall elements. An oil channel was used which permitted measurements very close to the wall at a Reynolds number of 7700. Space-time correlations in the direction normal to the wall showed a severe change of the flow structure in the viscous sublayer, produced by the physical presence of the moveable probe. A similar disturbance of the near-wall region has been observed by other investigators, but was not recognized as an artificially produced flow structure.

1. INTRODUCTION

It is well established that turbulent motions in the near-wall region in bounded turbulent shear flows show a quasi-ordered structure. The picture that we have today of this kind of flow has been formed in large part by the visual studies of Kline, Reynolds, Schraub and Rundstadler (1967), Corino and Brodkey (1969), Kim, Kline and Reynolds (1971), Nychas, Hershey and Brodkey (1973), Offen and Kline (1974) and more recently by Oldaker and Tiederman (1977). The work done by the hot-wire and hot-film method, as well as the interferometric technique used by Emmerling (1973), brought further insight into the characteristics of bounded turbulent shear flows. At this point it should not be necessary to name all the other authors who worked on this problem, because the two review articles by Laufer (1975) and Willmarth (1975) very well summarize the work that was done on the structure of turbulence in bounded turbulent shear flows. In the following, only the papers of immediate pertinence to the problem will be cited.

Space-time correlations of velocity fluctuations have often been used in turbulent flows to obtain an idea of the coherent structures. The advantage of this method is that it allows quantitative measurements of the convection and decay of these structures. The disadvantage is that two or more probes have to be inserted into the flow. Care always has been taken that no probe will be in the wake of another probe. Whether such probes will disturb, entirely change or even fully destroy the structures that should be investigated, cannot however be predicted.

Correlation measurements in the viscous sublayer and adjacent wall region that were carried out in the oil channel of the Max-Planck-Institut für Strömungsforschung in Göttingen by Kreplin, Eckelmann and Wallace (1974) and by Blackwelder and Eckelmann (1977a) showed severe probe interferences. These interferences were the result of the physical presence of the probe near the wall, where the probe seemed to cause a change in the existing structure in the wall area. It will be shown by two other examples that such interferences also have contaminated similar correlation measurements of other investigators.

2. EXPERIMENTAL TECHNIQUES

Any probe that is inserted into a flow field perturbs the flow, because the fluid must move around the sensor and the probe body. This is true for all kinds of probes (hot-wire, Pitot-tubes etc.). To minimize the inherent disturbance of the flow field at the location of the sensor, a probe is normally constructed such that the sensor is located in a sufficiently undisturbed area. But what happens to the flow field, if such an ideal probe is positioned very close to the wall? The flow between the probe and the wall will be accelerated or blocked. Both effects can be minimized by using a bent probe, such that sensor and probe body are displaced from each other by several body diameters, in a direction transverse to the mean flow direction. Such probes are known as boundary-layer probes.

The influence of the wall on hot-wire measurements has been investigated in detail by Wills (1962). This work, and also that of others not cited here, is restricted to the influence on mean values when hot-wire probes are positioned very close to a wall. The possible change of existing flow structures due to the presence of the probe, and hence the change in the measured values due to this effect, have to the knowledge of the author not been discussed. That a disturbance of the flow field near the wall was observed in our flow channel (where the diameter of the hot-film probe used was of the same size as the thickness of the viscous sublayer) indicated that even under these conditions a change of the flow structure due to the presence of the probe could be responsible for the deviations observed.

Before discussing further details, a brief description of the flow channel and the probes that were used for the measurements will be given. The data were all obtained in the oil channel described by Eckelmann (1970, 1974). At this point it is only necessary to repeat the main features of the channel.

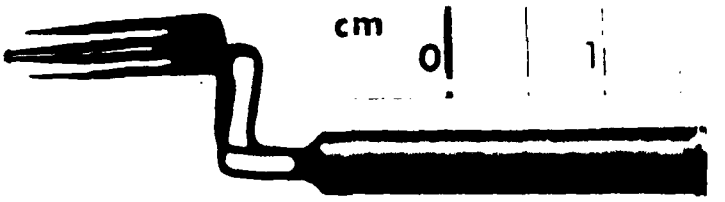

Figure 1. Photograph of the V-probe used for the experiments.

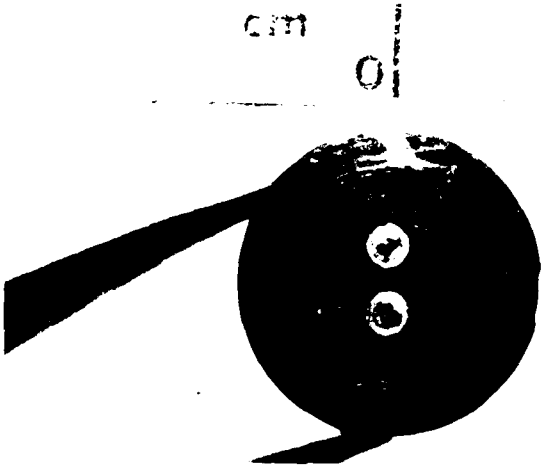

Figure 2. Photograph of the wall-element plug with two DISA type 55A93 probes.

The oil channel is 8.5 m long, 0.22 m wide and 0.79 m deep. The flow was tripped as it entered the channel. The measurements were made 32 channel-widths downstream and half way between the top cover and bottom of the channel, where the flow was fully developed. A portion of

the partition wall at the test section was replaced by a special wall that had several pairs of flush-mounted wall elements and a removable plug, into which special probe configurations could be placed. This wall was the same as that used by Kreplin (1976) and Blackwelder and Eckelmann (1977a).

The test fluid was oil of kinematic viscosity 0.06 cm^2/s at 25^oC. The Reynolds number based upon the channel width was 7700 and the friction velocity u_τ = 1.06 cm/s. At this Reynolds number a distance of 1 cm corresponded to a dimensionless distance of $\lambda^+ = \frac{1 \cdot u_\tau}{\nu} = 17$.

Measurements of the streamwise and spanwise velocity components, U and w, were made with quartz-coated hot-film probes. To avoid an influence of the mean gradient $\frac{\partial U}{\partial y}$ on the spanwise velocity component, two hot-film sensors were placed 90^o apart in one plane, in a V-configuration. To avoid errors when the probe was used near the wall, at distances down to $y^+ = 1$, the sensors were displaced by about 1 cm with respect to the probe body. Such V-probes are not commercially available. Figure 1 shows the V-probe used, designed by the author and his former co-worker Dr. Kreplin and built at the Max-Planck-Institut für Strömungsforschung using two 1 mm long and 50 µm thick TSI model 10121-20W sensors.

Heated wall elements were utilized to measure the two velocity gradients at the wall, $\left.\frac{\partial U}{\partial y}\right|_W$ and $\left.\frac{\partial w}{\partial y}\right|_W$. The wall elements are pairs of flat hot-films that are flush-mounted in a V-configuration in a wall plug. Figure 2 shows such a wall element consisting of two DISA type 55A93 probes. The sensors are quartz-coated, with dimensions of 0.75 mm long and 0.15 wide. To check for probe interference, an arrangement was used that consisted of a single hot-film probe mounted on a wall plug at a distance of $y^+ = 15$ and a wall element which was embedded in the wall at the same x-location, but separated in the spanwise direction by $z^+ = 17$. A perspective sketch of this arrangement is shown in Figure 5, together with the V-probe. The single hot-film probe was also made at the institute using the same TSI sensors as used for the V-probe.

The hot-films and wall elements were driven by DISA 55M01 anemometers coupled to DISA 55D10 linearizers. The overheat ratio of the hot-films was 1.01 and of the wall elements 1.02. The low overheat ratio was possible because the temperature of the entire laboratory including the oil channel was controlled.

The calibration of the V-probe was achieved by towing the probe at variable speeds through the oil channel with the oil at rest. The fixed velocity probe at $y^+ = 15$ (compare Figure 5) was calibrated together with the wall elements in situ by operating the channel at different speeds corresponding to known velocities at the location of the probe and known velocity gradients at the wall. Errors encountered due to free convection could be minimized by using the calibration technique

described by Blackwelder and Eckelmann (1977b). The streamwise velocity component from the V-probe and the streamwise gradient component from the wall element were obtained by using the sum of the linearized signals from the two sensors forming the probe in each case. Similarly, the spanwise components were derived from the differences. Since in a fully developed channel flow $\bar{w}$ and $\left.\frac{\partial \bar{w}}{\partial y}\right|_W$ are zero, the mean values of the difference signals were adjusted to be zero. To get an idea of a systematic error, the correlation coefficient between the streamwise and spanwise components was calculated. These values, which by homogeneity should be zero, were typically found to be less than 10 %. An additional technique was then used which slightly adjusted the calibration slopes of the individual sensors so that the correlation coefficients were made zero. This additional adjustment lay always within the range of scatter of the calibration data.

The various signals from the moveable V-probe, from the wall element and from the fixed probe at $y^+ = 15$ and $z^+ = 17$ were sent over analog lines to a multiplexer with analog-to-digital converter, were then digitized at a rate of 50 samples per second and finally stored on a magnetic disk. The subsequent processing of the data was accomplished by FORTRAN programs. A PDP-15 computer was used for both data acquisition and processing. Records of duration 30 minutes were evaluated at every V-probe position.

3. SPACE-TIME CORRELATION

Correlation measurements have been carried out in the oil channel for several years. Eckelmann (1970, 1974), Kreplin, Eckelmann and Wallace (1974), Kreplin (1976) and more recently Blackwelder and Eckelmann (1977a) made correlation measurements in conjunction with an investigation of the structure of the near-wall region. The thick viscous sublayer of the oil channel allowed measurements very close to the wall. Down to wall distances of about $y^+ = 1$, corresponding to $y \geq 0.5$ mm, an influence of the wall on the signal of a single hot-film probe could not be observed. Eckelmann (1970) showed that the fluctuations of the streamwise velocity u and the fluctuations of the streamwise velocity gradient at the wall $\left.\frac{\partial u}{\partial y}\right|_W$ are highly correlated in the viscous sublayer and in the adjacent buffer layer. In addition, both fluctuations are shifted in time such that the signal measured in the flow preceded the signal measured at the wall. Kreplin (1976) could show in his dissertation that also the spanwise fluctuations of the velocity w, and the fluctuations of the spanwise velocity gradient at the wall $\left.\frac{\partial w}{\partial y}\right|_W$, are correlated and shifted in time. However, the correlations decreased more rapidly with increasing wall distance than was observed for the streamwise components. Figure 3 shows the correlation functions

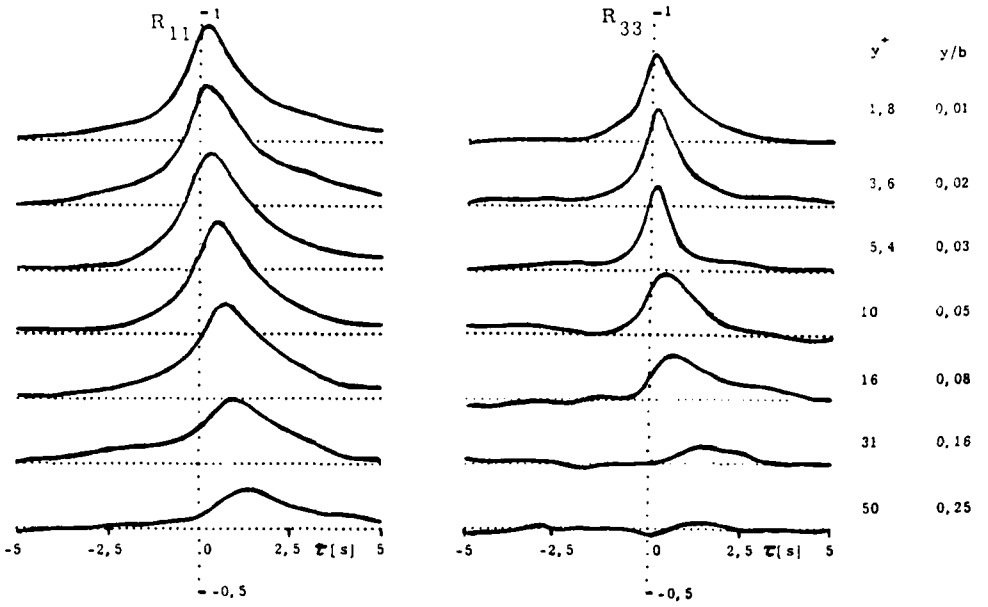

Figure 3. Space-time correlations of the streamwise velocity fluctuations u and the streamwise wall gradient fluctuations $\left.\frac{\partial u}{\partial y}\right|_W$ (left). Space-time correlations of the spanwise velocity fluctuations w and the spanwise wall gradient fluctuations $\left.\frac{\partial w}{\partial y}\right|_W$ (right). y is the separation normal to the wall and b the channel half-width. From Kreplin (1976).

$$R_{11}(y^+,\tau) = \frac{\overline{u(y^+,t) \cdot \left.\frac{\partial u(0,t+\tau)}{\partial y}\right|_W}}{u'(y^+) \cdot \left.\frac{\partial u'}{\partial y}\right|_W}$$

and

$$R_{33}(y^+,\tau) = \frac{\overline{w(y^+,t) \cdot \left.\frac{\partial w(0,t+\tau)}{\partial y}\right|_W}}{w'(y^+) \cdot \left.\frac{\partial w'}{\partial y}\right|_W}$$

which were measured by him. The denominators of the two correlation functions are formed using the products of the r.m.s. values. The probes used by Kreplin were the same as shown in Figures 1 and 2.

Finally, Blackwelder and Eckelmann (1977a) measured again the correlations $R_{11}(y^+,0)$ and $R_{33}(y^+,0)$ in conjunction with their investigation of streamwise vortices, which were associated with the bursting phenomenon. The paper of Professor Blackwelder, also presented at this workshop, reports in detail about these investigations. In these measurements it was observed that the correlation $R_{33}(y^+,0)$ displayed a very irregular behavior for $y^+ < 10$. In particular, sometimes very strong negative correlations were obtained with separations of $y^+ = 5$ and less. When the measurements were repeated under similar conditions, however, positive correlations were obtained. In Figure 4 the results of three different runs are plotted. The values $R_{11}(y^+,0)$ measured simultaneously and Kreplin's $R_{11}(y^+, \tau = 0)$ and $R_{33}(y^+, \tau = 0)$ obtained from Figure 3 are also represented in this Figure. The probes used for the investigation were those previously used by Kreplin.

Since the signals themselves did not show any obvious difference for positive and negative correlation $R_{33}(y^+,0)$, it was impossible to decide on the basis of $R_{33}(y^+,0)$ which the correct value was. The decision was made more difficult because the correlation $R_{11}(y^+,0)$ was independent of the sign of $R_{33}(y^+,0)$. Thus a new experiment was developed, with the probe arrangement shown in Figure 5. A fixed single probe and a wall-element were mounted on a wall plug. The V-probe was located directly above the wall element at various wall positions y^+. In addition to the correlation $R_{11}(y^+,0)$ and the suspect $R_{33}(y^+,0)$, shown in Figure 4, the correlations between the streamwise fluctuation velocity component at $y^+ = 15$ and $z^+ = 0$ and the two fluctuation components $\frac{\partial u}{\partial y}\Big|_W$, $\frac{\partial w}{\partial y}\Big|_W$ of the gradient at $y^+ = 0$ and $z^+ = 17$ were computed as the moving V-probe above the wall element approached the surface. With no probe interference, the two correlation functions

$$R^*_{11}(y^+,z^+,\tau) = \frac{\overline{u(15,0,t) \cdot \frac{\partial u(0,17,t+\tau)}{\partial y}\Big|_W}}{u'(15,0) \cdot \frac{\partial u'}{\partial y}(0,17)}$$

and

$$R^*_{13}(y^+,z^+,\tau) = \frac{\overline{u(15,0,t) \cdot \frac{\partial w(0,17,t+\tau)}{\partial y}\Big|_W}}{w'(15,0) \cdot \frac{\partial w'}{\partial y}(0,17)}$$

should show the same shape and magnitude independent of the V-probe location. The result of this new experiment was that again the shape of the correlation function $R^*_{11}(y^+,z^+,\tau)$ was not affected. However, the function $R^*_{13}(y^+,z^+,\tau)$ showed a remarkable change.

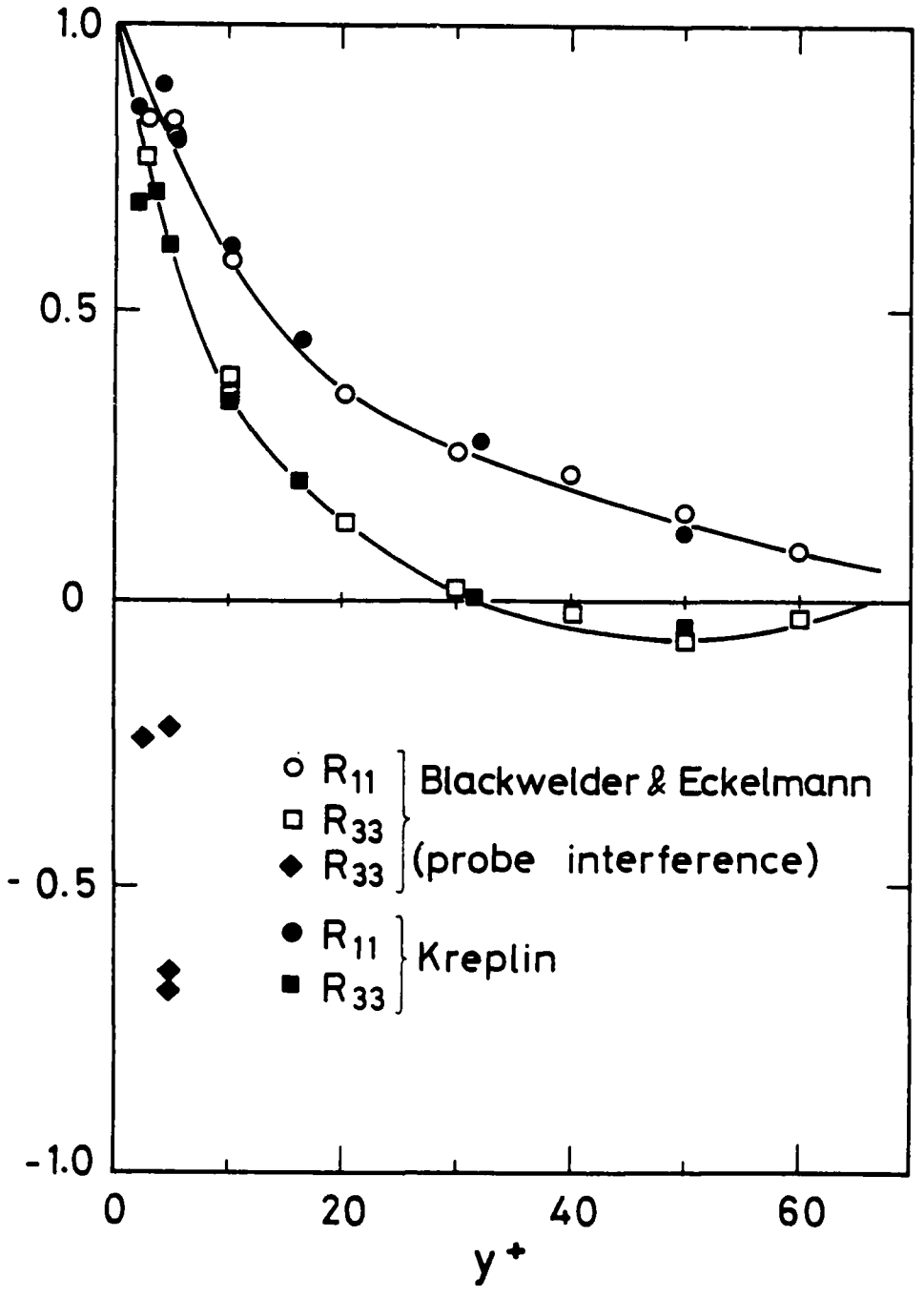

Figure 4. Spatial correlations of u and $\frac{\partial u}{\partial y}\Big|_w$ (R_{11}) and of w and $\frac{\partial w}{\partial y}\Big|_w$ (R_{33}) with separations normal to the wall.

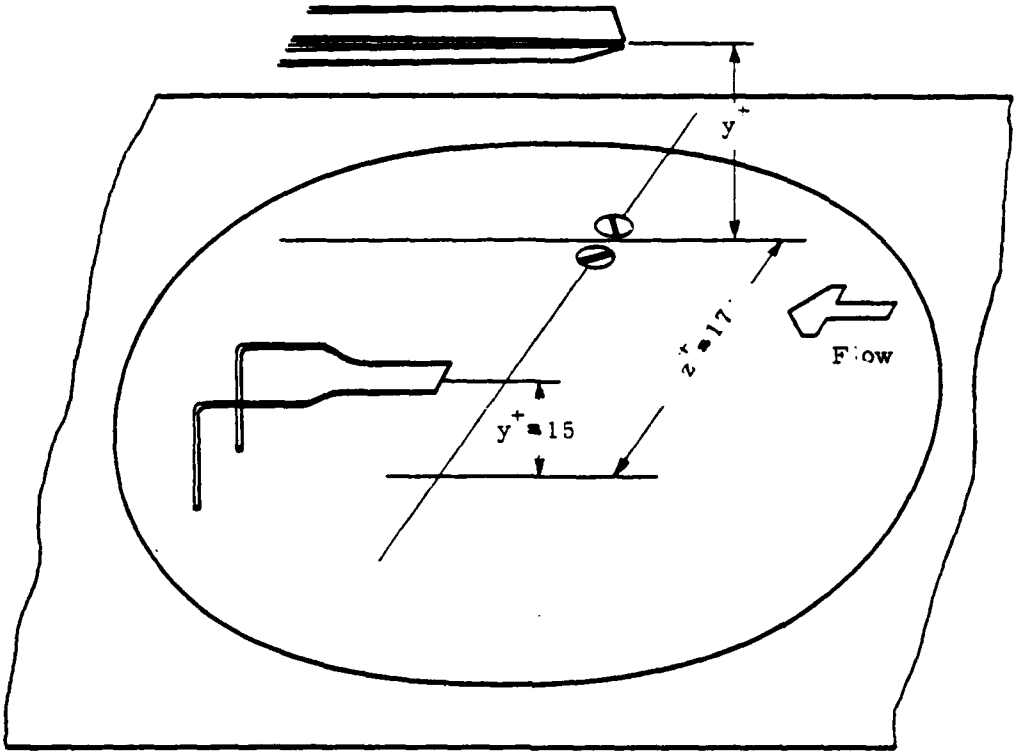

Figure 5. Sketch of the probe arrangement used to check for probe interference. Single hot-film probe (left), wall-element (right) and V-probe (middle).

The results are seen in Figure 6 for six different locations of the moveable V-probe. As long as the V-probe was at wall distances $y^+ > 10$ the correlation functions $R^*_{13}(y^+,z^+,\tau)$ did indeed show the same shape and magnitude. At $y^+ = 5$ the computed correlation was observed to have approximately the same shape and magnitude but an opposite sign. At $y^+ = 2.5$, both a positive and a negative correlation were observed in two different runs. Since the y^+ and z^+ separations could only be determined for these experiments within ± 0.5, it was believed possible that the positive correlation at $y^+ = 2.5$ was obtained at a slightly different position than the correlation with the negative value. The correlation functions $R^*_{13}(y^+,z^+,\tau)$ in Figure 6 were always negative whenever the correlation $R_{33}(y^+,0)$ in Figure 4 simultaneously yielded a negative value.

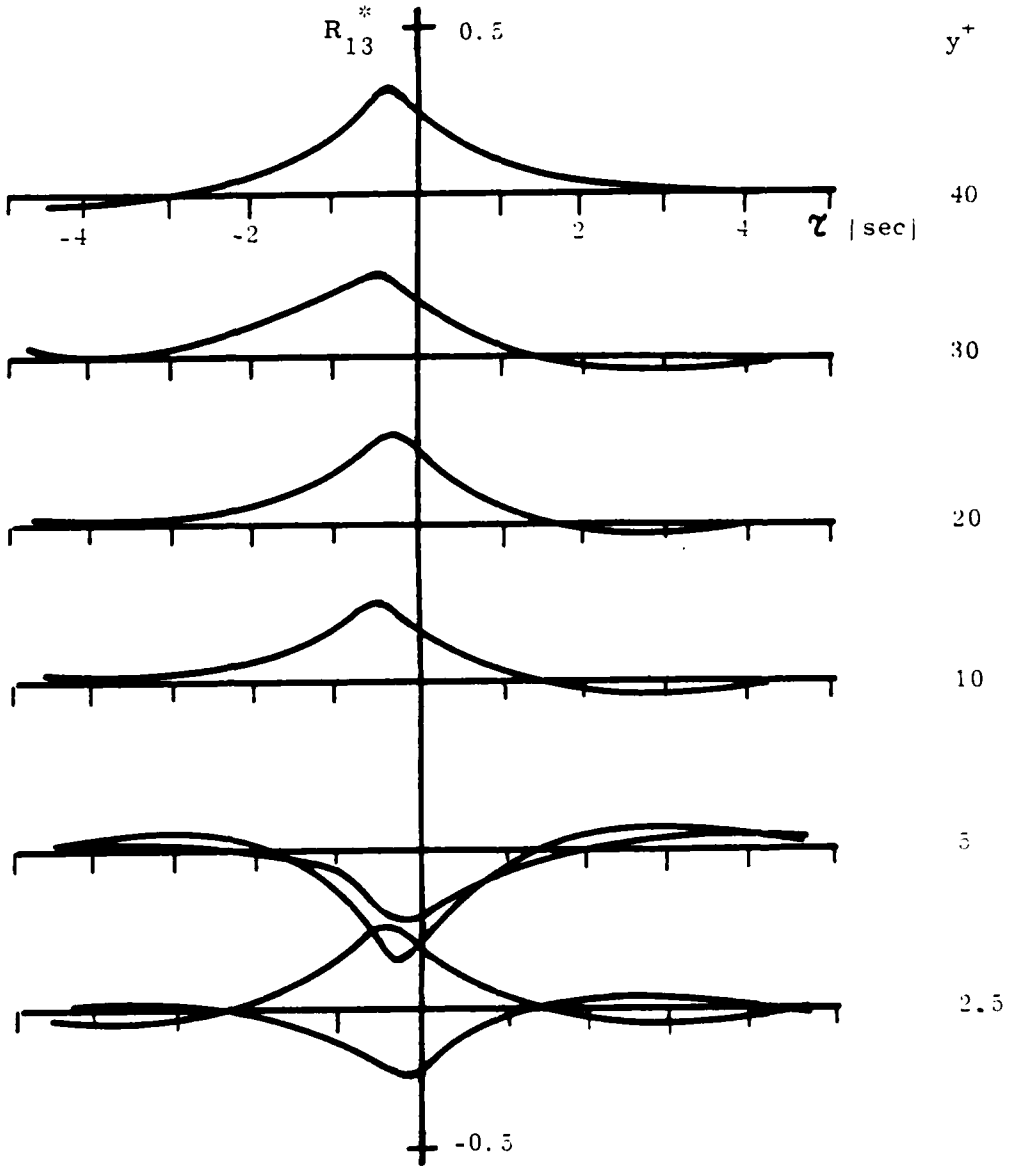

Figure 6. Space-time correlations of the streamwise velocity fluctuations at $y^+ = 15$ and $z^+ = 0$ (single hot-film probe) and spanwise velocity gradient fluctuations at $y^+ = 0$ and $z^+ = 17$ (wall element). The moveable V-probe was positioned at $z^+ = 17$ and at the indicated y^+ positions.

To be sure that the observed probe interference was not caused by electrical cross-coupling through a possibly defective quartz coating of the sensors the V-probe was first driven cold (anemometer in standby position) and then disconnected from all electrical leads (also from ground). Both experiments were made at $y^+ = 5$. However, the signals of the wall-element and the wall-probes, as well as the correlation R^*_{33} between them, were not affected. The conclusion that can be drawn from all these experiments is that the V-probe by its physical presence in the viscous sublayer causes a change in the existing flow structure. This change is such that the streamwise velocity and wall gradient components seem to be unaffected but the spanwise velocity and wall gradient components suffer a phase shift of 180^0. Knowing nothing about the probe inference, this could be misinterpreted as a new vortex structure inside the viscous sublayer, a structure which in reality does not exist. However, it can be assumed that the presence of the V-probe generates such a structure.

4. DISCUSSION AND CONCLUSIONS

Spatial correlations with separations normal to the wall have also been carried out by Gupta, who used for his experiments in air a fixed V-probe at $y^+ = 2.8$ and a moveable probe which he could place as close as $y^+ \sim 5$ from the wall. Lau worked with an iodine electrolyte. He used electrochemical wall electrodes to measure the streamwise and spanwise gradients at the wall and simultaneously a thermal probe in the flow field. Lau could also measure down to $y^+ \sim 5$. The Reynolds number in Gupta's experiment was three times and in Lau's experiment more than twice that in our oil channel. The correlations $R_{11}(y^+,0)$ obtained by Gupta and Lau are shown in Fig. 7, together with those of Blackwelder and Eckelmann. Gupta's and our measurements are in good agreement.

The spatial correlations $R_{33}(y^+,0)$ of the same three experiments are plotted in Fig. 8. It can be seen that the measurements of Gupta and Lau also show in the vicinity of the wall the same characteristic behaviour found in our measurements. It is almost certain that also in the case of Gupta and Lau a probe interference is causing the negative lobes of the correlation curves. These probe interferences, however, could not be recognized by them. because they did not simultaneously measure a third correlation that should be constant, independent of the location of the moveable probe. Just as in our case, the correlations $R_{11}(y^+,0)$ of Gupta and Lau were not affected by the probe interference.

In Fig. 8 the dependence of the Reynolds number can also be seen. With increasing Reynolds number, the influence of the probe on the near wall region starts sooner as the probe is approaching the wall. The disturbance a probe produces in the wall region depends on the (normalized) characteristic dimension and on the shape of the probe itself. In the oil channel the influence of the probe is restricted to the viscous

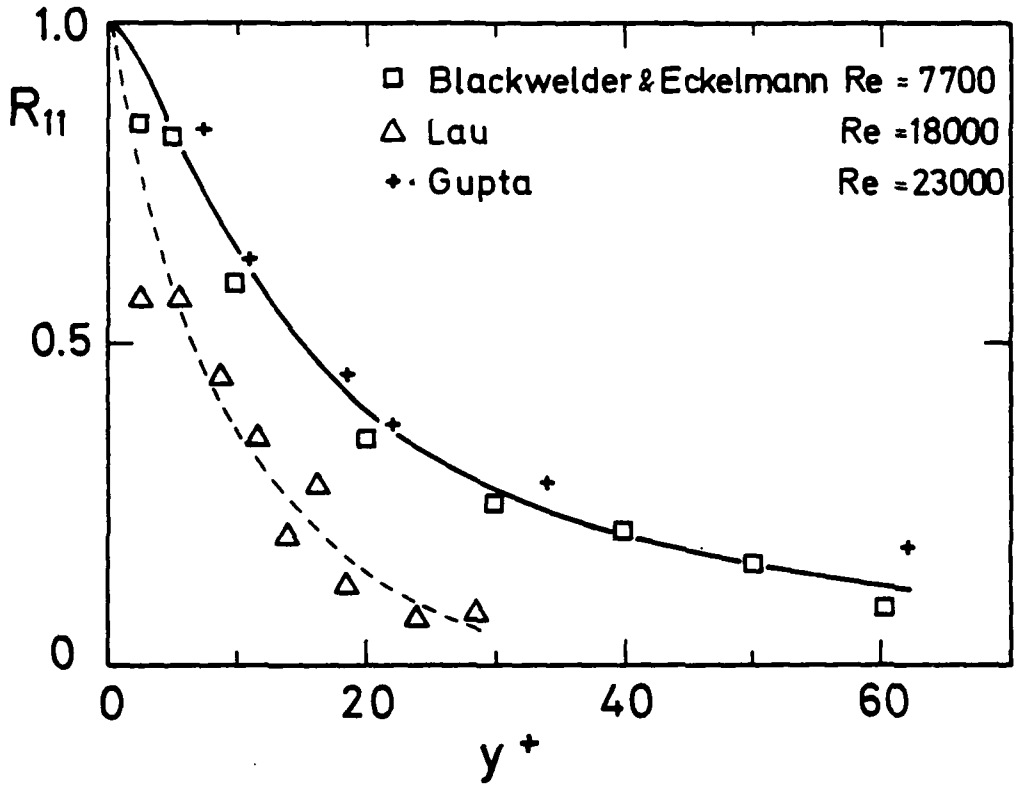

Figure 7. Spatial correlations of u and $\frac{\partial u}{\partial y}\Big|_W$ measured by Lau (1977) and Blackwelder and Eckelmann (1977) and of u and $u(y^+ = 2.8)$ measured by Gupta (1970) with separations y normal to the wall.

sublayer region ($y^+ \leq 5$) or is not observed, as in the case of Kreplin's measurements (Fig. 3). In the oil channel the thickness of the sublayer is about five times that of Gupta's wind tunnel where the probe interference already started in the buffer layer ($y^+ \leq 30$).

Space-time correlation measurements of Kreplin et al. (1974) also show that flow structures in the vicinity of the wall are probe interferences, that do not exist without a probe. The space-time correlations of the spanwise component R_{33} shown in Fig. 9 are not in contradiction with streamwise vortices that obviously are produced by the physical presence of the probe.

It is planed to continue this work to get further insight into the problem of probe interference in the near-wall region.

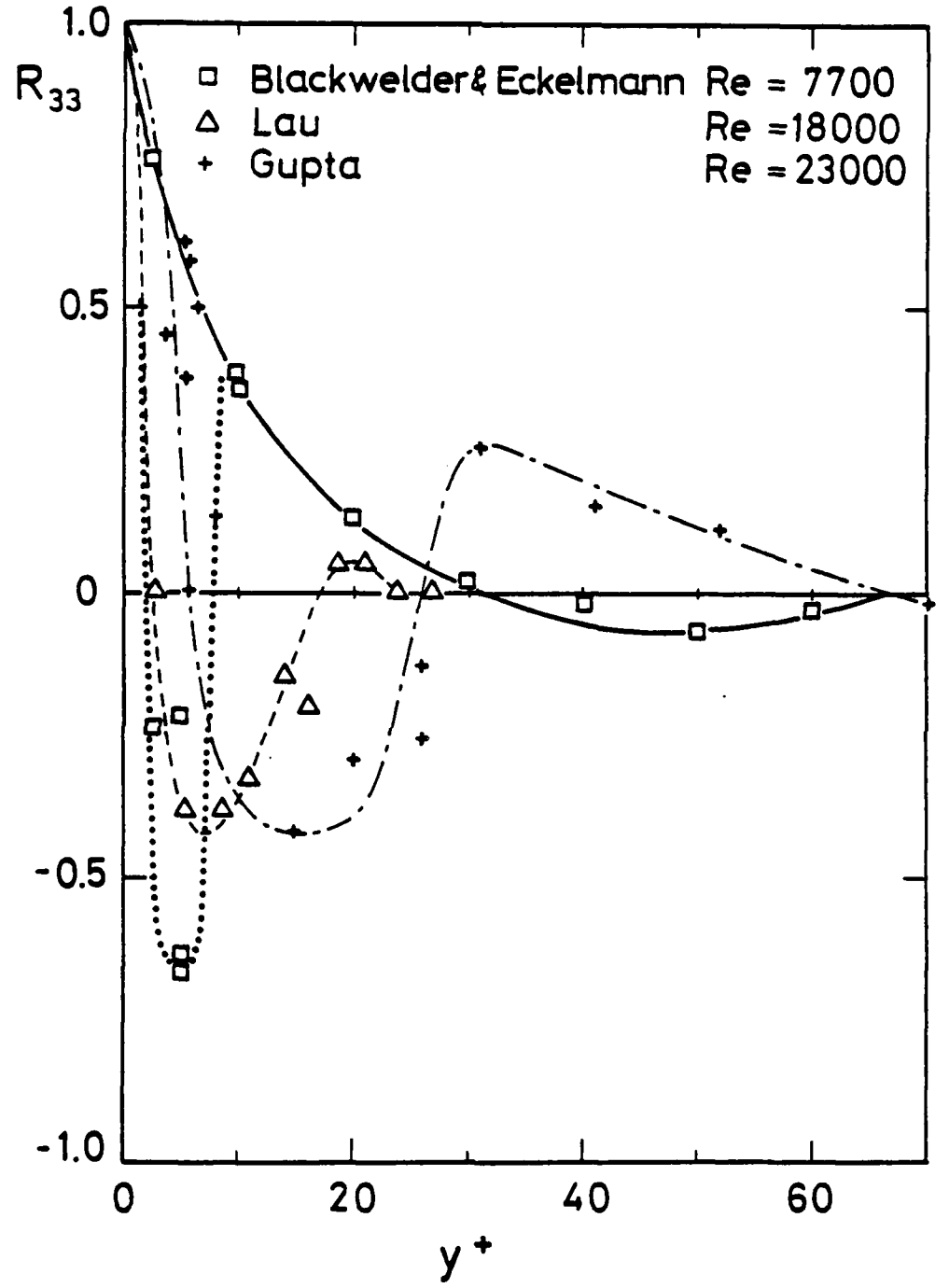

Figure 8. Spatial correlations of w and $\frac{\partial w}{\partial y}\Big|_w$ measured by Lau (1977) and Blackwelder and Eckelmann (1977) and of w and $w(y^+ = 2.8)$ measured by Gupta (1970) with separations y normal to the wall.

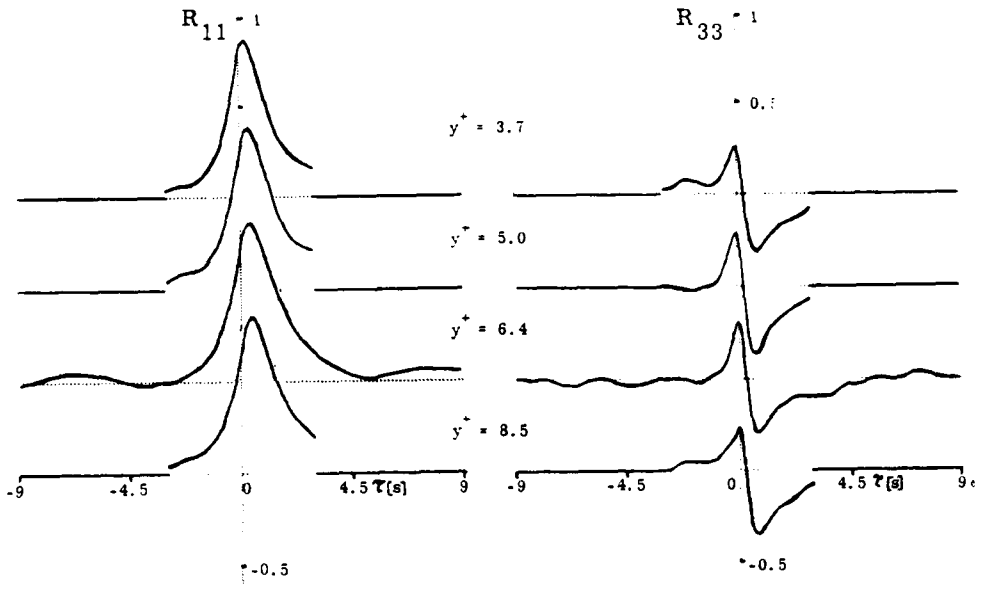

Figure 9. Space-time correlations of u and $\frac{\partial u}{\partial y}\Big|_W$ (left) and of w and $\frac{\partial w}{\partial y}\Big|_W$ (right) with separations y normal to the wall. From Kreplin, Eckelmann and Wallace (1974).

REFERENCES

1. Blackwelder, R.F., Eckelmann, H., 1977a. Streamwise vorticies associated with the bursting phenomen, submitted for publication in J.Fluid Mech.

2. Blackwelder, R.F., Eckelmann H., 1977b. Influence of the convection velocity on the calibration and linearization of heated surface elements, to appear in proceedings of EUROMECH 90, Nancy 1977

3. Corino, E.R., Brodkey, R.S., 1969. A visual investigation of the wall region in turbulent flow, J.Fluid Mech. 37, 1

4. Eckelmann, H., 1970. Experimentelle Untersuchungen in einer turbulenten Kanalströmung mit starken viskosen Wandschichten, Mitt. MPI Strömungsforschung and AVA, Göttingen, No. 48 (available in English)

5. Eckelmann, H., 1974. The structure of the viscous sublayer and the adjacent wall region in a turbulent channel flow, J.Fluid Mech. 65, 439

6. Emmerling, R., 1973. Die momentane Struktur des Wanddruckes einer turbulenten Grenzschichtströmung, Mitt. MPI Strömungsforschung and AVA, Göttingen, No. 56

7. Gupta, A.K., 1970. Ph.D. Thesis, University of Southern California

8. Kim, H.T., Kline, S.J., Reynolds, W.C., 1971. The production of turbulence near a smooth wall in a turbulent boundary layer, J. Fluid Mech. 50, 133

9. Kline, S.J., Reynolds, W.C., Schraub, F.A., Runstadler, P.W., 1967. The structure of turbulent boundary layers, J.Fluid Mech. 30, 741

10. Kreplin, H.-P., Eckelmann, H., Wallace, J.M., 1974. Propagation of perturbations in the viscous sublayer, unpublished lecture, Colloquium on Coherent Structures in Turbulence, Southampton 1974

11. Kreplin, H.-P., 1976. Experimentelle Untersuchungen der Längsschwankungen und der wandparallelen Querschwankungen der Geschwindigkeit in einer turbulenten Kanalströmung, MPI Strömungsforschung and AVA, Göttingen, No. 63 (Ph.D. Thesis 1976 University of Göttingen)

12. Lau, K.K., 1977. M.S. Thesis, University of Illinois

13. Laufer, J., 1975. New trends in experimental turbulence research, Ann.Rev.of Fluid Mech. 7, 307-326. Annual Reviews, Inc.

14. Nychas, S.G., Hershey, H.C., Brodkey, R.S., 1973. A visual study of turbulent shear flow, J.Fluid Mech. 61, 513

15. Offen, G.R., Kline, S.J., 1974. Combined dye-streak and hydrogen bubble visualization of a turbulent boundary layer, J.Fluid Mech. 62, 223

16. Oldaker, D.K., Tiederman, W.G., 197 . Spatial structure of the viscous sublayer in drag-reducing channel flows, Phys.Fluids Supplement 20, 133

17. Willmarth, W.W., 1975. Structure of turbulence in boundary layers. Advances in Appl.Mech. 15, 159-254. Academic Press

18. Wills, J.A., 1962. The correction of hot-wire readings for proximity to a solid boundary, J.Fluid Mech. 12, 388

DISCUSSION

Hanratty:

I guess I'm glad to see this paper because we've been worried about our previous measurements ourselves and for other reasons than what you have mentioned. We intend to go back and reproduce some of them. So with the information you have here, this might forewarn us of what we should do if we go back and remeasure.

Brodkey:

It is noteworthy that not only people doing visualization work have troubles. However, by the same token I've been involved jointly with some of the work Helmut presented here. I wonder if you would comment, could this in some way account for the difference very close to the wall of the measurements made in the oil channel in Goettigen by you and Jim (Wallace) and myself, and the measurements with the x-probe made by Bill Willmarth --- in particular, on the different direction of the quandrant split for only a y^+ of 10 and below.

Eckelmann:

Very good question. If I weren't a speaker here, I would have brought this up. I think maybe we should bring Bill's problem into this because it might be that the probe may also cause some flow structure change. It may not have come out that clearly from my lecture, the u-velocity is not affected as far as the correlations were concerned. Maybe the v-component, I mean the v component which Willmarth measured, isn't affected either, but if it is a rotating structure, than v and w should go together and be consistent.

Willmarth:

Well, I don't think that what I was seeing with the small x-probe is related to this. I didn't have other things in the flow, just one hot wire. Also, I saw this anomaly that I talked about all the way out to y^+ of 400.

Eckelmann:

I think it is the scale of the sublayer thickness or a scale of $y^+ = 5$ to 15 that is involved, and it is restricted to the wall for measurements at high Reynolds numbers.

THE BURSTING PROCESS IN TURBULENT BOUNDARY LAYERS

R.F. Blackwelder

Department of Aerospace Engineering

University of Southern California

Los Angeles, California 90007

ABSTRACT

Much of the research in turbulent boundary layers during the last decade has been concerned with the sequence of events that occur near the solid boundary. This important sequence, collectively called the bursting phenomena, is responsible for most of the turbulent evergy production within the boundary layer. The important aspects of the bursting process are discussed as well as the interaction between this dynamical structure and the coherent eddies in the outer region. Similarities between the bursting phenomena and corresponding events in a transitioning boundary layer suggest a dynamical resemblance between these two flow fields.

THE BURSTING SEQUENCE

Hama (see Corrsin[1]) first observed an organized eddy structure near the boundary by carefully injecting dye through a slot in the wall. Downstream of the slot, the dye was observed to coagulate into long narrow regions aligned with the mean velocity, $\bar{u}$, in the x direction. (The normal and spanwise directions will be denoted by y and z with velocities v and w.) Since the dye at the wall initially marked the low momentum fluid, these regions have been called "low-speed streaks". Kline, et al.[2] visualized these structures by using a hydrogen bubble wire aligned perpendicular to the mean velocity and parallel to the wall. They also found that the bubbles collected into long streamwise streaks characterized by a deficit of streamwise momentum and suggested that this was due to the spanwise velocity component. The streaks were observed below $y^+ = 10$ and occurred randomly in space and time. They found a mean spacing between the streaks of approximately $\lambda_z^+ = 100$ ($\lambda_z^+ = \lambda_z u_\tau/\nu$). Later evidence, e.g. Kim, et al.[3], Gupta, et al.[4], Lee, et al.[5], and Oldaker and Tiederman[6], found that the spanwise spacing is a random variable with a probability density function similar to a Rayleigh distribution having a mean of $\lambda_z^+ \approx 80$.

Gupta, et al.[4] used an array of hot-wires and found that the spanwise correlation function, $R_{uu}(\Delta z)$, was quite periodic when measured over a short time period. Since the wavelength, λ_z, is random, however, the periodicity disappeared as the averaging time was extended.

In another visualization study, Corino and Brodkey[7] used neutrally buoyant particles to study the wall region of a turbulent pipe flow. They observed the particle motions in the x-y plane by filming the flow with a high speed motion picture camera in a convected frame of reference. They observed a sequence of events that began with a gradual deceleration near the wall. This was followed by a large scale region of high speed fluid called a "sweep" that seemed to have been associated with the outer flow field. The low speed fluid and the sweep were often observed to be separated by less than $\Delta z^+ = 20$ in the spanwise direction giving large spanwise velocity gradients. The interaction with the sweep manifested itself by the ejection of low speed fluid away from the wall followed by a strong and violent mixing in the logarithmic region. Kline, et al.[2] reported a similar sequence that involved a "lift-up" of the low speed streak from the wall, followed by a characteristic oscillation leading to a random chaotic motion. Both of these studies reported that most of the production of turbulent energy was related to the bursting phenomenon.

In the Eulerian frame, Willmarth and Lu[8] and Blackwelder and Kaplan[9] showed that these events could be detected with hot-wire anemometers and studied using conditional sampling techniques. The first authors verified that the tangential Reynolds stress associated with the bursting phenomenon was indeed large compared to its mean value. The latter authors found one of the most striking features of this phenomenon to be a sharp acceleration of the streamwise velocity as reported also by Wallace, et al.[10] The strength and extent of this aspect of the motion is seen by referring to the data in figure 1 taken with a rake of 10 hot-wires at different y^+ locations. The simultaneous velocity traces associated with the sharp acceleration show a high degree of correlation normal to the wall, with the acceleration appearing earlier at the higher elevations. The data of Blackwelder and Eckelmann,[11] indicate that the low speed streaks manifest themselves as the velocity defects that appear before the sharp accelerations. These defects can extend outward beyond $y^+ = 100$ as seen in figure 1. They typically require a time period of $25<\tau^+<150$ to pass a fixed probe which implies a streamwise length scale of $300<x^+<2000$; thus they are long indeed.

The spanwise extent of the events in the bursting phenomenon has not been explored as fully as their motion in the x-y plane. Several authors have suggested that the wall region is inhabited by streamwise counter-rotating vortices as sketched in figure 2. Bakewell and Lumley,[12] used hot-film anemometers to study this region of a pipe flow. By using an orthonormal decomposition of space-time correlations, they found that the most energetic velocity fluctuations were consistent with the vortices shown in figure 2. Lee, et al.[5] and Hanratty, et al.[13] have measured regular quasi-periodic variations of the velocity gradients at the wall and have proposed a model similar to that suggested by figure 2. To study how these vortices are related to the bursting process, Blackwelder and Eckelmann,[11], [14] used a series of flush mounted wall elements sensitive

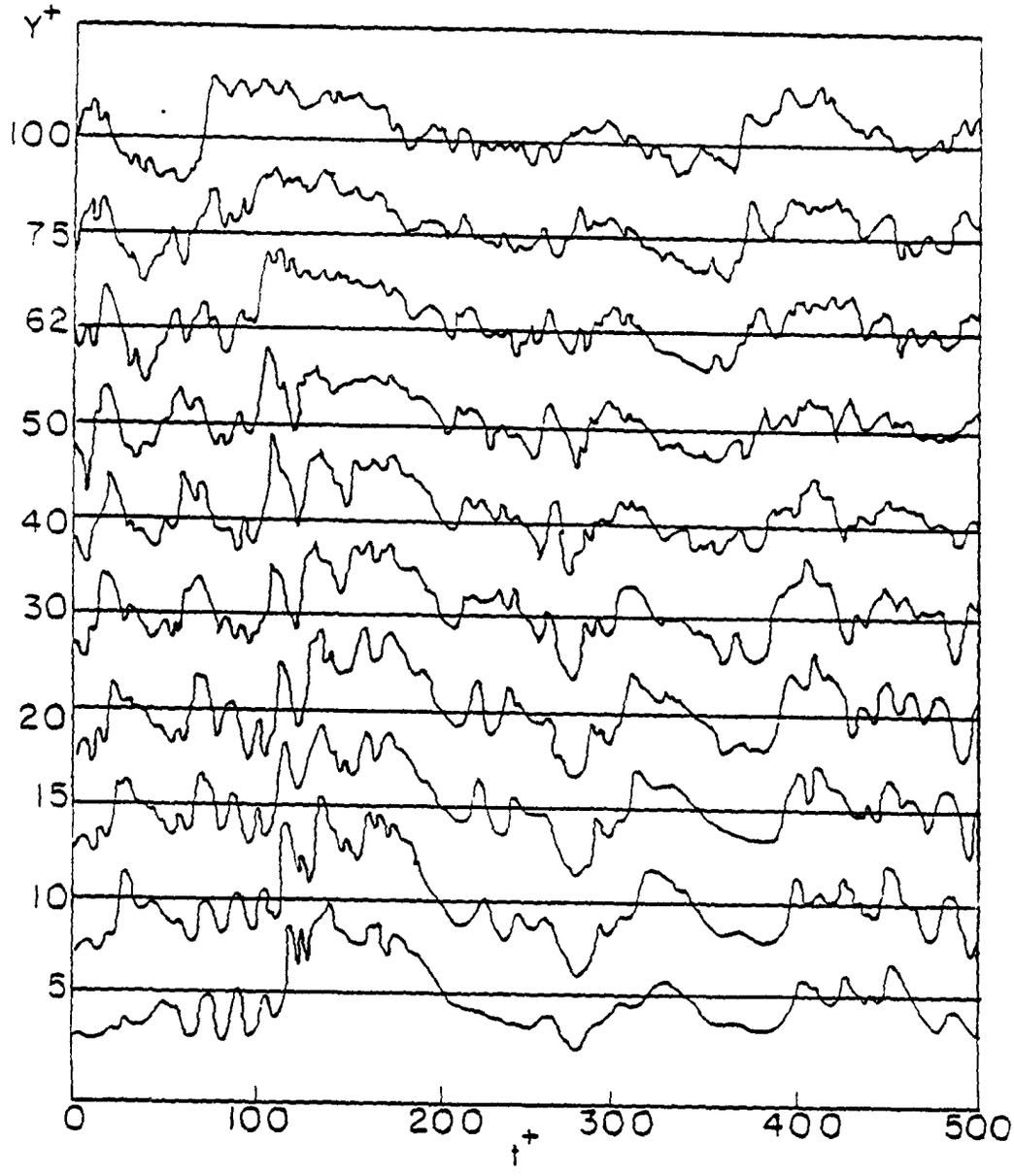

Figure 1. Simultaneous streamwise velocity signals at 10 locations in the wall region.

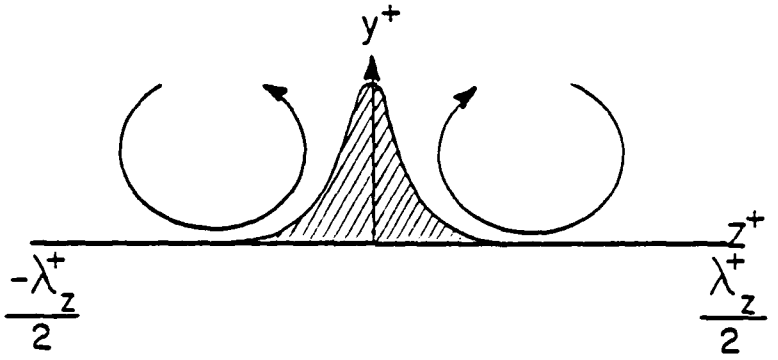

Figure 2. Cross-sectional view of a low speed streak lying between two counter-rotating streamwise vortices.

to $\partial u/\partial y|_0$ and $\partial w/\partial y|_0$ and traversed other probes in the y-z plane. An example of their instantaneous velocity gradients on the wall at $\Delta z = \pm 9$ and a single hot-film sensitive to the streamwise velocity at $y^+ = 15$ is shown in figure 3. Before the acceleration occurs at $y^+ = 15$ the streamwise velocity gradients on the wall are less than the mean value and the spanwise gradients are of opposite sign consistent with a pair of counter-rotating vortices. Their conditional averages indicated that this pattern consistently occurred before the sharp acceleration. A pattern recognition scheme based upon the wall gradient signals indicated that the vortices occur at least 50% of the time at a fixed streamwise location and $R_\theta \approx 400$. Furthermore, their results suggest that the vortices "pump" low speed fluid toward $z^+ = 0$ and away from the wall, as illustrated in figure 2 thus accounting for the strong velocity defects observed in figure 1. The large streamwise extent of these measured velocity defects, $\Delta x^+ > 1000$, and their narrow spanwise length scale, $\Delta z^+ \approx 20$ (reference 15) suggest that they are the low-speed streaks observed in the visualization studies. The pumping action and the low-speed streaks disappear when the sharp acceleration occurs as seen in figure 3. The acceleration and the high speed sweep is observed to reach the wall later because this structure is skewed in the x-y plane.

The spanwise velocity associated with the bursting phenomenon have been measured by Blackwelder and Eckelmann,[11] and some of their conditionally averaged results are replotted in figure 4. The bursts were detected using the technique of Blackwelder and Kaplan,[15] at $y^+ = 15$ and the conditional average of the detector probe at that location is shown at the bottom of the figure. The spanwise velocity component was measured using a "V" probe of two hot-films traversed normal to the wall at $\Delta z^+ = 17$ and 34. It was verified that the conditionally averaged profiles of w were antisymmetrical in Δz^+; thus only the results of $\Delta z^+ > 0$ are plotted for several values of the time delay τ^+. As the

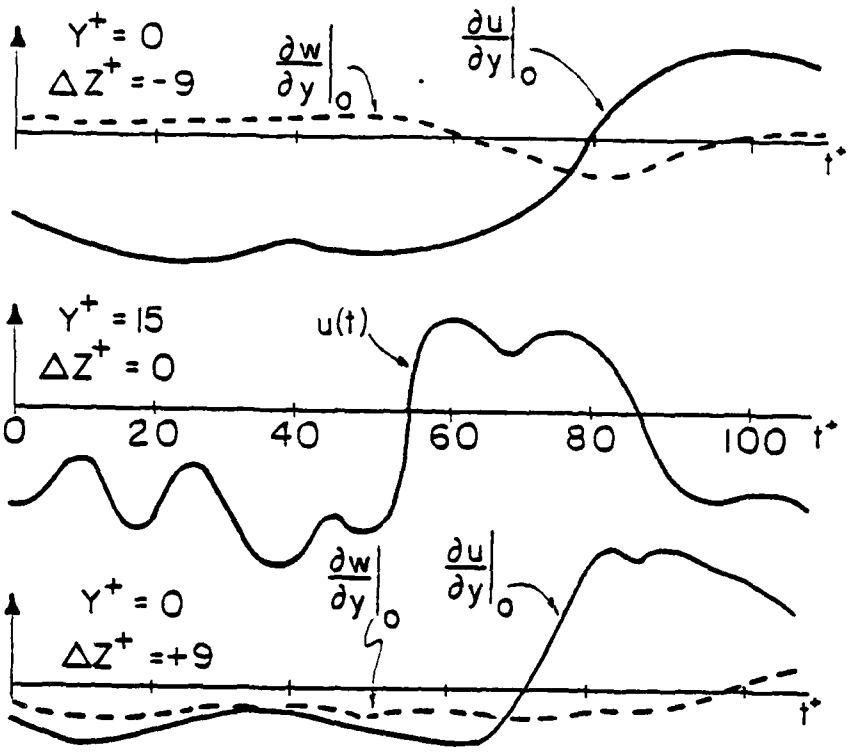

Figure 3. Simultaneous streamwise and spanwise velocity gradients on the wall at $\Delta z^+ = \pm 9$ and the streamwise velocity at $y^+ = 15$ and $\Delta z^+ = 0$. The mean values have been subtracted from all signals.

magnitude of the spanwise velocity increases, so does the streamwise velocity defect at $y^+ = 15$, consistent with the counter-rotating vortices. An estimate of the strength of the streamwise vorticity indicates that its maximum is approximately an order of magnitude less than the mean spanwise vorticity at the wall.

INFLUENCE OF THE OUTER FLOW FIELD

Narahari Rao, et al.[16] noted that the frequency of occurrence of the bursts scaled with the outer flow variables, δ and U_∞, and not with the inner variables, ν and u_τ. Laufer and Badri Narayanan,[17] further showed that the bursting frequency was approximately the same as the frequency of passage of the large scale structures in the outer flow field, thus suggesting a possible relationship between these two diverse phenomenon. To explore this possibility, Chen and Blackwelder,[18] (see also Chen[19]) slightly heated the entire boundary and used the

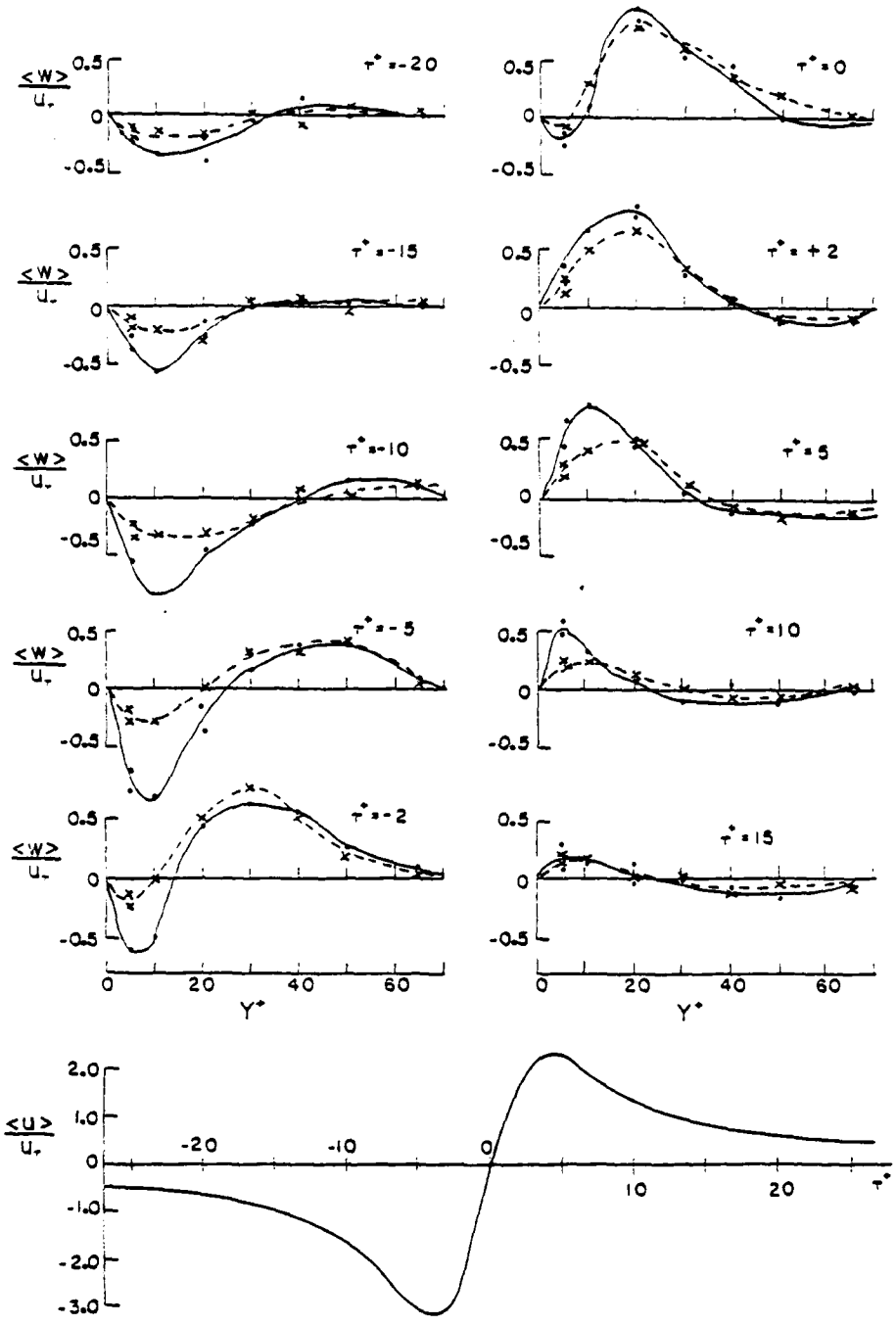

Figure 4. Conditionally averaged spanwise velocity profiles, $\langle w(y) \rangle$; —●—, $z^+ = 17$; -x--x-, $z^+ = 34$. The time delay τ^+ is with respect to the detection of the bursts. For reference, the conditional average of the streamwise velocity at $y^+ = 15$ is shown below.

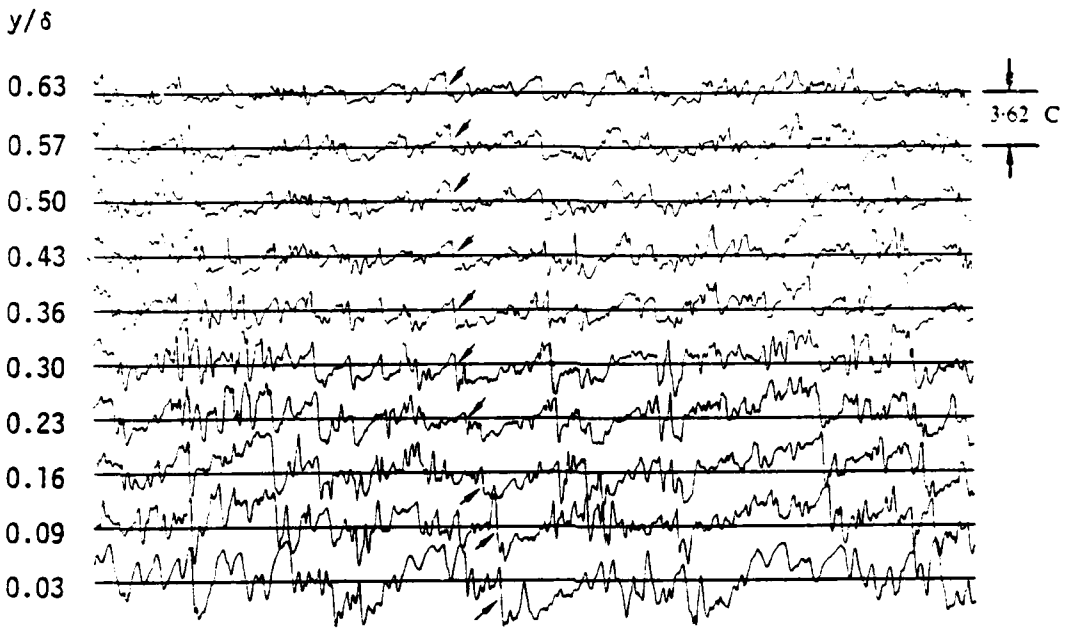

Figure 5. Simultaneous temperature traces at ten positions in a slightly heated turbulent boundary layer. The horizontal span is $U_\infty t/\delta = 18.7$.

temperature as a contaminant tracer. They observed the large scale structures, called "bulges", in the outer flow field as studied by Kaplan and Laufer [20], Kovasznay, et al.[21] and others. In addition, they discovered that these structures extend into the logarithmic and wall regions. This is vividly seen by the instantaneous temperature signals in figure 5 obtained from a rake of sensors spanning $0.03\delta<y<0.63\delta$. The most striking features are the sharp temperature decreases extending throughout the layer. By studying simultaneous temperature and velocity data, they ascertained that the sharp temperature fronts were coincident with the backsides of the bulges in the outer flow field. Because the outer structures are not two-dimensional, the sharp temperature fronts did not usually span the entire boundary. The angle between the temperature front in the x-y plane and the wall is a random variable that seems to decrease with the age of the bulge. The velocity signals associated with the temperature fronts indicated that each "back" coincided with a vortex sheet across which a sharp change in the streamwise and normal velocity appeared, in agreement with the visual results of Nychas, et al.[22]. Falco [23] and Brown and Thomas [24] have also concluded that the upstream sides of the large scale outer structures are the most energetic regions of these eddies. Chen and Blackwelder[18] observed that the velocity signature of the backs was similar to that of the

bursts, i.e., a region of relative low speed momentum followed by an acceleration and high speed fluid. The strength of the velocity signals increased as the wall was approached. By using conditional sampling and other sophisticated data processing techniques, they plausibly argued that the "backs" of the outer flow structure were directly related to the bursting process in the wall region.

A MODEL OF THE BURSTING PHENOMENON

The available knowledge of the bursting process can be summarized by the model shown in figure 6. The streamwise vortices are indicated by their corresponding vortex lines. Only two vortices are illustrated although others exist in the spanwise direction with a quasi-periodic spacing of $\lambda_z^+ \approx 100$. The distribution, strength, height and other characteristic parameters of the vortices are assumed to be random variables with fluctuations about their mean values. Near the wall the vortices move low speed fluid toward z = 0 and "pump" this fluid away from the wall. This action leads to the formation of the low speed streak that is broad near the wall and narrower in the spanwise direction at higher elevations. The visualization studies have observed streaks with lengths often exceeding $\Delta x^+ = 1000$. However, as they move downstream, the streaks meander in the spanwise direction, thus explaining why fixed probes yield streamwise length scales less than $\Delta x^+ = 1000$. For example, a meandering of only 1^0 for a streak with a width of $\Delta z^+ = 20$ implies that a probe fixed in the laboratory coordinates will measure its length to be $\Delta x^+ \approx 1000$ even though the streak may be infinite in extent. Higher speed fluid is moved toward the wall by the model vortices at $z = \pm\lambda_z/2$, however, this aspect is less important to the dynamics because it does not create an unstable velocity profile.

The long length of these structures indicates that they are relatively stable. However, they are randomly disturbed by the sweep of high speed fluid associated with the large scale structure in the outer flow field which interrupts the pumping action. The interface between the low-speed fluid of the streak and the higher speed sweep manifests itself as the observed sharp acceleration. The convection velocity of this interface is also random and has a value of approximately $0.8U_\infty$ at $y^+ = 15$ (Blackwelder[25]) indicating that it is associated with the outer flow field. The interface forms angles of 20^0 to 45^0 with respect to the wall in the x-y plane. Since it is associated with the outer flow structure, the interface must have a spanwise length scale of δ. As it is convected downstream its interaction with the wall structure is most predominate where large velocity differences occur; i.e., between it and the low speed streaks. As the interface passes, the instantaneous velocity profile is inflexional because of the high speed sweep above and the low speed streak near the wall. Blackwelder and Kaplan[15] found that the conditional average over approximately 300 such events was strongly inflexional, indicating that this is a predominate feature of these events. Their averaged profile along z = 0 is sketched in figure 6. The available evidence (see also Kline, et al.[2] and Corino and Brodkey[7]) indicates the inflexional profile is only a local phenomemon

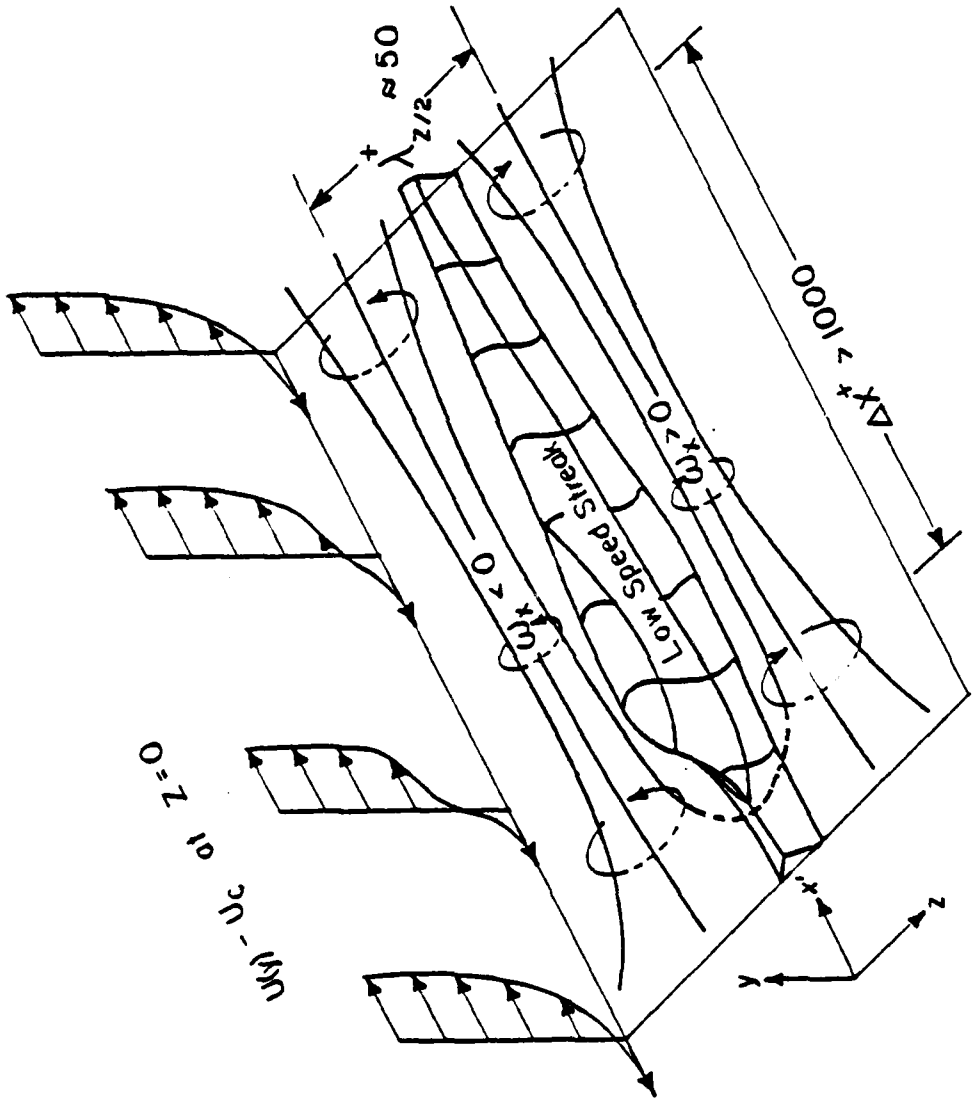

Figure 6. Model of the counter-rotating streamwise vortices with the resulting low-speed streak. The velocity profiles are from Blackwelder & Kaplan.[15]

with a spanwise extent of $\Delta z^+ \approx 20$. After passage of the sharp acceleration, a general momentum excess associated with the sweep exists over the entire boundary layer.

The steep velocity gradients in the normal and spanwise direction suggest that the inflexional profile may be related to an isolated two-dimensional free shear layer instability as indicated in figure 7. Michalke,[26] and Greenspan and Benney [27] have shown that a two-dimensional free shear layer has a most amplified wave of $\alpha\Delta = .4$ where 2Δ is the thickness of the layer. The instability has a wave length of $\lambda_x^+ = 2\pi/.4\Delta^+$ where Δ^+ is the non-dimensional half thickness. The inflexional profiles of Blackwelder and Kaplan give $\Delta^+ \approx 10$; thus λ_x^+ 150. This value compares favorably with the experimentally observed oscillations in Table 1.

	R_θ	λ_x^+
Blackwelder and Kaplan (figure 1)	2550	200
Emmerling[28]	1800	200
Kim, et al.[3]	660	240
Oldaker and Tiederman*	500	120
Blackwelder and Eckelmann (figure 3)	400	160

TABLE 1

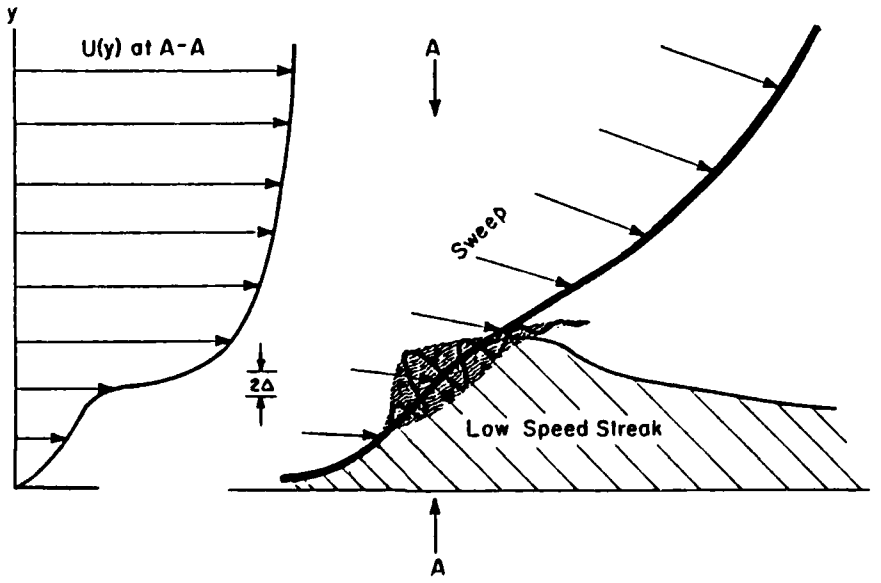

Figure 7. Sketch of the localized shear layer instability between the sweep and low-speed streak. The concomitant inflexional profile at section A-A is shown at the left.

*Obtained from the 8mm movie film accompanying reference 6.

It should be noted that these characteristic oscillations will be difficult to find with a single probe at a fixed spatial location. However, once they are found, the oscillation may occur in either the high- or low-speed fluid as in figure 1, or both, e.g. figure 3. Because of their random appearance in space and time, they will also be relatively rare events when several probes are used. However, after the instability has grown to sufficient amplitude, the oscillation should influence a large region so that it could be observed by several nearby probes as in figure 1 at $t^+ \approx 100$. This structure should be more readily observable in visualization experiments that view an entire plane of the flow as in references 2, 3 and 6.

As depicted in figure 7, the instability will cause the spanwise vorticity, ω_z, to grow, suggesting that some of the vortex lines in figure 6 may close to form a hairpin or horseshoe vortex as indicated by the dashed vortex line. On the other hand, the interface between the sweep and the streak is highly three-dimensional, so the strongest gradient, and hence, the principal instability, may develop in a different plane leading to other orientations of the vorticity.

The next stage of development in the bursting process corresponds to the "breakup" event defined by Kim, et al.[3] as a more chaotic motion characterized by strong mixing. Although not illustrated in figures 6, or 7, this event is possibly the nonlinear stage of the free shear layer instability accentuated by the inherent three-dimensional nature of the flow field.

DISCUSSION

The origin of the streamwise vortices is one of the major remaining questions of the bursting phenomenon. In 1974, Coles (see Cantwell, Coles and Dimotakis[29]) suggested that they may be due to a Taylor-Görtler type instability in which the centrifugal force is due to the large scale structure in the outer flow field. It is not difficult to show that the Görtler instability parameters associated with the streamline curvature of a steady laminar boundary layer can be satisfied. One example illustrating this feasibility uses the curvature of the locus of maximums of the space-time correlations of Favre, et al.,[30] which yield a radius of curvature of $R \simeq 40\delta$. Using a length scale relevant to the wall region, a super-critical Görtler parameter is obtained with a wave length near $\lambda_z^+ \approx 100$. However, it is not obvious that the steady state stability analysis of Taylor and Görtler for fields homogeneous in the flow direction can be applied to the unsteady flow field near the wall.

The sequence of events in the bursting phenomenon is qualitatively similar to the events leading to the formation of a spot in a transitioning boundary layer as described by Klebanoff, et al.[31] They observed an initial Tollmien-Schlichting wave and a spanwise periodic system of counter-rotating streamwise vortices. The vortices were similar to those of the bursting phenomenon (as can be seen by comparing figure 4 with figure 16 of Klebanoff, et al.) but had a finite

streamwise length imposed upon them by the Tollmien-Schlichting wave. As these vortices grew, they also seemed to pump low speed fluid away from the wall into a localized region. This action continued until terminated by the occurrence of a localized velocity "spike" analogous to the ejection phase of the bursting phenomenon. The instantaneous velocity profiles accompanying the spike were measured by Kovasznay, et al.[32] They had an infection point and were qualitatively the same as the profiles of Blackwelder and Kaplan.[15] The spike and subsequent high frequency oscillations have been described by Greenspan and Benney [27] as due to an unsteady shear layer similar to that suggested above. In the transitioning boundary layer there was no unsteadiness in the outer flow field so the spike and subsequent oscillations occurred in a regular and repeatable manner. In the turbulent boundary layer, the unsteady large scale structure in the outer flow field determines the spatial and temporal location of the inflexional profile and subsequent breakdown. Although the length scales in these two flows are slightly different, a better understanding of the dynamics in boundary layer transition may prove useful in modelling the bursting phenomenon.

The support of the U.S. Army Research Office - Durham under Grant DA-ARO-DAAG29-76-G-0297 is gratefully acknowledged.

REFERENCES

1. S. Corrsin, Symp. on Naval Hydrodyn, Publ. 515, NAS-NRC 373, 1957.

2. S.J. Kline, W.C. Reynolds, F.A. Schraub & P.W. Runstadler, J. Fluid Mech., 30, 741, 1967.

3. H.T. Kim, S.J. Kline and W.C. Reynolds, J. Fluid Mech., 50, 133, 1971.

4. A.K. Gupta, J. Laufer and R.E. Kaplan, J. Fluid Mech., 50, 493, 1971.

5. M.K. Lee, L.D. Eckelman and T.J. Hanratty, J. Fluid Mech., 66, 17, 1974.

6. D.K. Oldaker and W.G. Tiederman, Phys. Fluids Supplement, 20, S133, 1977.

7. E.R. Corino and R.S. Brodkey, J. Fluid Mech., 37, 1, 1969.

8. W.W. Willmarth & S.S. Lu, NATO-AGARD Conf. Proc. No. 93, London; Technical Editing & Reproduction Ltd., 1972.

9. R.F. Blackwelder and R.E. Kaplan, NATO-AGARD Conf. Proc. No. 93, London; Technical Editing & Reproduction Ltd., 1972.

10. J.M. Wallace, R.S. Brodkey and H. Eckelmann, J. Fluid Mech., 83, 673, 1977.

11. R.F. Blackwelder and H. Eckelmann, submitted to J. Fluid Mech., 1979.

12. H.P. Bakewell and J.L. Lumley, Phys. Fluids, 10, 1880, 1967.

13. T.J. Hanratty, L.G. Chorn and D.T. Hatziavramidis, Phys. Fluids, 20, S112, 1977.

14. R.F. Blackwelder and H. Eckelmann, To appear in Symposium on Turbulence in Lecture Notes in Physics, Springer Verlag, 1978.

15. R.F. Blackwelder and R.E. Kaplan, J. Fluid Mech., 76, 89, 1976.

16. K. Narahari Rao, R. Narasimha and M.A. Badri Narayanan, J. Fluid Mech., 54, 39, 1971.

17. J. Laufer & M.A. Badri Narayanan, Phys. Fluids, 14, 182, 1971.

18. C.H.P. Chen & R.F. Blackwelder, J. Fluid Mech., to appear, 1978.

19. C.H.P. Chen, The large scale motion in a turbulent boundary layer: a study using temperature contamination, Ph.D. thesis, University of Southern California, Los Angeles, 1975.

20. R.E. Kaplan and J. Laufer, Proc. IUTAM, Cong., Stanford, p. 236, Springer, 1969.

21. L.S.G. Kovasznay, V. Kibens & R.F. Blackwelder, J. Fluid Mech., 41, 283, 1970.

22. S.G. Nychas, H.C. Hershey & R.S. Brodkey, J. Fluid Mech., 61, 513, 1973.

23. R.E. Falco, Phys. Fluids, 20, S124, 1977.

24. G.L. Brown and A.S.W. Thomas, Phys. Fluids, 20, S243, 1977.

25. R.F. Blackwelder, Phys. Fluids Supplement, 20, S232, 1977.

26. A. Michalke, J. Fluid Mech., 23, 521, 1965.

27. H.P. Greenspan and D.J. Benney, J. Fluid Mech., 15, 133, 1963.

28. R. Emmerling, "Die Momentane Struktur des Wanddruckes einer turbulenten Grenzschictstromung." Mitt. MPI Stromungsforsch u. Aerodyn. Versuchsanst., Gottingen, no. 56, 1973.

29. B. Cantwell, D. Coles and P. Dimotakis, Cal Tech. Interim Report, 1977.

30. A.J. Favre, J.J. Gaviglio and R. Dumas, J. Fluid Mech., 3, 344, 1958.

31. P.S. Klebanoff, K.D. Tidstrom and L.M. Sargent, J. Fluid Mech., 12, 1, 1962.

32. L.S.G. Kovasznay, H.Komoda and B.R. Vasudeva, Proc. Heat Transfer and Fluid Mech., Inst., Stanford U. Press, Palo Alto, 1962.

DISCUSSION

Kovasznay:

If this indeed has an analogy to transition and the little argument we made in 1962 regarding pressure, couldn't you infer from that what kind of pressure fluctuations you should see under the boundary layer? Can you make a back-of-the envelope analysis?

Blackwelder:

No, I have not done that yet. I looked at the structure of the velocity signals and I established that they're analogous enough. I couldn't see that there would be any gross difference.

Donaldson:

Thank you. I haven't followed this work all that closely for the past few years. I've been off playing with aircraft vortices. I think some of the teachings that one finds when they look at vortices near surfaces have a very important bearing on just what's been discussed here, in the way of a model. It has generally been assumed that when an airplane flys by and leaves a pair of trailing vortices,that they roll up at the center of the shed vorticity, they come together, and descend. Then you ask what happens when they get in the vicinity of a surface. And when the question was asked, everybody said it was the same thing, they're just vortices and they go on across the airport, and if there's a cross flow, they move with the flow, but that isn't so at all. The vortices as they approach a surface have in them the mechanism for their own demise and also for the fact that they do not move across parallel to the surface, but that they rise again. For many years, everybody threw out data showing that they rose, because obviously they shouldn't. The attitude was: "there must be something wrong with the instrumentation, so we won't publish the results". And here's the mechanism. As a trailing vortex moves downward, it induces a flow due to a viscous boundary condition on the surface. The viscous boundary layer that develops on that surface has a vorticity which is of an opposite sign to the original vortex. As the flow in the boundary layer moves into the adverse pressure gradient that is set up by the original vortex, the flow separates and comes up off the surface with a velocity component which turns the original vortex upward, with the two vortices then merging. And if these viscous "spawned" vortices continuously feed in opposite

Donaldson: (Cont'd)

vorticity through this merging process, they really contribute to the death of the original vortex. For real flows over real airports, it only depends on how rough the surface is, it doesn't matter how big the airplane is. In general, the decay time for a vortex is just three minutes. The situation described in this paper is the inverse of the situation I described and if, indeed, you have a counter-rotating vortex pair, then the flow that is moving into the center region continually has the opposite vorticity. The spawned vortex in turn will cause the original to rise, which wouldn't occur if you didn't look for the induced vorticity on the surface. The spawned vortex must upwash on the original vortex which is just equal to the downwash from the other counter-rotating leg of the original vortex pair. Thus, these spawned vortices not only have in them the ability to raise the original vortices, they also have in them the ability to kill them.

Blackwelder:

If the structure were allowed to exist long enough that might indeed happen, and remember the transition work of Klebanoff in which he actually had a picture of vortices of type of shape you show. However, in his case, the flow was not disturbed by the outer structure. I think this streak would stay there for a lot longer period of time, if it were not disturbed by the outer structure. But it's a disturbance by the outer structure that kills it off and forms the oscillations or ejections. I would say to answer your question, I would doubt that these vortices would be there long enough for that type of flow to develop.

Landahl:

I think first of all one ought to distinguish between a low speed region and a vortex, because the indication is that once these regions have formed, that fluid doesn't rise quickly, which indicates that the vorticity is really rather small after the regions are formed. So, I think one should distinguish between longitudinal vorticity and a long streaky, low-speed region, because once the low speed region has formed, its upper edge doesn't lift very fast. Which indicates that the vorticity lifting it up is rather weak after that.

Blackwelder:

What would you call weak, in terms of the mean gradient?

Landahl:

Well, I wouldn't like to put any figures on it.

Eckelmann:

Did you calculate the revolutions that your vortex would make say over the length of low-speed streak? If not, we did one in the colloquia.

Blackwelder:

No, I calculated that after I got back and found that it makes one rotation maybe every $1000x^+$ downstream.

Eckelmann:

That's why I want to comment on the previous speaker...because, it's not a tip vortex, it is only a slowly revolving vortex.

Blackwelder:

The other thing is that these vortices don't have to exist for the full length of the low-speed streak. I think the vortices can be much shorter. I feel that they bring the low-speed fluid up and it essentially lays there until this large scale structure comes along and strikes it. I did forget to mention that with this structure that I have presented, you are going to get high-speed regions off to the side. The reason I didn't mention it is because they obviously are not as important to the subsequent dynamics because they give you a stabler mean velocity profile instead of a less stable one.

Kovasznay:

It is becoming very clear to me that this is the point where we should have a committee. And I think the committee should really address itself to the question of who means what regarding instability and burst. It should clarify what everybody's position is. I would like to propose the topic of "what are the main distinguishing features of different breakdown models and to what extent they are measureable". For starters, I would like to have as members Martin Landahl, Ron Blackwelder, Bob Brodkey, Don Mc Elligot, and Steve Kline. [This is committee report 4. Ed.]

Kline:

Could I make a comment. First of all, I agree with what Marten Landahl said. In that long series of visual studies that we did, we did not see longitudinal vortices below a y^+ of 10 and I don't think we ever saw one go around as much as 3 times. If it got around once or twice, that would be very strong. Usually you just see it going up. That means, of course, there is some x vorticity but you wouldn't describe it as a wing tip vortex, which is really very strong. Where we do see strong vorticity is in the next layer after it lifts in the buffer layer, the lower log zone,

Kline: (Cont'd)

Then you see something that looks like vortices, if we could make this distinction.

I'd like to make a comment also on the relationship to transition. Enter a note of caution there. There is some difference between the transition case and the fully turbulent case when you go clear back to the very first formation stage. That is, to the Klebanoff-Tidstrom spot breakdown stage. In particular, those thing are running in a laminar environment, they're not heavily disturbed. Secondly, there is a distinct change of scales. The visual studies of say Elder & Meyer for example, show that you do get what looks like a lifted low-speed streak, but it's of the order of the whole laminar boundary layer in terms of characteristic length. This low speed fluid begins to oscillate and drops down and socks the wall. At that point, you get a turbulent spot with seven or eight sub-layer streaks forming immediately, such that there's a wholly different order of scale. So you've got at least two differences there which make me think that this ought to be an analogy rather than an exact replication.

Blackwelder:

In many ways, a closer analogy of the geometry per se is that with a transition or laminar instability of the Gortler vortex type or that of a slightly heated boundary layer. In both cases, you do have a slow formation of a practically stagnant region in the middle, and then you have an interaction of the outer flow, without any large scale. It's still an interaction of the outer flow which is potential. I think that if people are always going to be looking back to Klebanoff, Tidstrom, and Sargent, I think they should be looking at the equally correct pictures of, for example Gortler and others. In just the last issue of the Journal of Heat Transfer of February of this year, there is a visualization technique from two sides showing streaks from above and the beginning of the large scale formation of vortices in a heated water layer. Now I think we have been stuck too much on the single experience of Kelbanoff, Tidstrom, and Sargent.

SESSION III

ANALYSIS AND PREDICTION

Session Chairman:

William C. Reynolds

THE ROLE OF COHERENT STRUCTURE IN TURBULENT BOUNDARY-LAYER ANALYSIS

Morris W. Rubesin

Ames Research Center, NASA

Moffett Field, California 94035

ABSTRACT

The influence of experiments examining coherent or organized structure on turbulent boundary-layer analysis is reviewed historically. The main trends in Reynolds stress prediction are outlined and shown to ignore the dynamical experimental observations. The newly developed method of large eddy simulation is shown to possess considerable potential as a predictive and analytical tool, and it is argued that this method will provide the focus to coordinated experimental, theoretical, and numerical research in the near future.

SYMBOLS

D_{11} dissipation rate of normal Reynolds stress, $\overline{u'u'}$, $D_{11} = 2\nu \left(\overline{\frac{\partial u'}{\partial x}}\right)^2$

r_i two-point correlation separation distance in ith direction

R_{11} correlation function $R_{11}(x_i,r_i) = \lim_{T\to\infty} \dfrac{\int_0^T u(x_i)\, u(x_i+r_i)dt}{\int_0^T u^2(x_i)dt}$

t time

T integration period

u velocity in stream direction

u_τ	friction velocity, $\sqrt{\tau_w/\rho}$
v	velocity perpendicular to a surface
w	velocity parallel to surface, normal to stream
x, x_1	coordinate in stream direction
y, x_2	coordinate perpendicular to surface, in channel measured from centerline
z, x_3	coordinate perpendicular to x, y in Cartesian system
Δ	grid spacing
δ	boundary-layer thickness, or half channel width
λ	wave length of feature
ν	kinematic viscosity of fluid
τ_w	surface shear
< >	averaged over horizontal plane in computational volume, then time averaged over a cycle of large-scale turbulence (conditional average)

Superscripts

+	wall region coordinate, lengths measured from surface and normalized by ν/u_τ, velocities by u_τ
—	filtered or resolvable quantity
'	fluctuating or subgrid scale quantity

INTRODUCTION

In a consideration of the role played by our knowledge of coherent and organized turbulence structures in the analysis of turbulent boundary layers, it is important to first define the scope of analyses being considered. Analyses can be placed into two categories. First, there are analyses that try to explain particular physical mechanisms that are observed in experiments, and here the relationship between the largely idealized analysis and experimental observations is rather clear. On the other hand, there are analyses that provide engineering methods for predicting the behavior of turbulent fields, and here the link between the analyses and the latest experimental evidence on organized structure becomes more tenuous. Engineering predictions usually employ the simplest and least costly methods that satisfy the

designer's needs. In practice, more complex methods are introduced only when earlier methods fail to define some behavior required of a particular design. Developers of the predictive methods, as contrasted to the designer, are often motivated to use more complex methods in the belief they inherently may be more universal and applicable to a larger variety of flows. Thus, predictive methods, themselves, resolve into tuned "zone" and attempted "global" methods. In either case, the more modern of these methods are primarily based on the numerical solution of the statistical Reynolds-averaged equations, with the distinction between the different methods lying in the complexity of establishing the Reynolds stresses. At present, these methods generally do not account for the organized structure observed in the experiments other than in a statistical sense. This situation led Professor Kovasznay to observe, in 1971, that workers in the field of turbulence consist either of experimentalists who do not want to know about predictions, or predictors who do not want to know about turbulence. As Professor Kovasznay has worked as both an experimenter and predictor during his distinguished career, his sensitivity to this dichotomy must be taken seriously and one should not be blinded by the wit of the remark and miss its message, namely, that advancements in the fields of turbulence require close collaboration of the experimentalist, analyst, and the predictor, and a mutual understanding of the needs of each by the others. This view is supported here and it will be shown that the trends of turbulence analysis are conducive to the attainment of such collaboration in the future.

A vehicle for such collaboration will be the need for the rapid development of methods for numerically simulating the large eddy structure within flow fields of technological importance. These needs are being forced by the complexity of the design problems that require solution and the desirability for a globally applicable technique to accurately describe the interaction of several disparate types of flow fields. As an example, the prediction of the separation at the root of an aircraft wing in the presence of a vortex generated by an upstream strake is a very real design problem. Another example of a real but complex problem beyond any prediction method other than numerical simulation is the problem of the means of actively delaying transition, as will be addressed in Professor Orszag's paper that follows.

It is generally accepted that in the foreseeable future no computer will have the storage capacity and speed to permit the numerical solution of the time-dependent, three-dimensional Navier-Stokes equations resolved to the smallest scales of turbulence required for an accurate energy balance at Reynolds numbers of technological interest. Numerical simulation, then, means the direct computation of the dynamics of only the large eddy structure while accounting by theory or modeling for the effects of the scales of turbulence that cannot be resolved by the computer. Optimism for the universality of this approach is based on the experimental observation that the large-scale structures of turbulence are characteristic of the flow field in which they are generated, whereas the small-scales appear to have a universal character. The numerical simulation method, then, calculates what is unique to the flow and employs models for its universal portions, where modeling can be expected to be more rigorous. Another inherent feature of the method is that for a given flow field the reliance on the modeling diminishes with the increase in computer power so that an evolutionary development of computer hardware and softwear is tied systematically with the convergence of the

technique. Alternatively, as the subgrid models are improved, a lesser fraction of the turbulence has to be calculated so that with a given computer larger flow fields of technological interest can be encompassed.

At present, numerical simulation is very costly in computer time and cannot be considered an engineering tool. With anticipated improvements in computers, this situation may change in a decade or two. Presently, the technique is being used to develop numerical methods and subgrid scale models appropriate to the computation of flows of technological interest. The testing of the models requires careful comparison with the latest experimental data to assure that physically established effects are captured in the computations. In addition, the analytical idealized computations that focus on particular events, such as those to be described in the workshop papers by Professors Landahl and Walker, will provide guidance to the numerical simulations by defining mesh sizes required to capture the important events and providing standards for assessing the accuracy of the computation technique. In turn, the numerical simulations can contribute to the experiments and the analyses. The large amount of information available in the numerical data, more than is possible to determine in experiments employing a limited number of discrete sensors, will help explain past experiments and suggest and guide new experiments. Again, the numerical simulation will indicate regions of flow or events requiring more critical analysis. Finally, the numerical simulation may provide insights into improving Reynolds stress modeling and thereby provide assistance to the predictor employing less costly methods.

To develop the bases for these remarks this paper is divided into four parts. The first gives a brief historical view of turbulent boundary-layer analyses and their interrelationship with the experimental data that preceded them. The papers by Professors Orszag, Landahl, and Walker are placed in context here. The second part is a discussion of the present trends in Reynolds stress evaluation and prediction techniques. It is shown that the methods are becoming more complex in their attempts at universality. Some conclusions of comparisons with experimental data on attached boundary layers are given. In addition, some of their shortcomings and the directions being taken to improve the methods are indicated. Finally, the limitations of current Reynolds stress modeling applied to separated regions in compressible flows are shown. The third part of this paper is devoted to the display of recent results from a large eddy simulation of the flow in a rectangular channel that was performed at Stanford University. Unlike previous simulations of channel flows (Refs. 1 and 2) where some "law of the wall" is utilized, these computations are extended completely to the surface and cover regions where bursting phenomena are observed experimentally. In the fourth part, conclusions are given regarding the focusing of viewpoints by the predictor, analysts, and experimenters. The gains that can be derived from strong interactions between the experimentalist and the analyst in the planning and execution of their individual activities are indicated.

BRIEF HISTORICAL VIEW

A brief sketch of the historical development of turbulent boundary-layer analyses is given in Figure 1. No attempt at completeness is made because

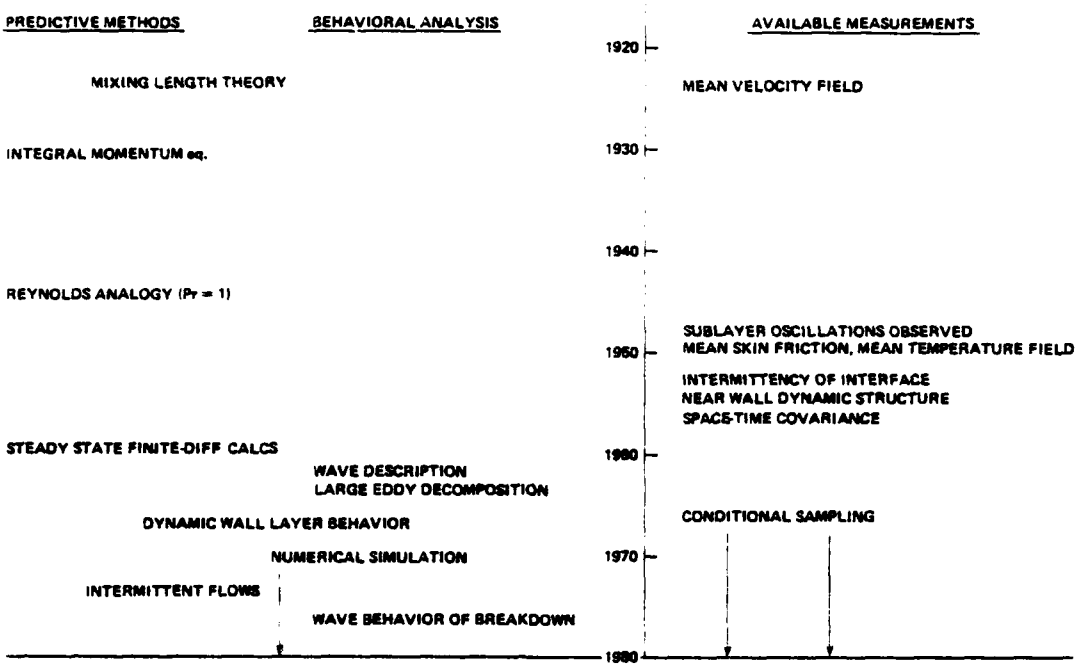

Figure 1. History of turbulent boundary-layer analysis.

the detail would confuse the main trends that emerge from this figure. The technical papers in the Workshop Session on Analysis and Prediction are placed relative to the field as a whole. The figure is constructed in three columns: predictive methods of engineering use; behavioral analyses with their emphasis on explaining physical behavior; and the state of available measurements. The time line format is intended to display the dependence of the analytical methods on the understanding of turbulence mechanisms developed by experiments and the time lag between an experimental discovery and its reflection in the analyses.

The chart is started in 1920 to avoid collapsing the information into the bottom of the figure. Osborn Reynolds' enormous contributions to the field starting in about 1880 can be considered the beginning of a serious scientific approach to turbulent flow studies (Ref. 3). Prandtl's work in unifying the fields of "inviscid hydrodynamics" and "engineering hydraulics" began at the turn of the twentieth century. At this time, predictive methods were based on formulas derived from correlations of experimental data or their graphical counterparts. The German and English groups at this time were developing mixing length theories to explain the mean velocity measurements in pipes and boundary layers that were being conducted concurrently. In Prandtl's group, especially, the need for the close interaction between the experimentalist and the analyst or theoretician was well understood even at that early time (e.g., Refs. 4 and 5). Pipe-flow measurements were emphasized for their technological importance and the ease of measuring skin friction. In the mid-1930's, activity began in the prediction of aerodynamic flow fields by using the momentum integral methods (Ref. 6), an idea introduced in 1910 by von Karman. Predictors were content to use empirically established mean velocity profiles and skin-friction laws based on boundary-layer thickness

Reynolds numbers. Shape factors had to be related to pressure gradients empirically and depended critically on experimental data. This approach continued for over three decades and its latter forms were contending methods at the Stanford Conference of 1968 (Ref. 7). Compuations with these methods could be done by hand or at minimal cost on the computers available in the 1950's.

In the 1940's, workers in heat transfer were developing modified Reynolds analogies for pipe flow and boundary layers (e.g., Refs. 8 and 9). These were based on the mean flow measurements taken in the vicinity of the pipe surface, called the laminar sublayer and buffer region in the terminology of the time. The emphasis on the near wall region reflected the rather large fraction of resistance to heat transfer that occurs there. The new "physics" introduced by the predictors related to assumptions regarding "turbulent" Prandtl numbers, for which measurements did not exist at that time, expecially in fluids such as liquid metals. It is interesting that at this time Professor Hans Einstein observed that the laminar sublayer was really unsteady (later reported in Ref. 10). This observation caused the developers of Reynolds' analogies considerable frustration as the mathematical tools available to them could not possibly handle such complications. All they could do was ignore the experimental observation and hope that its effect on the transfer of heat was negligible. Subsequent heat-transfer tests supported the accuracy of the computations and justified ignoring some of the experimentally observed details. This example indicates that experimental evidence of a physical phenomenon that is beyond the mathematical levels of predictive analysis is bound to be rejected until mathematical techniques are developed that can account for the features of the phenomenon and that a need for the added analytical complication is demonstrated.

In the post-war era of the late 1940's and early 1950's the need for boundary-layer prediction methods became critical in America's missile programs. The conditions these vehicles experienced could not be simulated completely within wind tunnels and flight measurements were extremely difficult. Accuracy was required in predicting aerodynamic heating rates as design safety factors were kept to a minimum by weight limitations. The methods of prediction used mixing-length theory, assumed profiles of shear across the boundary layers, used local density in the Reynolds shear stress, and assumed turbulent Prandtl numbers. Integration across the boundary layer yielded velocity and temperature profiles and wall skin friction and heat-transfer coefficients at given stations. This information was then used in integral relations to define distributions of the skin friction and heat transfer over the missile bodies. A significant contribution here was van Driest's unification of the sublayer and buffer layer through his damping function (Ref. 11). Despite the crudeness of these prediction methods, they permitted the design of successful missiles and could even be extended (Ref. 12) to account for, in an engineering sense, the effects of surface transpiration, ablation, and small angles of attack. Some failures to describe the effects of compressibility observed in experiments in transpiration, led predictors (Ref. 13) to reexamine the available low-speed flow data. This suggested a two-layer model of the boundary layer, reflecting the "law of the wall" and "law of the wake" resolution developed by Coles for incompressible flows over impervious surfaces (Refs. 14 and 15). These ideas were extended for use in prediction methods by use of two-dimensional finite-difference computations using parabolic marching schemes in the downstream direction of the boundary

layer. Compressibility was handled, again, by adding an energy equation and utilizing a local density in the turbulence model. The power of these methods was demonstrated at the 1968 Stanford Conference (Ref. 7); they are still the mainstay of design in the aircraft industry.

During the middle and late 1950's, with the development of improved experimental equipment, evidence began to emerge that the turbulent boundary layer was not a quasi-steady, randomly disorganized field, but that it possessed some organized structure, was intermittent in its character at its outer edge and, although very dynamic near the wall, could be described by a repeatable sequence of dynamic events (Refs. 16 and 17). Predictors, again, ignored these discoveries because they revealed facets of turbulence that were beyond the available mathematical tools and because the prediction techniques generally satisfied the design requirements of the time.

The late 1950's saw an increased level of experimental research. Space-time or space covariance measurements came into being and gave a new view of the temporal and length scales in the boundary layer (e.g., Refs. 18 and 19). The 1960's saw the introduction of data conditioning by many of the participants of this workshop. Analysts began to attempt to understand and explain the mechanisms leading to the features observed and measured in the laboratory. Principal in this activity is Professor Landahl, who is presenting a following paper. He and his colleagues have used an earlier developed wave mechanics description of turbulence (Ref. 20) to describe the mechanisms of the "bursting" phenomenon observed in the near wall regions of the turbulent boundary layers (Refs. 21 and 22). Another enlightening view of the structure of turbulence was due to Professor Lumley with his method of large-eddy decomposition as applied to covariance data (Ref. 23). Insights into the statistically principal large-scale structure in the wake of a cylinder and in a flat-plate boundary layer (Refs. 24 and 25) have resulted from application of this method. Also, examinations are under way to determine if the remaining small-scale turbulence can be represented with an eddy viscosity (Ref. 26).

One of our workshop coordinators, Professor Abbott, and an author of a workshop paper in behavioral analysis, Professor Walker, examined the dynamic behavior of the near-wall region of a boundary layer between successive bursts through leading order analysis of the time-dependent, three-dimensional Navier-Stokes equations (see Ref. 27 for the latest developments of this work). They found the leading order expression for the axial velocity to have the form of the one-dimensional transient diffusion equation containing the molecular diffusivity. The mean axial velocity in the near-wall region of the boundary layer could be represented by the time average of the solutions of the instantaneous velocity in the period between bursts. This period, made dimensionless by the time scale based on wall parameters, was established from detailed comparisons with boundary-layer data. From the viewpoint of a complete theory, the weakness of this method lay in its inability to handle the violent bursting period and to account for the intense Reynolds stresses that develop there. In this workshop, Professor Walker describes his recent analysis toward bridging this gap. In this study, the reaction of a viscous fluid in the vicinity of a surface to a large, inviscid vortex moving along the surface with its axis transverse to the flow is computed with a finite difference technique. For this two-dimensional problem, Professor Walker demonstrates that physically stable solutions cannot occur.

Late in the 1960's, the power of electronic computers rose to the point where the calculation of the largest features of turbulence became a possibility. Pioneers in this field were the atmospheric physicists at the National Center for Atmospheric Research (e.g., Ref. 28). Professor Orszag, a contributor to this workshop, worked with the NCAR group (e.g., Ref. 29) and is responsible for many of the mathematical advances this area of research has enjoyed. In his paper for this workshop he will demonstrate that these techniques have developed to the point where predictors can even attempt to determine the means or the conditions required for dynamically inhibiting the transition process!

Another interesting development in predictive analysis has been the development of a statistical theory of turbulence by Prof. Paul Libby that accounts for intermittencies within the flow (Ref. 30). This approach is still in its early stages but should prove to be a powerful tool for studies of chemically reacting flows and mixing processes.

Finally, there have been several developments in the field of large-eddy simulations of flows of interest to those involved in studies of turbulence structure. The work at NCAR expanded from atmospheric studies to include the computation of the flow within a channel (Refs. 1 and 2). Although this early work did not attempt to resolve the flow in the near-wall region, but used near-wall models instead, some structural features seemed to develop. At Stanford University, a research program in large eddy simulation has been under way for about 6 years. The most recent computation performed also addresses the turbulent channel flow (Ref. 31). This work, however, no longer models the near-wall flow, it computes the eddy structure directly to the surface. It is encouraging that features akin to experimentally observed coherent structures develop in these calculations.

From this brief historical review, certain important trends are evident. First, experiments had to precede either predictive or behavioral analysis. Predictive analysis needed the statistical experimental results to reintroduce much of the phase and wavelength information lost in the Reynolds averaging process, and the behavioral analysis needed experimentally observed phenomena to explain. A second point that emerges from this review is that predictive analysis is constrained to the mathematical tools available at the time. Experimental discoveries of features that cannot be handled mathematically are generally ignored as unnecessary complications of the predictor's orderly world. Finally, it appears that the rapid development of computers has allowed the analyst to begin computing the boundary layer in a more physically realistic manner that captures some of the time-dependent features observed in the laboratory, resulting in a smaller gap between the states of the art in experimentation and prediction.

TRENDS IN REYNOLDS STRESS EVALUATION

Except for the method described in Ref. 27, predictive analyses are based on the solution of Reynolds-averaged or long-time-averaged steady-state boundary-layer equations. The coherent or large-scale turbulence structure, observed experimentally, is accounted for only in a statistical manner in that the time-averaged Reynolds stresses are modeled according to time-averaged experimental data. It is not clear how general such a statistical approach

will be for boundary layers experiencing different environments, such as pressure gradients, curved surfaces, or three dimensions. Under these conditions, the large-scale structure may be modified considerably from that on a flat plate, thereby altering the elements within the statistical mix. Since data on structure have been obtained principally within flat-plate boundary layers, they provide no guide to means of broadening the range of applicability of Reynolds stress modeling. As a consequence, predictors are forced to base their models on measurements of mean quantities. The status of a Reynolds stress modeling assessment based on the author's experience with a variety of models applied to attached boundary-layer flows is indicated in Figure 2. The figure is divided into three columns: the modeling level, the types of data that were used to establish modeling coefficients, and the observations that have resulted from comparisons with experimental data for the hierarchy of modeling levels.

The lowest level of modeling indicated in the figure describes techniques of representing the Reynolds shear stress in the mean momentum equation with a constitutive relationship depending on the product of an eddy viscosity and the local mean rate of strain. It is called first-order closure because the modeled constitutive relationship is applied directly in the mean momentum equation, a first-order equation. Since algebraic expressions are used to relate the eddy viscosity to the variables of the mean motion and the appropriate length scales, these are also called zero-equation models in that they introduce no additional partial differential equation to describe the boundary-layer flow. It has become customary to divide the boundary layer into two layers for modeling the eddy viscosity. In the inner region close to the surface, the eddy viscosity is most commonly expressed in terms of the Prandtl mixing length, $\ell_m = ky$, reduced by the van Driest damping factor. In the outer region, the eddy viscosity usually is treated as uniform across the entire boundary layer at a value scaled with the kinematic displacement thickness and the boundary-layer edge velocity (Clauser model). Alternatively, the mixing length can be treated as uniform at a value scaled with the boundary-layer thickness (Escudier model). The scaling or modeling constants that are used in the eddy viscosity or mixing length expressions are based on

MODELING LEVEL	DATA SOURCE	OBSERVATIONS FROM DATA COMPARISONS
FIRST-ORDER CLOSURE	$\bar{u}(y)$, c_f	• MAINSTAY OF ENGINEERING METHODS
(0 - eq. MODEL)		• FINE TUNED FOR BOUNDARY LAYERS WITH SMALL dp/dx
		• POOR FOR SEPARATED FLOWS
SECOND-ORDER CLOSURE		
1 - eq. (ℓ or τ)	+ DISSIPATION RATE	• WITHOUT MODEL TUNING, MODERATELY IMPROVED ACCURACY FOR SUBSONIC AND SUPERSONIC FLOW IN MILD PRESSURE GRADIENTS
2 - eq. (ℓ, SCALE)	+ τ/ℓ	• FOR SUPERSONIC FLOWS WITH LARGE ADVERSE PRESSURE GRADIENTS, IMPROVED PREDICTIONS IN REGIONS OF RISING SKIN FRICTION
R.S.E. $(\overline{u_i u_j})$	+ $\frac{\overline{u_i u_j}}{q^2}$ $i = 1,2,3$	• FOR MEAN QUANTITIES, NO PREFERENCE BETWEEN 2 - eq. OR R.S.E.
		• R.S.E. MODELS STILL REQUIRE IMPROVEMENT IN THE NEAR WALL REGION
		• UNIVERSALITY OF R.S.E. MODELS IN QUESTION

Figure 2. Status of Reynolds stress modeling.

measurements of mean velocity profiles through the boundary layer and on local skin-friction coefficients backed out from momentum balances or measured by some type of surface gage.

This type of modeling, although blind to the actual dynamics of turbulence, is still the mainstay of aerodynamic design methods (Ref. 32). Extension to three-dimensional boundary layers has been accomplished in most cases by treating the eddy viscosities as scalars being equal in the direction along and across the flow. Increased accuracy of prediction has been achieved by fine tuning the Karman "constant" and the van Driest damping parameter to be functionally dependent on the local pressure gradients to improve comparisons with experimental data.

Predictors have not been content with this level of modeling primarily for two reasons: first, there is an implied equilibrium between the turbulence and the mean flow regardless of the rapidity of changes in boundary conditions, and, second, the length scales utilized in establishing the eddy viscosity apply to a simple attached boundary layer and must be modified rather drastically if an additional length scale is introduced. An example of the latter situation would be the boundary layer downstream of a tangential film cooling slot or on a wing flap. Both of these equilibrium and length-scale effects make this level of modeling quite poor for separated flows.

Attempts at improving the turbulence models to overcome the inherent weaknesses of the first-order closure models has led to methods where the closure is achieved within the partial differential equations representing one or more of the second moments of the turbulence fluctuations. As these equations are usually solved in the steady state, only the gradual rate processes in the development of the turbulence are being considered. This level of modeling also ignores the details of the organized structure of turbulence. Over the years, a hierarchy of models of increasing complexity has developed. The simplest utilize a single differential equation to define a particular turbulence quantity. For example, the Glushko model (Ref. 33) expresses the kinetic energy of the turbulence with a differential equation. This kinetic energy and an algebraically defined length scale are combined to yield an eddy viscosity. Alternatively, Bradshaw et al. (Ref. 34) utilize a single differential equation to define the turbulent shear stress directly, thereby avoiding the use of the eddy viscosity concept and thus allowing shear to exist in regions of zero velocity gradients. Bradshaw's closure model also requires an algebraically defined length scale.

Because the length scale of turbulence itself may be out of equilibrium with the mean flow, two-equation models have been developed where both ingredients of the eddy viscosity, the intensity and the length scale, are represented by differential equations. Modeling in these equations usually requires experimental knowledge of the ratio of the local shear to kinetic energy in addition to the mean velocity profile (see the second column of Figure 2). Although these models can treat turbulence intensity and scale out of equilibrium with the mean flow, their use of an eddy viscosity still links changes of the Reynolds stresses tightly to rapid changes of the mean rate of strain. To loosen these ties and to avoid forcing the alignment of stress and strain, several models have been developed that compute the individual components of the Reynolds stress tensor (e.g., Refs. 35 through

37). For an incompressible fluid, these methods involve at least six additional partial differential equations. To establish the modeling coefficients in these equations, use is made of ratios of the normal Reynolds stresses obtained either from a homogeneous shear flow experiment (Ref. 38), or from measurements in the logarithmic region of a flat-plate boundary layer (Ref. 39).

During the past few years rather extensive comparisons have been made between experimental data and predictions based on the hierarchy of second-order closure models (e.g., Refs. 40-42). Because the modeling coefficients are based to a large extent on data from flat-plate experiments, it is not surprising that the models "predict" the mean flow over flat plates and surfaces experiencing small pressure gradient quite well. Even the effects of compressibility are correctly accounted for up to Mach numbers of about 5, either through the use of Favre mass-weighted dependent variables (Ref. 43), or with primitive variables and additional modeling coefficients in equations for turbulent heat flux and the intensity of thermal fluctuations (Ref. 36). In regions of intense adverse pressure gradients at supersonic speeds, these methods predict the rise in local skin friction that agrees with data better than predictions based on the first-order closure models. For the mean flow quantities, velocity profile, skin friction, etc., there seems to be no advantage in the full Reynolds stress models, at this time, over the two-equation eddy viscosity models. That the full Reynolds stress models still require improvements to accurately describe the anisotropy of boundary-layer turbulence and to enhance their potential for universal application will become evident from the figures that follow.

Figure 3 shows a profile of the component of the dissipation tensor D_{11} measured in a low-speed flat-plate boundary layer by Klebanoff (Ref. 39), compared with predictions of the full Reynolds stress turbulence model originated by Donaldson and expanded in Reference 36. The dissipation tensor component $D_{11} = 2\nu\left(\frac{\partial u'}{\partial x}\right)^2$ was chosen for this comparison because it is a directly measured quantity when the Taylor hypothesis is invoked to relate traces of the u velocity in time to velocity gradients in space. Other measures of dissipation require approximations; the turbulence kinetic energy dissipation, for example, requires additional assumptions regarding the isotropy of the dissipation process to account for terms such as $(\partial w/\partial z)$

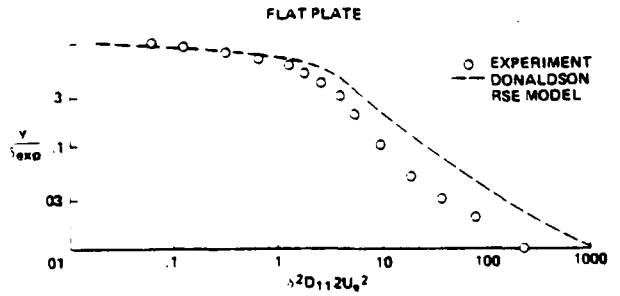

Figure 3. Comparison of experimental and modeled dissipation rate tensor component.

which cannot be measured directly. The ordinate in Figure 3 is the distance from the wall y normalized by the experimental boundary-layer thickness. It is observed, that the dissipation increases greatly as the surface is approached. Of course, this ordinate stops short of the sublayer region next to the surface where the dissipation of the turbulence again diminishes. In the region of large dissipation near the wall, it is observed that the computational method overpredicts the dissipation rate by a factor of about 3. The turbulence model in this particular calculation was based on a scalar dissipation length scale, equal in magnitude in all directions. It was demonstrated in Reference 41 with a near-wall asymptotic analysis, however, that the dissipation length scale adjacent to the surface should really be a vectorial quantity having significantly different values normal and parallel to the surface. To account for this anisotropic character, a differential equation model for a tensor length scale is currently under development (Ref. 44).

The table in Figure 4 shows another direction that modeling of the full Reynolds stress equations is taking to broaden their range of application. The author is indebted to Professor Launder for the information in this table. The figure shows a comparison of the relative measured spreading rates of a plane jet, a plane asymmetric wake, and a round jet with corresponding predictions based on the most general Reynolds stress model in existence (Ref. 45). The column labeled "Single Scale" refers to calculations based on the turbulence kinetic energy dissipation rate or scale equation of Reference 45. From this column, it is seen that the model gives an excellent prediction of the spreading of the plane jet. Incidentally, the modeling constants employed throughout the computations were essentially the same as those used in successful predictions of attached boundary-layer flows. Thus, the same model can predict both the attached boundary layer and the plane jet. When the model is applied to computing the plane asymmetric wake, it is found to underpredict the spreading rate by 1/3. For the round jet, it overpredicts the spreading rate by about 3/2. Professor Launder identified the source of inaccuracies in these applications in the use of a single-scale equation. In some preliminary work, Launder and his colleagues have extended a two-equation eddy-viscosity model to include a scale or dissipation equation that is divided into two equations; the first represents the energy dissipation rate transferred to the small scales from the large, and the second, the rate of dissipation at the small scales. The effect of this bimodal scaling is to introduce some spectral information into the modeling. The improvements achieved by this modification,

FLOW FIELD	SPREADING RATE		
	EXPERIMENTAL	SINGLE SCALE	DUAL SCALE*
PLANE JET, $\frac{d\delta}{dx}$	1.0	1.0	1.0
PLANE ASYMMETRIC WAKE, $\frac{\Delta u}{u}\frac{d\delta}{dx}$	90	60	.88
ROUND JET, $\frac{d\delta}{dx}$	79	1.10	95

*PRELIMINARY RESULTS FROM LAUNDER

Figure 4. Measured and Reynolds stress predicted spreading rates of jets and wakes.

in its preliminary form, are estimated to be as indicated in the column "Dual Scale" in Figure 4. Significant improvement in the predicted spreading rate of the different flow fields results from these changes. Thus, the introduction of spectral information, especially, the spectral changes between different positions in the flow, may contribute to making the Reynolds stress models more universal. Experimental information on the large coherent structure throughout different flow fields could prove to be most helpful in such new modeling endeavors.

Second-order Reynolds-stress modeling has recently been introduced into the time- or Reynolds-averaged compressible Navier Stokes equations to permit the solution of flow fields where strong interactions occur between the inviscid and viscous portions of the field. An example of such a calculation is shown in Figure 5. The flow field computed is indicated schematically at the top of the figure. Air is introduced into a cylindrical test section through a nozzle that produces a flow of Mach 1.4. A standing normal shock wave is generated within the test section with a controllable downstream obstruction (Ref. 46). The shock wave so created was thought to possess sufficient strength to separate the turbulent boundary layer on the walls of the test section and create a test zone of separated flow. The skin friction was measured in this experiment with a buried wire gage (Ref. 47) located at a single station. Surface pressure was also measured at this location. By

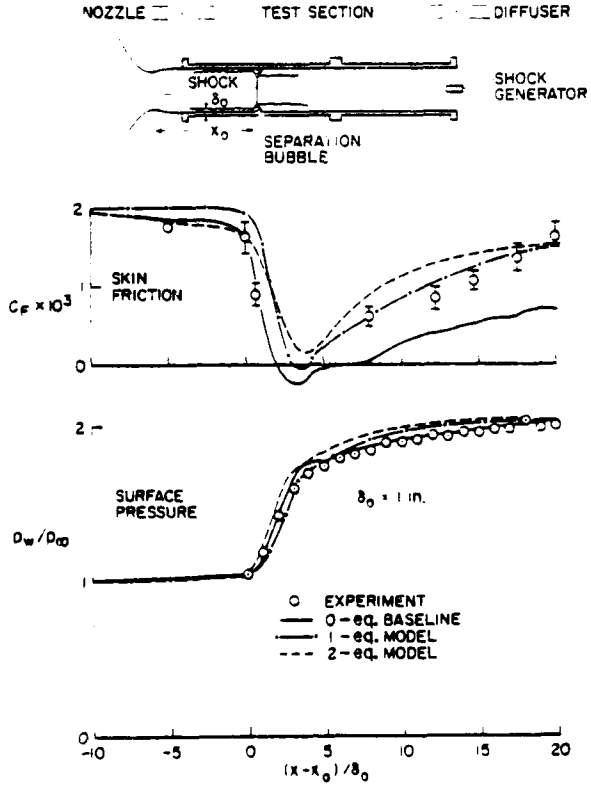

Figure 5. Reynolds stress modeling in Navier-Stokes equations for shock-wave boundary-layer interaction.

small variations in the axial position of the shock generator, the normal shock wave could be moved in a controlled manner axially along the test section relative to the pressure tap and skin-friction gage providing the means of mapping the profile of data indicated on the skin friction and surface pressure plots. The calculations shown are from Reference 48 and include the first-order model described earlier and two second-order models of one equation (Refs. 33 and 49), and two equations (Ref. 37). From the lowest part of the figure, it is observed that the surface pressure distribution is well represented by all of the models, though the first-order zero-equation model yields the best agreement with the data. From the skin-friction plot, however, it is seen that the first-order model fails to capture the rise of skin friction in the data in the downstream portion of the interaction zone. Of the second-order models, the one-equation model is the better in predicting the skin friction in this region, but is the poorer at the upstream portion. At this point in time, then, if interest centers on the boundary-layer development downstream of separation and reattachment it appears that one must utilize second-order models to achieve proper predictions. Recent reinterpretation of the data of Ref. 46 by G. Mateer suggests that the flow was not separated in the experiment; this would allow the tentative suggestion that the two-equation model may be the best of the three for defining the conditions for incipient separation.

From this brief description of the status of Reynolds stress modeling, it is evident that considerable improvement is needed before the method can be considered universally applicable. Improved definitions of the anisotropic and spectral character of the turbulence are the main directions the research is taking. However, it is not clear that the increasingly complex models are converging onto a universal global model. Can a method that treats turbulence as a steady-state phenomenon be expected to handle turbulence in a global fashion?

It is this question that has led to an acceleration of research into methods in which the large eddies of a particular flow field are simulated on a computer. The next section describes such a simulation of incompressible flow in a channel.

SIMULATION OF INCOMPRESSIBLE TURBULENT FLOW IN A TWO-DIMENSIONAL CHANNEL

The author is indebted to Mr. Moin and Professors Reynolds and Ferziger for allowing him to use the material in this section prior to its publication in Reference 31. As grant monitor of this research, I found the results to be most exciting because they revealed many features akin to those observed in experiments of coherent structure and bursting phenomena. I knew they would be of particular interest to the participants of this workshop and am pleased that they could be included here. These computations also offer the opportunity to emphasize one of the themes of this paper, namely, that advances in computational fluid dynamics is closing the time lag between experimental discoveries and analysis, both theoretical and numerical, and the time is approaching when collaboration between the different investigative processes will be most fruitful.

The principal objective of the research of Reference 31 was to simulate the large eddy structure of the turbulent flow within a two-dimensional channel, but to be different from the work of References 1 and 2 by numerically resolving the near wall region and thereby avoiding the need for invoking some sort of instantaneous "law of the wall." The latter was done in References 1 and 2 and many of the real aspects of physical behavior that exist in the real wall region were missed. The computational volume used to represent the flow in the two-dimensional, rectangular channel of height 2δ is indicated in Figure 6. A Cartesian coordinate system is employed with its x-axis aligned in the streamwise direction of the mean flow, the z-axis is parallel to the channel walls, and the y-axis is normal to the walls with its origin on the channel centerline. Because pseudospectral methods are employed in evaluating the partial derivatives of the dependent variables, u, v, w, and p in the x and z directions, it is required that the conditions at opposite faces of the computational volume to be periodic. For such boundary conditions, it is necessary to use a computational volume large enough in the x and z directions to avoid having the bulk of the flow within the volume dominated by the boundary conditions. Experience with computations of homogeneous isotropic turbulence (Ref. 50) indicated this can be achieved by setting the length of a side of a computational volume to be about twice the experimentally determined two-point correlation length in that direction. Experimental data from a channel flow experiment of Compte-Bellot (Ref. 51) indicates that when $r_1 > 3.2\delta$ and $r_3 > 1.6\delta$ $R_{11}(r_1, o, o)$ and $R_{11}(o, o, r_3)$ are both negligible. Distances approximately twice these were chosen as the lengths of the sides of the computational parallelopiped in these computations. In the y direction, the computational volume extends from the lower to the upper channel wall.

The next stage of the computation involves the selection of the computational grid configuration, subject to the constraints imposed by the capacity of a CDC 7600 computer limited to about 32^3 grid points for computations of an incompressible flow field. The relatively low Reynolds number experiment of Hussain and Reynolds (Ref. 52) was selected for simulation, and this fixed $u_\tau\delta/\nu = 640$. Data on coherent structures near surfaces (e.g., Ref. 53)

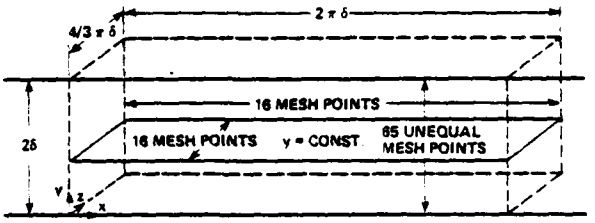

EXPERIMENTAL CONDITIONS

$\frac{u_\tau\delta}{\nu} = 640$, $\lambda_z^+ \cong 100$, $\lambda_x^+ \cong 440$

COMPUTATIONAL RESOLUTION $\Delta_z^+ = 16$ $\Delta_x^+ = 251$

COMPUTATIONAL SCHEME
- PSEUDOSPECTRAL, FILTERED IN x, z DIRECTION
- SECOND-ORDER FINITE DIFFERENCE IN y DIRECTION
- SECOND-ORDER EXPLICIT, IMPLICIT IN TIME

Figure 6. Computational volume employed in large eddy simulation of channel flow.

indicate spacings of features to be $\lambda_z^+ \cong 100$ and $\lambda_x^+ \approx 440$ in wall unit notation. To resolve these features, with 4 mesh points per wave length, would require 37 and 82 grid points in the x and z directions, respectively. Because the intended improvement of these calculations over those of References 1 and 2 was the resolution of the near wall region, Moin et al. (Ref. 31) wanted to reserve 65 grid points for the y direction. The total number of grid points needed to resolve the flow field accurately exceeded the capacity of the computer, so that a compromise had to be adopted. Moin et al. elected to use 16 grid points in both the x and z directions, which in wall units meant grid spacings of $\Delta_z^+ = 168$ and $\Delta_x^+ = 251$. Thus, the real features in the z direction cannot be resolved, and any structure shown in this direction has to be interpreted in a qualitative sense. Although the failure to resolve the real structure in the x direction is less severe, care must still be exercised in interpreting the calculational output because of this "anisotropic" resolution.

The basic equations in this large-eddy simulation are the Navier-Stokes equations in primitive variables, the three velocity components, and the pressure, that have been filtered (Ref. 54) in the x and z direction. Thus the new, filtered dependent variables are weighted means over elemental areas parallel to the channel surface. Their spatial derivatives in x and z are obtained by pseudospectral methods, whereas those in the y direction are established from a second-order finite-difference scheme.

The filtering process yields equations similar to the original Navier-Stokes equations but with additional terms based on scales of turbulence comparable to and smaller than the grid-spacing dimensions. Since the computations are "blind" to these scales of turbulence, these terms must be the modeled. Moin et al. (Ref. 31) adopted the Smagorinsky model (Ref. 55) for the bulk of the channel, but near the surfaces they modified the model to include the effects of molecular viscosity. The scaling constant in the latter model is evaluated by requiring the two models to yield the same subgrid eddy viscosity averaged over the plane where $y^+ = 27$. The length scale in the subgrid model is then taken as either the cube root of the grid element volume or the Prandtl mixing length, whichever is smaller. The authors recognize the heuristic nature of this model, but feel the overall behavior of the computations are not seriously compromised by its adopted form.

The manner of starting the calculation required additional decisions. In nature, the fluid attains its fully turbulent character after having undergone a transition process in the entrance of the channel. The simulation of this process in itself is a major undertaking and is avoided here. What Moin et al. do is start their computations with an initial dynamic flow field that can extract energy from the mean field and sustain the turbulence. In time this field loses its initial identity and establishes a fully developed, stationary turbulence field. The computations begin with a velocity field composed of three superimposed elements: (1) the two-dimensional mean-velocity profile observed in the channel; (2) an initial three-dimensional large-eddy field made up of the principal eigensolutions of the Orr-Sommerfield equation employing the mean velocity profile; and (3) a random phased velocity field with an amplitude about 10% of the large eddy. The authors had to adjust the intensity of the Orr-Sommerfield eddy upward and reduce the magnitude of the Smagorinsky modeling constant below that for decaying isotropic flow before

solutions would result in which the turbulence would not decay to a vanishingly small value but maintain itself and achieve a self-sustaining stationary dynamic character. The results of such a calculation are indicated in the figures that follow.

Figure 7 shows the resolvable velocities $\frac{\bar{u}}{u_\tau}$ and $\frac{\bar{v}}{u_\tau}$, at a representative point x, z, over half of the channel width at two instances in time. These values were obtained after the solution developed into a stationary dynamic state and the two times are when the velocities represent close to the extremes in maximum and minimum values during a cycle of the large-eddy structure. The corresponding $\bar{u}/u_\tau$ and $\bar{v}/u_\tau$ velocity components are coded with the same lines. The crosses represent the mean axial velocity over two cycles of oscillation. It is observed that when the $\bar{u}/u_\tau$ is less than the mean, the corresponding $\bar{v}/u_\tau$ is generally positive, indicating an overall lifting of retarded fluid. Very close to the surface, $y/\delta > 0.93$, the $\bar{v}/u$ is downward for this case, and it is not clear what this signifies or if it is a usual occurrence. At the other extreme, when $\bar{u}/u_\tau$ is greater than the mean, $\bar{v}/u_\tau$ is everywhere negative or sweeping downward. This last description is analogous to the conditions that prevail at the end of a "sweep" in an experimentally observed bursting sequence. The lifting of the retarded fluid also has its experimental counterpart.

To date, the numerical data have not been analyzed sufficiently for other values of x and z to be able to establish a characteristic three-dimensional pattern of the dynamic flow field; however, a few spot checks at other values

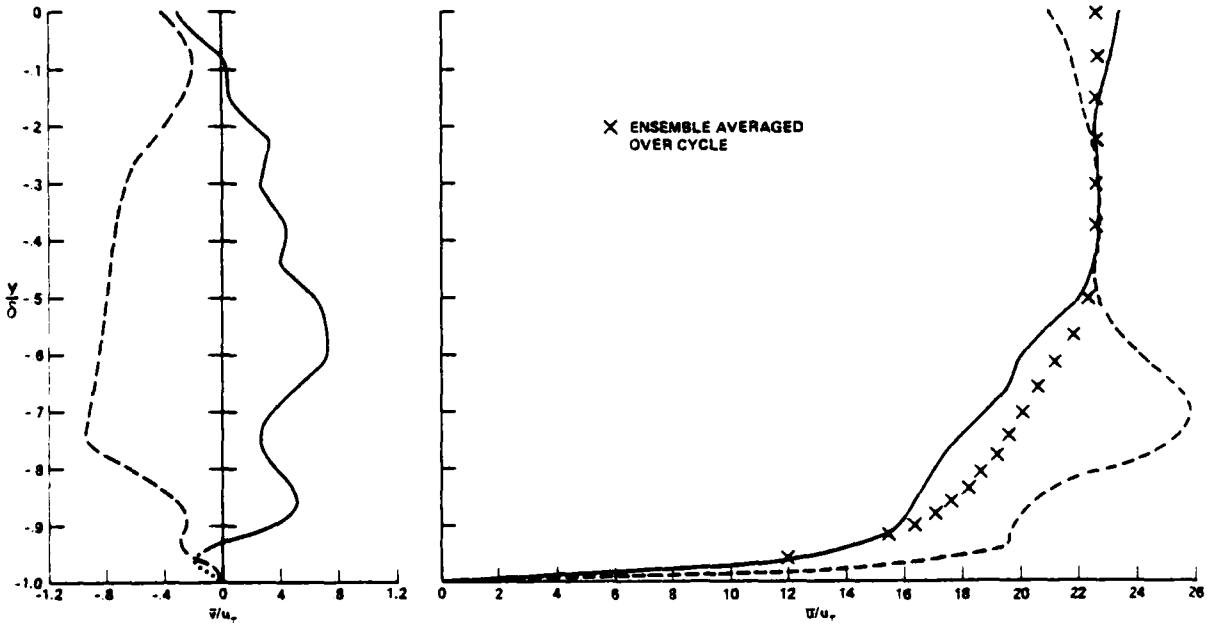

Figure 7. Instantaneous resolvable velocity profiles at a representative point in x,z.

of x and z, at the same instant of time, show variations in the local velocities comparable to those indicated on this figure at different times.

Figure 8 shows the instantaneous values of $\bar{u}/u_\tau$ across the channel at a value of $y^+ = 3.78$ and at several x positions along the computational volume. The patterns at each of the x stations are similar. The variation in $\bar{u}/u_\tau$ in the z direction is quite large. This implies regions of slow-moving fluid between jets along the surface. It should be recalled that the numerical resolution in the z direction in these calculations was inadequate to resolve the streaks observed experimentally; however, it is most encouraging that the calculations show features that are akin to the experimentally observed streaks. Further examination of the numerical data is required to learn if the low-speed portions of the streaks rise during the bursting process as is believed to occur in the experiments. Further examination of the numerical data will also reveal if the streaky character of the near-wall fluid motion contains a significant amount of axial vorticity and if it moves up and down as would be suggested by the horseshoe vortex models.

The behavior of the instantaneous Reynolds stress averaged over eacn y - plane in the computational volume is shown in Figure 9 at three instances

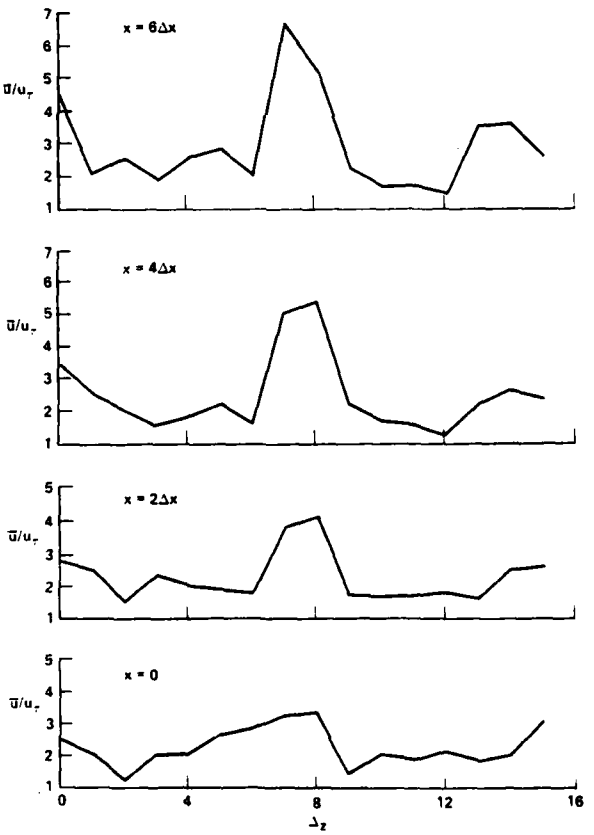

Figure 8. Instantaneous axial velocity profiles across computational volume at four stations, $y^+ = 3.78$.

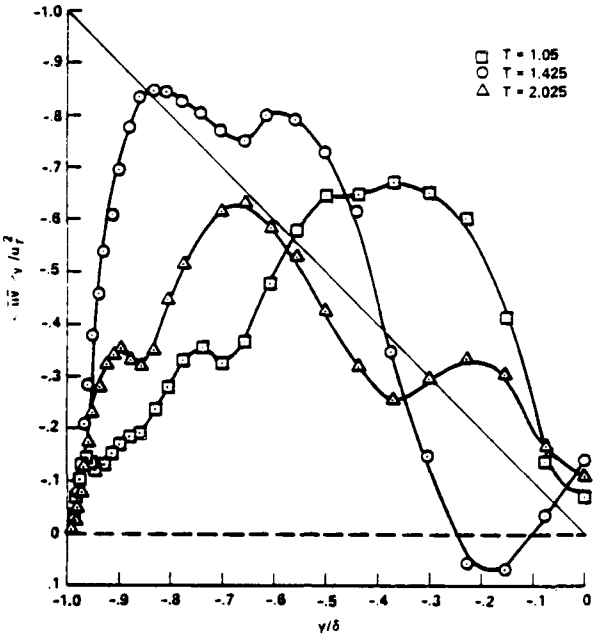

Figure 9. Instantaneous profiles of Reynolds shear stress averaged over horizontal plane of computational volume.

during a representative cyclic period of the large eddies. Here the time indicated, T, has been made dimensionless by division with ν/u_τ^2, and the Reynolds stress has been normalized by u_τ^2. The straight line diagonally across the figure represents the time-averaged shear stress distribution that occurs over a half channel width. The results indicate large changes in the instantaneous, planar-averaged Reynolds stress from time to time during the cycle. If the numerical data were not planar-averaged the changes from time to time would even be larger. To date, no correlation has been made between these numerical data and the velocities themselves to establish the portions of the oscillation period of the large eddies that produce the largest contributions to the Reynolds shear stress.

If the data of Figure 9 are conditionally averaged in time over a specific period of the large structure oscillation, the Reynolds shear stress distribution indicated in Figure 10 results. Again, the diagonal line represents the time averaged total shear stress that balances the applied mean pressure gradient. If many periods of large eddy structure were averaged this straight line would be expected to result. Near the surfaces, $y/\delta = \pm 1$, the total shear stress is made up largely of laminar stress and this accounts for the approach by the Reynolds stresses to a zero value there. The data represented by the open symbols represent the contributions of the resolvable scales of the turbulence, whereas the solid symbols include the contributions of the modeled subgrid scales as well. Over the center half of the channel, the modeled subgrid contribution is negligibly small. Near the surfaces, at $y/\delta \cong \pm 0.7$, their contribution rises to about 10% of the total turbulent stress. It should be recalled that the contribution of the subgrid model is

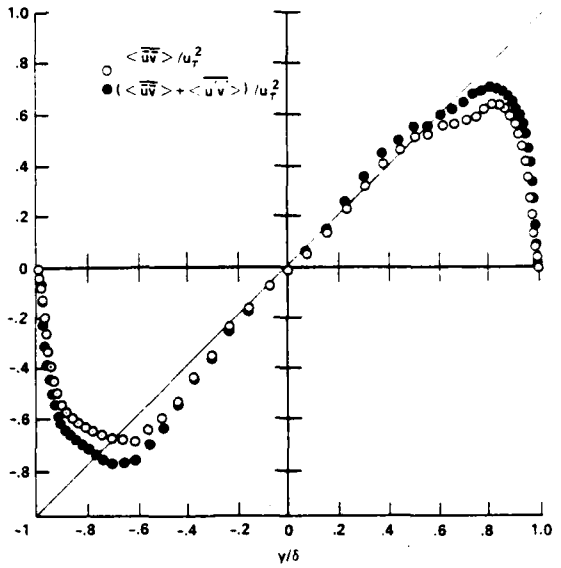

Figure 10. Planar and conditional averaged Reynolds shear stress.

very dependent on the particular grid system and subgrid model employed, so that the results of this figure are not general. A small subgrid contribution, however, indicates the present calculation is capturing the bulk of the Reynolds stress producing eddies.

Figures 11-13 show a comparison of the computed Reynolds normal stresses in the near-wall region and data from the experiments of Clark (Ref. 56), Hussain and Reynolds (Ref. 52), Compte-Bellot (Ref. 51), and Laufer (Ref. 57). Two abscissas are utilized: the value of y/δ corresponds to the numerical results of Reference 31, and the wall distance parameter, $y^+ = \frac{(\delta-y)u_\tau}{\nu}$, corresponds to each of the experiments and the numerical results. The latter coordinate is the more significant. The ordinates in these figures are $\sqrt{\langle(\bar{u} - \langle\bar{u}\rangle)^2\rangle}/u_\tau$, $\sqrt{\langle\bar{v}^2\rangle}/u_\tau$, and $\sqrt{\langle\bar{w}^2\rangle}/u_\tau$, respectively, where the bracket $\langle\ \rangle$ indicates combined spatial average over a horizontal plane, y = const., and conditionally averaged in time over a cycle. Again, the open circles represent the resolvable terms alone and the closed symbols include the subgrid modeling.

Figure 11 compares the computed component of turbulence intensity in the axial direction (x) with experimental data from three experiments (Refs. 51, 52, and 56) in the near-wall region where $y^+ < 128$. The intensity is normalized with u_τ. Although it would be expected that use of the near-wall coordinates would collapse the data of the three experiments, even though they cover a rather large range of Reynolds number, the data do not collapse onto a single curve but show differences of about 30% in intensity. The peak experimental intensities occur in the range $12 < y^+ < 22$. Though

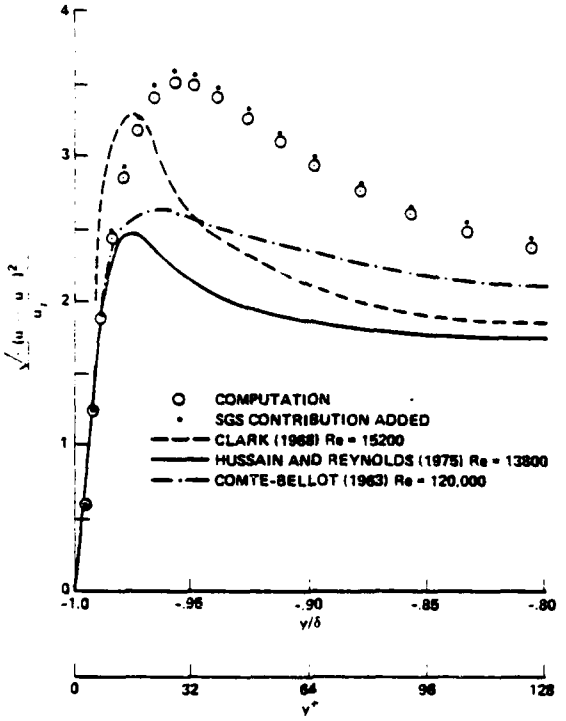

Figure 11. Planar-averaged and conditional-averaged Reynolds normal stress in axial direction.

somewhat higher than the experimental data, the numerical results possess the same general character as the experimental data and peak at $y^+ = 25$, which is rather close to the point where the experimental data are maximum. The subgrid contribution here is very small and, therefore, the calculated large-scale turbulence represents the bulk of the normal stress in this direction.

Figure 12 shows a comparison of the normal intensity in the z direction across the channel with the data of References 56 and 57. Although the use of near-wall coordinates does not collapse these data either, the two sets of data show a similar character, but seemingly displaced by about a $\Delta y^+ = 30$. Again, the computed results possess the same general character as the data, though with somewhat higher values. It is observed that the subgrid contribution is larger for this component of intensity than in the previous figure.

Figure 13 shows the behavior of the normal intensity perpendicular to the surface. The agreement between the data of the experiments of References 56 and 57 is remarkable when it is considered how difficult v measurements are. Here, the directly computed large-eddy structure does not behave as the data. Only when the rather large contribution of the subgrid model is added do the computed results fall into general agreement with the experimental data. It appears from the last three figures that the calculations in their present form are not handling the normal Reynolds stresses uniformly. The subgrid model dominates the component perpendicular to the surface, whereas it makes

little contribution to those components parallel to the channel surfaces. This suggests that subgrid scale modeling modifications are required to account for the anisotropy of the turbulence in a more uniform manner. In

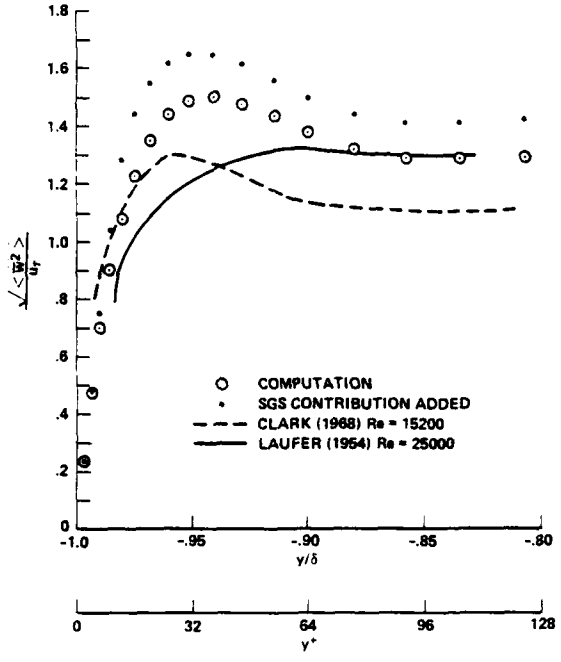

Figure 12. Planar-averaged and conditional-averaged Reynolds normal stress in crossflow direction.

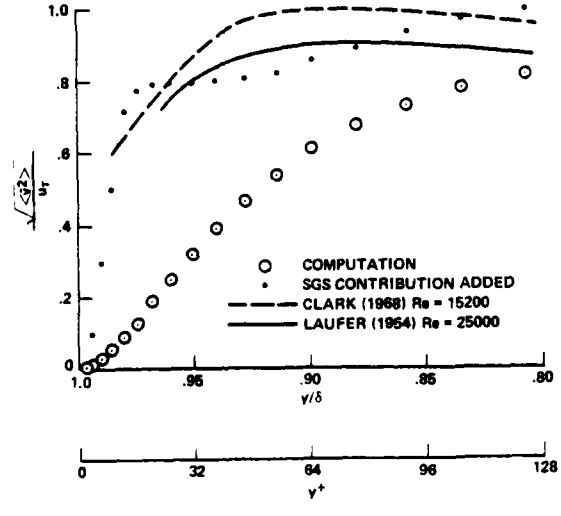

Figure 13. Planar-averaged and conditional-averaged Reynolds normal stress in direction perpendicular to surface.

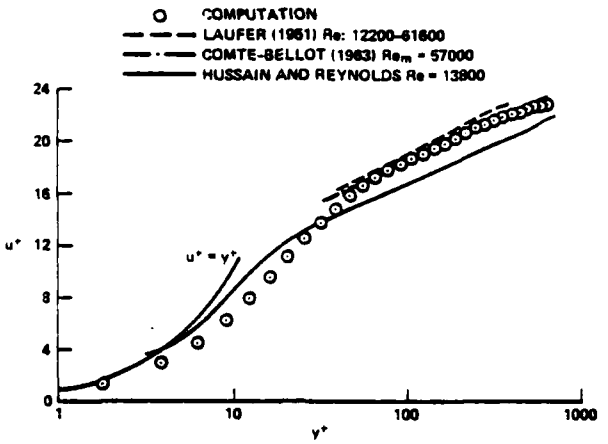

Figure 14. Mean velocity profiles in channel.

particular, the assumption regarding the length scale as the cube root of the element of grid volume may be the weakness indicated here.

As a final assessment of the large-scale simulation, Figure 14 shows a comparison of the long-time-averaged results in the classic wall layer coordinates with the mean velocity profiles measured in References 51, 52, and 57. It is noted that the near-wall coordinates do not collapse the experimental data at $y^+ > 50$. At these values of y^+, the results of the numerical simulation lie about 12% higher than the Hussain and Reynolds experimental data at the same Reynolds number, but are lower than Laufer's data, which also include the computed Reynolds number. Toward the surface at $y^+ < 50$, the numerical results cross over the Hussain and Reynolds data and approach the sublayer at values a little below $u^+ = y^+$. For a first attempt at computing the $y^+ < 100$ region, these results are most encouraging.

CONCLUDING REMARKS

A review of the state of boundary-layer analysis for engineering predictions reveals very little reliance in the past on the dynamic experimental observations of coherent and organized structure. Computational techniques generally available have been inadequate to account for these dynamic physical effects. Predictive techniques have had to rely mainly on Reynolds averaged equations developed from statistical experimental data in a sequence of more complex methods.. Current design needs, however, are forcing consideration of more global techniques, and it is not entirely clear that a global model is within the capabilities of the most complex of the Reynolds stress models, even if new effects such as spectral changes or nonisotropic scales can be included. Rapid evolution in the capacity and speed of computers has raised the prospect of a more general alternative to the Reynolds stress approach. This is the simulation of the larger scales of turbulence on a computer in a three-dimensional time-dependent calculation. A rather successful simulation has been presented here. The practicality of ultimately using such a method

in real design problems depends critically on defining the minimum three-dimensional spatial resolution required to capture the essential character of the turbulence in a variety of flow fields. This process cannot be performed with the computer alone, but will require guidance from the experimentalist, the behavioral analyst, and the theoretician. Some of this interplay between the computational needs and experimental data are shown in the example of large eddy simulation described herein. The behavioral analyst, by employing theory and/or detailed zonal numerical computations, can contribute much to the definition of the minimum resolution required in a larger global problem. A good subgrid theory will push the required grid resolution toward practicality at an earlier date. Even if the prospect of an early application of large-eddy simulation to design is proven to be poor, continued application of the method for simple flow fields, such as a flat-plate boundary layer, will prove to be an enormously valuable research tool. Provided the method can be verified against experimental data, the wealth of information contained within the solution should be most useful to the experimentalist by filling in the information between his discrete sensors and providing him with an overall picture of the processes in a variety of frames of reference or dependent variables. These computations should also suggest new critical experiments. Numerical simulation of simple flows also can provide the predictor with improved Reynolds stress models. Thus, numerical large eddy simulation has the potential of focusing our research in turbulence by drawing upon the most detailed experimental and analytical investigations and, in turn, returning information where the experimental techniques and theoretical methods, themselves, are limited. The day when the predictor can choose to be oblivious to the observed details of turbulence, or the experimentor can ignore the needs or the findings of the analyst is rapidly drawing to a close.

REFERENCES

1. Deardorff, J. W.: A Numerical Study of Three-Dimensional Turbulent Channel Flow at Large Reynolds Number. J. Fluid Mech., Vol. 41, 1970, p. 453.
2. Schumann, U.: Subgrid Scale Model for Finite Difference Simulations of Turbulent Flows in Plane Channels and Annuli. J. Comp. Physics, Vol. 18, 1975, pp. 376-404.
3. Reynolds, O.: On the Dynamical Theory of Incompressible Viscous Fluids and the Determination of the Criterion. Phil. Trans. A, Vol. 186, 1895, pp. 123-164.
4. Prandtl, L.: Über die ausgebildete Turbulenz. ZAMM, Vol. 5, 1925, p. 136.
5. Nikuradse, J.: Untersuchungen über die Geschwindigkeitsverteilung in turbulenten Strömungen. Thesis, Göttingen, 1926.
6. Schlichting, H.: Boundary Layer Theory. Chap. XXII, McGraw-Hill Book Co., New York, 1960.
7. Kline, S. J., et al., eds.: Proceedings of AFOSR-IFP-Stanford Conference on Computation of Turbulent Boundary Layers - 1968, Stanford University, Calif., Aug. 18-25, 1968.
8. von Karman, Th.: The Analogy between Fluid Friction and Heat Transfer. Trans. ASME, Vol. 61, 1939, pp. 705-710.
9. Martinelli, R. S.: Heat Transfer to Molten Metals. Trans. Amer. Soc. Mech. Engrs., Vol. 69, 1947, pp. 947-959.

10. Einstein, H. A. and Li, H.: The Viscous Sublayer along a Smooth Boundary. Proc. Amer. Soc. Civ. Engrs., Paper 945, 1956.
11. van Driest, E. R.: On Turbulent Flow Near a Wall. J. Aero. Sci., Vol. 23, No. 11, 1956.
12. Rubesin, M. W. and Inouye, M.: Forced Convection, External Flows. Handbook of Heat Transfer, W. M. Rohsenow and J. P. Hartnett, eds., McGraw-Hill, New York, 1973.
13. Kendall, R. M., Rubesin, M. W., Dahm, T. J., and Mendenhall, M. R.: Mass, Momentum, and Heat Transfer within a Turbulent Boundary Layer with Foreign Gas Mass Transfer at the Surface. Part I - Constant Fluid Properties. Vidya Report No. 111, 1964, AD 619209.
14. Coles, D.: The Law of the Wall in Turbulent Shear Flow. Sonderdruck aus "50 Jahere Grenzschichtforschung," H. Görtler and W. Tollmien, eds., Verlang Friedr. Vieweg and Sohn, Braunschweig, Germany, 1955.
15. Coles, D.: The Law of the Wake in Turbulent Boundary Layer. J. Fluid Mech., Vol. 1, 1956, p. 191-226.
16. Kim, H. T., Kline, S. J., and Reynolds, W. C.: The Production of Turbulence Near a Smooth Wall in a Turbulent Boundary Layer. J. Fluid Mech., Vol. 50, 1971, pp. 133-160.
17. Kline, S. J., Reynolds, W. C., Schraub, F. A., and Runstadler, P. W.: The Structure of Turbulent Boundary Layers. J. Fluid Mech., Vol. 30, 1967, pp. 741-773.
18. Favre, A. J., Gaviglio, J. J., and Dumas, R. J.: Space-Time Double Correlations and Spectra in a Turbulent Boundary Layer. J. Fluid Mech., Vol. 3, 1958, pp. 344-356.
19. Grant, H. C.: The Large Eddies of Turbulent Motion. J. Fluid Mech., Vol. 4, 1958, pp. 149-190.
20. Landahl, M. T.: A Wave Guide Model for Turbulent Shear Flow. J. Fluid Mech., Vol. 29, 1967, pp. 441-459.
21. Landahl, M. T.: Wave Breakdown and Turbulence. SIAM J. Appl. Math., Vol. 28, 1975, pp. 735-756.
22. Bark, F. H.: On the Wave Structure of the Wall Region of a Turbulent Boundary Layer. J. Fluid Mech., Vol. 70, 1975, pp. 229-250.
23. Lumley, J. L.: The Structure of Inhomogeneous Turbulent Flows. Proceedings Inter. Colloq. on Fine Scale Processes in the Atmosphere. Doklady Akademia Nauk SSR, Moscow, 1966.
24. Payne, F. P.: Large Eddy Structure of a Turbulent Wake. Ph.D. Thesis, Pennsylvania State University, 1966.
25. Lemmerman, L. A.: Extraction of the Large Eddy Structure of a Turbulent Boundary Layer. Ph.D Thesis, University of Texas at Arlington, 1976.
26. Chuang, S. L.: Large Eddy Component Removed from the Total Measured Two-Point Reynolds Stress Tensor and Subsequent Small Eddy Viscosity Calculation. M.S. Thesis, University of Texas at Arlington, 1978.
27. Walker, J. D. A., and Abbott, D. E.: Implications of the Structure of the Viscous Wall Layer. Turbulence in Internal Flows, S. N. B. Murthy, ed., Hemisphere Publishing Corp., Washington, 1977.
28. Lilly, D. K.: The Representation of Small-Scale Turbulence in Numerical Simulation Experiments. Proceedings of IBM Scientific Computing Symp. on Environmental Sciences, 1967.
29. Orszag, S. A.: Numerical Methods for the Simulation of Turbulence. Phys. Fluids, Supplement II, 1969, pp. 250-257.
30. Libby, P. A.: On the Prediction of Intermittent Turbulent Flows. J. Fluid Mech., Vol. 68, 1975, pp. 273-295.

31. Moin, P., Reynolds, W. C., and Ferziger, J. H.: Large Eddy Simulation of Incompressible Turbulent Channel Flow. Stanford University Report TF-12, 1978.
32. Cebeci, T. and Smith, A. M. O.: Analysis of Turbulent Boundary Layers. Academic Press, New York, 1974.
33. Glushko, G. S.: Turbulent Boundary Layer on a Flat Plate in an Incompressible Fluid. Bull. Acad. Sci. USSR, Mech. Ser. 4, 1965, pp. 13-23.
34. Bradshaw, P., Ferriss, D. H., and Atwell, N. P.: Calculation of Boundary-Layer Development Using the Turbulent Energy Equation. J. Fluid Mech., Vol. 28, 1967, p. 593.
35. Launder, B. E., Reece, G. J., and Rodi, W.: Progress in the Development of a Reynolds-Stress Turbulence Closure. J. Fluid Mech., Vol. 68, 1975, pp. 537-566.
36. Sullivan, R. D.: GYC: A Program to Compute the Turbulent Boundary Layer on a Rotating Cone. A.R.A.P. Working Paper 76-2, Aeronautical Research Associates of Princeton, Inc., Princeton, N.J., 1976.
37. Wilcox, D. C., and Rubesin, M. W.: Progress in Turbulence Modeling for Complex Flowfields. Prospective NASA TN, 1978.
38. Champagne, F. H., Harris, V. G., and Corrsin, S.: Experiments on Nearly Homogeneous Turbulent Shear Flow. J. Fluid Mech., Vol. 41, 1970, p. 81.
39. Klebanoff, P. S.: Characteristics of Turbulence in a Boundary Layer with Zero Pressure Gradient. NACA Report 1247, 1955.
40. Rubesin, M. W., Crisalli, A. J., Horstman, C. C., Acharya, M., and Lanfranco, M.: A Critique of Some Recent Second Order Closure Models for Compressible Boundary Layers. AIAA Preprint 77-128, AIAA 15th Aerospace Sciences Meeting, Los Angeles, Jan. 24-26, 1977.
41. Rubesin, M. W., Crisalli, A. J., Lanfranco, M. J., and Acharya, M.: A Critical Evaluation of Invariant Second-Order Closure Models for Subsonic Boundary Layers. Symposium on Turbulent Shear Flows, Pennsylvania State University, University Park, Penn., April 18-20, 1977.
42. Higuchi, H. and Rubesin, M. W.: Behavior of a Turbulent Boundary Layer Subjected to Sudden Transverse Strain. AIAA Preprint 78-201, AIAA 16th Aerospace Sciences Meeting, Huntsville, Ala., January 16-18, 1978.
43. Wilcox, D. C., and Traci, R. M.: A Complete Model of Turbulence. AIAA Preprint 76-351, AIAA 9th Fluid and Plasma Dynamics Conf., San Diego, Calif., July 14-16, 1976.
44. Sandri, G.: A New Approach to the Development of Scale Equations for Turbulent Flows. Report No. 302, Aeronautical Research Associates of Princeton, April, 1977.
45. Launder, B. E., Reece, G. J., and Rodi, W.: Progress in the Development of a Reynolds Stress Turbulence Closure. J. Fluid Mech., Vol. 68, 1975, p. 537.
46. Mateer, G. G., Brosh, A., and Viegas, J. R.: A Normal Shock Wave Turbulent Boundary-Layer Interaction at Transonic Speeds. AIAA Paper 76-161, AIAA 14th Aerospace Sciences Meeting, 1976.
47. Rubesin, M. W., Okuno, A. F., Mateer, G. G., and Brosh, A.: Flush-Mounted Hot-Wire Gage for Skin Friction and Separation Detection Measurements. Int'l Congress on Instrumentation in Aerospace Simulation Facilities, Ottowa, Sept. 22-24, 1975, IEEE Publication 75 CHO 993-6 AES, 1975.

48. Viegas, J. R. and Horstman, C. C.: Comparison of Multi-Equation Turbulence Models for Several Shock Separated Boundary Layer Interaction Flows. AIAA Paper 78-1165, AIAA 11th Fluid and Plasma Dynamics Conf., Seattle, Wash., July 10-12, 1978.
49. Rubesin, M. W.: A One-Equation Model of Turbulence for Use with the Compressible Navier-Stokes Equations. NASA TM X-73,128, April, 1976.
50. Ferziger, J. H., Mehta, U. B., and Reynolds, W. C.: Large Eddy Simulation of Homogeneous Isotropic Turbulence. Symposium on Turbulent Shear Flows, Pennsylvania State University, University Park, Penn., April 18-20, 1977.
51. Compte-Bellot, G.: Contribution a l'etude de la turbulence de conduite. Thesis, Univ. of Grenoble, 1963.
52. Hussain, A. K. M. F. and Reynolds, W. C.: Measurements in Fully Developed Channel Flow. J. Fluids Eng., Vol. 97, 1975, p. 568.
53. Clark, J. A., and Markland, E.: Vortex Structures in Turbulent Boundary Layers. Aeronaut. J., Vol. 74, 1970, p. 243.
54. Leonard, A.: On the Energy Cascade in Large-Eddy Simulations of Turbulent Fluid Flows. Adv. in Geophysics, Vol. 18A, 1974, p. 237.
55. Smagorinsky, J.: General Circulation Experiments with the Primitive Equations. Mo. Weather Rev., Vol. 93, 1963, p. 99.
56. Clark, J. A.: A Study of Incompressible Turbulent Boundary Layers in Channel Flow. J. Basic Eng., Vol. 90, 1968, p. 455.
57. Laufer, J.: Investigation of Turbulent Flow in a Two-Dimensional Channel, NACA Rep. 1053, 1951.

DISCUSSION

Orszag:

In the large eddy simulation, how accurate was the predicted wall skin friction? Secondly, was anything special done in the sub-grid model close to the wall?

Rubesin:

An indication that the mean skin friction was predicted well is implied by the law of the wall, which was predicted relatively well. We still have a great deal to learn about what to do near the walls, where the mesh shapes are very anisotropic.

Reynolds:

May I add to that just a little bit? The calculation was [illegible] run with the [illegible]in friction specified, and the mean flow [illegible] accele[illegible]ed) to match that. So what you really [illegible] accuracy of the through-flow, and that [illegible]ent. The Smagarinsky model assumes equi-[illegible] large eddies and the small eddies, and the

Reynolds: (Cont'd)

Smagarinsky model used in the outer region is based on inertial scaling for the dissipation. Near the wall the dissipation scales on viscous parameters, and so the modified Smagarinsky model was modified near the wall to bring in the viscous parameters at low turbulence Reynolds numbers. The details are in Dr. Moin's Dissertation.

Bradshaw:

The calculated log law looked rather higher than the standard log law as evidence, for instance, by the Hussain and Reynolds data. However, the bulk Reynolds number of the flow was pretty low, and it is known from the work of Patel and Head, for example, that at low bulk Reynolds numbers in duct flows,the log law does indeed start to rise. It might be worthwhile cross-checking calculations with the Patel and Head work to see whether you are really getting the right rise in log law.

One of the most encouraging things about the large eddy simulations is the way that one can get pressure fluctuation data from them. In particular, you can get specific measurements of the pressure-strain correlation which is what one would like to put in ones Reynolds stress models.

Reynolds:

I brought the pressure-strain curves with me and will give them to you.

Hussain:

Could computed large-scale streaky structure near the wall be utilized to determine the instantaneous vorticity distribution or contours?

Rubesin:

Yes. The streamwise vorticity contours showed a concentration of vorticity very close to the surface was followed over an interval of time by a lifting off and a sort of a spreading. This region of vorticity was observed to grow and collapse repetitively. However, I caution that we can't really look at these answers quantatively because the resolution in the z direction in this particular computation was not sufficient to resolve the experiments. This technique shows potential, but I don't think we really want to start comparing it with detailed fluctuation data at this stage.

Morokovin:

I would like to suggest that we should shift our attention from trying to understand the large scale eddies in one very special equilibrium flow (which is what we had all day yesterday) to examining whether that understanding will allow us at least physical ideas of what happens for all sorts of other flows. This is particularly important, for example, when the large scale eddies are subjected to changes from one condition to another via pressure gradients of various kinds. I am particularly interested in whether you have any comments on the possible role of the large eddy in understanding reattachment of a boundary layer. Do you really need to have additional scales associated with presumably large scale phenomena?

Rubesin:

The limited objective of our particular group is to be able to model the near field of a three-dimensional separation. This is a particular problem which raises the questions that Mark mentioned and is an example of how design needs are forcing more reality into our predictive techniques.

Landahl:

The large-eddy simulation indicated that the small-scale contribution to the Reynolds stress was fairly small except near the wall. How was this determined?

Rubesin:

It's my understanding that the sub-grid stresses were computed in the calculation and were imposed on the large-scale field.

Reynolds:

That's correct.

Eckelmann:

You said you did have very good agreement, but you had a large Reynolds number range in the data, and you made the comparison on a y/δ basis. I think you should make all comparisons on the basis of y^+ values. The experimental data will behave this way too if you plot them on the basis of y^+ instead of on the basis of y/δ basis. I think you should make all comparisons on the basis of y^+, which requires replotting of all experimental data on a y^+ scale. If you do this, the maximum is shifted towards higher y^+ values. The experimental data will behave this way. Plot them on the basis of y^+ instead of on the basis of y/δ. When plotted vs. y/δ, the maximum is dependent on the Reynolds number. Thus, the higher the Reynolds number, the closer the maxima is to 0.

Rubesin:

Well, in this particular example, the Reynolds number of the computation agreed with the Reynolds number of the experiments, so there is still a disagreement as to where the maxima appear.

Reynolds:

The curves near the wall were plotted on a y^+ basis, and then y/δ scale was added for the Reynolds number of the computations. Unfortunately, the y^+ scale subsequently disappeared.

MODEL OF BURST FORMATION IN TURBULENT BOUNDARY LAYERS

Steven A. Orszag

Department of Mathematics

Massachusetts Institute of Technology

ABSTRACT

A numerical model of turbulent boundary layer flows over compliant walls has been investigated. The model is based on Burton's observation that turbulent bursts produce large pressure fluctuations that tend to produce low speed 'streaks' near the wall. These streaks undergo space-time retardation and a new burst appears when the velocity profile becomes highly inflectional. The idea of the model is that the compliant wall motion interrupts this feedback loop of burst formation and that short wavelength wall motions can possibly delay burst formation long enough for the favorable gradient part of the pressure pulse caused by previous bursts to effect a decrease in the burst frequency. The results of our calculations indicate that certain small wavelength wall motions can have a significant effect upon the stability of the turbulent boundary layer. This result suggests that novel structural dynamics will be an essential component of successful drag reduction by compliant walls.

1. INTRODUCTION

In this paper, we discuss the formulation, development, and some applications of a numerical model of the effect of compliant walls on turbulent boundary layer flows. Since skin-friction drag accounts for about half the drag on long-haul aircraft, any reduction in this drag is of great importance in improving fuel economy and aircraft range as well as increasing payload efficiency and decreasing environmental pollution.

The current state of experimental and theoretical research on compliant walls and their effect on turbulent boundary layers has been reviewed by Fischer,Weinstein, Ash & Bushnell[1] and by Bushnell, Hefner & Ash[2]. In summary, the current state of both experiments and theory is inconclusive. Some experiments show a substantial effect of compliant walls on drag, while others do not. It is not clear whether conventional materials can serve as suitable compliant boundaries to give drag reduction, though there do seem to be some attractive possibilities. It is only clear that drag reduction by compliant walls is not as simple a phenomenon as may be suggested by cursory consideration of the hydrodynamical efficiency of dolphins.[3] Evidently, the dynamical characteristics of the wall are crucial in determining whether drag reduction or drag enhancement will result; the response of the wall must be matched in some dynamical sense still to be elucidated to the characteristics of the turbulent boundary layer over it. One of the principal purposes of the present work is to help in identifying the nature of the effect of the wall motions on the drag so that design of suitable walls can be expedited.

There have been several theoretical investigations of turbulent boundary layer flows over moving walls; a survey is given in Ref. 2. One of the most attractive ideas[2] for explaining the drag reduction by compliant walls is that the wall influences the turbulent burst phenomenon by providing a pressure field that tends to inhibit bursts when they normally occur. This idea leads to significant qualitative understanding of the effect of compliant walls. In this paper, we discuss a numerical model based on the above idea and report quantitative tests of it as a mechanism of compliant wall drag reduction.

In Sec. 2, we discuss the proposed mechanism of compliant wall drag reduction. In Sec. 3, we discuss the numerical model of the mean flow motion. Then, in Sec. 4, we discuss techniques for the investigation of the stability of the predicted mean flow profiles and for the prediction of burst frequency. In Sec. 5, we present results of the present model for turbulent boundary layer velocity profiles during the burst phenomenon and use these results to fix various parameters of the model by comparison with experimental results. Then, in Sec. 6, we present numerical results for the combined mean-flow and stability analysis of the turbulent boundary layer flow over a compliant wall. In this analysis, we use a crude burst predictor based on amplification factors. Finally, in Sec.7, we summarize the current state of research on the turbulence flow model investigated here.

2. A PROPOSED MECHANISM OF COMPLIANT WALL DRAG REDUCTION

In the last decade, there has accumulated a wealth of experimental evidence that the process of burst formation in turbulent boundary layer flows is not completely random, but rather can be correlated with a set of reasonably well-ordered

dynamical events. Thus, a plausible coherent sequence of events for formation and regeneration of bursts is as follows:[4-6]

1.'Old' bursts produce a large adverse pressure pulse that moves at a speed of roughly $0.8U_\infty$ and has an amplitude of roughly $3p'_{rms}$, where p'_{rms} is the rms wall pressure intensity.[4]

2. The adverse pressure gradient retards the flow near the wall and produces a low-speed streak.

3. A new burst is created when the low-speed streak creates highly inflectional velocity profiles in the wall region.

4. The favorable part of the large-scale pressure pulse due to previous bursts tends to assist the new burst in 'sweeping' out away from the wall. Most of the Reynolds stress and turbulence production occurs during the burst and sweep process, with relatively low turbulence activity between bursts.

5. The 'new' burst sets up conditions similar to those discussed in 1. above and the whole sequence of events is repeated.

Bushnell[2] has proposed that the above sequence of events can be used to formulate a quantitative flow model for the prediction of properties of turbulent boundary layers. The idea is to impose the experimentally measured pressure pulse due to 'old' bursts, to model the background turbulence between bursts using a crude turbulence model, and then to calculate the inflectional mean-velocity profiles produced by the pressure pulse using a two-dimensional Navier-Stokes equation computer code. Finally, the occurrence of new bursts can be investigated in this flow model by calculating the growth of Tollmien-Schlicitng waves and using an amplitude-growth criterion[7] to predict the onset of new bursts.

Bushnell's turbulent boundary layer model also suggests a mechanism for drag reduction by compliant walls. If the wavelength of the wall motions is small (at most the wavelength of the imposed pressure pulse), the wall motion can interrupt the feedback loop outlined above somewhere between steps 2. and 4. If the short wavelength wall motions can delay burst formation through the adverse part of the imposed pressure pulse, then the favorable part of the imposed pressure pulse may inhibit bursting. In this case, turbulence production and turbulent boundary-layer drag are reduced.

The present work is motivated by the above ideas of Bushnell.[8] The model seeks to determine quantitatively whether realistic wall motions and imposed pressure pulses interact in a time-dependent environment in such a way as to decrease burst frequency and wall drag. We investigate numerically the mean velocity profiles produced by the imposed

pressure pulse. We use two techniques to investigate the stability of the resulting profiles (see Sec. 4): 1) local quasi-steady analysis via the Orr-Sommerfeld equation and 2) study of the full linearized Navier-Stokes equations.

It seems that if the wavelength of the wall motions is large (of order the length of the imposed pressure pulse), there is no drag reduction. However, if the wavelength of the wall motions is small (at most several sublayer thicknesses), drag reduction may occur. Future work must test the flow model further, particularly with respect to parameter sensitivity and three-dimensional effects(neglected here).

3. NUMERICAL MODEL FOR THE MEAN FLOW

In this Section, we discuss the numerical techniques used to solve the equations of Bushnell's turbulent boundary layer model discussed in Sec. 2. We solve the two-dimensional Navier-Stokes equations with a background turbulence model, inflow-outflow boundary conditions, and an imposed large-scale pressure pulse at 'infinity'. The resulting mean-flow profiles show the effect of the pressure pulse in distorting (retarding) the mean profiles and in producing inflectional profiles.

The two-dimensional Navier-Stokes equations for incompressible flow are

$$\frac{\partial \vec{v}}{\partial t} + \vec{v}\cdot\vec{\nabla}\vec{v} = -\vec{\nabla}p + \vec{\nabla}\cdot\underset{\sim}{I} + \vec{f}, \tag{3.1}$$

$$\vec{\nabla}\cdot\vec{v} = 0, \tag{3.2}$$

where $\vec{v}(x,y,t)$ is the two-dimensional velocity field, $p(x,y,t)$ is the pressure, $\underset{\sim}{I}$ is the stress tensor, and $\vec{f}$ is an imposed external force. We solve (3.1) in a channel: $0 \leq x \leq L$ and $0 \leq y \leq H$. In a typical run, the values of L and H are L=600 and H = 200-400 in units non-dimensionalized by the length ν/U_τ where U_τ is the friction velocity and ν is the viscosity.

We approximate the stress tensor $\underset{\sim}{I}$ by retaining only its x-y component:

$$T_{xy} = -\overline{u'v'} + \nu\frac{\partial \bar{U}}{\partial y}, \tag{3.3}$$

where ν is the viscosity, $\bar{U}$ is the mean velocity, and u' and v' are the x and y components, respectively, of the velocity fluctuations. The Reynolds stress, $-\overline{u'v'}$, is then evaluated by Van Driest's empirical formula[9] so that

$$T_{xy} = \left[B(.4y)^2\left|\frac{\partial \bar{U}}{\partial y}\right|(1 - e^{-AyU_\tau/\nu})^2 + \nu\right]\frac{\partial \bar{U}}{\partial y} \tag{3.4}$$

where the constant A is chosen to be 0.04 in agreement with experimental measurements of turbulent boundary-layer mean-velocity profiles. The constant B is an <u>ad hoc</u> correction

to the usual Van Driest formula that accounts for the fact that the turbulence level between bursts is small; a typical value for the constant B in our calculations is B = 0.05.

Boundary conditions

The boundary conditions to be imposed on (3.1-2) require detailed consideration. Each of the four boundaries x = 0, L and y = 0, H poses its own special kind of boundary condition problem. A detailed analysis of these boundary conditions has been given in a preliminary version of this paper[10] and will not be repeated here. Our conclusions are as follows:

x = 0

Here the flow is assumed to enter the computational domain. Since the boundary is an inflow boundary, it is both physically and mathematically reasonable to assume that both components of the velocity field are known at x = 0. Thus, we assume that u(0,y,t) and v(0,y,t) are known for all y and t.

x = H

This boundary is an outflow boundary. Since the only non-vanishing component of the Van Driest Reynolds stress tensor (3.4) that we retain is T_{xy}, it follows that the Navier-Stokes equations (3.1-2) are parabolized in the x direction. Therefore, only the outflow component of the velocity, u(L,y,t), need be imposed.

However, imposition of boundary values on u(L,y,t) directly will give some difficulty because it will generate boundary layers near the outflow point x = L. Therefore, we impose the weaker boundary condition

$$u_{xx}(L,y,t) = 0. \tag{3.5}$$

Boundary conditions like (3.5) are known to have small upstream influence so they do not disturb the main region of computation which is away from the downstream boundary x = L.

y = 0

This is the location of the compliant wall. If the wall were rigid, we would impose the boundary conditions

$$u(x,0,t) = v(x,0,t) = 0. \tag{3.6}$$

There are two effects of a moving boundary at y = 0. First, the boundary location is shifted to y = η(x,t). Second, the wall motion as a function of t requires that the relative fluid velocity at the wall vanish, not the fluid velocity itself.

We impose boundary conditions at the moving wall by assuming linearized wall motion. This assumption is a great simplification and is justified because the wall motions of

interest are not large compared to the sublayer thickness. [A modified version of the mean flow code is now being developed to handle nonlinear wall boundary conditions using techniques for fast conformal transformation recently developed by the author.] It follows that the vertical wall motion is

$$v = \frac{D\eta}{Dt} = \frac{\partial \eta}{\partial t} + U\frac{\partial \eta}{\partial x} , \qquad (3.7)$$

where $U = Dx/Dt$ is the component of the wall motion in the direction tangent to the wall. Eq. (3.7) for the vertical wall motion is true nonlinearly. Linearization of the wall motion implies that all quantities in (3.7) may be evaluated at the undisturbed wall location $y = 0$.

In order to complete the specification of boundary conditions at $y = 0$, it is necessary to know $U(x,t)$, the tangential component of the wall motion. This quantity depends on the physical model of the compliant wall, and must be specified in addition to the vertical wall motion $\eta(x,t)$. Thus, if the wall motion is achieved by physically sliding the boundary in the x-direction, then U will be non-zero and significant. On the other hand, if the wavy wall motion is obtained by means of suitably phasing the vertical wall motion with no concomitant x-motion then U=0. In the present work, we do not determine the wall motions self-consistently, in the sense that we impose $\eta(x,t)$ and do not determine the effects of wall pressure fluctuations due to the turbulent boundary layer flow on the motion of the wall.

Most of the materials of current interest for compliant wall drag reduction applications are flexible materials that can 'stretch' in the y-direction but have little lateral freedom for movement in the x-direction. Therefore, because of the lack of specific information on this point, we have chosen the wall boundary condition to be $U = 0$. Admittedly, this is oversimplified, but a detailed model of the wall is necessary before this boundary condition can be improved.

It is not generally recognized that both $\eta(x,t)$ and $U(x,t)$ must be specified to determine the wall motion. However, consider the simple wall motion $y = \eta(t)$, independent of x. The motion of the wall in its plane $y = \eta(t)$ can be arbitrary and the proper tangential boundary conditions are $u(x,\eta,t) = U(x,t)$.

$y = H$

The boundary conditions imposed at the top of the boundary layer $y = H$ are the most unusual, and the most difficult to get right. In order to model the large- scale pressure pulse due to old bursts, we want to impose the value of the pressure $p(x,H,t)$ at the top of the layer. According to the mathematical analysis of flow boundary

conditions, the pressure $p(x,H,t)$, and the normal velocity, $v(x,H,t)$, may be specified if the boundary $y = H$ is an inflow boundary.

On physical grounds, we expect the magnitude of the normal velocity at the top of the layer to have profound effects on our ability to model the bursting process. In fact, we have found by numerical experimentation with the model (see Sec. 5) that there is strong sensitivity of the model to $v(x,H,t)$. We have assumed that

$$v(x,H,t) = - V \tag{3.8}$$

where V is a non-negative constant.

The imposition of the boundary conditions that $p(x,H,t)$ and $v(x,H,t)$ are specified has proved satisfactory in practice, except for some slight difficulty near the intersection of the outflow boundary $x = L$ and the lid $y = H$; this difficulty is evidently due to a very thin outflow boundary layer and was cured by introducing additional dissipation locally.

Another difficulty with the top boundary conditions was encountered first in running computations with compliant walls with wavelengths intermediate between the sublayer thickness and the pressure pulse wavelength. An instability developed that was evidently due to the interaction of wall pressure fluctiations produced by the moving boundary at $y = 0$ with the imposed pressure pulse at $y = H$. This problem was solved by implementing a variable grid map[11] in the y-direction to allow larger values of H with the same number of degrees of freedom in y. Thus, by moving the lid from $y_+ = 200$ to $y_+ = 400$, all trace of the previous instability was removed.

Numerical methods

Eqs. (3.1-2) with the boundary conditions discussed above have been solved using a mixed spectral-finite difference method. The vertical (y) direction is resolved using expansions in Chebyshev polynomials, while the x-direction is resolved using a second-order staggered-grid finite-difference scheme. Thus, in the unmapped case, we represent the velocity field by

$$v(j\Delta x,y,t) = \sum_{n=0}^{N} u_n(j\Delta x,t)T_n(2y/H-1) \tag{3.9}$$

where Δx is the grid separation in x and $T_n(y)$ is the Chebyshev polynomial of degree n. A detailed review of the spectral and finite-difference methods used here has been given elsewhere[12,13]

We use Adams-Bashforth time differencing of the nonlinear terms, together with a semi-implicit time differencing scheme for the diffusive terms of the Van Driest Reynolds stress and for the inflow terms at $y = 0$ and $y = H$. Because the

Chebyshev polynomial expansions have so much resolution at the top and bottom of the channel, they would give extremely stringent time-step restrictions on the Adams-Bashforth scheme. The semi-implicit method avoids these time-step restrictions.[13]

The code is also formulated in such a way that a moving coordinate system in x can be used as an option. This option is not used, however, in the calculations reported in Sects. 5-6.

4. NUMERICAL METHODS FOR STABILITY CALCULATIONS

Once the mean flow profiles are calculated by the computer code described in Sec. 3, we study the stability of the resulting flow in two ways. We solve the Orr-Sommerfeld equation for temporally growing disturbances in steady, plane-parallel two-dimensional incompressible flow, and we also solve the linearized Navier-Stokes equations. The first procedure involves three important approximations. First, we calculate only temporally growing disturbances, so we must convert between temporal growth and spatial growth using a complex group-velocity transformation.[15] In some early calculations, we were even cruder; instead of the group-velocity transformation in Runs 1-7 reported below, we transformed using the phase velocity instead of the group velocity. Later runs have all used the group velocity transformation.

Second, by assuming the mean-flow to be steady we neglect possibly very important phase-coherence effects which could strongly affect growth rates. In the Orr-Sommerfeld stability analyses, time variation of the mean flows is included only by using different mean profiles at different times in the evolution of a wave packet. The justification for the approximation of steady flow is weak a priori; a posteriori, the results of the linearized Navier-Stokes analysis seem to agree well with the local quasi-steady analysis. However, we have made a detailed comparison only in one case to date and this agreement may be fortuitous. The third approximation of the Orr-Sommerfeld stability analysis is the assumption that the flow is plane parallel in x; this defect is also remedied in the linearized Navier-Stokes calculations.

The Orr-Sommerfeld equation is solved by expanding the eigenfunction in a series of Chebyshev polynomials and then applying either global QR matrix eigenvalue routines or local Rayleigh quotient iteration routines.[16,17] These procedures are very efficient and accurate.

The results of the linear stability analysis are used to predict the occurrence of a burst as follows. First, we calculate the stability chracteristics of various profiles at a fixed location x and various values of the time t. These calculations proceed until a time t_0 is found at which the profile is unstable. From that time onwards, we calculate

the amplification ratio by the formula

$$\frac{A}{A_0} = \exp \int \mathrm{Im}\ \omega/c_g \ dx \ , \tag{4.1}$$

where c_g is the complex group velocity of a mode with wavenumber α and (complex) frequency ω. The profiles whose stability is calculated are related in space-time by following a wavepacket using the relation

$$\Delta x = \mathrm{Re}(c_g)\ \Delta t \ . \tag{4.2}$$

Next, the Michel-Smith criterion[7] for occurrence of a burst is applied; a burst is presumed to occur if

$$\frac{A}{A_0} \gtrsim e^M \tag{4.3}$$

where M is a number of order 10. This empirical correlation has worked well for a variety of trnasition flows, but it is very crude and the number M that best fits experimental data may vary over the range 5-15 or wider.[18]

We have also developed a computer code for solution of the linearized Navier-Stokes equations. Presently, the code solves the linearized Navier-Stokes equations using a Fourier series representation of the flow field in x and a Chebyshev series representation of the flow field in y, with rigid boundary conditions imposed at the wall y = 0 and the lid y = H and periodic boundary conditions imposed at x = 0 and x = L. Another linearized Navier-Stokes code is under development that allows imposition of inflow-outflow boundary conditions in x, as described in Sec. 3. The present linearized Navier-Stokes code is a linearized version of a full Navier-Stokes code used by the author and L. Kells to study transition and turbulence in planar shear flows.[19]

The linearized Navier-Stokes equation code is currently being used in the following way. The mean-flow code is used to generate a set of mean velocity profiles for all x at a time t when the pressure pulse has propagated through a distance L/2. The profiles used in the linearized Navier-Stokes code at later times is obtained by convecting this fixed set of velocity profiles through the grid at a speed equal to the phase speed of the pressure pulse. (We have also made a run using the speed U_∞ and the results changed by less than 15%.) The evolution of a mode of the linearized equations is then studied as a function of time for a fixed x. The motivation for this somewhat contrived procedure is simply to minimize the amount of data handling. A combined code that marries the mean flow code to the stability analyzer with no external data transfers is under development.

5. FLAT PLATE RESULTS

In this Section, we report a number of numerical experiments performed to tune the Bushnell turbulent boundary layer model for flow over a flat plate. First, in Fig. 1, we show the results of a numerical experiment performed to test the accuracy of the Van Driest Reynolds stress (3.4) with B = 1 (full strength) in reproducing a turbulent boundary layer mean-velocity profile. The calculation (as well as other calculations reported in this paper) used 33 Chebyshev polynomials to resolve the boundary layer (y) direction and 257 staggered grid points to resolve the downstream (x) direction. For the experiment (Run 1) plotted in Fig. 1, we impose the boundary conditions $p = v = 0$ at $y_+ = H = 200$. It is apparent from Fig. 1 that a turbulent boundary layer profile is well preserved in evolution from the upstream boundary at $x = 0$ to $x_+ = 200$ (and even beyond). This calculation shows that the upstream influence effect of the downstream boundary at $x_+ = 600$ is minimal -- in fact, no appreciable upstream influence of the boundary at $x_+ = 600$ is discernible beyond $x_+ = 500$.

The next set of runs were designed to adjust the background turbulence level constant B in (3.4) and the inflow velocity -V at $y_+ = H$, as well as to test the form of the required pressure pulse to achieve reasonable mean velocity profiles. The goal of these experiments is to match the development of turbulent boundary layer profiles between bursts as measured by Blackwelder & Kaplan.[20] Some of the experimental data for conditionally averaged velocity profiles before, during, and after the period of burst formation are shown in Fig. 2. Observe the very strong inflectional profiles at a time delay of -3.1 ms. This profile is strongly unstable and gives rise to a burst a short time later.

In Fig. 3, we plot the form of the pressure pulse used in our calculations of the Bushnell model. The magnitude of the pulse is chosen to be $3p'_{rms}$, in agreement with Burton's data[4] and to occur over a time period of 25 (in units of ν/U_τ^2). The triangular form of this pulse is an arbitrary choice, but it is not inconsistent with available experimental data. In some of the numerical experiments reported below, the amplitude of the pressure pulse is $2.5p'_{rms}$ and in some others the length of the pulse is decreased to 20.

In Fig. 4, we plot the results of a numerical calculation using the code described in Sec.3 with B = 0.05 and v = 0 at $y_+ = H$, together with the imposed pressure pulse. The agreement with the Blackwelder profiles shown in Fig. 2 is not very good.

In Fig. 5, we plot the results of a similar experiment in which the vertical dimension is truncated to H = 100 with the pressure pulse applied at $y_+ = 100$. The agreement with the experimental data is even worse. We conclude from this

AD-A100 632 PURDUE RESEARCH FOUNDATION LAFAYETTE IND F/G 20/4
WORKSHOP ON COHERENT STRUCTURE OF TURBULENT BOUNDARY LAYERS.(U)
NOV 78 D E ABBOTT, C R SMITH AFOSR-76-3015
UNCLASSIFIED AFOSR-TR-78-1533 NL

4 OF 6
AD
A100632

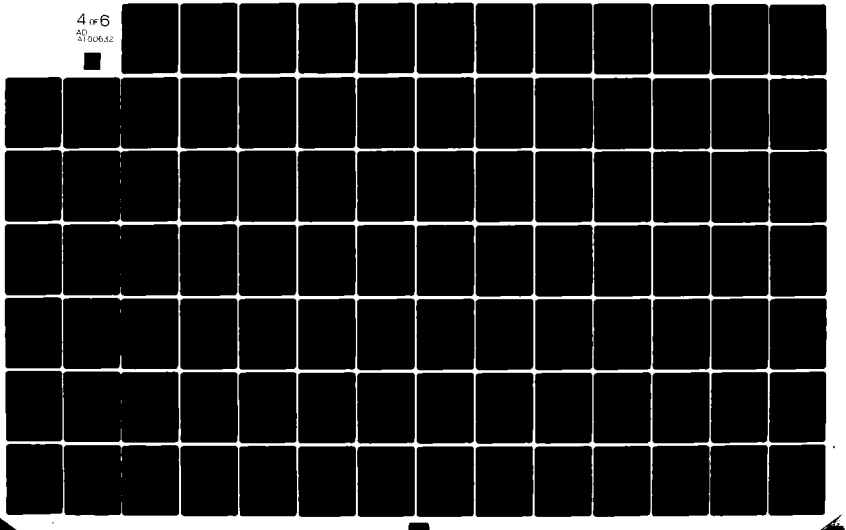

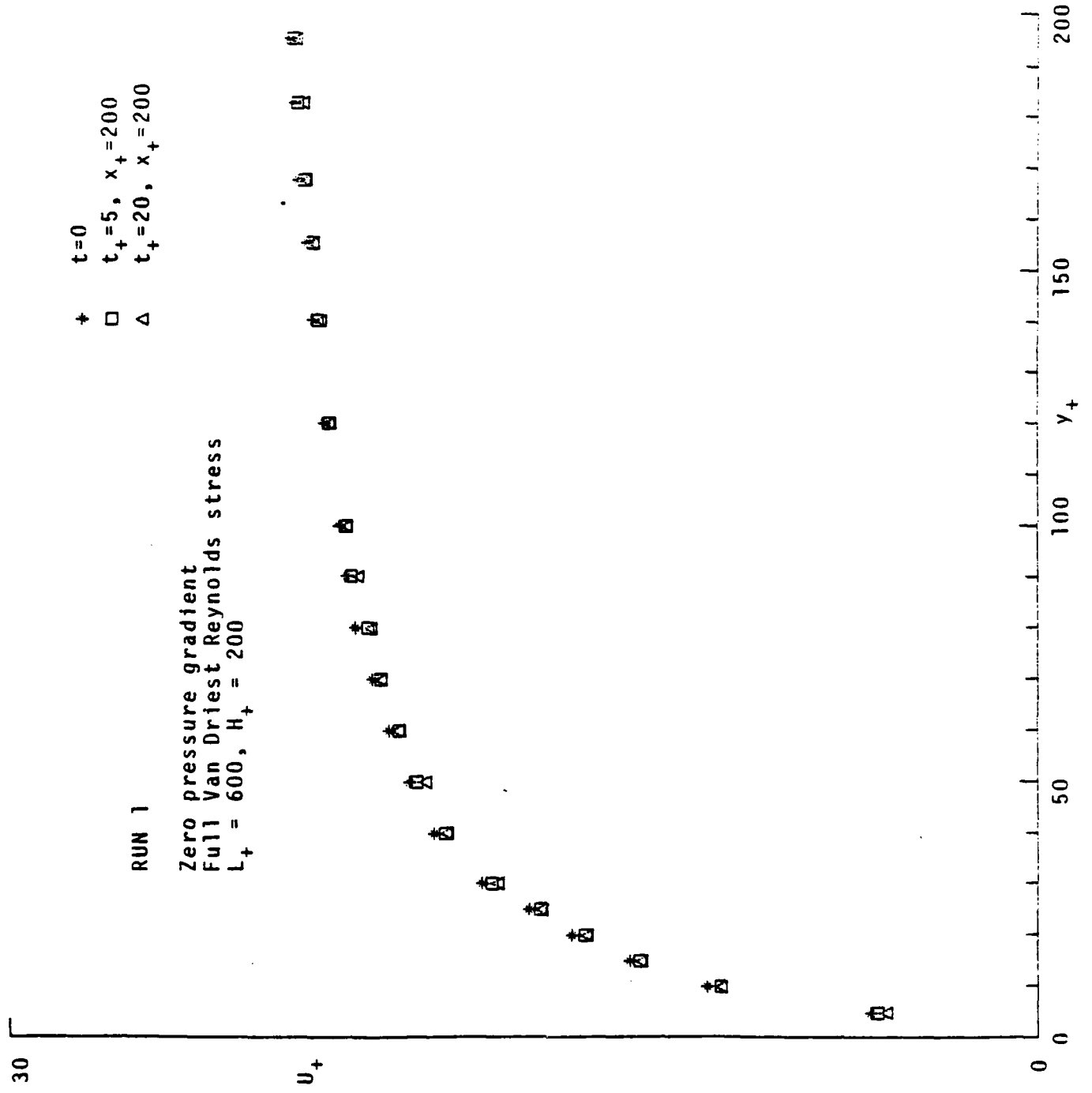

Figure 1. A plot of the calculated mean-velocity profiles for Run 1.

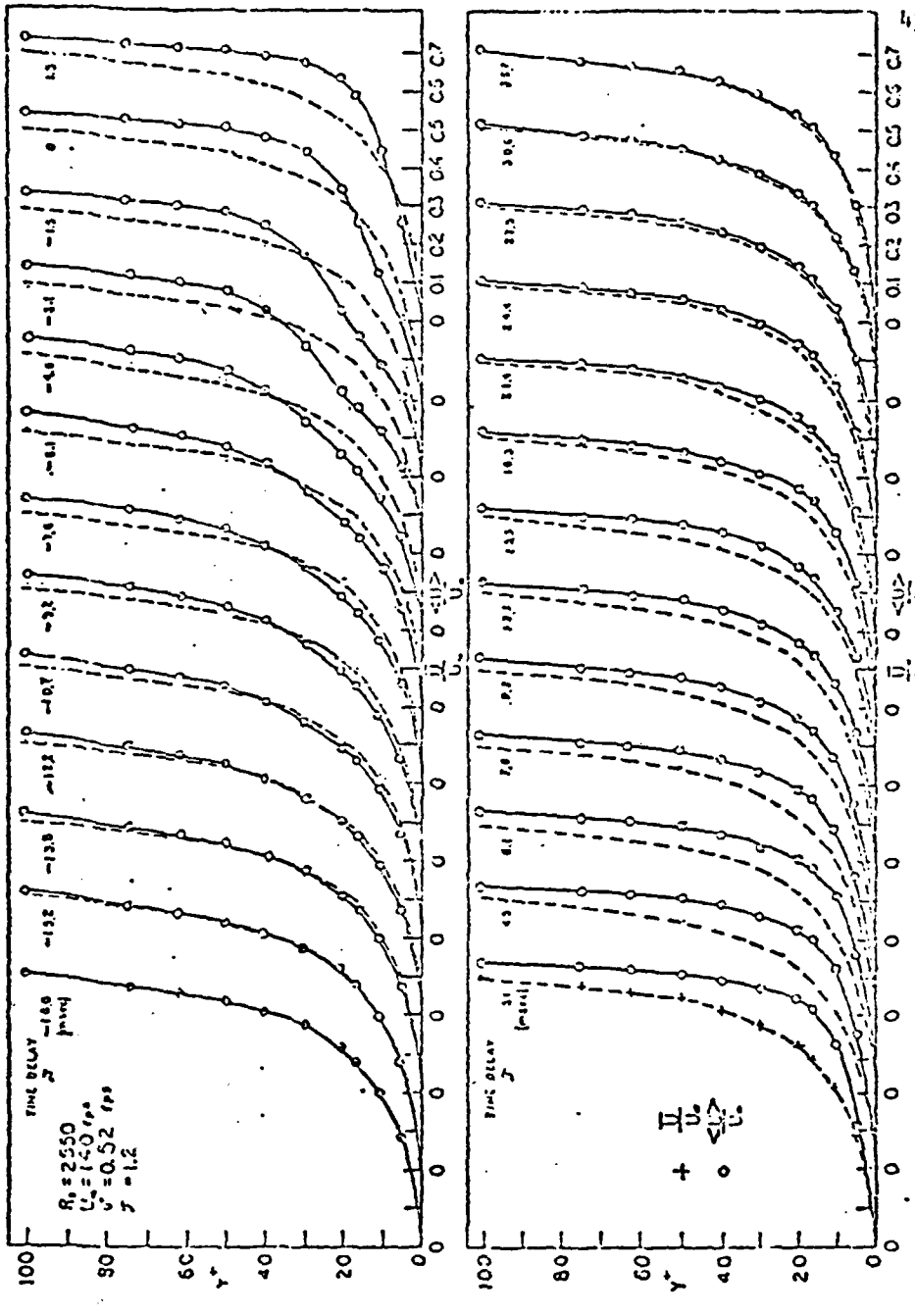

Fig. 2 - Conditionally averaged and mean velocity profiles with positive and negative time delay from the point of detection.(From Ref. 20).

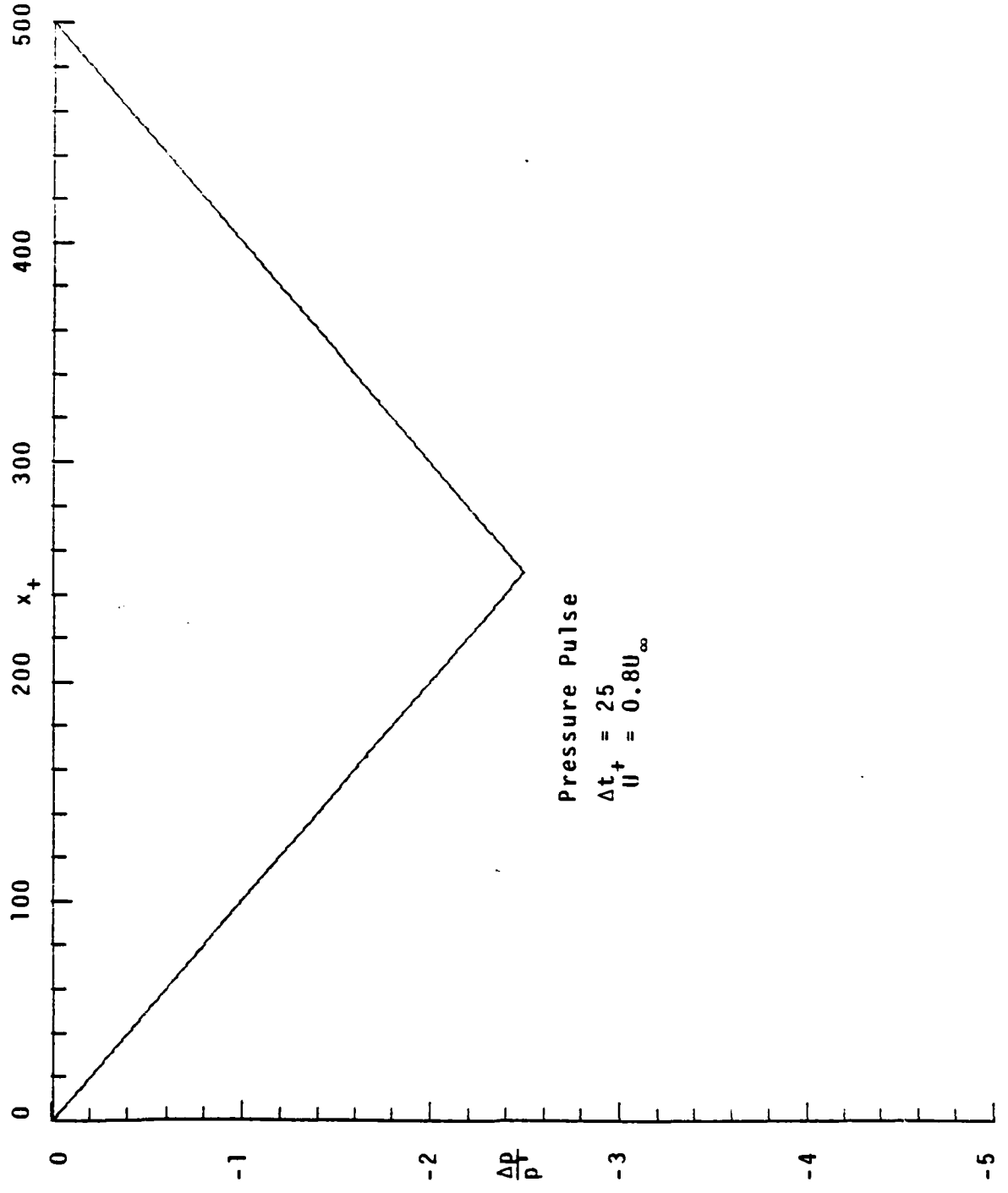

Figure 3. A plot of the imposed pressure pulse at $y_+ = H$. The form of this pulse is in good agreement with that measured by Burton.[4]

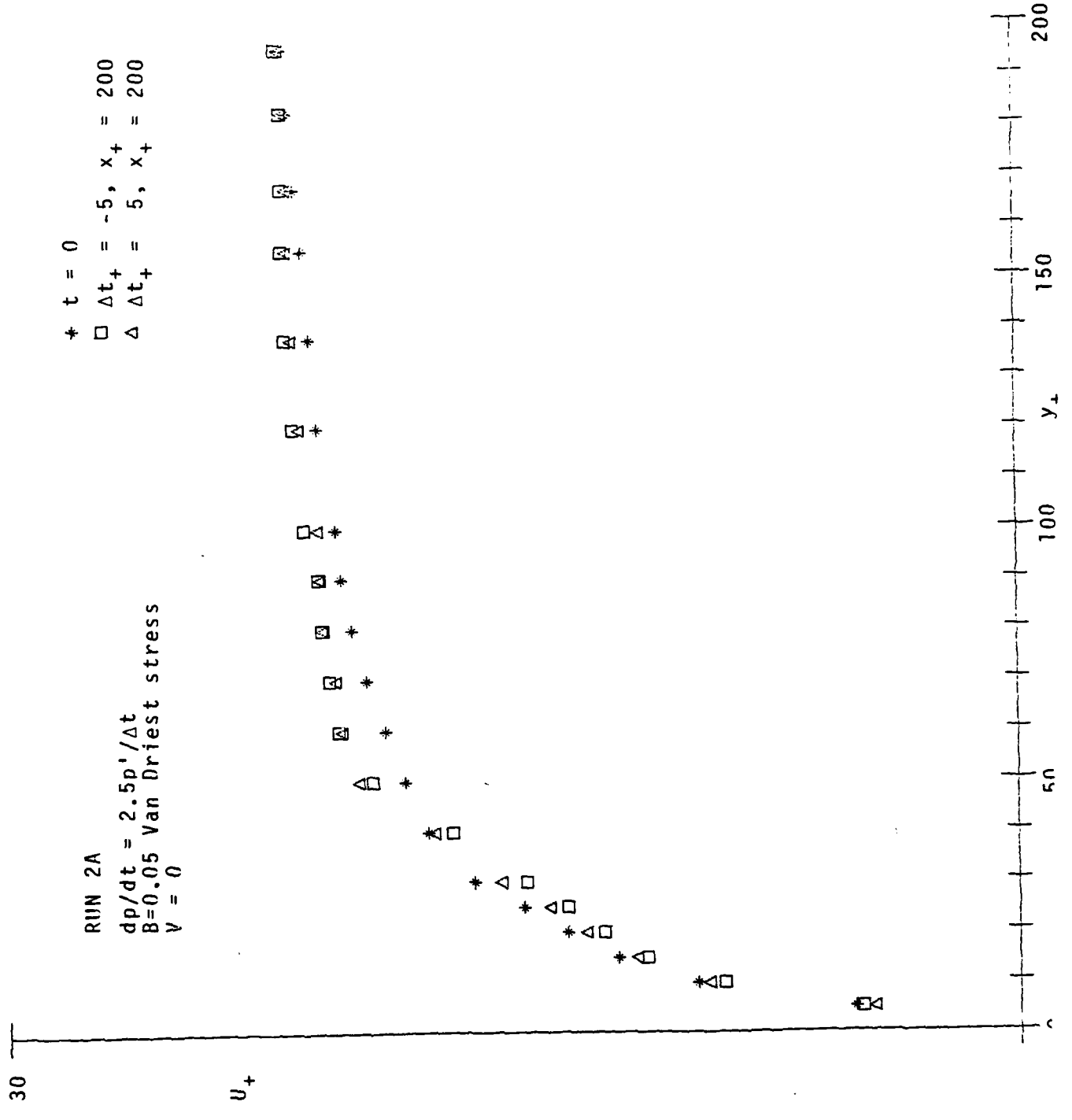

Figure 4. A plot of the calculated velocity profiles for Bushnell's model of the turbulent boundary layer. Time differences are measured from passage of the peak of the adverse pressure gradient pulse. The boundary conditions at the top of the layer are $v = 0$.

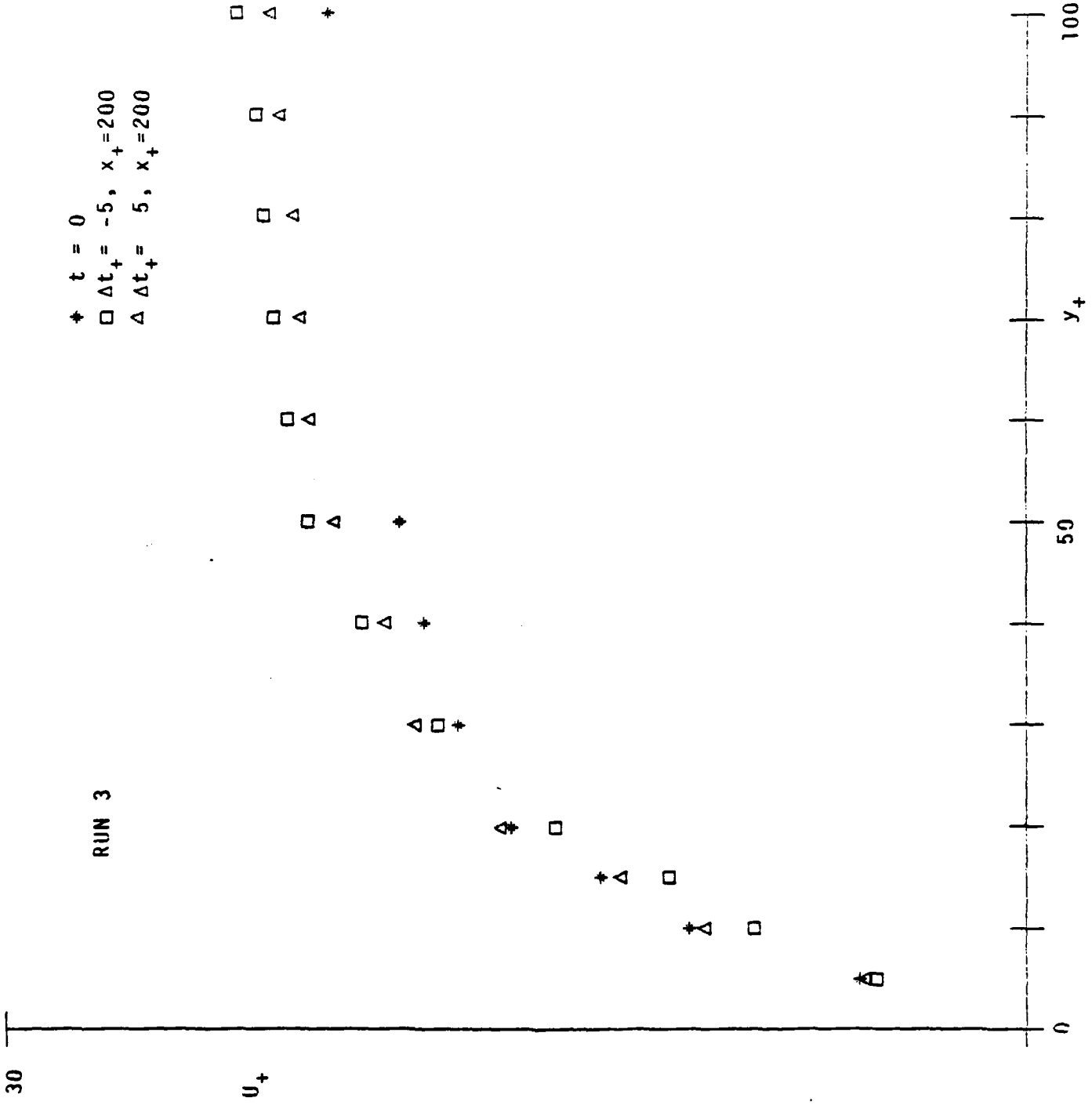

Figure 5. Same as Figure 4, except that the pressure pulse is applied at $y_+ = 100$ instead of $y_+ = 200$.

comparison that the pressure pulse must be imposed in the region y_+ 200 and certainly not so close to the wall as $y_+ = 100$.

In Fig. 6, we plot the results of a calculation similar to that shown in Fig. 4, except that the imposed inflow velocity at the top of the layer is $v_+ = -0.5$ ($V = 0.5$ U). In this case, the retardation due to the imposed pressure pulse is much larger than that shown in Fig. 4 and is in qualitative agreement with the experimental results of Ref. 20. Then, in Fig. 7, we plot the results of a calculation similar to the calculations plotted in Figs. 4 and 6, except that the inflow velocity at the top of the layer is $v_+ = -2$. In this case, the inflectional profile is very strong and even our two-dimensional mean-flow code with background turbulence model went unstable near the peak of the adverse pressure gradient pulse. This difficulty with Run 5 (shown in Fig. 7) is, we believe, unrelated to the calculational difficulties with the unmapped grid for intermediate wavelength compliant wall problems discussed in Sec. 3. We believe that the breakdown of Run 5 is due to the small value of $B = 0.05$, so that the background turbulence cannot stabilize (by diffusion) the unstable profile produced by the pressure pulse.

The conclusion to be drawn from Figs. 4-7 is that the strength of the inflectional profiles produced by the passage of the pressure pulse is a very strong function of the inflow velocity V at the top of the boundary layer. It seems that $V_+ \simeq 0.5$ gives results in reasonable agreement with the experimental data of Ref. 20.

6. COMPLIANT WALL RESULTS

We have performed about a dozen runs to study the effect of a compliant wall with imposed wall motion on the structure of a turbulent boundary layer. In all the experiments performed to date, we have assumed that the component of the wall motion in the direction of the mean flow vanishes: $U(x,t) = 0$. As discussed in Sec. 3, the justification for this approximation is that typical compliant boundaries have supports that stiffen the medium to lateral deformation. Our computer code has now run successfully in cases involving a wide variety of wavelengths of the wall motion. For very short and very long wavelength motions, stable results have been achieved with $H_+ = 200$, while we have had to use our variable grid map with $H_+ = 400$ to handle intermediate wavelength cases (see Sec. 3). For example, in Fig. 8, we plot the results of a numerical calculation for a flow over a compliant boundary whose surface motion was a short wave,

$$\eta(x,t)_+ = 5 \sin(2x_+ - 30t_+). \qquad (6.1)$$

This wave is as short as can be resolved on our grid with 257 grid points in x. (In fact, it is surely not resolved accurately on this grid, so the results for Run 7 are qualitatively correct at best.)

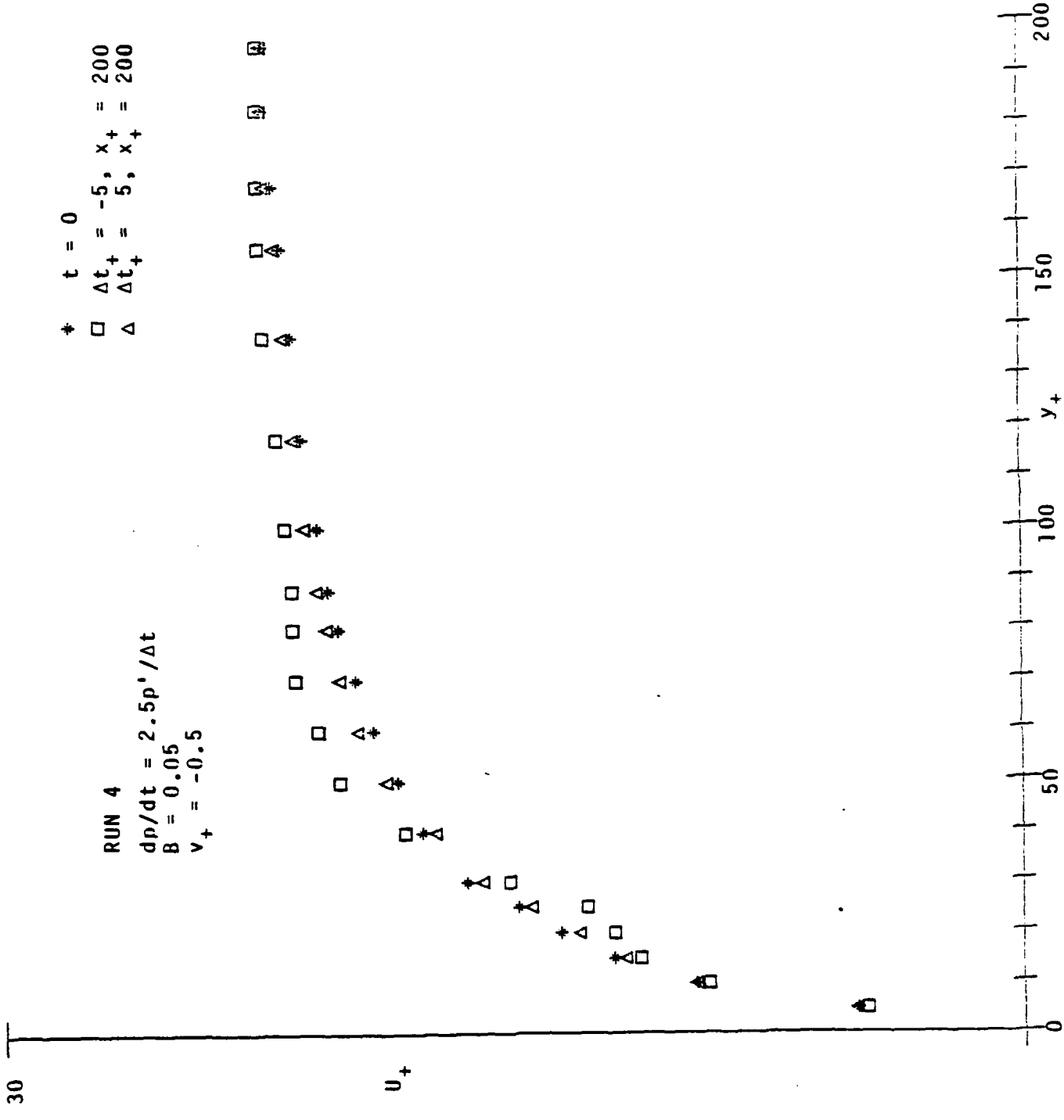

Figure 6. Same as Figure 4, except that an inflow velocity -0.5_+ is imposed at the top of the calculational domain $y_+ = 200$.

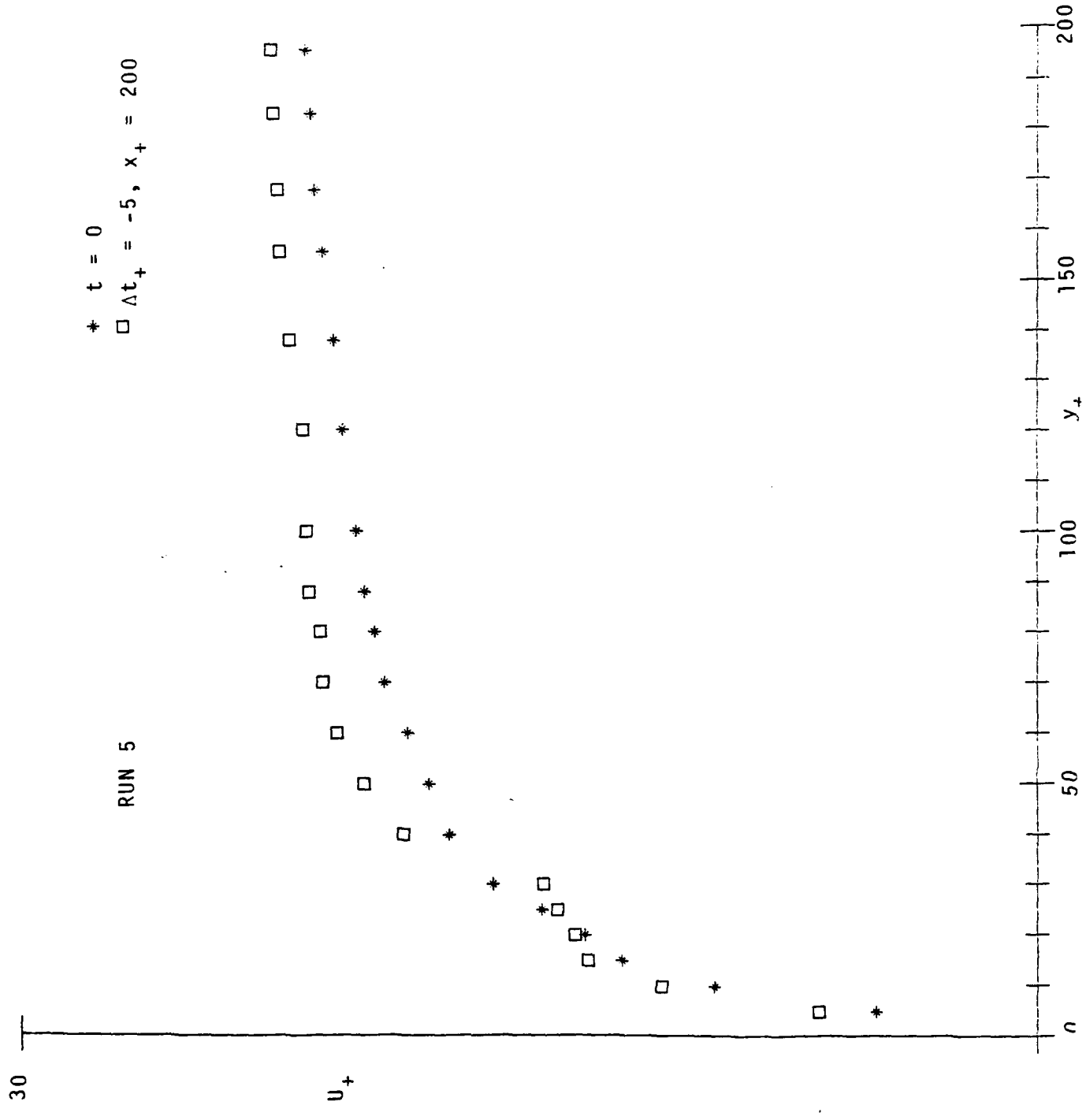

Figure 7. Same as Figure 4, except that an inflow velocity $V_+ = 2$ is imposed at the top of the calculational domain $y_+ = 200$.

The characteristics of our compliant wall test runs reported here are listed in Table 1. For all runs but Run 7, $H_+ = 400$ and a variable grid map is used in y. In this Table, λ_+ is the wavelength of the imposed sinusoidal wall motion, c is its phase speed, and A is its amplitude, all in sublayer(+) units.

TABLE 1. COMPLIANT WALL TEST MATRIX

Run	λ_+	c_+	A_+
7	3	15	5
10	30	15	5
11	20	20	5
12	60	15	5
13	30	10	5
14	20	10	5
15	40	10	5
16	40	10	10
17	40	20	5
18	40	20	15
19	80	15	5

We have performed stability calculations for these flows over compliant moving walls. The amplification ratio A/A_0 is calculated as described in Sec. 4 for a wave that is initially most rapidly growing and the Michel-Smith correlation is used to predict the occurence of a burst. We assume that the drag on the turbulent boundary layer is proportional to the burst frequency, so that if the burst frequency is decreased then the drag is decreased proportionately.

In Fig. 9, we plot the amplification ratio vs time for a wavepacket originating at $x_+ = 200$ for Runs 4 (Fig. 6) and 7 (Fig. 8), in order to demonstrate the effect of a compliant wall. In Fig. 9, we plot the data in two ways: the squares and triangles indicate the amplification factors obtained by local stability analysis following the most unstable wave using a phase speed transformation; the crosses and circles indicate the amplification factors obtained at a fixed location $x_+ = 200$, not following the wave.

The effect of the wall motion in decreasing the growth rate of disturbances in the boundary layer is apparent from the results plotted in Fig. 9 both following the wave and fixed in space. Also, the growth rates obtained following the wave are larger than those obtained fixed in space, apparently because when the wave packet moves it stays in a region of large amplification rate for a longer time and does not quickly encounter the favorable gradient part of the pressure pulse.

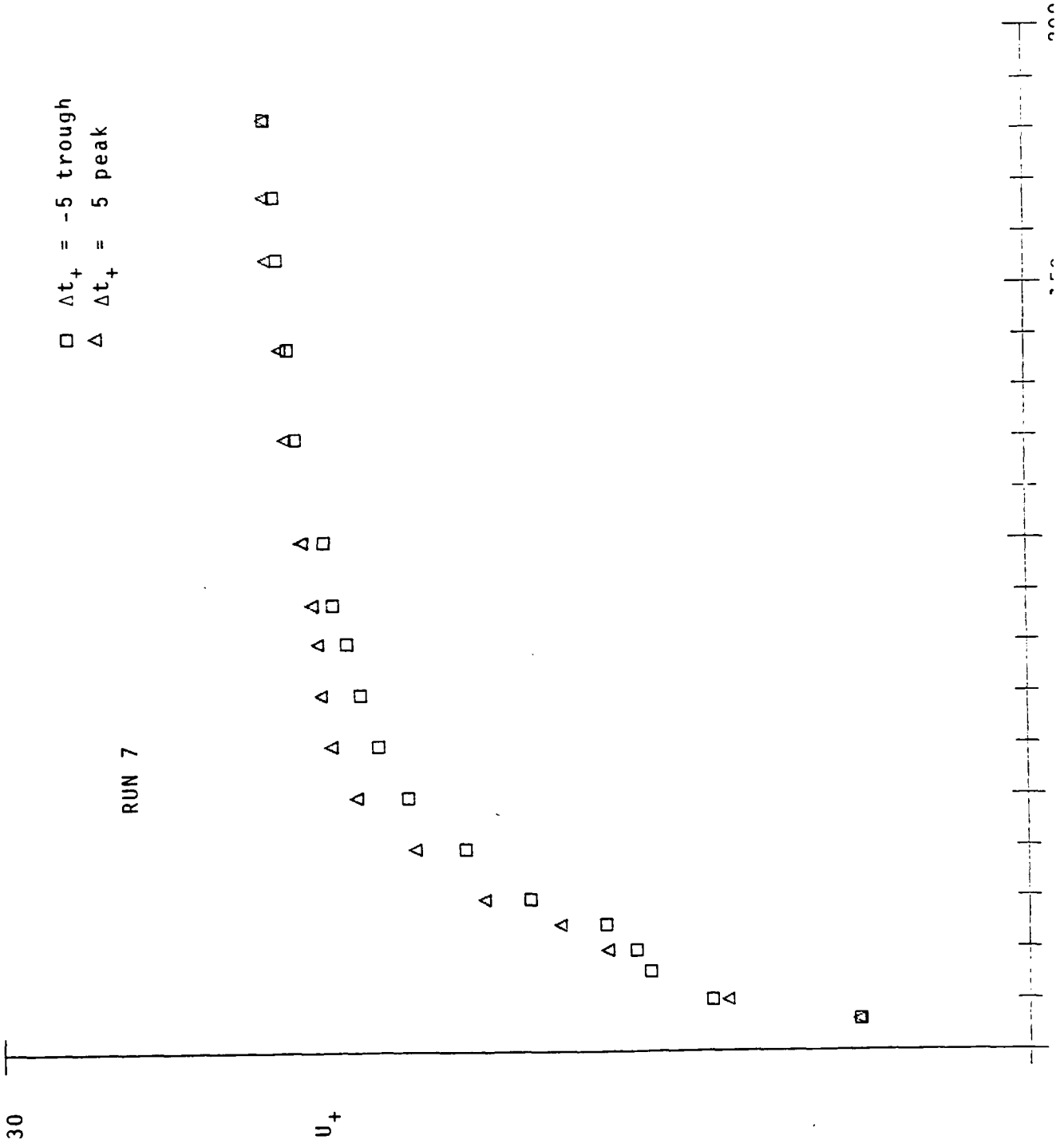

Figure 8. A plot of the calculated velocity profiles for Bushnell's model of the turbulent boundary layer over a moving wall. The imposed wall motion is a travelling sinusoid of amplitude $\eta_+ = 5$ and wavelength $\lambda_+ = \pi$ (short compared with the sublayer thickness).

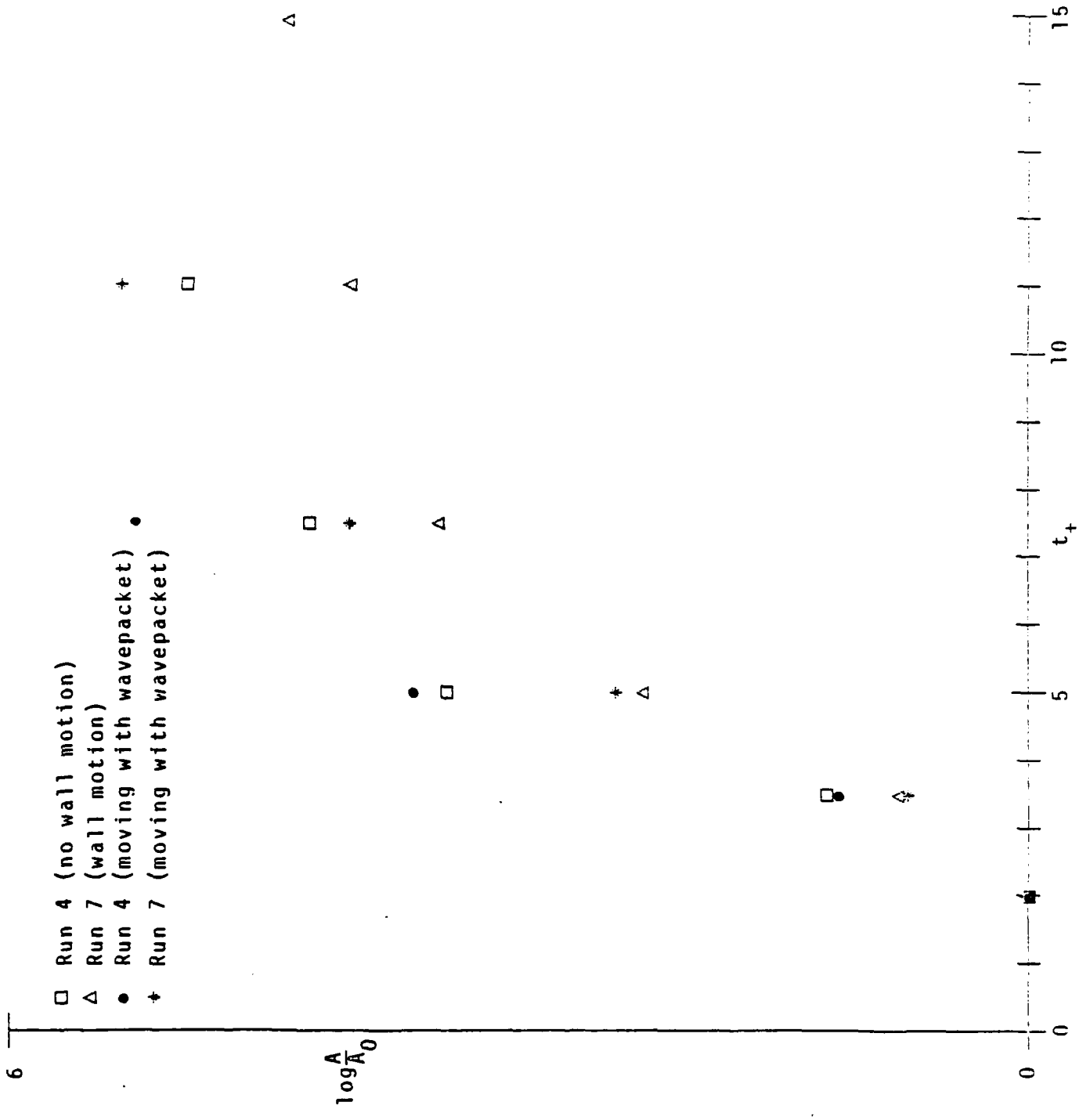

Figure 9. A plot of the amplification ratios of the most unstable disturbances of the boundary layer profiles of Runs 4 and 7, which are identical except that Run 7 has a short wavelength imposed wall motion. Results are presented for disturbances following the wavepacket and for disturbances fixed at $x_+ = 200$.

The results of our quasi-steady stability analyses of the runs tabulated in Table 1 are plotted in Fig. 10. The best result for a run in which the spatial resolution was adequate to give good results is for Run 14. It is disturbing that our results are so sensitive to the parameters of the wall motion. Perhaps the safest conclusion that can be made from these results is that drag reductions in excess of 25% or so may be available from compliant walls, but that the walls will have to be very carefully tuned to achieve such results.

In Fig. 11, we compare the results of a quasi-steady stability analysis of Run 13 with analysis based on the linearized Navier-Stokes equations. Apparently, while the detailed growth rates of the quasi-steady analysis may be significantly in error, the cumulative effect of the linearized stability analysis is quite well predicted by the quasi-steady analysis. Until further verification can be made of this result by performing more runs, we must regard this agreement as fortuitous. However, if it should survive further test, major simplification of future calculations can result.

Similar calculations with even longer wavelengths have been performed. If the wavelength is of order the length of the pressure pulse, we have found drag enhancement of the order of 10-25%.

7. SUMMARY AND CONCLUSIONS

We have developed a set of computer codes to test Bushnell's boundary layer model. One code computes the evolution of mean velocity profiles during the period between bursts as forced by an imposed large-scale pressure pulse due to earlier bursts. Another code computes stability characteristics of these mean flows using the Orr-Sommerfeld stability equation. Still another stability code solves the linearized Navier-Stokes equations. Typical calculations involved the use of 33 Chebyshev polynomials to resolve the y direction and 257 grid points (or Fourier modes) to resolve the x-direction.

By carefully choosing the shape of the imposed pressure pulse, the level of the background turbulence, the height of the computational box, and, especially, the inflow velocity at the top of the boundary layer, we are able to achieve reasonable agreement with experimental measurements of mean velocity profiles during the burst process on a flat plate.

Stability calculations of the resulting mean velocity profiles show that compliant moving walls with relatively short wavelengths may have an appreciable effect in stabilizing the boundary layer to further bursts. On the other hand, long wavelength wall motions do not seem to limit the burst process, and therefore do not appear good candidates for drag reduction.

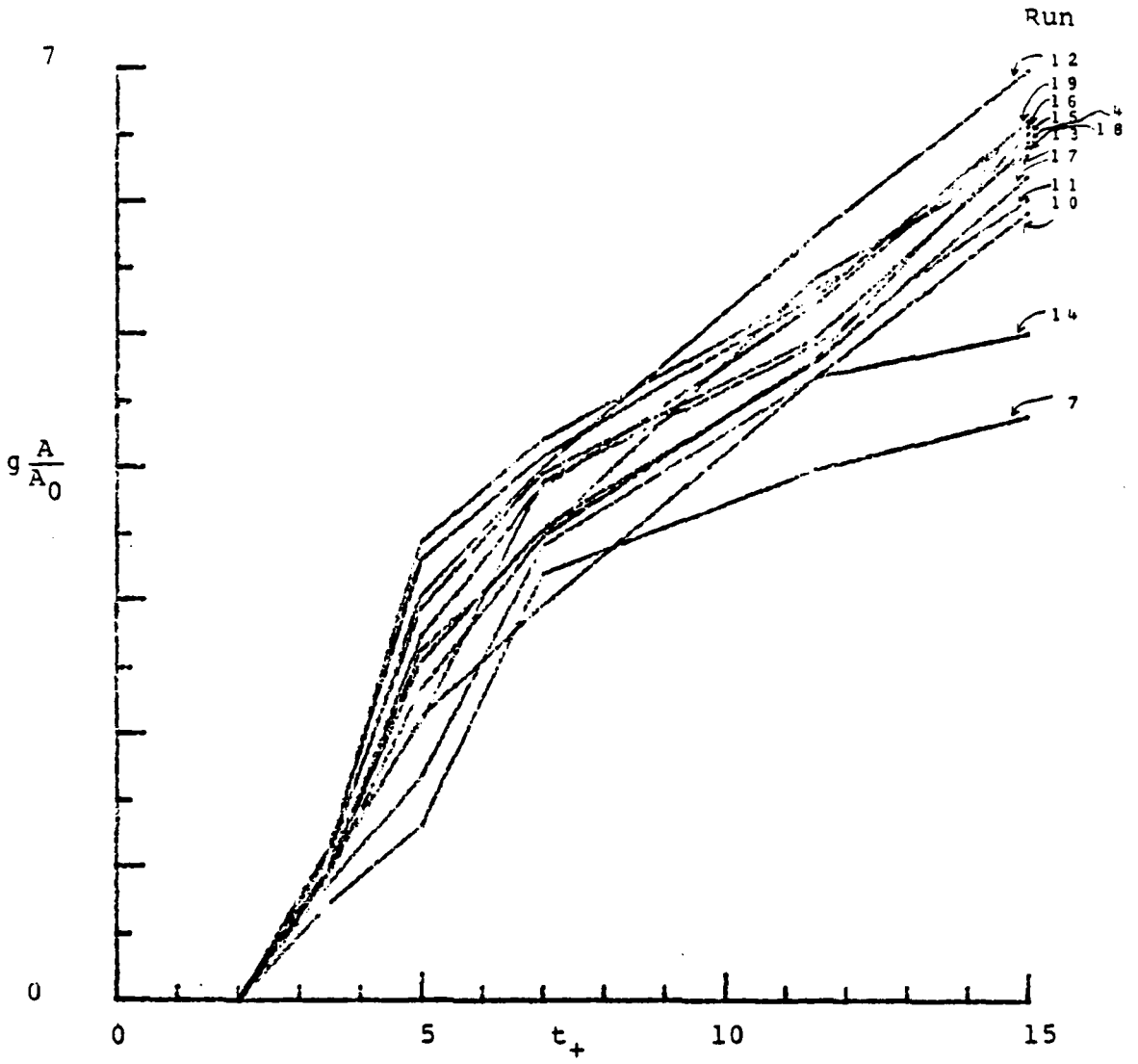

Figure 10. A plot of the results of quasi-steady stability analysis for the runs listed in Table 1. Note that Run 4 is for no wall motion. According to the Michel-Smith criterion for production of a burst, the burst frequency should be inversely proportional to the time required to achieve an amplification factor e^M with M of order 10. For all runs, the amplification factor is measured at $x_+=200$ in a fixed coordinate frame.

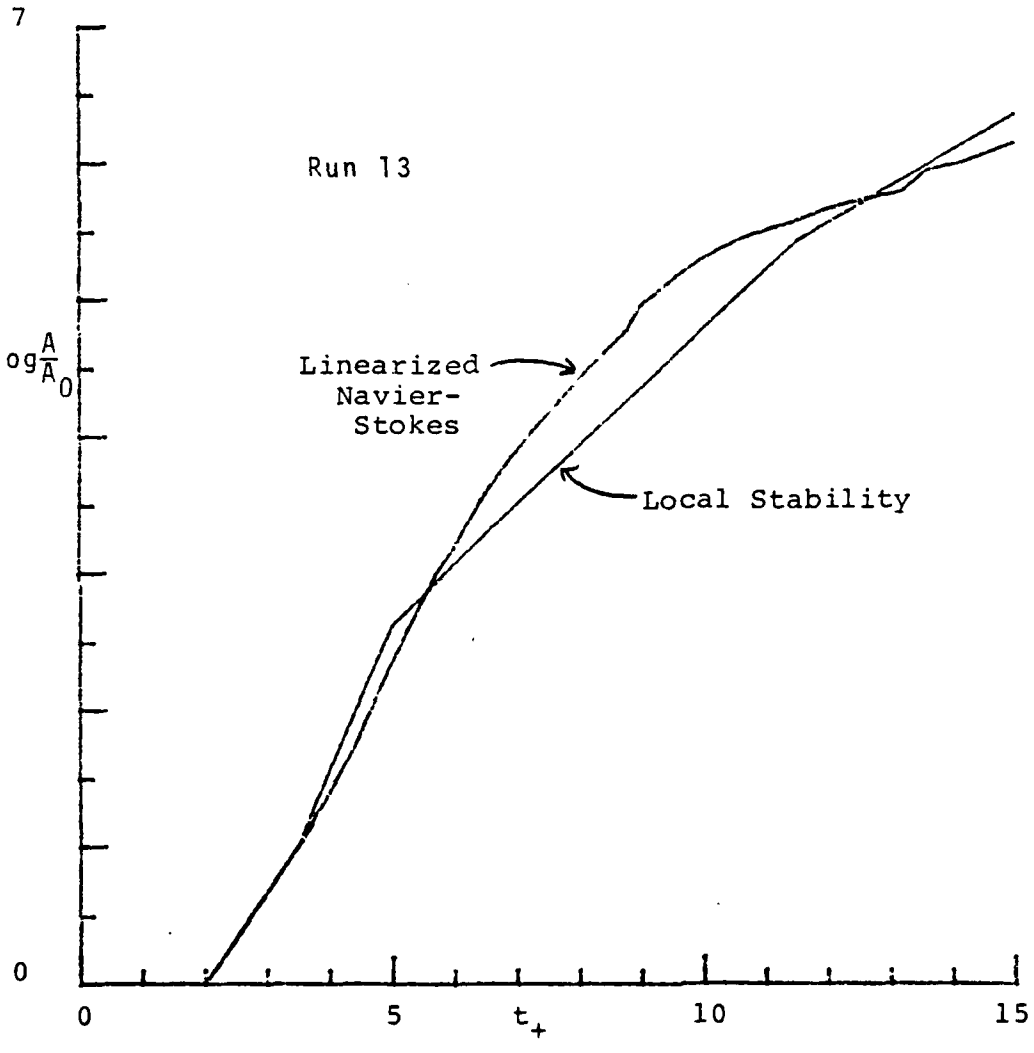

Figure 11. A comparison between the results of quasi-steady stability analysis using the Orr-Sommerfeld stability equation and the results of solution of the linearized Navier-Stokes equations (with periodic boundary conditions in x) for Run 13. The results are computed at $x_+ = 200$ in a coordinate frame fixed in space.

This work was done at Cambridge Hydrodynamics, Inc., Cambridge, MA with support by NASA Langley Research Center under Contracts NAS1-14275 and NAS1-14906. A preliminary version of this paper is given in NASA CR-2311 (Ref. 10 below).

REFERENCES

1. M.C. Fischer, L.M. Weinstein, R.L. Ash and D.M. Bushnell, "Compliant Wall-Turbulent Skin-Friction Reduction Research." AIAA Paper No. 75-833 (1975).

2. D.M. Bushnell, J.N. Hefner and R.L. Ash, "Compliant Wall Drag Reduction for Turbulent Boundary Layers." Phys. Fluids 20, S31 (1977).

3. M.O. Kramer, " Hydrodynamics of the Dolphin." Adv. in Hydroscience 2, 111(1965).

4. T.E. Burton, " The Connection Between Intermittent Turbulent Activity Near the Wall of a Turbulent Boundary Layer with Pressure Fluctuations at the Wall." Sc.D. Thesis, M.I.T. (Cambridge, MA, 1974).

5. J. Laufer, "New Trends in Experimental Turbulence Research." Ann. Rev. Fluid Mech. 7, 307 (1975).

6. W.W. Willmarth, "Structure of Turbulence in Boundary Layers." Adv. in Appl. Mech. 15 (1975).

7. N.A. Jaffe, T.T. Okamura and A.M.O. Smith, "Determination of Spatial Amplification Factors and Their Application to Predicting Transition." AIAA Journal 8, 301 (1970).

8. S.A. Orszag, D.M. Bushnell and J.N. Hefner, "Model of Drag Reduction by Compliant Walls." Phys. Fluids 20, S289(1977).

9. E.R. Van Driest,"On Turbulent Flow Near a Wall." J. Aero. Sci. 23, 1007 (1956).

10. S.A. Orszag,"Prediction of Compliant Wall Drag Reduction-Part I." NASA CR-2911 (1977).

11. C.E. Grosch and S.A. Orszag, "Numerical Solution of Problems in Unbounded Regions: Coordinate Transforms." J. Comp. Phys. 25, 273 (1977).

12. S.A. Orszag and M. Israeli, "Numerical Simulation of Viscous Incompressible Flows." Ann. Rev. Fluid Mech. 6, 281 (1974).

13. D. Gottlieb and S.A. Orszag, Numerical Analysis of Spectral Methods: Theory and Applications. NSF-CBMS Monograph No. 26, SIAM (Phila., PA, 1977).

14. S.A. Orszag, "Fourier Series on Spheres." Mon. Weather Rev. 102, 56 (1974).

15. A. Michalke, "On Spatially Growing Disturbances in an Inviscid Layer." J. Fluid Mech. 23, 521 (1965).

16. S.A. Orszag, "Accurate Solution of the Orr-Sommerfeld Stability Equation." J. Fluid Mech. 50, 689 (1971).

17. D.J. Benney and S.A. Orszag, "Stability Analysis for Laminar Flow Control-Part I." NASA CR-2910 (1977).

18. A. Srokowski and S.A. Orszag, "Mass Flow Requirements for LFC Wing Design." AIAA Paper No. 77-1222 (1977).

19. S.A. Orszag and L. Kells, "Transition to Turbulence in Planar Shear Flows." To be published.

20. R.F. Blackwelder and R.E. Kaplan,"On the Wall Structure of the Turbulent Boundary Layer." J. Fluid Mech. 76, 89(1976).

DISCUSSION

Thomas:

On the question of the pressure gradient and turbulent bursting, I undertook some pressure measurements myself with a view toward clarifying this question. I found that the pressure gradients were not of the correct sign or character to play the role that you've suggested.

Orszag:

I haven't seen your results, however, if the pressure gradients have the opposite sign this mechanism can't work.

Thomas:

I agree.

Landahl:

Did you also do your calculation without a pressure gradient, but with an in-flow condition, to determine whether that alone could produce the inflection?

Orszag:

In all those calculations, the pressure pulse was imposed and the shape of the pressure pulse was determined beforehand to match what we considered to be the correct experimental results.

Quinn:

Could you extend your comment on compliant walls? I believe your conclusion was that you needed to build a wall capable of maintaining very small wave-length oscillations in order to achieve the control you wanted. If that's so, I wonder if you think you could control the transition by using acoustic waves?

Orszag:

The conclusions from the model, if the model is correct, indicate that fairly short wave-length wall motions are necessary to effect the bursting process. In the case of acoustic waves, the only data I'm familiar with are those of Paul Shapiro on the transition process. I'm not sure of the effects of acoustics on the turbulent boundary layer. According to the results I heard yesterday from Wygnanski, if linear perturbations are imposed on the turbulent boundary layer, the perturbations would die out fairly fast and not affect things like spots.

Landahl:

No, perturbations don't die out.

Orszag:

Wygnanski told me earlier that they do die out. Did I quote you wrong on that?

Wygnanski:

It depends on the amplitude of the perturbation. Essentially, what I was quoting were the experiments of Gaster and Grant where perturbations were introduced at a point, and along the center they were found to die out providing that they were not of sufficient amplitude initially.

Orszag:

However, in the case of transition the experimental results do indicate that there is a substantial effect, but one that can be explained on the basis of essentially linear theory.

Kline:

There is a big difference between the transition case and the turbulent boundary layer case, with respect to disturbances. As we know, there is some kind of inherent global instability in the transition process, in the sense that you put a small disturbance in and it grows and you get a wholly different flow condition---- turbulence. In the turbulent case, there are some experiments by Lissin and I, in which very large disturbances were impressed on a turbulent flow with the result being a relatively small response. There have been a number of attempts experimentally to modulate the turbulent flow by inputting disturbances, but it's difficult. In some cases, we've put 40 per cent disturbances on the outer flow and not much happens. In the case of transition, any kind of disturbance you put in will ultimately take over and grow. Thus, there certainly is a very clear difference, and one has to be careful of the analogies one draws.

Kline: (Cont'd)

Another comment-there have to be local pressure gradients somewhere down near the wall, after all, the pressure does go up and down.

Thomas:

Well, that's because the pressure pulse has the pressure going up and down.

Kline:

Yes, so if it goes down it's got to go back up again.

Thomas:

The question is which one occurred first.

Kline:

Yes, there's the question of phase and all that. If you direct a jet at the wall, as an example of the sweeps one sees in Bob Brodkey's movies and in George Offen's movies, this creates a quasi-stagnation point. Somewhere underneath that there has to be a local region of high pressure; I just don't see how that's avoidable. So there has to be a rising pressure in there somewhere.

Reynolds:

We've seen, I think, in Rubesin's talk and in Orszag's talk some examples of what computer simulation can do to help the understanding of the physics. Let me just mention three points, two that we've seen and one that we haven't. First, Orszag was able to suppress three-dimensional disturbances in one of his computations. Thus, he was able to look at what happens if you only have two-dimensional mechanisms active, and he was able to show that the wrong things happen unless you have three-dimensions. It's very hard in the experiment to make it two-dimensional; it's easy in the computation to make it two-dimensional. He also was able to suppress the small-scales, in that he's not using a small-scale model. When his transition calculation breaks down one interpretation might be that this is the point where you must start to put in some small scales. We have found much the same behavior in transition simulations. The third thing we have been able to do is suppress the large-scales. And we find, for example, in the two-stream mixing layer and the channel flow, that if we don't start the calculation out with the large-scales present in the initial field, but we do have small-scales present, everything just dies out. The large scales are essential to the maintenance of the turbulence flow in both of those cases. These are examples of the way that computer simulations are now beginning to provide insight into physics.

Bushnell: (To Reynolds and Orszag)

In your large eddy simulations, did you ever do any conditional sampling of your numerical information? Did, you in fact, look for bursting rates and if so, what was the bursting frequency from your calculations?

Reynolds:

Do you want to answer that first Steve--on the basis of your transition work?

Orszag:

I can make a comment on the differences between large eddy calculations and direct calculations. I suspect that the effective Reynolds number in your large eddy simulation may be as low--if not lower--than the effective Reynolds number in the direct calculations. When I claimed that there was no accuracy after breakdown, I was claiming detailed accuracy. I claimed that as I doubled the number of modes in each space direction, the details of the flow changed. The statistics of the flow do not change. There is statistical insensitivity...but there is detailed sensitivity. Now, you cannot claim by the very nature of the equations you are solving that the large eddy simulations are ever an accurate flow simulation. You may have a statistically accurate flow simulation, but it cannot be in detail accurate, because you're putting in a statistical model. Another point. We've learned that in doing transition calculations, that it is harder, I think, to do a transition calculation than to do a turbulence calculation. The reason is that in turbulence things happen pretty fast. It is my experience that when I do turbulence calculations, I can get interesting results after 20 time steps, where the full run is a couple of hundred time steps. By contrast, for these transition calculations we took of the order of 10,000 time steps. In the latter calculations, we're interested in detailed phase relations between the modes, and if you want to maintain accuracy, you have to be careful.

Reynolds:

To answer Bushnell's questions, we have indeed done some other things. For example, we have looked at the RMS wall pressure and we're starting to examine some conditional sampling techniques. We believe that we have established the large-eddy simulation concept and now want to do a finer-mesh calculation that will yield more of the features and have more resolution.

Orszag:

I have one more point, and that is as you increase the resolution in a numerical calculation, it turns out surprisingly, you get less randomness, not more. It's easy to get random solutions with low resolution. However, when you increase the resolution, the degree of randomness in the calculations goes away.

Coles:

I know one flow that I think is a prime candidate for a large-eddy calculation, that is the puff in a pipe. And it could even be the periodic problem, because there is a stable configuration in a pipe at one very special Reynolds number with a train of puffs. In this case the turbulent region is roughly 15 diameters long and the puffs are separated by laminar regions of about 20 diameters. I think the computer might be able to tell us some very interesting things regarding the flow. The puff to me is a vortex ring going down the pipe. I can see this in Wygnanski's measurements, but I'm not certain that he can see it. I'd be particularly interested in the pressure behavior for that flow.

Abbott:

Doug Abbott. Wouldn't it be useful in some of these time-dependent computations to put in a simulated hydrogen bubble-wire and compare with flow visualizations?

Reynolds:

It's a good suggestion and we expect to do that as Ames gets better graphics. We have already done some particle tracing.

SHEAR LAYER BREAKDOWN DUE TO VORTEX MOTION

T. L. Doligalski & J. D. A. Walker

Department of Mechanical Engineering and Mechanics and

Center for the Application of Mathematics

Lehigh University, Bethlehem, Pa., 18015, U.S.A.

ABSTRACT

The nature of the time-dependent flow in a two-dimensional time-mean turbulent boundary layer and the relationship of this flow to the time-mean quantities is discussed. Although the bursting phenomenon is known to be a dominant feature of the time-dependent flow, it is pointed out that, as yet, there is no satisfactory explanation as to why bursting occurs. The present paper reviews numerical solutions for the unsteady boundary-layer flow induced by a transverse vortex convecting in a uniform flow above a plane wall; these studies are of a fundamental nature and were undertaken as a search for a possible physical mechanism for bursting in a turbulent boundary layer. The numerical solutions strongly suggest that the boundary layer will erupt behind the convecting vortex for all convection speeds. It is conjectured that, as the erupting fluid from the boundary layer penetrates into an inviscid region of cross flow above the wall, a roll-up phenomenon into another vortex structure will occur. This physical process thus gives a possible explanation for the observed regeneration of vortex structures in a turbulent boundary layer. It is important to emphasize that the phenomena discussed in this paper develop and take place in a frame of reference convecting with the vortex and consequently can only be properly observed in a moving reference frame; recent experiments where flow visualization has been carried out in a convecting reference frame are discussed and these experiments support a number of the conjectural aspects of this paper. Finally the expected nature of the boundary layer due to the motion of a convected three dimensional vortex structure is discussed.

1. INTRODUCTION

Effectively inviscid flows with vorticity occur in a wide variety of applications in fluid mechanics; however relatively little is known on a theoretical basis about such flows and how they interact with a solid wall. In this paper, the primary interest is in rotational disturbances in an effectively inviscid flow which are not small and how a boundary layer may be expected to respond to such a disturbance. In particular, it is of interest to ascertain whether the boundary layer can be expected to remain passive for all time or whether a breakdown can be expected to occur. Here, following Riley [1], the term breakdown is understood to imply a catastrophe with respect to the boundary-layer flow in which the notion of a thin boundary layer embedded in an effectively inviscid flow fails. Such a breakdown will result in a viscous-inviscid interaction between the boundary layer and the outer inviscid flow and can be expected to substantially alter the inviscid flow. Two areas where a good understanding of such phenomena should prove useful are boundary-layer transition and the turbulent boundary layer.

Although boundary-layer transition is not well understood, it is known that the extirpation of order in a two-dimensional laminar flow can have its genesis in at least two different effects, namely both small and finite amplitude disturbances. In carefully designed experiments where the free stream turbulence level is maintained at low levels, the onset of turbulence is heralded by the appearance of two-dimensional Tollmein-Schlichting waves; there then ensues a period of wave amplification which ultimately becomes highly nonlinear and three-dimensional and culminates in the production of a turbulent spot. This process has been described in detail by Morkovin [2] who catalogues a number of different factors which influence the process of spot formation.

In boundary-layer transition, once spots are formed they are convected downstream and at this stage the flow may be considered to be double structured, consisting of an effectively inviscid flow with vorticity in the form of spots above a viscous boundary layer near the wall. This is the type of problem which is primarily of interest in this paper, corresponding to rotational disturbances in the inviscid flow which are not small. Once spots appear they seem to be able to reproduce structures similar to themselves in a complex interaction with the boundary-layer flow and as the flow becomes increasingly complicated, transition to fully turbulent flow follows. It is of interest to understand how this reproductive process can occur; moreover, the regenerative process is possibly related to the second known cause of spot formation. When the initial mainstream is contaminated with large enough disturbances, spot formation can occur without recourse to Tollmein-Schlichting wave amplification, a phenomenon which Morkovin [2] (see also Reshotko [3]) has termed the "high intensity bypass". Thus although the end product of a turbulent spot appears to be essentially the same, it appears that there are at least two physical causes for the phenomenon.

The gross overall features of a turbulent spot have been investigated experimentally; those portions of the spot where the vorticity is largest may be made visible by various techniques and the spot appears as a wedge or U-shaped structure which is convected downstream. The nature of the instantaneous internal motion within the spot is not well established although in recent times progress has been made in this area by Coles and Barker [4] and Wygnanski [5]; these authors have created disturbances believed to be similar to naturally occurring turbulent spots and have measured velocities downstream at various points within the symmetry plane of the spot. At each point the measured velocities are time-averaged with the view of obtaining a representative picture of the instantaneous flow within the spot. These measurements show at least one recirculation zone within the spot and suggest that a simple loop vortex filament may be a useful idealization of the spot. This point will be discussed in more detail subsequently but at this stage it is worthwhile to remark that the motion of a spot is probably much more involved than that described by the motion of a convecting, stretching vortex loop. Since the measurements reported in [4] and [5] are ensemble-averaged, it is entirely possible that some significant details have been averaged out. A series of photographs by Falco (R. Falco, private communication) in which spots are visualized using smoke in air clearly show a streamwise streaky structure associated with the spot itself; these photographs strongly suggest some type of irregular multiple eddy motions within the spot. Perhaps at the time of creation of a spot, the flow field associated with a spot may be approximated as a simple loop filament of vorticity; as the loop stretches and convects downstream, it is possible that wavelike instabilities of some nature develop. The study of Widnall and Tsai [6] does demonstrate that a ring vortex in motion in an unbounded fluid becomes unstable at high Reynolds numbers and the instabilities observed in [6] do bear a very superficial resemblance to the observed flow patterns in visualization studies of spots. At the same time, visualization also suggests that the flow field associated with the spot is much more complicated than for the vortex rings observed in [6] and that the spot may consist of an intricate conglomeration of many vortex loops.

A problem common to all visualization methods is that the vorticity itself cannot be visualized and only the effects of vorticity can; consequently in using visualization methods or ensemble-averaged probe measurements, the instantaneous streamline patterns must be extrapolated. Regretfully instantaneous volume measurements are beyond the scope of modern experimental methods and interpretations based on current experimental techniques are bound to remain controversial. Clearly the phenomena associated with a spot are rather complex and despite a wealth of beautiful experimentation are not well understood at present.

The process of spot formation from either small or finite amplitude disturbances is also a difficult theoretical problem. The appearance of the Tollmein-Schlichting waves and their subsequent linear amplification may be explained on the basis of small disturbance linearized stability theory. The ensuing nonlinear growth period

is not as well understood but an important contribution on this aspect has been made by Hocking, Stewartson and Stuart [7]. These authors consider the case of plane Poiseuille flow for $Re \geq R_c$ where Re is the Reynolds number and R_c is the critical Reynolds number below which small disturbances will be damped out; the authors [7] show that an initially small disturbance, which the linear theory predicts will travel downstream spreading outwards and increasing in amplitude, will eventually focus energy toward the center of the disturbance as nonlinear effects become important. As the solution focuses toward a singularity the theory is no longer valid; however it was noted [7] that the explosive nature of the solutions bore at least a superficial resemblance to the observed formation of turbulent spots. Although the authors [7] admit that it would be premature to claim more than this, the theory is important because it demonstrated for the first time and in a rational manner how nonlinear effects can lead to the focusing of an initially infinitesimal disturbance. Due to the complex nature of the phenomenon the importance of a self-consistent theoretical approach is evident and the objections to some of the previous theories are discussed in [7]. It would seem that the approach of reference [7] might be pursued to demonstrate how a spot can occur although it is clear that the theoretical problem is substantial. At present there is no theory which explains spot formation via the "high intensity bypass".

The implication of this discussion is that the theoretical description of what a spot is and how such a structure originates is quite incomplete; thus at present it is only possible to speculate on the basis of experimental evidence that at least at the time of creation the spot may be similar to a three-dimensional loop vortex.

Another important area, where an event occurs that appears qualitatively similar to spot formation, is the fully developed turbulent boundary layer. This is the bursting phenomenon wherein intermittent, rapid and violent ejections are observed to occur from the wall layer at isolated streamwise and spanwise locations. One result of the bursting appears to be the creation of a vortex structure. This characteristic feature of the wall layer flow was first observed in detail by Kline et al. [8] and a review article by Willmarth [9] details the numerous experimental contributions in this area.

The turbulent boundary layer is known to be a composite double layer consisting of (1) a relatively thick outer layer whose dimensionless thickness is $O(1/\log R_e)$ and (2) a thin inner wall layer whose dimensionless thickness is $O[U_o/(u_\tau R_e)]$. Here U_o and u_τ are the local mainstream and friction velocities respectively and Re is the Reynolds number. The orders of magnitude describing the thickness of each layer are asymptotic estimates valid in the limit $Re \to \infty$ and are based on the work of Fendell [10], Mellor [11] and Yajnik [12]. These authors have considered the mathematical structure (in the limit $Re \to \infty$) of the equations governing the time-mean flow in a turbulent boundary layer which is two-dimensional and nominally steady. There are a number of important aspects of these papers which have a bearing on the possible consideration of the time-dependent flow in a turbu-

lent boundary layer and which will be discussed briefly here.

First the authors [10], [11], [12] using an apparently minimum appeal to experiment are able to develop a self-consistent set of asymptotic expansions describing the leading order mean velocity components and turbulence terms. In the second place, it is shown that the viscous terms in the outer layer and the convection terms in the inner layer are negligible to leading order; both of these results may be viewed as constraints and need to be kept in mind when the time-dependent flow in a turbulent boundary layer is considered theoretically. While these and other results in the cited references are strongly suggested by experiment and can be obtained by intuitive order of magnitude arguments, this latter type of approach has been and will continue to be the source of numerous controversies. On the other hand, the method of matched expansions is a technique for constructing self-consistent and uniformly valid solutions. Indeed even the most fundamental unsteady laminar boundary-layer problems, such as the impulsively started semi-infinite flat plate, have only been understood through the use of such methods (see for example reference [1]). The modern view of boundary-layer problems is that the solution of the laminar boundary-layer equations represents the leading terms in an asymptotic expansion of the Navier-Stokes equations for large Reynolds number. Consequently the laminar boundary-layer equations, for example, are not to be regarded as an approximation but are exact in the limit $Re \to \infty$. Although the theoretical problem is admittedly substantial, ideally one would like to carry this type of rational approach over to the turbulent boundary layer and references [10], [11] and [12] are an important step in this direction.

A second point is that because the cited references [10], [11] and [12] start from the time-mean equations, they can offer only a partial resolution of the closure problem; that is to say, although the order of magnitude of the Reynolds stress term is fixed in terms of the Reynolds number, a functional form must still be obtained for this term. The popular approach in the past (which has been somewhat disappointing) has been to simply postulate a functional form based on a mixing length or eddy viscosity formulation. Another alternative is to carry out an analysis of time-dependent motions which are representative of the motions observed in a turbulent boundary layer; such solutions could then be suitably time averaged in order to arrive at a constitutive relation. In revealing a remarkable degree of coherent structure in the turbulent boundary layer, experiments have suggested to an ever increasing extent that this second alternative may be viable. At the same time, it is not reasonable to expect that a complete solution to boundary-layer turbulence may be developed from first principles; this point has been clearly discussed by Cebeci and Smith [13], p. 41. Because a number of varied phenomena, some of which occur at very small physical scales, are observed within the time-dependent flow, consideration of all features of the flow by a numerical solution of the full Navier-Stokes equations appears to be an impossible task. However it may be possible to consider the dominant features of the turbulent flow and the method of matched expansions has the potential of definitively isolating which effects are

important and which are not. Consequently the argument for the use of such methods is even more compelling than in the case of the time-mean equations since the time-dependent flow is necessarily three-dimensional and is governed by a set of more complicated equations. Unfortunately the theoretical problems are formidable and at present there are a number of difficulties which are mainly associated with the nature of the time-dependent flow in the outer layer and which will be discussed subsequently.

It is possible to make some progress with the wall layer flow. If the thickness of the wall layer in the time-mean sense is $O(\nu/u_\tau)$ then it is reasonable to expect that this length scale is appropriate for a large majority of the time in the time-dependent flow; this is confirmed by experiment and that period of time when the integrity of the wall layer flow is maintained has been defined as the quiescent period by Kline et al. [8]. During this period of time no important interaction occurs with the outer layer and the streak structure discussed in [8] is observed to be in place and relatively stable. By assuming the dimensionless streak spacing λ^+ is large for large Reynolds numbers, Walker and Abbott [14] have argued that the equations governing the three velocity components in the wall layer during the quiescent period are linear and of the heat conduction type. A consequence of this result is that the principle of superposition of solutions applies; thus in the consideration of which solutions make a direct contribution to the time-mean streamwise profile, oscillatory Stokes-like solutions (which may be present in the time-dependent flow and which arise from apparently random fluctuations at the outer edge of the wall layer) need not be considered since such solutions can make no net contribution to the mean profile. Walker and Scharnhorst [15] go on to consider the possible similarity solutions of the governing equations which correspond to the organized motion observed between the streaks during the quiescent period. These solutions take into account the three-dimensional nature of the flow and consist of an infinite set of eigenfunctions; the arbitrary constants associated with these eigenfunctions can in theory be chosen to represent any initial velocity distribution in the latter stages of the sweep. In [15] these similarity solutions are time-averaged to obtain an approximation for the time-mean profile in the wall layer and this profile has been extensively compared with measured data in [16].

In obtaining the model profile in [15], the contribution due to the burst-sweep sequence was neglected and it was argued that this was justifiable on the grounds that these events are of relatively short duration. The burst (wherein fluid from the wall layer is ejected into the outer layer) and subsequent sweep may be regarded mathematically as a localized breakdown of the wall layer flow. During this period of time, a viscous-inviscid interaction occurs between the inner and outer layer and a distinction between an inner and outer layer cannot be made. Since the boundary layer is double structured in the time-mean sense, it is not expected that events for which the wall layer is not distinguishable can give rise to a dominant contribution to the time-mean profile in the wall layer. Moreover, it is worthwhile to mention that the asymptotic analyses [10], [11] and [12]

establish certain constraints that need to be kept firmly in mind in any description of the time-dependent flow in the wall layer. In particular the fact that the convective terms do not enter the leading order time-mean equations is important in the sense that any attempted solution for the wall layer flow must time average to give results compatible with the theory in [10], [11] and [12].

It is of interest however to understand how the wall layer breakdown can occur and what physical mechanism causes the observed eruptions. The model profile in [15] was obtained using a number of assumptions which were based on experimental observation; in the theoretical description of the wall layer flow it was argued that the majority of the contribution to the time mean profile and the intensities $\overline{u'^2}$ and $\overline{w'^2}$ arise during the quiescent period. However the normal component of velocity is too small to account for any leading order contribution to either $\overline{v'^2}$ or $\overline{u'v'}$. At present this picture seems compatible with experiment which shows the majority of production occurs during the breakdown. However an expression for $\overline{u'v'}$ can be calculated indirectly from the time-mean streamwise momentum equation and this was carried out in [14]. Clearly to complete any description of the wall layer flow it will be necessary to treat the breakdown problem and to understand why the breakdown occurs. In particular it is important to identify theoretically the Reynolds number dependence of the time scale associated with the burst-sweep sequence. Moreover to obtain an expression for the Reynolds stress in the outer layer from consideration of representative time-dependent motions, it is crucial to be able to analyze the bursting phenomenon and thus to be able to calculate the $\overline{u'v'}$ term directly. The breakdown problem is rather difficult since as the discussion of section 3 of this paper shows, no laminar breakdown problem has ever been successfully considered. In any case the breakdown problem cannot be resolved without a detailed consideration of the outer layer flow; consequently it is crucial to be able to develop a good understanding of the dynamics of the outer layer.

It is observed experimentally that the outer layer flow is dominated by (1) the motion of vortex structures believed by some investigators to be similar in certain respects to transition spots and (2) the burst-sweep phenomenon in which similar structures appear to be generated through intermittent eruptions from the wall layer. Of these two effects it is the latter which is believed to make the dominant contribution to the Reynolds stress in the outer layer. To a limited extent this is to be expected; certainly a vortex filament which remains at an essentially horizontal level in motion past a probe cannot make any net contribution to the Reynolds stress. However a vortex filament which possesses a significant component of vertical velocity will make a contribution.

Just as in transition there are at least two possible ways in which a wall layer breakdown could occur. It is possible that the wall layer flow is an inherently unstable flow and that some process similar to Tollmein-Schlichting wave amplification occurs. Certainly this type of process cannot be ruled out but there are a number of

reasons to suspect that another explanation is possible. In view of the apparently dominant linear behavior of the wall layer argued in [14] which is compatible with the results of [10], [11] and [12], the manner in which a small scale disturbance could amplify is not clear. Moreover, in transition Tollmein-Schlichting wave amplification is only observed to be the dominant spot producing effect when the outer flow is maintained at an essentially irrotational level; because the outer layer of a turbulent boundary layer contains a substantial amount of vorticity, an analogy between transition and the turbulent boundary layer for this type of mechanism is disquieting. Finally it is difficult to find examples in fluid mechanics where an inner boundary layer, in and of itself exerts such a strong measure of control over an outer layer.

The other possibility is that the wall layer responds to the rotational flow in the outer layer in such a way that a localized breakdown of the wall layer flow occurs; there is experimental evidence to indicate this possibility is viable. Nychas et al. [17] suggest that the eruptions of the wall layer were associated in some way with the passage of a vortex structure in the outer layer. Recently visualization studies have been carried out by Smith [18] in a convected reference frame moving with a vortex structure in the outer layer. Using hydrogen bubble wires to visualize the relative flow field, fluid was observed to pile up behind the leading head of the vortex. As time increased this erupting fluid appears somewhat like an ocean wave of growing amplitude; eventually the erupting fluid is observed to roll up into another vortex structure in a process which appears somewhat like the breaking of an ocean wave. This is also the type of breakdown phenomenon that will be suggested by the results of this paper.

In considering the possible motions that may lead to a breakdown in a turbulent boundary layer, there are a number of theoretical difficulties which are associated to a large extent with the outer layer. One problem is associated with the observed logarthmic behavior of the time-mean profile near the overlap zone; a number of arguments, which are discussed in detail by Weigand [19], have been given over the years to demonstrate this behavior. Unfortunately none of these arguments are entirely satisfactory and in any case they give little insight as to the nature of the time-dependent flow which gives rise to the logarithmic behavior of the mean profile. The turbulent boundary layer is a rather challenging singular perturbation problem apparently involving a rather unusual matching principle between the inner and outer layer and to what extent the matching principle discussed in [10] carries over to the time-dependent flow is unclear. It might be expected that the time-dependent streamwise profile contains the logarithmic behavior within the turbulence for a majority of the total time (otherwise a time-mean logarithmic behavior would not be possible). However it is not obvious that this description of the flow in the overlap zone is appropriate during the breakdown process.

In addition the leading order equations for the time-dependent

flow in the outer layer should in principle be derived from the Navier-Stokes equations. While the studies [10], [11] and [12] of the time-mean equations give some guidance as to how this might be done, the proper leading order equations are unknown at present. It might be thought that one possible way out of the aforementioned difficulty is to write the time-dependent velocity components as a sum of a mean and fluctuating term; time-averaged experimental measurements could then be used to give some guidance as to the orders of magnitude of each term in the governing equations. However, this procedure could be dangerous in the sense that a structure in the outer layer could produce no net contribution in the mean and yet be responsible for an eruption of the wall layer; thus a significant term in the governing equations might be neglected. Moreover this type of approach is somewhat circular because at a certain stage it is necessary to assume some model for either the time-mean profile or the Reynolds stress term (see for example Landahl [20][†], [21], [22], Bark [23]); from a practical point of view, it is precisely information in regard to the Reynolds stress term calculated directly from a time-dependent analysis that would be most useful in forming improved constitutive models for the prediction of the time-mean flow. Such information cannot be obtained from a theoretical analysis of the time-dependent flow in which a time-mean profile or a functional form for the Reynolds stress is assumed; this latter type of analysis should be regarded as indirect and may or may not be useful in identifying the basic processes in turbulent boundary-layer flows. Finally, the appropriate initial flow in considering the dynamics of the outer layer should presumably involve the flow in the latter stages of the transition zone. As already indicated this flow region is not well understood at present.

Despite these theoretical difficulties in describing the outer layer flow it is possible to consider flows of a more fundamental nature which possess a number of features which are qualitatively similar to the observed eddy motion in the outer layer of a turbulent boundary layer. Some evidence that this is the case may be found in the experimental study of Coles and Barker [4] in which the authors create what they term a synthetic turbulent boundary layer. This is accomplished by creating vortex structures by injecting a finite slug of fluid from the wall into an otherwise laminar boundary layer. Presumably the method of creating the disturbance is not crucial to the results of the experiment and alternatively, rotational disturbances could be introduced from above the existing laminar boundary layer. Preliminary experiments using this alternate method have been carried out by Prof. C. R. Smith at Purdue and there appears to be a wide variety of different ways to create the wedge-shaped disturbance which looks like a transition spot. An important aspect of the study of Coles and Barker [4] is that measurements of the time-mean

[†]The objections to the theory of reference [20] have been discussed in detail by Stewartson [24]. Note also that the term breakdown is used in a context in references [20], [21], [22] which is different from that used in this paper.

streamwise profile downstream yield a profile which is very similar to measured profiles in a turbulent boundary layer. Thus it would seem important to understand the motion of such a structure above an otherwise laminar boundary layer.

The observed gross features of the turbulent spot suggest that an appropriate vortex structure to consider is the loop filament sketched in figure 1 which is being convected to the right in a uniform flow. The arrows show the sense of the rotation and the parts of the vortex tube where the vorticity is strongest are made darkest. The location where the vorticity is strongest occurs at the head of the structure (labeled A) and this is the region where the vortex tube is most highly stretched. Along the arms of the filament (labeled B and C) the vorticity weakens from right to left and is weakest along the trailing portion of the loop (labeled D). Such a vortex structure would produce the wedge-shaped flow which is observed experimentally. It should be mentioned that because the vorticity is relatively weak on the trailing portion of the loop it is difficult to get a clear definition from experiment of the characteristics there and in view of this the part of the curve labeled D in figure 1 is conjectural; however the filament sketched in figure 1 is believed to be a reasonable possibility. Experimentally only the head and arms of the vortex are readily made visible and presumably this has given rise to the terms "horseshoe" and "hairpin" vortices; such model structures are

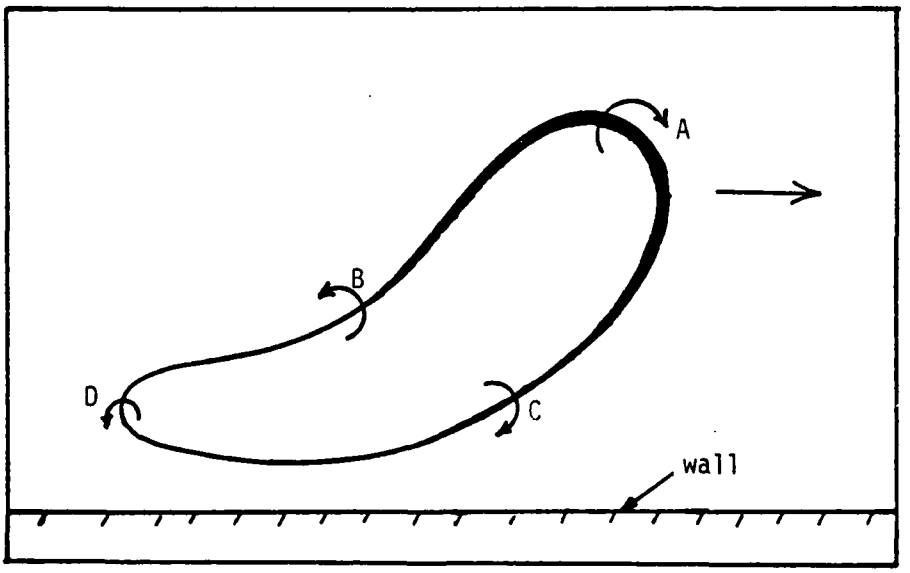

Figure 1. Schematic diagram of instantaneous vorticity distribution in a loop filament convected to the right (darkest parts of filament represent locations of strongest vorticity).

often sketched with the arms either terminating on the wall or bending sharply near the wall with the filament meandering off aimlessly away from the wall. However as the discussion by Lighthill [25] makes clear a vortex filament must form a closed loop in any real fluid and it is useful to consider how this occurs. In this respect the arms of the filament B and C cannot bend toward the wall and terminate there as suggested by Roshko [26] in his discussion of the experiments in [4].

At present the inviscid solution describing the motion of a filament of the type depicted in figure 1 is not available analytically. The distribution sketched in figure 1 is instantaneous and will change with time as the structure is convected in the uniform flow. It is possible to calculate such a motion numerically using the approximate methods due to Leonard [27] and the resultant unsteady laminar boundary layer induced by such a structure could then be considered. However the boundary-layer flow is expected to be rather complex owing to the three-dimensional, time-dependent nature of the flow and the accurate calculation of such a boundary-layer flow is expected to involve an extremely large number of mesh points. (The reason for this statement will be made clear subsequently.)

At this stage our purpose is to demonstrate the effect that a moving disturbance containing concentrated vorticity (in an otherwise irrotational flow) has on a boundary-layer flow. Because relatively little is known theoretically about such flows a very fundamental problem will be considered here, corresponding to a rectilinear vortex of negative rotation which is convected to the right in a uniform flow above a plane wall. It will emerge that the boundary-layer flow is rather complex and involves a variety of unusual separation effects which take place in a frame of reference convecting with the vortex. Moreover in all cases considered the two-dimensional unsteady flow eventually evolves into a state wherein very intense variations in the flow field occur; this situation requires a relatively large number of mesh points in order to accurately describe the flow development. Consequently it was believed that before the more complicated problem depicted in figure 1 could be understood it was important to understand the nature of the two-dimensional problem first; in addition because of the novel and complex phenomena discussed in this paper, we are unwilling at this stage to compromise numerical accuracy to consider the three-dimensional loop filament.

At a number of places in the paper we shall point out certain features of the flow which are similar to the motions observed in turbulent boundary layers. However it seems wise to interject a note of caution in this respect. Because the vortex flows considered in this paper are two-dimensional, no account is taken of the vortex stretching and the possible development of instabilities that are expected to occur in the effectively inviscid motion sketched in figure 1. However it is important to first develop an understanding of the motion of the line filament and we shall subsequently speculate in §4 on the nature of the boundary-layer flow induced by the loop filament in figure 1.

The boundary-layer flow due to a rectilinear line filament of positive rotation in motion above a plane wall has been considered by Walker [28]; in this case the fluid is at rest at infinity and the inviscid theory predicts that the filament will remain at constant height above the wall and will move with constant velocity to the right. It was demonstrated that no steady boundary-layer solution exists, even in a frame of reference which convects uniformly with the vortex, and that the boundary-layer flow is inherently unsteady. To investigate the nature of the unsteady boundary-layer flow, a problem was considered wherein the plate was imagined to be inserted in the flow at time $t = 0$; in this way the effects of viscosity become important near the wall abruptly. It was found that a short time after the initiation of the boundary-layer motion, separation occurred in the boundary layer in the form of a recirculating eddy of negative rotation. This separation phenomenon is novel in the sense that it develops and takes place in a frame of reference moving with the vortex. The calculated numerical solutions show possible explosive growth of the boundary layer and it was conjectured [28] that the eddy spawned by the parent vortex (in the inviscid region) would erupt from the boundary layer intact and would strongly influence the motion of the parent vortex, slowing it down and driving it away from the wall. This problem has direct application to the effect of trailing aircraft vortices near the ground and has been studied experimentally by Harvey and Perry [29]. In these experiments the trailing vortex is curved and three dimensional. However the main observed features of the flow are predicted by two-dimensional theory and the conjecture of [28] was substantiated; a secondary vortex was observed to form and be ejected from the boundary layer, strongly influencing the motion of the trailing vortex in the process. The violent ejection observed by Harvey and Perry [29] bears some resemblance to the bursting in a turbulent boundary layer and the theory in [28] demonstrated how this can occur.

In this paper, problems which are somewhat more relevant to the vortex motions observed in a turbulent boundary layer will be considered; these problems concern the boundary-layer motion induced by a vortex of negative rotation convected to the right in a uniform flow. Define the convection velocity of the vortex to be V_c and the speed of the uniform flow in which the vortex is embedded to be U. Then if $V_c = \alpha U$, α represents the ratio of the convection velocity of the vortex to the speed of the flow far upstream of the vortex. The coherent structures observed in turbulent boundary layers may be similar to the loop filament sketched in figure 1; a typical speed of the head A is about 80% of the mainstream speed. The arms B and C are thought to slowly spread outward. Consequently values of the parameter α in the range $0 \leq \alpha < 1$ are of interest in this study.

The plan of the paper is as follows. In §2 the problems to be considered are formulated and in §3 the results of the numerical calculations for the unsteady boundary-layer flow induced by the vortex motion are discussed. In some cases, particularly at the lower values of α in the range $0 < \alpha < 1$ an unusual separation effect occurs in a frame of reference convecting with the vortex; for $\alpha \geq 0.75$ a dramatic change takes place in the character of the unsteady boundary-layer flow

and no separation takes place in the boundary layer. However in all cases the boundary layer enters a period when rapid and substantial growth occurs in a direction normal to the wall; thus it is suggested that the boundary-layer flow will not remain passive for any α but an eruption is to be expected along with a concomitant modification of the inviscid flow. Because a space limitation precludes a detailed discussion, a more complete description of the results may be found in Doligalski and Walker [30] and only a brief synopsis is included here. Finally in §4 and on the basis of the results in §3 we speculate on the nature of the boundary-layer flow which will be induced by the filament sketched in figure 1.

2. STATEMENT OF THE PROBLEM

Consider the construction of the inviscid flow due to a vortex of negative rotation convected in a uniform flow above a plane wall which is illustrated schematically in figure 2. The inviscid solution (Milne-Thompson [31], p. 359) predicts that the vortex pair illustrated in figure 2 will move with constant velocity to the left with

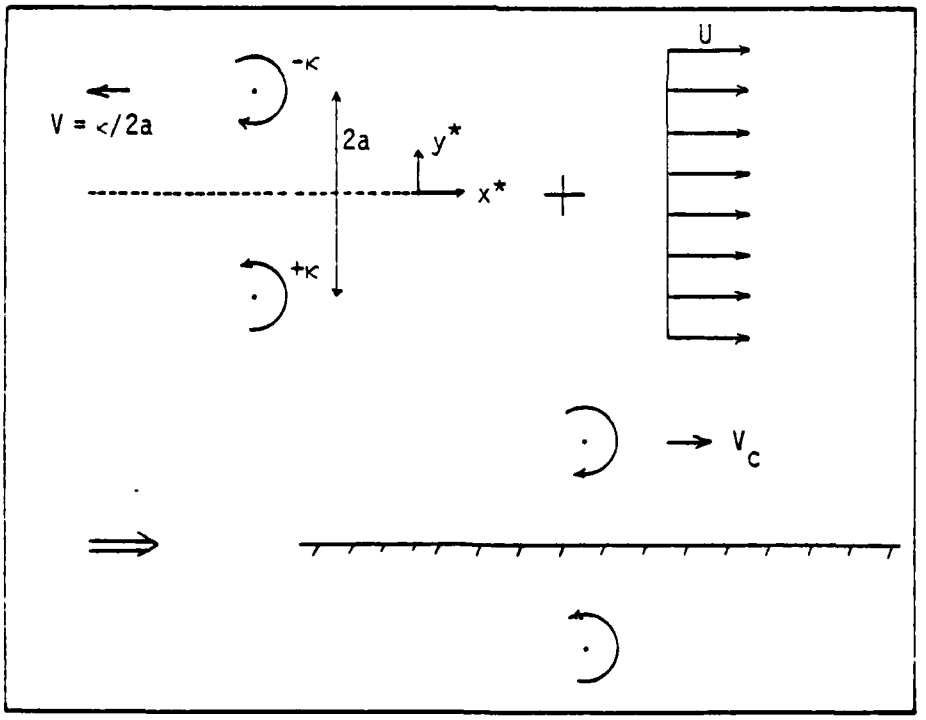

Figure 2. Sketch of geometry and construction of inviscid flow due to a vortex of negative rotation convected to the right above an infinite plane wall in a uniform flow.

each vortex remaining at a constant distance from the symmetry plane $y^* = 0$. The vortex in the upper half plane has negative rotation $-\kappa$ while its image in the plane $y^* = 0$ has positive rotation $+\kappa$. If a uniform flow of sufficient speed U is superimposed to the right the net result is a vortex pair of negative rotation convected to the right. Because the plane $y^* = 0$ is a streamline for the unsteady inviscid flow, it may be replaced by a solid wall. In the upper half plane ($y^* > 0$) the rectilinear vortex convects to the right with speed

$$V_c = U - \kappa/2a \ . \tag{1}$$

Define $V_c = \alpha U$; consequently the ratio of convection rate to the speed of the uniform flow is given by

$$\alpha = 1 - \frac{\kappa}{2aU} \ . \tag{2}$$

In this paper the primary interest is in values of α in the range $0 < \alpha < 1$; it may be inferred from equation (2) that the stronger the vortex or the closer the vortex is to the wall, the slower the relative convection speed.

The unsteady stream function corresponding to the inviscid flow is given in [30] and here the instantaneous streamline patterns are

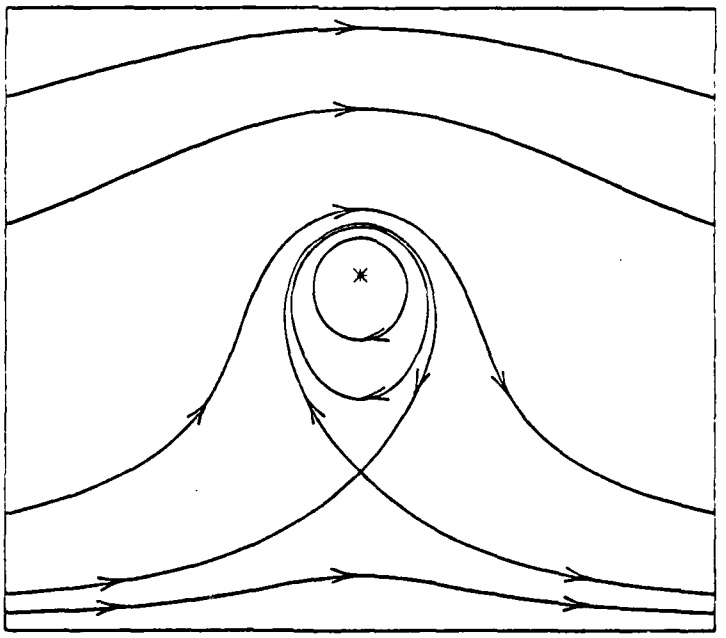

Figure 3(a). Instantaneous streamlines in the laboratory frame for the inviscid flow for a vortex convected at 80% ($\alpha = 0.80$) of the mainstream speed.

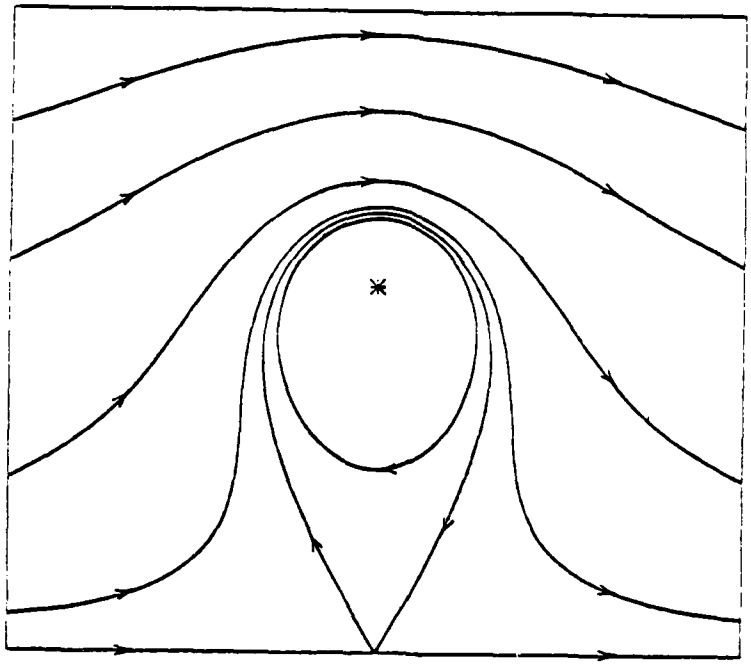

Figure 3(b). Instantaneous streamlines in the laboratory frame for the inviscid flow for a vortex convected at the critical value of 75% ($\alpha = 0.75$) of the mainstream speed.

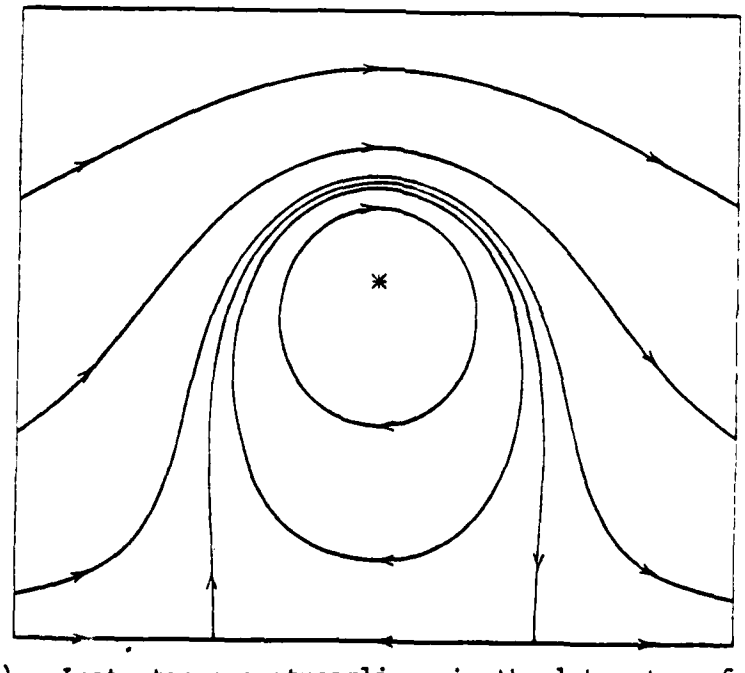

Figure 3(c). Instantaneous streamlines in the laboratory frame for a vortex convected at 70% ($\alpha = 0.70$) of the mainstream speed.

plotted in figures 3. In figure 3(a), the instantaneous streamline patterns are given for $\alpha = 0.8$; this figure corresponds to the streamlines that an observer in the laboratory frame would see for the inviscid flow. In figure 3(b) the case $\alpha = 0.75$ is plotted and it may be inferred from this figure that this value of α is a critical case; for a convection rate corresponding to 75% of the mainstream value the effect of the vortex spreads to the wall and a single stagnation point appears in the laboratory frame in motion along the wall. In figure 3(c) the instantaneous streamlines are plotted for $\alpha = 0.7$ and it may be observed that now there are two stagnation points associated with the inviscid flow in the laboratory frame. The plots in figures 3 are to scale and on the same scale.

As α decreases the effect of the vortex appears to become more spread out in the laboratory frame and the two stagnation points move to limiting values at $x' = \pm\sqrt{3}a$. Here $x' = x^* - V_c t^*$ where t^* is the time and x^* measures distance in plane $y^* = 0$; moreover it is assumed the vortex passes the point $x^* = 0$ at $t^* = 0$. The case $\alpha = 0$ corresponds to the physical situation of a vortex held stationary in a crossflow;

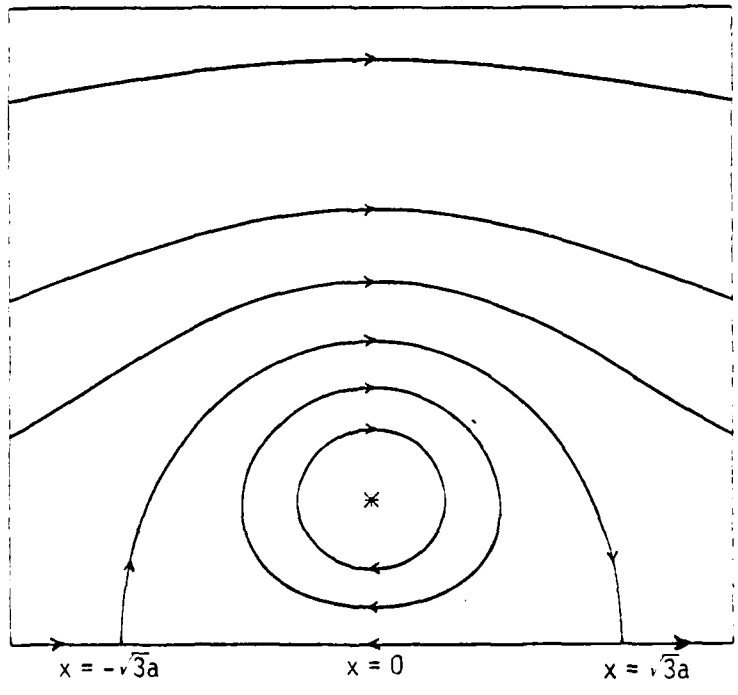

Figure 4. Instantaneous streamlines for a vortex held stationary in a crossflow ($\alpha = 0$). Also streamline pattern for all α in a frame of reference convecting with the vortex. Note that the scale of this figure is 2½ times smaller than in figures 3.

the streamlines of the inviscid flow for this limiting case are plotted in figure 4. This figure is also to scale but the scale is reduced by a factor of 2.5 from figures 3. Note that in figures 3 and 4 the asterisk denotes the location of the vortex center.

In regard to the boundary-layer flow, it is the unsteady inviscid velocity in the x*-direction (u_w^*) near the wall which is important and it is shown in [30] that this is given in the laboratory frame by

$$\frac{u_w^*}{U} = 1 - \frac{4a^2(1-\alpha)}{x'^2+a^2} \tag{3}$$

This distribution is plotted in figure 5 for various values of α and it may be seen that for all $\alpha < 0.75$, reversed flow is observed in the laboratory frame near the wall in the region immediately below the vortex. In all cases the point of minimum velocity occurs immediately below the vortex and an absolute minimum of $u_w^*/U = -3$ occurs for the case $\alpha = 0$.

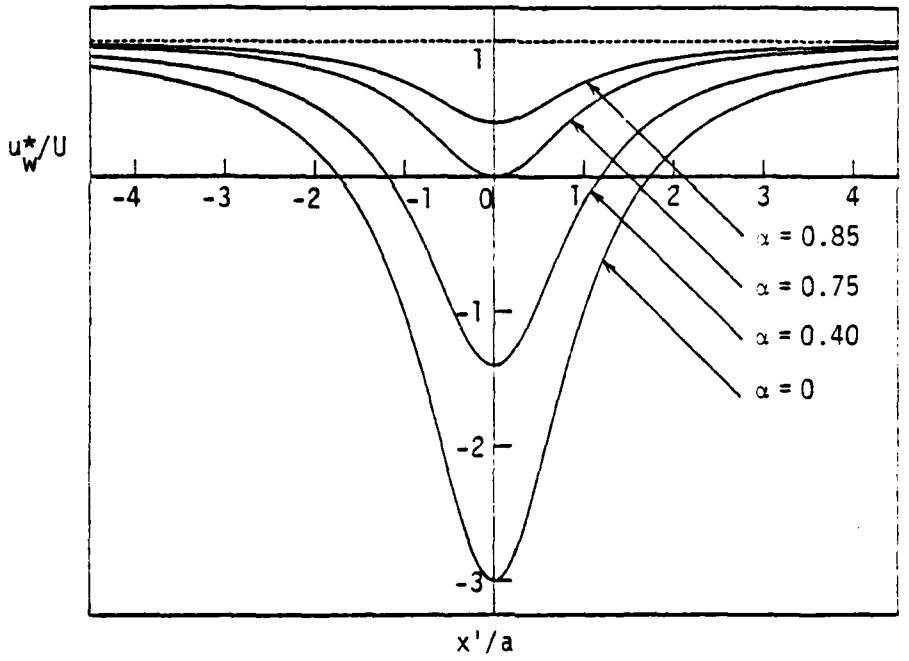

Figure 5. Instantaneous inviscid velocity distribution near the wall in the laboratory frame for various values of the relative convection speed of the vortex.

In the laboratory frame of reference the inviscid flow is unsteady; however in a frame of reference which convects uniformly with the vortex the inviscid flow appears as a steady flow; moreover, in this moving coordinate system the wall moves to the left with velocity $-V_c = -\alpha U$. The relative streamline patterns are easily obtained [30]

in the moving reference frame by superimposing a uniform flow $-V_c$ to the left. For all values of α the inviscid flow relative to the vortex is identical to that depicted in figure 4. A number of features of the relative inviscid flow are worthy of note. Recall that the scale of figure 4 is 2.5 times smaller than that of figures 3; thus it may be seen that the main effects of the vortex are more spread out than is suggested by the instantaneous streamline patterns in the laboratory frame depicted in figures 3. A second point concerns the relative stagnation points depicted in figure 4. The first of these at $\sqrt{3}a$ is termed the leading relative stagnation point and is characterized by flow toward the wall; on the other hand the trailing relative stagnation point is characterized by flow away from the wall. If u_w^* now denotes the streamwise inviscid velocity distribution near the wall in the moving reference frame, the curve labeled $\alpha = 0$ in figure 5 gives [30] the velocity $u_w^*/(1-\alpha)U$. It may be observed that there is a deceleration from upstream infinity to the leading relative stagnation point followed by a strong reverse acceleration underneath the vortex to an absolute minimum at $x^* = 0$. A similar type of behavior has been observed in turbulent boundary layers in a convected reference frame experimentally by Nychas et al. [17] and also in the water channel at Purdue by Prof. C. R. Smith. Again it should be remarked that the visualization carried out in these studies is in a plane through a three-dimensional structure and we only note here that the behavior in figure 4 is qualitatively similar to that observed in the visualization. Behind the vortex center the velocity decreases monotonically to zero toward the trailing relative stagnation point and a slow acceleration ensues toward downstream infinity.

To consider the nature of the unsteady boundary-layer flow near the infinite plane wall at $y^* = 0$, the following dimensionless variables are defined,

$$\left.\begin{aligned} x = x^*/a \ , \quad y = (y^*/a)Re^{\frac{1}{2}} \ , \quad t = U(1-\alpha)t^*/a \\ u = \frac{u^*}{U(1-\alpha)} \ , \quad v = \frac{v^*}{U(1-\alpha)} Re^{\frac{1}{2}} \ . \end{aligned}\right\} \qquad (4)$$

Here the quantities with the asterisk denote dimensional quantities and (u^*,v^*) are the components of velocity in the (x^*,y^*) directions respectively; the Reynolds number is defined as $Re = (1-\alpha)Ua/\nu$ where ν is the kinematic viscosity. The typical velocity $(1-\alpha)U$ which is used to define the dimensionless variables in equations (4) is a particularly convenient choice and corresponds to the inviscid velocity near the wall at infinity in the convected reference frame. The laminar boundary-layer equations, which are exact in the limit $Re \to \infty$, are

$$\left.\begin{aligned} \frac{\partial u}{\partial t} + u\frac{\partial u}{\partial x} + v\frac{\partial u}{\partial y} = U_\infty \frac{dU_\infty}{dx} + \frac{\partial^2 u}{\partial y^2} \ , \\ \frac{\partial u}{\partial x} + \frac{\partial v}{\partial y} = 0 \ , \end{aligned}\right\} \qquad (5)$$

where

$$U_\infty(x) = 1 - \frac{4}{1+x^2}. \tag{6}$$

The boundary conditions associated with equations (5) are

$$u = -\beta, \quad v = 0 \quad \text{at} \quad y = 0; \quad u \to U_\infty(x) \quad \text{as} \quad y \to \infty, \tag{7}$$

where

$$\beta = \frac{\alpha}{1-\alpha}.$$

Here the parameter β is the ratio of the convection velocity of the vortex to the inviscid velocity near the wall at infinity in the moving reference frame.

The motivation for the choice of dimensionless variables in equations (4) is evident from equations (6) and (7); in these variables the velocity in the inviscid flow near the wall is the same for all α but the wall moves at different speed to the left. For the inviscid flow near the wall an absolute minimum of -3 occurs in $U_\infty(x)$ at $x = 0$. At convection rates such that $\alpha < 0.75$, $\beta < 3$ and thus the wall moves to the left at a slower velocity than -3; however at $\alpha = 0.75$, $\beta = 3$ and the wall moves at the same rate as the maximum inviscid speed. Finally for $\alpha > 0.75$, $\beta > 3$ and the wall moves at a greater rate than any speed in the inviscid flow near the wall. Thus it is expected that a critical case will be the situation of a vortex convecting at a rate of 75% of the uniform flow speed; it will subsequently be shown that the boundary-layer development is radically different for α greater or less than the critical value $\alpha = 0.75$. Finally it should be noted that as $\alpha \to 1$, $\beta \to \infty$ and the dimensionless variables in equations (4) are not appropriate; however this singular behavior is apparent rather than real. The case $\alpha \to 1$ is of no interest since there is no vortex in this limit.

The subsequent analysis could be carried in terms of the x coordinate but it is convenient to introduce a new streamwise coordinate, ξ, defined by the Göertler-type transformation

$$\xi = \frac{1}{2\pi}\int_x^\infty \frac{4}{1+x^2}dx = 1 - \frac{2}{\pi}\arctan x, \tag{8}$$

whereupon the mainstream velocity (6) becomes

$$U_\infty(x) = 1 - U_e(\xi)$$

where $U_e(\xi) = 2(1 - \cos\pi\xi)$. This transformation is one-to-one and compresses the doubly infinite range of x to the finite range [0,2] for ξ; this is convenient for carrying out the numerical calculations. Since the coordinate ξ will be used throughout the paper it is worthwhile to summarize the effect of the transformation for some of the critical x locations in the flow and this is done in Table 1.

Table 1. Effect of the Transformation (8)

x	ξ	streamwise location
$+\infty$	0	upstream infinity
$\sqrt{3}$	1/3	leading relative stagnation point
0	1	vortex center
$-\sqrt{3}$	5/3	trailing relative stagnation point
$-\infty$	2	downstream infinity

This transformation was used in reference [28] and the motivation for its use is the same as discussed there.

Although the boundary conditions (6) and (7) are independent of t it is evident that no steady solution to the problem exists in view of the vortex sheet type flow at upstream and downstream infinity. To investigate the nature of the unsteady flow the following unsteady problem is considered. For $t < 0$ a vortex pair is convected to the right in a uniform flow; at $t = 0$ the plate is abruptly inserted on the symmetry plane $y^* = 0$. For all $t > 0$ a thin unsteady boundary layer will develop on the plate in order to satisfy the no slip condition and in §3 the nature of this boundary layer will be considered.

It should be remarked that such an initial condition is virtually impossible to produce experimentally. It is selected here primarily as a mathematically convenient state from which the boundary-layer development may be calculated forward in time. Our object here is to determine whether or not the boundary layer responds to the vorticity in the inviscid flow in such a way so that a breakdown of the boundary-layer flow is to be expected along with a subsequent interaction of the inviscid flow. Consequently since it will emerge that the latter possibility is the correct one the particular initial condition selected is not important insofar as demonstrating the basic effect. It is also worthwhile to remark that the inviscid flow is not disturbed initially by the sudden appearance of the plate. The numerical solutions which are summarized in §3 and reported in [30] strongly suggest that breakdown will occur in all cases and in each case we speculate on the nature of the ultimate breakdown.

3. NATURE OF THE BOUNDARY LAYER DUE TO A CONVECTED RECTILINEAR VORTEX

3.1 INTRODUCTION

At this point it is worthwhile to describe in somewhat more detail the term breakdown. In the classical picture of laminar flow at high Reynolds numbers, the flow field is double-structured consisting

of (1) an outer region in which the effects of viscosity are negligible to leading order, and (2) a viscous boundary layer region near all solid walls. The laminar boundary layer has a thickness $O(Re^{-\frac{1}{2}})$ and on the scale of the inviscid flow and in the limit $Re \to \infty$, the boundary layer is a region of zero thickness. However the notion of a thin boundary layer embedded in an inviscid flow is known to fail in a number of circumstances; one example is the catastrophic separation observed behind bluff bodies in which boundary-layer separation leads to a large rotational wake region. To understand why and how such catastrophic separation occurs, the fluid motion due to bluff bodies impulsively started from rest has been studied both theoretically and experimentally. One such problem is the impulsively started circular cylinder which has been discussed by Riley [1] and which will serve here as an illustrative example. Immediately upon initiation of the motion a thin viscous boundary layer forms on the cylinder; a short time later separation occurs in the boundary layer near the rear stagnation point of the cylinder and as time increases, the separation bubble increases in directions both tangential and normal to the cylinder boundary. Up to and including this latter period of time the concept of a thin boundary layer is still appropriate; indeed as Proudman and Johnson [32] have argued the initial value mathematical problem for the unsteady boundary-layer flow is well posed. Moreover, provided a singularity does not develop in the solution at finite time, once the limit $Re \to \infty$ is taken the boundary-layer flow cannot influence the inviscid flow at any finite time. However it is observed in the numerical calculations discussed in [1] that once separation in the boundary layer occurs, the effective boundary-layer thickness near the separation zone begins to increase substantially. This effect is believed to be explained by Proudman and Johnson [32]; these authors modeled the unsteady boundary-layer flow near the rear stagnation point of bluff body by considering the boundary-layer flow due to an outflow inviscid stagnation point near an infinite plane wall. It was demonstrated in [32] that for large time the boundary-layer thickness grows exponentially with time, a phenomenon which we term explosive boundary-layer growth. In cases for which the Proudman-Johnson [32] model is appropriate, Riley [1] argues that an eruption of the boundary-layer flow into the inviscid region is expected on the dimensionless time scale $t = O(\log Re)$; this event is understood to occur when the boundary-layer thickness becomes comparable to the length scale of the body itself. The phenomenon of breakdown for a cylinder is illustrated schematically in figure 6.

Another type of boundary layer breakdown is also believed to occur in the motion of fluid past bluff bodies in the two separate cases of magnetohydrodynamic flow and flow in a rotating environment. This type of breakdown is illustrated schematically in figure 7. When a strong radial magnetic field is present, the Lorentz force inhibits the type of flow separation illustrated in figure 6 and at a critical level discussed in [33], [34] and [35] no separated bubble occurs within the boundary layer. As the magnetic field strength is further increased a second critical level is reached beyond which a steady boundary-layer flow solution is possible. The nature of the boundary-layer flow in the intermediate range has been considered theoretically

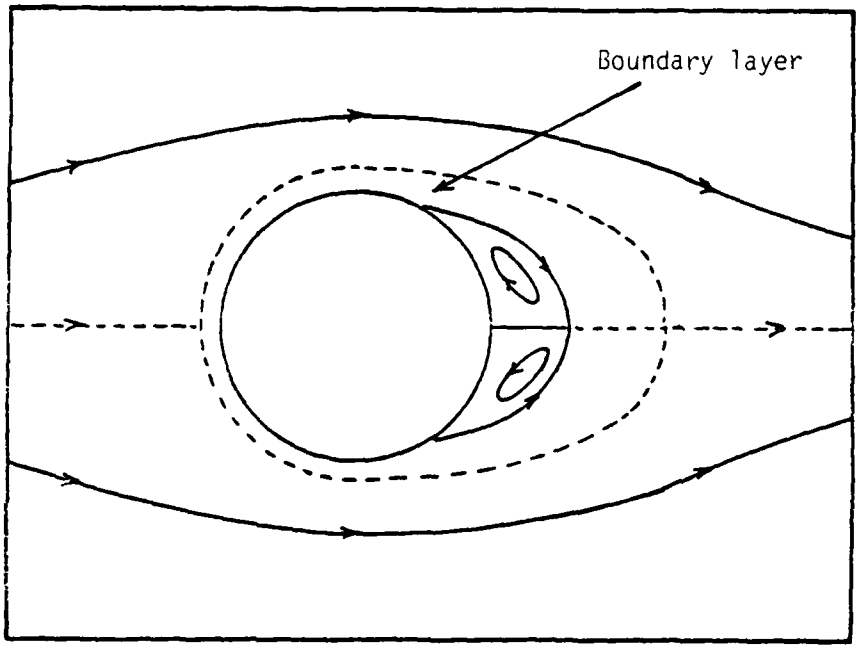

Figure 6. Schematic sketch of boundary-layer breakdown taking place in the impulsive motion a bluff body and involving a separation effect; the boundary layer region is not to scale. Breakdown occurs when the boundary layer thickness becomes comparable to the length scale of the cyliner.

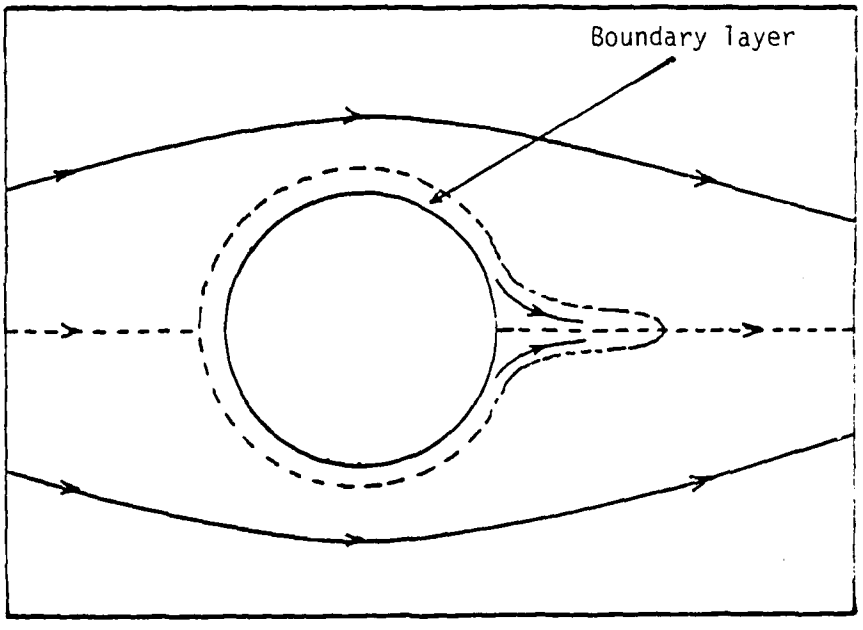

Figure 7. Schematic sketch of boundary-layer breakdown taking place without a separation effect; see text for examples.

by Leibovich [33] and Buckmaster [34], [35] and although the flow in this parameter range is not completely understood these investigations suggest: (1) an inherent unsteadiness in the boundary-layer flow in a thin region near the rear stagnation point, and (2) an extreme thickening of the boundary layer there. The numerical calculations of Crisalli and Walker [36] (where the case of flow in a rotating frame of reference is discussed) support the idea of the existence of a steady boundary-layer flow above the second critical level as well as substantial boundary-layer growth in the intermediate range. Physically the type of breakdown illustrated in figure 7 may be thought of as a jet-like eruption of the boundary layer flow into the inviscid region. Another example where breakdown of the boundary-layer flow occurs in a localized location without a separation effect is the boundary layer on a spinning sphere near the equator (Stewartson, [37]).

It is worthwhile to point out that, although the breakdown phenomenon illustrated in figure 6 may be readily observed experimentally, there are substantial theoretical difficulties in considering the actual breakdown process. It is possible to numerically compute the solution in the boundary layer up to and beyond the time of separation in the case illustrated in figure 6; however once the separation bubble begins to grow significantly in the direction normal to the cylinder, formidable difficulties are encountered in continuing the numerical integrations with good accuracy (see for example, Belcher et al. [38]). There is persuasive evidence in the numerical integrations reviewed by Riley [1] that the Proudman-Johnson model describes the boundary-layer flow at large times in the case of the circular cylinder. However, in theory it is necessary to compute the boundary-layer solution to large times in order to consider the ultimate breakdown problem and to date this has not been possible. At present there has been no successful rational treatment of the breakdown problem in any situation where a separating unsteady boundary layer ultimately interacts with the outer inviscid flow. At present it has only been possible to calculate solutions in the boundary layer at relatively early times. However the character of these solutions gives some insight as to the type of boundary layer breakdown that should be expected and it is then possible to speculate on the nature of the inviscid-viscous interaction that will eventually follow with the outer flow.

In the present paper, the numerical integrations strongly suggest that for all cases considered, breakdown of the boundary-layer flow induced by the vortex motion will occur. The nature of the flow in the case of vortex motion is similar in some respects to the bluff body situations sketched in figures 6 and 7 but with two important differences. First in the case of vortex motion the events which ultimately lead to breakdown, develop and take place in a frame of reference which convects uniformly with the vortex. In the second place, in the situation illustrated in figure 6 the growing region of reversed flow is expected to lead to breakdown wherein the erupting boundary layer simply displaces the outer inviscid flow; in figure 7 the eruption is expected in a direction which at any stage is

approximately the same as the direction of the local inviscid flow. In the case of a vortex motion, the events which are expected to lead to breakdown are somewhat localized and the eruption is expected to take place into a crossflow in the inviscid region in the convected reference frame. Consequently the ultimate breakdown in the case of vortex motion is believed to be somewhat more complex and violent than in the classical separation depicted in figure 6, possibly leading to a roll-up phenomenon in which another vortex is created.

Finally it is important to mention a third possibility other than the two sketched in figures 6 and 7 regarding boundary-layer breakdown. Sears and Telionis [39] have postulated what they intend to be a general model of unsteady laminar separation; this model is known as the Moore-Rott-Sears model and is discussed in references [1], [28] and [40]. The model is based on the conviction that a singularity develops in the solution of the boundary-layer equations at finite time in all cases of unsteady separation. In the Moore-Rott-Sears model the term boundary-layer separation is reserved for the phenomenon we have termed breakdown. In the present paper, we shall adopt the classical definition of boundary-layer separation and the term separation is understood to imply the first appearance of a closed recirculating eddy in the boundary-layer flow. It should be noted that for any situation described by the Proudman-Johnson model [32], breakdown occurs explosively as the boundary layer thickens exponentially but only in the limit $t \to \infty$; on the other hand in any case of breakdown described by the Moore-Rott-Sears model [39], breakdown will occur much more abruptly. This is because if a singularity begins to develop at finite time, the outer inviscid flow must begin to respond in such a way so that a singularity in the boundary-layer solution never occurs.

3.2 THE CONVECTED VORTEX

In the study by Doligalski and Walker [30], the case of a vortex held stationary in a crossflow ($\alpha = 0$) has been considered; in this case boundary-layer separation occurs a short time after the insertion of the plate in the flow. This separation is in the form of an eddy attached to the wall and occurs in the region between the trailing stagnation point at $\xi = 1.67$ and the vortex center at $\xi = 1$. After the flow in the boundary layer separates, the separated bubble grows in a direction tangential and normal to the wall. Once the normal growth of the eddy becomes significant, eventually a point is reached in the numerical integrations where the calculations could not be continued further; the reasons for the failure of the numerical calculations are believed to be similar to those discussed in reference [28]. Moreover the results are suggestive that an eruption of the boundary-layer flow should be expected. Because the eddy created in the boundary layer is of positive rotation it might be anticipated that one modification to the inviscid flow in this case is that the parent vortex will be displaced and driven away from the wall as is the case for the problem treated in [28].

In reference [30], a number of cases corresponding to a convected rectilinear vortex of negative rotation were considered. Here only a brief summary of the results and calculation procedure can be given and complete details may be found in [30]. An unsteady stream function $\psi(\xi,y,t)$ is defined in terms of the velocity components (u,v) in the frame of reference convecting with the vortex according to,

$$u = \frac{\partial \psi}{\partial y} , \quad v = \frac{1}{2\pi} U_e(\xi) \frac{\partial \psi}{\partial \xi} , \tag{9}$$

where $U_e(\xi) = 2(1 - \cos \pi\xi)$. Rayleigh variables are defined by,

$$\eta = \frac{y}{2\sqrt{t}} , \quad \psi = 2\sqrt{t}\, \Psi(\xi,\eta,t) , \tag{10}$$

and the boundary layer equations (5) become

$$\frac{\partial^3 \Psi}{\partial \eta^3} + 2\eta \frac{\partial^2 \Psi}{\partial \eta^2} - 4t \frac{\partial^2 \Psi}{\partial \eta \partial t} = 4t \left[- 2 \sin \pi\xi (1 - \cos \pi\xi) - \frac{U_e(\xi)}{2\pi} \frac{\partial \Psi}{\partial \eta} \frac{\partial^2 \Psi}{\partial \xi \partial \eta} + \frac{U_e(\xi)}{2\pi} \frac{\partial \Psi}{\partial \xi} \frac{\partial^2 \Psi}{\partial \eta^2} \right] . \tag{11}$$

The boundary conditions on the wall and at the mainstream are respectively:

$$\Psi(\xi,0,t) = 0 , \quad \frac{\partial \Psi}{\partial \eta} (\xi,0,t) = - \beta , \tag{12}$$

and

$$\frac{\partial \Psi}{\partial \eta} (\xi,\eta,t) \to 2 \cos \pi\xi - 1 \quad \text{as} \quad \eta \to \infty . \tag{13}$$

Recall here that the parameter β is related to the fractional convection rate α by $\beta = \alpha/(1 - \alpha)$. As $\xi \to 0,2$ the right side of equation (11) vanishes and the solution satisfying conditions (12) and (13) is

$$\frac{\partial \Psi}{\partial \eta} = - \beta + (1+\beta) \operatorname{erf} \eta . \tag{14}$$

The boundary layer solution at infinity given by equation (14) may be interpreted as follows. At upstream and downstream infinity (corresponding to $\xi = 0$ and 2 respectively) the inviscid mainstream velocity in the convected frame is unity because of the normalization used to define the dimensionless variables in equation (4). Once the plate is inserted in the flow it appears to move to the left with velocity $-\beta$ in the convected frame; thus the situation at upstream and downstream infinity is analogous to a vortex sheet flow. The boundary layer solution given by equation (14) provides the smooth transition in the boundary layer between the left moving plate and right moving uniform flow. This boundary-layer solution is a typical Rayleigh-type flow and the boundary layer at infinity thickens continuously and in proportion to $\sqrt{t}$ upon insertion of the plate.

To obtain the proper initial conditions, an exact solution of equations (11), which is valid for small time, may be calculated by

writing the solution as a power series in time according to,

$$\Psi = \Psi_0(\xi,\eta) + t\Psi_1(\xi,\eta) + \ldots \quad . \tag{15}$$

This procedure is well known and will not be discussed in detail here. The solution for the first term in equation (15) is

$$\frac{\partial \Psi_0}{\partial \eta} = -\beta + (\beta + 2\cos\pi\xi - 1)\operatorname{erf}\eta \quad , \tag{16}$$

which describes the initial solution at $t = 0^+$ for all ξ and η. The solution for Ψ_1 is given in reference [30].

Equation (11), with boundary conditions given by equations (12) and (13) at $\eta = 0$ and as $\eta \to \infty$ respectively and equation (14) at $\xi = 0,2$, defines the nonlinear parabolic problem to be solved for various values of the parameter β. The initial velocity field at $t = 0^+$ is described by equation (16) for all ξ and η and starting from this initial solution, equation (11) may be integrated numerically forward in time. Calculations were carried out in this manner; however it eventually proved convenient to write the velocity as a linear combination of the Rayleigh flow at infinity plus a term due to the disturbing vortex motion according to,

$$\frac{\partial \Psi}{\partial \eta} = U_R(\eta) - U_e(\xi)U(\xi,\eta) \quad , \tag{17}$$

where

$$U_R(\eta) = -\beta + (1+\beta)\operatorname{erf}\eta \quad . \tag{18}$$

The boundary conditions for $U(\xi,\eta)$ follow from equations (12) and (13) and are,

$$U(\xi,0) = 0 \quad , \quad U(\xi,\eta) \to 1 \quad \text{as} \quad \eta \to \infty \quad . \tag{19}$$

One motivating factor for the transformation (17) is that the variable U varies from 0 at the wall to 1 at the boundary-layer edge; consequently U may be interpreted as a normalized velocity which is convenient for computational purposes.

3.3 THE NUMERICAL METHOD

A rectangular grid in the (ξ,η) plane was defined with uniform mesh spacings in the ξ and η directions denoted by h_1 and h_2 respectively; in all cases h_1 was selected so that mesh lines were located at the ξ stations $\xi = 1/3$ and $5/3$ which correspond to the streamwise locations of the leading and trailing relative stagnation points, respectively. The last of conditions (19) must be enforced at some large but finite value of η, say $\eta = \ell$, as an approximation and ℓ must be increased until there is no significant change in the solution at any value of t. Throughout the early stages of the integrations, for each value of β, a value of $\ell = 6$ was found to be adequate. In all cases, substantial boundary-layer growth was eventually observed in the vicinity of the trailing relative stagnation point and it was necessary to increase ℓ to 8 and in some cases larger values in the

latter stages of the integrations.

Equation (11) with the transformation (18) is of the form

$$4t \frac{\partial U}{\partial t} = \frac{\partial^2 U}{\partial \eta^2} + P \frac{\partial U}{\partial \eta} + RU + Q \frac{\partial U}{\partial \xi} + \Gamma , \qquad (20)$$

where the coefficients P, R, Q and Γ are functions of U, w and ξ and η. A Crank-Nicolson scheme which is essentially the same as that described in reference [28] was used to advance the solution in time.

A number of different mesh sizes and time steps were used as a check on the accuracy and agreement between successive solutions was excellent. In the initial phases of the motion, variations with time are relatively large and a small time step k was used. The time step k was progressively increased from k = 0.001 to 0.025 at t = 0.025 and held constant through the balance of the integration as described in [28]. As a check on the accuracy two sets of mesh sizes for (h_1, h_2) were used corresponding to (0.0167, 0.1) and (0.0111, 0.0667).

In the latter stages of the integrations, substantial difficulties were encountered in continuing the numerical procedure. In some of the cases, flow separation occurs within the boundary layer and similar difficulties were encountered as described in reference [28]. In all cases considered, intense variations in the flow field ultimately develop in the range $1.67 < \xi < 1.0$ and eventually the numerical scheme based on the standard Crank-Nicolson scheme failed to converge. This is a well known difficulty which has been experienced in many other unsteady boundary layer problems (see for example reference [38]).

The basis of the standard Crank-Nicolson scheme is illustrated schematically in figure 8. Here we use the Southwell notation to label a typical point in the (ξ,η) mesh by 0 and surrounding points by 1, 2, 3 and 4 in the current time plane at t. The corresponding points in the previous time plane at t-k are labeled with a Γ risks and on this time plane the solution is assumed known. The partial differential equation (20) is approximated at the midpoint of the time planes at the point labeled 0^{**} in figure 8. In the standard Crank-Nicolson scheme the term $Q\partial U/\partial\xi$, for example, is evaluated at 0^{**} and a simple average is taken along the line labeled (a) in figure 8, to obtain

$$Q \left.\frac{\partial U}{\partial \xi}\right|_{0^{**}} = \frac{Q_0^{**}}{2} \left\{ \left.\frac{\partial U}{\partial \xi}\right|_0 + \left.\frac{\partial U}{\partial \xi}\right|_{0^*} \right\} . \qquad (21)$$

Here the subscripts and asterisks denote the point of approximation of the appropriate terms. The simple average in equation (21) is second-order accurate in the time step k. To evaluate the coefficient Q_0^{**}, which contains values of the dependent variables, simple averages are used so that the dependent variables are evaluated at points in the mesh. At this stage the derivatives in equation (21) are approximated by central differences in the appropriate time plane; for example

$$\left.\frac{\partial U}{\partial \xi}\right|_0 = \frac{U_1 - U_3}{2h_2} + O(h_2^2) . \qquad (22)$$

As indicated previously, in the latter stages of the integrations difficulties were experienced in continuing the numerical integrations using this type of method; consequently an alternate forward-backward differencing scheme was used. This method is similar to a scheme developed by Cebeci [41] in the calculation of flow past an implusively started circular cylinder. It will also be seen that the method of differencing is similar to a technique used in an algorithm known as "MacCormack's method" for inviscid supersonic flow calculations (see for example [42], [43]). The main feature of this forward-backward method affects only the evaluation of the terms $P\partial U/\partial\eta$ and $Q\partial U/\partial\xi$ in equation (20). Here the main features of the method for the term $Q\partial U/\partial\xi$ will be sketched; the details for $P\partial U/\partial\eta$ are easily inferred from this discussion.

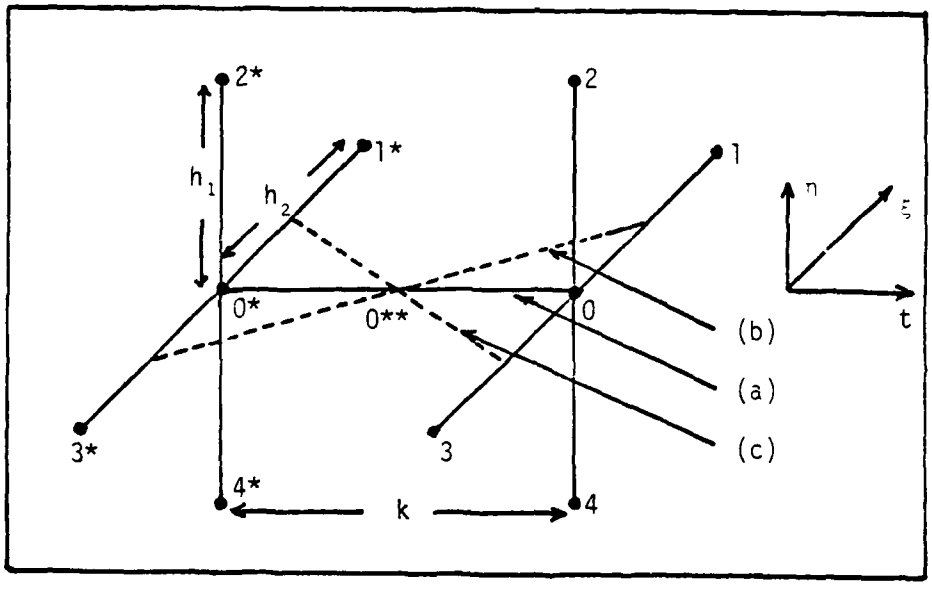

Figure 8. Schematic diagram of grid structure at a typical mesh point 0 in the (ξ,η) plane; see text for explanation of labels.

For the evaluation of $Q\partial U/\partial\xi$ at the point 0**, it can be shown that an average along a line passing through the point 0** is second order accurate in the time step k. In particular consider the lines labeled (b) and (c) in figure 8 which intersect the lines connecting mesh points 0 and 1 and 0 and 3 at the midpoints respectively. The $\partial U/\partial\xi$ term may then be approximated on the appropriate time plane with second order accuracy in h_2. The choice of line (b) or line (c) is dictated by the sign of the current value of Q_0^{**}, if $Q_0^{**} > 0$, the following difference approximation for $Q\partial U/\partial\xi$ at the point 0** is used,

$$\frac{Q_o^{**}}{2}\left\{\frac{U_1-U_o}{h_2}+\frac{U_o^*-U_3^*}{h_2}\right\} \quad . \tag{23}$$

On the other hand if $Q_o^{**} < 0$, the difference approximation used is,

$$\frac{Q_o^{**}}{2}\left\{\frac{U_o-U_3}{h_2}+\frac{U_1^*-U_o^*}{h_2}\right\} \quad . \tag{24}$$

The similarity of this method to a technique known as upwind-downwind differencing should be noted; however the approximations in (23) and (24) are second order accurate in both k and h_2. It may be inferred that the matrix problem associated with this method of differencing is always diagonally dominant.

To test the alternate differencing scheme, calculations were carried out in the early stages of the motion using both methods and the results were virtually identical. However an important feature of the alternate method is that it was possible to extend the numerical integrations to larger times, beyond the point where the standard Crank-Nicolson method failed to converge.

3.4 CALCULATED RESULTS

In reference [30] calculations were carried out the the cases $\alpha = 0$, 0.2, 0.4, 0.55, 0.7, 0.75 and 0.80. Here some results for two representative cases ($\alpha = 0.4$ and $\alpha = 0.8$) will be presented and the results for other cases in [30] summarized.

In order to plot the instantaneous streamlines, the stream function ψ is defined by equation (10) and consequently a plot of lines of constant Ψ gives the instantaneous streamlines; in the subsequent figures the labels correspond to constant Ψ values. It is worthwhile to emphasize that the streamline patterns that will be presented here are relative to the vortex and thus the vortex is towing the developing boundary-layer patterns as it moves along the plate. The subsequent plots are given in the (ξ,η) plane which is convenient to illustrate the flow patterns over the entire range from upstream to downstream infinity. Note however that in this plane, because of the transformation (8) there is a distortion of the flow patterns corresponding to a relative compression of the far field flow and an exaggeration of the region below the vortex.

In figures 9(a), 9(b), 9(c) and 9(d) the boundary-layer development for the case $\alpha = 0.4$ is illustrated. In figure 9(a) the instantaneous relative streamline patterns are plotted at $t = 0.2$, where the direction of relative flow is indicated by arrows. For $0 < \xi < 0.33$ the motion in the upper portion of the boundary layer is downward and toward upstream infinity. The streamline labeled -0.12 in figure is a limiting streamline emanating from near the inflow stagnation point and proceeding to upstream infinity; on the lower branch of this limiting streamline the direction of flow is to the left all the

way to downstream infinity at $\xi = 2.0$. Below the lower branch of this limiting streamline all flow is to left and the arrows on the wall emphasize the fact that the wall is moving to the left in the convected coordinate system. For $2 < \xi < 1.67$ the flow on the upper branch of the limiting streamline as well as for all streamlines above is upward toward the trailing relative stagnation point. Between the inviscid stagnation points, $0.33 < \xi < 1.67$, the flow patterns are characterized by downflow near the leading relative stagnation point at $\xi = 0.33$ and subsequent upflow near the trailing stagnation point at $\xi = 1.67$. The flow pattern is almost symmetrical and this behavior is typical of all values of α in the early stages of development of the boundary layer.

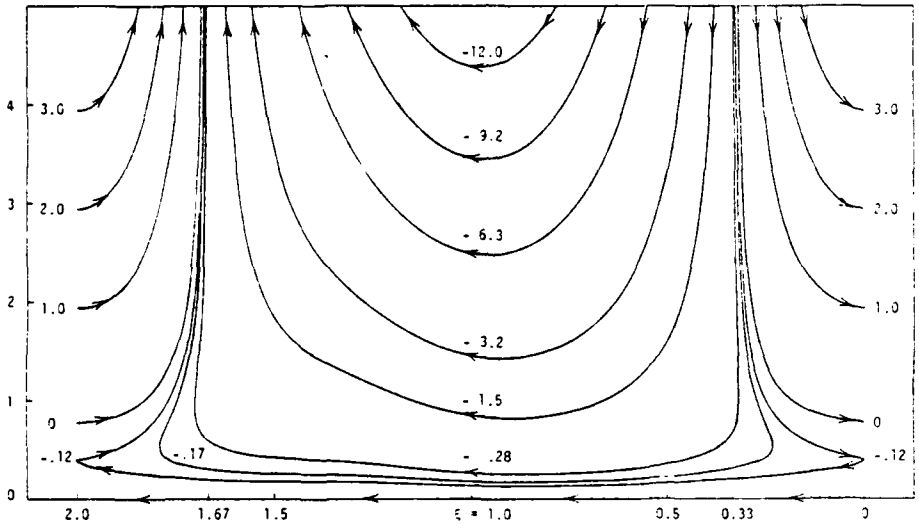

Figure 9(a). Instantaneous streamlines in the boundary layer relative to the vortex for $\alpha = 0.4$ at $t = 0.2$. (Labels correspond to lines of constant Ψ.)

In figure 9(b) the flow patterns in the convected frame are plotted at $t = 0.4$ for $\alpha = 0.4$. It may be observed that near the vicinity of the trailing relative stagnation point the streamlines are developing a kink. This feature of the flow is typical for all values of $\alpha < 0.75$; this behavior may be explained as follows. For $\alpha < 0.75$, the speed of the wall to the left $\beta = \alpha/(1 - \alpha)$ is less than 3; however in the defined dimensionless coordinates the maximum inviscid velocity at $\xi = 1.0$ is -3 to the left which is greater in magnitude than the wall speed. Consequently, the net effect of this larger inviscid velocity is to lift the relative streamlines up and may be thought of as a reaming and lifting action by the vortex on the boundary layer; however as the trailing relative stagnation point is approached from the left the magnitude of the inviscid velocity decreases and the moving wall acts to drag the fluid to the left.

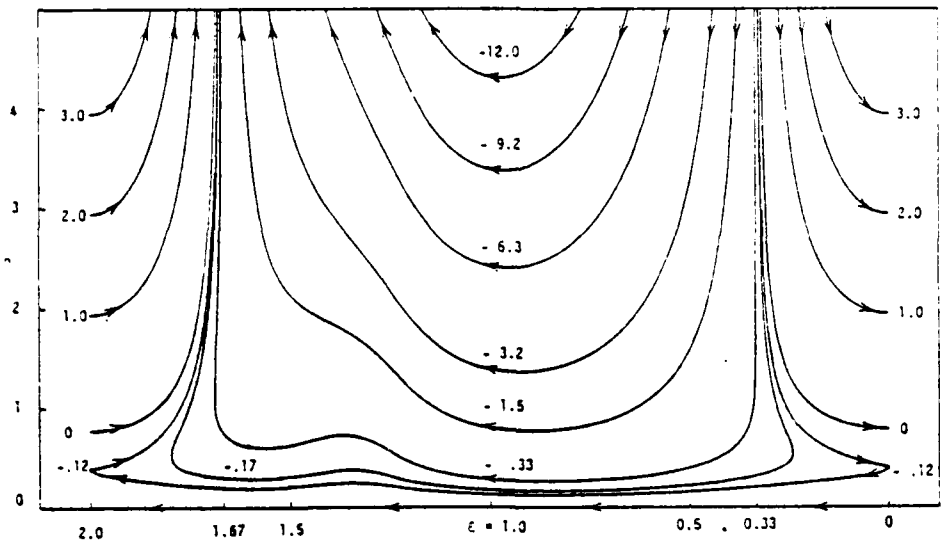

Figure 9(b). Instantaneous streamlines in the boundary layer relative to the vortex for $\alpha = 0.4$ at $t = 0.4$. (Labels correspond to lines of constant Ψ.)

In figure 9(c) the relative streamlines are plotted at $t = 0.6$ where it may be observed that separation has occurred in the form of a closed recirculating eddy in the flow field. There are two stagnation points associated with the eddy: one at the eddy center and one on the limiting streamline labeled -0.07 defining the eddy edge. It may be observed that the eddy has appeared in the pocket that was observed forming between the kinking streamlines in figure 9(b) in the region $1.0 < \xi < 1.67$. The time-dependent development of the eddy is typical of that observed in the classical separation problems involving bluff bodies. The eddy rapidly grows in the tangential direction and then a period of accelerated and rapid growth in a direction normal to the wall ensues. Note that the growing eddy increasingly pushes up the limiting streamline labeled -0.12.

Shortly after $t = 0.6$ the standard Crank-Nicolson procedure failed to converge and the calculations could only be carried further in time using the forward-backward differencing scheme described in §3.3. Eventually this scheme fails to converge as well at around $t = 0.775$. The reason for the failure of the numerical procedure is evident from figure 9(d) where the instantaneous streamlines are plotted at $t = 0.7$. The streamlines near the right edge of the eddy and throughout the field upward have begun to develop a spike-like behavior. This same type of behavior was noted in the terminal stages of the integrations reported in [28] where various attempts using forward-backward differencing were used to extend the integrations to higher times. The streamline behavior illustrated in figure 9(d) is suggestive of the early stages of the development of a singular behavior in the boundary

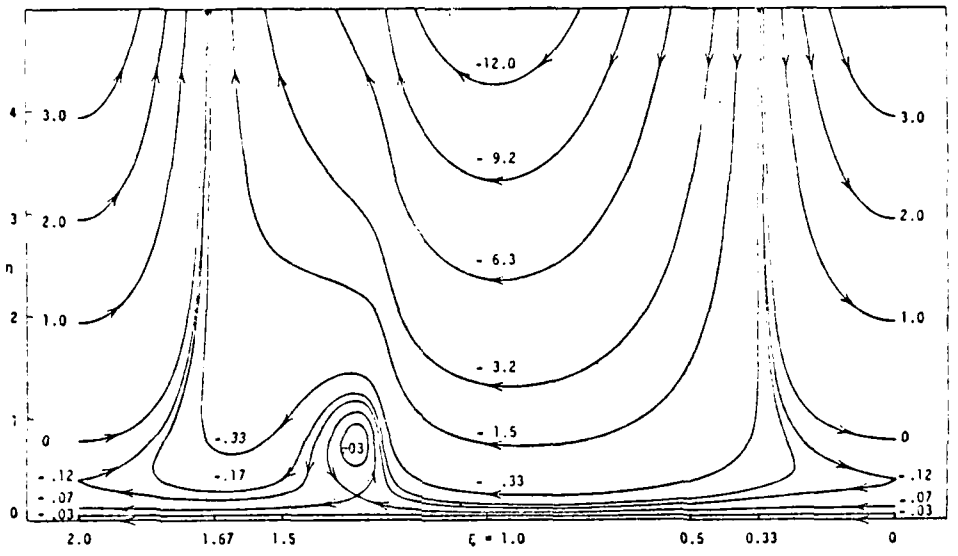

Figure 9(c). Instantaneous streamlines in the boundary layer relative to the vortex for $\alpha = 0.4$ at $t = 0.6$. (Labels correspond to lines of constant Ψ.)

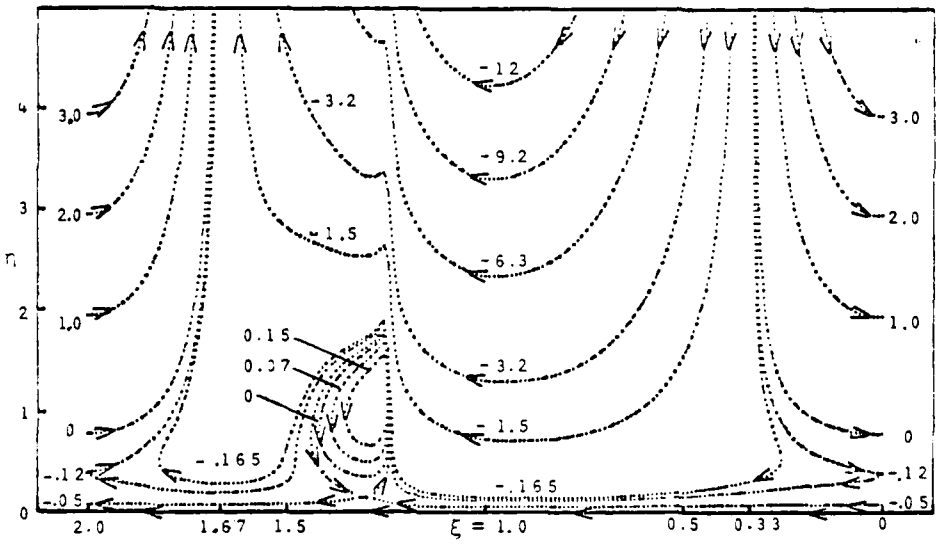

Figure 9(d). Instantaneous streamlines in the boundary layer relative to the vortex for $\alpha = 0.4$ at $t = 0.7$. (Labels correspond to lines of constant Ψ.)

layer solution. At the stage of the integrations in figure 9(d) the outer boundary was $\eta = 8$ and this value appears adequately large in the calculations; for this reason it does not appear that the thickening boundary layer near the eddy is the major problem in continuing the integrations. The major problem with continuing the integrations appears to be associated with the developing intense variation in the flow field near the right edge of the eddy. The calculations were carried out using a CDC 6500 and at the point of termination of the integrations there were approximately 22,000 points in the mesh. Because of core limitations the mesh could not be reduced further; thus it is possible but not likely that the apparently developing singular behavior in figure 9(d) is a symptom of numerical error. It is also possible that a singular behavior is truly developing although it would be premature to claim anything more than this.

Although the nature of the large time solution for the boundary layer is not known, it may reasonably be concluded that a breakdown will occur for $\alpha = 0.4$ and it is possible to speculate on the nature of the breakdown. It appears likely that in the moving reference frame, a boundary-layer eruption will occur to the right of the trailing relative stagnation point. Note that the eddy in figure 9(c) is of positive rotation and it might be expected that one effect of the growing eddy will be to drive the parent eddy (which is of negative rotation) away from the wall. However if the spawned eddy in the boundary layer does emerge intact from the boundary layer it is also worthwhile to note that the ejection will take place into a relative crossflow (see figure 4) and some type of roll-up behavior into a more complex eddy structure might be anticipated.

Whether or not the separated eddy in the boundary layer is rolled up into a more complex multi-celled eddy as it is ejected from the boundary layer, for all cases $\alpha < 0.75$, is not known; presumably this depends on the size and strength of the eddy in the boundary layer. In reference [30] a complete description of the calculations in the range $\alpha < 0.75$ is given. The boundary-layer eddy always appears in the range $1.67 < \xi < 1.0$ and has maximum tangential dimensions at the lower values of α. As α increases the size of the eddy decreases and it moves progressively closer to the streamwise location of the trailing relative stagnation point. In the case $\alpha = 0.55$ the streamwise dimensions of the boundary-layer eddy are very small. In the case $\alpha = 0.7$ no separation was observed to occur; however a pronounced kinking of the streamlines occurs near the trailing relative stagnation point.

For $\alpha \geq 0.75$ a dramatic change occurs in the flow; in these situations $\beta > 3$ and the wall moves at a rate to the left which is faster than the maximum inviscid velocity near the wall of -3. For these cases no kinking of the streamlines occurs and a representative example is $\alpha = 0.8$ at $t = 1.1$ which is illustrated in figure 10. In the cases for $\alpha \geq 0.75$ substantial boundary-layer growth always occurs near the trailing relative stagnation point; in these cases the boundary-layer integrations could be continued for relatively long times provided the outer boundary $\eta = \lambda$ was moved to progressively large values as

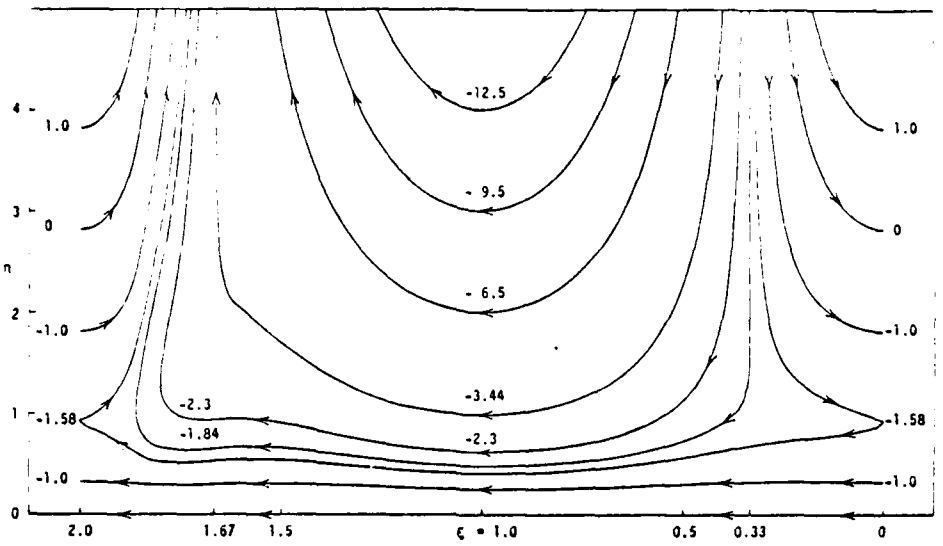

Figure 10. Instantaneous streamlines in the boundary layer relative to the vortex for $\alpha = 0.8$ at $t = 1.1$. (Labels correspond to lines of constant Ψ.)

the integration proceeded.

The boundary-layer growth is not readily apparent in the streamline patterns in figure 10 for $\alpha = 0.8$; to illustrate this feature of the flow a conventional displacement thickness is defined with respect to the velocity in the laboratory frame according to

$$\delta^* = \int_0^\infty \left\{ 1 - \frac{(u+\beta)}{2\cos \pi\xi - 1 + \beta} \right\} dy \ . \qquad (25)$$

The time dependent development of δ^* is plotted in figure 11 where the accelerated boundary layer growth near the trailing relative stagnation point should be noted. The displacement effect illustrated in figure 11 corresponds to the effect that an observer in the laboratory frame would see at fixed values of time. It is interesting to note that in the laboratory frame the effect could be interpreted as a moving wave of growing amplitude although whether this is a useful interpretation is questionable.

Preliminary experiments in the water channel at Purdue by Prof. C. R. Smith have confirmed the general features of the displacement thickness effect illustrated in figure 11. These experiments will be reported elsewhere but the main ideas and preliminary results will be summarized here as follows. A two dimensional vortex was created by abruptly tilting an airfoil which was located upstream of a flat plate

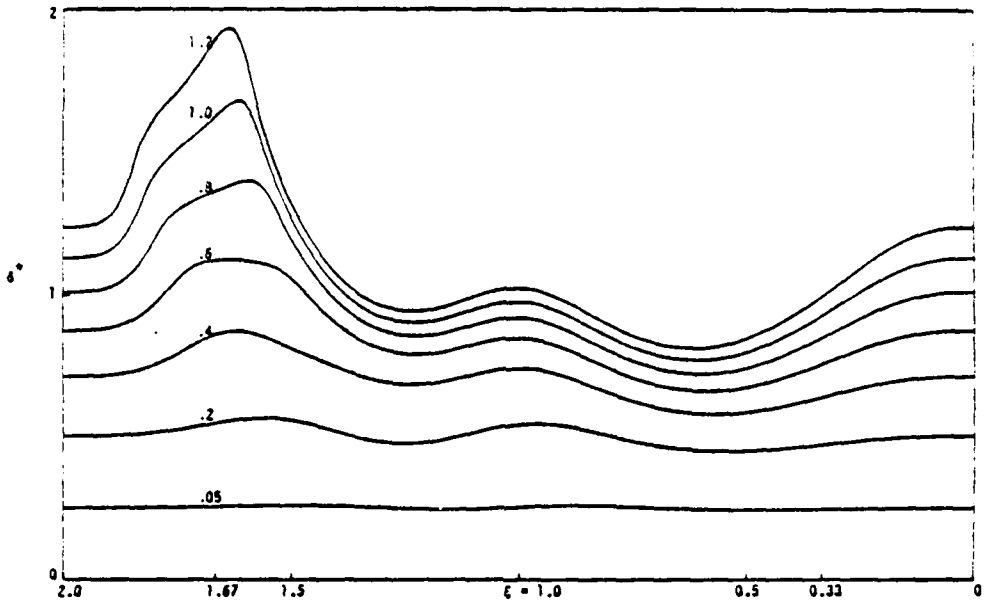

Figure 11. *Temporal development of displacement thickness for* $\alpha = 0.8$. (Labels correspond to values of t.)

in the water channel at Purdue. The effect of the vortex on the boundary layer was then observed as the vortex passed over the flat plate; the flow visualization was carried out using hydrogen bubble wires and in a convected reference frame as reported in [18]. To date it has only been possible to create a relatively well controlled two-dimensional vortex which is somewhat weak and which convects at about 95% of the mainstream speed above the plate. In every case, an upwelling was observed from the boundary layer and behind the vortex in accordance with the present theory. As time increased the upwelling behind the vortex became more pronounced and eventually a phenomenon, which appeared to be a roll-up into another vortex structure, was observed; in the television pictures taken in the convected reference frame, this phenomenon appeared to resemble the cresting and breaking of an ocean wave. Once the roll-up occurs the inviscid flow above the plate is significantly altered and while the cited experiments are as yet of a preliminary nature, the correspondance with the present theory (and the conjectures made in regard to the ultimate nature of the proposed inviscid-viscous interaction) is very encouraging.

4. DISCUSSION

In view of the results of §3.4 and reference [30], it is reasonable to conclude that the laminar unsteady boundary layer induced by a convected vortex will not remain passive but will eventually react in

such a way that an interaction will eventually occur with the outer flow for any convection speed. For a rectilinear line filament a critical value corresponds to the situation when the convection speed of the vortex is 75% of the uniform flow speed. For convection rates such that $\alpha < 0.75$, a kinking always occurs in the streamline patterns near the streamwise location corresponding to the position of the trailing relative stagnation point in the convected reference frame. At the lower values of $\alpha \leq 0.55$ a separation phenomenon was observed to initiate near the wall and eventually grow in the direction normal to the wall; the eddy created in the boundary layer is of positive rotation. As α increases the relative width of the separation zone diminishes and at $\alpha = 0.7$ no separation was observed. In view of the difficulties discussed in §3.1 associated with consideration of the actual breakdown problem, we are unable at present to consider the ultimate inviscid-viscous interaction which we believe will occur with the outer flow in all cases. However it is possible to speculate on what should eventually transpire. It seems possible that for the lower values of α, the eddy created in the boundary-layer flow may eventually emerge from the boundary layer intact; because the spawned eddy is of positive rotation one effect may be that the parent vortex will be driven away from the wall. As α approaches 0.75 the width of the region (where events are taking place that are expected to lead to a penetration of the inviscid region) narrows and the width of the positive rotation eddy created in the boundary layer decreases. For these latter values of α it is possible that the relatively narrow band of upwelling fluid from the boundary layer is rolled up into another vortex structure. It is well known that the injection of a finite slug of fluid into an otherwise stagnant fluid can lead to the formation of a vortex ring. It is possible that if such an ejection occurs in a frame convecting with the parent vortex, that some type of more complex vortex creation would occur; in this case the created vortex would be of negative rotation. For $\alpha > 0.75$, the development of the boundary-layer flow is somewhat more gradual but again substantial thickening of the boundary layer occurs. In these cases there is a tendency for the flow to develop into a jet-like behavior near the trailing relative stagnation point. This is similar in some respects to the breakdown phenomenon illustrated in figure 7. In these cases, a roll-up phenomenon is also expected and the experiments discussed in §3.4 support this idea. Finally it is important to note that it is only possible to properly perceive the phenomena discussed in this paper in the convected reference frame; streamline patterns in the laboratory frame have been given in reference [30] and these tend to be somewhat misleading insofar as interpretation of events transpiring within the boundary layer is concerned.

The rectilinear line filament represents one limit of inviscid flow with vorticity in which the vorticity is concentrated in a very localized region. For two dimensional vortex motions, it is natural to inquire whether the phenomena described in this paper are peculiar to only the rectilinear vortex. Batchelor [44], p. 534 has described the other possible limit of two dimensional vortex motion in which the vorticity is distributed over a finite area in the inviscid flow. Let (r,θ) be polar coordinates measured from an origin on an infinite

plane wall and define a stream function in terms of the corresponding velocity components (u_r, u_θ) by $u_r = r^{-1}\partial\psi/\partial\theta$, $u_\theta = -\partial\psi/\partial r$. A solution of the inviscid equations which has the zero vorticity for $r > b$ and is proportional to ψ for $r < b$ is given by

$$\begin{aligned} \psi &= V\left(r - \frac{b^2}{r}\right)\sin\theta \qquad \text{for} \quad r > b\,, \\ &= \frac{2VJ_1(kr)}{kJ_0(kb)}\sin\theta \qquad \text{for} \quad r \leq b\,. \end{aligned} \tag{26}$$

Here J_1 and J_0 are Bessel functions and $k = \lambda_i/b$ where λ_i is the ith zero of the Bessel function J_1. This inviscid solution represents a vortex flow embedded in a uniform flow having speed V at infinity with vorticity spread out over a finite area, namely the half-circle $r = b$.

If the wall is now imagined to move to the left, an observer on the wall would see a vortex of negative rotation convected to the right. A variety of solutions are possible corresponding to the particular value of λ_i. Consider the first zero given by $\lambda_1 = 3.8317$; the relative streamlines corresponding to this situation are plotted in figure 12. The location of the vortex center is at $r_0 = 0.480b$ and in preparing this figure the same scale was used as in figure 4 with r_0 being used to make lengths in equations (26) dimensionless. The inviscid flow patterns are essentially similar to that for the rectilinear vortex in figure 4. Insofar as the boundary-layer flow is

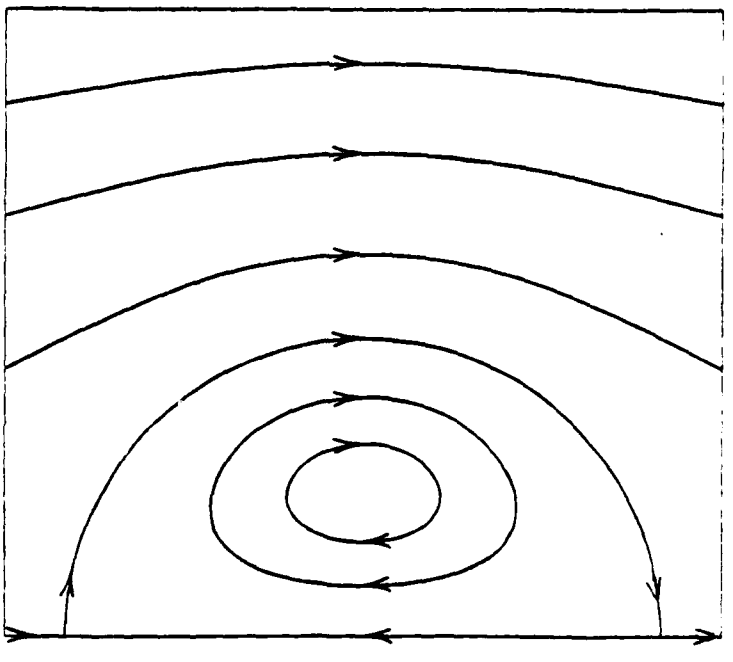

Figure 12. Relative streamlines in inviscid flow for vortex flow given by equation (26).

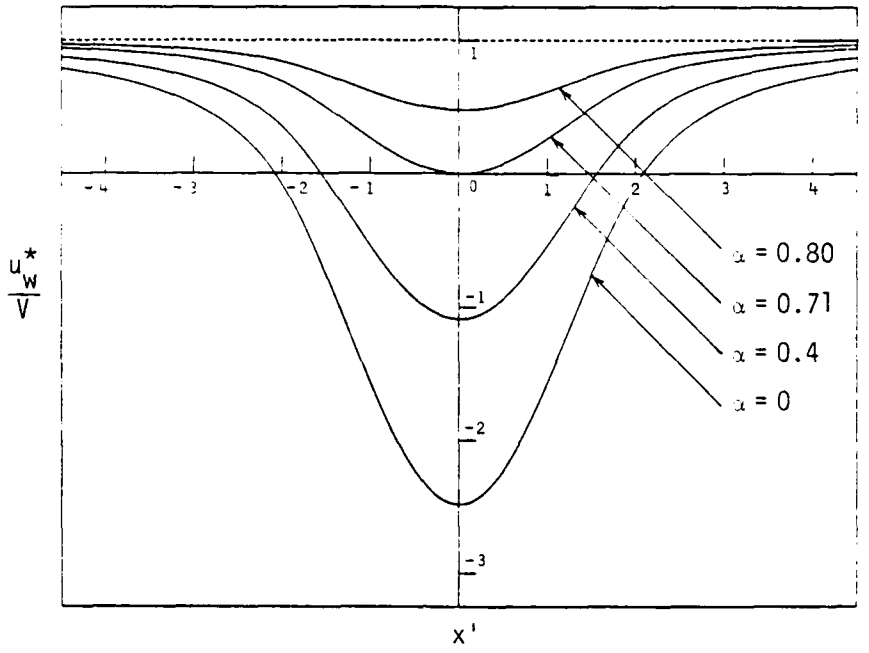

Figure 13. Streamwise velocity distribution in the inviscid flow in laboratory frame for vortex flow given by equation (26).

concerned, the relevant feature is the distribution of the inviscid velocity near the wall. This is sketched in figure 13 for various values of the relative convection rate; note the similarity to the analogous figure 5 for the rectilinear vortex. In this case the critical convection rate can be calculated as $\alpha = 0.713$ rather than 0.75 for the rectilinear filament. The effects of the vorticity are slightly more spread out than in the case of the rectilinear vortex with the stagnation points occurring at $x = \pm 2.09 r_0$ rather than $x = \pm 1.73a$ as in figure 4. Because of the close similarity of these two limiting cases the boundary-layer development for this type of single-celled vortex is expected to be similar to that of the rectilinear vortex.

For $\lambda_1 = \lambda_2 = 7.0156$ the double-structured vortex illustrated in figure 14 is obtained and more recirculation zones can be obtained by taking successively higher zeros of J_1. In the case illustrated in figure 14, the boundary-layer development is expected to be more complex because of the multiple stagnation points in the relative inviscid flow. However in view of the fact that two outflow stagnation points are present in the inviscid flow depicted in figure 14, it seems likely that the wall boundary layer will erupt in response to the vortex motion above it; however in this case the nature of the

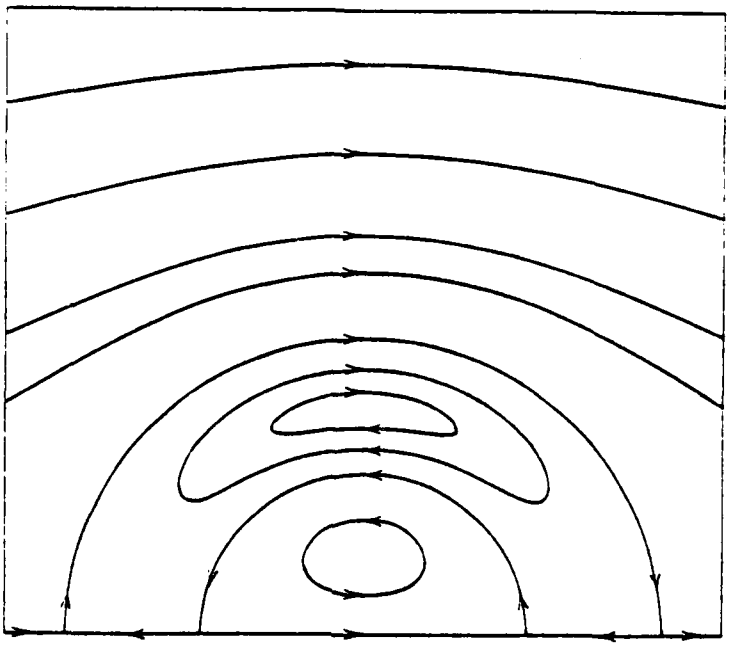

Figure 14. Relative streamlines in inviscid flow for distributed vortex flow given in equation (26) with $\lambda = \lambda_2$.

eruption will be more complex and will possibly occur at two locations.

In §1 of this paper we discussed why it would be desirable to develop an understanding of the nature of the flow due to a loop filament above an otherwise laminar boundary layer. At the very least this will give some insight as to the nature of the flow in the transition zone and possibly the flow in a turbulent boundary layer. It seems apparent from the results in this paper that a laminar boundary layer cannot remain intact when the inviscid flow contains convected two-dimensional vortices; eventually the boundary layer will respond to the motion of the vortex in such a way that eruption of the boundary layer occurs along with an inviscid-viscous interaction with the outer flow. Consideration of the loop filament in figure 1 is a more substantial theoretical problem; the inviscid flow due to such a structure is not well understood theoretically and because no analytic solution is available for the type of motion depicted in figure 1 it would be necessary to compute such an inviscid flow numerically. Even if it supposed that such an inviscid calculation could be carried out, the associated boundary-layer problem is at best difficult; due to the relatively large number of mesh points required in the present two-dimensional study to accurately describe the boundary-layer flow, the accurate calculation of the three-dimensional unsteady

flow due to the loop in figure 1 is a formidable problem.

At the same time on the basis of the results of this paper it is possible to make some speculations regarding the three-dimensional problem. In figure 15 the anticipated instantaneous streamline patterns due to a three-dimensional loop filament are sketched as viewed by an observer in a convected reference frame. As in figure 1 the vortex filament is shown as a solid line with the darkest portions of the closed loop indicating the locations of strongest vorticity and the sense of the vorticity is indicated as in figure 1. The three-dimensional inviscid streamlines near the wall are indicated by the broken lines with the direction of relative flow indicated by arrows. The instantaneous stream surfaces above the wall are indicated by the dotted lines and for simplicity only those in the foreground of the symmetry plane of the loop are sketched. An instantaneous relative stagnation point near the wall is expected and because the vorticity is strongest at the head (A) and weakens along the arms of the loop (B and C), the location of this instantaneous stagnation point is expected near the trailing portion of the loop at the point labeled O. Consequently, the zero stream surface is expected to be a tilted, lopsided umbrella-like surface; underneath this surface and above the wall a recirculating loop eddy motion is anticipated which is centered on the loop filament of vorticity. Because of the relatively weak vorticity near the trailing portion, the portion of the eddy in this region may be very difficult to observe experimentally. Near the point labeled E near the wall the maximum reverse acceleration occurs

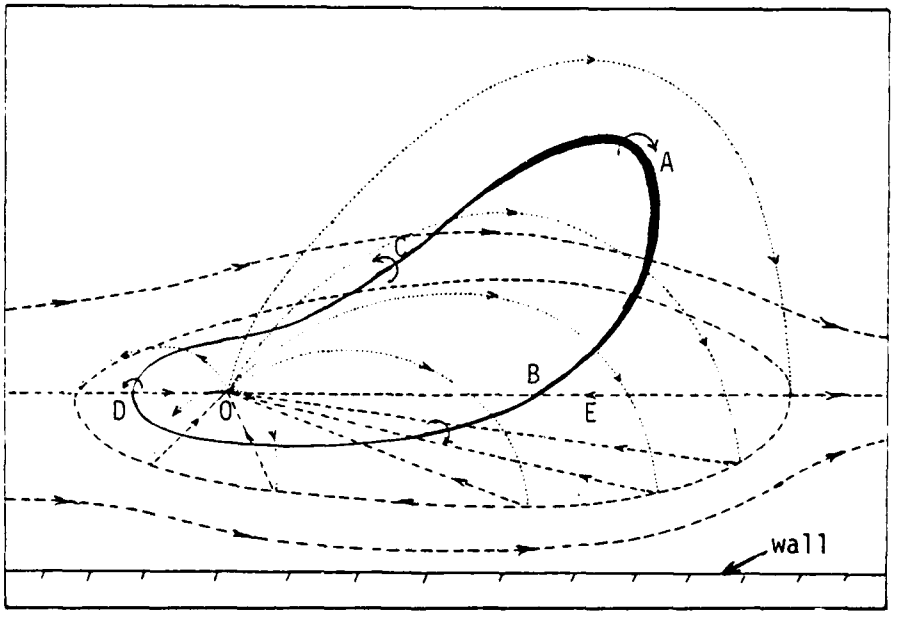

Figure 15. Intuitive sketch of instantaneous relative flow due to a loop filament of vorticity (see text for explanation of flow patterns).

in the symmetry plane of the loop. Of course the sketch in figure 15 is instantaneous; as time increases the distribution of vorticity will change as the loop stretches. Moreover, wave-like instabilities may well develop on the loop as it is convected downstream. However it is reasonable to expect that the stagnation point will move along the wall as well and be present at each instant.

It is worthwhile to emphasize that the sketch in figure 15 is intuitive and is the expected instantaneous streamline pattern that would be observed in a frame of reference which convects at or near the speed of the vortex head (labeled A in figure 15). One difficulty associated with the motion of the loop depicted in figure 15 is that all portions of the loop move at different speeds as the loop stretches and consequently the definition of a single convection speed which is characteristic of the loop is difficult (unlike the case for a two dimensional vortex). However it is reasonable to expect that the dominant effects of the loop are associated with the locations of strongest vorticity (the head A and the arms B and C). If the convection speed of the observer is at or near the convection speed of the vortex head, the zero stream surface should appear as in figure 15 but the orientation will vary as the convection speed is varied. It will be rather difficult to obtain a complete three dimensional picture of the flow associated with the loop in figure 15 using current experimental visualization techniques; for example hydrogen bubble wires produce a picture of the instantaneous flow in a plane and a plane parallel to the streamwise direction would cut the loop in such a manner that an observer would appear to see a transverse two-dimensional vortex. Finally it should be pointed out that the nature of the loop near D (the trailing portion) is conjectural but is believed to be realistic. In one other model [26], the vorticity distribution in a spot was inferred from the ensemble-averaged velocity measurements reported in [4]; presumably this inference was carried out by identifying significant deviations from the mean velocity with local regions of significant vorticity. However because strong upwelling occurs near the wall and behind the vortex head, it cannot legitimately be assumed that the vortex filament bends and ends on the wall as in [26]; this latter idea is the familiar concept of a horseshoe vortex which bends sharply toward the wall and joins its image at the plate. Because it is a theoretical impossibility for any vortex tube to end on a wall in any real fluid [25], the notion of a horseshoe vortex as a useful model for flow in a turbulent boundary layer or anywhere else should be abandoned. It is often remarked in defense of the horseshoe vortex that the model is inviscid and, since the inviscid equations permit a vortex tube to close on a wall, that the model is a reasonable approximation; however near any wall a viscous boundary layer will exist. If a vortex tube is imagined to enter the boundary layer, the manner in which the tube closes back on itself without crossing the wall needs to be explained; clearly such an explanation is difficult and for this reason the loop filament depicted in figure 15 is believed to be the most realistic vorticity distribution.

In any case, for a laminar boundary-layer flow below the vortex

structure depicted in figure 15, the upwelling toward the stagnation point 0 is believed to be an inherently unstable situation which will ultimately lead to breakdown of the boundary-layer flow. The lifting action of the vortex is expected to continually draw fluid from the boundary layer until the erupting fluid penetrates the inviscid flow near the instantaneous location of the point 0. We suggest that when this sequence of events occur, since the eruption takes place into a relative cross flow, a roll-up phenomenon could take place and another loop vortex would be created. There is some evidence that this type of regenerative process does occur in turbulent boundary layers. In the experiments of Smith [18], the flow due to vortex motion in a turbulent boundary layer was visualized using hydrogen bubble wires in a frame of reference convecting with a vortex structure in the outer layer. The upwelling and subsequent roll up was repeatedly observed to take place behind the head of the vortex structure. Again it should be pointed out that such a phenomenon will only be readily apparent in a convected reference frame.

The calculations presented in this paper are for a two-dimensional vortex and solutions for a three dimensional loop of vorticity must await further work. For such a loop filament of vorticity, vortex stretching is expected to play an important role in the inviscid dynamics of the loop; however a primary effect of vortex stretching would be to alter the convection speed of various portions of the loop. In the present paper we have demonstrated that at least a laminar boundary layer cannot withstand the massaging action of a two dimensional vortex convected at any speed; for this reason it appears rather unlikely that the effect of vortex stretching can negate the basic eruptive phenomena described in this paper. Finally it is worthwhile to point out that a vital feature of the proposed mechanism is that viscosity is important in triggering the eruptions of the wall layer although the ultimate interaction with the outer flow is probably inviscid in character.

Whether the physical mechanism proposed in this paper is the primary production process in a turbulent boundary layer is hypothetical at this point; we suggest this mechanism here as a reasonable possibility on the basis of the current theoretical and experimental evidence. The dynamics of the turbulent boundary layer are very complex and further research into the possibility suggested here is required.

ACKNOWLEDGMENT: The authors gratefully acknowledge support of this work by AFOSR under Grant Number 74-2707.

REFERENCES

[1] Riley, N., "Unsteady Laminar Boundary Layers", SIAM Review 17, pp. 274-297, 1975.

[2] Morkovin, M. V., Air Force Flight Dyn. Lab. Rep. AFFDL-TR-68-149, 1969.

[3] Reshotko, E., "Boundary Layer Stability and Transition", Ann. Rev. Fluid Mech. 8, pp. 311-349, 1976.

[4] Coles, D. & Barker, S. J., "Some Remarks on a Synthetic Boundary Layer", in Turbulent Mixing in Nonreactive and Reactive Flows, S. N. B. Murthy, ed., Plenum Press, pp. 285-293, 1975.

[5] Wygnanski, I., Sokolov, M. & Friedman, D., "On a Turbulent 'Spot' in a Laminar Boundary Layer", J. Fluid Mech. 78, pp. 785-819, 1976.

[6] Widnall, S. E. & Tsai, C., "The Instability of a Thin Vortex Ring of Constant Vorticity", Phil. Tran. Roy. Soc. Lond. A, 287, pp. 273-305, 1977.

[7] Hocking, L. M., Stewartson, K. & Stuart, J. T., "A Nonlinear Instability Burst in Plane Parallel Flow", J. Fluid Mech. 51, pp. 705-735, 1972.

[8] Kline, S. J., Reynolds, W. C., Schraub, F. A. & Runstadler, P. W., "The Structure of Turbulent Boundary Layers", J. Fluid Mech. 30, pp. 741-773, 1967.

[9] Willmarth, W. W., "Structure of Turbulence in Boundary Layers", Adv. Appl. Mech. 15, pp. 159-254, .

[10] Fendell, F. E., "Singular Perturbation and Turbulent Shear Flow Near Walls", J. Astro. Sci. 20, pp. 129-165, 1972.

[11] Mellor, G. L., "The Large Reynolds Number Asymptotic Theory of Turbulent Boundary Layers", Int. J. Engrg. Sci. 10, pp. 851-873, 1972.

[12] Yajnik, K. S., "Asymptotic Theory of Turbulent Shear Flows", J. Fluid Mech. 42, pp. 411-427, 1970.

[13] Cebeci, T. & Smith, A. M. O., Analysis of Turbulent Boundary Layers, Academic Press, New York, 1974.

[14] Walker, J. D. A. & Abbott, D. E., "Implications of the Structure of the Viscous Wall Layer", in Turbulence in Internal Flows, S. N. B. Murthy, ed., Plenum Press, pp. 131-167, 1977.

[15] Walker, J. D. A. & Scharnhorst, R. K., "Solutions of the Time-Dependent Wall Layer Flow in a Turbulent Boundary Layer", in Recent Advances in Engineering Science, G. C. Sih, ed., Lehigh University Press, pp. 541-552, 1977.

[16] Scharnhorst, R. K., Walker, J. D. A. & Abbott, D. E., "Comparisons of Theoretical Profiles for a Two-Dimensional Time-Mean Turbulent Boundary Layer With Experimental Data", CFMTR-77-1, School of Mechanical Engineering, Purdue University; also AFOSR-TR-77-0877, 1977.

[17] Nychas, S. G., Hershey, H. C. & Brodkey, R. S., "A Visual Study of Turbulent Flow", J. Fluid Mech. 61, pp. 513-540, 1973.

[18] Smith, C. R., "Visualization of Turbulent Boundary-Layer Structure Using a Moving Hydrogen Bubble-Wire Probe", Proc. Workshop on Coherent Structure in Turbulent Boundary Layers, C. R. Smith and D. E. Abbott, ed., Lehigh University, May, 1978.

[19] Weigand, G. G., "Forced Convection in a Two-Dimensional Nominally Steady Turbulent Boundary Layer", Ph.D. thesis, Purdue University, 1978.

[20] Landahl, M. T., "Wave Mechanics of Breakdown", J. Fluid Mech. 56, pp. 775-802, 1972.

[21] Landahl, M. T., "Wave Breakdown and Turbulence", SIAM J. Appl. Math. 28, pp. 735-756, 1975.

[22] Landahl, M. T., "Dynamics of Boundary Layer Turbulence and the Mechanism of Drag Reduction", Phys. Fluids 20, pp. S55-S63, 1977.

[23] Bark, F. H., "On the Wave Structure of the Wall Region of a Turbulent Boundary Layer", J. Fluid Mech. 70, pp. 229-250, 1975.

[24] Stewartson, K., "Some Aspects of Nonlinear Stability Theory", Fluid Dynamics Transactions, Vol. 7, pt. 1, Polish Academy of Sciences, Institute of Fundamental Technological Research, Warsaw, pp. 101-128, 1973.

[25] Lighthill, M. J., "Introduction. Boundary Layer Theory", in Laminar Boundary Layers, L. Rosenhead, ed., Oxford University Press, p. 51, 1963.

[26] Roshko, A., "Structure of Turbulent Shear Flows: A New Look", AIAA Journal 14, pp. 1349-1357, 1976.

[27] Leonard, A., "Numerical Simulation of Interacting, Three Dimensional Vortex Filaments", Proc. 4th Int. Conf. on Num. Methods in Fluid Dynamics, R. D. Richtmyer, ed., Springer Verlag, pp. 245-250, 1975.

[28] Walker, J. D. A., "The Boundary Layer Due to a Rectilinear Vortex", Proc. Roy. Soc. Lond. A 359, pp. 167-188, 1978.

[29] Harvey, J. K. & Perry, F. J., "Flowfield Produced by Trailing Vortices in the Vicinity of the Ground", AIAA Journal 9, pp. 1659-1660, 1971.

[30] Doligalski, T. L. & Walker, J. D. A., "The Boundary Layer due to a Convected Rectilinear Vortex", submitted for publication.

[31] Milne-Thomson, L. M., Theoretical Hydrodynamics, 4th ed., New York, MacMillan, 1960.

[32] Proudman, I. & Johnson, K., "Boundary Layer Growth Near a Rear Stagnation Point", J. Fluid Mech. 12, pp. 161-168, 1972.

[33] Leibovich, S., "Magnetohydrodynamic Flow at a Rear Stagnation Point", J. Fluid Mech. 29, pp. 401-413, 1967.

[34] Buckmaster, J., "Separation and Magnetohydrodynamics", J. Fluid Mech. 38, pp. 481-498, 1969.

[35] Buckmaster, J., "Boundary Layer Structure at a Magneto-Hydrodynamic Rear Stagnation", Q. J. Mech. Appl. Math. 24, pp. 373-386, 1971.

[36] Crisalli, A. J. & Walker, J. D. A., "Nonlinear Effects for the Taylor Column for a Hemisphere", Phys. Fluids 19, pp. 1661-1668, 1976.

[37] Stewartson, K., "On Rotating Laminar Boundary Layers", Proc. Symp. Boundary Layers Res., Int. Union Theoret. Appl. Mech. Freiburg i Br., pp. 59-71, 1957.

[38] Belcher, R. J., Burggraf, O. R., Cooke, J. C., Robins, A. J. & Stewartson, K., "Limit-less Boundary Layers", Recent Research on Unsteady Boundary Layers, Quebec, Canada, Laval University Press, pp. 1444-1466, 1971.

[39] Sears, W. R. & Telionis, D. P., "Unsteady Boundary-Layer Separation", Recent Research on Unsteady Boundary Layers, Quebec, Canada, Laval University Press, pp. 404-447, 1971.

[40] Williams, J. C., "Incompressible Boundary Layer Separation", Ann. Rev. Fluid Mech. 9, pp. 113-144, 1977.

[41] Cebeci, T., "The Laminar Boundary Layer on a Circular Cylinder Started Impulsively from Rest", to appear in J. Comp. Physics, 1979.

[42] MacCormack, R. W., "The Effect of Viscosity in Hypervelocity Impact Cratering", AIAA Paper 69-354, Cincinnati, Ohio, 1969.

[43] Warming R. F. & Beam, R. M., "Upwind Second-Order Difference Schemes and Applications in Aerodynamic Flows", AIAA J. 14, pp. 1241-1249, 1976.

[44] Batchelor, G. K., An Introduction to Fluid Dynamics, Cambridge University Press, 1967.

DISCUSSION

Coles:

I want to show a slide from a paper which was in press in JFM by Cantwell, Coles and Dimotakis. This is a picture of particle trajectories in and near a turbulent spot in the plane of symmetry. These are obtained under the touchy assumption that the continuity equation applies in a two-dimensional plane. The picture

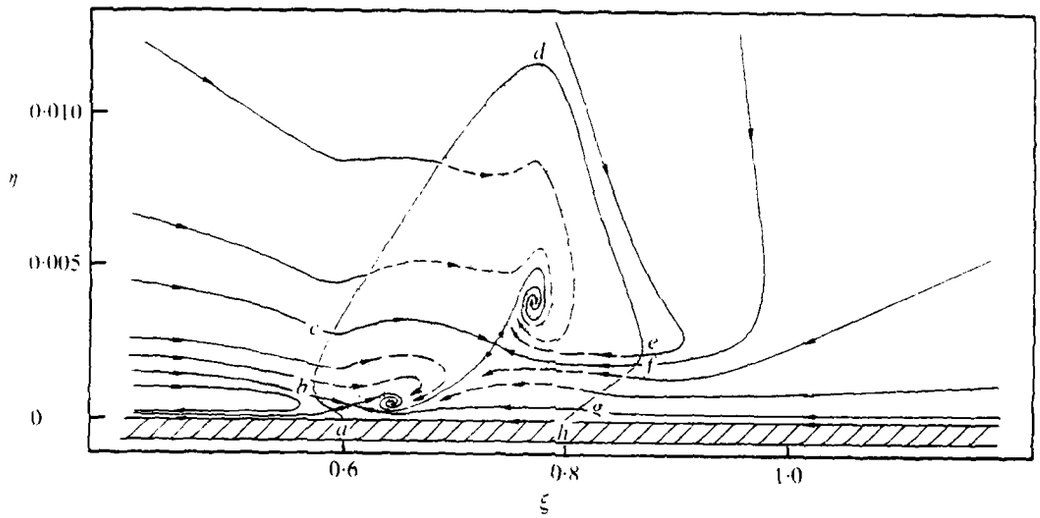

you see is in coordinates which normalize the size of the spot. The observer is zooming away from the spot as the spot grows in time in such a way that it's apparent size remains fixed. The coordinates ξ and η are really x/t and y/t, and the stream function has to be taken as Ψ/t. The velocity is derived from Ψ in the usual way. The fact that the amount of fluid inside the boundary of the spot is increasing with time means that the vortex appears as a focus. Notice that the entrainment is all at the rear. There is no entrainment at the front, except near the wall where the laminar boundary layer under-runs the spot or the spot over-runs the laminar boundary layer. The fluid which is entrained at the rear in the outer region rolls up into the main vortex, which is the focus roughly in the center of the figure. There is another small singularity and two separate stagnation points in the flow. These are particle trajectories remember. It's taken us quite a while to get so that we really understand the difference between streamlines and particle trajectories in unsteady flow and even then in only two-dimensions. The point is that the topology of outer part of this spot picture is not too much different from the speaker's results, except I think it would be interesting to have particle trajectories

rather than the streamlines in his results.

Walker:

I would agree that it is extremely difficult to understand what's going on in an unsteady flow, however, I feel more comfortable with streamlines than particle trajectories. I guess I would like to ask a question about your spot picture. If the head of the spot is a vortex, and this picture is a two-dimensional cut of a vortex-loop of which the head is the leading portion, is the upstream vortex we see the trailing part of that loop? If it is the trailing portion of a loop, the rotation is incorrect.

Coles:

Well, I must say that puzzles us, too. We have pictures like this at three different times in the evolution of the spot. That particular singularity is only visible in the latest stage in the evolution.

Landahl:

Don (Coles), would it be appropriate to point out that you have compressed the x-scale tremendously, such that if you were to plot this with equivalent x and y scales, you wouldn't see anything that looked like concentrated vorticity.

Coles:

Yes, this thing is really very flat. It's at least 10 to 1, maybe 20 to 1. The vortex structure is a very flat, very long eliptical structure--not round at all. The second singularity we just don't understand at the moment.

Kovasznay:

But is it entirely with the boundary layer? At least at the vortex part?

Coles:

Well, there isn't any (turbulent) boundary layer. This is a single turbulent spot. The laminar boundary layer you can detect by the way the particle trajectories in front turn over and start toward the left. The particle trajectories in an absolutely irrotational uniform flow would all head for the point 1 on the abcissa, which they all essentially do in this figure, subject to displacement effects. But where they stop doing that and turn back to the left is the deceleration processes as they enter the laminar boundary layer. I might add that we looked for the wave

packets in our photographic evidence, and could not find them.

Morkovin:

How many turbulent boundary layer thicknesses long is the spot?

Coles:

On the order of 15.

Morkovin:

And no more?

Coles:

Well, I don't have a turbulent boundary layer thickness. I have the thickness of the spot. This thing should be about 15 to 1 when you make the scales equal.

Morkovin:

But in principle, it should go on and on if it is the only spot.

Coles:

If I don't have wave packets and drop offspring and so on-it's something to do.

Morkovin:

The reason I am asking is I'm trying to find out whether your vortex is the same vortex Dave Walker was trying to simulate, which would be related to a single burst. This would presumably have a number of bursts underneath would it not, if it's that long?

Coles:

I believe so. We have looked at the streaky structure under a spot and confirmed Kline's original statement that the bottom of a spot looks like the bottom of a boundary layer. The same streaks are present.

Kline:

There are a number of streaks under each spot?

Coles:

Oh yes,under this thing there would be hundreds. Well, at least 50 to 100 streaks across the width to this spot.

Morkovin:

So your vortex is some sort of a global vortex, and hence I don't believe it is the same as what Dave Walker is trying to simulate.

Coles:

The reason I showed this slide after hearing Dr. Walker's talk is that I think this is the real situation that he is trying to model. It happens to be a spot and not a vortex in a boundary layer.

Walker:

Well---no, those filaments that I was drawing were vortices in a boundary layer. The emerging belief that is coming from the experiments of Chuck Smith and I think independently from Bob Falco is that what is creating these small bursts or filaments is a lot smaller than the ensemble average spot you show.

Walker:

I think it's possible to observe from Bob Falco's pictures [See Figure 2 of paper by Falco in this proceedings. Ed.] that in fact, these large spots may be agglomerations of many small filaments. There's certainly a lot of action going on within one of these spots that is time-averaged out or ensemble-averaged out. You can see a lot of action going on in the plan-view spot of Falco's. I find it very difficult even to define a symmetry plane in something like this. Perhaps Bob Falco would like to describe this picture?

Falco:

That is a turbulent spot growing in a laminar boundary layer. The Re_x is the order of about 5×10^5 and the laminar boundary layer is filled with smoke and the spot is sucking the smoke up into it.

Walker:

In making an ensemble average one averages out a lot of the details. In his pictures, you can see what Falco calls pocket instabilities indicating, I think, an upflow from the clear fluid underneath. I'm also possibly suggesting that a spot is an agglomeration of a number of these loop-like filaments.

Morkovin:

And your (Walker's) model seeks to simulate those loop-like small things?

Walker:

I'd like to be able to treat one loop filament first. The problems are substantial. I'm talking about 22,000 points in a two-dimensional calculation. The inviscid solution for a loop is not known and you have to treat that problem numerically as well. I think we could expect an order or two orders of magnitude more mesh points for a three-dimensional loop. The problems are not easy.

Abbott:

What Dave is getting, if this is a possible mimicing of a regeneration method, is the following. He has a primary vortex with one sense of vorticity which is spawning a secondary vortex of the opposite sense. Now, if this is a regeneration mechanism, the second vortex grows, moves out, and will interact with the boundary layer which will produce presumably a third vortex of the same sense of vorticity as the first one. Thus, the third vortex will be the same as the first and this process could then represent a cyclical, regenerating mechanism.

Wygnanski:

What Don (Coles) proposed was the advantage of particle trajectories vis-a-vis streamlines and I agree. In the case of a structure which keeps on growing, I would like to have Coles' comment or perhaps the speakers comment, too, on what happens if we have interacting structures? Is the streamline description then convected in the proper frame? Would that be adequate?

Coles:

Let me first make a point about the philosophy of the averaging processes as experimenters use them. If you look at an ensemble of these spots, which I have shown in this picture, there is an absolutely incredible standardization of the turbulent spot, no matter where or how it originates. Obviously, nature is trying to tell us something. If you do an ensemble average and you see nothing, then you have to look again at the details without averaging. If you look at an ensemble average and you see something, then we could go to the next stage since we know the particle trajectories and we have equations for what happens to fluid when you follow a fluid element. I claim that we saw something--we saw a vortex and we got a feeling for entrainment--and thus, we know where the fluid element is going.

Coles: (Cont'd)

The next stage is to move the Reynolds averaging one step down and talk about the stresses in the spot, where the stresses in the spot are produced by details. The main structure, the surviving part of the dynamics, seems to be a separate issue.

Wygnanski:

My question was related to the calculation. In the case of the spot, I think that particle trajectories provide something which is not describable by some pseudo streamlines. I say pseudo streamlines because of the difficulty one encounters due to spot growth. But in a case when we have interacting spots in tandem, where the structure is essentially of a fixed size, how relevant is the calculation that determines the particle trajectory vis-a-vis a simple streamlines?

Coles:

I can tell you what our philosophy is in attacking an undefined next stage. Cantwell has a paper in JFM recently which looks to be a paper on similarity arguments and group theory. Actually, it is an attempt to find and define a non-steady similarity which would be relevant in reducing a turbulent spot or a vortex in a vortex streak or vortex in a mixing layer to a conical form, so that you can handle particle trajectories and follow processes going along those trajectories. That's the point of that paper and the picture I showed you of the spot was an example of the canonical similarity in action. This appraoch is where we think there is a contribution to be made.

Reynolds:

Let me suggest that we ought to have a group take a look at the spot question and what can we learn about boundary layers from spots. I'd like to suggest that Don Coles take part in that discussion and Wygnanski and Dave Walker and Falco. We'll let the committee decide on it's own Chairman, but I'll ask Falco to call the meeting.

Brodkey:

This isn't a question to anybody, it's to the new spot committee. In a number of photographs that Don Coles, Falco, and others have shown me, I have often seen, depending on the visualization technique, the streaky structure considerably upstream of the spot. The appearance is of something that is swept under the spot, like under the rug, and I wonder if you might also ask yourself what is going on--- Is something propagating upstream?

Willmarth:

In your paper, Dave (Walker) the thing that struck me was that you have a mechanism with a vortex for getting a stagnation flow towards the wall, giving you a very strong shear layer. Could you get that same shear layer near the wall without the vortex?

Walker:

Even in the 0.75 cases, you get a developing shear layer near the rear stagnation point.

Willmarth:

So, I'm leaving you with the question, could the highly sheared region become unstable in the Kelvin-Helmholtz sense and erupt, forming its own vortex?

Walker:

Whether the high-shear region leads to an instability or not, I don't know, but it certainly develops. Whether you can go that one step further is still under study.

Abbott:

Of course, once that secondary vortex leaps off, continuity tells us that something has to rush back down toward the plate.

Donaldson:

I'd just like to point out a little experience we have had with computed vortices. First of all, you do get this opposite vortex and we find that the shear layers are so powerful that there's no way that you can proceed with the computation with laminar viscosity in the kind of grid sizes that we have. If you put in any kind of disturbance in the complete second-order closure with scale, you'll find those are regions of extreme production of turbulence, wherever those high-shear layers develop. It's not turbulence, but the high-shear layers are very unstable in the Kelvin-Helmholtz sense and are a very strong producer of turbulence. If you put a secondary vortex in, the shear layers can't get that strong and we've been able to calculate the secondary vortex as it goes all the way through the process of rolling up into the primary vortex and killing it.

MODELING OF COHERENT STRUCTURE IN BOUNDARY LAYER TURBULENCE

M. T. Landahl

Dept. Aero. & Astro., Mass. Inst. Technology, Cambridge, Mass. 02139 and

Dept. Mechanics, Royal Inst. Technology, S-10044 Stockholm 70, Sweden

ABSTRACT

The large-scale coherent motion associated with turbulent bursting in a boundary layer is studied with the aid of an inviscid model. The space-time evolution of a disturbance of large horizontal dimensions compared to the wall layer thickness is analyzed under the assumption that the mean flow is parallel. The initial velocity field is assumed to be set up by the action of the turbulent stresses produced by a patch of secondary instablity. For short and moderate times, the effects of viscosity and pressure are small, and the evolution of the disturbance is conveniently studied with the aid of Lagrangian techniques. The model is able to reproduce qualitatively many of the observed features of the bursting motion such as the formation of longitudinal streaks, the rapid acceleration after initiation of bursting, and the strong y-coherence of the u-fluctuations. In particular, the model demonstrates how action by the mean shear makes the disturbance eventually evolve into a thin internal shear layer, thus making possible the appearance of a new region of inflexional instability and hence burst regeneration-downstream of the original burst.

1. INTRODUCTION

The discovery of recent years that turbulence in the wall region of a boundary layer is highly intermittent and possesses a quasiperiodic and fairly distinct "bursty" structure (see Frenkiel et al. 1977 for a number of recent papers on this subject) has pointed to the necessity of analyzing in depth the dynamical processes involved in the generation of turbulent fluctuations in this region. This requires the adoption of a deterministic rather than a statistical approach since the usual statis-

tical methods are not suitable for dealing with such highly intermittent processes. Because the flows under consideration are extremely complicated unsteady three-dimensional ones dominated by strong nonlinearity and rotation, the development of a successful theory necessitates a very careful choice of a theoretical model, one that it is simple enough to analyze, yet incorporates the major dynamical effects. Early such efforts emphasizing different aspects of the dynamics were those of Theodorsen (1952), Einstein & Li (1956) and Sternberg (1965).

Since turbulence may in some sense be regarded as a manifestation of flow instabilities, it is of considerable theoretical interest to try to relate the dynamical processes in the fully developed turbulent flow to those studied in hydrodynamic stability theory. This approach (Landahl, 1967, Bark, 1975) has proven partially successful in explaining some of the observed statistical properties of fluctuating pressures and velocities in terms of the propagation characteristics of linear waves. Later findings (Landahl, 1975, 1977) indicate, however, that other types of disturbances besides waves of the Tollmien-Schlichting type must be incorporated in order to model properly the fluctuation field. On basis of a two-scale model (first proposed in Landahl, 1973), in which the main nonlinear interaction was assumed to occur through a coupling between small and large scales of motion, it was concluded that large-scale motion in a localized region, a "coherent structure", would result from nonhomogeneous mixing in a patch of secondary instability of the inflectional type. In addition to waves of scales typical of the dimension of the patch, the large-scale eddy produced by the mixing will also contain a convected portion which will move downstream with the local mean velocity. The shearing of the convected eddy was found to lead to the formation of a new thin shear layer further downstream (Landahl, 1975), thus giving rise to a new inflectionally unstable region downstream of the original burst, and thereby making burst regeneration possible.

In the present paper a more detailed analysis of the dynamics of a large-scale coherent structure formed by the action of localized mixing is given. The approach taken is to treat the flow as an initial value problem with initial conditions provided by the large-scale momentum transfer caused by the mixing due to secondary instability. Since the processes involved are primarily inertial, viscosity is neglected. On the assumption that strong nonlinearity is primarily confined to the initial time period during the secondary instability phase, the evolution of each coherent structure could be analyzed separately, independently of other large-scale motion and statistical superposition used to model the random fluctuating flow field, if so desired.

2. FORMULATION OF THE MODEL

The theoretical model will be formulated on basis of the two-scale model proposed by Landahl (1973). The fundamental ideas underlying this model and some of the conclusions which can be drawn from it have been discussed earlier (Landahl, 1975, 1977). Here we shall only give a brief review

of its main features and draw some conclusions from it regarding the overall characteristics of the initial large-scale velocity field.

To understand the characteristics of the initial large-scale velocity field we must first discuss the behavior of the small-scale motion. The secondary instability giving rise to the small-scale motion is assumed to be of the Kelvin-Helmholtz type arising locally on a thin internal shear layer formed in the flow. The secondary instability, and hence the small-scale turbulence production, draws its energy from the velocity difference across the shear layer, and the resulting mixing will be such as to tend to remove the velocity difference (Landahl, 1975). The instability, and hence the turbulence production, will therefore eventually be quenched when the small-scale mixing has removed the local inflection in the large-scale velocity distribution. After an initial period of growth, the small-scale motion will therefore begin to decay slowly due to viscous dissipation. After the completion of the initial nonlinear growth phase, the motion will thus consist of a large-scale field on which is superimposed a slowly decaying small-scale velocity field, and the interaction between the large and small scales then becomes weak. The subsequent evolution of the large-scale velocity field may therefore be analyzed with the effects of the small-scale motion neglected. Furthermore, since the mechanisms involved are primarily inertial, the effects of viscosity may be omitted, at least during a moderate time period after the creation of the coherent structure. Since observed typical dimensions of the large-scale eddies are of the order the boundary layer thickness, the downstream rate of change of the mean properties of the boundary layer may be neglected in the analysis and therefore the parallel-flow assumption adopted for the mean flow. With disturbance velocities u_i ($u_1 = u$, $u_2 = v$, $u_3 = w$), pressure p, and mean velocity $U(y)$ the equations of motion may thus be written

$$\frac{D(u_i + \delta_{1i}U(y))}{Dt} = -\frac{1}{\rho}\frac{\partial p}{\partial x_i} \tag{1}$$

$$\frac{\partial u_i}{\partial x_i} = 0 \tag{2}$$

The boundary conditions are that the component $u_2 = v$ is zero at the wall ($y = 0$) and that the disturbances vanish at large distances. The region occupied by the disturbance shall be assumed to be localized and have a typical horizontal dimension of ℓ, which will be assumed to be large compared to the thickness δ of the wall layer. Since the mean shear outside the wall and buffer regions is quite small compared to what it is inside this region, one may treat the mean flow in the wall layer as a separate boundary layer having a free-stream velocity equal to the value at the edge of the wall layer which may be taken to be located at approximately $y^+ = 50$.

Consider now the effect of a small-scale secondary instability occurring over a patch of typical horizontal dimension ℓ and confined within the wall region (see Fig. 1).

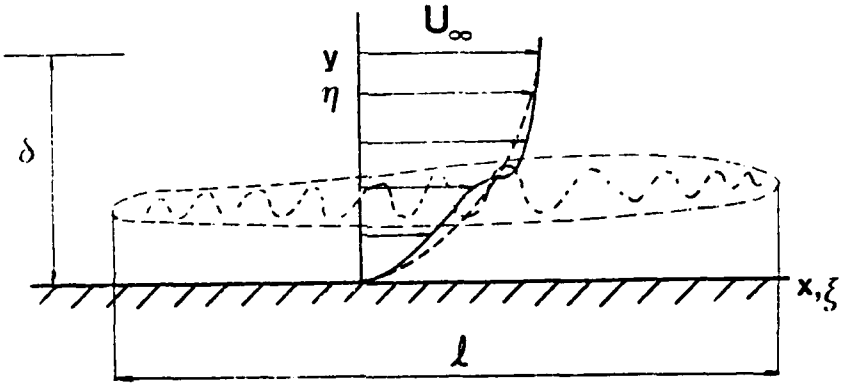

Figure 1. Two-scale model (conceptual) for initiation of coherent structure.

By integration of (1) and (2) over planes $x_2 = y = \text{const.}$ the following relations may be shown to hold:

$$\int_{-\infty}^{\infty}\int v\,dx\,dz = 0 \tag{3}$$

$$\int_{-\infty}^{\infty}\int xv\,dx\,dz = -\int_{t_i}^{t}dt\int_{-\infty}^{\infty}\int uv\,dx\,dz \tag{4}$$

$$\int_{\infty}^{\infty}\int xp_w\,dx\,dz = -\rho\int_{0}^{\infty}dy\int_{-\infty}^{\infty}\int uv\,dx\,dz \tag{5}$$

where t_i is the time of initiation of the disturbance and p_w the wall pressure. In deriving these results it has been assumed that the disturbances drop off with distance from the center of the patch fast enough to make boundary terms vanish. A localized event producing Reynolds stresses of the usual sign ($\langle uv\rangle<0$) will thus impart a moment of momentum to the flow, through the action of the surface pressure, so as to give it a forward rotation in a sense opposite to the mean shear (Landahl, 1975, 1977). Large instantaneous Reynolds stresses are produced only as long as the small-scale instability persists; thus the right-hand side of (4) will receive its major contribution during the secondary growth stage, and the non-

linear effects from the small-scale motion will be small thereafter. Therefore, the subsequent evolution of the large-scale flow may be treated independently from the small-scale motion, and each coherent structure analyzed separately.

3. EVOLUTION OF THE COHERENT STRUCTURE

Following the discussions in the previous section we shall analyze the large-scale motion as an initial value problem with initial conditions u_0, v_0, w_0 specified at $t_0 = 0$ and selected so as to be commensurate with the properties of the secondary instability. Thus

$$\int_{-\infty}^{\infty}\int xv_0 dxdz > 0$$

Also the initial u_0-distribution should be such that the streamwise velocity $(U + u_0)$ is free from inflection. (For simplicity, u_0 will be taken to be zero in the numerical example to be treated below). A formal solution of the system (1), (2) is most easily constructed on basis of material ("Lagrangian") coordinates

$$\xi_i = (\xi,\eta,\zeta)$$

defining the position of each fluid element at $t = 0$ (see Fig. 1). From the first and third of (1) it follows that

$$u + U = u_0(\xi,\eta,\zeta) + U(\eta) - \frac{1}{\rho}\int_0^t p_x Dt_1 \tag{6}$$

$$w = w_0(\xi,\eta,\zeta) - \frac{1}{\rho}\int_0^t p_z Dt_1 \tag{7}$$

where $\int \doteq Dt_1$, denotes integration following a fluid element, i.e., holding ξ_i constant. The laboratory ("Eulerian") coordinates are then determined from

$$x = \xi + (U + u_0)t - \frac{1}{\rho}\int_0^t (t-t_1)p_x Dt_1 \tag{8}$$

$$z = \zeta + w_0 t - \frac{1}{\rho}\int_0^t (t - t_1)p_z Dt_1 \tag{9}$$

The pressure is found by integration of the second momentum equation along x, z = const.,

$$p = \rho \int_y^\infty \frac{Dv}{Dt}\, dy \tag{10}$$

The second velocity component, finally, is found from the requirement that continuity must be satisfied. The transformation of a volume element from laboratory to material coordinates is given by

$$dxdydz = Jd\xi d\eta d\zeta \tag{11}$$

where J is the Jacobian

$$J = \det\left(\frac{\partial x_i}{\partial \xi_j}\right)$$

For a fluid of constant density we must have that

$$J = 1 \tag{12}$$

(Lamb, 1932, section 15). Hence, upon expansion of (12) it follows that

$$A_1 y_\xi + A_2 y_\eta + A_3 y_\zeta = 1 \tag{13}$$

where

$$A_1 = x_\zeta z_\eta - z_\zeta x_\eta \equiv \left(\frac{d\xi}{dy}\right)_{x,z} \tag{14a}$$

$$A_2 = x_\xi z_\zeta - x_\zeta z_\xi \equiv \left(\frac{d\eta}{dy}\right)_{x,z} \tag{14b}$$

$$A_3 = x_\eta z_\xi - x_\xi z_\eta \equiv \left(\frac{d\zeta}{dy}\right)_{x,z} \tag{14c}$$

The identities expressed in the last column of (14) are found by direct calculation setting dx = dz = 0 and making use of (13). One may easily solve (13) by the method of characteristics, or equivalently, by direct integration of (14 b), which gives

$$y = \int_0^\eta \frac{d\eta_1}{(A_2)_{x,z}} \tag{15}$$

where the boundary condition that y = 0 for η = 0 has been taken into account. By substituting (8) and (9) into (14 b) we find

$$A_2 = (1 + tu_{o\xi} - I_{1\xi})(1 + tw_{o\zeta} - I_{3\zeta}) - (tu_{o\zeta} - I_{1\zeta})(tw_{o\xi} - I_{3\xi}) \tag{16}$$

where

$$I_1 = \frac{1}{\rho}\int_0^t (t - t_1)p_x Dt_1 \tag{17}$$

and

$$I_3 = \frac{1}{\rho}\int_0^t (t - t_1)p_z Dt_1 \tag{18}$$

It is convenient to define the quantity

$$\ell_m \equiv y - \eta = \int_0^\eta \left(\frac{1-A_2}{A_2}\right)_{x,z} d\eta_1 \tag{19}$$

which gives the displacement of the fluid element in the direction normal to the wall, the quantity of primary interest in Prandtl's (1925) mixing-length theory. From this, the y-component of the perturbation velocity may be directly obtained

$$v = \frac{D\ell_m}{Dt} \tag{20}$$

and then the pressure from (10).

The formal solution given by (6) - (10) and (16) - (20) is exact within the framework of inviscid theory but can only be evaluated by an iterative procedure. Fortunately, the problem considered allows one to introduce some simplifying assumptions which make the evaluation much more tractable. The assumption of a large horizontal scale compared to the thickness of the wall layer allows one to neglect the pressure variation through the boundary layer (the usual boundary layer assumption) so that one may set

$$p \simeq p_\delta = \rho\int_\delta^\infty \frac{Dv}{Dt}\, dy \tag{21}$$

throughout the layer, where p_δ is the pressure at the edge of the boundary layer. The flow outside the layer may be taken to be irrotational, provided the initial disturbance is such that fluid elements originating inside the shear layer do not penetrate outside $y = \delta$. From the equations for an irrational flow one finds that

$$\frac{p_\delta}{\rho} = -\left(\frac{\partial}{\partial t} + U_\infty \frac{\partial}{\partial x}\right)\Phi - \frac{1}{2}\left(\Phi_x^2 + \Phi_z^2 + v_\delta^2\right) \tag{22}$$

where U_∞ is the velocity outside $y = \delta$, Φ the velocity potential, and subscript δ denotes values at $y = \delta$. The velocity potential may be calculated in terms of v_δ from the integral

$$\Phi = -\frac{1}{2\pi}\iint_{-\infty}^{\infty} \frac{v_\delta(x_1, z_1, t)\, dx_1 dz_1}{\sqrt{(x-x_1)^2+(z-z_1)^2}} \tag{23}$$

Taking ℓ/U_∞ to be a typical time scale of evolution for the large-scale motion one may estimate the pressure to be of order (for times which are not large compared to ℓ/U_∞)

$$\frac{p}{\rho} = O(U_\infty v_0') \tag{24}$$

where v_0' is a measure of the amplitude of the initial motion. Using this, one finds that the pressure integrals I_1 and I_3 are of the order

$$I_{1,3} = O\left[t^2 U_\infty v_0'/\ell\right] \tag{25}$$

and their contribution to the integrand in (19) of order (taking only the linear terms)

$$t^2 U_\infty v_0'/\ell^2 \tag{26}$$

This will be negligible compared to the linear term

$$-t(u_{0\xi} + w_{0\zeta}) = t\, v_{0n}$$

which is of order $t\, v_0'/\delta$, whenever

$$t\, U_\infty/\ell \ll \ell/\delta \tag{27}$$

Hence, for $\delta/\ell \ll 1$ the effects of pressure may be neglected for times which are not large compared to the time needed for the disturbance to be convected downstream a distance equal to its own length.

In the analysis which follows the perturbations are assumed to be small so that terms involving products of the initial velocity components may be neglected in the solution (19). From (16) it follows that this is permissible provided

$$v_0' t \ll \delta \tag{28}$$

For times of order δ/v_0' and larger, nonlinear selfdistortion effects may become important. Only for very weak disturbances such that

$$v_0'/U_\infty \ll (\delta/\ell)^2 \tag{29}$$

will the nonlinear effects be small compared to those of the pressure. If (29) is not satisfied, the solution may be obtained by iteration on the pressure as follows. First, the solution (19) is calculated by neglecting I_1 and I_3 in (16), Second, the pressure is obtained from (22) and (23), I_1 and I_3 are computed, and then an improved value of ℓ_m determined, etc. It is difficult to assess the convergence properties of such a method, however. Possibly, a step-by-step procedure in time in which after each time step a new initial velocity field is calculated could be used to study the flow behavior for large times.

To investigate the qualitative effects of pressure for large times, we have here instead made use of the linearized solution. Neglecting all terms which are quadratic in the initial velocity components we find from (10) - (19)

$$\ell_m = t \int_0^y v_{on}(\xi_1,\eta_1,z)d\eta_1 - \frac{1}{\rho}\nabla_2^2 \int_0^y dy \int_0^t (t-t_1)p(\xi_1,t_1,z)dt_1 \tag{30}$$

$$\equiv \ell_m^{(1)} + \Delta\ell_m$$

where

$$\nabla_2^2 = \partial^2/\partial x^2 + \partial^2/\partial z^2$$

and

$$\xi_1 = x - U(\eta_1)(t-t_1) \qquad (t_1 = 0 \text{ in the first term})$$

Here, use has been made of continuity of the initial velocity field and the approximations

$$x \simeq \xi + U(y)t \ , \ y \simeq \eta \ , \ z \simeq \zeta \tag{31}$$

The first term, $\ell_m^{(1)}$, in (30) may be regarded as the purely convected solution. The second term, $\Delta\ell$, gives the lowest-order correction due to the pressure. The pressure is now approximated by

$$\frac{p}{\rho} \simeq \frac{1}{2\pi}\left(\frac{\partial}{\partial t} + U_\infty \frac{\partial}{\partial x}\right) \iint_{-\infty}^{\infty} \frac{v_\delta \, dx_1 dz_1}{\sqrt{(x-x_1)^2 + (z-z_1)^2}} \tag{32}$$

and the perturbation velocity components by

$$u \simeq u_o(\xi,y,z) - \ell_m U'(y) - \frac{1}{\rho}\int_0^t p_x Dt_1 \tag{33}$$

$$v \simeq \left(\frac{\partial}{\partial t} + U_\infty \frac{\partial}{\partial x}\right) \ell_m \tag{34}$$

$$w \simeq w_o - \frac{1}{\rho}\int_0^t p_z \, Dt_1 \tag{35}$$

4. LARGE-TIME BEHAVIOR

We shall now consider the large-time behavior of the solution (19) under certain simplifying assumptions. It follows that for moderately large times such that (27) and (28) are satisfied both the pressure and nonlinear terms may be neglected in (19) so that the fluid element vertical displacement may be approximated by the linearized expression

$$\ell_m \equiv \ell_m^{(1)} = t\int_0^\eta v_{on}(\xi_1,\eta_1;z)d\eta_1 \tag{36}$$

where

$$\xi_1 = x - U(\eta_1)t$$

By change of integration variable to ξ_1 this may be written

$$\ell_m = \int_\xi^x \frac{1}{U_1'} v_{on}(\xi_1,\eta_1;z)d\xi_1 \tag{37}$$

where $\xi = x - U(y)t$, and where U_1' is given by

$$U_1 \equiv U(\eta_1) = (x - \xi_1)/t \tag{38}$$

Consider now $x/\ell >> 1$ and large times (but within the limits set by (27) and (28)). Since sizeable contributions to the integral (37) come only for regions $\xi_1 = O(x/\ell)$, one may set

$$U_1 \simeq x/t \tag{39}$$

and η_1 may thus be replaced by a constant in (37) giving

$$\ell_m \simeq \frac{1}{U_1'} \int_{\xi}^{\infty} v_{on}(\xi_1;\eta_1;z)d\eta_1 \tag{40}$$

where we have replaced the upper limit by infinity since v_{on} approaches zero for $x/\ell >> 1$. The solution for ℓ_m will have the character illustrated in Fig. 2.

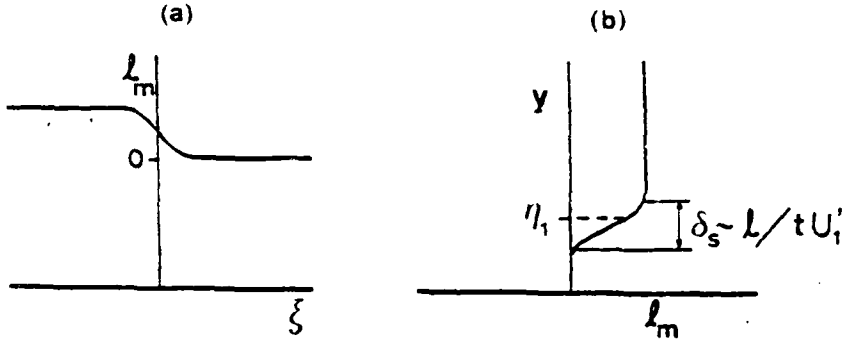

Figure 2. The fluid element displacement, ℓ_m , in the direction normal to the wall for large times (conceptual):
a) as function of $\xi = x - U(y)t$
b) as function of y. $U_1 \equiv U(\eta_1) = x/t$.

For large negative ξ (corresponding to large y) the range of integration will include the whole streamwise range of nonzero values of v_o, so that ℓ_m tends to a limiting nonzero value (provided $\int_{-\infty}^{\infty} v_o d\xi \neq 0$) above $y = \eta$. For large positive ξ, on the other hand, (corresponding to small y) the lower limit will tend to $+\infty$ and the integral, and hence ℓ_m, will become zero. The fluid element displacement will hence vary rapidly, when $tU' >> 1$, in a region around $y = \eta$, with a thickness of order $\ell/U't$. Since, when the pressure term is neglected in (33)

$$u \simeq u_0(\xi,y,z) - \ell_m U(y) \tag{41}$$

it follows that a thin shear layer, of thickness $\delta_s = \ell/U't$, decreasing as the inverse of time, will form. It also follows from the second term of (41) that the streamwise velocity will show a strong y-coherence for $y>\eta_1$. Such coherence has been observed in the experiments by Blackwelder & Kaplan (1976).

For the nonlinear case one must include the possibility that A_2 could become zero in some point for large times such that $v_o'/\delta = 0(\delta)$. the conditions under which this may arise have not been investigated, however.

The long-time effects of pressure may be studied on basis of the linearized equations (30) - (35). Application of Fourier transform in x, z and t to (30), (32) and (34), with

$$\hat{\ell}_m = \iiint_{-\infty}^{\infty} e^{-i(\alpha x + \beta z - \omega t)} \ell_m dx dz dt \tag{42}$$

gives

$$\hat{\ell}_m = \int_0^y \frac{v_{on}(\eta_1)d\eta_1}{[i\alpha(U_1-c)]^2} - k^2 \frac{\hat{p}}{\rho} \int_0^y \frac{d\eta_1}{[i\alpha(U_1-c)]^2} \equiv \hat{\ell}_m^{(1)} + \Delta\hat{\ell}_m \tag{43}$$

$$\frac{1}{\rho}\hat{p} = -\alpha^2(U_\infty - c)^2 \hat{\ell}_{m\delta}/k \tag{44}$$

In these, caret denotes triple Fourier transform as in (42), tilde a transform with respect to x and z, only, e.g.

$$\tilde{v}_o = \iint_{-\infty}^{\infty} e^{-i(\alpha x + \beta z)} v_o dx dz \tag{45}$$

and

$$U_1 = U(\eta_1)$$

$$c = \omega/\alpha$$

$$k = \sqrt{\alpha^2 + \beta^2}$$

The behavior of the solution for $\delta/\ell << 1$ is obtained from the transformed solution for small values of α and β. Similarly, the large-time behavior may be determined from the transform for small c. From the solutions for ℓ_m and p the velocity components may be found from (33) - (35), so only these quantities will be considered.

Combination of (43) and (44) gives

$$\hat{\ell}_{m\delta} = \frac{\hat{\ell}^{(1)}_{m\delta}}{1 + k(U_\infty - c)^2 \int_0^\delta (U_1 - c)^{-2} d\eta_1} \tag{46}$$

Hence,

$$\Delta\hat{\ell}_m = - k(U_\infty - c)^2 \hat{\ell}^{(1)}_{m\delta} \frac{\int_0^y (U_1 - c)^{-2} d\eta_1}{1 + k(U_\infty - c)^2 \int_0^\delta (U_1 - c)^{-2} d\eta_1} \tag{47}$$

where

$$\hat{\ell}^{(1)}_{m\delta} = \int_0^\delta [i\alpha(U_1 - c)]^{-2} \tilde{v}_0(\eta_1) d\eta_1 \tag{48}$$

Expansion of the denominator in (46), (57) for small c and k yields

$$1 + k(U_\infty - c)^2 \int_0^\delta (U_1 - c)^{-2} d\eta_1 \simeq 1 - \tag{49}$$

$$- \frac{k(U_\infty - c)\, U_\infty}{c\, U_c'} - \frac{k(U_\infty - c)^2}{U_c'^3} U_c'' \ln\left(\frac{U_\infty - c}{-c}\right)$$

Index c denotes values at $\eta = \eta_c$, where η_c is defined by $U(\eta_c) = c$. That branch of the logarithm in the second term which is obtained by going below the integral must be chosen. This follows from the treatment of the problem as an initial-value one; convergence of the Fourier time integral then requires that αc has a positive imaginary part. (This difficulty is familiar in the theory of hydrodynamic instability for an inviscid flow, see Lin, 1955). For small k it is found that

(49) has a zero for $c = c_o$, where

$$\frac{c_o}{U_\infty} \simeq \frac{q}{1 + q\,[1 - U_\infty U_c''\,(\pi i - \ln q)/U_c'^2]} + O(k^2) \tag{50}$$

$$\simeq k\,U_\infty/U_c' + \pi i k^2 U_\infty^3\,U_c''/U_c'^4 + O(k^2) \equiv (c_{or} + i c_{oi})/U_\infty$$

where $q = k\,U_\infty/U_\infty'$. This gives the eigenvalue for an infinite wave train of (a small) wave number k in an inviscid parallel shear flow. (The approximation underlying (50) is the same as the one employed in the early analytical approaches to hydrodynamic stability theory. In fact the integral in (49) is identical to the integral K_1 in Lin, 1955 , p. 44). For $U_c'' > 0$, which will occur when the velocity profile has an inflection point somewhere, the imaginary part of c_o is positive and the waves will grow, i.e. the flow is unstable to small disturbances. The mean velocity profile of interest here has $U'' < 0$ everywhere, hence the flow is stable in the hydrodynamic sense. From (50) it follows that

$$c_{oi}/c_{or} \simeq \pi\,k\,U_\infty^2\,U_c''/U_c'^3 \tag{51}$$

which is of order δ/ℓ for $k = O(1\ell)$ and thus small under the assumptions of the present theory.

For the study of the long-time behavior of a disturbance of large horizontal scale we need only retain the lowest-order terms in k and c, provided all poles in the transform are properly represented. By approximating the integrals in (47) and (48) through expansion of the integrand about the point y_c in the same manner as that employed in (49) and retaining only poles, but not logarithmic terms in c and U-c (which give rise to contributions varying as inverse powers of t), we obtain

$$\hat{\ell}_m \simeq \frac{\tilde{v}_{on}(\eta_c)}{\alpha^2\,U_c'}\,\frac{U}{(c - c_o)(U - c)} \tag{52}$$

But from (43) we find in the same manner

$$\hat{\ell}_m^{(1)} \simeq \frac{\tilde{v}_{on}(\eta_c)}{\alpha^2\,U_c'}\,\frac{U}{c(U - c)} \tag{53}$$

Hence, we may set, within the same approximation,

$$\hat{\ell}_m \simeq \frac{c}{c - c_o}\,\hat{\ell}_m^{(1)} \tag{54}$$

After inversion, the results may be cast in form of the following convolution integral:

$$\ell_m = \frac{\partial^2}{\partial x \partial t} \int_0^t dt_1 \iint_{-\infty}^{\infty} G(x-x_1, z-z_1, t-t_1) \ell_m^{(1)}(x_1, y, z_1, t_1) dx_1 dz_1 \tag{55}$$

where G is the inverse transform of

$$\hat{G} = \frac{1}{\alpha^2 (c - c_0)} \tag{56}$$

An asymptotic analysis for $x, t \to \infty$ under the assumption that $c_{qi} < 0$ for all non-zero wave numbers, but that $|c_{oi}|/c_{or} \ll 1$ (which is consistent with the assumption $\delta/\ell \ll$, see (54), gives the following simple approximate result:

$$G = \frac{1}{\pi z} \sin\left[\frac{x z U_c'}{U_\infty (t U_\infty - x)}\right] \cdot H(t U_\infty - x) \tag{57}$$

Here, $H(x)$ is the Heaviside step function and $U_c' = U'(y_c)$ is defined by (c.f. (39))

$$U_c \equiv U(y_c) = x/t \tag{58}$$

In deriving (57), use has been made of (the first of) (50) with the imaginary part neglected, i.e. taking

$$c_0/U_\infty \simeq q/(1 + q) \tag{59}$$

It follows from (55), (57) that the effects of the pressure causes the leading edge of the disturbance to propagate with the free-stream velocity U_∞ . This is in accordance with the finding by Gustavsson (1978), in which it is shown that the continuous spectrum of the solution for a disturbance initiated in a boundary layer gives rise to a portion propagating with the free-stream velocity, both in the viscous and in the inviscid cases. It can also be shown from (55), (57) that ℓ_m tends to zero as t^{-2} or faster as $t \to \infty$ for fixed x, in accordance with the result of Gustavsson (1978).

Of possible significance is also that (57) shows a definite span-

wise periodicity with a wave length increasing with time. This will also cause a cut-off for the larger spanwise scales, so that they tend to propagate with a lower velocity ($tU_\infty - x$ larger) than those with small spanwise scales. That the highest propagation velocities are attained by the disturbances of the smallest spanwise scales is a consequence of the form of the approximate dispersion relation (50). This was derived under the assumption of a large horizontal scale, so that the propagation velocities near U_∞ predicted for the small scales are not correctly given by this theory.

An interesting limit is that for $t\to\infty$ with $x/t = U_c$ held fixed. The argument of the sine in (57) then tends to a fixed value, and one can show that ℓ_m approaches a nonvanishing value for $t\to\infty$, provided $U(y)<U_c<U_\infty$. Hence, the streamwise dimension of the disturbed region will grow as $t(U_\infty - U(y))$. Since the largest differences between the free tream velocity and the local mean velocity $U(y)$ are found near the wall, one would thus expect the most highly elongated disturbances to appear there. This may provide a possible explanation for the streaky structure observed to occur in the turbulent boundary layer in the region close to the wall. However, in a real viscous flow the pressure cannot give rise to nondecaying disturbances, unless neutrally stable or growing waves are present because of instability. In the inviscid case, waves of $\alpha\to 0$ will always be nondecaying, even if the flow is hydrodynamically stable, and they provide the main contributions to the nondecaying disturbances in the limit of $t\to\infty$. In the viscous case, the waves with $\alpha\to 0$ will be decaying, and the disturbed region will therefore not continue to grow forever, but decay will set in at some finite value of streamwise to spanwise wave length.

It is of interest to estimate the time required for viscous effects to become important. By comparing the rate at which viscosity diffuses the internal shear layer with the rate at which it is being thinned by stretching of spanwise mean vorticity, Landahl (1977) arrived at the following estimate of the time t_v at which viscous diffusion and stretching balance:

$$t_v \sim (\ell^2/\nu U'^2)^{1/3} \tag{60}$$

In terms of wall variables, taking for U' the value at the wall one finds

$$t_v^+ \sim (\ell^+)^{2/3}$$

which shows that viscous effects are likely to become important before the disturbance has travelled a distance downstream many times its own streamwise length. The time required for viscous diffusion from the wall to be felt in the flow is given by

$$t_{vw} \sim y^2/\nu$$

which in terms of wall variables gives

$$t_{vw}^+ \sim y^{+2}$$

which appears to give a somewhat less severe restriction, except in the immediate neighborhood of the wall ($y^+ < 5$, say).

5. NUMERICAL EXAMPLE

A numerical example will be used to illustrate the application of the simplified model and a comparison made with experimental data. From (3) it follows that the initial v-distribution must be such that the net vertical flow across a plane y = const. must be zero. According to (4) the moment of v_0 with respect to the z-axis should on the average be positive, since $\langle uv \rangle$ is negative, typical v_0-distribution will thus have values that are positive downstream and negative upstream of the center of the disturbance. Also, since the Reynolds stresses drop to zero for y = 0 and for y = δ, the initial v-distribution must be zero in these limits and have a maximum near the position of maximum turbulence production. For the calculations presented here, the following v_0-distribution which satisfied these conditions was chosen :

$$v_0 = C_0 \left(\frac{x^+}{\ell_1^+}\right) \left(\frac{y^{+2}}{\ell_2^+}\right) \exp\left[-\left(\frac{x^+}{\ell_1^+}\right)^2 - \left(\frac{y^+}{\ell_2^+}\right)^2\right] \tag{61}$$

In this, ℓ_1^+ and ℓ_2^+ are scaling factors to be suitably selected. The plus superscript is used to indicate that viscous wall variables will be used in the presentation of the results. Fig. 3 shows numerical values for

$$C_0 = \sqrt{2}\, e^{3/2}, \quad \ell_1^+ \simeq 50 \quad \text{and} \quad \ell_2^+ = 16$$

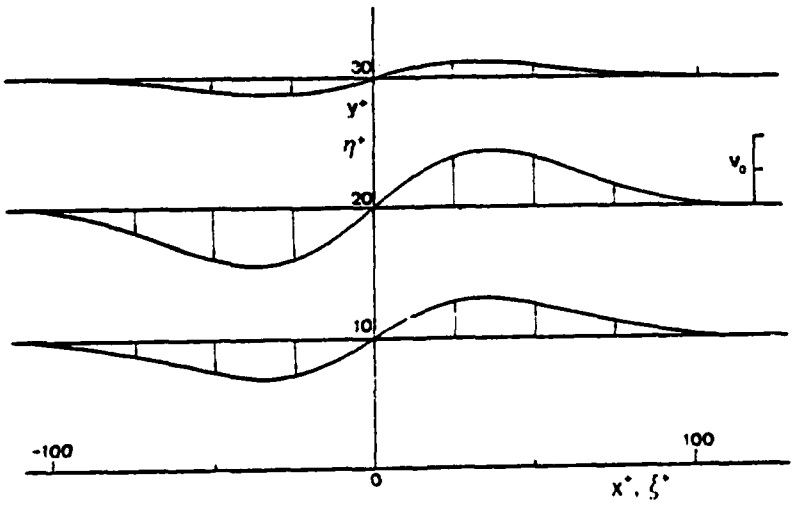

Figure 3. Initial condition used in numerical example $u_0 = 0$, v_0 from (61).

This v_0-distribution has a maximum at $y^+ = 16$ and an overall streamwise dimension of approximately 200 in wall units, values which are not inconsistent with experimental data. The value of C_0 was selected to make the maximum of v_0 equal to unity (i.e. equal to the wall friction velocity in dimensional form). At $y^+ = 40$, v_0 is about 0.03 and hence of negligible magnitude above this y^+-value. The character of the solution depends primarily on the scaling factor ℓ_2^+; by a simple linear rescaling the results for a given parameter combination may be applied to any other desired combination of C_0 and ℓ_1^+. For a representation of the mean velocity distribution the simple exponential approximation proposed by Schubert & Corcos (1965)

$$U^+ = 16\,(1 - e^{-y^+/16}) \tag{62}$$

was found to give adequate accuracy for the present purpose.

Fluid element displacements ℓ_m, and from this the u-perturbations, were calculated with pressure effects ignored. Sample results are shown in Fig. 4 and 5. At first, the streamwise velocity perturbation grows rapidly, and the flow pattern is stretched out in the streamwise direction. A shear layer is seen to form and intensify as it is convected downstream. For $t^+ = 5$ it is just beginning to appear between about $x^+ = -50$ and $x^+ = 0$, and for $t^+ = 15$ it is most intense at around $x^+ \simeq 50$.

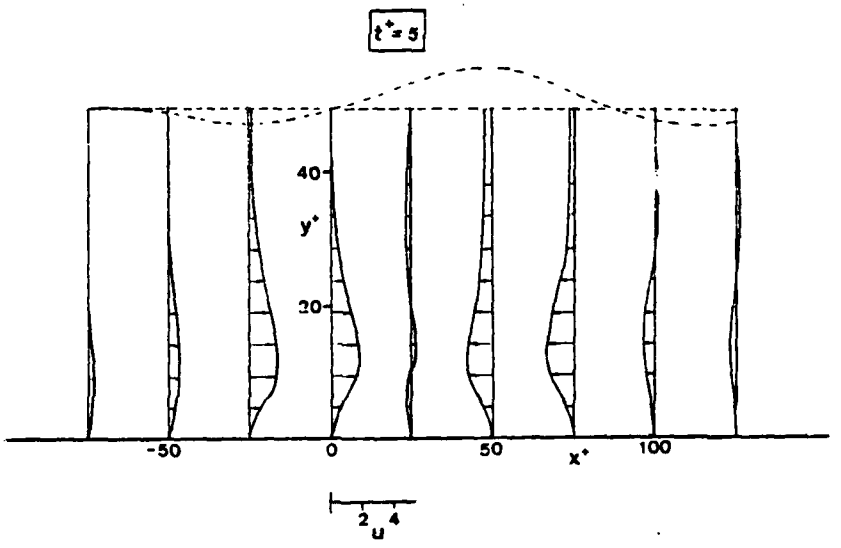

Figure 4. Distribution of streamwise velocity perturbation u at $t^+ = 5$ for model example. Dotted line gives position of fluid elements originally located along $y^+ = 50$.

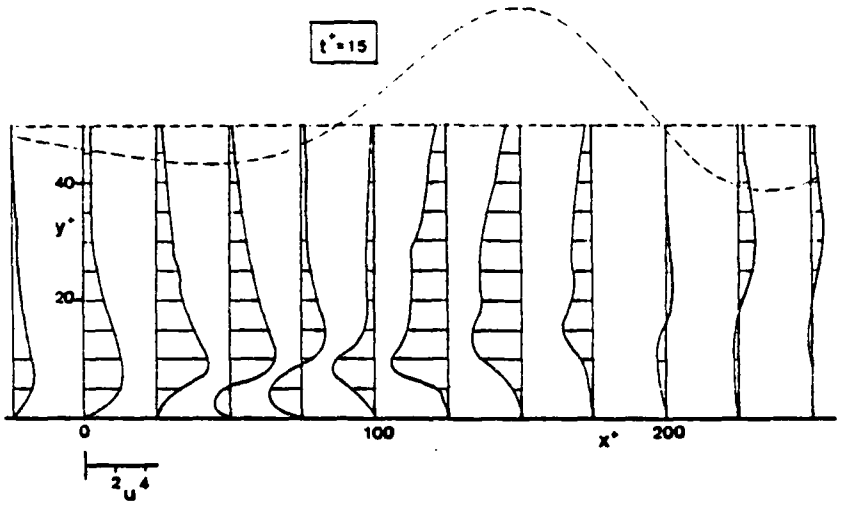

Figure 5. Distribution of streamwise velocity perturbation at $t^+ = 15$. Dotted line gives position of fluid elements originally located along $y^+ = 50$.

The displacement of the outer edge of the wall layer (taken to be located at $y^+ = 50$) is also indicated in both figures. For $t^+ = 15$ the displacement has become so large that the validity of the linearized theory may be seriously in doubt for this choice of initital velocity amplitudes. Nevertheless, the characteristic features shown by the theory such as the appearance of a bulge next to a depression further downstream are likely to be correctly represented. The depression and bulge will be convected downstream with a velocity less than U_∞, and the fluid riding over the outer edge of the wall layer will induce a pressure pattern which could be expected to consist of an overpressure in the region below the depression and an underpressure below the bulge. This pattern will then disperse as waves.

Perhaps the most revealing way to present the results is to show how the perturbation velocity distribution at a given downstream location varies with time. This would be what would be seen in experiments such as those of Blackwelder & Kaplan (1976) in which instantaneous velocity distributions were measured by a hot-wire rake. The variable-interval time-averaging (VITA) detection and sampling method employed by them could be expected to pick out structures which have formed just upstream of the measurement station. Accordingly, the station $x^+ = 50$, a position about half-way downstream of the center of the initial disturbance, was chosen as one which might correspond qualitatively to the experimental situation. In Fig. 6 are shown the streamwise perturbation velocities as function of y^+ at various nondimensional time t^+ after the initiation of the disturbance. One sees first a velocity defect extending throughout the whole layer. This arises because the station considered is first affected by fluid elements which have been lifted up by the initial v_0-distribution. At $t^+ = 10$ the regions further out from the wall have begun to receive fluid elements travelling towards the

wall, and an accelerated region begins to fill up the whole y^+ -range. The perturbation velocities then decay slowly to zero.

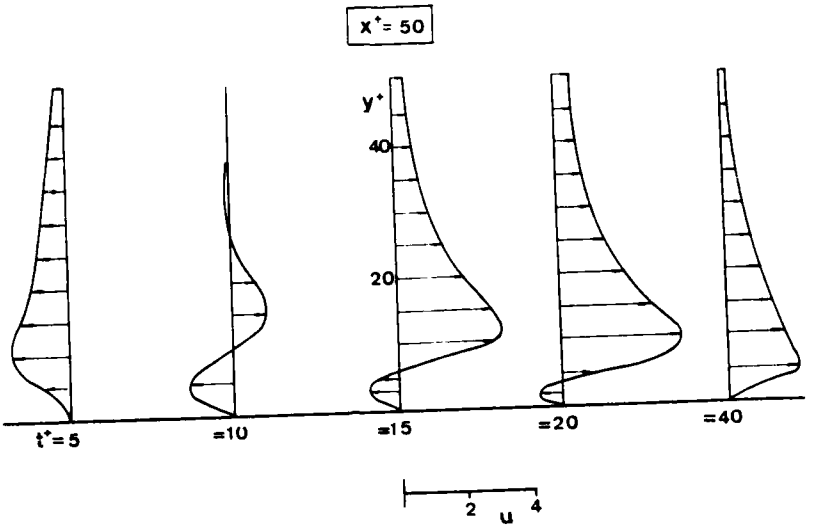

Figure 6. Streamwise perturbation velocity profile for $x^+ = 50$ at various instances of time.

The model calculations may be compared to the conditionally sampled perturbation velocities obtained by Blackvelder & Kaplan (1972) using their VITA procedure. These are reproduced in Fig. 7. As seen, the results obtained from the theoretical model are remarkably similar to the experimental ones. The most characteristic features of the measured data, which are correctly represented by the theory, is the strong shear layer, which appears to propagate towards the wall, and the very rapid acceleration associated with the passage of the shear layer. The experiments also show the predicted slow deceleration back to the undisturbed mean flow. The main qualitative difference is the observed excess velocity in the outer layer for early times which is not included in the simplified model. This velocity excess is probably a manifestation of the wallward motion (the sweep) which has been observed to precede the bursting (Corino & Brodkey, 1969 Offen & Kline, 1974) and which appears to be essential for the initiation of the lift-up and subsequent bre k-up of the flow in the wall region. This sweep is believed to originate in a previous burst further upstream. Since it was assumed for the initial conditions that $u_0 = 0$, the calculated results will show small streamwise perturbations in the outer region for small times.

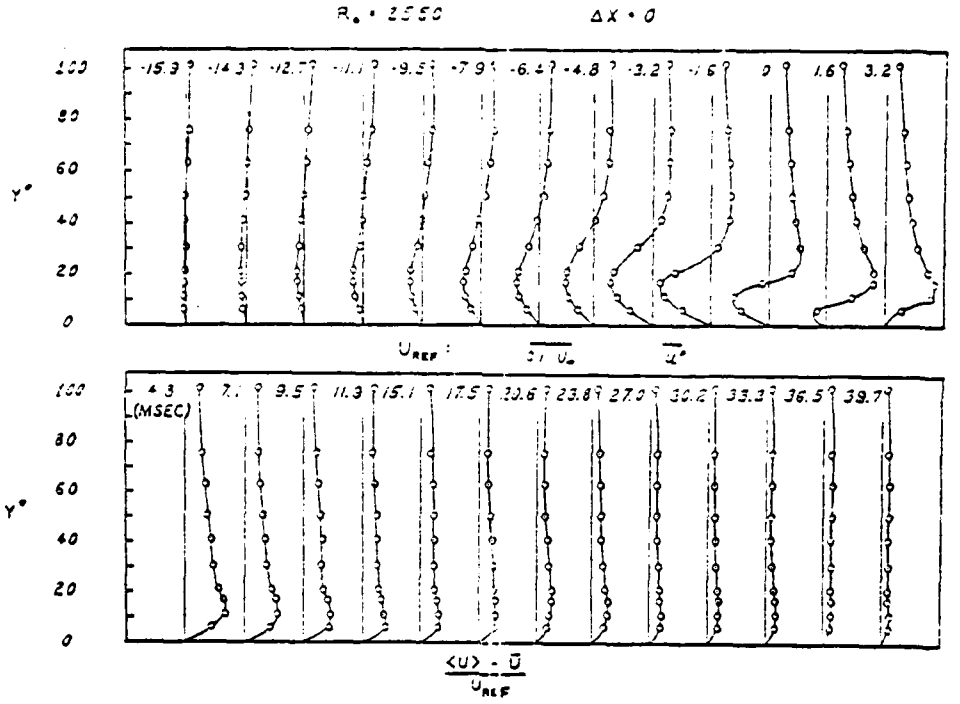

Figure 7. Conditionally (VITA) averaged u-perturbation velocity profiles with positive and negative time delay τ relative to the time of detection obtained in experiments by Blackwelder & Kaplan [29].

The sign predicted by the present theory for the perturbation velocity in the outer region caused by an earlier upstream burst may be determined from the approximate asymptotic solution (40). For values of y greater than the value $y_{|v_0|max}$ for which v_0 has its largest magnitude, v_{on} is negative for the downstream region in ξ and positive for the upstream region. Therefore, the integral in (40) will be negative, and the fluid elements therefore tend to be displaced towards the wall in this region (see Fig. 8), i.e. a velocity excess occurs. For the region closer to the wall, for $y<y_{|v_0|max}$, the opposite situation prevails. Thus, a velocity excess tends to develop in the outer region for large times, and this may travel downstream to interact with a new burst.

For large times the effects of pressure must be taken into account, which may be accomplished through application of (55). By substituting into (57) the exponential approximation (62) for the velocity profile, G becomes, expressed in wall variables

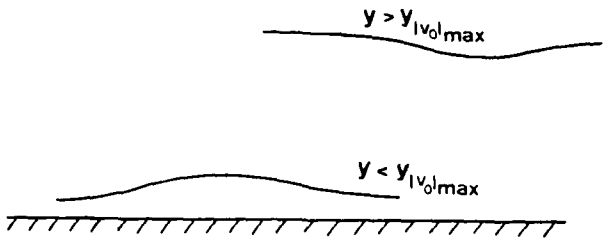

Figure 8. Typical streak lines. Upper curve, y greater than value $y_{|v_0|max}$ for which $|v_0|$ is maximum. Lower curve, $y < y_{|v_0|max}$.

$$G^+ = \frac{1}{\pi z^+} \sin\left[\frac{x^+ z^+}{U_\infty^+ t^+ \delta^+}\right] H\,(t^+ U_\infty^+ - x^+) \tag{63}$$

in which, in accordance with (62), $U_\infty^+ = 16$ and $\delta^+ = 16$. With $x^+/t^+ = U_c^+$, this gives a spanwise wave length of

$$\lambda_z^+ = 2\pi\delta^+ U_\infty^+ / U_c^+ \simeq 100\, U_\infty / U_c \tag{64}$$

Since initial disturbances of finite spanwise scales always give rise to propagation velocities less than the free-stream velocity, this expression gives a somewhat larger spanwise streak spacing than the accepted experimental value of $\lambda_z^+ \simeq 100$ (see Gupta et al., 1971). However, for such a small scale the basic assumption of the theory, namely that the horizontal scale is large compared to the thickness of the wall layer, is of questionable validity. Even more serious is the neglect of viscosity for this case, since it is likely to have a considerable effect on the dispersion characteristics of the pressure waves. Therefore, the fairly good quantitative agreement between theory and experiments in this case is probably fortuitous.

6. CONCLUSIONS

The simple theoretical model presented here is based on the assumption that the interaction mechanism responsible for the generation of turbulent fluctuations is basically inviscid and involves the interaction of eddy motion of two disparate length scales, a large-scale one, typically of a dimension of the order of the boundary layer thickness, and a small-scale one, of a dimension smaller than the thickness of the wall layer. The large-scale eddy is set into motion by the action of the nonuniform Reynolds stresses produced by inflectional instability

of a thin internal shear layer. The turbulent mixing due to this instability can be shown to induce a slow forward rotation of the large-scale flow, in a sense opposite to the mean shear. That bursting regions indeed show such a rotation has recently been found in pipe-flow experiments by Sabot & Comte-Bellot (1976).

Under the assumption that the horizontal dimensions of the large-scale field are large compared to the thickness of the wall layer it can be shown that the effects of pressure and of nonlinearity on the evolution of the large-scale eddy may be neglected during short and moderate times after its initiation. By use of a Lagrangian analysis a simple formula for the displacement of the fluid element in the direction normal to the wall could then be derived. From this, one may then easily calculate the streamwise perturbation velocity in the spirit of Prandtl's mixing-length theory.

From the approximate theory one can demonstrate that a localized disturbance tends to develop into a thin shear layer during its downstream travel. A numerical example presented to illustrate the theory shows clearly this tendency and also gives qualitative agreement with conditionally averaged data obtained in the experiments by Blackwelder & Kaplan (1972). For large times after the intitiation of the disturbance, measured in terms of the time it requires to be convected downstream a distance equal to its own length, nonlinearity, pressure, and viscosity may all become important. Nonlinear effects may be handled fairly easily by the theory for cases for which the pressure gradient effects are small.

The effects of pressure, which provide the most intricate part of the analysis, were studied on the basis of linearized equations. It was found that for large times the pressure waves will give rise to an elongated pattern whose streamwise length will continue to grow as the long waves become more and more dominant. The flow will thus become increasingly two-dimensional in planes normal to the x-axis within this pattern. From (30) it therefore follows that the pressure effect will depend primarily on p_{zz}. At a spanwise pressure maximum, p_{zz} will be negative, and the contribution to ℓ_m will be negative, i.e., the flow will be speeded up. The opposite will be true for a pressure minimum. Since a region of $p_{zz} < 0$ must always have neighboring spanwise regions of $p_{zz} > 0$, a high-speed streak could be expected to be located between two low-speed streaks. That low-speed streaks tend to occur in pairs is consistent with observations of the streaky structure in the viscous sublayer (see Gupta et al., 1971). The present theory also gives an estimate of the spacing between longitudinal streaks in terms of the wave propagation characteristics for waves of large streamwise wave lengths.

It has been proposed by Offen & Kline (1975) and others that the inflectional region preceding breakdown is caused by a large-scale travelling pressure disturbance, originating in the outer portions of the boundary layer, which will retard the fluid elements near the wall through the action of a local adverse pressure gradient. Measurements reported by Willmarth (1975) show that intermittent Reynolds stress pro-

duction is associated with the passage of a large-scale pressure minimum which would indicate that the fluid near the wall, having a velocity less than the convection velocity of the pressure, had been subjected to retardation by a positive pressure gradient just before bursting. An estimate on basis of the present inviscid theory gives, in contrast, that this effect tends asymptotically to zero as the time of travel of the disturbance tends to infinity. The result of the present theory that a large lift-up would occur at a spanwise minimum of the pressure is not inconsistent with the experimental findings, however.

Simple estimates show that viscosity is likely to become important at about the same time pressure effects begin to be felt. From comparisons between the viscous and inviscid stability analysis, it could be expected that the propagation characteristics of the waves induced during the large-scale motion will be changed considerably by viscosity. An initial-value analysis similar to the one carried out here but with viscosity taken into account would therefore be desirable. Some initial efforts in this direction have been made by Gustavsson (1978) but the analysis becomes considerably more complicated than the one presented here and the results much more difficult to interpret.

ACKNOWLEDGEMENT

The work reported in this paper was supported in part by the Air Force Office of Scientific Research under Grant AFOSR 74-2730.

My special thanks go to Mrs. Gunnel Nordenfelt and Mrs. Ingrid Pramberg for an expert typing job under trying circumstances .

AD-A100 632 PURDUE RESEARCH FOUNDATION LAFAYETTE IND F/G 20/4
WORKSHOP ON COHERENT STRUCTURE OF TURBULENT BOUNDARY LAYERS.(U)
NOV 78 D E ABBOTT, C R SMITH AFOSR-76-3015
UNCLASSIFIED AFOSR-TR-78-1533 NL

5 of 6
AD
A100632

REFERENCES

Bark, F.H. 1975 J. Fluid Mech. 70, 229

Blackwelder, R.F. & Kaplan, R.E. 1972 "The intermittent Structure of the Wall Region of a Turbulent Boundary Layer" Paper presented at the 13th IUTAM Congress, Moscow

Blackwelder, R.F. & Kaplan, R.E. 1976 J. Fluid Mech. 76, 89

Corino, E.R. & Brodkey, R.S. 1969 J. Fluid Mech. 37, 1

Einstein, H.A. & Li, H. 1956 Proc. ASCE, J. Eng. Mech. Div. 82, EM 2

Frenkiel, N.F., Landahl, M.T. & Lumley, J.L. 1977 Phys. Fluids, 20, No. 10, Pt. II

Gupta, A.K., Laufer, J. & Kaplan, R.E. 1971 J. Fluid Mech. 50, 493

Gustavsson, L.H. 1978 On the evolution of disturbances in boundary layer flows, TRITA-MEK-78-02, The Royal Inst. Technology, Stockholm, Sweden

Lamb, H. 1932 Hydrodynamics, 6th ed., Cambridge University Press

Landahl, M.T. 1967 J. Fluid Mech. 29, 441

Landahl, M.T. 1973 in Proceedings of the 13th IUTAM Congress, 177 Springer Verlag

Landahl, M.T. 1975 SIAM, J. Appl. Math. 28, 735

Landahl, M.T. 1977 Phys. Fluids 20, No. 10, Pt. II, S55

Lin, C.C. 1955 The Theory of hydrodynamics Stability, Cambridge University Press

Offen, G.R. & Kline, S.J. 1974 J. Fluid Mech. 62, 233

Offen, G.R. & Kline, S.J. 1975 J. Fluid Mech. 70, 209

Prandtl, L. 1925 Z. angew. Math. u. Mech. 5, 136

Sabot, J. & Comte-Bellot, G. 1976 J. Fluid Mech. 74, 767

Sternberg, J. 1965 AGARD-ograph 97

Theodorsen, T. 1952 in Proc. of the Second Midwestern Conference of Fluid Mechanics, Ohio State University

DISCUSSION

Kline:

Marten (Landahl), you said that you were basically working off the inflectional profile, but you wanted also to have the condition that the group velocity of the finer-scales was the same speed as the phase velocity of the larger motion. Can you give us some simple reason why you want that condition? Does it arise out of your assumption that a finer scale has to feed back into a larger-scale?

Landahl:

No, it's simply a result of kinematic waves. When the wave group comes to a position where it's group velocity is equal to the phase velocity it tends to compress, it's an accordian effect, and the amplitudes tend to go up.

Kline:

In other words, you need that (the accordian effect) in order to get the increase in amplitude?

Landahl:

I suspect that it isn't required for a violent instability, and this may constitute an explanation as to why not every inflectional profile leads to a burst.

Reynolds:

I guess it is worth noting that in two-dimensions, it generally is understood that the cascade goes in the other direction, from high wave numbers to low wave numbers.

Brodkey:

Marten, I'm just a little confused. The first part of the analysis is for very short-times, and yet when you brought in the last part, you ignored the branch, which would be $1/t$, which turns the analysis around and makes it long-time. I don't quite understand what time is in the total solution, because one part of the analysis is for short-times and the other is for long-times.

Landahl:

Large time means large time in terms of how far the structure travels in terms of it's own dimension.

Brodkey:

I'd call that a short time.

Landahl:

Well, not necessarily, because the smaller scales can travel several times their own scale downstream. If you look at Emmerling's pressure measurements, you'll see this.

Falco:

Marten (Landahl), you say that to get a sufficiently rapid event, that we should be considering an inviscid process. Would you comment on that in light of Dave Walker's talk a little bit earlier in which he showed a fairly rapid process which was brought about because of the no-slip condition on the wall and viscous action?

Landahl:

I really don't have a feel for the time-scales involved in that case. Of course, one thing you have to realize is that the vorticity regions that you see in the boundary layer are always flattened out. They are not concentrated vortices, and that, of course, sets the time-scale of the evolution of the viscous effects, also. If you noted, my estimate of the effect of viscosity on the large-scales involved a characteristic length, and for very short lengths of course, viscosity effects will set in fairly rapidly.

Blackwelder:

I am curious as to how you get a length-scale in the spanwise z-direction. Did you make some specific assumptions which brought that in?

Landahl:

No, not really. It came from the dispersion relationship of the inviscid waves. Of course the shortest length-scale is involved with propagational waves, which propagate at a velocity close to the free stream, and the theory isn't good for that regime. That's the reason that I say it's probably a coincidence that the results are of the right order of magnitude. However, once you have identified that this is a wave property, you can go ahead and perform the wave calculation for the completely viscous case. If you do that, you find that there are spectral peaks which correspond to a spanwise, wave-length which is roughly consistent with experimental data, perhaps 50% greater. The predicted stream-wise lengths are about 6 or 7 times as long.

Blackwelder:

Have you looked at the span-wise velocity component then?

Landahl:

No.

Walker:

I'd like to comment in response to the matter of concentrated vorticity. I think it's clear from some of Falco's work that those typical eddies are pretty concentrated regions of vorticity.

Landahl:

They become concentrated eddies once they lift-up and that could come about either through instability or through something else. What happens once you get them concentrated is, of course,another story. I'm just considering the condition for initiation of the strong secondary instability.

Walker:

The second question I have focuses on your appraoch. I'm not clear what equations you are solving to begin with. You neglected the viscosity and there doesn't seem to be any composite inner and outer layer in what you start off with.

Landahl:

Well, I'm analyzing the inner layer.

Walker:

And neglecting viscosity?

Landahl:

Sure. That's perfectly okay as long as I stick to short times relative to the initiation of the large-scale distrubance. The estimate of the time-scales was what I gave in one of the first slides.

Walker:

What is it that you expect to happen once the shear layer or the profile develops an inflection?

Landahl:

Once it develops a shear layer, I expect that a secondary instability would set in.

Walker:

Yes, but what physically is going to happen? Are we going to see an explosion or what?

Landahl:

There will be a strong mixing which relieves the internal shear layer, and sets off the next large-scale disturbance.

Walker:

So, in your view of things, there is nothing initiating this in the outer layer; this is a small disturbance?

Landahl:

I'm not saying that nothing initiates this instability in the outer-layer. The thing that initiates the breakdown of the outer-layer is most probably a pressure disturbance passing by, because pressure has the right propagation characteristic for producing focusing of secondary instabilities.

Zakkay:

Are there any limitations in U_∞ or Reynolds number? I'd like to know because there was some discussion of these yesterday. I think Professor Kline mentioned that the effective Reynolds number is not that important. Very little experimental results are being obtained in higher Reynolds number ranges, and I think that we really need to redefine our conditions at very high Reynolds numbers, especially the sublayer condition.

Landahl:

As to the effect of viscosity, although I present the results in wall variables, that's only incidental to the theory. The evolution of the disturbance is completely controlled in this theory by the mean flow. The reason why the wall variables come into the picture is because you can express the velocity distribution in the inner wall region by wall variables. That's the only reason for them. And thus U_∞ really implies the velocity at the edge of the wall-layer.

Zakkay:

But what limitations can it have on the Reynolds number?

Landahl:

The limitation on Reynolds number has to do with the limitation on viscosity and that's contained in this analysis. I'm just following a large-scale distrubance from its initiation by small scale mixing. Viscosity will set in and, in particular, viscosity will be important for the smaller scales.

Orszag:

I would just like to suggest that one of the panels consider the question of precisely what flow equations we can use when considering a turbulent boundary layer. Is it okay to use the boundary layer equations to analyze such things as a spot or turbulent burst? Can we neglect viscosity or do we have to use the full Navier-Stokes equations? We've heard a couple of talks today where approximations have been made, and we need to ascertain the limitations of such analyses.

Reynolds:

Okay, the question to a committee is "Which equations should be used to characterize certain features of the flow?" Perhaps there might be more than one feature or more than one recommendation on the kinds of equations.

[Reynolds appoints committee of Orszag, Ormand, and Reshotko to examine question; see committee report number one. Ed.]

Landahl:

Let me point out, that there is a boundary-layer assumption involved in my analysis, namely that the stream-wise lengths of the disturbance are large compared to the thickness of the layer. That's precisely the boundary-layer assumption. This allows one to assume that the induced pressure is effectively constant through the layer.

Kline:

I wanted to inquire a little farther into your (Landahl's) remarks about the pressure coming down to the wall. We all recognize,of course, that you can describe it as vorticity or as a vortex sheet or as velocity, but it might also be well to remember that Euler's equations, tell us that pressure perturbations are also velocity perturbations. What I want to ask you is are you visualizing pressure distrubances as initiating streaks or initiating lift-ups? The two would be quite different, presumably.

Landahl:

The equations for the large-time behavior due to the pressure indicates that the lift-ups will extend in the stream-wise direction at the rate proportional to the U_∞ minus a local velocity and they will remain fixed in time after that. So you will then have a string of fluid elements having been lifted-up. You will have the opposite effect in the neighboring regions, because this behavior is proportional basically to the second span-wise derivative of the pressure. So you'll always find uplifted regions in streaks, neighboring with down-press (or flow) regions. I think that's fairly consistent with the experimental picture.

Kline:

Then you're saying that the streak structure itself comes out of the pressures in your theory.

Martin:

Right.

Kline:

That's what I wanted to find out...thank you.

Landahl:

A pressure pulse passing by will leave a lifted-up region or a depressed region, depending where you are in span-wise location.

Coles:

I have a question actually for the speaker and I think for the audience to consider. I heard the speaker use the words coherent structure and large eddy. I point out that for many years we have thought of boundary layers as having two characteristic scales. There's the sublayer scale and there is an overall scale.

Coles: (Cont'd)

Now I think these words coherent structure and large eddy are being used relative to both of those scales. I think a lot of confusion has arisen because some of the early flow visualization was done at such low Reynolds numbers that the scales are not distinct. I want to know if the speaker agrees on the necessity of making a distinction?

Landahl:

I think it's very difficult to pinpoint what you call a large and a small-scale if you want to do it by definition in any very strict manner. As I mentioned in the beginning, I took the small-scales to consist of motion of the order of a tenth of the wall units, whereas the large-scales would incorporate scales of the order of say the boundary-layer thickness or the displacement thickness. I don't want to stick my neck out and give a more precise definition of what I consider one or the other. Obviously, a two-scale model like this represents an idealization. In real flows, you have interactions between neighboring scales, but that's too difficult to analyze. So I want to first point out this particular interaction mechanism which I feel should be pursued.

SESSION IV

SHORT PRESENTATIONS

Session Chairman:

Douglas E. Abbott

APPLICATION OF A SMOKE-WIRE VISUALIZATION TECHNIQUE TO TURBULENT BOUNDARY LAYERS

H. M. Nagib, Y. Guezennec & T. C. Corke

Mechanics & Mechanical & Aerospace Engineering Department

Illinois Institute of Technology, Chicago, IL 60616

A flow visualization technique, utilizing a "smoke-wire" for introducing controlled sheets of smoke streaklines, has been used over the last two years in several three-dimensional and turbulent flowfields to produce high quality records of the flow. The results of its first application to study the turbulent boundary layer on a flat-plate are presented for Reynolds numbers based on momentum thickness of up to 3000. The recorded images are compared to similar ones obtained in the same wind tunnel by the technique employed recently by Falco [1].

The smoke-wire is mounted on a portable probe in the traversing mechanism of the wind tunnel and used to generate vertical or horizontal sheets of smoke streaklines. The location of the wire can be changed to visualize vertical sheets of smoke at any lateral position of the boundary layer or to observe and record horizontal sheets of streaklines at any height from the surface of the flat plate. This procedure can be repeated at various downstream locations to study the development of the boundary layer.

The surface of the 0.1 mm diameter wire is coated with uniformly spaced minute droplets of oil which are vaporized by its resistive heating, resulting in sheets of discrete streaklines. A synchronization circuit controls the duration of the time the wire is supplied with the heating current and triggers the camera and lights after an adjustable delay. The synchronization circuit can be triggered manually or by an external input signal which can be provided from the output of a transducer sensing the flowfield. For example, this trigger signal could be obtained by conditioning the output from a hot wire in the boundary layer or a pressure transducer in the surface of the flat plate. The smoke wire is operated from outside the wind tunnel without interruption of the experiment. Applications of the smoke-wire technique

to study flows near building models in simulated atmospheric turbulent boundary layers, to investigate wakes of bluff bodies, to examine the transition downstream of a protuberance in a laminar boundary layer, and to record the shear layers instability and turbulence downstream of grids have been presented by Nagib et. al. [2-5]. Preliminary analysis of some of these visualization records by digital computers will soon be presented by Nagib et. al. [6]. The recorded images of the smoke sheets are digitized on a drum scanner to facilitate this analysis.

The turbulent boundary layers are developed naturally on a 2.6 m long flat plate suspended in the 0.6 x 0.9 x 3 m test section of the wind tunnel. The smoke wire permits the visualization of boundary layers over a large range of Reynolds numbers which extends to values higher than those available by traditional smoke techniques or by hydrogen bubbles visualization in water tunnels. Using free stream velocities ranging from 1.5 to 10 m/s with the shear layers developed naturally on the plate, the estimated Reynolds numbers based on the boundary layer development length and momentum thickness range from 2×10^5 to 1.6×10^6 and from 600 to 3600 respectively. All of the photographs presented in Figs. 1 and 2 were recorded using stroboscopic illumination to obtain an instantaneous image of the boundary layer over approximately 0.5 m of the flat plate near its trailing edge.

Based on our preliminary experience with this application of the smoke wire the following conclusions can be made. The photographs of Figs. 1 and 2 support these conclusions.

1. As in all of its other applications, the smoke wire provides a reliable technique which leads to high quality records with far less smoke contamination of the wind tunnel. These records can be obtained at any desired instant in any location and cross section of the flow with very high resolution in the plane of the smoke sheet and minimum interference from flow conditions outside this cross section. Simultaneous qualitative (or possibly quantitative) hot-wire measurements can be obtained with probes positioned in the plane of the smoke sheet with much less interference from the smoke droplets as compared to the case of conventional smoke. As in the case of the hydrogen bubble technique, positioning the wire in the region of interest permits the direct observation and recording of changes in the unsteady flow from the wire to nearby downstream locations.
2. Boundary layers can be visualized at Reynolds numbers higher than those possible by other techniques, e.g., hydrogen bubbles and conventional smoke methods, because of the high velocity capability and the local introduction feature of the technique.
3. The edge of the boundary layer is clearly defined by this technique.
4. Information regarding the potential flow in the intermitent region of the boundary layer and in the free stream above it is readily available from the recorded images.

5. Using the smoke wire simultaneously with conventional smoke, introduced downstream of the leading edge of the boundary-layer plate to mark the "vortical part of the shear layer," provides direct comparison between the two methods and sheds some light on the question of coincidence of the boundary layer edge and the boundary of the region marked by the conventional smoke.

ACKNOWLEDGMENTS

The research was partly supported by NSF Grant ENG 76-04112 and USAF OSR Contract F44620-76-C-0062.

REFERENCES

[1] Falco, R. E., "Coherent Motions in the Outer Region of Turbulent Boundary Layers," J. Phys. of Fluids, 20, 11, 1977, p. 5124.

[2] Corke, T., Koga, D., Drubka, R. and Nagib, H., "A New Technique for Introducing Controlled Sheets of Smoke Streaklines in Wind Tunnels," Proceedings of International Congress on Instrumentation in Aerospace Simulation Facilities, IEEE Publication 77 CH1251-8 AES, 1977, p. 74.

[3] Nagib, H. M., "Visualization of Turbulent and Complex Flows Using Controlled Sheets of Smoke Streaklines," Proceedings of the International Symposium on Flow Visualization, Tokyo, Japan, October 1977.

[4] Nagib, H. M., Merati, P. and Crawford, A. C., "Visualization of Turbulent Atmospheric Flows," Proceedings of the Third U.S. National Conference on Wind Engineering Research, Gainesville, Florida, February, 1978.

[5] Corke, T. C., Nagib, H. M. and Crawford, A. C., "Visualization of Turbulent Flows Using Controlled Sheets of Smoke Streaklines," 30th Physics of Fluids Meeting of the American Physical Society, APS Bulletin, November, 1977.

[6] Nagib, H., Corke, T., Helland, K. and Way, J., "Computer Analysis of Flow Visualization Records Obtained by the Smoke-Wire Technique," Proceedings of the Dynamic Flow Conference, Baltimore, Maryland, September, 1978.

Re_θ = 1200

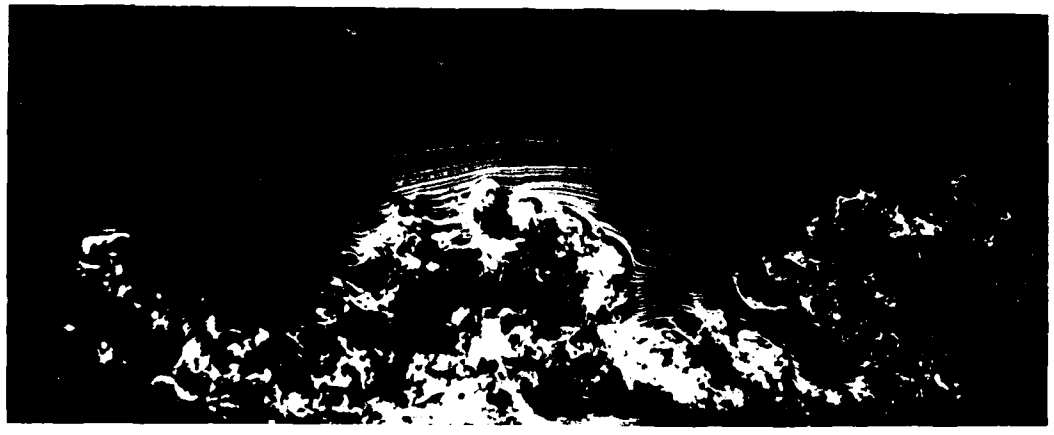

Re_θ = 1800

Re_θ = 2600

Flow

Fig. 1. Turbulent Boundary Layers Visualized By Smoke Wire at Different Reynolds Numbers Based on Momentum Thickness

Conventional

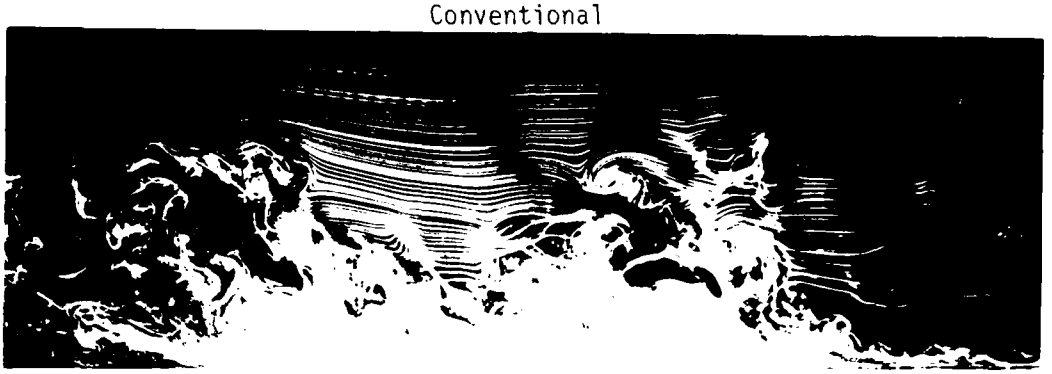

Simultaneous Conventional and Wire
Re_θ = 600

Conventional

Simultaneous Conventional and Wire
Re_θ = 800

Flow

Fig. 2. Comparison Between Conventional Smoke and Smoke Wire Visualization Techniques at Two Reynolds Numbers Based on Momentum Thickness.

DICUSSION

Brodkey:

The difference between those two last pictures should be discussed.

Nagib:

Yes, I would like Bob Falco to comment on it, but my feelings are like this. We tried some things, we talked to Bob Falco, we made changes and we found out that it was very difficult to get the two to match unless you introduce the smoke in a laminar boundary layer and you don't trip it. I'm referring to the edge of what you see using conventional smoke techniques and the edge that you define from what looks like a potential part and a vortical part from the smoke wire. If in introducing the smoke, you trip the boundary layer so that it's going through transition as you are introducing the smoke, they don't seem to match. Bob had suggested that we really should introduce the smoke within the laminar boundary layer and then trip it. We have not been able to do that but that is only due to our difficulty of setting up the experiment in our facility within the limited time.

Falco:

I guess you said what I wanted to. The piece of evidence that we have is this: we've done simultaneous hot wire measurements in the smoke filled boundary layer by first introducing smoke into a laminar boundary layer, through discreet holes in the tunnel wall and across the span of the boundary layer, and then tripping it. What we found is that there is a reasonably close correspondence between what you observe and the hot wire signals, going from the very low fluctuation levels to very high fluctuation levels (or vice versa) as you cross the boundary of the smoke. The correspondence was by no means exact, but it was fairly close. Some of the earlier pictures I have seen of Nagib's, and even the ones he showed here, show that there are times when the two techniques seem to correspond and at other times they do not.

Nagib:

We have tried, and all that I can say right now is that it is very difficult for us to get the two to coincide.

Falco:

It's very clear that if you have a turbulent boundary layer and you introduce the smoke at some position downstream of the origin of the turbulence, then you have a separate boundary layer developing

Falco: (Cont'd)

and the two only asympototically agree. It's the same problem, of course, with temperature contamination so you have to be very careful how you introduce the smoke. I think if you are careful, you can get reasonable correspondence. May I ask a question? Are you suggesting to us that you figured out a way to get a turbulent shear flow which has an extremely low outer intermittency?

Nagib:

You saw pictures. The design of that manipulator was intended to take the large scale motion out, and as I showed you in the pictures, it did.

Falco:

Does it grow more slowly than a normal turbulent boundary layer?

Nagib:

It's practically not growing at all. I looked at it for about 12 deltas on length and it's almost parallel to the wall.

Falco:

You don't have probe measurements?

Nagib:

No, not yet.

Willmarth:

Is the reason it works because the pressure gradient over that step is very favorable?

Nagib:

The case with the step I don't understand as well, actually. I did the one with the step after having discussions with Mark Morokovin. But the one with the four plates was based on our experience with honeycombs for taking out large scale motion. I designed it the same way I would design a honeycomb for a wind tunnel and it worked.

Kline:

Two things. First, I'd like to remind you that in Runstadler's work we used time lines from a bubble wire, which are essentially

Kline: (Cont'd)

very close to your smoke technique. And we did in that case actually map out intermittency, making corrections for the fact that there's a difference in interpretation. So that in one case you've got volumes and in the other case you've got Eulerian vectors and you have to correct about 15% in some cases, but not more than that. But if you make that correction, then you get a very good agreement with the measured intermittency factors. Secondly, I'd like to ask that in making these comparisons, you make them quantative and identify the parameters because I don't know what you mean by differences. The gross pictures don't look that different, but is δ different? Are the velocities you see different? What differences are you talking about and how much in magnitude?

Nagib:

I have no measurements in these boundary layers. It basically was a preliminary study trying to investigate what you can visually determine within the boundary layer. In regard to the first of your questions, I am familiae with your work at Stanford. But what I'm saying is that with this technique you do get a better visualization of the potential part of the flow than you do with the hydrogen bubble wire. It's very interesting that you can see this so clearly in many of our photographs. Now in reference to the measurements, we haven't made them. But what I'm saying right now is you can compare these two photographs (and its not just one picture---we have something like 50 pictures) in each case there is definite absence of the large scale motion and you can see that the imprint on the boundary layer near the floor does look different between the two.

Bushnell: (Showing a slide)

The manipulator in this case came from consideration of some work presented at the Berlin meeting last year. I don't know if you can see this clearly, but these are measurements with screens just across the boundary layer (not across the whole flow). The result is that the skin friction is down by about 50% with the screens. The relaxation distance is the order of 60 to 100 boundary layer thicknesses, rather than 4 to 10 if you're just taking out the momentum. The visual evidence from these kind of experiments at Langley is that this sort of manipulator may work on the large scale structure.

[Ed. Comment: See panel presentation by Bushnell for further discussion of turbulence manipulators.]

ON THE PERIOD OF THE COHERENT STRUCTURE IN BOUNDARY LAYERS AT LARGE REYNOLDS NUMBERS

M. A. Badri Narayanan* and Joseph G. Marvin

Ames Research Center, Moffett Field, California 94035

ABSTRACT

The period of the large coherent structure in a subsonic, compressible, turbulent boundary layer was determined using the autocorrelation of the velocity and pressure fluctuations for Reynolds numbers R_θ between 5,000 and 35,000. As observed previously by Laufer and Badri Narayanan, in low Reynolds number flows the overall correlation period ($\bar{T}$) scaled with the outer variables -- namely, the free-stream velocity U and the boundary-layer thickness δ. Also, the value of $U\bar{T}/\delta$ was nearly constant, approximately 6 ± 1, and it agreed with previous measurements.

SYMBOLS

U	free-stream velocity
U^*	friction velocity $= \left(\frac{\tau_w}{\rho}\right)^{1/2}$
u	mean velocity
u'	fluctuating velocity in the direction of the free stream
p'	fluctuating static pressure
w	subscript w means wall conditions
δ	boundary-layer thickness at 99.5% of U
θ	momentum thickness

*National Research Council.

R_θ $\quad \frac{U\theta}{\nu}$

ν kinematic viscosity

ρ density

τ_w wall shear stress

c_f skin-friction coefficient = $\frac{\tau_w}{(1/2)\rho U^2}$

$R_{zz}(t)$ autocorrelation coefficient = $\left[\frac{\overline{Z(t)Z(t+\Delta t)}}{\overline{Z(t)^2}}\right]$

$\bar{T}$ period of the second zero in $R_{zz}(t)$

1. INTRODUCTION

The existence of some well-defined patterns in the velocity fluctuations in a turbulent boundary layer such as the wall bursts and the wavy motion in the outer region have been well established (refs. 1-4). Investigations by Laufer and Badri Narayanan (ref. 5), by Badri Narayanan, et al. (ref. 6), and by Brown and Thomas (ref. 7) have clearly shown the existence of a near-cyclic flow motion across the boundary layer suggesting that the wall bursts and the outer wavy motion are just two phases of the same process. This cyclic macrostructure could be considered as the largest eddy in the flow or as a coherent structure, a terminology coined after the well-organized eddy patterns observed in a free mixing layer by Brown and Roshko (ref. 8). Various techniques employed for the identification of the coherent structures from the overall random fluctuations in a turbulent boundary layer have suggested that the average length of the coherent structure of a flat plate turbulent boundary layer is nearly five to six times the boundary layer thickness, and is independent of Reynolds number. Information so far available in the literature is mainly confined to incompressible boundary layers having R_θ less than 10,000. The main aim of this investigation was to extend the data to high R_θ as well as to compressible flows. The experiments were conducted in a 10.2 cm by 15.2 cm wind tunnel capable of producing Mach numbers and Reynolds numbers (R_θ) up to 0.5 and 35,000, respectively. The autocorrelation technique was employed for determining the period of the coherent structure. Major details of the experimental setup, as well as the procedures, are described in ref. 9.

2. RESULTS AND DISCUSSION

Some of the measured mean velocity profiles are plotted in figure 1 in the standard semilogarithmic form, U/U^* versus yU^*/ν, where U^* is the friction velocity. The skin-friction coefficients for the above plots were obtained by using the Ludwig-Tillman formula, namely

$$c_f = 0.246/R_\theta^{-0.268}\ 10^{-0.678\ H} \qquad (1)$$

with Van Driest's correction for Mach number. All the profiles exhibit a definite logarithmic region which follows the law, $U/U^* = 5.6 \log_{10} yU^*/\nu + 5.4$, indicating that the values of c_f, obtained using Ludwig-Tillman's formula, agree well with those inferred from the profile measurements. The maximum velocity defect of nearly 2.60 is a good indication of the fully developed nature of the boundary layer (ref. 10).

The autocorrelation measurements of velocity fluctuations made at the wall and in other regions of the boundary layer, at R_θ of 10,000 are shown in figure 2. All across the boundary layer, the curves look similar. Correlation curves corresponding to different Reynolds numbers measured at $x = 3.0$ m at 0.1 mm away from the wall are given in figure 3. Measurements made using pressure fluctuation data showed similar results (ref. 9).

The aim of the present investigation is to study the period of the coherent structure in a boundary layer using the measured autocorrelation $R_{zz}(t)$

$$R_{zz}(t) = \left[\frac{\overline{Z(t)Z(t + \Delta t)}}{\overline{Z(t)^2}}\right] \tag{2}$$

The value of $R_{zz}(t)$ reaches zero rapidly, extending to the negative region and returning to zero once again (figs. 2 and 3). Beyond this period, low-magnitude oscillatory traces are observed. The second zero, corresponding to the end of the negative portion of R_{zz}, is of considerable importance in determining the period of the coherent structure. Laufer and Badri Narayanan (ref. 5) used the extent of this second zero to represent the overall correlation time $\bar{T}$ and the same method is adopted in the present investigation.

The determination of $\bar{T}$ from the experimental correlation curve has a certain amount of uncertainty due to the oscillatory nature of the correlation curve. In the present investigation, the curves were smoothed to evaluate $\bar{T}$. The correlations were obtained with an averaging period of 10 sec; the results were repeatable within the uncertainty level indicated in figure 4.

The values of $\bar{T}$ obtained from the present experiments at and near the wall are plotted in figure 4, in the nondimensional form $U\bar{T}/\delta$ versus R_θ for Reynolds number and Mach number ranges of 5,000 to 35,000 and 0 to 0.5, respectively. These new data have about the same scatter band as those from previous studies. No definitive trends with Reynolds number can be established. The present interpretation is that $U\bar{T}/\delta$ is essentially constant with increasing Reynolds number having a value approximately equal to 6 ± 1.

At any given Reynolds number, the variation in $\bar{T}$ with position across the boundary layer is also nearly single-valued, as shown in figure 5. Such a result is significant since it indicates, though not directly, that a coherent structure exists throughout the boundary layer as a whole. The recent investigation of Brown and Thomas (ref. 7) supports this view.

3. CONCLUSIONS

The period $\bar{T}$ of the large-scale, coherent structure in a flat-plate boundary layer was obtained from the autocorrelation measurements of the fluctuating pressure and the longitudinal velocity. Measurements were made in the range of Reynolds number R_θ and Mach numbers from 5,000 to 35,000 and from 0 to 0.5, respectively. The value of $U\bar{T}/\delta$ was nearly constant, approximately 6 ± 1, all across the boundary layer, independent of Reynolds number and Mach number.

4. REFERENCES

1. Kline, S. J. et al.: The Structure of Turbulent Boundary Layers. J. Fluid Mech., vol. 30, 1967, p. 74.

2. Corino, E. R.; and Brodkey, R. S.: A Visual Investigation of the Wall Region in Turbulent Flows. J. Fluid Mech., vol. 37, 1969, p. 1.

3. Wallace, J. M. et al.: The Wall Region in Turbulent Shear Flow. J. Fluid Mech., vol. 54, 1972, p. 39.

4. Rao, K. Narahari et al.: The Bursting Phenomenon in a Turbulent Boundary Layer. J. Fluid Mech., vol. 48, 1971, p. 33.

5. Laufer, John; and Badri Narayanan, M. A.: Mean Period of the Turbulent Production Mechanism in a Boundary Layer. Physics of Fluids, vol. 14, 1971, p. 182.

6. Badri Narayanan, M. A. et al.: Some Experimental Investigations of the Fine Scale of Turbulence. Dept. of Aero. Engr. Report 74 FM15, Indian Institute of Science, Bangalore, India, 1974.

7. Brown, G. L.; and Thomas, A.S.W.: Large Structure in a Turbulent Boundary Layer. Phys. Fluids, vol. 20, 1977, p. 5243.

8. Brown, G. L.; and Roshko, A.: On Density Effects and Large Structure in Turbulent Mixing Layers. J. Fluid Mech., vol. 64, 1974, p. 775.

9. Badri Narayanan, M. A.; and Marvin, J. G.: On the Period of the Coherent Structure in Boundary Layers at Large Reynolds Numbers. NASA Technical Memorandum 78477, April 1978.

10. Coles, D. E.: The Turbulent Boundary Layer in Compressible Fluids. U.S. Air Force, Project Rand, Report No. R403-PR, 1962.

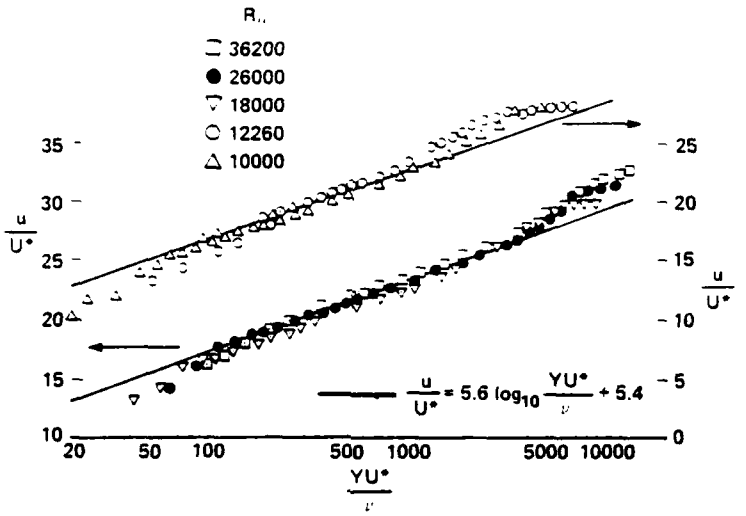

Figure 1. Mean-velocity profiles in the boundary layer.

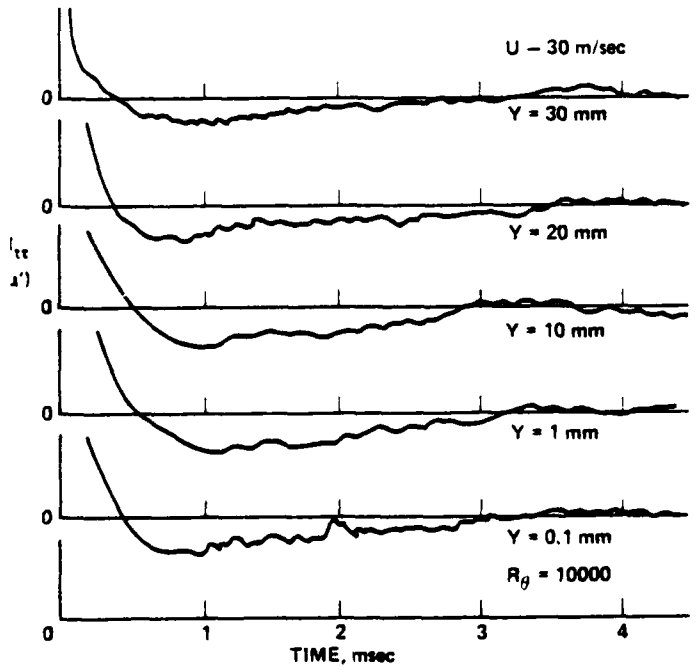

Figure 2. Autocorrelation of u' across the boundary layer.

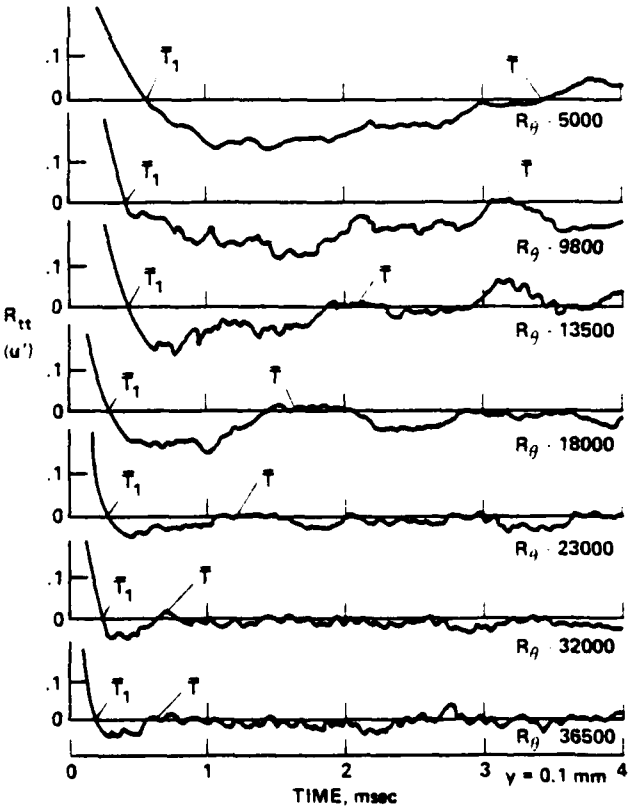

Figure 3. Autocorrelation of u' at various Reynolds numbers.

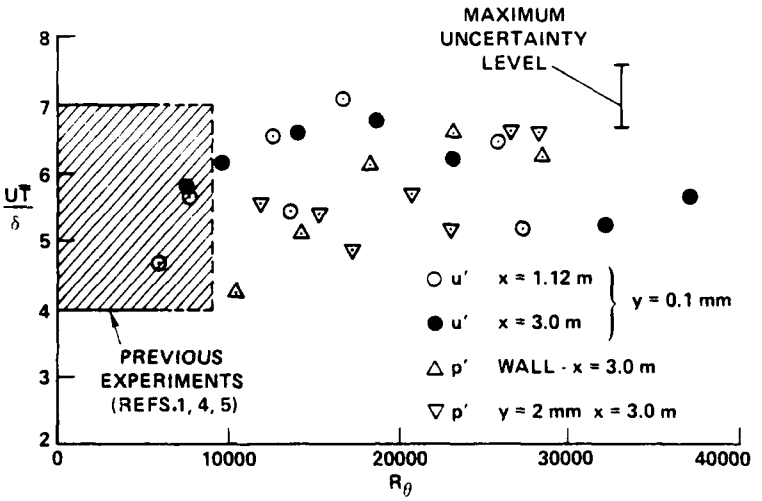

Figure 4. Variation of $\overline{UT}/\delta$ with Reynolds number.

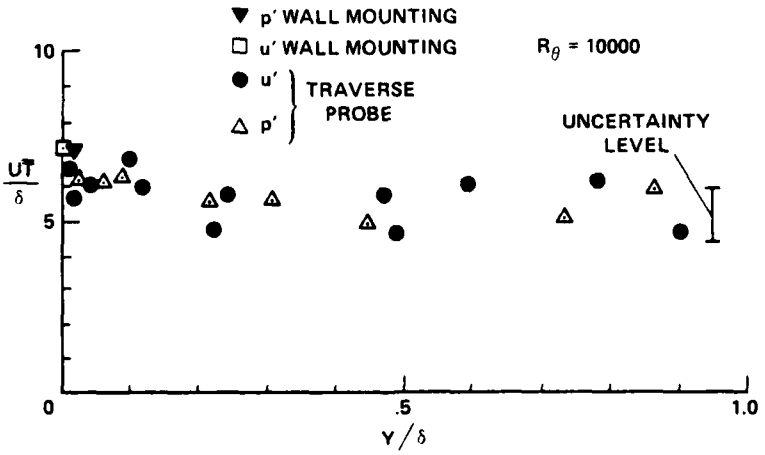

Figure 5. Variation of $\overline{UT}/\delta$ across the boundary layer.

DISCUSSION

Kovasznay:

As I recall your previous work, the principal result was that these filaments near the wall scaled with outer variables. Now, when you showed these diagrams, both when you had the T and later on you had the other variables, you plotted using outer variables.

Narayanan:

That's right.

Kovasznay:

Do you have it plotted against wall variables, too, just to see how much worse it is?

Narayanan:

We did that on the original paper in 1971.

Kovasznay:

But not now.

Narayanan:

Not now, but it will follow the same pattern. I don't have it here, but I did it.

Bradshaw:

May I point out, that if you're going to talk about time-scales, and take measurements in fixed axes, you really ought to convert them into wave lengths. That is to say, your basic variable ought to be local convection velocity, let's say local mean velocity in most cases, multiplied by T. So to say that something scales on U times T over, let's say delta is not necessarily saying anything about inner layer or outer layer variables. You're just converting correctly to a wavelength and then dividing by delta.

Narayanan:

That is true.

COHERENT STRUCTURE OF TURBULENCE AT HIGH SUBSONIC SPEEDS

V. Zakkay, V. Barra & C.R. Wang

New York University

Westbury, N.Y.

ABSTRACT

Simultaneous measurements of velocity, wall-pressure and wall-shear fluctuations in a turbulent boundary layer at $M_\infty = 0.64$ and $Re_{\delta^*} = 108{,}000$ have been analyzed to obtain a description of the coherent or quasi-ordered structures called turbulent bursts. It has been determined that the mean period between bursts, when scaled by flow velocity and boundary layer thickness, agrees with values obtained by other investigators for substantially lower free stream velocities. However, preliminary results indicate that the scaling length for the vertical dimension of the bursts is not ν/u_τ, as suggested by studies at low velocities, but rather the boundary layer thickness. It is also found that the duration of the burst event scales better with δ^*/U than with ν/u_τ^2.

RESULTS & DISCUSSION

New York University Aerospace and Energetics Laboratory has conducted experimental research under AFOSR-76-2497 for the past two years in order to obtain information concerning the possible role of pressure fluctuations on the bursting processes of the turbulent boundary layer. In order to accomplish this an extremely low noise ($u'/U_\infty = .008$) induction wind tunnel having a one foot diameter test section was designed, built and calibrated. The essentials and details of this facility are presented in Ref. 1. Simultaneous measurements of velocity, wall-pressure and wall-shear were carried out. In this manner, an improvement on the spatial resolution of the bursts is obtained. The results presented here were obtained for flow conditions which differ significantly from those in previous studies. The free stream velocity is in the high subsonic regime and the Reynolds number is an order of magnitude higher than that for which the burst phenomenon has been previously investigated (see Table I).

TABLE I

TEST CONDITIONS AND DATA SAMPLING DENSITIES FOR TWO TYPICAL INVESTIGATIONS AND THE PRESENT STUDY

	U_∞ (ft/sec)	δ^* (ft)	Re_θ	u_τ^2/ν (sec^{-1})	$\frac{\Delta t\, u_\tau^2}{\nu}$	$\frac{\Delta t\, U_\infty}{\delta^*}$
Blackwelder & Kaplan (Ref. 2) (Velocity)	14	.031	2550	1.33×10^3	1.0	.30
Emmerling (Ref. 3) (Wall-Pressure)	25	.015	2000	7.64×10^3	1.0	.24
Present Study (Velocity, Wall-Pressure and Wall-Shear)	675	.047	108000	1.61×10^6	8.0	.070

Δt = Data Sampling Interval

Based on mean flow measurements, the velocity boundary layer thickness (δ), displacement thickness (δ^*), momentum thickness (θ) and wall friction velocity (u_τ) were computed. The parameters of the boundary layer flow in the test section are summarized below:

$M_\infty = .64$ $\quad \delta = 0.334$ $\quad Re_\theta = 1.08 \times 10^5$

$U_\infty = 675$ ft/sec $\quad \delta^* = 0.047$ ft $\quad u_\tau^2/\nu = 1.61 \times 10^6$ sec^{-1}

$q_\infty = 2.9$ psi $\quad \theta = 0.032$ ft $\quad u_\tau/\nu = 9.06 \times 10^4$ ft^{-1}

The test configuration for the results presented here is shown in Fig. 1. The details of the instrumentation, data acquisition, and data analysis can be found in Ref. 1.

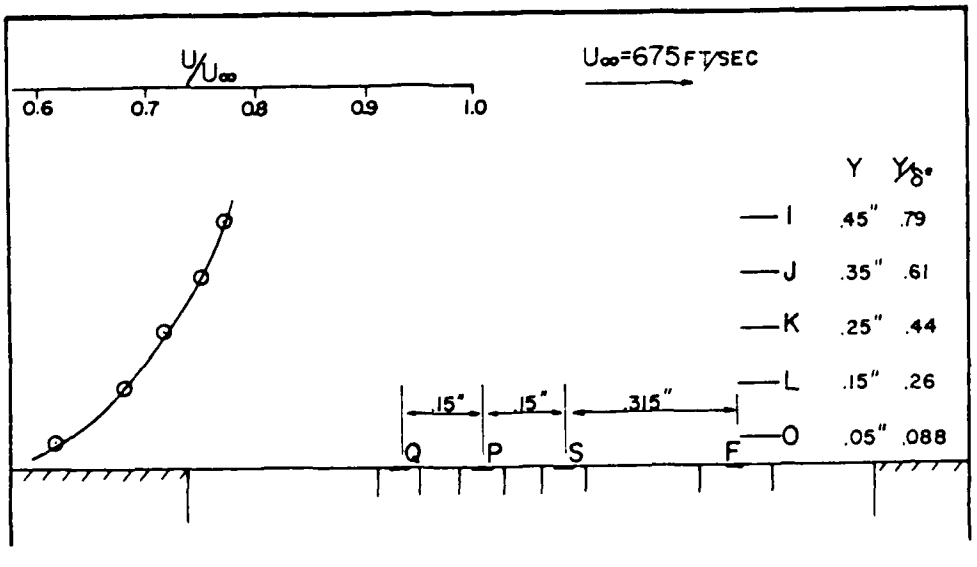

Fig. 1 Test Configuration

correlation. The correlations of the three wall-pressure fluctuation measurements in the streamwise direction indicate that the overall streamwise convection velocity of disturbances travelling along the wall is given by $U_c/U_\infty = 0.59$. The correlation of Q and P ($\Delta x = .26\delta^*$) and Q and S ($\Delta x = .52\delta^*$) both yielded approximately the same value for the convection velocity. The value obtained here falls within the range $U_c/U_\infty = .5 - .8$ found in other investigations depending on the streamwise separation between measurements and on the frequency characteristics of the fluctuations correlated

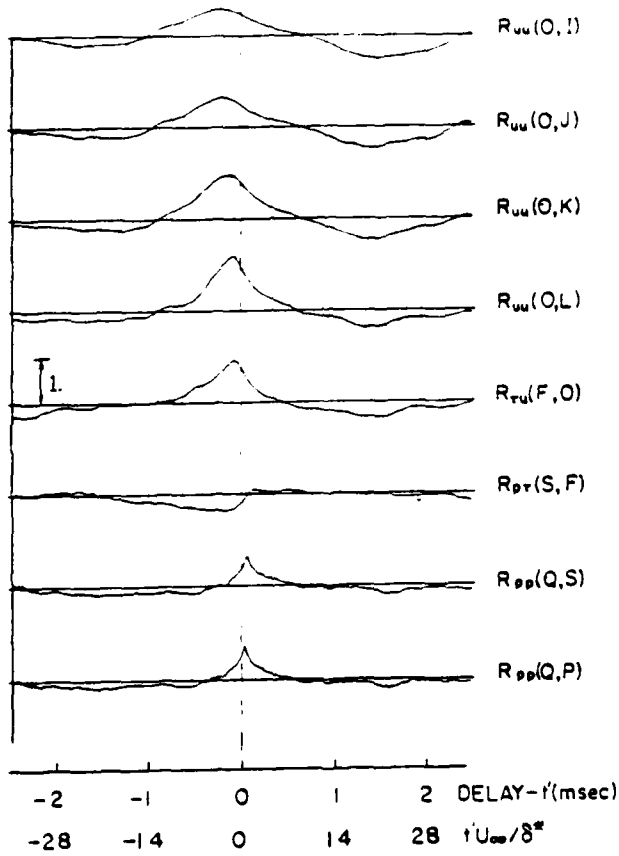

Fig. 3 Normalized Cross-Correlations Between Velocity.Shear and Pressure Fluctuations

The four velocity-velocity correlations and the velocity-shear correlation show that disturbances in the flow tend to arrive first at points away from the wall and at increasingly later times as the wall is approached. This can be interpreted either as a propagation of the disturbances from the outer part of the boundary layer toward the wall or as a tendency for the disturbance fronts to be leaning forward in the flow.

A sample plot of the digitized fluctuations is presented in Fig. 2. Approximately 21 msec ($tU_\infty/\delta^* = 294$) or 4200 points of data are shown for each of the nine fluctuating quantities. This represents about 1/14 of the total amount of data available for this test. Using the symbol α to represent one-half of the vertical distance between adjacent zero lines in Fig. 2, the vertical scales of the plots are as follows: for the velocity fluctuations $\alpha = 0.13\ U_\infty$, for the shear fluctuations $\alpha = 0.27\ \rho u_\tau^2$, and for the pressure fluctuations $\alpha = 0.024\ q_\infty$.

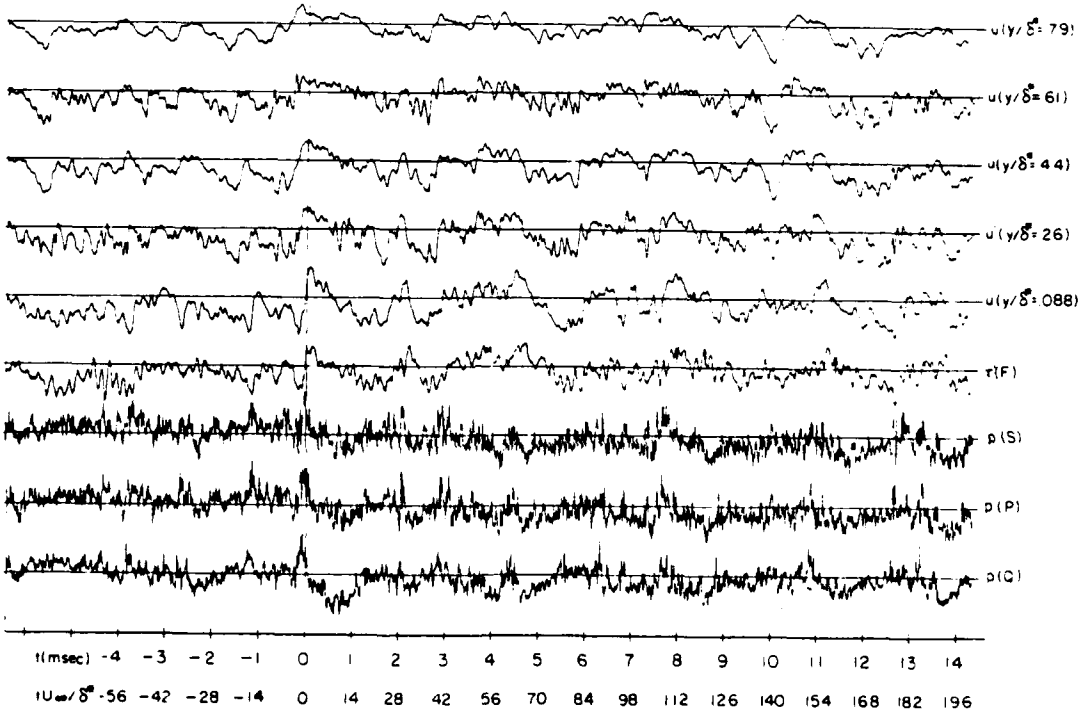

Fig. 2 Sample Plot of Digitized Data Showing Velocities, Shear and Pressures

As can be seen from Table 1, the time increment between samples for the data of Fig. 2 can be expressed as either $\Delta t\ U_\infty/\delta^* = 0.070$ or $\Delta t\ u_\tau^2/\nu = 8.0$. In terms of the scaling parameter δ^*/U_∞ our increment is much smaller than that used in the other investigations. The opposite is true when ν/u_τ^2 is used as the scaling parameter. For the velocity and shear fluctuations our sampling density is clearly more than sufficient, whereas for the pressure fluctuations it is much less so but still acceptable.

Various normalized cross-correlations between the fluctuating quantities were calculated once the fluctuations were digitized. Some of the more interesting correlations are presented in Fig. 3. All of the correlations shown were calculated for time delays ranging from -2.5 msec to + 2.5 msec ($-35 < tU_\infty/\delta^* < +35$). The time delay was imposed on the second of the two measurements listed in the parenthesis for each

By applying a conditional sampling analysis described in Ref. 1 to the digitized fluctuations it was possible to determine the average time interval between bursts detected in each of the fluctuating quantities. The mean period between bursts was found to be in the range of $\bar{T} U_\infty/\delta^* = 30\text{-}36$. This result compares well with those obtained by others at much lower free stream velocities.

A sequence of perturbation velocity profiles centered about the time $t = 0$ are shown in Fig. 4. The entire sequence is for an interval of 700 μsecs with an increment between profiles of 20 μsecs ($tU_\infty/\delta^* = 0.28$). Also shown at each time is the instantaneous shear fluctuation on the wall as measured by the flush mounted hot-film sensor. The development of the perturbation velocity profiles during this sequence is typical of the bursting event as depicted by other investigators doing both theoretical and experimental work. In particular, the profiles shown in Fig. 4 and those obtained by Blackwelder and Kaplan (Ref. 2, Fig. 5) for a boundary layer with U_∞ = 14 ft/sec and Re_θ = 2550 exhibit a great many similarities. They both indicate that the flow near the wall decelerates before bursting, that the total velocity profile will be inflectional just prior to the detection of the burst ($t = 0$), and that a strong acceleration of the flow occurs afterwards. This acceleration, which leads to large positive fluctuation velocities, is then followed by a slow relaxation nearly back to zero. The time involved for the entire process is approximately $tU_\infty/\delta^* = 10$ or $tu_\tau^2/\nu = 1150$ in our case and $tU_\infty/\delta^* = 15$ or $tu_\tau^2/\nu = 50$ for the Blackwelder and Kaplan results. This again seems to point to the fact that ν/u_τ^2 is not the appropriate scaling parameter for time.

A similar inconsistency occurs in terms of the scale of the burst in the direction normal to the wall. Although the range of y/δ^* for our measurements and those of Blackwelder and Kaplan is approximately the same (i.e. 0.088-0.79 and 0.059-1.08, respectively), the range of yu_τ/ν is different by an order of magnitude (i.e., 375-3375 and 5.5-100, respectively). This seems to imply that the burst structure in the direction normal to the wall scales with δ^* and not with ν/u_τ. It could be argued that what we are measuring here is some structure in the outer region of the boundary layer and overlooking a finer structure close to the wall. However, the excellent correlation between the perturbation profiles and the instantaneous shear fluctuations measured at the wall tends to dispute this argument.

Plans are being made to repeat the measurements at several lower velocities in order to check the validity of these conclusions.

REFERENCES

1. Zakkay, V., Barra, V., and Wang, C.R., "The Nature of Boundary Layer Turbulence at High Subsonic Speeds," paper presented at the 16th AIAA Aerospace Sciences Meeting at Huntsville, Alabama, January 16-18, 1978. AIAA Paper # 78-198.

2. Blackwelder, R.F. and Kaplan, R.E., "The Intermittent Structure of the Wall Region of the Turbulent Boundary Layer," U. Southern California A.E. Report No. 1-22, 1972.

3. Emmerling, R., "The Instantaneous Structure of the Wall Pressure Under a Turbulent Boundary Layer," Max-Planch-Institut fur Stromungschung Report No. 9, 1973.

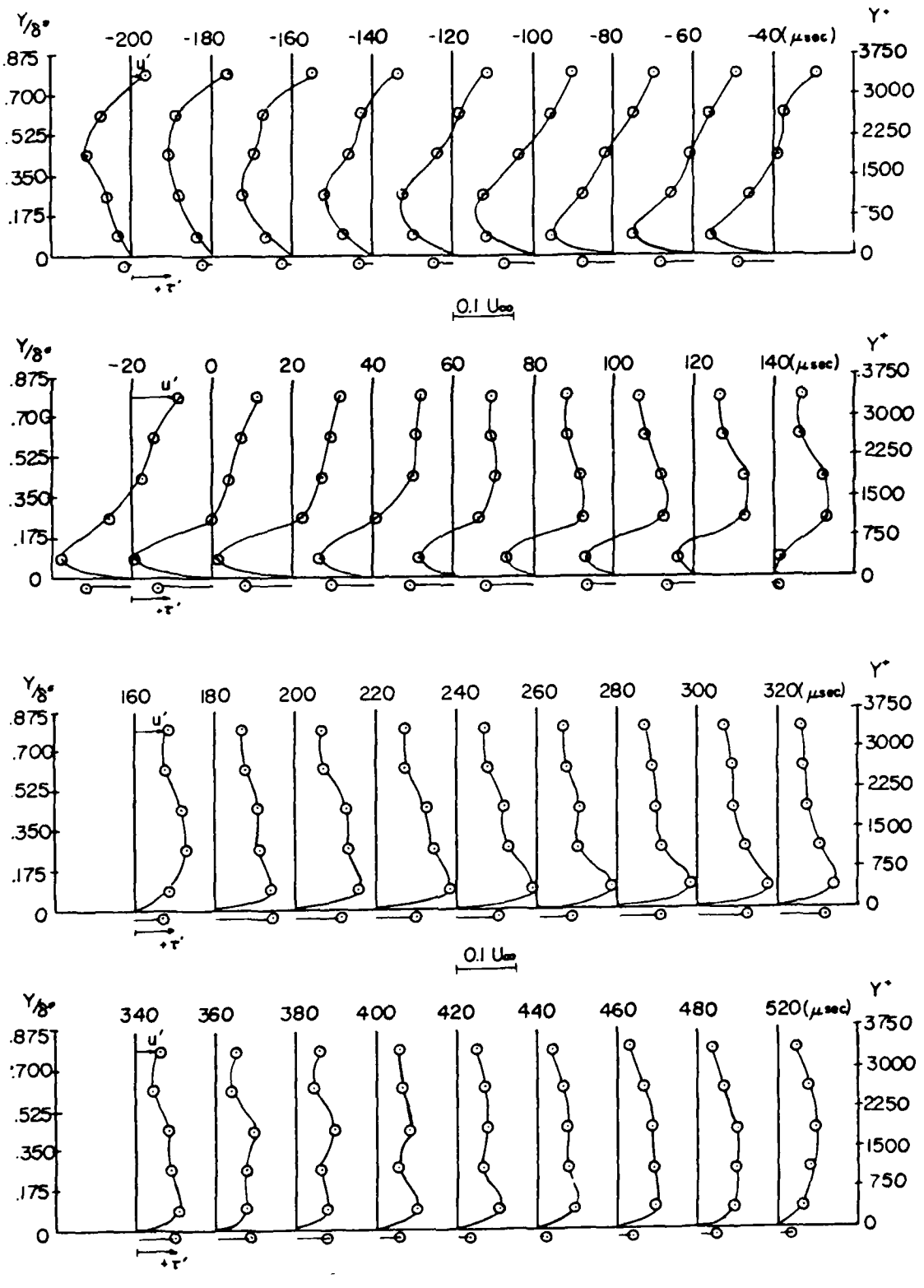

Fig. 4 Sequence of Perturbation Velocity Profiles and Fluctuating Shear During a Burst

DISCUSSION

Kline:

Two things. First of all, I think since you're starting at y+ of 400, one wants to be careful of identifying those as bursts. Our total layer only went out to about 700 to 900 so that you might want to call what you measure an event. Secondly, your event looks more like a Brodkey sweep -- it's coming in -- whereas what we were talking about yesterday, was going out. I think these events are related, but there is a question of phase time and identification that is important, as I was discussing yesterday. A further comment.....there is inherent in the bursting process at least two different times.....one of them is the time of the whole cycle..... the period of the cycle.....the other is the duration of either on-time or off-time of some particular event.....and those also need to be straightened out or we'll wind up in confusion.

Barra:

I think the point we're trying to make is that if the sequence shown by Blackwelder and Kaplan is for the bursting process, our measurements show the same process, whether it's in the outer region or near the wall. Obviously....it's in the outer region. But the process is very similar or shows the same history.

Kline:

Let's discuss that later.....I don't quite understand that.

Wygnanski:

Would it be correct to say that both your acceleration events and deceleration events originated in the outer part and moved with time towards the surface?

Barra:

No, no....Deceleration is near the wall, as you can see.

Wygnanski:

I thought I observed the opposite. (Refers to a slide corresponding to Fig. 4). Look at the first profile. The bulge is at a y/δ^* of about 0.525, then it moves down towards the surface...then it rests at the surface for a while.

Barra:

The first one here at t = 200?

Wygnanski:

Yes, at a y/δ^* of 0.525. Then it moves to a 175, then its very near the surface.

(There followed considerable discussion of Fig. 4 regarding what was acceleration, deceleration and how to interpret the figure. While an agreement was not reached, Professor Wygnanski raised several significant questions. Ed.)

Wtgnanski:

I'm sorry--perhaps I've confused you--but I think that I observed in some cases of our own data for individual velocity profiles that the velocity profile also originated from high up and moved towards the wall. Perhaps, however, that should not be confused with fluid material. The direction the fluid is moving depends on your reference frame. The fluid may be moving from the surfact outward!

(The following is a response to the previous discussion, written by Professor Zakkay after the conference, and dated May 5, 1978. It is included so as to help clarify conclusions of the paper. Ed.)

"We wish to emphasize that the results presented in our short paper concerning the coherent structure of turbulence at high Reynolds numbers were preliminary in nature. The available data at high Reynolds number and comparable measurements made at much lower velocities are in the process of being more thoroughly analyzed to clarify our picture of the structure. We also wish to make clear what we are concluding that our data shows.

It is obvious that our velocity measurements are made outside of what has been called the wall region ($y+<50$) with respect to the so-called "bursting" process at low Reynolds numbers. (In our case, a $y+$ of 50 corresponds to a vertical distance from the wall of .006 inches.) However, the great similarity between the fluctuation velocity profiles we presented in Fig. 4, and those obtained by Blackwelder and Kaplan (USC A.E. Report No. I-22, 1972) at a much lower Reynolds number, seems to indicate that the detection scheme being used in the two cases triggers on the same type of flow structure and that this flow structure scales in the direction normal to the wall width with δ^* and not ν/u_τ. This conclusion is supported by our shear measurement at the wall which shows an excellent correlation with the assumption we have made concerning the shape of the profiles from the wall to the first velocity measurement. In addition, the mean period between detected events when scaled by δ^*/U_∞ is in good agreement with other estimates of the mean period between quasi-cyclic, recognizable patterns in both wall and boundary layer fluctuation measurements.

We would agree with the claim that further study is required to determine whether the flow phenomenon which our profiles represent is part of the large-scale structure of the outer boundary layer, or is a representation of a "bursting" process which exists in high-velocity, high-Reynolds number flows.

However, we disagree with the argument that the Blackwelder and Kaplan profiles necessarily depict the wall layer "bursting" process. If it should be determined that our profiles represent part of a large-scale structure which extends down to the wall, the Blackwelder and Kaplan results would have to be reexamined in light of the arguments made above concerning the similarity with our data. In particular, it should be emphasized that while a comparison of the vertical scale of the fluctuation profiles in the two cases shows a great discrepancy in terms of the parameter ($y+ = yu_\tau/\nu$), an almost exact agreement occurs when the profiles are looked at in terms of y/δ^*.

It seems from the presentations made at the conference that a significant emphasis is being placed on low velocity experiments in this area, and very little work is being conducted in high-velocity, high-Reynolds number flows. Additional research at these flow conditions would be very useful in helping to resolve some of the questions raised during the meeting and for practical applications in aerodynamics."

EFFECTS OF HEATED COHERENT STRUCTURES ON MEASUREMENTS BY LASER DOPPLER ANEMOMETRY

J. A. Stabile & D. M. McEligot

Aerospace and Mechanical Engineering Department

University of Arizona, Tucson, Ariz. 85721 USA

ABSTRACT

The transient temperature and velocity signals were measured by a hot film anemometer and a laser Doppler anemometer, respectively, near $y^+ = 17$ in a heated, low Reynolds number turbulent boundary layer in water. Examination of the traces showed that the velocity signal tended to be lost most frequently during bursts and regained most frequently during sweeps.

1. INTRODUCTION

Horizontal turbulent flow over a heated horizontal surface is considered, as in the recent measurements of coherent structures in thermal boundary layers by Antonia and co-workers [1977], and others. In these works at low heating rates, hot wire anemometry has been applied to measure the velocity components. However, when extending measurements to conditions where gas properties vary substantially, meaningful calibration of the hot wire anemometer becomes difficult [Shehata and McEligot, 1977] so there is an incentive to apply laser Doppler anemomentry (LDA) which conceptually allows measurement of velocity components directly without a need for calibration [Durst, Melling and Whitelaw, 1976]. The latter approach was adopted by McEligot, Pils and Durst [1976] in conjunction with hydrogen bubble flow visualization for a study of the turbulent thermal boundary layer in a water channel.

Since coherent thermal structures cause coherent local fluctuations in the index of refraction of a fluid, the paths of the laser beams bend and fluctuate as well. Further, the line of sight from the

intended measuring control volume to the receiving optics becomes distorted. The signal is lost whenever the beams do not intersect in the region viewed. In the present note, the phases of the coherent motion will be described as (1) a "burst" of heated, low momentum fluid away from the wall, (2) a "sweep" of higher velocity, cooler fluid towards and along the wall and (3) a relatively "quiescent" period as the flow decelerates gradually. If the thermal structure is such that the signal is lost preferentially during one of these phases, the results of normal signal processing techniques will be biased accordingly.

In normal operating practise with LDA systems, the optics are aligned for optimal performance at the beginning of the experiment and are then traversed together without further resetting. The objective of the present study is to determine experimentally whether the heated coherent structures cause preferential sampling and consequent biasing of mean results when the LDA is operated in this manner.

2. APPARATUS

Measurements were taken in a small, horizontal, rectangular water tunnel. Heating was initiated after the boundary layer was partially developed but before the mean profile became invariant.

The velocity component in the streamwise direction (u) was measured with an LDA system consisting of a 5 mw He-Ne laser, dual beam optics by OEI with an S-20 phototube in the photomultiplier assembly, and a TSI 1090/1091 frequency tracker. The instantaneous temperature was determined with a TSI 1218-20W hot film boundary layer probe connected to a Disa 55D01 anemometer operated in the constant current mode. The two signals were recorded with a dual beam storage oscilloscope and Polaroid camera or with a Hewlett-Packard twin pen strip chart recorder.

3. CONDITIONS

Measurements were obtained in adiabatic flow and at two heating rates. The nominal flow rate led to a Reynolds number of about 12,600, based on twice the plate spacing. Adiabatic data showed a mean velocity profile as expected for a normal turbulent flow.

The wall shear stress was obtained by determining the slope in the linear layer, $u^+ = y^+$, for the adiabatic runs. For the heated data, this method was not possible; therefore, all references to wall law coordinates correspond to adiabatic conditions.

Comparison of mean velocity profiles for adiabatic flow and moderately heated flow showed an increase in the velocity which was largest near $y = 3.8$ mm, corresponding to $y^+ \approx 17$. The transient temperature and velocity signals were then measured at this location.

The Reynolds numbers based on boundary layer thickness, displacement thickness and momentum thickness were approximately 3160, 380 and 220 for the adiabatic flow. The flow rate was kept constant throughout.

Characteristic conditions of the three runs are presented in Table 1; the Grashof number is based on thermal boundary layer thickness.

Table 1. Comparison of experimental conditions.

Heating rate	$q\left(\frac{\text{watts}}{\text{cm}^2}\right)$	$t_w - t_\infty$, °C	Grashof number	Bursts cm	Samples sec	Signal loss, per cent
Adiabatic	0	0	0	--	140	4.5
Low	0.473	8	2.5×10^6	--	53	5.7
Moderate	1.06	21	6.6×10^6	0.6	--	40

4. RESULTS

Typical temporal traces are shown in Figure 1 for the three experiments. In each oscillograph the upper trace presents the LDA velocity trace and the lower is the temperature signal from the hot film sensor. Upward deflections represent increases in velocity and temperature. The sampling rate was determined from oscillographs at a high sweep rate so that individual samples could be identified and counted on the LDA traces.

Examining the signals for the low heating rate, one may observe that usually when there is a significant increase in temperature there is a decrease in velocity, as expected. The warmer bursts from the wall carry low momentum fluid, i.e., lower velocity. This correlation was observed for about 80 per cent of heated pulses; presumably the others correspond to heated fluid carried from upstream. On this photograph two periods occurred where the LDA lost the signal for substantial time intervals and held the previous voltage (velocity). In both instances the velocity was decreasing and the temperature increasing at the time, i.e., during a burst. The signal was regained as the velocity increased and the temperature decreased, which could be interpreted as a sweep. The thermal boundary layer was thin so that the sweep usually brought water at freestream temperature past the sensor. For this particular record, the deduced mean voltage would indicate a higher mean velocity than apparently occurred. However, by estimating the trend of the velocity signal from other regions of the trace and considering the length of time the signal was lost, one can see that the error in mean velocity would only be of the order of one per cent for this trace. As the moderate heating rate the situation is more difficult; the loss of signal is more frequent and longer.

The records of the two heated flows were examined to determine whether one phase corresponded to a loss of signal more frequently than did others. In the present study, apparent bursts and sweeps were interpreted as above. The signal was considered lost if the frequency tracker output held constant for about 0.1 sec. or more. Results are presented in Table 2. Quiescent deceleration observations represent a

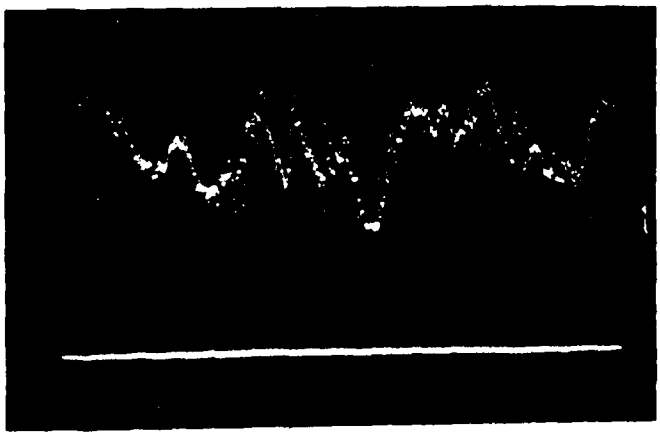

Adiabatic

Low heating

Moderate heating
(temperature scale
reduced)

Figure 1. Typical temporal traces of velocity (upper) and temperature. Sweep rate 1 cm/sec.

Table 2. Number of occurrences of events.

Heating rate	LDA Signal lost during				LDA Signal regained during			
	Burst	Sweep	Quies-cent	Un-certain	Burst	Sweep	Quies-cent	Un-certain
Low	9	4	6	3	5	11	5	1
Moderate	31	24	18	4	17	35	18	7

slight temperature change with no sharp gradients with respect to time. Uncertain determinations correspond to freestream temperature with insufficient velocity information to estimate the trend.

While this examination was not exhaustive and was only semi-quantitative, it does show preferential loss of velocity signal during the bursts and preferential regaining of the signal during sweeps, particularly for the low heating rate experiment. For moderate heating, the burst process does not appear to be as dominant a circumstance during loss events when the number of events are compared, accounting for 42 per cent of the events. However, the length of time lost due to the bursts was half of the time loss or 20 per cent of the total time. Again the dominant phase in regaining the tracking was the sweep phase. One expects that failure to measure the velocity partially during the quiescent phase will not modify the deduced mean significantly, while missing the more energetic events will. Overall in this experiment, the tendency appeared to be to lose the velocity signal during bursts and regain it during sweeps, so the mean velocity would be biased upward.

5. CONCLUSION

Unless sufficient care is taken, measurements by laser Doppler anemometry in flows with heated coherent structures can give misleading mean profiles and statistics, particularly in the viscous layer.

ACKNOWLEDGMENTS

The financial support of the National Science Foundation and the Office of Naval Research is gratefully acknowledged.

1. Antonia, R.A., H.Q. Danh and A. Prabhu, J. Fluid Mech., 80, 153-177 (1977).
2. Shehata, A.M. and D.M. McEligot, Bull. A.P.S., 22, 1280 (1977).
3. Durst, F., A. Melling and J.H. Whitelaw, Principles and Practises of Laser Doppler Anemometry, Academic Press, 1976.
4. McEligot, D.M., E. Pils and F. Durst, Bull., A.P.S., 21, 1220-1 (1976).

DISCUSSION

Bradshaw:

Don, (McEligot) I didn't quite get what your laser anomometry geometry was like. Are you getting dropouts because your crossed beams aren't crossing, or are your fringes moving, or what?

McEligot:

My feeling, which isn't proven yet, is that in general the drop-out is probably due to a failure of the beams to cross. If you look at the far side of the channel, you see that due to the turbulent fluctuations---index of refraction fluctuations---the beams are deflected upwards, which will effect the counting rate. Secondly, they're jiggling about like mad. I'd like to take some motion pictures, but haven't done so yet, to see whether they tend to be in phase or mostly out of phase in that process. If they're out of phase, they're not crossing very much.

Bradshaw:

A few years ago, a clever guy from AEDC, who was troubled with vibrations of his Schlaren knife edge fixed up a photo cell and feedback arrangement whereby he jiggled his knife edge up and down in sympathy with the vibrations in the tunnel. I wonder if you can have a few more photo cells to track your beam and wave your laser around---in other words, wave your optics around to get the beam in the right place?

Mr. Eligot:

I think we can improve our signal by readjusting the receiving optics for each new position, by using the hot film anomometer as a measuring point to see how much the measuring position moved upward relative to where we think it is and perhaps improve things.

Adrian:

I certainly agree with your conclusion. There may be a couple of other difficulties than just beam misalignment or wave fronts. The optical path lengths are being distorted and they're fluctuating randomly in these flows and the angles are changing and so on. So even if you get the components to stay in line, you have all those other things to worry about. One thing that helps in these situations is to keep the beam angles narrow so that the two beams are going into correlated regions of fluid. This tends to cancel things out, but you still have the problem of the measurement volume wavering around introducing a spurious velocity, with respect to the fluid.

EXPERIMENTAL INVESTIGATION OF LARGE SCALE STRUCTURES IN TURBULENT JET MIXING LAYERS

Otto Leuchter and Khoa Dang

Office National d'Etudes et de Recherches Aérospatiales (ONERA)

92320 Châtillon (France)

ABSTRACT

A simple method of conditional sampling for identifying coherent structures in the mixing layer of turbulent jets is used for characterizing the effects of initial conditions, such as turbulence and boundary layers, on the behaviour of these structures. The method uses conventional hot wire instrumentation combined with a correlator operating in the signal recovery mode. The ensemble averaging is initiated from the spikes occurring either in the hot wire signal to be analyzed or in a separate signal proceeding from a trigger probe. Some typical results obtained with both operating modes will be presented, illustrating several characteristic features of the coherent structures in jet mixing layers.

1. INTRODUCTION

In the last few years concentrated research effort has been devoted to the phenomena of coherent large scale structures in turbulent shear layers. It was realized that further progress in the field of turbulence modeling, particularly for aeroacoustical applications, implies a better understanding of these phenomena and further refinements in the description of the turbulence structure. A large amount of experimental data is now available which bring to light the existence of regular flow structures in the mixing layer of undisturbed turbulent jets, whose basic pattern may be conceived as an array of more or less evenly spaced vortices convected downstream at a definite speed. In the present paper some typical features related to the identification of these structures will be discussed in the context of fundamental research work conducted at ONERA on the effects of particular initial conditions, such as turbulence and initial boundary layers, on the structure of turbulent jets.

2. INSTRUMENTATION

Owing to the deterministic features of the large scale structures, conditional sampling techniques have to be employed for identifying the nature of the structures. Standard hot wire instrumentation was used in the present study together with an eduction technique developed first by Lau and Fisher [1] . It is based on the identification of individual upward or downward spikes in the longitudinal velocity signal, which are then used to initiate the eduction. A spike detector was designed specifically for the purpose of the present study. It converts the time intervals between successive spikes in the hot wire signal into a series of discrete voltage levels which are then available for further processing. A schematic representation of the different stages of signal processing performed in the spike detector is given in Figure 1. The individual instants at which the selected spikes reach their peak value are first detected from the zero crossing of the derivative of the low-pass filtered signal The criterion for the selection consists in retaining only spikes with a peak value exceeding a given predetermined level, which in practice is of the order of the r.m.s. value of the input signal.

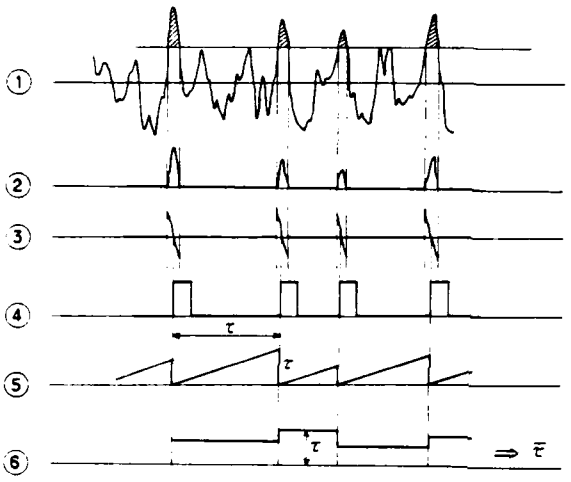

Figure 1. Principle of the spike converter.

Sawtooth voltage ramps are generated at the precise instants the peak values are reached. As the slope of the ramps is constant, the final values of the ramp voltage give a direct measure of the time intervals between the spikes. Each final value is then maintained constant until a new ramp is generated. It may thus be sampled and fed to a computer or a correlator, where the probability density function (p.d.f.) of the time interval is computed. From the p.d.f. one can determine then the most probable and the mean intervals. The intermediate output ④ is used to trigger the sampling of the ramp voltage ⑥. Downward or upward spikes can be processed indifferently by this apparatus.

The correlator can also be used in the signal recovering mode allowing repetitive components to be recovered from a general random signal. This is achieved by simultaneous computation of the ensemble averages at 400 different values of the phase, the origin of which is defined from the triggering signal ④ of the spike detector. A block diagram of the measuring circuit as a whole is given in Figure 2. The correlator is connected to a mini computer (as is the spike converter) which carries out the computation of the mean energy contribution of the recovered pattern to that of the unfiltered input signal.

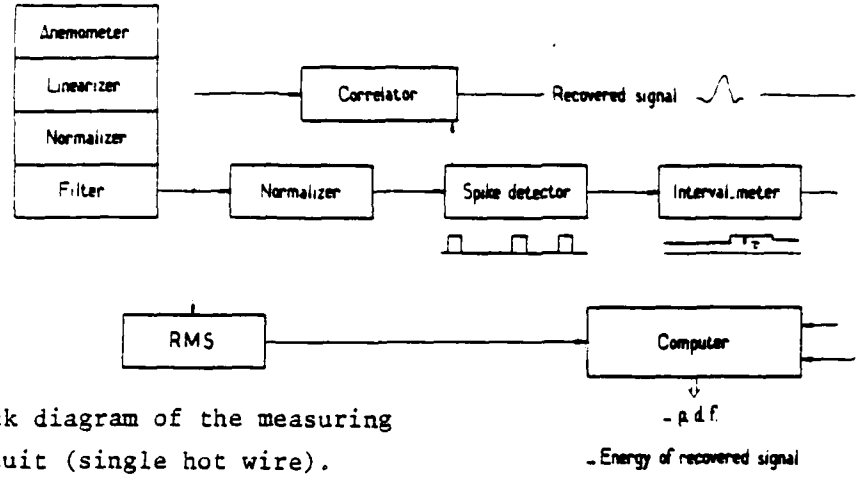

Figure 2. Block diagram of the measuring circuit (single hot wire).

3. EXPERIMENTAL CONDITIONS

The experiments were conducted in a coaxial jet facility equipped with two concentric nozzles of 30 (or 50) and 100 mm diameter respectively. The maximum velocity of the inner jet is 100 m/s, corresponding to a maximum jet Reynolds number of 3.10^5. The outer to inner velocity ratio U_e / U_i lies in the range between 0 and 0.5, which corresponds to practical applications relevant to jet noise. This facility offers further the possibility of creating either thick initial boundary layers (up to $\delta/D = 0.25$) or initial free stream turbulence by means of grids of appropriate mesh size placed into the ducts. Typical values of the turbulence intensity level lie between 5 and 10%, whereas the longitudinal integral scale normalized with the diameter of the inner jet ranges from 0.05 to 0.15.

4. DISCUSSION OF THE RESULTS

Examples of recovered signals are shown in Figure 3 for a velocity ratio of 0.25. The recovery hot wire, placed at the radial position $y/D = 0.5$, was used also as the triggering probe, the eduction being initiated by the downward peaks of the hot wire signal. Therefore the recovery process is conducted in two stages from the previously tape recorded signals by playing the tape first in the direct and then in the reversed sense. About 16,000 samples have been processed for obtaining the educed shapes shown in the figure. A continuous widening of the patterns can be observed as the probe is moved downstream in the mixing layer. The mean values of the time intervals $\bar{\tau}$ as deduced from the corresponding p.d.f.'s grow correspondingly, as indicated in the figure. The mean contribution of the educed signals to the total energy of the input signal as evaluated from these diagrams is shown in Figure 4 in terms of the r.m.s. values. It may be seen that the recovered shapes contribute to somewhat about 30 and 40 percent of the total r.m.s. value and this contribution varies only slightly as the probe is moved downstream. It was further observed that this rate was rather independent of the presence of initial turbulence in the jet (in the present case of about 5% intensity).

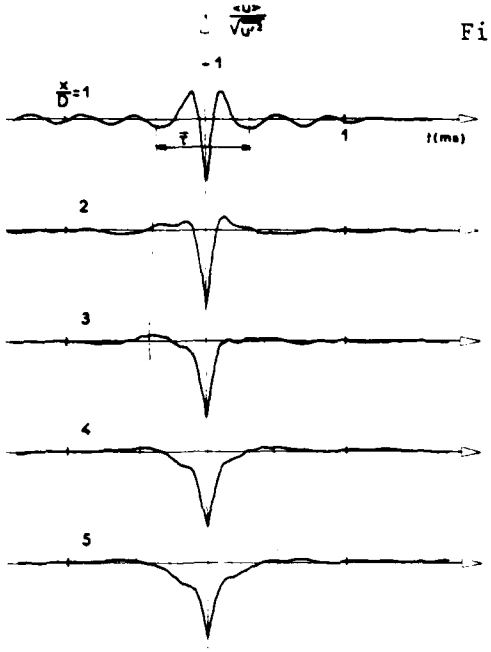

Figure 3. Examples of recovered signals (single hot wire).

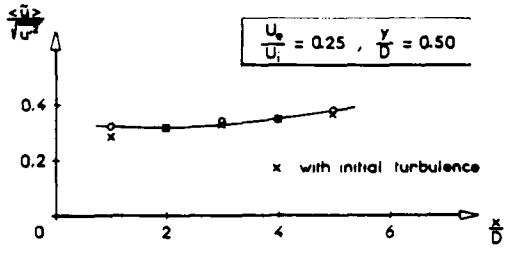

Figure 4. Contribution of the recovered signal to the r.m.s. value.

It has been realized in the course of this study that the efficiency of identifying regular flow patterns from single probes placed in the mixing layer is relatively poor, as a consequence of the high apparent randomness of the velocity signals in this region. This may be explained by the fact that the successive vortices (even when regularly spaced) do not follow exactly identical trajectories. This effect becomes however less and less important as the probe is moved away from the vortex cores, and that is why the hot wire signals detected in the potential core generally present a much higher degree of regularity than those extracted from the mixing layer itself. It was therefore considered to trigger the recovering process of the mixing layer signal with an auxiliary probe placed at an appropriate position inside the potential core. The corresponding block diagram is similar to that of Figure 2, except that it is now the signal of the auxiliary probe which is fed into the spike detector and that filtering is no longer necessary.

An additional advantage resulting from this procedure is the possibility of gaining phase informations about the coherent structure, as is illustrated in Figure 5 for a free jet ($U_e/U_i = 0$). Here the triggering hot wire is at a fixed position on the jet axis (y=0) at 1 diameter downstream of the nozzle, whereas the recovery hot wire is held at the fixed radial position y/D = 0.5 and successively placed at particular axial positions. The downward spikes of the triggering hot wire were used here for initiating the eduction. Several interesting features may be recognized from Figure 5 :

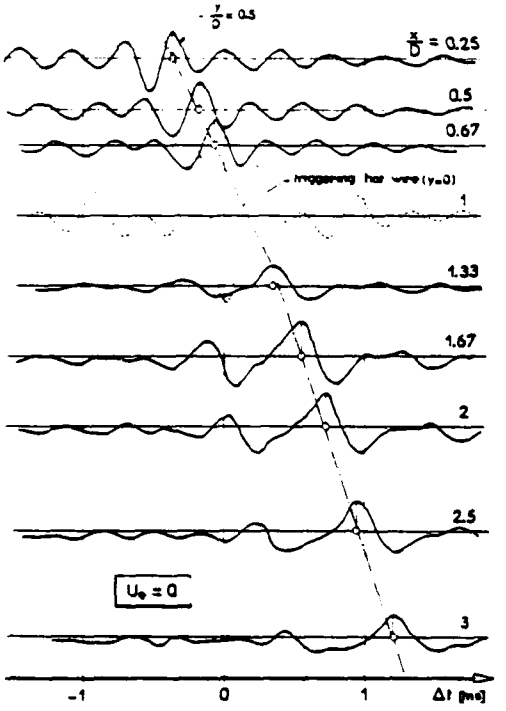

Figure 5. Examples of recovered signals (two hot wires).

- The recovered signals have a nearly sinusoidal shape, in contrast to those shown in Figure 3. This may reflect the fact that the time differences between the instants when the eduction is triggered on the axis and the instants when the corresponding spike of the eduction signal occurs are not necessarily constant.
- A rather large number of periods are recovered, especially in the early stages of the mixing process, indicating that there must prevail a relatively regular spacing of the vortices.
- The maximum amplitudes of the educed signals are continuously moving along the time-axis as the probe in the mixing layer is displaced downstream. This suggests the existence of a definite velocity at which the vortices are convected downstream.
- One observes further a sudden increase of the wavelength downstream of about 1 diameter from the nozzle, suggesting that this could be attributed to the phenomena of vortex pairing.

It is significant that the Strouhal number as deduced from the wavelength of the recovered signals downstream of the pairing process is of the order of 0.4 and that the convection velocity (as determined from the displacement of the peaks in the recovered signals) is about 0.6 times the jet efflux velocity. This is consistent with what is usually determined from space-time correlations in the mixing layer. In contrast to these values the Strouhal number is 0.8 in the early stage of mixing and the convection velocity only 0.42 times the jet velocity. This double valued Strouhal number has been confirmed by the p.d.f.'s measured in the potential core. No significant Reynolds number effect on this pattern could be revealed in the present study for the range of Reynolds number investigated. The influence of boundary

layers and initial turbulence on this particular structure will further be investigated in the course of this study and no final conclusion may be drawn at the present time regarding these influences. In Figure 6 are shown the trajectories of the positive and the negative peaks of the educed signals presented in the previous figure, from which the regular vortex pattern and the pairing process may be clearly recognized.

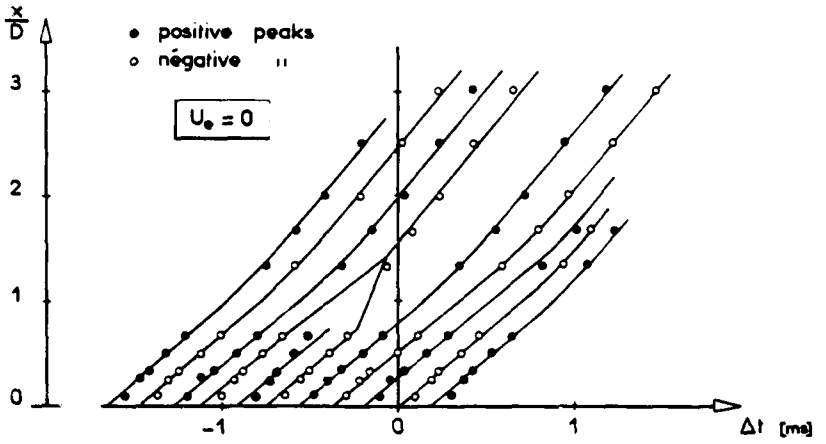

Figure 6. Trajectories of the peaks of the recovered signal in the x-t plane.

5. CONCLUDING REMARKS

The few examples shown in the present paper have been selected to illustrate the capability of relatively simple conditional sampling techniques for identifying and characterizing coherent structures in turbulent free shear layers. These may of course also be applied for investigating coherent structures in wall boundary layers. Owing to the use of a numerical correlator together with an appropriate spike detector, this type of investigation may be conducted without any particular computational equipment. Only a x-y plotter ought to be connected in this case to the correlator. Many typical features concerning coherent structures, as e.g. those relevant to the noise generation, may be studied by this technique. It is intended, in the context of fundamental research work on turbulence structure in free shear layers, to make an extensive use of these techniques, especially for characterizing the effects of initial conditions as mentioned above on the coherent structure of jet mixing layers and on the noise generation associated with this structure.

6. REFERENCE

[1] J.C. Lau and M.J. Fisher - J. Fluid Mech. (1975), Vol. 67, p. 299.

DISCUSSION

Kovaszny:

Did you try to condition the sample and detect your sound field from a microphone?

Leuchter:

No---not yet. It will be done.

Hussain:

I would like to ask two short questions. First, Brune in his recent JFM paper has shown that the structure determined by triggering from the upper spike (which is the ejected fluid from center to the outer part of the jet) and the coherent structures from the downward spikes are completely different. Do you have an explanation for this apparent discrepancy.

Leuchter:

The apparatus can operate in two directions. It can trigger from upward spikes or from downward spikes. We have not yet triggered with upward spikes---only with the downward spikes.

Hussain:

Yes, but Brune has shown that the coherent structures educted are completely different, depending on which signal he uses for eduction or triggering.....The second question concerns your reference to Lau & Fisher. Lau has found that there are actually two different vortex strings, one radiating away from the jet center axis and the other one converging. Do you have any such evidence in your measurements?

Leuchter:

The study is not yet far enough along to have more details on this. I have to remark that the Reynolds number of this experiment is quite high; on the order of 300,000.

Hussain:

That's about what Lau used. He had about 500,000 and I would suggest that you look for this rather peculiar and surprising phenomon that he's claiming.

Birch:

I'd like to make a comment which is very similar to the one Steve Kline made recently and that is that there is no real dispute, I think,

that these mixing layers contain a large structure of some type and that it's size increases as you go downstream. But when you start using terms like "vortex" and "large eddy" and "pairing", different people mean different things by these terms and I think it's important to define precisely what you mean.

Leuchter:

The regular spacing of the vortices came out from the reduction process. It is not directly connected to the spreading of the jet. You may have spreading, say linear spreading, which is consistent with with regular vortex spacing.

Birch:

I appreciate that. What I'm referring to is when you use a term such as "pairing", which is observed at low Reynolds numbers. It is true at High Reynolds numbers that the size does increase on the average, however, "pairing" as such, or at least the mechanism for the growth of the eddies, isn't as clear.

UNIVERSAL LAWS OF VORTEX MERGER IN THE TWO-DIMENSIONAL MIXING LAYER

R. Takaki

Tokyo University of Agriculture and Technology

Fuchu-shi, Tokyo, Japan

ABSTRACT

Two universal laws are proposed which are considered to govern the dynamics of vortex merger. One is a dependence of the rate of merger of two vortices on their spacing. The other is about a growth of the vortex size during the merger. These laws are examined by numerical simulations and, for the latter, also by a rough experiment.

1. INTRODUCTION

In order to predict dynamical behaviors in a turbulent flow with coherent structure, a statistical treatment of an ensemble of the organized structures is a powerful method. In the case of the two-dimensional mixing layer, the vortices arranged in a row correspond to the structures. In the statistical treatment, it is necessary to assume certain universal laws governing interactions between them, i.e. the vortex merger. The word 'universal' means here that the law dominates the dynamics at any stage so long as the viscosity is negligible.

One example is the following power law which is assumed by the author and Kovasznay in order to obtain a distribution of spacings in a row of vortices, whose mean quantities are assumed uniform in the streamwise direction (1978):

$$\text{rate of merger} \propto \xi^{-2},$$

where $\xi = l/\bar{l}$, l is the spacing between two vortices and $\bar{l}$ is a mean spacing in the row. In that work detailed mechanism of the merger is not discussed. One of the purpose of this paper is to examine the validity of this power law by numerical simulation of the vortex merger.

When one tries to predict the spreading rate of the mixing layer based on the statistical treatment, one must assume certain laws about a growth of vortex through entrainment during the merger process. The second purpose of this paper is to propose a law about the area of the vortex based on results of the numerical simulation and an experiment by a simple apparatus.

In the numerical simulation one puts, as an initial condition, a row of vortices on the x-axis, where two vortices, which are to merge, are at $x = \pm \ell/2$, and the other vortices at regular positions with equal spacing ℓ. Circulations are assumed uniform (say Γ). By changing ℓ one can take an effect of an irregularity in the vortex cofiguration into account. Each of the two vortices is replaced by a group of 43 point vortices with size 0.8ℓ. Effect of the other vortices is replaced by a background stationary shearing field

$$u = -ky, \quad v = -kx, \quad k = 0.298\ \Gamma/\ell^2 .$$

Each point vortex moves with a superposition of the velocity induced by the other point vortces and the background velocity.

Experimental apparatus is composed of a towing tank filled with water and a curved plate travelling at the middle level of the rest water. A velocity jump is produced behind the plate, and the flow is visualized.

2. EXAMINATION OF THE POWER LAW

Results of the numerical simulation are as follows. Two groups of point vortices come close and amalgamate. This procedure is similar to results obtained by several authors in the past. The center of each group moves on a nearly elliptical path. Speed of the motion depends much on

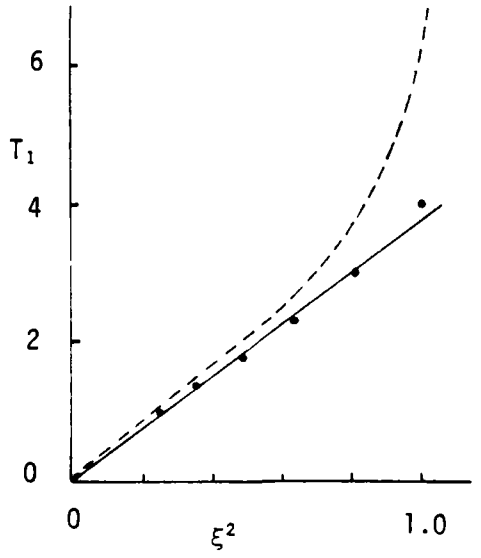

Figure 1. Dependence of the time T_1 measured by a unit ℓ^2/Γ on ξ.

ξ, and increases as ξ decreases. The speed is considered to give the rate of merger of the two vortices in question. For the sake of convenience it is measured in terms of the time T_1 for the center of each group to come on the y-axis. Fig.1 shows results of the numerical simulations, from which one can say that the rate of merger ($\propto T_1^{-1}$) is proportional to ξ^{-2} for $\xi<1$. The dashed line is the result for the case where each of the two vortices is replaced by a single point vortex with circulation equal to Γ. Clearly the power law is more effective for the vortex pair with finite scale.

3. CHANGE OF VORTEX SIZE DUE TO THE MERGER

Two groups of the point vortices become a single group with nearly elliptical shape and larger size. Fig.2 shows a ratio of the area of the new group to the sum of the areas before merger. The measurement of the area contains a certain amount of error, but one can say from this figure that the total area is nearly conserved for small ξ. After the merger the area of the single vortex increases slowly. Considering this fact and that the group of point vortices with larger ξ moves slower, one may say that the total area does not have a stepwise growth by the occurrence of merger but grows continuously.

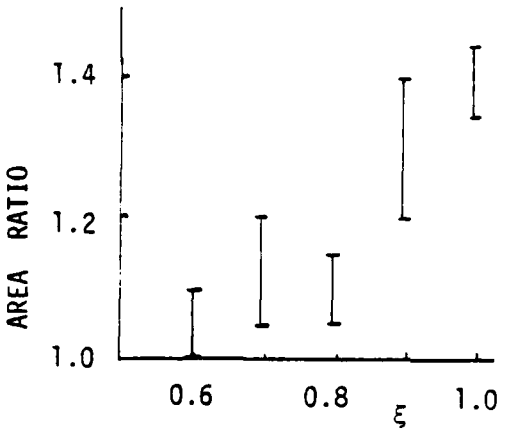

Figure 2. Ratio of the total area after merger to that before merger. Vertical line segments show errors in measuring area.

In the experiment the area is measured from photograph of the visualized flow. Growths of the total area and the vertical size of the merging pair are shown in Fig.3(a) and (b) respectively, where the sum of the sizes is plotted in (b) for the vortices before and during the merger. Arrows in the figure show beginning and end of the merger. The vortices in the experiment were arranged relatively regular. This situation corresponds to the case $\xi=1$ in the numerical simulation. This figure shows

that the total area changes continuously but the total size does not.

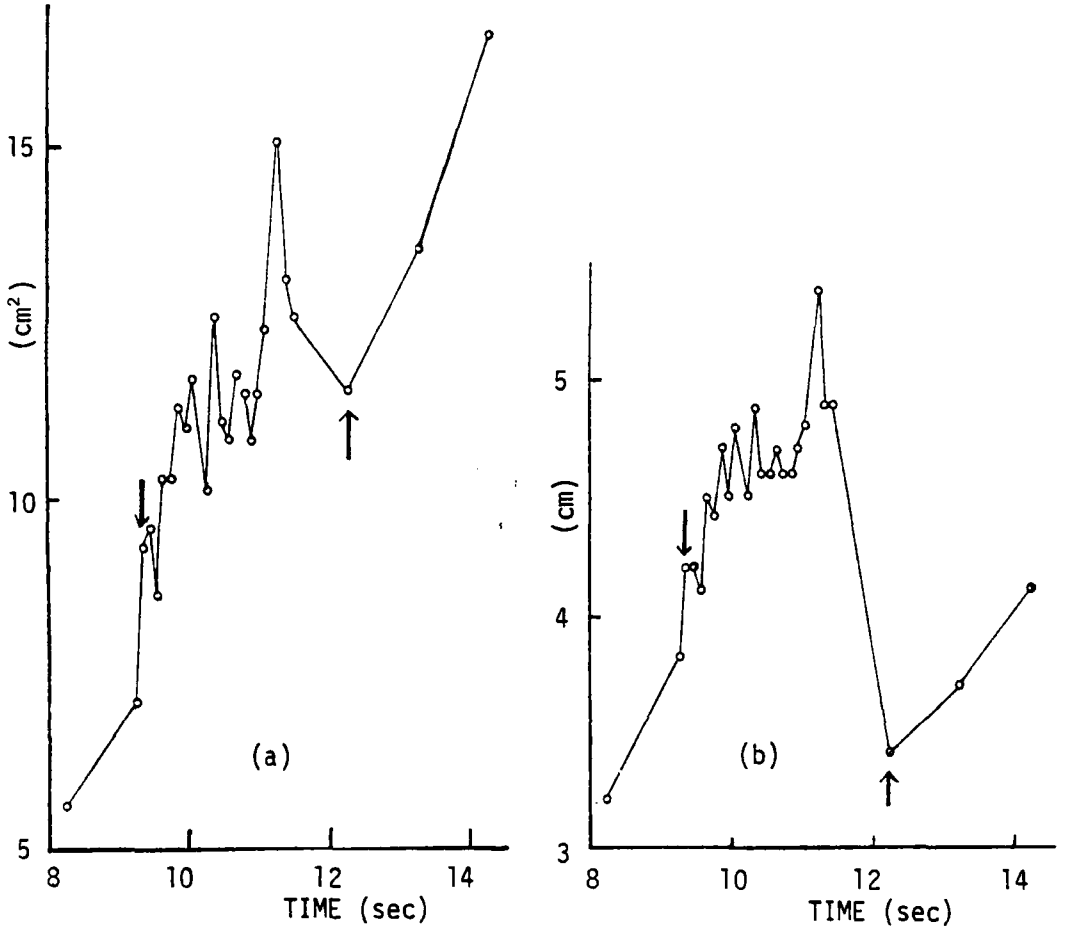

Figure 3. Growths of the total area(a) and the total size(b). The merger occurs in the interval marked with arrows.

Both numerical simulation and experiment suggest that the area of vortex is an important variable, and that the merger process obeys a law of continuous growth of area.

ACKNOWLEDGMENT

The author thanks to Mr. Y. Tanaka and Mr. K.Hasegawa for their help in computer calculation and experiment.

REFERENCE

1. Takaki, R. and Kovasznay, L. S. G., to appear in Phys. Fluids(1978).

DISCUSSION

Donaldson:

I guess I should mention that you might look up some work by Vernon Rossow of NASA TMX 62-304 and by Alan Bilanin A.R.A.P., both of whom have done the same numerical calculations that you have done. They consider tne conditions as to whether two vortices will continue to rotate around themselves forever, or whether they will capture themselves, and the time required for capture. The line that divides the two cases was considered and they show that two point vortices will rotate around themselves forever; they'll never capture each other. There has to be some distribution of the vorticity in order for them to capture themselves. Vernon Rossow did the numerical simulation of how big that distribution of vorticity had to be and how it affected the capture time and Alan Bilanin has done the analytical solution to that particular problem.

Takaki:

Thank you very much for your comment.

Kovasznay:

I would like to amplify on the Author's statement. For the earlier work which he referred to, the ξ^{-2} merger rate was assumed. It was an assumption and it was consistent with an experiment in the scaleless nondimensional probability density distribution of the Brown & Reshko results. In order to justify the assumption, he made the numerical simulation with the finite vortices. Indeed the final finite cloud of point vortices confirmed the intuitive assumption as Donaldson well pointed out. So I think that all fits very well with what Coleman just said.

Hussain:

I was wondering Dr. Takaki, are some of the other integral measures of the mixing layer predicted by your numerical technique? Namely, spread rate or the entrainment rate.

Takaki:

The spread rate I have not tried. I have begun work on such comparison.

Hussain:

The other things are what Reshko talks about; the life expectancy of each vortex and the probability density distribution.

Kovasznay:

What really fixes the merge rate, is the similarity law and the similarity law with minus two power of the merge rate gives the probability density distribution. Therefore, the picture looks forever the same. It's a high Reynolds number approximately, and therefore, automatically follows the rate of killing or merging of vortices---or lifetime, if you like. One adjustable constant which was adjusted came from Roshko & Brown.

Donaldson:

I also should say that in addition to those inviscid calculations, which yours are also, the merging of two vortices has been calculated with a complete second order closure model. It is very interesting that when two vortices of the type that you have in a shear flow merge, and each of them has a certain amount of turbulent energy in them before they merge, not only is the scale larger, but they produce turbulent kinetic energy at just the rate required to increase the turbulent energy that you would have in the shear layer.

Kovasznay:

Reference?

Donaldson:

The first publication is in a NATO monograph on vortex wakes of large airplanes some years ago by Donaldson and Balinin.

STRUCTURAL INFORMATION OBTAINED FROM ANALYSIS USING CONDITIONAL VECTOR EVENTS: A POTENTIAL TOOL FOR THE STUDY OF COHERENT STRUCTURES

Ronald J. Adrian

Department of Theoretical and Applied Mechanics

University of Illinois at Urbana-Champaign 61801

ABSTRACT

The flow event of type E_1, in which the velocity at a fixed point is required to assume a prescribed vector value, is considered in regard to its ability to extract information about the structure of a turbulent flow. The amount of structural information that can be obtained is demonstrated by a simplified conditional analysis of isotropic turbulence which predicts, on the basis of empirical correlation data, a conditional flow pattern in the form of a dual vortex ring. It is concluded that E_1 based conditional analyses would yield at least as much information in more highly structured flows. Further work is needed to establish firmly the relationship between these conditional flow patterns and current conceptions of coherent flow structures.

1. INTRODUCTION

In a previous paper (Adrian, 1975) it was suggested that conditional averages based on conditional events involving the velocity vector in the form

$$E_1 = \{ \underset{\sim}{c} \leq \underset{\sim}{u}'(\underset{\sim}{x},t) < \underset{\sim}{c} + d\underset{\sim}{c} \}$$

could possibly provide useful quantitative information about the structure of coherent flow patterns. Here $\underset{\sim}{u}'(\underset{\sim}{x},t)$ is the fluctuating velocity at $\underset{\sim}{x}$, and $\underset{\sim}{c}$ is an arbitrarily prescribed vector value. This speculation was motivated more by the desirable properties of conditional averages given E_1 type events, than by the available experimental evidence. (The properties of conditional averages such as the average of $\underset{\sim}{u}'(\underset{\sim}{x}+\underset{\sim}{r},t)$ given E_1, denoted by $<\underset{\sim}{u}'(\underset{\sim}{x}+\underset{\sim}{r})|\underset{\sim}{u}'(\underset{\sim}{x})>$, are discussed in detail in Adrian 1975, 1978. See also Tevlev 1970, and Dopazo 1975.) In fact, measurements of the scalar, time delayed conditional average

$< g(\underset{\sim}{x},t+\tau)|g(\underset{\sim}{x},t) >$, where g was either the streamwise velocity component or the fluctuating static pressure in the driven mixing layer of a round jet, showed that this quantity contained little more information than the autocorrelation function (Adrian, Chung, Jones and Nithianandan, 1976). Hence, the scalar version of the E_1 event did not appear suitable for coherent structure analysis.

The purpose of this paper is to explore the possibility that conditional analyses based on the full vector event, E_1 , may provide structural information of sufficient detail to warrant their use in coherent flow studies. As a severe test of this hypothesis we shall consider the E_1 based conditional analysis of isotropic turbulence, a flow which presumably possesses less structure than any other turbulent flow.

2. CONDITIONAL ANALYSIS OF ISOTROPIC TURBULENCE

In the mean square sense the best conditional analysis of the velocity vector field around the point $\underset{\sim}{x}$ given the value of the velocity vector at $\underset{\sim}{x}$ is $< \underset{\sim}{u}'(\underset{\sim}{x}+\underset{\sim}{r})|\underset{\sim}{u}'(\underset{\sim}{x}) >$ (the time dependence is suppressed). That is, $< \underset{\sim}{u}'(\underset{\sim}{x}+\underset{\sim}{r})|\underset{\sim}{u}'(\underset{\sim}{x}) >$ is the least mean square error estimate of $\underset{\sim}{u}'(\underset{\sim}{x}+\underset{\sim}{r})$ in terms of the known velocity, $\underset{\sim}{u}'(\underset{\sim}{x})$. In incompressible isotropic turbulence the vector field given by $< \underset{\sim}{u}'(\underset{\sim}{x}+\underset{\sim}{r})|\underset{\sim}{u}'(\underset{\sim}{x}) >$ is a non-linear function of $\underset{\sim}{u}'(\underset{\sim}{x})$ that is independent of $\underset{\sim}{x}$, axisymmetric about the direction of $\underset{\sim}{u}'(\underset{\sim}{x})$ and solenoidal with respect to $\underset{\sim}{r}$ (Adrian 1975). Direct experimental measurements of $< \underset{\sim}{u}'(\underset{\sim}{x}+\underset{\sim}{r})|\underset{\sim}{u}'(\underset{\sim}{x}) >$ have not been made for isotropic turbulence, so in order to examine the structural information content of this quantity an approximation is necessary that permits its evaluation in terms of data that are available.

The simplest approximation is obtained by truncating the Taylor series expansion of $< \underset{\sim}{u}'(\underset{\sim}{x}+\underset{\sim}{r})|\underset{\sim}{u}'(\underset{\sim}{x}) >$ about $\underset{\sim}{u}'(\underset{\sim}{x}) = 0$ after the first order term, leaving the linear estimate,

$$< u_i'(\underset{\sim}{x}+\underset{\sim}{r})|\underset{\sim}{u}'(\underset{\sim}{x}) >^{(1)} = A_{ij}(\underset{\sim}{r})\, u_j'(\underset{\sim}{x}) \ , \tag{2}$$

wherein the coefficient $A_{ij}(\underset{\sim}{r})$ is determined by minimizing the mean square estimation errors $<(< u_i'(\underset{\sim}{x}+\underset{\sim}{r})|\underset{\sim}{u}'(\underset{\sim}{x})> - A_{ij}u_j'(\underset{\sim}{x}))^2 >$ for $i = 1,2,3$. This implies that A_{ij} must satisfy a set of nine linear algebraic equations

$$< u_\ell'(\underset{\sim}{x})u_i'(\underset{\sim}{x}+\underset{\sim}{r}) > = A_{ij}(\underset{\sim}{r}) < u_j'(\underset{\sim}{x})u_\ell'(\underset{\sim}{x}) > \tag{3}$$

(Adrian 1975). In isotropic turbulence $< u_j'(\underset{\sim}{x})u_\ell'(\underset{\sim}{x}) > = u^2\delta_{j\ell}$, and the solution of eqn. (3) is simply

$$A_{ij}(\underset{\sim}{r}) = < u_j(\underset{\sim}{x})\, u_i(\underset{\sim}{x}+\underset{\sim}{r}) > /u^2 \ . \tag{4}$$

Combining the usual expression for the isotropic two point correlation tensor (Batchelor, 1960, eqn. 3.4.5) with eqns. (2) and (4) yields

$$< u_i'(\underset{\sim}{x}+\underset{\sim}{r})|\underset{\sim}{u}'(\underset{\sim}{x}) >^{(1)} = \left[(f-g)\frac{r_i r_j}{r^2} + g(r)\delta_{ij}\right] u_j'(\underset{\sim}{x}) \ , \tag{5}$$

where $f(r)$ is the longitudinal correlation function, $g(r) = f + \frac{1}{2} r df/dr$ is the transverse correlation function, and $r = |\underset{\sim}{r}|$.

Since the conditional vector field given by eqn. (5) is axisymmetric about $\underset{\sim}{u}'(\underset{\sim}{x})$, its streamlines may be found by computing the Stokes' streamfunction corresponding to eqn. (5). The result is

$$\psi^{(1)} = \frac{1}{2} u'(\underset{\sim}{x})\, f(r)\, r^2 \sin^2\theta \quad , \tag{6}$$

where θ is the polar angle measured from the direction of $\underset{\sim}{u}'(\underset{\sim}{x})$. For isotropic turbulence, the particular choice of the direction is, of course, arbitrary. Hence, the structure of the linearly estimated vector field can be calculated using only one piece of empirical information, $f(r)$.

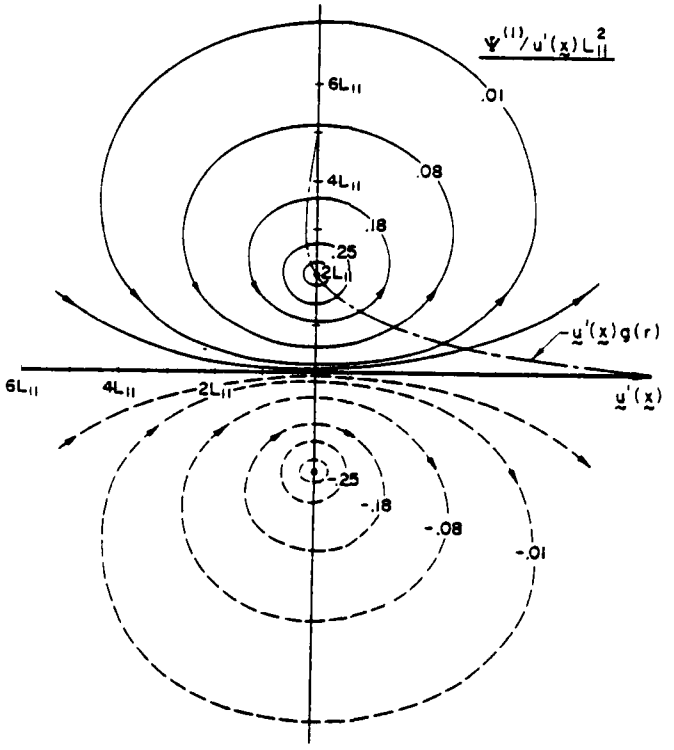

Figure 1. Streamlines of the linearly estimated conditional flow field given the value of $\underset{\sim}{u}'(\underset{\sim}{x},t)$. $f(r) = \exp - |r|/L_{11}$. Numbers indicate the value of $\psi^{(1)}/u'(x)L_{11}^2$.

3. CONDITIONAL STRUCTURE

Consider for a first example the well known model correlation function

$$f(r) = \exp - |r|/L_{11} \tag{7}$$

having integral length scale L_{11} . The streamlines of constant $\psi^{(1)}/u'(\underset{\sim}{x})L_{11}^2$ plotted in Fig. 1 reveal a vortex ring structure whose center is at $\underset{\sim}{x}$. In the $\theta = 90°$ plane the conditional velocity vector is given by $\underset{\sim}{u}'(\underset{\sim}{x})\, g(r)$ which is indicated by the dashed-dotted line in Fig. 1. The core of the vortex ring occurs in the plane at $r = 2L_{11}$, coincident with the zero value of $g(r)$. According to this model the negative regions of the transverse correlation function are associated with the return flow of the vortex ring.

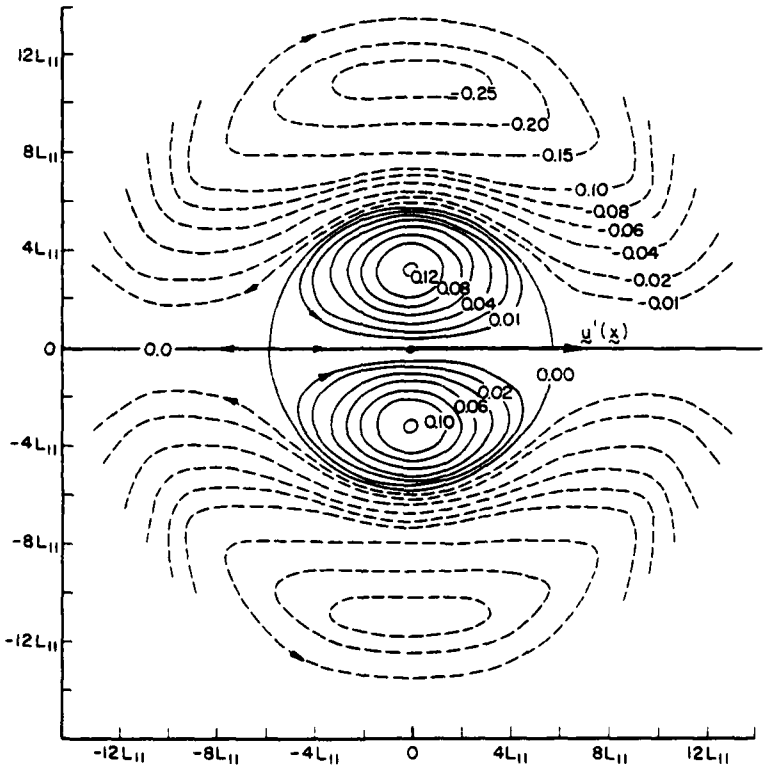

Figure 2. Streamlines of the linearly estimated conditional flow field computed from eqn. (6) using Van Atta and Chen's (1968) correlation data for $x/M = 48$. $L_{11} = 0.54M$ is the integral scale. Numbers indicate the value of $\psi^{(1)}/u'(\underset{\sim}{x})L_{11}^2$.

A more realistic and significantly more interesting structure is found by using Van Atta and Chen's (1968) correlation data from the initial decay law region of grid turbulence. Their $f(r)$ curve differs qualitatively from the simple exponential in eqn. (7) in that it crosses zero at $r \cong 5.2L_{11}$ with the consequence that the transverse correlation function calculated from $f(r)$ possesses two zeroes. The difference is manifested in Fig. 2 by the appearance of a second, counter rotating vortex ring that surrounds the inner ring and has a core center located at the second zero of $g(r)$. The large diameter of the outer ring core,

approximately $22L_{11}$, emphasizes the importance of the tails of the correlation functions when considering large scale structure. It also suggests that the integral scale L_{11} may not be even a good order of magnitude estimate of the scale of the turbulent structure.

4. DISCUSSION AND CONCLUSIONS

The application of conditional analysis based on the event E_1 to isotropic turbulence results in a suprisingly detailed and not unreasonable picture of conditional patterns in a flow that is often considered relatively featureless. On the basis of this result is seems likely that E_1 type events could be useful in the experimental study of much more highly structured flows such as turbulent boundary layers.

It is obvious that E_1 based conditional analyses must yield some sort of conditional flow structure for turbulent boundary layers. It is less obvious, indeed unproven, that these structures would coincide with the Lagrangian type of flow entities that are sometimes implied by the term coherent structure. This would depend upon whether or not a particular coherent flow entity could be characterized uniquely on average by given values of the velocity vector at some point in its volume. Experimental studies using E_1 based conditional analysis would appear to be the best way to resolve this question.

REFERENCES

Adrian, R. J. 1975, On the role of conditional averages in turbulence theory. Proc. 4th Symposium on Turbulence in Liquids (ed. Zakin and Patterson), pp. 323-32, Princeton: Science Press.

Adrian, R. J. 1978, Turbulence models based on conditional averages as optimal estimates. Submitted to J. Fluid Mech.

Ievlev, V. M. 1970, Approximate equations of turbulent motion in incompressible fluids. Iz. Mekh. Zhid i Gaza, Akad. Nauk SSSR, No. 1, 91.

Dopazo, C. 1975, Probability density function approach for a turbulent axisymmetric heated jet. Centerline evolution. Phys. Fluids 18, 397.

Adrian, R. J., Chung, M. K., Jones, B. G., and Nithianandan, C. K., 1976, Linear estimation closure of two-point conditional averages. Bull. Amer. Phys. Soc. 21, 1233 (Abstract).

Batchelor, G. K. 1960, Theory of Homogeneous Turbulence. Cambridge Univ. Press.

Van Atta, C. W., and Chen, W. Y. 1968, Correlation measurements in grid turbulence using digital harmonic analysis. J. Fluid Mech. 34, 497-515.

DISCUSSION

Kovasznay:

Two comments. One of them is a statement of fact that a quantity very closely related to what you describe is referred to as contingency. Namely, if you take two functions (a two-point correlation) and you define the probability so that if function X is above a fixed value A and function Y is also above a fixed value B, and the correlation properly normalized so that there is complete coincidence of the two events if the value is one and zero if they are strictly independent, then you have contingency of the two functions X and Y. Contingency has been measured by the Marsailles turbulence group for several flows ....that's a comment. Second is a question....have you made any attempt to do what you describe in any truly three-dimensional shear flow?

Adrian:

Yes, we're doing it right now.

Kovasznay:

Does it reveal anything?

Adrian:

Well, subject to the proviso that it is all tentative, I can say that right now our direct measurements of pipe flow structure using two cross-wire probes in which we do compute these conditional averages (and we also do linear estimation and non-linear estimation but we haven't an updated map of structure yet so we don't know if we can identify this yet with large scale structure), we are finding at least that the linear estimates are very accurate. So I can only take that to imply that these curves are close estimates of the conditional averages. Now what the conditional averages mean as such, I think we have to wait on because these are not Lagrangian pictures.

Kovasznay:

Sure. A third comment. Is not surprising that you get a vortex ring, a diffused vortex ring type of structure because isotropic turbulence has been described as random oriented vortex rings by several people, the most elaborate of them being Chou Pe Yuan in Peking.

Adrian:

I should mention that without any approximation this must be the case because you have specified an isotropic field once you say you're going to specify a given direction for the velocity vector. It has to be an axisymmetric field.

REYNOLDS AVERAGING AND LARGE EDDY STRUCTURE

Stanley F. Birch
Boeing Aerospace Company
Seattle, Washington

INTRODUCTION

The objective of these remarks is to briefly discuss the roles of detailed experimental measurements and Reynolds averaged based turbulence models in basic turbulence research. Although the development of reliable prediction methods for use in industrial design is probably the major motivation for most turbulence research, the present discussion of prediction methods will be restricted primarily to a discussion of their role as a tool in basic research; not because the former function is unimportant, but because the latter function is less frequently discussed and sometimes overlooked.

A convenient point from which to start such a discussion is the relationship between understanding and predictions mentioned by Bradshaw (1) in his Reynolds-Prandtl lecture. It is argued, here, that prediction and understanding are closely related concepts. This relationship will be discussed from two points of view. The role of understanding, in the restricted sense of an accumulation of empirical facts, in the development of prediction methods will be discussed first, and then the role of prediction methods in the development of understanding, in a broader sense, will be examined.

THE ROLE OF UNDERSTANDING IN PREDICTION

It would seem that some understanding of a system is always necessary if we are to predict, in any meaningful sense of the word, its behavior; and understanding requires, at minimum, the accumulation of a certain quantity of empirical information about the system. This was not always accepted as fact. Indeed one can argue that the development of the modern scientific method was due largely to the slow realization that "Pure logical thinking cannot yield us any knowledge of the empirical world; all knowledge of reality starts from experience and ends

in it. Propositions arrived at by purely logical means are completely empty as regards reality," (2).

Within the more limited context of the prediction of turbulent flows, the experimental study of turbulence structure plays a much more direct role. This is perhaps most easily demonstrated by considering the relations.

$$\overline{u'v'} = \alpha_1 q \tag{1}$$

$$\overline{u'v'} = \alpha_2 q^{\frac{1}{2}} \ell \frac{\partial u}{\partial y} \tag{2}$$

Here q is the turbulence kinetic energy, ℓ is a characteristic length scale for the turbulence, $\partial u/\partial y$ is the mean velocity gradient and α_1 and α_2 are constants. Both relations are known to be approximately valid for a fairly wide range of flows (References 3 and 4). Both have been successfully used in the development of Reynolds averaged based turbulence models, but here we will discuss them as experimental observations, without reference to any particular turbulence model. Combining (1) and (2) yields

$$q \propto \ell^2 \left(\frac{\partial u}{\partial y}\right)^2 \tag{3}$$

or, if we take $q^{\frac{1}{2}}/\ell$ to be a measure of the strength of the large eddie ω, we can write

$$\frac{\omega}{\Omega} = \text{const.} \tag{4}$$

since

$$\Omega = \left(\frac{\partial u}{\partial y} - \frac{\partial v}{\partial x}\right) \approx \frac{\partial u}{\partial y} \tag{5}$$

for most boundary layer flows. What this says is that any major change in the structure of a flow, for which equations (1) and (2) are valid, must be due to variations in the size of the large eddies, since equation (4) implies that the strengths of eddies remain in equilibrium, in a statistical sense, with the local mean vorticity.

Now the Reynolds equations for the single point correlations contain no length scale information. Therefore, the formal study of these equations cannot tell us anything about the nature of this change. The performance of any turbulence model, based on the Reynolds equations, for such flows must depend on the accuracy of the method used to specify the length scale ℓ. One can, or course, derive an equation for a length

scale containing quantity, but because of the complexity of these equations and the almost complete lack of experimental information on the terms which appear in them, the development of any model equation must of necessity be highly empirical. Therefore, the model is ultimately based directly on experimental measurements. The Reynolds equations themselves, it would appear, provide little more than a convenient framework within which such a model can be constructed. For a more detailed discussion, see Reference (5).

It is true that equations (1) and (2) are not universally valid, and even for the range of flows over which they are approximately valid, the intent of the above remarks is not to imply that the behavior of turbulent flows can be completely described by a consideration of just the turbulence length scales. The objective is merely to demonstrate that in turbulence models based on the Reynolds equations, much of the real physics of the flow is carried by the empirical closure assumptions, rather than by the Reynolds equations themselves. The obvious conclusion which follows from this is that the continuing development of such models depends on the availability of new experimental data.

THE ROLE OF PREDICTION IN UNDERSTANDING

Although experimental data is required in the development of prediction methods, understanding, in general, implies more than the simple accumulation of data; it implies a knowledge of the causal relationships between the observed phenomena. Experimental observations may suggest possible relationships, but they do not provide such knowledge directly. How is such knowledge acquired? The classical method is to attempt to predict the behavior of the flow under different circumstances, based on some assumption about the causal relationships. These predictions are tested against new experimental data. If they prove to be correct, then an attempt is made to predict a larger range of flows. If not, a new hypothesis is formulated and the process is repeated. In this way, hypotheses are developed which are valid for a wider and wider range of flows. Obviously, it is important to assure that the predictions follow rigorously from the assumptions, and as the range of flows which must be considered increases, it becomes necessary to develop a formal prediction procedure. This procedure must be reasonably tractable. It is also desirable that its formulation does not precommit one to a particular point of view, since one does not know initially which hypothesis will prove to be correct. These criteria are satisfied by turbulence models based on the Reynolds equations.

Note that the objective is not to predict the detailed structure of the flow. The objective is to establish the

validity of certain assumptions about the basic physics of the flow. A model of the turbulence of some sort is implicit in any detailed discussion of experimental data in which the results of one experiment are compared and contrasted with those of other experiments. The formal use of turbulence models simply makes the procedure more systematic and scientific.

Developments in numerical methods and turbulence models over the last 10-15 years have had two important effects. First, the development of efficient methods for the solution of sets of coupled partial differential equations has led to the development of turbulence models which are valid for a much wider range of flows than the older models. None of the models developed to date are universally valid, and it is unlikely that any such model will be developed, but the better methods are now capable of predicting a fairly wide range of flows. As the accuracy of these models has increased, their importance in the design of experiments and the interpretation of results has also increased. This has been exploited with considerable success by a number of groups in recent years.

The second effect of the improvements in numerical methods has been that the range of flows which can be studied numerically has greatly increased. But this has led to experimental problems. Our experience from the study of classical two-dimensional flows over the last 50 years has made it clear that an experimental description of the more complex flows of practical importance is not going to progress very far if we approach the problem in the same way. To completely document such flows experimentally is out of question. If we are to make any progress with these flows, we must use a combination of numerical calculations and detailed experimental measurements. To be practical the experimental measurements in these flows must be confined to trying to resolve new problems which arise, rather than trying to completely document the flows.

CONCLUDING REMARKS

The objective of this discussion was to attempt to show that the roles of detailed experimental measurements and numerical turbulence models are largely complimentary, and to suggest that continued progress, particularly for the more complex flowsencountered in most practical applications, will require the combined use of both.

REFERENCES

(1) Bradshaw, P. The Understanding and Prediction of Turbulent Flow. Aero. J. 76, 1972.

(2) Einstein, A. On the Method of Theoretical Physics. The Herbert Spencer Lecture, Oxford, June 10, 1933. Published in Mein Weltbild, Amsterdam: Querido Verlag. 1934.

(3) Harsha, P. T. and Lee, S. C. Correlation Between Turbulent Kinetic Energy and Turbulent Shear Stress. AIAA J., 8, 8, 1970.

(4) Rodi, W. A Review of Experimental DATA of Uniform Density Free Turbulent Boundary Layers. Studies in Convection, Academic Press, 1975.

(5) Birch, S. F. Turbulent Length Scales in Non-Equilibrium Flows. Numerical Methods in Laminar and Turbulent Flow. Swansea, July 1978.

DISCUSSION

Patterson:

This gives me an opening to make a comment and ask a general question. The thing that I've been wondering throughout this conference is how all this knowledge that we're accumulating on the coherent structures of turbulence is going to contribute to our ability to do the kind of engineering modeling that Birch is talking about. My interests, for instance, are primarily in mixing and in shear flows with additives and, to a larger extent, in modeling these kinds of flows. I'd like to have suggestions from anyone about how the simplier engineering type modeling efforts (two-equation and simpler) can benefit from the knowledge that's been accumulated. Do you have any comments on this, or anyone else?

Birch:

I think that's a pretty complicated question to answer right off. All I'm saying is, there has to be a connection or else we're not going anywhere. We have to try and interest the people who are developing models to look at experimental work, and the people who were making measurements to try to relate those measurements to the sort of information we need to develop models. That is the problem. I can't solve that.

Abbott:

I have a quote here from Cebeci & Smith's book (Academic Press, 1974) that I think is relevant to this discussion. Would you like to read that into the record Amo?

Smith:

Yes, thank you. In fact, I happened to write this part myself. I was thinking of the airfoil-like 28 foot long body investigated by Schubauer and Klebanoff (1950) at nearly full-scale Reynolds number. Since the average boundary-layer thickness was of the order of 3½ inches, and if you argue that you need, say, 10 nodal points to describe the smallest eddy, then for a typical two-dimensional calculation you must use 20,000 steps in X, 1200 in Y and 4800 in Z. If you assume 100 time steps will give average characteristics and solve the complete Navier-Stokes equations from first principles, the calculation would require 1.15 X 10^{13} computation steps. For a CDC 7600 this would require 1.85 x 10^{10} minutes or 35,000 years! Corrsin and Emmon's have made similar estimates. Later I found out from Deardorff that 1000 time steps are probably necessary, and it would take 10 times longer if you had a real three-dimensional problem!

Reynolds:

I'd just like to kind of counter that comment of Amo's because I think it could be misleading. The two things we have learned from experiments are that the large-scale structures are very different from flow to flow, and in fact they affect all of the statistics that are important. So if you try and perform a calculation by going to more and more higher-ordered closure terms, you're still involving the large-scale structures. Since they are all different from flow to flow, there's no way to model them. The other thing we've learned from experiments is that small-scale structures are very nearly the same from flow to flow. So this is the whole idea behind large eddy simulation....you model small-scale structures and compute the large-scale ones that are different, and I don't think that it takes as many points as you've indicated to do that.

McElligot:

I can think of one case somewhere along the lines Bill Reynolds just described where the modeling could help and that is when we try to predict heat transfer which is primarily wall dominated. What we need is a fairly good understanding of how the viscous sublayer is modified, and I'd like to do that from an understanding of what are the dominant features in the viscous sublayer --- meaning at a y^+ of 30 in the unheated flow and y^+ of 50 to 100 in some of the strongly heated flows. Once I have a reasonable treatment for

the sublayer, I think we can patch it in with any outer flow treatment which gives an approximately decent answer and we'll come up with good predictions for heat transfer and wall friction which is what many engineers want.

Brodkey:

The reason that I got involved myself in all of this coherent structure work was the recognition that it was impossible really to model it. The modeling you're talking about is modeling without understanding. This is what you need really to bulldoze your way through a problem with a computer bigger than all the computers added together in the world. And the only reason that many of us are in this area of study, starting with Steve Kline and others, is to provide some of the understanding which makes the problem manageable.

Abbott:

I disagree with your contention that it's impossible to model the details of turbulent flow; there are a number of us that are doing just that. Whether solving a complete problem will prove computationally feasible was AMO's point, and in all fairness he wrote that back before 1974. Maybe Bill Reynolds is right.

Peter Bradshaw:

Can I just refer to that highly unfamiliar equation I just wrote up on the board and point out that the main stumbling block in solving this shear stress transport equation is the term with the pressure fluctuation. (No record was made of the equation Ed.) Now I'm not convinced that one can necessarily model this term just by plugging in a simple length scale. A pressure fluctuation isn't really a locally determined quality anyway. So I'd like to take issue with what Stan Birch said about the length-scales in effect containing all the information. We haven't really worried much about pressure fluctuations except for what Marten Landahl said this morning, but somehow or other we have either got to predict those pressure fluctuations or we've got to solve the Poisson equation and plug that into the equation before we start modeling.

Birch:

I don't think I said, at least I hope I didn't say, that all you have to do is solve for a length scale and plug it in. I'm agreeing with you. The pressure velocity correlations are important terms, but they're not terms that you can solve with the Reynolds equations--they're empirical input.

ON THE FEASIBILITY OF A VORTEX MODEL OF THE TURBULENT BOUNDARY LAYER BURST PHENOMENA

J. E. Danberg

Department of Mechanical & Aerospace Engineering

University of Delaware, Newark, DE 19711

ABSTRACT

A limited feasibility study is described involving the modeling of turbulent streak and burst phenomena using vortex configurations imbedded in a mean turbulent flow field. Two situations are considered, first, the development of a hairpin vortex attached to the wall and, second, two elongated vortex rings one above the other. The hairpin is found to grow away from the wall and form a vortex ring with several features resembling streak development (upward growth, leading edge oscillations, speed of 80% of mean speed). The two ring system shows vertical motion 10 times larger than that of the hairpin, a characteristic which would be required to describe the burst phenomena.

1. INTRODUCTION

Several aspects of flow visualization studies and hot wire measurements of the streak-burst-sweep sequence in turbulent boundary layers suggests the presence of vortices. Theodorsen[1] was the first to suggest horseshoe vortices as a flow pattern underlying turbulence. Many other researchers have proposed models or "pictures" which explain the observations, most notably those of Kline and his associates[2]. However few attempts have been made to quantify these models into a theory. Analyses of vortex motion have been made by Hama[3], Thomson[4] and Stuart[5] but with transition in mind.

In the present study it is proposed that a hairpin shaped vortex is formed in the laminar sublayer and that the vortex moves with the fluid and as a result of self-induced velocities. An image vortex is introduced to satisfy the impermeable wall condition. The prongs of the hairpin are assumed fixed to the wall. As the prongs elongate they are induced to approach each other creating a ring like structure with a

smaller hairpin behind. The stretching and movement away from the wall corresponds to streak formation and lift up. Waves are observed to develop on the vortex which could correspond to the oscillations observed in flow visualization studies. If the formation of the vortex ring coincides with the passage of a similar vortex in the flow away from the wall, the mutual attraction produces a rapid upward movement of the ring modeling the burst phenomena. Finally the circulation around the trailing edge of the ring produces a sweep-like wallward directed flow.

As a preliminary attempt to formulate such a model the different phases are considered separately. The first model is that of the development of the hairpin vortex in the sublayer. A second model consists of two ring vortices separated in the y-direction.

MODEL FORMULATION

The vortex system as shown in Figure 1 is divided into nodal points so that (n, n+1) defines a segment of the vortex. Both the primary vortex and its image are assumed symmetric to the z = 0 plane.

The curved vortex loop segments are approximated by straight line elements where the motion of the end points are computed using the Biot-Savart law. The vortex is fixed at x = 0 but all other points are convected by the mean flow $\bar{u}(y)$ (based on Coles[6]) and by the self induced velocities. The computations are carried out in wall region non-dimensional variables. The initial hairpin was assumed to be a half ellipse $x^+_{max} = 100$, $z^+_{max} = 10$ and inclined at 4.6° to the wall. The circulation strength was chosen as $\Gamma^+ = 10$ ($\Gamma^+ = \Gamma/\nu$) which resulted in a growth rate roughly compatible with streak growth rates.

Figures 2 and 3 illustrate the results obtained where Fig. 2 shows the side view and 3 the plan view. Note that the ordinate and abscissa have very different scales. The vortex is shown every 6 time units ($t^+ = u^2_\tau t/\nu$). Fig. 3 shows the "neck down" and formation of a ring from the leading edge of the hairpin. Fig. 2 shows the instability of the leading edge which resembles the oscillation observed in the later stages of streak development. The x-direction velocity of the leading edge of the vortex is found to be approximately 80% of the mean flow speed which is consistent with hot wire measurements of turbulence propagation.

RING MODEL

Fig. 4 illustrates the results obtained for a pair of elongated ring vortices separated in y. For this calculation the overhead vortex was assumed fixed at $y^+ = 50$ and convected at 80% of the local mean speed. Both rings were elongated ellipses approximately of the dimensions of the ring formed from the hairpin system. The duration of this calculation is $\Delta t^+ = 10$ compared with the $\Delta t^+ = 60$ of the previous figures. The vertical velocity of the lower ring can be estimated as 10 times the vertical speed of the hairpin system.

CONCLUDING REMARKS

Further details of the analysis are available in Reference 7 and additional studies are planned to consider the effects of other choices of parameters such as segment length, initial vortex configuration and circulation strength. A more complete model is being developed including both a hairpin and overhead ring so as to give a more complete picture of the interaction of the elements of the system.

ACKNOWLEDGMENT

Support for this work was provided by the National Aeronautics and Space Administration, Langley Research Center.

REFERENCES

1. Theodorsen, T., "Mechanism of Turbulence" Proceedings of the Second Midwestern Conference on Fluid Mechanics, Ohio State University (1952).

2. Kline, S. J., Reynolds, W. C., Schraub, F. A., and Runstadler, P. W., "The structure of turbulent boundary layers", J. Fluid Mech. 30, p. 741 (1967).

3. Hama, F. R., "Progressive deformation of a curved vortex filament by its own induction", Phys. Fluids, 5, p. 1156 (1962).

4. Thomson, K. D., "The prediction of inflectional velocity profiles and breakdown in boundary layer transition", WRE Rept. 1052 (WR&D), Dept. of Supply, Australian Defense Scientific Service, Weapons Research Establishment (1973).

5. Stuart, J. T., "The production of intense shear layers by vortex stretching and convection", AGARD Rept. 514 (1965).

6. Coles, D., "The law of the wall in turbulent shear flow", 50 Jahre Grenschicht forschung (Ed. H. Görtler and W. Tollmien) pp. 153-163 (1955).

7. Danberg, J. E., "On the Feasibility of a Vortex Model of the Turbulent Boundary Layer Burst Phenomena," Technical Report No. 208, Department of Mechanical & Aerospace Engineering, University of Delaware (1977).

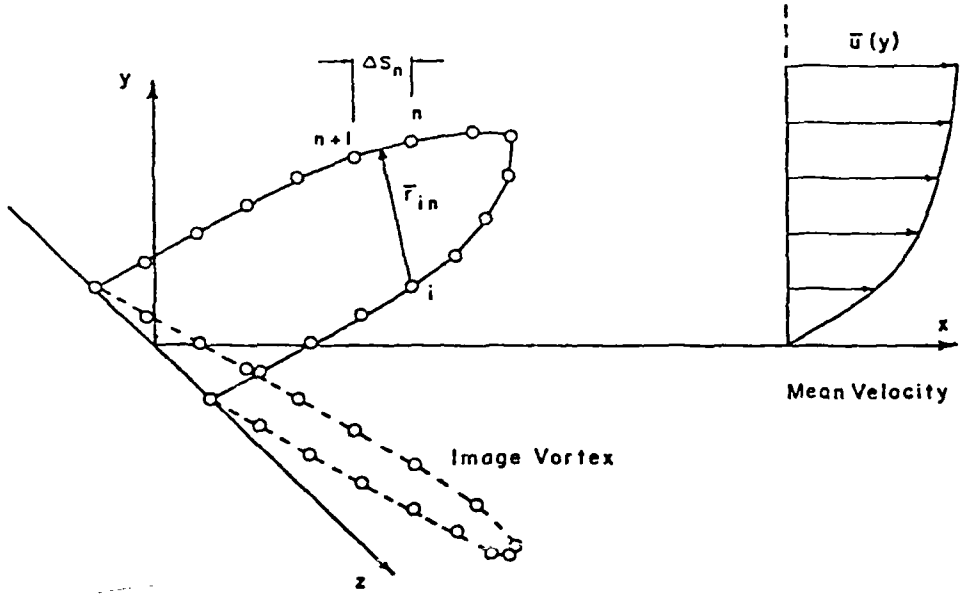

Fig. 1 Sketch of coordinate system for hairpin vortex

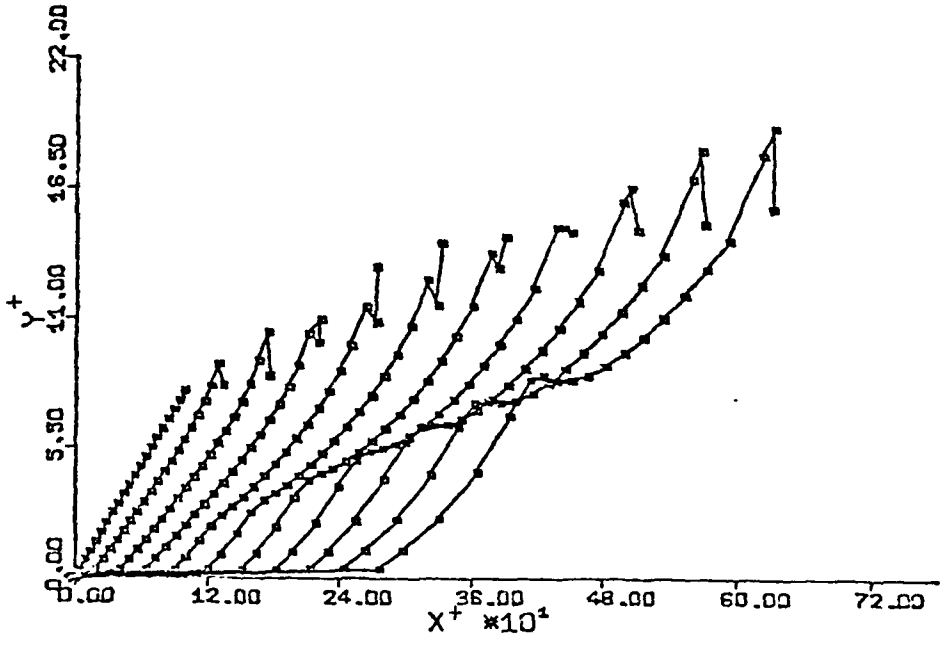

Fig. 2 Side view of hairpin vortex at successive times

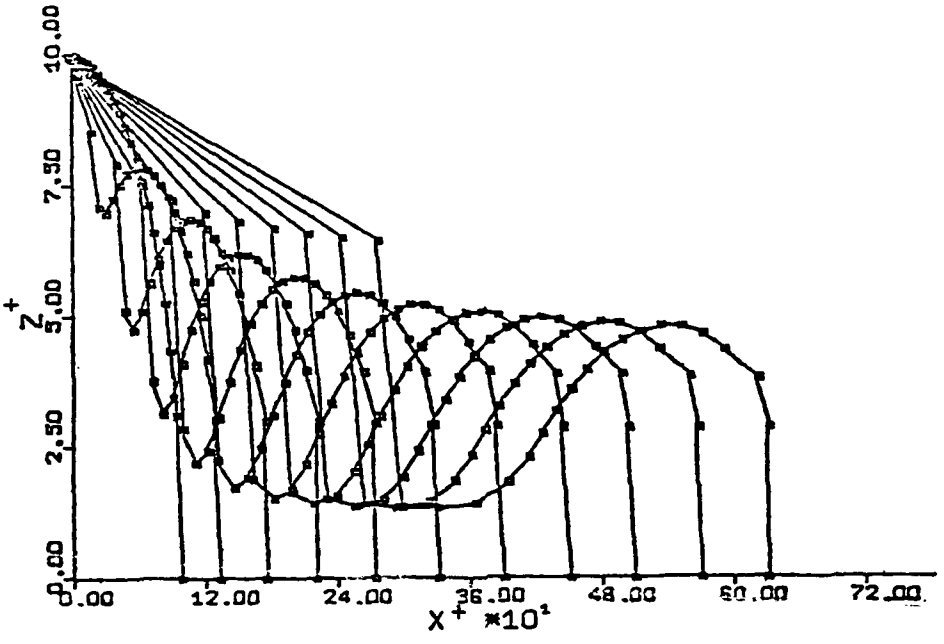

Fig. 3 Plan view of hairpin vortex at successive times

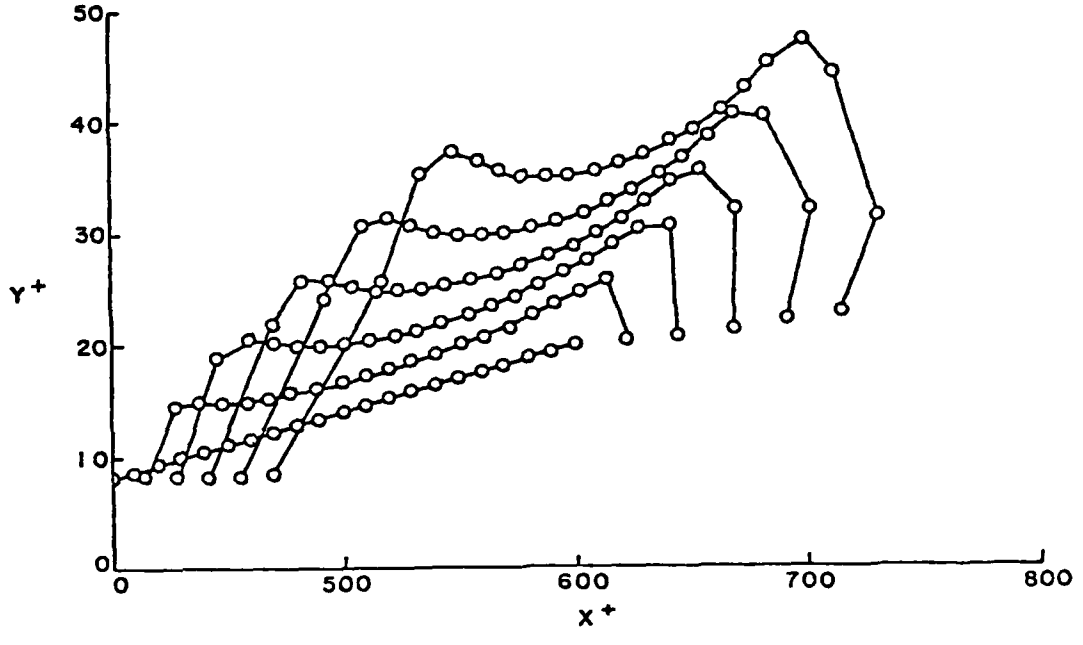

Fig. 4 Side view of elongated ring vortex under the influence of a second vortex at $y^+ = 50$

DISCUSSION

Abbott:

Jim, (Danberg) I'd like to ask you a question. You have your hairpin vortices ending on the wall now, right? I think we all pretty well understand that this can't be true for viscous flows. I can give you a very simple proof of this if you want; is there any question about it now? No? *OK. So we can take your work as a schematic model of something that is not quite right.

(The proof, in its simplest form, can be outlined as follows: If a vortex is to end on a wall (or connect to its image), there must be a non-zero value of ω_y at the wall. But $2\omega_y = (\partial u/\partial z - \partial \omega/\partial x)$, and since u and ω are zero at the wall in a viscous flow, their gradients in the plane of the surfact are zero. Hence, in a viscous flow, since ω_y is a zero at the wall, a vortex cannot end on the wall. Ed.)

Danberg:

Yes, it's strictly an inviscid flow. There was no viscosity in our model.

Abbott:

There was no viscosity, but a profile. A rotational profile?

Danberg:

Yes, correct.

Landahl:

I wasn't quite sure what you assumed about the core of the vortex. Was this a line vortex? Yes? Well, then the question arises, since a curved line vortex has infinite self-induction velocities on it, what did you do with that?

Danberg:

Well, when you approximate the curved vortex with a line element, then of course the line elements adjacent to the point have to be excluded from the calculation of the induced velocity.

Landahl:

Okay, but the point I guess is that a line element consisting of straight-line pieces doesn't behave the same as a curved element.

Danberg:

That's right

Knight:

In relation to Marten Landahl's question, did you make any observations about what happened when you increased the number of segments on your vortex hairpin? Were your results different?

Danberg:

Yes, but I haven't a complete picture on that. That's one of the obvious things that we want to do. It does change things but it doesn't change the overall picture.

Knight:

You still see the formation of the vortex ring and it's lifting off the wall?

Danberg:

Yes, and of course that's controlled to a large extent by the choice of circulation strengths that you select. We tried to look at a range of circulation strengths that might be reasonable. We want to of course pick a fairly low strength, a very weak vortex. Apparently, in a range of between five and say eighteen in this non-dimensional circulation strength, we get a ring formation, but the rate at which the ring forms is controlled by the magnitude of that number.

Bradshaw:

This first slide shows the way in which a vortex loop more or less artificially introduced into a laminar boundary layer, will grow (it's growing downward). The flow is from right to left and it's at the top of a wind tunnel if you like. The second slide is a laminar boundary layer flowing left to right. There are some suction holes in the surface which stretch the curved "vortex lines" in the laminar boundary layer spanwise causing little vortex horseshoes to form between the suction holes. They also make most of the smoke disappear. The horseshoes are then shed at intervals and as you can see they move downstream periodically, although we need concentrate on only one of them. The smoke, i.e. the vortex lines, more or less just trail down (behind) in what would be the viscous sublayer in a turbulent flow. It looks like a couple of snail trails, so maybe this elephant is really going downstream on a skateboard and leaving a trail behind it. I thought you might be interested, those of you who haven't had these slides peddled out to you before, to see the correspondence between the flow visualization and Professor Danberg's nice calculations.

Abbott:

Where are the suction holes?

Bradshaw:

Here is one layer. The next one is up here. So you're getting a vortex line, a kind of stretching between the two suction holes. That is, the vortex lines in the laminar boundary layer get stretched out sideways.

Reynolds:

Peter, is there any indication of any interaction between those nice clean vortices (that are marching downstream) as you go further downstream? Do they come together at all?

Bradshaw:

I don't believe they do. This was all done about 15 years ago when we were working on laminar flow control. I think they just wander downstream without anything else very much happening to them until we run out of wind tunnel. As you can see, they're pretty widely spaced. The fact that they look as though they are in echelon is, I think, just a coincidence. There's certainly a streamwise periodicity, but its set by an oscillation down on the side. But that is not turbulence! That's a laminar flow with artificially introduced vortex loops at the beginning--croquet hoops if you like--which then go downstream and form into the same sort of horseshoe vortex shape that Professor Danberg has been showing us.

Danberg:

I certainly wish I had seen that Figure before I started my talk. It would have been a useful addition.

Wallace:

I want to ask Professor Danberg to what extent he feels that modeling a hairpin vortex in a shear layer without viscosity gives insight into the dynamics of a horseshoe vortex in a viscous shear layer?

Danberg:

Well, if I knew all the answers I guess I could answer that question, but I felt it was necessary to start some place and look at what happened. There is much discussion in the literature about horseshoe vortices as a description of what is going on, but no one, as far as I am aware, has tried to quantify this before.

Wallace:

This wasn't meant as a criticism but just a question: did you have a specific motivation?

Danberg:

Well, just as a learning process at this stage.

Falco:

Two questions for both Peter Bradshaw and the speaker. First, do you see your horseshoes closing into rings, as the calculation suggests. And second, do those things lift off the wall or do they just convect at roughly a fixed height the whole of the time.

Bradshaw:

I don't think there's any interaction between them. I don't think there's any real tendency to come together into complete loops; remember, each of these has got an image, underneath anyway, so a horseshoe on the top and a horseshoe on the bottom is a complete loop from an inviscid point of view.

Abbott:

The answer is no?

Bradshaw:

Correct. They popped out of the laminar boundary layer and then they just formed downstream with nothing else to do. So they were effectively fixed patterns of smoke going downstream.

Falco:

So they were effectively inert after they formed?

Bradshaw:

Yes.

Danberg:

Well, let me just mention one thing. What you are describing is very sensitive to the circulation strength that is put in. And the experimental situation that was illustrated was a result of a fairly low circulation strength, so that the arms would pinch off very slowly or perhaps not at all. That is what we get for very low circulation strengths as well.

THE INTERPRETATION OF THE VISCOUS WALL REGION AS A DRIVEN FLOW

Dimitrius T. Hatziavramidis and Thomas J. Hanratty

Department of Chemical Engineering

University of Illinois, Urbana, IL. 61801

ABSTRACT

A model for the kinematics of a turbulent flow close to a solid boundary has been explored. Good agreement is obtained between the calculated flow field and experimental results. This agreement suggests that the flow oriented eddies in the viscous wall region can be represented as being coherent and as being driven by flow deviations from the mean flow direction in a well mixed outer region. The observed "bursting" phenomenon is pictured as the result of the motion of a strong shear layer from the region of coherent flow to the outer flow.

1. DESCRIPTION OF THE MODEL

This paper is concerned with the viscous wall region of a turbulent flow ($y^+ < 30$-45). The two dominant theoretical notions that have been used to describe this region have been that the flow is driven by the outside flow or that the events are due to a hydrodynamic instability. We explore the first of these.

The field is assumed to be homogeneous in the direction of mean flow. The equations of motion are solved numerically for a flow which is periodic in time and in a direction transverse to the direction of mean flow. The period is taken to be the time interval between "bursts" and the wave length the spacing of the streaky structure close to the wall observed by a number of investigators.

The average flow is assumed parallel to the x-direction. By using the assumption of homogeneity in the x-direction the velocity field is given by the equations

$$\frac{\partial w}{\partial t} + w\frac{\partial w}{\partial z} + v\frac{\partial w}{\partial y} = -\frac{1}{\rho}\frac{\partial p}{\partial z} + \nu\left(\frac{\partial^2 w}{\partial z^2} + \frac{\partial^2 w}{\partial y^2}\right),$$

$$\frac{\partial v}{\partial t} + w\frac{\partial v}{\partial z} + v\frac{\partial v}{\partial y} = -\frac{1}{\rho}\frac{\partial P}{\partial y} + \nu\left(\frac{\partial^2 v}{\partial z^2} + \frac{\partial^2 v}{\partial y^2}\right),$$

$$\frac{\partial U}{\partial t} + w\frac{\partial U}{\partial z} + v\frac{\partial U}{\partial y} = \nu\left(\frac{\partial^2 U}{\partial z^2} + \frac{\partial^2 U}{\partial y^2}\right)$$

$$\frac{\partial w}{\partial z} + \frac{\partial v}{\partial y} = 0$$

These are to be solved subject to boundary conditions

$z = 0 \quad \lambda/2 \qquad w = 0, \quad \frac{\partial v}{\partial z} = 0, \quad \frac{\partial U}{\partial z} = 0$

$y = 0 \qquad w = v = U = 0$

$y = y_o \qquad w = w_L \sin\frac{2\pi z}{\lambda} \cos \omega t,$

v from continuity,

$U = \bar{U} + u = U_L,$

where U_L is the measured time average velocity at y_o. For this purpose we used the average velocity measurements given by Laufer (1954). For initial conditions we took w, v from the inviscid irrotional solution and $U = \bar{U}(y)$.

Finite difference methods have been used to solve these equations. Calculated values of U, v, w were found to vary periodically with time after 4-5 periods. The characteristics of this periodic solution are discussed in this paper.

2. CALCULATED STREAMLINES

Examples of calculated stream lines for the conditions $y_o^+ = 45$, $\lambda^+ = 100$ and $\tau^+ = 100$ are shown in figures 1 and 2. Here τ is the period defined as $2\pi/\omega$. For $t = 0$, the flow is inward at $z = 0$ and outward at $z = 0.5\lambda$. At $t = 0.21\tau$ a separation bubble appears at $z = 0.5\lambda$ as indicated in figure 1. Because of the imposed outer boundary condition the w- velocity reverses direction at $t = 0.25\tau$. At $t = 0.26\tau$ a streamwise vortex larger than the separation bubble appear close to the upper boundary. In subsequent times the streamwise vortex and the separation bubble increase in size until at $t = 0.31\tau$ the vortex occupies the whole region of coherency. At $t = 0.32\tau$ the v- velocity reverses direction at the upper boundary. In subsequent times the separation bubble and the streamwise vortex shrink in size until they eventually disappear. During this period the outflow $z = 0$ and the

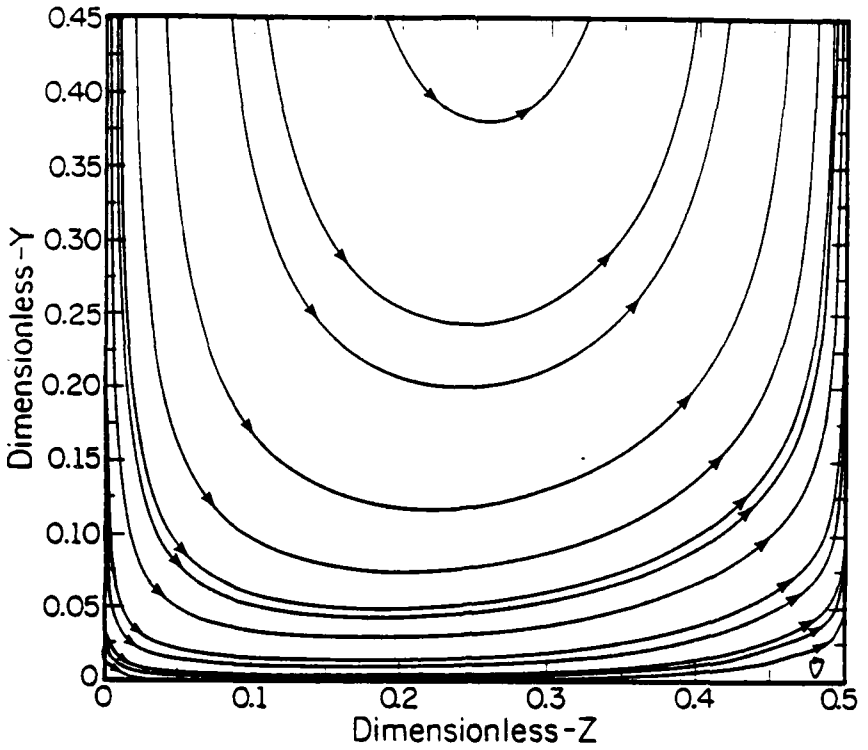

Figure 1. Calculated secondary flow pattern ($y_o^+ = 45$, $\lambda^+ = 100$ and $T_B^+ = 100$) at $t = 0.21\ T_B$.

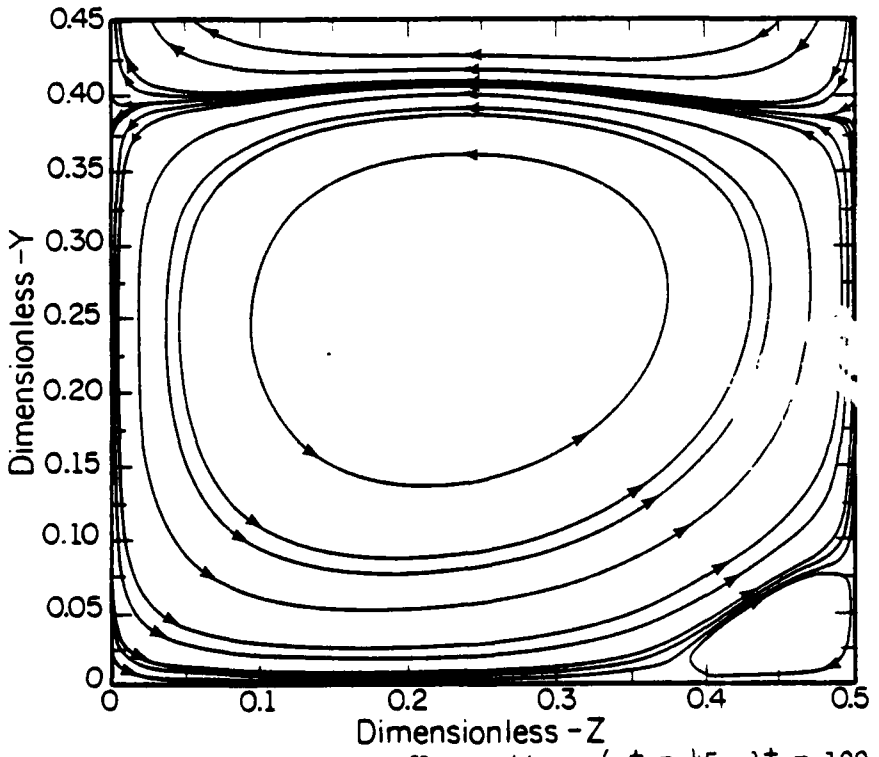

Figure 2. Calculated secondary flow pattern ($y_o^+ = 45$, $\lambda^+ = 100$ and $T_B^+ = 100$) at $t = 0.34\ T_B$.

inflow at $z = \lambda/2$ become stronger and the secondary flow pattern shows phase changes as well as shear layers. At $t = 0.50\tau$ the pattern is the same as for $t = 0$ except that the direction of flow is reversed.

The flow lines shown in figure 1 would suggest that dye injected through a wall slot would initially form a rising plume at $\frac{\lambda}{2}$. At about $t = 0.39\tau$ this plume would disappear at $\frac{\lambda}{2}$ and would start to appear at $z = 0$ at about $t = 0.44\tau$. However, before disappearing at $\frac{\lambda}{2}$, its leading edge would recede backward, (see figure 2), perhaps giving the appearance of an oscillation, and have lateral movement. This resembles in some ways the description of breakup given by Offen and Kline. (See figure 2 of their paper, 1975).

The streamwise vortices observed over a part of the cycle are different from the counterrotating eddies proposed by Townsend (1956) and Bakewell and Lumley (1967). They are not associated with intense outflows and inflows in the region of coherent motion. They appear only during transitional stages separating periods of high activity.

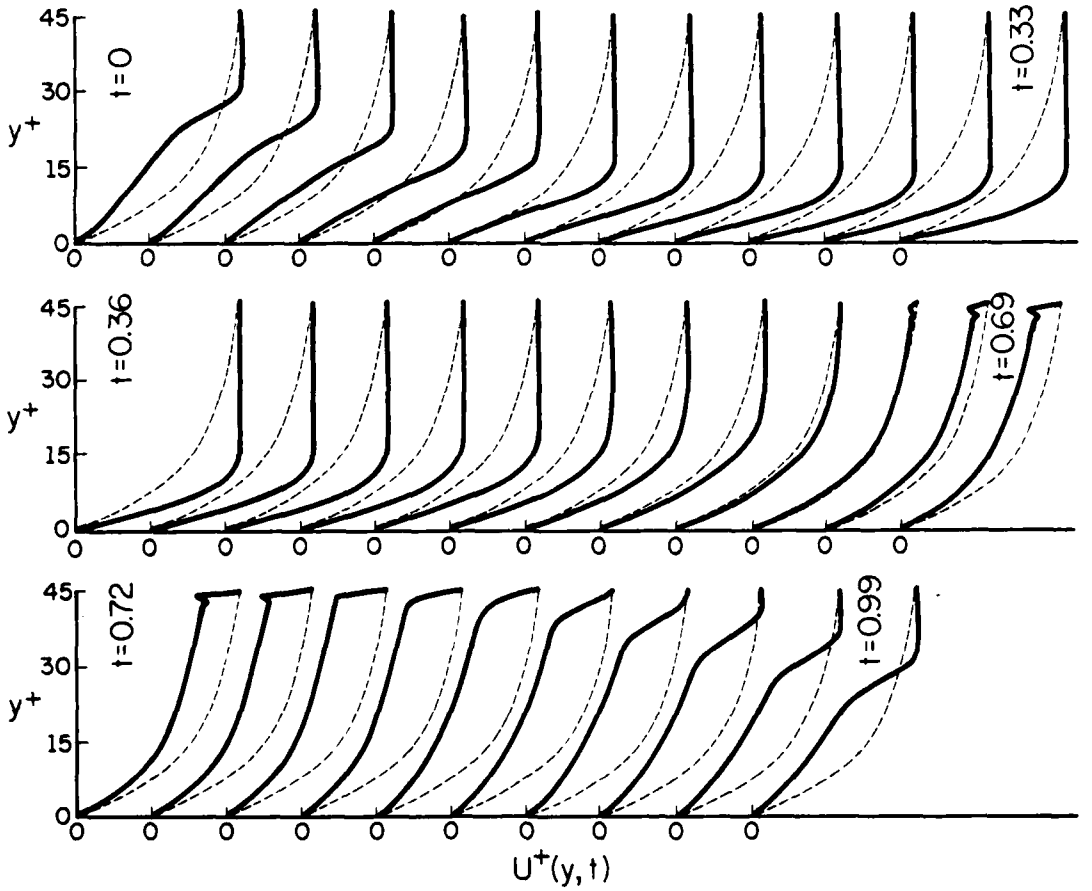

Figure 3. Calculated instantaneous axial velocity profiles ($y_o^+ = 45$, $\lambda^+ = 100$, $T_B^+ = 100$) at $Z^+ = 0$ and for times $t = 0$ to $t = 0.99T_B$.

3. DEFINITION OF BURSTING

Calculated instantaneous axial velocity profiles at z = 0 are shown in figure 3. In this figure the time averaged velocity profiles are indicated by dashed lines.

The instantaneous axial profiles at $z^+ = 0$ show positive deviations from the mean velocity profile far from the wall and negative deviations close to the wall at the beginning of the period (t = 0 to t = 0.13τ). Over the time t = 0 to t = 0.34τ increases in the axial velocities are noted. This acceleration is stronger far from the wall. It is noted that this acceleration occurs at the same time that strong inflows occur at z = 0, so that it is associated with the convection of momentum from the outer flow to the wall region. During the acceleration inflexion points gradually disappear from the axial velocity profile. The velocity gradient at the upper boundary also disappears and this results in a blunt velocity profile with a region of uniform velocity expanding from the upper boundary toward the wall.

At $t \cong 0.35\tau$ a deceleration of the axial velocity profile begins and continues to $t \cong 0.79\tau$. This deceleration occurs over the period that outflows are occurring at z = 0. At $t \cong 0.63\tau$ the axial velocity profile is the same as the mean profile. At subsequent times (t = 0.65τ to 0.84τ) a distinct shear layer is present at the upper boundary which separates the regions of coherent flow from the outer flow, as evidenced by a strong discontinuity in the axial velocity profile right at the upper boundary. Negative deviations of the instantaneous axial velocity from the mean velocity profile are observed at all values of y for t = 0.84τ to t = 0.91τ. However, no shear layer is present at the upper boundary.

There seems to be some differences in the literature in the definition of the actual event of bursting. We have chosen to define bursting as that period of time that the instantaneous axial velocity at z = 0 has steep discontinuities at the upper boundary, t = 0.65τ to t = 0.84τ. (At z = 0.50τ, it occurs from t = 0.15τ to t = 0.34τ.) It is to be noted that according to the above definition dye streamers formed at a wall slot would disappear from the z = 0 location shortly after the bursting. Thus we estimate that bursting occurs about 20 percent of the time. This result is in agreement with an estimate of 18 percent by Corino and Brodkey (1969). The calculated profiles shown in figure 3 are in striking agreement with measured velocities for y < 0.4 in. presented by Kim, et al (1971) in figure 6 of their paper.

Calculated instantaneous profiles at z = 0.22λ do not show steep discontinuities (shear layers) at the upper boundary as do the instantaneous profiles at z = 0. These results suggest a thickness of the bursting region of $\Delta z^+ < 44$.

4. CALCULATED STATISTICAL PROPERTIES

A number of statistical properties of the calculated velocity field were calculated. For this purpose averages at a given y^+ were obtained by averaging over one period in time and one wave length in z. Several aspects of these calculated results are in agreement with measurements.

The calculated average velocity profile is in good agreement with measurements of Laufer (1954) for $y^+ < 25$. The region $y^+ > 25$ matches the relation

$$\bar{U}^+ = 5.60 \log y^+ + 5.0 \quad .$$

A maximum in the intensity of the velocity fluctuations in the direction of mean flow is obtained at $y^+ = 10$. The ratio of the root mean squared values of the axial, $(\overline{s^2}_x)^{1/2}$, and transverse, $(\overline{s_z^2})^{1/2}$, fluctuating velocity gradients at the wall are calculated to be approximately equal to three. The calculated skewness of the axial velocity fluctuations is calculated as positive for $y^+ < 12$ and negative for $y^+ > 12$.

As in Willmarth and Lu (1971) and Wallace, et al (1972), calculated time averaged values of the product uv have been classified according to the sign of its components u and v. Quadrant IV ($u > o$, $v < o$) is identified as inflows of high speed fluid, quadrant II ($u < o$, $v > o$), as ejections of low speed fluid and quadrants I ($u > o$, $v > o$) and II ($u < o$, $v < o$) as interactions between inflows and outflows. The calculations agree with experiments (Brodkey, et al 1974) in that quadrants IV and II each contribute approximately 70% of the Reynolds stress and quadrants I and II contribute -40%. Also in agreement with experiments the quadrant IV contribution is greater than the quadrant II contribution for $y^+ < 22$.

ACKNOWLEDGMENT

This work is supported by the Office of Naval Research under Grant NR 062-558.

REFERENCES

Laufer, J. 1954 NACA Rep. 1174.

Offen, G. R. & Kline, S. J. 1974 J. Fluid Mech. 62, 223.

Townsend, A. A. 1956 The Structure of Turbulent Shear Flow.

Bakewell, H. P. & Lumley, J. L. 1967 Phys. Fluids 10, 1800.

Corino, E. R. & Brodkey, R. S. 1969 J. Fluid Mech. 37, 1.

Kim, H. T., Kline, S. J. & Reynolds, W. C. 1971 J. Fluid Mech. 50, 133.

Willmarth, W. W. & Lu, S. S. 1971 J. Fluid Mech. 55, 481.

Wallace, J. M., Eckelmann, J. & Brodkey, R. S. 1972 J. Fluid Mech. 54, 39.

DISCUSSION

Abbott:

Tom, one thing that immediately comes to mind would be a very important test; are you getting, in your time averages, the log-law in the outer portions of your profiles?

Hanratty:

Of course we only go out to about a y^+ of 45 and so we can't really get the log-law, but it does roughly suggest a match up with the log-law.

Reynolds:

Tom, this work looks very nice. Is the flow independent of x ?

Hanratty:

Yes.

Reynolds:

Does that mean that there's not a u, or is there a u in there too?

Hanratty:

There is a u in there, but we assume homogenity in the x-direction.

Reynolds:

So is there a Reynolds stress?

Hanratty:

Yes, there is a u and there's fluctuation in u. What we did is to solve the equations for a homogeneous flow in the x-direction until we got a periodic solution.

Reynolds:

Now isn't the u problem uncoupled from the v and w problems in that homogeneous case? What did you do about the u; did you prescribe the u?

Hanratty:

No. After we calculated v and w, we then solved the new momentum equations to get u.

Reynolds:

Oh---they're coupled that way. Okay--fine.

Brodkey:

What does the Reynolds stress come out to be?

Hanratty:

The Reynolds stress is just the average of v times the fluctuating u.

Brodkey:

Does it come out to be reasonable?

Hanratty:

Well -- we didn't look to see. We just calculated the average velocity and I don't know how the Reynolds stress would come out. I suppose it wouldn't come out right on the nickel, because if it did, then you'd be suspicious. I think the intensities did not come out right, as you noticed, but we were looking for the semi-quantitative and the qualitative descriptions of the features that you should have. What we thought was more important was the quandrant analysis; i.e., what percentage of the Reynolds stress is due to burst, what percentage is due to sweep, and what percentage is due to interaction. And, also, how these vary through the layer!

Coles:

You have the full Navier-Stokes equations, subject to this decoupling process?

Hanratty:

Right.

Coles:

I wish you'd explain how these things are energized. I see this flashing back and forth, but I can't put it together.

Hanratty:

It's a boundary condition for the equation.

Wallace:

You chose this driving velocity function as a boundary condition--at the upper boundary of your space.

Hanratty:

Right.

Wallace:

Did you have some sort of physically intuitive reason for that choice, or was that just an arbitrary choice?

Hanratty:

Well no, not arbitrary. First of all the intuition was that the length scale was the streak spacing and the time scale was the period of bursting. We picked a cosine function because that looked as good as any other choice from data that we had of velocities that were measured near the wall.

Wallace:

So, you're picking a simple periodic function in time and space that hopefully will produce a solution which will give the kind of time and space description that one observes close to the wall.

Hanratty:

Right. It was consistent with the two basic structural parameters that I see coming out of wall measurements (the bursting time and a lateral spacing) and we tried to use those two parameters.

Wallace:

Together with the assumption that the flow is being driven by something above the wall layer?

Hanratty:

Right. So, as I said, I think the theoretical intuition that we put into the problem is that this is just a consequence of an oscillation in the outer flow. Now what causes that oscillation, I don't know. That is, what causes the microscale of turbulence (which is a measure of the zero crossings) to be whatever number it is at, say, a y^+ at 45. That would be the question. I don't know the answer.

Landahl:

What did your boundary condition on the upper edge of the wall layer mean as regards to the pressure? I didn't see the pressure in the boundary condition. I guess that's zero, isn't it?

Hanratty:

I don't know what the implication of the pressure up there would be. That didn't enter in because we assumed no pressure variations in the direction of the mean flow, because of the homogenity. So the only pressure variations would be in the y and z direction and we never directly cal-

culated them. We just eliminated pressure between the v and w momentum equations and never really looked at the implications of the upper boundary conditions with reference to pressure. So I can't answer your question.

Landahl:

So you cannot tell what the pressure corresponding to that boundary condition would be?

Hanratty:

No, I can't answer that question.

Brodkey:

When you're calculating v and w , you then put them into the u equation. You can then calculate u, but you must have a boundary condition on u at the outer edge!

Hanratty:

Right. I did go through that rather rapidly. We just used the notion of a well-mixed layer. We used whatever the average velocity a person would measure for a turbulent flow at y_o, that is at a y^+ of 35 or 40.

Brodkey:

So, basically then, you just have three constants: y_o , x^+, and the bursting time to select?

Hanratty:

Yes. It's an oversimplification in the sense that we're assuming a complete coherent structure and then a wall-mixed outer region. Now, obviously that isn't what you really have.

Reynolds:

I note that there was no pressure-strain term (pdu/dx) in your equation, which is a very important term.

Hanratty:

That's true, since du/dx is zero. I think that one of the real weaknesses of the model is this assumption of homogenity in the x direction. That would be the next step if you wanted to play further with this type of analysis. However, I think there are so many features that come out, even with the homogenity assumption, that are qualitatively and semi-quanitatively in agreement with what people observe, both visually and quantitatively, that it's worth thinking about anyway.

THE ROLE OF OUTER FLOW COHERENT MOTIONS IN THE PRODUCTION OF TURBULENCE NEAR A WALL

R.E. Falco

Department of Mechanical Engineering

Michigan State University

ABSTRACT

Experiments showed that in the sublayer of a turbulent boundary layer a double structure exists; the well-known long streaky structure, and a much more energetic flow module which at some point in its evolution appears as a short streak pair which is joined to form an upstream apex. These flow modules are called pockets. An experiment was performed in which the formation of pockets in a laminar boundary layer being buffeted by a wake was studied using combined simultaneous visual/hot-wire anemometry. The results showed that a sequence of events which very closely resembles both the bursting sequence (see Kline, in this symposium) and the sweep event, is associated with the occurence of pocket flow modules. Since the boundary layer was a two-dimensional laminar boundary layer, no streamwise vorticity was present to produce low speed streaks, and thus neither the streaks nor the concurrent inflectionary velocity profiles were factors in the process.

1. INTRODUCTION

This paper describes an experiment whose purpose is to isolate a mechanism which appears to be associated with the production of turbulence near a wall under a turbulent boundary layer. The experiment was inspired by the correspondence between observations of a flow module which appeared in several transitional flows, and descriptions of the turbulence production process (Offen and Kline (1973; 1975), and Corino and Brodkey (1969), as well as papers in this symposium). This flow module appears to be the footprint on a wall of a Typical Eddy flow module described by Falco (1977). The suggestion that a direct interaction between a vortical outer layer flow module and the wall could lead to the lift up, oscillation and breakdown phases of the wall layer bursting process has already been made by Offen and Kline (1973) and Nychas,

Hershey and Brodkey (1973). The length scales of the outer layer vortices are roughly 100 wall layer units, which corresponds to the Typical Eddy flow module scale (see Falco 1977). These facts combined with the fact that the average spacing of the streaky structure in the sublayer is approximately 100 wall layer units, led to an experiment in which movies were taken with a plane of light which was parallel to the wall and in the sublayer of a fully developed turbulent boundary layer into which oil fog "smoke" had been introduced more than 50 boundary layer thicknesses upstream. It was found that flow features in the sublayer were more clearly visible (because of higher contrast) just after the smoke which fills the boundary layer was turned off. Turning the smoke off resulted in a period in which there was a significant amount of smoke in the sublayer, but very little in the outer part of the boundary layer, because the higher velocities in the outer part of the layer convect the smoke in that region downstream faster. Under these conditions the streaky structure was clearly observed, but more careful observation showed that there is a double structure in the sublayer consisting of short rapidly evolving streaks, which come in pairs and appear to be joined together at an upstream apex, (see Figure 1) and a longer streaky structure. The former flow module appears as a "pocket". (The forms taken during the evolution of the flow module can also be seen in figures 2, 3, 6 and 8; figure 6 should be studied first for orientation.) The streak pairs which formed the sides of the pockets were spaced approximately 100 viscous lengths. When this was discovered, old hydrogen bubble photos of the sublayer flow taken by Runstadler, Kline and Reynolds (1963) were examined, and with hindsight, the pockets are clearly visible and are seen to comprise a significant fraction of the streaks they counted. The formation of a pocket consisted of a "hole" (region in which there was no smoke) forming in the smoke filled sublayer which very quickly grew into the pocket shape. The movies showed pockets forming in between the long streaks as well as right on them with roughly equal frequency. Since the flow in between the long streaks has a more stable instantaneous velocity profile (assuming that streaks are regions of upflow between pairs of streamwise vortices), the formation of the rapidly evolving pockets in between streaks suggested that the current understanding that ejections of sublayer fluid are the result of an instability of the instantaneous inflected velocity profile which results from the upflow between the long streamwise vortices that produce the long streaks might be incomplete or perhaps wrong.

Several questions have been answered which give us a better understanding of these new sublayer observations. The ones addressed are: Is a pocket the response to a disturbance from the outer layers? If so, what was the scale of the disturbance, and was a highly vortical disturbance required? If the transport of outer layer fluid was not directly involved, what role did streamwise vorticity observed at the edge of the sublayer play? What role did the long low-speed sublayer streaks play? Was significant Reynolds stress associated with the formation and evolution of a pocket? Was the bursting sequence, as described by Kline in this symposium associated with pocket flow modules? And finally, do velocity and instantaneous Reynolds stress signatures agree with those found by other investigators of the bursting process.

Several transitional flows were investigated in the hope that as

many variables as possible could be kept fixed. From previous experiments (Falco, unpublished) it was known that pockets were present in the laminar boundary layer before the leading edge of turbulent spots (see figure 2) and in the nonlinear stages of natural transition (see figure 3). Furthermore, pockets were also observed in a smoke marked laminar boundary layer being buffeted by the wake of a two-dimensional cylinder placed several boundary layer thicknesses above the layer.

It was decided that buffeting a two-dimensional laminar boundary layer with a turbulent wake that was two-dimensional in the mean had a lot in common with the interactions between the viscous sublayer and the outer region flow in a fully turbulent boundary layer. Since it is known that the outer flow of a fully turbulent boundary layer has a "wake like" mean velocity profile, if forcing from the outer region was the cause of the pockets, assuming they marked the regions of high turbulence production, similar flow modules should appear in a laminar boundary layer being buffeted by a turbulent wake, which then undergoes transition to turbulence. This transition is observed to occur at any spanwise location immediately after a pocket forms. Komoda (1967) has extensively studied similar wake/laminar boundary layer interacting flows and also concluded that transition (the production of turbulence) resulted from the creation of flow modules that, with hindsight, resemble pockets (rather than from the classical Tollmien-Schlichting wave breakdown).

2. WAKE/WALL INTERACTION EXPERIMENTS

Experiments were performed in the flow visualization tunnel at Michigan State University which is capable of continuous volume flow marker operation. A laminar boundary layer was formed on the test wall of the tunnel, which is 122 cm wide. The high degree of uniformity and two-dimensionality achieved was demonstrated by the fact that when smoke (see Falco 1977) was injected into the layer, we observed the layer to remain uniform and laminar as it grew over the 7.3 meter test section length at a tunnel velocity of 1.1 meters/sec. A 1.27 cm circular cylinder was placed across the tunnel 4.6 cm above the test wall. Figure 4 shows details of the arrangement, giving all relevant dimensions. An array of 4 hot-wires was placed in the laminar boundary layer (also see figure 4). It consisted of a u-wire near the outer part of the layer, an x-wire near the center of the layer and a u-wire just above the wall. It was hoped that this arrangement would allow us to determine whether sweep (u(+), v(-)) and burst (u(-), v(+)) events were occuring during the pocket flow module evolution; to determine the extent of the wallward moving disturbances which appeared to be associated with the formation of pockets; and to measure the reaction of the fluid closest to the wall. The anemometers used were TSI 1054b, and signals were low pass filtered at 1000Hz. Analog equipment was used through the experiment, except for wire calibrations, which used algorithms written by Foss (unpublished). Two types of experiments were performed. The first consisted of marking the laminar boundary layer with smoke and not marking the turbulent wake, so that a camera located on the top of the tunnel could look through the cylinder wake and record the disturbances produced in the laminar boundary layer beneath it which were illuminated with general lighting. Both visual, and combined simultaneous visual/hot-wire experiments were performed of this type. In the later, four hot-wire signals, u(wall), u(x-wire), uv

and u(1.75 cm) were displayed on a storage scope and simultaneously recorded. (This data was reduced by hand, although we now have a semiautomated digital data acquisition system).

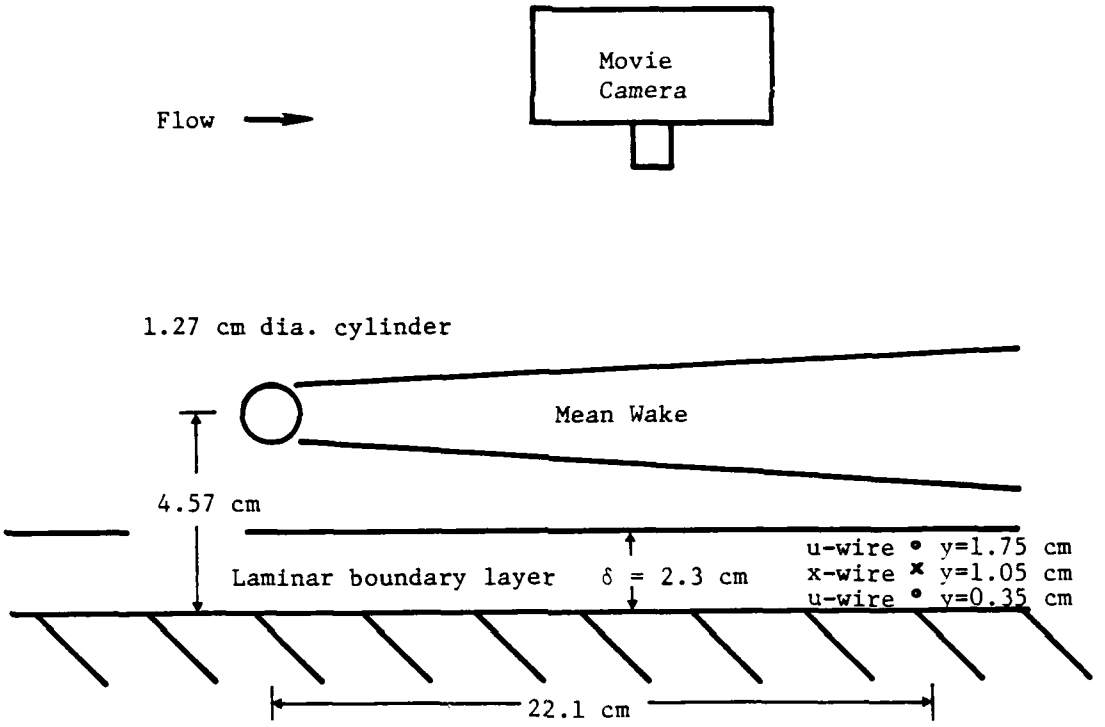

Figure 4. Schematic of the turbulent wake/laminar boundary layer interaction. Note placement of four wire array.

The second type of experiment involves recording visual data in two mutually orthogonal sheets of light. These were produced by splitting the output of a 10 watt argon ion laser and redirecting the light by suitably placed mirrors and scanners. The sheets were approximately 3mm wide. The light scattered from the smoke particles in the sheets was oriented to a single pin registered camera via two systems of mirrors and prisms. A split-field view was obtained which allowed us to observe both the evolving patterns in the laminar boundary layer and, by simultaneously oozing smoke into the wake of the cylinder, to observe the excursions in the wake which were associated with them.

A low cylinder Reynolds number was chosen so that the Typical Eddies generated in the wake would be of a scale large enough that the wire array did not seriously effect the expected interaction event with the wall. The wake Reynolds number (R_D) was 770. This is high enough to be fully turbulent, and indeed several detailed turbulent structure experiments have been performed at even lower R_D (see, for example, Hinze 1975). At

this Reynolds number, vortices could be observed to shed alternately from the cylinder, some staying coherent for several cylinder diameters. The Strouhal period was .067 sec, and the time between successive frames was set at .018 sec.

3. OVERALL FLOW MEASUREMENTS AND VISUAL RESULTS

Figure 5 shows the velocity profile before the cylinder was put in place (it is offset for convenient comparison) and the velocity profile and turbulent intensity profile with the cylinder in place 22.1 cm upstream of the measurement location and 4.6 cm above the approximately 2.3 cm thick boundary layer.

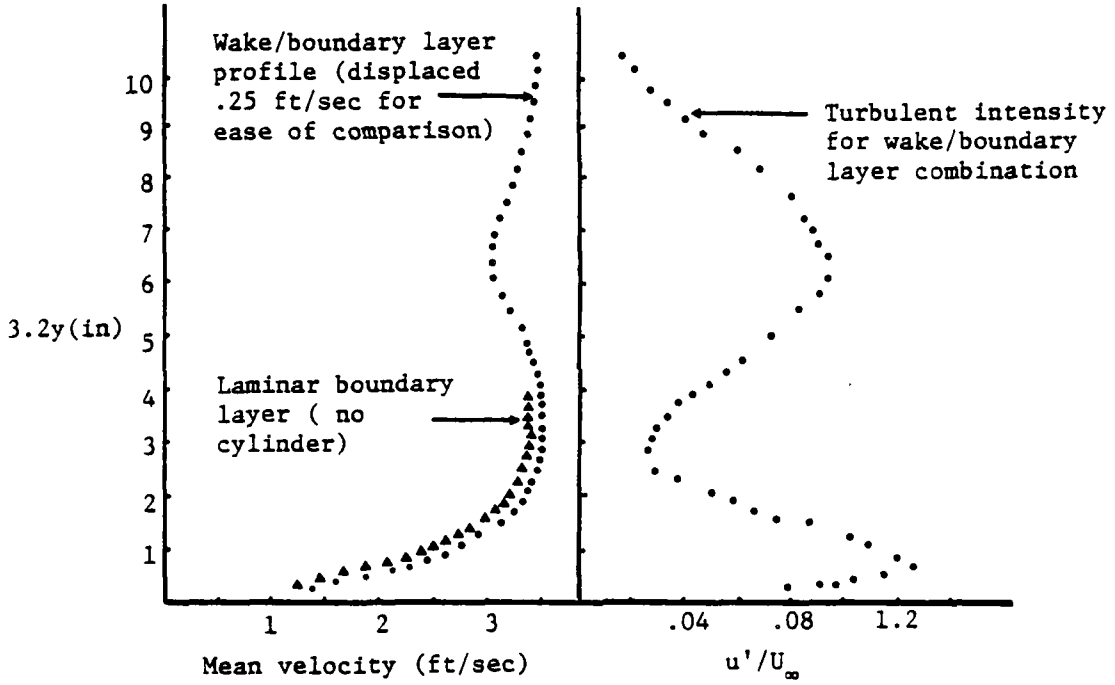

Figure 5. Mean velocity profiles, with and without the cylinder in place (they are displaced for ease of comparison), and the turbulent intensity profile with the cylinder in place (see figure 4 for geometry).

It is interesting to note that although a turbulence intensity of more than 12% is measured at this station, which is just upstream of the position of intersection of the mean wake and the laminar boundary layer, the mean velocity profile in the boundary layer appears to be remarkably Blasius (this was also found to be true when they were compared on a displacement thickness basis). Figure 6 is an enlargement from a 16 mm movie showing the evolution of a pocket flow module resulting from the turbulent wake/laminar boundary layer interaction. (No smoke is being released from the cylinder). An important aspect to be noted in these pictures is that the laminar boundary layer appears to be uniform for several cylinder diameters downstream of the cylinder. From movies of this type it was

discovered that although the wake excites the laminar boundary layer with a continuous range of scales, the laminar layer appears to be least stable with respect to a surprisingly narrow range of wavenumbers of the forcing spectrum, resulting in the narrow range of scales of the pocket flow module and the remarkably similar evolution of each pocket. These observations were made both several boundary layer thicknesses before the mean position of intersection and as far downstream as the illumination permitted. Furthermore, the scale of the pocket decreased as the cylinder Reynolds number increased. This behavior suggests that it is not the large scale eddies interacting with the laminar boundary layer that are responsible for the pockets, but Reynolds number dependent coherent motions (for example, Typical Eddies). It was also interesting to note that no visual indication of shedding at the Strouhal frequency was observable in the smoke marked boundary layer.

The crossed light sheet visual information allowed a direct correspondence between the wake flow and the boundary layer disturbances to be made. Figure 7 shows a sketch of a sequence of three split-field frames, in which a pocket flow module formed at the intersection of the two mutually perpendicular light planes. The sketch is a blowup of the interaction event captured in the photographic sequence shown in figure 8. The sketches of figure 7 actually depict events between frames 8a and 8b. The following description will be keyed to the photos in figure 8, but it is expected that the sketches will be needed to make the photos more easily comprehensible. Little effort was expended to obtain high quality records because of the preliminary nature of the experiment but the essential information can be seen. The first frame of figure 8 (8a) shows an excursion of wake fluid approaching the wall in the side view (light plane parallel to the flow and normal to the wall). No detail is observable at the corresponding streamwise position in the top view (light plane parallel to the wall and in the laminar boundary layer). In the second frame of figure 8 the module which came from the wake can no longer be seen but an extending tail of smoke marked fluid shows where its remains have been convected to. Immediately upstream of this extending tail we can see a small region of laminar boundary layer fluid, marked by a dense concentration of smoke beginning to lift up. In the top view of this frame, the pocket shaped flow module can be readily seen. It appears that the lift-up/ejection occurs at the downstream end of the pocket. Note that the first and second frames of figure 8 are separated by .1 sec whereas the second and third frames are separated .02 sec. The third frame of figure 8 clearly shows the lift-up/ejection of boundary layer fluid that results.

Restating this sequence of events in current boundary structural language, first we see a sweep approach the wall, the sweep interacts with the wall and a lift-up/ejection of low speed fluid results. The pocket appears to be the footprint of the sweep as it initially approaches and convects over the wall. An interaction then occurs in which the sweep, as initially identified, can no longer be followed and the ejection is seen where the upstream boundary of the sweep would be expected. These visual results answered several questions posed in the introduction. Clearly, the pocket is a response to a disturbance which is convected towards the wall. Typical Eddies appeared in the two instances in which pockets formed precisely at the intersection of the two light planes in our 100 foot roll of film. Several others, portions of which touched the intersection of the light planes (a necessary condition if both views

are to appear) helped to confirm the general sequence, but did not allow classification of the portion of wake fluid approaching the wall. We could state that this process, in which a rapid ejection of wall layer fluid occurs does not depend upon the existence of low-speed streaks. Indeed, the laminar boundary layer from which they emerged appeared to be accurately two-dimensional, and thus no streamwise vorticity was present.

4. SIMULTANEOUS VISUAL/HOT-WIRE DATA

Data from the four wire array was conditionally sampled to the pocket flow modules. The objectives were to confirm the visual impressions, and to quantify the interactions marked by the pockets. It was also hoped that a correspondence could be made between the pocket signatures and signatures of the bursting sequence obtained by Offen and Kline (1973).

Figure 9 shows "typical" tracings of the u(wall), u(x-wire) and uv signals obtained.

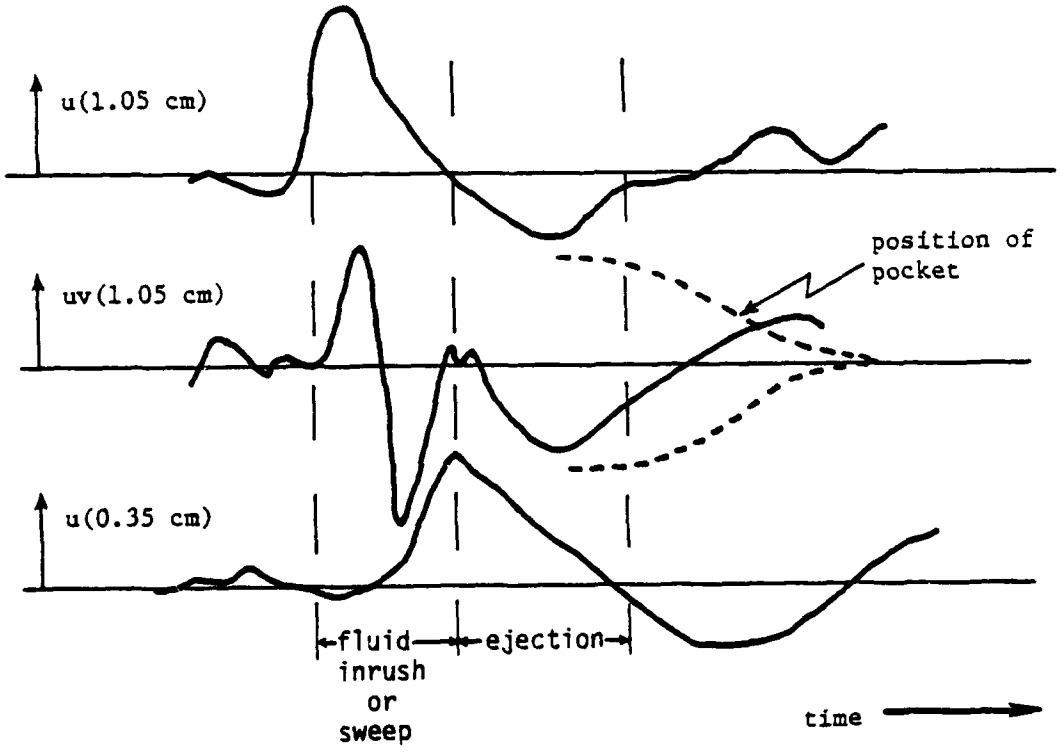

Figure 9. Tracings of simultaneously recorded perturbation velocity signatures from the x-wire and the wall u-wire, conditionally sampled to a fully developed pocket, the outline of which is traced (assuming a Taylor hypothesis).

A sketch of a fully developed pocket has been drawn to indicate the relative position of the signals to the pocket (this is approximate because Taylor's hypothesis does not accurately hold for these events).

Ensemble averages were not formed because when this data was acquired digitization could only be done by hand, but several hundred "hits" were examined. In those "hits" in which the pocket was fully developed and centered with respect to the probe array, u(wall) varied little from the signature of the event traced in figure 9. The streamwise perturbation from the x-wire also showed little variation from that shown in figure 9. The instantaneous Reynolds stress (center signature) always showed two distinct regions of large perturbation phased with respect to the two other signatures as indicated (the regions are bounded by dashed lines). The negative peak at later times, was a consistent feature, however, the shape of the signal in the earlier region of activity was sometimes as indicated, and sometimes completely negative. The streamwise perturbation measured by wire 2, at the top of the array, was not repetitive, and therefore is not shown.

The phasing of these signatures is completely consistent with the visual observations made previously. They indicate that at a given streamwise location a disturbance with high streamwise velocity first passes over the x-wire then over the wall probe. The uv signals indicate that either a vortex is passing over the probes or a wallward moving flow module. This corresponds to the sweep event. This is followed by the ejection of boundary layer fluid which results in u(-) and v(+) at the x-wire. Although the layers closer to the wall respond to this, there is a well defined lag. The ejection occurs at the downstream end of the pocket as indicated previously from the crossed light sheet experiments. Both the sweep and ejection result in significant uv contributions. The fact that the wire furthest from the wall did not have a signal which was well correlated with the others suggests that the length scale of the sweep event is the order of 1.6 cm or less in the direction normal to the wall. Furthermore, measurements of the pockets indicated that the average streamwise length (from apex to downstream end of the "legs") is 3.89 cm and the average width was 2.13 cm. Combining these signatures with the visual information discussed earlier, it is clear that the flow module which approaches the wall interacts with the wall in a manner which results in the ejection of boundary layer fluid, the fully developed pocket representing a pointer which locates the events. However, the pocket also locates the position where significant interaction between the wall and the outer region flow module was initiated. The discrepancy between the center of the pocket and the measured positions of uv peaks simply reflects the fact that the outer region flow module is convecting faster than the wall layer fluid and that the interaction takes a finite time before concluding in an ejection. Both the visual data and the anemometry data suggest that the ejection is a direct result of an instability of the boundary layer fluid caused by the interaction of the sweep with the wall. This picture of the pocket as a passive marker is not entirely correct. It has been observed that after the ejection occurs the legs of the pockets, which apparently have a streamwise vorticity component, occasionally spiral up. This aspect of the interaction was not investigated further.

5. DISCUSSION AND CONCLUSIONS

If the ejction discussed above is a part of the bursting process observed over the wall under a turbulent boundary layer, then the representative signatures in figure 9 should have something in common with the ensemble averaged signatures centered around visually identified bursts reported by Offen and Kline (1973). Although quantitative comparisons can't be made, qualitatively the ejection portion of the pocket flow module signatures look remarkably similar to the Offen and Kline signatures, especially with respect to the phasing of the uv peak from the x-wire with the negative slope of the u-wire placed closest to the wall.

Several points remain to be further investigated, and direct measurement in a fully turbulent boundary layer is clearly desirable, but it must be noted that the mechanism of the interaction has not been illuminated by these experiments. One possible explanation was put forth by Falco (1977). It relied upon the viscous instability that vortex rings undergo when they come into contact with a wall. The first steps could be made to verify this hypothesis by measuring the relative vorticity content of the wallward moving flow modules.

It appears that many of the essential features of the turbulence production process are produced when a disturbance from a turbulent wake propagates into a laminar boundary layer. Both visual data and conditionally sampled hot-wire data suggest that the interaction is of the same type as observed to occur in the viscous sublayer. It appears that this interaction does not depend upon the presence of sublayer streaks, longitudinal vorticity or an instability that may result fron an instantaneous inflection in the velocity profile.

6. ACKNOWLEDGEMENTS

It is our pleasure to acknowledge that this work has been supported in part by ONR Fluid Dynamics Program under Contract No. N000 1477 C0348.

7. REFERENCES

Corino, E.R. and Brodkey, R.S., 1969. "A visual investigation of the wall region in turbulent flow." J. Fluid Mech. 37, pp. 1-30.

Falco, R.E., 1977. "Coherent motions in the outer region of turbulent boundary layers." Phys. of Fluids 20, pp. S124-S132.

Hinze, J.O., 1975. Turbulence. McGraw-Hill.

Komoda, H., 1967. "Nonlinear development of disturbance in a laminar boundary layer." Phys. of Fluids 10, pp. S87-S94.

Nychas, S.G., Hershey, H.C. and Brodkey, R.S., 1973. "A visual study of turbulent shear flow." J. Fluid Mech., 61, pp. 513-540.

Offen, G.R. and Kline, S.J., 1973. "Experiments on the velocity characteristics of 'bursts' and on the interactions between inner and outer regions of a turbulent boundary layer." Rep. MD-31, Thermosciences Div., Mech. Engr. Dept., Stanford University.

Offen, G.R. and Kline, S.J., 1975. "A proposed model of the bursting process in turbulent boundary layers." J. Fluid Mech. 70, pp. 209-228.

Runstadler, P.W., Kline, S.J., and Reynolds, W.C., 1963. "An experimental investigation of flow structure of the turbulent boundary layer." Report MD-8, Thermosciences Div., Mech. Engr. Dept., Stanford University.

Figure 1. Streaky structure of the wall region of a turbulent boundary layer visualized using smoke. Note the long streaks and the pocket flow module (located by arrows). Flow is from left to right.

Figure 2. A turbulent spot at $Re_x \approx 4 \times 10^5$. Note the pocket flow modules which form along the leading edges.

Figure 3. A pocket forming downstream of naturally occuring streamwise irregularities growing in a smoke marked laminar boundary layer. This patch of disturbances eventually developed into a spot. Flow is from left to right. This is a negative print.

AD-A100 632 PURDUE RESEARCH FOUNDATION LAFAYETTE IND F/G 20/4
WORKSHOP ON COHERENT STRUCTURE OF TURBULENT BOUNDARY LAYERS.(U)
NOV 78 D E ABBOTT, C R SMITH AFOSR-76-3015

UNCLASSIFIED AFOSR-TR-78-1533 NL

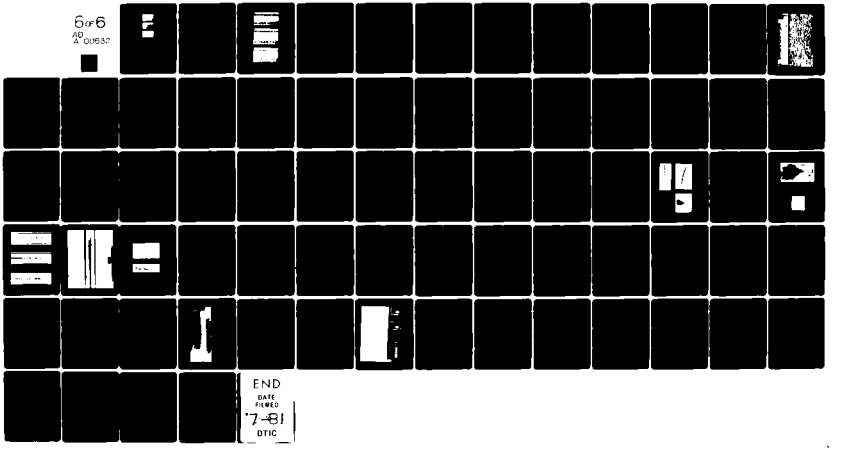

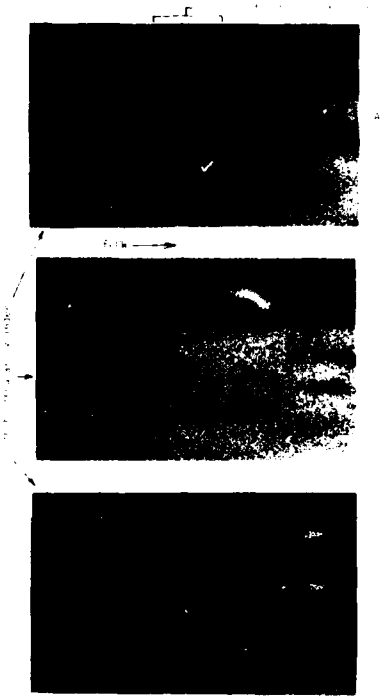

Figure 6. An enlargement from a 16mm movie showing a "pocket" flow module forming in a laminar boundary layer which is being buffeted by the wake from a two-dimensional circular cylinder approximately 2.5 δ above the wall. In this sequence of three frames we see the footprint of a disturbance which has been convected from the wake toward the wall. The lower part of the laminar boundary layer is filled with smoke. In frame A we see the first indication of a disturbance forming in the laminar boundary layer which previously was uniform at this location and at all locations upstream of this position. In frame B this fluid displaces the smoke marked laminar boundary layer fluid. Hot-wire signals recorded when this phase of the event occurs at the probe array indicate that high speed fluid is moving towards the wall. Frame C shows the fully developed pocket form. When events at this stage of evolution passed over the hot-wire array, it was found that low speed fluid was moving away from the wall! By the time the flow module evolves to the condition of frame C it has the appearance of a pair of short streaks. Note that the laminar boundary layer appears to be uniform for several cylinder diameters downstream of the cylinder. For these conditions the direct effect of the cylinder on the laminar boundary layer is small; there is no evidence of separation or streamwise vorticity near the cylinder.

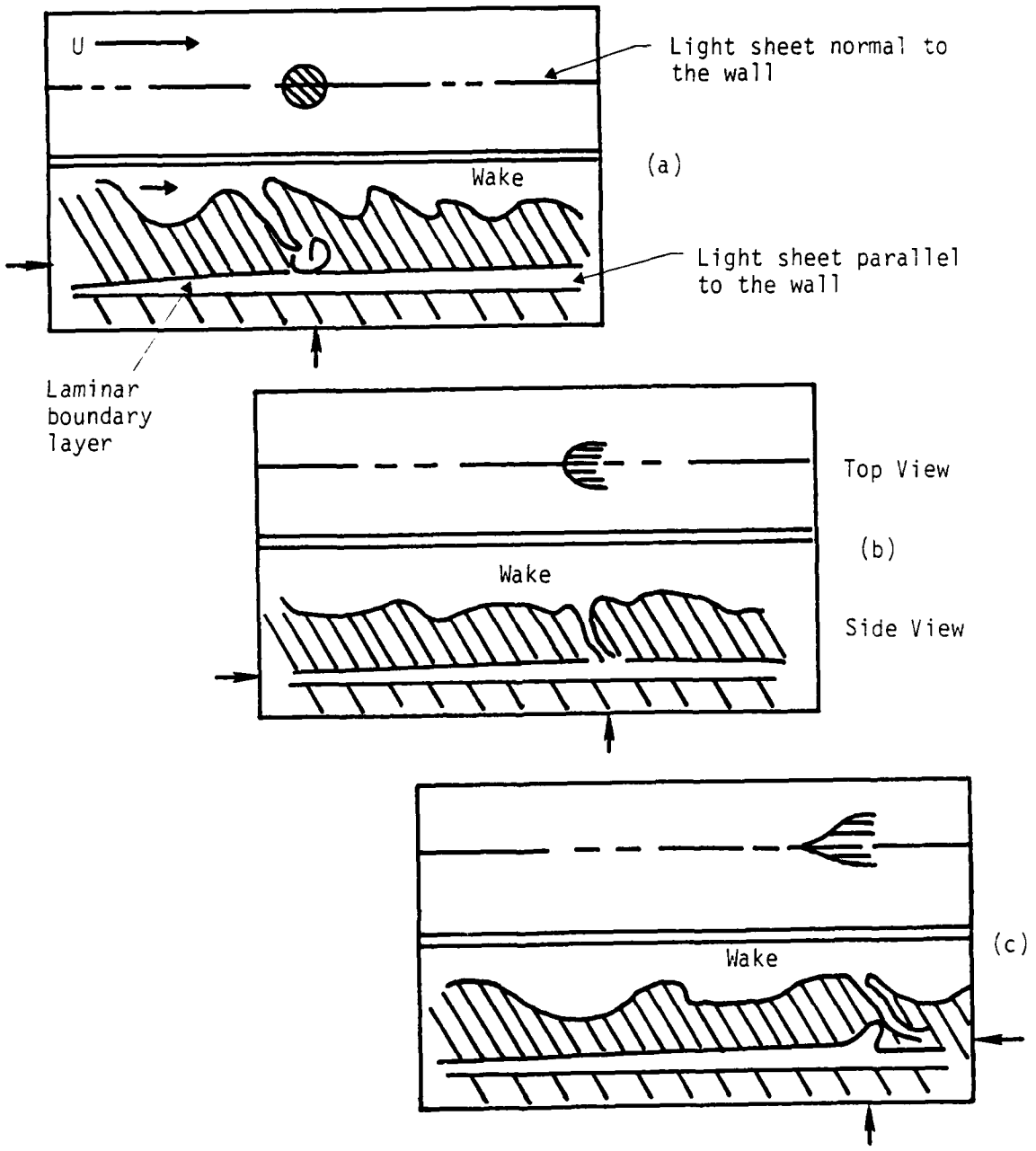

Figure 7. A sequence of three split-field frames showing, in schematic form, an excursion of fluid from the turbulent wake approaching the wall, the creation of a pocket, and the ejection of fluid from the boundary layer.

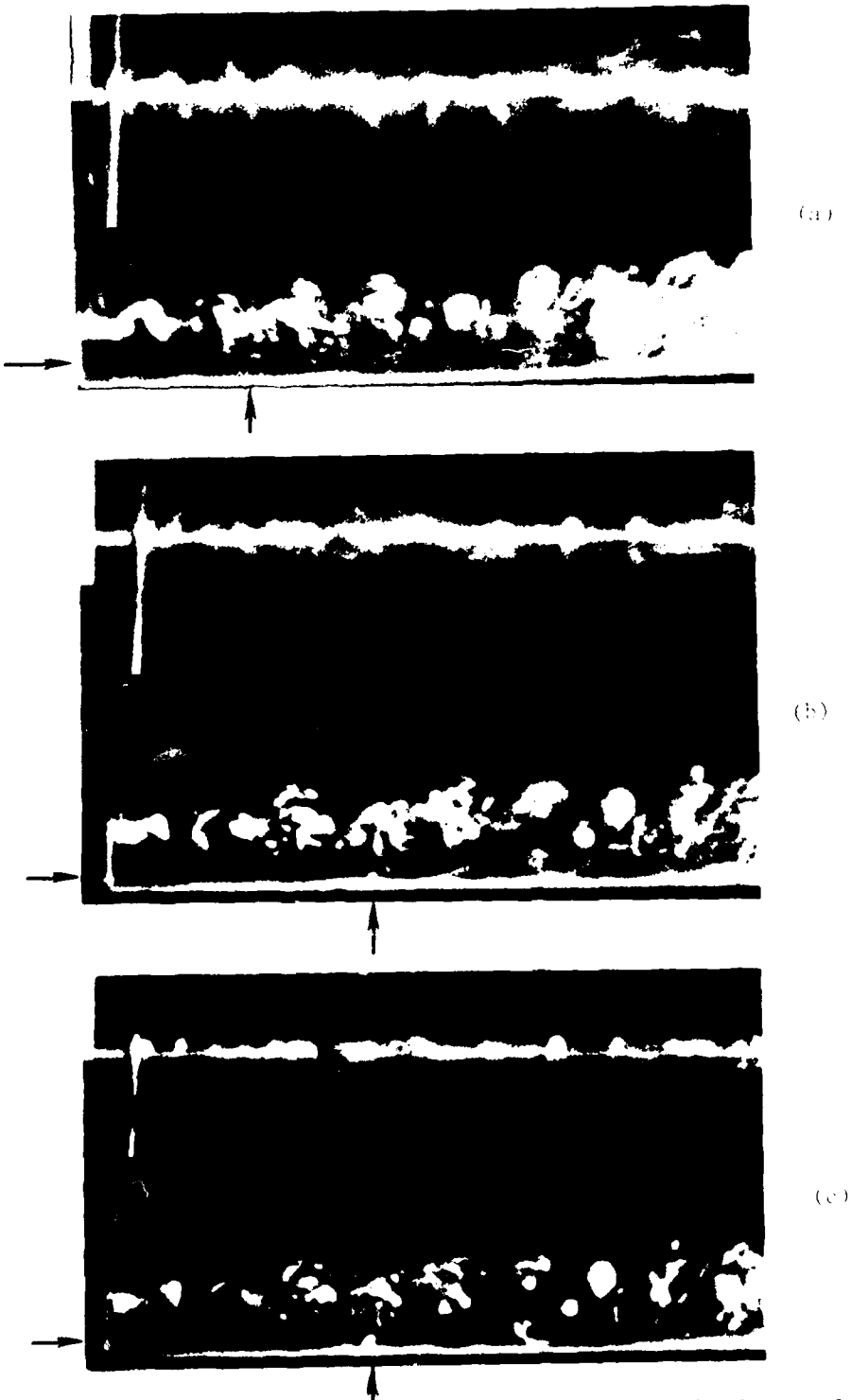

Figure 8. Photographs of a sequence of three split-field frames from a 16mm movie showing an excursion of fluid from the turbulent wake approaching the wall, the creation of a pocket, and the ejection of fluid from the boundary layer. See figure 7 for orientation.

A MODEL FOR FLOW IN THE VISCOUS SUBLAYER

Donald Coles

California Institute of Technology

Pasadena, California

ABSTRACT

A model based on Taylor-Görtler instability is proposed to describe the flow in longitudinal sublayer vortices. Reasonable fidelity is achieved in representing measured velocity fluctuations. The main conclusion is that there are three mechanisms at work in the sublayer. At the wall, the mechanism is purely viscous. Below $y^+ = 15$, approximately, sublayer vortices account for all of the momentum transport by fluctuations, but not for all of the fluctuation energy. Between $y^+ = 15$ and $y^+ = 50$, approximately, the mechanism shifts from transport by sublayer vortices to transport by large eddies in the outer flow. These outer eddies are assumed to drive the Taylor-Görtler instability. The instability, however, is described mostly in terms of its difficulty.

MODEL FLOW

Work on coherent structure in the turbulent boundary layer has come to share with earlier work on similarity laws the notion of outer and inner length scales, say δ and ν/u_τ. I am concerned here only with inner coherent structure, which I take to be the sublayer streaks first documented at Stanford (e.g., Kline et al. 1967). Although my conjecture for some time has been that these streaks are longitudinal counter-rotating vortices resulting from an instability of Taylor-Görtler type, I am not yet able to argue quantitatively for the instability, for the ubiquity of the resulting vortices, or for the mechanisms which maintain (on the average) a constant finite amplitude. I have here a much more limited objective, which is to show that such vortices are compatible with much of what is known about fluctuations in the sublayer.

The model proposed here assumes a finite-amplitude secondary motion similar to the motion resulting from Taylor instability in circular

Couette flow or from Görtler instability in the boundary layer on a curved surface. A similar model was used by Taylor (1932) for a different purpose, to draw some conclusions about pressure fluctuations at a wall from the fluid-motion-microscope observations then being made by Fage and Townend (1932). Roughly speaking, the inner cylinder (the edge of the sublayer) is rotating and the outer cylinder (the wall) is at rest. The gap (the sublayer thickness) is d and the axial (spanwise) wave length is λ. The coordinates are (x,y,z), with x in the general flow direction and y normal to the wall. The velocities are (u,v,w), with $u = \bar{u} + u'$, etc., The overbar indicates an average at constant x and y over one wave length in the z-direction.

Let the flow be steady and independent of x. Then the secondary motion (v', w') is described by a stream function which I represent approximately and heuristically by

$$\psi' = \frac{A}{\pi} \lambda \, u_\tau \left(\frac{y}{d}\right)^2 e^{-4y^2/d^2} \sin(2\pi\frac{z}{\lambda}), \tag{1}$$

where A is a dimensionless constant. The exponent has been scaled to place the vortex center at $y/d = 1/2$; thus

$$v' = \frac{\partial\psi'}{\partial z} = 2A \, u_\tau \left(\frac{y}{d}\right)^2 e^{-4y^2/d^2} \cos(2\pi\frac{z}{\lambda}) \; ; \tag{2}$$

$$w' = - \frac{\partial\psi'}{\partial y} = - \frac{2A}{\pi} \frac{\lambda}{d} u_\tau \frac{y}{d} \left(1 - 4\frac{y^2}{d^2}\right) e^{-4y^2/d^2} \sin(2\pi\frac{z}{\lambda}) \; . \tag{3}$$

I take the remaining component of the secondary motion as

$$u' = - B \, u_\tau \frac{y}{d} e^{-4y^2/d^2} \cos(2\pi\frac{z}{\lambda}) \; . \tag{4}$$

In dimensionless form, the rms fluctuations are

$$u^{+\prime} = \frac{B}{2^{1/2}} \frac{y}{d} e^{-4y^2/d^2}; \tag{5}$$

$$v^{+\prime} = 2^{1/2} A \left(\frac{y}{d}\right)^2 e^{-4y^2/d^2} \; ; \tag{6}$$

$$w^{+\prime} = \frac{2^{1/2}}{\pi} A \frac{\lambda^+}{d^+} \frac{y}{d} \left|1 - 4\frac{y^2}{d^2}\right| e^{-4y^2/d^2}; \tag{7}$$

and the contribution to the stress is

$$\tau^+ = AB \left(\frac{y}{d}\right)^3 e^{-8y^2/d^2} \; , \tag{8}$$

where $u^{+'} = (\overline{u'u'})^{\frac{1}{2}}/u_\tau$, $\tau^+ = -(\overline{u'v'})/u_\tau^2$, $d^+ = u_\tau d/\nu$, $\lambda^+ = u_\tau \lambda/\nu$, etc.

These equations have been designed to have the proper y-dependence to leading order as $y \to 0$. They express $u^{+'}$, etc., as functions of $y^+ = u_\tau y/\nu$ and of four dimensionless parameters, which I take to be d^+, λ^+, and the two (positive) amplitudes A and B. I determine these by the four conditions

(a) $\lambda^+ = 100$;

(b) $u^{+'}/w^{+'} \to 2.75$ as $y^+ \to 0$, from the data of Fortuna and Hanratty (1972) and Py (1973);

(c,d) $\bar{u}^+$ and $d\bar{u}^+/dy^+$ match Spalding's sublayer profile (1961) at the maximum in τ^+.

Conditions (c) and (d) require evaluation of the mean streamwise momentum equation,

$$\tau_w = \rho u_\tau^2 = -\rho\overline{u'v'} + \mu \frac{d\bar{u}}{dy} \quad . \tag{9}$$

Substitution for $\overline{u'v'} \sim \tau^+$ from (8) gives

$$\frac{d\bar{u}^+}{dy^+} = 1 - AB \left(\frac{y}{d}\right)^3 e^{-8y^2/d^2} \quad , \tag{10}$$

and integration gives

$$\bar{u}^+ = y^+ - d^+ \frac{AB}{128} \left\{1 - \left(1 + 8\frac{y^2}{d^2}\right) e^{-8y^2/d^2}\right\} \quad . \tag{11}$$

As mean sublayer profile I take Spalding's implicit formula,

$$y^+ = \bar{u}^+ + e^{-\kappa c} \left\{e^{\kappa\bar{u}^+} - 1 - \kappa\bar{u}^+ - \frac{1}{2}(\kappa\bar{u}^+)^2 - \frac{1}{6}(\kappa\bar{u}^+)^3\right\} \quad , \tag{12}$$

which also has the proper y-dependence to leading order as $y \to 0$. With $\kappa = 0.41$ and $c = 5.0$, the four parameters are found to be

$$\lambda^+ = 100;$$

$$d^+ = 33.7;$$

$$A = 2.76;$$

$$B = 14.3.$$

In the figures below, the distributions for $\bar{u}^+$, $u^{+'}$, τ^+, etc. obtained from this model are shown as dotted lines. The rms fluctuations turn out (as planned) to bear a reasonable resemblance to the eigenfunctions calculated by Smith (1955, second method) for Görtler instability of a

Blasius boundary layer on a curved wall.

EXPERIMENTAL EVIDENCE

A search of the experimental literature has turned up about 50 papers (listed in the adjacent table) which contain information about velocity fluctuations in the sublayer. The information in question is displayed in Figure 1 for the case of the circular pipe, the rectangular channel, and the boundary layer at constant pressure. Large discrepancies are common, and I have therefore indicated by line weights the weight which I give to the data in each instance (this judgment refers only to the circumstances of skill and luck which may have attended the difficult measurements in the sublayer, not to other results of the research in question).

The streamwise fluctuations $u^{+'}$ in Figure 1 usually have a definite maximum at about $y^+ = 15$. Figure 2 shows the value of this maximum plotted against δ^+, where $\delta^+ = u_\tau \delta/\nu$ is based on pipe radius, channel half-width, or estimated boundary-layer thickness. No clear influence of Reynolds number appears in the figure. What does depend on Reynolds number is the value of $u^{+'}$ outside the sublayer (say at $y^+ = 50$), relative to the maximum near $y^+ = 15$. This relative amplitude, shown in Figure 3, appears to increase steadily from about 0.6 for δ^+ near 10^2 to about 0.9 for δ^+ near 10^4.

I also have some experimental evidence of my own. Figure 4 is a photograph taken by Brian Cantwell of the sublayer of a turbulent boundary layer as viewed from below (Cantwell, Coles, and Dimotakis 1978). The visualization technique uses a very dense, almost opaque suspension of aluminum flakes in water. The flow is from right to left. The Reynolds number $u_\infty \theta/\nu$ based on momentum thickness is estimated to be about 1100; the sublayer scale λ^+ (measured by an optical correlation method) is about 85; the depth of view is about 15 in wall units.

The photograph confirms an implicit observation by Kline et al. (1967), that sublayer streaks or vortices are present everywhere beneath a turbulent boundary layer. The photograph also illustrates the mixture of order and disorder which confronts an experimenter or analyst attempting to classify part of the motion in the sublayer as coherent.

Figure 1 (opposite). Collected experimental data for velocity fluctuations and momentum transport in the sublayer. The dotted lines represent the model flow defined by equations (5)-(8), with $\lambda^+ = 100$, $d^+ = 33.7$, $A = 2.76$, and $B = 14.3$. For references and other information about the experiments, see the table.

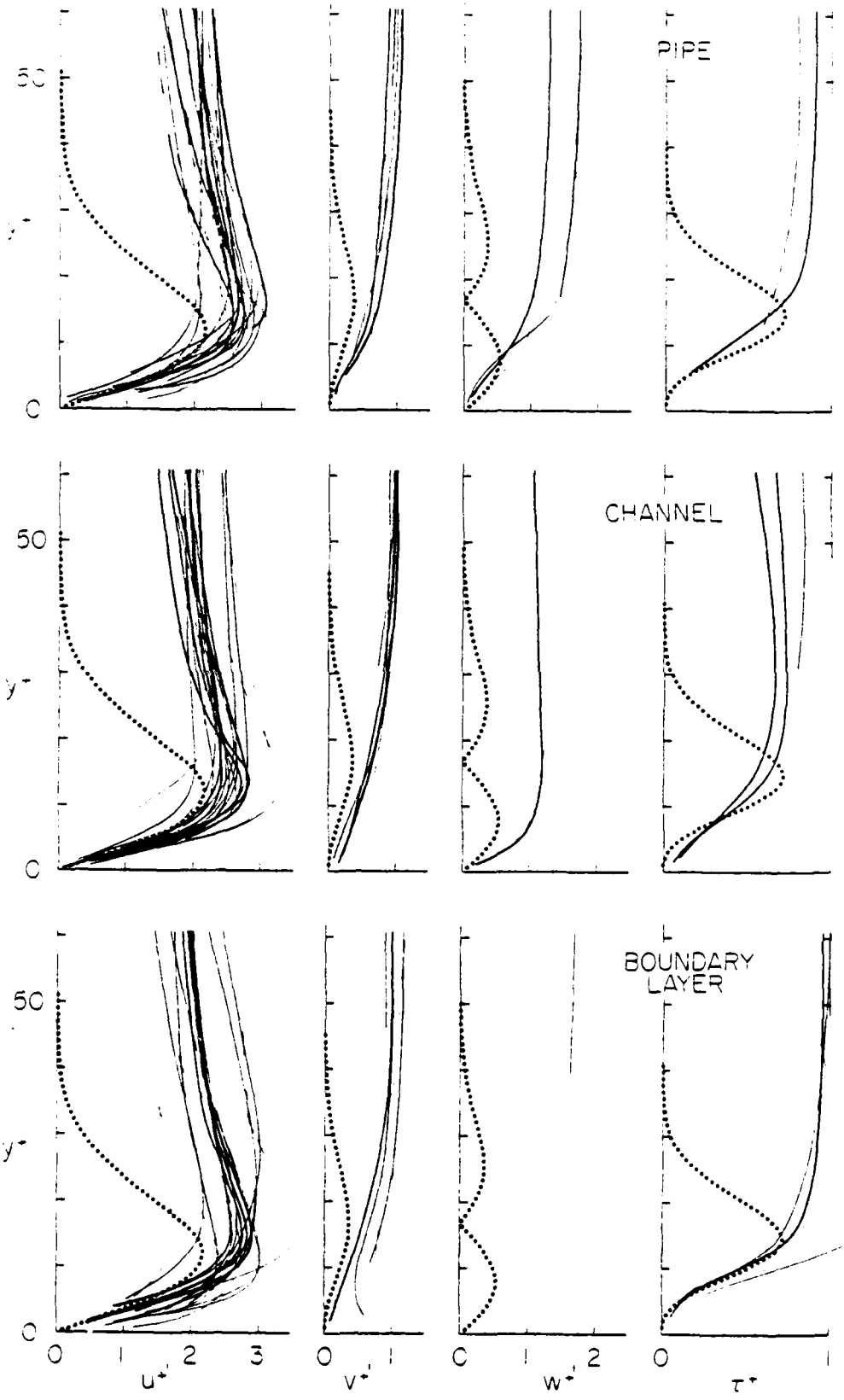
PIPE
CHANNEL
BOUNDARY LAYER
50
0
y^+
0
1
2
3
u^+
0
1
v^+
0
1
2
w^+
0
1
τ^+

COLLECTED EXPERIMENTAL DATA

Author	Date	Reference	Flow
AlSaji	1968	Ph. D. Thesis, Univ. Utah	b. layer
Andersen et al.	1972	Stanford Univ., Rep. HMT-15	b. layer
Bakewell and Lumley	1967	Ph. Fl. 10. 1880	pipe
Blinco and Partheniades	1971	IAHR J. Hydr. Res. 9, 43	flume
Blinco and Sandborn	1973	3rd Rolla Symp., 403	flume
Bogar	1977	Ph. Fl. 20, No. 10/II, S9	b. layer
Bremhorst and Walker	1973	J. Fl. Mech. 61, 173	pipe
Clark	1968	J. Basic Eng. 90D, 455	channel
Coantic	1966	Thesis, Univ. Aix-Marseille	pipe
Comte-Bellot	1965	Pub. Sci. Tech. No. 419	channel
Eckelmann	1974	J. Fl. Mech. 65, 439	channel
Elena	1977	I. J. Heat Mass Tr. 20, 935	pipe
Grass	1971	J. Fl. Mech. 50, 233	flume
Gupta and Kaplan	1972	Ph. Fl. 15, 981	b. layer
Hanjalic and Launder	1972	J. Fl. Mech. 51, 301	channel
Heidrick et al.	1971	2nd Rolla Symp., 149	pipe
Hussain and Reynolds	1975	J. Fluids Eng. 97I, 568	channel
de Iribarne et al.	1969	Ch. Eng. Prog. (S65, 91), 60	pipe
Karpuk and Tiederman	1974	2nd LDV Workshop II, 68	channel
Khabakhpasheva	1968	Heat Mass Tr. in B. L. II, 573	square pipe
Kim et al.	1971	J. Fl. Mech. 50, 133	b. layer
Klebanoff	1954	NACA TN 3178	b. layer
Kreplin	1976	Mitt. MPI/AVA Nr. 63	channel
Kudva and Sesonske	1972	I.J. Heat Mass Tr. 15, 127	pipe
Lau	1977	M. S. Thesis, Univ. Illinois	pipe
Laufer	1950	NACA TN 2123	channel
Laufer	1953	NACA TN 2954	pipe
Liu et al.	1966	Stanford Univ., Rep. MD-15	b. layer
Logan	1973	3rd Rolla Symp., 91	square pipe
Milliat	1957	Pub. Sci. Tech. No. 335	channel
Mizushina and Usui	1977	Ph. Fl. 20, No. 10/II, S100	pipe
Morrison and Kronauer	1969	J. Fl. Mech. 39, 117	pipe
Nicholl	1970	J. Fl. Mech. 40, 361	b. layer
Orlando et al.	1974	Stanford Univ., Rep. HMT-17	b. layer
Patterson et al.	1977	Ph. Fl. 20, No. 10/II, S89	pipe
Pennell et al.	1972	I. J. Heat Mass Tr. 15, 1067	pipe
Perry and Abell	1975	J. Fl. Mech. 67, 257	pipe
Powe and Townes	1971	2nd Rolla Symp., 123	pipe
Reichardt	1938	Naturwiss. 26, 404	channel
Reischman and Tiederman	1975	J. Fl. Mech. 70, 369	channel
Rollin and Seyer	1973	3rd Rolla Symp., 56	pipe
Rudd	1972	J. Fl. Mech. 51, 673	square pipe
Runstadler et al.	1963	Stanford Univ., Rep. MD-8	b. layer
Schildknecht et al.	1975	4th Rolla Symp., 56	pipe
Sherwood et al.	1968	Chem Eng. Sci. 23, 1225	pipe
Smith	1962	Sc. D. Thesis, MIT	b. layer
Ueda and Hinze	1975	J. Fl. Mech. 67, 125	b. layer
Van Thinh	1967	C. R. Acad. Sci. A264, 1150	channel
Weissberg and Berman	1955	Proc. HTFMI (UCLA), Paper 14	pipe

ON FLUCTUATIONS IN THE SUBLAYER

u	v	w	T	δ^+	Technique	Method for u_τ	Remarks
x				780-1020	hot film	Clauser plot	blowing
x				850	hot wire	$-\rho\overline{u'v'} + \mu d\bar{u}/dy$	mass transfer, dp/dx
x				260	hot film	dp/dx?	correlations
x				490-1600	hot film	handbook	roughness
x	x		x	230-1100?	split hot film	$(d\bar{u}/dy)_w$	
x	x		x	4100	hot wire	Clauser plot	joint pdf of u,v
x	x		x	1100	tandem wire	dp/dx?	spectrum of uv
x	x	x		650-1700	hot wire	$(d\bar{u}/dy)_w$	
x				1100-8000	hot wire	dp/dx	
x				2400-8100	hot wire	dp/dx	
x	x		x	140,210	hot film	$(d\bar{u}/dy)_w$	thick sublayer
x				920?	hot wire	dp/dx	heat, mass transfer
x	x		x	420	bubbles	$-\rho\overline{u'v'} + \mu d\bar{u}/dy$	roughness
x	x		x	770	hot wire	Clauser plot	
x				850	hot wire	Stanton tube	one rough wall
x				700-2600	hot film	dp/dx?	
x				650-1500	hot wire	dp/dx	vibrating ribbon
x				160-520	photolysis	$(d\bar{u}/dy)_w$?	
x				220,400	LDV	$(d\bar{u}/dy)_w$	
x	x			200-900?	particles	dp/dx?	polymer
x	x		x	270?	bubbles	Clauser plot	bursting
x	x	x		2300	hot wire	$-\rho\overline{u'v'} + \mu d\bar{u}/dy$	energy balance
x		x		200	hot film	$(d\bar{u}/dy)_w$	thick sublayer
x				180	hot film	dp/dx	heat transfer
x		x		520,850	hot film	dp/dx	polymer
x				520-2300	hot wire	$(d\bar{u}/dy)_w$	energy balance
x	x	x		1100	hot wire	dp/dx	energy balance
x				320	hot wire	Clauser plot	roughness
x	x			570	LDV	dp/dx	polymer
x				910	hot wire	$(d\bar{u}/dy)_w$	diffuser
x				330	LDV	dp/dx	polymer
x				770-3700	hot wire	dp/dx?	cross spectra
x	x			150,220	hot wire	$d\theta/dx$?	stratification
x				490	hot wire	$-\rho\overline{u'v'} + \mu d\bar{u}/dy$	suction, dp/dx
x	x			170-1070	split hot film	dp/dx	polymer
x				110-560	hot film	Blasius law	
x				1600	hot wire	Clauser plot	similarity
x	x	x		4000?	hot wire	dp/dx	roughness
x	x		x	410?	hot wire	dp/dx	
x				300-780	LDV	Clauser plot	polymer
x	x			1100	bubbles	dp/dx	polymer
x		x		320?	LDV	dp/dx	polymer
x				400-900?	hot film	$(d\bar{u}/dy)_w$	flow visualization
x	x		x	500	hot wire	dp/dx	suction
x		x		260-1400	particles	dp/dx	
x				290-870	hot wire	$d\theta/dx$	blowing
x				500,1300	hot wire	$(d\bar{u}/dy)_w$	
x				1700	hot wire	Preston tube	
x				1500-3900	hot wire	dp/dx	suction

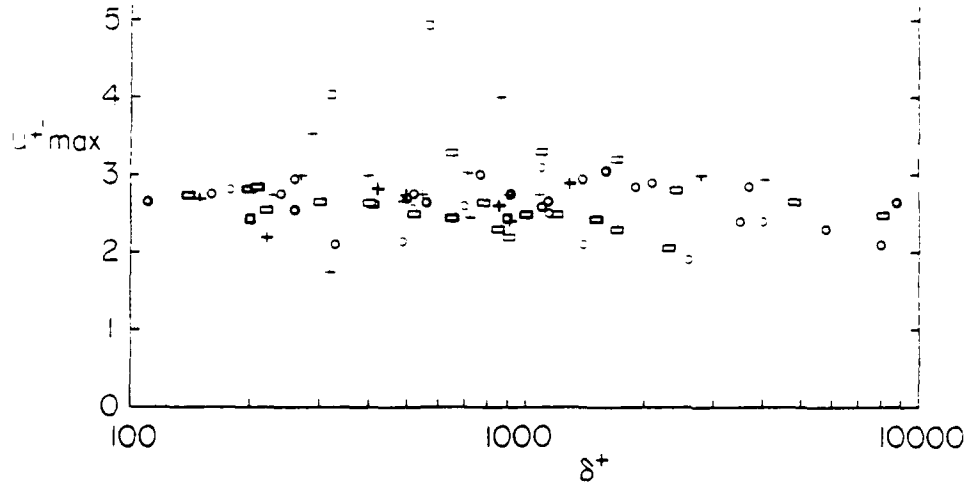

Figure 2. The maximum value of the streamwise fluctuation $u^{+'}$ in the sublayer as measured (usually) at about $y^+ = 15$. Crosses, boundary-layer flow. Rectangles, channel flow. Circles, pipe flow.

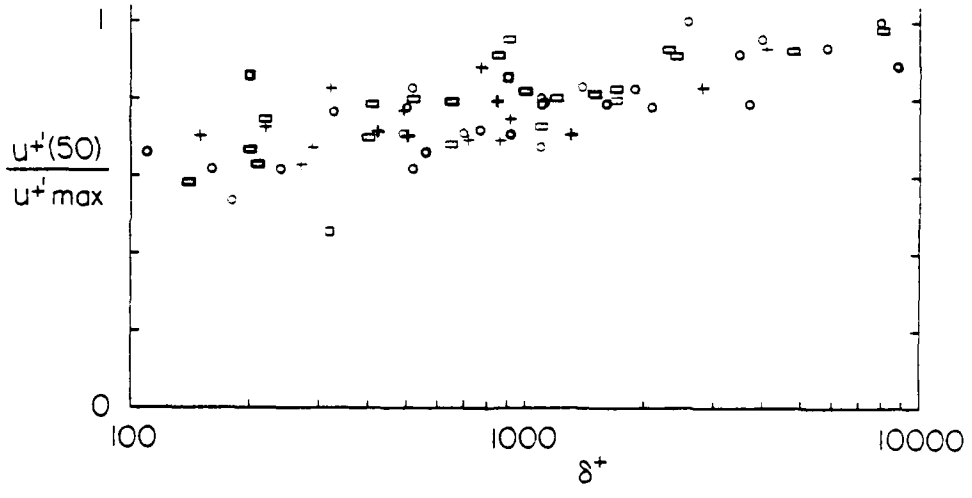

Figure 3. The value of $u^{+'}$ at $y^+ = 50$ relative to the maximum value of $u^{+'}$ at about $y^+ = 15$. The symbols are the same as in Figure 2.

Figure 4 (opposite). Visualization of sublayer flow using a dense suspension of aluminum flakes in water (photograph courtesy of B. Cantwell). The flow is from right to left and is viewed horizontally through the vertical glass side wall of a rectangular channel. Only the motion below about $y^+ = 15$ is visible. The sublayer area photographed is about 28 cm by 57 cm. A mirror is mounted above the channel at 45° to include a view of the motion in the free surface.

Figure 4

DISCUSSION

The essence of the present model is expressed by Figure 5. At the left, the mean model profile is compared to Spalding's formula (the solid line) and to its linear and logarithmic asymptotes (the dashed lines). The model flow should only be taken seriously below the matching point at $y^+ = 3^{1/2}\, d^+/4 = 14.6$, because in the model the transport mechanism above this point reverts to a purely viscous one, whereas in the real flow the mechanism must shift to transport by other kinds of fluctuations. In the center of Figure 5, the rms fluctuation $u^{+'}$ for the model is compared to a hypothetical fluctuation profile (the solid line) representing a concensus of the experimental data in Figure 1 for flow at intermediate Reynolds numbers. At the right in Figure 5, the constant total stress is divided into conventional laminar and turbulent components by the solid line, and the turbulent component is further divided into a contribution from sublayer vortices (the dotted line) and from other fluctuations (the dashed line).

The flow visualization in Figure 4 suggests that the model vortices may be energetic enough to encounter a second instability (well known to students of circular Couette flow) which leads to a varicose, doubly-periodic pattern traveling in the direction of the outer flow. The main message of Figure 4, however, is that the model vortices, if they exist, are being rudely knocked about by outer turbulence of larger scales. I therefore see little point at present in exploring the jungle of measured correlations, power spectral densities, and celerities for the sublayer.

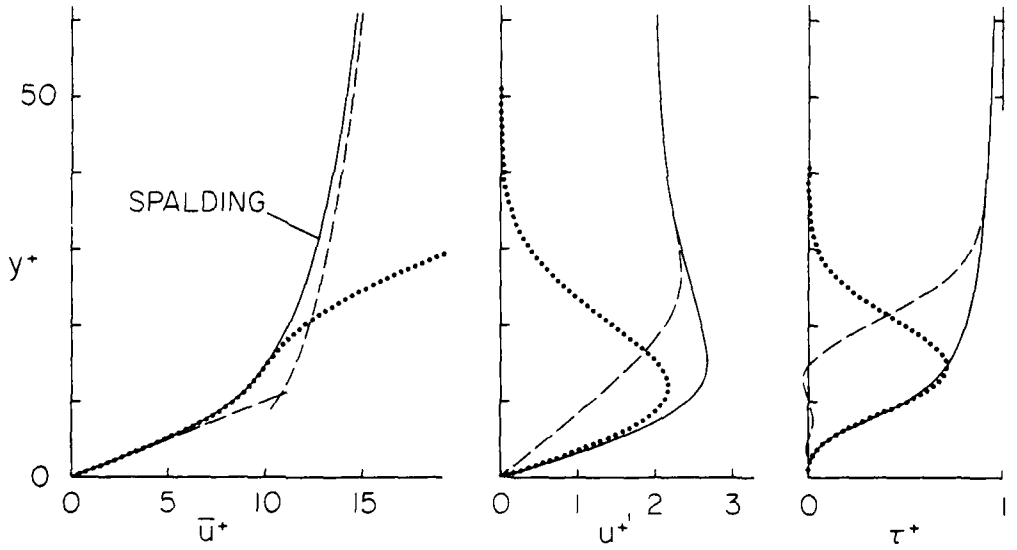

Figure 5. The essence of the sublayer model. At the left, the mean-velocity profile for the model (dotted line) is a good fit to the Spalding profile (solid line) out to about $y^+ = 15$. In the center, the observed fluctuations $u^{+'}$ (solid line) are resolved into a model component (dotted line) and a statistically independent outer component (dashed line). On the right, the shearing stress is similarly resolved.

It is not that I doubt the Reynolds averaged equations of motion; I only doubt that these equations are informative about structure unless used with great caution. Using great caution, I propose to draw one quantitative conclusion from the measured mean and variance of the flow field near the wall.

Note in Figure 5 that τ^+ is fully accounted for by the model out to $y^+ \sim 15$, but $u^{+\prime}$ is not. From Equations (2) and (4), the correlation

$$R = - \frac{\overline{u'v'}}{(\overline{u'u'})^{\frac{1}{2}} (\overline{v'v'})^{\frac{1}{2}}} \tag{13}$$

for the model is identically equal to unity, whereas measurements by Eckelmann (1970) show a nearly constant correlation of 0.4 in the lower part of the sublayer (I am aware that measurements by Kutateladse et al. (1977) dispute this result; I assume for the purposes of the argument which follows that Eckelmann's data are reliable). The discrepancy in correlation seems to be of one piece with a proposal made by Townsend (1961), and later developed by Bradshaw (1967), that flow near a wall can be divided into an active and a passive component. The test is not the fluctuation level but the contribution to momentum transport. A coherent version of this idea therefore suggests itself for application in the lower part of the sublayer.

Suppose that the fluctuations in the lower sublayer have an active part u', v' (given by the model; perfectly correlated; $R' = 1$) and a statistically independent passive part u'', v'' (associated with damping at the wall of outer eddies of larger scale; uncorrelated for $y^+ < 15$; $R'' = 0$). When u' and v' in the definition (13) are replaced by $u' + u''$ and $v' + v''$ and the combined correlation is taken as 0.4, it is found that

$$\left[1 + \frac{(u^{+\prime\prime})^2}{(u^{+\prime})^2}\right]\left[1 + \frac{(v^{+\prime\prime})^2}{(v^{+\prime})^2}\right] = \frac{1}{(0.4)^2} = 6.25 \quad .$$

Given Figure 1, my rough guess as to values which are consistent with this condition is $u^{+\prime\prime} = u^{+\prime}/2$, $v^{+\prime\prime} = 2\, v^{+\prime}$. In other words, about 80 percent of the u-energy (and of the w-energy, pending clarification of condition (b) for the model flow), but only about 20 percent of the v-energy, is accounted for by the model. The dashed curve in the center part of Figure (5), calculated from the difference in variance for the other two curves, seems a reasonable estimate for the contribution of the outer flow to the measured rms fluctuation $u^{+\prime}$, at least for $y^+ < 15$.

The discussion so far is based entirely on the concept of Reynolds averaging, which discards all phase information and thus all structural information. There is ample experimental evidence that fluctuations in the sublayer are bimodal, or at least non-Gaussian, and that the Reynolds stress $-u'v'$ in particular is highly intermittent close to the wall, with a flatness factor many times larger than the Gaussian value of 3 (e.g.,

Gupta and Kaplan 1972). This property must be important for understanding the mechanism which creates and maintains the sublayer vortices.

* Brown and Thomas (1977) favor the Taylor-Görtler instability mechanism and attempt to estimate directly the curvature of mean fluid trajectories. I think this attempt is premature, but I am willing at least to estimate, using properties of the average flow, what curvature is required. Like Brown and Thomas, I take as point of departure my linearized stability criterion $2\bar{\omega}\bar{\zeta} = -\nu^2/L^4$ (Coles 1967). This criterion says that at the stability boundary the mean angular velocity $\bar{\omega}$ and the mean vorticity $\bar{\zeta}$ must have opposite signs, and that the geometric mean of their periods must be of the same order as the diffusion time L^2/ν, where L is some suitable fraction of the vortex scale d. Here I take $\bar{\omega} = \bar{u}_s/r$, with $\bar{u}_s$ a characteristic sublayer velocity (at the matching point, say) and r the unknown mean radius of curvature. From Equation (10), I take $\bar{\zeta} = -(1 - \tau^+_{max})\, u^2_\tau/\nu$. Then the Taylor number can be written

$$T = \left(\frac{d}{L}\right)^4 = 2\left(1 - \tau^+_{max}\right)\bar{u}_s^{\,+}\,\frac{(d^+)^4}{r^+} \quad . \tag{14}$$

Taking $T = T_c = 1708$, $\tau^+_{max} = 0.71$, $\bar{u}_s^{\,+} = 10$, and $d^+ = 33.7$, I obtain the estimate

$$r^+ = \frac{u_\tau r_c}{\nu} = 4400 \quad .$$

In Figure 4, for example, this estimate implies a value for r about eight times larger than the boundary-layer thickness δ.

It is not enough to show that this curvature actually occurs in the sublayer. The maintenance of finite vorticity is almost certainly a non-linear effect. In circular Couette flow, for example, the amplitude A of the secondary motion is governed by the Landau-Stuart equation (e.g., DiPrima and Rogers 1969),

$$\frac{dA}{dt} = \sigma A + \alpha A^3 \quad , \tag{15}$$

---

*At this meeting, Hatziavramidis and Hanratty have proposed a non-linear model in which the longitudinal vorticity in fixed sublayer cells is caused to oscillate in strength and direction by an outer boundary condition which specifies a substantial part of the line integral defining the circulation. As long as this boundary condition is not justified a priori, such a model stands on the same uncertain ground as the model discussed in this paper.

where α is a negative constant. Close to $T = T_c$, the linear amplification factor σ varies like $T - T_c$. For an initial-value calculation with fixed $(T - T_c)$, therefore, the final steady-state amplitude is either $(-\sigma/\alpha)^{\frac{1}{2}}$ or zero. In a real sublayer flow the Taylor number T varies in time and space about a mean value which is manifestly not T_c, but zero. It is therefore implicit in the Taylor-Görtler model that T must not only reach T_c but must exceed it by a very substantial amount during part of each cycle, to overcome the fact that the vortices decay during the remainder of the cycle (one analogy which comes to mind is that of a child pumping a swing). Since dA/dt must also have essentially zero mean, the real issue is the combined effect of excursions in $\bar{\omega}$, $\bar{\varepsilon}$, and L on the local Taylor number T and thus on σ in Equation (15) or in some more relevant equation. Unstable excursions presumably occur when high-speed outer fluid moves close to the wall, over-running and thinning the sublayer and making fluid trajectories locally concave outward over an area large enough in the spanwise direction to include at least several pairs of sublayer vortices. I doubt that this issue can be resolved without a specific model for the large-scale motion in the outer flow. In any event, the non-linear mixed Eulerian-Lagrangian two-timing problem epitomized by Equation (15) is a formidable obstacle to progress.

In summary, to keep the sublayer vortices energized, the Taylor-Görtler instability must occur intermittently. It must involve a close approach to the wall of high-speed eddies which are not necessarily of outer scale, but are probably at least one order of magnitude larger than the sublayer-vortex scale (perhaps the same eddies which are responsible for the success of the mixing-length theory in accounting for the logarithmic mean profile). At large Reynolds numbers, therefore, it is a major difficulty in the Taylor-Görtler model that local instability regions might become numerous in the signature of a single large outer structure. The intensity of the sublayer vortices should be highest at the end of the energizing process. The energizing process itself should be accompanied by a moving local maximum in the stress at the wall, as argued by Brown and Thomas. Such a maximum should be readily detectable by a surface element having a transverse dimension of 90 to 100 in wall units. If this energizing process is what is called bursting, as I believe to be the case, it becomes urgently necessary to consider how the arguments given here should be modified so that bursting can scale on outer rather than inner variables.

Whatever model and mechanism for sublayer vortices may eventually prevail, I expect my conclusion to stand that it is necessary to divide the transport mechanism near the wall into three components, as in Figure 5, rather than two. My own conjecture is that, for some reason, the transport mechanism cannot shift smoothly from bulk or eddy transport in the outer flow to purely viscous transport right at the wall and, at the same time, satisfy the boundary conditions which have to be imposed on the turbulence at the wall. To bridge the gap, nature has invented the sublayer vortex structure. It goes almost without saying that further studies of sublayer structure are best formulated in terms of factors which directly influence this structure, such as roughness, heat transfer, compressibility, mass transfer, longitudinal curvature, and especially the presence of polymer additives.

REFERENCES

Bradshaw, P. 1967 "Inactive" motion and pressure fluctuations in turbulent boundary layers. J. Fluid Mech. 30, 241-258.

Brown, G.L. and Thomas, A.S.W. 1977 Large structure in a turbulent boundary layer. Phys. Fluids 20, No. 10, Part II, S243-S252.

Cantwell, B., Coles, D., and Dimotakis, P. 1978 Structure and entrainment in the plane of symmetry of a turbulent spot. (to appear in J. Fluid Mech.)

Coles, D. 1967 A note on Taylor instability in circular Couette flow. J. Appl. Mech. 34, 529-534.

DiPrima, R.C. and Rogers, E.H. 1969 Computing problems in nonlinear hydrodynamic stability. Phys. Fluids 12, Suppl. II, II/155 - II/165.

Eckelmann, H. 1970 Experimentelle Untersuchungen in einer turbulenten Kanalströmung mit starken viskosen Wandschichten. Mitt. M-PI und AVA, Nr. 48.

Fage, A. and Townend, H.C.H. 1932 An examination of turbulent flow with an ultra-microscope. Proc. Roy. Soc. A135. 656-677.

Fortuna, G. and Hanratty, T.J. 1972 The influence of drag-reducing polymers on turbulence in the viscous sublayer. J. Fluid Mech. 53, 575-586.

Gupta, A.K. and Kaplan, R.E. 1972 Statistical characteristics of Reynolds stress in a turbulent boundary layer. Phys. Fluids 15, 981-985.

Kline, S.J., Reynolds, W.C., Schraub, F.A., and Runstadler, P.W., 1967 The structure of turbulent boundary layers. J. Fluid Mech. 30, 741-773.

Kutateladse, S.S., Khabakhpasheva, E.M., Orlov, V.V., Perepelitsa, B.V., and Mikhailova, E.S. 1977 Experimental investigation of the structure of near-wall turbulence and viscous sublayer. Proc. Symp. on Turbulent Shear Flows, Penn. State Univ., 17.13 - 17.22.

Py, B. 1973 Étude tridimensionnelle de la sous-couche visqueuse dans un veine rectangulaire par les mésures de transfert de matiére en paroi. Int. J. Heat Mass Transf. 16, 129-144.

Smith, A.M.O. 1955 On the growth of Taylor-Görtler vortices along highly concave walls. Quart.Appl. Math. 13, 233-262.

Spalding, D.B. 1961 A single formula for the "law of the wall". J. Appl. Mech. 28, 455-457.

Taylor, G.I. 1932 Note on the distribution of turbulent velocities in a fluid near a solid wall. Proc. Roy. Soc. A135, 678-684.

Townsend, A.A. 1961 Equilibrium layers and wall turbulence. J. Fluid Mech. 11, 97-120.

SESSION V(A)

COMMITTEE REPORTS

Session Chairman:

Douglas E. Abbott

AD HOC COMMITTEE REPORTS

COMMITTEE 1

Question: WHICH EQUATIONS OF MOTION ARE SUITABLE FOR PREDICTION OF COHERENT STRUCTURE?

Spokesman: ELI RESHOTKO

During a lunch meeting of our committee there was universal agreement contrary to the remarks of Hans Mark. We agreed completely that the Navier-Stokes equations are the proper fundamental equations for our investigation, and that since we are looking at scales that are many times mean free paths we do not expect to encounter phenomena that would require a higher order set of equations. We also agree that to the best of our knowledge, no information on turbulence which is useful to us, has been obtained from kinetic theory, at this point.

A question was raised as to whether boundary layer equations were adequate for certain kinds of description. If you think of the boundary layer equations as stretching one dimension to get detail on viscous effects, then that already puts a preferred direction into a calculation, namely the direction normal to a wall. If, in conjunction with turbulence studies, one finds that there are small scale features which are aligned in such a manner that the scales are not necessarily normal to the wall, then there are other directions for which the viscous effects must be included. Eventually you are driven to the Navier-Stokes equations if you want to introduce viscous effects on structure which is evolving rapidly in directions other than normal to the wall. So that as long as there is a preferred direction, i.e. if you're phenomenon is elongated in the streamwise direction near the wall, then perhaps the boundary layer equation will suffice. But if you have small scale features which require resolution, then you probably have to go to Navier-Stokes equations. These comments were motivated by Dave Walker's work where it looked like fronts were developing which were steep in a non-normal direction to the wall, and which could be better resolved using Navier-Stokes equations.

Our discussion was not meant to be necessarily practical, but only to explore what are probably the most appropriate sets of equations. For example, it may not be practical for Dave Walker to do calculations using the Navier-Stokes equations, but we only wanted to point out that better resolution for his phenomenon might be obtained using the Navier-Stokes equations.

The Committee was formed in response to Martin Landahl's presentation in order to attempt to decide which equations he was solving and what was relevant. Landahl's method essentially involves boundary layer equations. In fact, he is looking at an inviscid stability equation that is entirely contained within unsteady boundary layer considerations. Our intrepretation is that this approach could predict the general shape of a phenomena as long as small scales are not involved. However, once you want to obtain small scale details on velocities and pressure fluctuations, then you again have to resort to a Navier-Stokes formulation or derivative thereof, including all the longitudinal variables.

COMMITTEE 2

Question: WHAT IS UNIVERSALLY UNDERSTOOD REGARDING TURBULENT SPOTS?

Spokesman: C.W. VAN ATTA

Our committee met two or three times over the past two days. There was a rather small group, about five or six usually, and the main combatants were Donald Coles, Bob Falco, and Israel Wygnanski, in alphabetical order. The main kibbitzers were myself, Mark Morokovin and a couple of other people. Our discussions can be broken down into two areas: 1) The things we agreed on, and 2) What we decided were interesting things to look at. This latter point led immediately to a series of experiments that should be done, which was probably the main contribution of the committee.

What do we agree on? We agree that we do not know what causes spots to grow linearly which leads to a number of interesting possible experiments to carry out which I will get to in the last part of the report. There was general agreement that the mean velocity profiles which are measured in the middle of single spots, in the tandem spots, and in Cole's synthetic boundary layer seem to look very much like that of a fully developed turbulent boundary layer. In addition, many of the correlations appear similar to the boundary layer as well. And as the spot goes by, a lot of the main features of the flow field look similar to what you might see in the bulges. This has been well discussed in the literature already so I won't go into any details on that.

The vortex, if it exists, is very flattened and elongated in the x direction. As Wygnanski pointed out yesterday, this means that it probably turns over maybe once or twice at most during its entire lifetime. It's a very weak, flattened motion, It doesn't appear that way in most of the common methods of presentation which employ non-linear or non-symmetric axes, but the vortex is actually very flat.

One important conclusion we reached last night was that the CCD picture (the Cantwell-Coles-Dimotakas picture) [See discussion of Walker paper, Ed.] is inconsistent with rapid transport away from the wall. In dye pictures and in aluminum pigment pictures, fluid appears to move up and away from the wall very quickly. Let me just refresh you on what is observed by CCD. Now the main entrainment is at the back of the spot, but if you observe the mean stream lines in the CCD spot, there is no way that the fluid can get rapidly out into the main body of the spot. This is because the fluctuations in the spot are on the same order as the total velocity difference from the boundary to the main stream. And these fluctuations are the things which really transport the momentum very quickly. However, when you draw the mean streamlines from an ensemble average, you don't see the fluctuations and you get the false impression that everything is nicely organized the way it appears in the CCD spot. What do you do to retain the information regarding fluctuations leads to a number of other experiments which I'll discuss in a moment.

What the above discussion leads to are important experiments which need to be done. Bob Falco suggested we add the hair back onto the vortex. Don (Coles) called it a hairy vortex a couple of years ago and proceeded to denude it into the CCD spot, removing all the hair so it's a bald vortex. How to put the hair, i.e. it's transport mechanisms, back on it, is not really clear. One way would be to try to examine the Reynolds stress field throughout the spot, and it's not clear how to do that. Wygnanski doesn't like the idea of determining fluctuations by means of ensemble averaging, and I guess that's why no fluctuation data appear in his papers. So how do you define the Reynolds stress field, and the transport field in the spot and relative to what?

The next experiments that were suggested are connected with the way the spot grows. We don't know why it grows the way it does, so we should try to place some external conditions on the spot which will make it grow differently. We should make these as strong as possible and try to force the spot into another mode, which it may like or dislike. Several possible experiments which would examine a spot in a negative pressure gradient were suggested. The first was to examine what would happen to a spot in a boundary layer subject to a negative pressure gradient. Perhaps this spot could be kept invariant in size in one direction or another. Now, to keep it invariant in size, another possibility might be to use a wedge flow with the boundary layer thinning because of a favorable pressure gradient. What will the spot do? Will it get smaller in the axial direction? And

what will it do laterally if it does that and so on? It is interesting to speculate on. Those then are two pressure gradient type experiments.

Wygnanski pointed out that there is a lot of information about puffs in three-dimensions in pipe flows and there's a lot of information about spots in three-dimensions in boundary layers. He suggested that an intermediate type of experiment be performed where you have essentially a puff with two-dimensional boundary conditions between two parrallel walls. Thus, this third type of experiment would try to bridge that gap in our understanding.

A fourth experiment is closely related to the third, and is an examination of a two-dimensional spot in a laminar boundary layer, which Don Coles has been talking about for a year or two. Coles found one accidentally and he feels he could possibly generate one artificially. When Coles fired off his little disturbance generators all at the same time, he found one spot which traveled down the plate and grew as a two-dimensional spot. It is turbulent in the spot and it would be very interesting to examine the stream-lines within the spot. It would remove the mean three-dimensionality in an ensemble sense and that might help in developing some understanding.

Then there are a whole group of experiments that would be possible on spot interactions. There is general disagreement with the idea of Elder that the spots don't interact strongly, because several people have already observed a number of times that when the spots get close together they do influence each other. They don't just grow linerally right into each other. The boundaries start to pull back and they behave differently in a crowd. You can interact spots in many ways. You can build a cross-beam experiment like a nuclear physicist would do or you can do it in a more general fluid mechanical way. I just think I'll leave it at that, interacting spots.

Another area that is somewhat different - say experiment number 6 - would be to examine the effects of additives on spots, and that's obviously connected with ideas on drag reduction. Apparently work is beginning on this, but I haven't seen any results yet. These experiments should be done in a boundary layer, but not on a thin water table because the spots look different in a thin water table. The experiments could probably be done in air, by adding something to the air - dusty gas or whatever. Something should be done in an air boundary layer, on a water table, and in a pipe flow.

Experiment number 7 is to redo the Gastor-Grant experiment, but carry it out for a longer time. They put in a small disturbance which produced beautiful waves which were mapped. The waves were two-dimensional, but they weren't followed very far, and they weren't followed long enough to see a spot form. Recently, Amini in Grenoble has done a very similar experiment, but he pushed it a little too hard and the spot formed a little too soon, so he didn't see all the intervening waves. It would be good to do this experiment over again and to get the full picture for the long development time.

I added one of my own ideas on experiments which we didn't talk about. The general focus would be the wave field around the spots. There are waves behind, and there are probably waves underneath the spot near the front. The waves behind have been seen now by three people that I know of. Kaplan being the first, Wygnanski, and Hertenes. Amini saw them in his work and I saw them recently in a heated spot within a heated laminar boundary layer where they're very strong. So the general idea would be to examine the waves, how important are they, and what they do.

Discussion

Morkovin:

First of all, I think it's not too difficult to twist Gastor's arm a little bit and I am willing to undertake the job when I visit him in October. He does have the experiment going again in London with considerably more detail and more accuracy. He showed me last year that by simply turning up the amplitude of his disturbing spots he can definitely see the early breakdown. Now, he was interested in the experiment at that time, but first he wants to complete the mapping of the present data he has.

A second item, with respect to two-dimensional spots. Those two-dimensional spots have been observed in oscillating flows. They are two-dimensional with a certain amount of zig-zag of the leading edge and the trailing edge. The zig-zags are something on the order of a couple of boundary-layer thicknesses; they are not uniform across. I don't think the sparking would make it uniform all across anyway. From the point of view of the size of the spot, they are definitely much more two-dimensional than anything else. Some discussion of this, although not in any detail, is in the Abramski-Fejer report on unsteadiness in transition.

Van Atta:

How are the spots triggered?

Morkovin:

You have flat plates and the free stream oscillates plus or minus 10 to 20 per cent.

Van Atta:

But it's natural then in that sense?

Morkovin:

It's natural. You can roughen it up, if you want, but it's natural.

Kline:

I wanted to mention that there is some data in the work of Johnston and three of his students with the effect of Coriolis forces on turbulence which is similar to the experiments you mentioned with regard to accelerating flow. In these cases, we do see spots. That is, if you visualize a flow in which you increase the Coriolis force systematically from zero in a rotating channel,then one wall destabilizes the other wall stabilizes. After a while you don't see anything on the stabilized wall, but there is an intermediate region in which the large eddies peeling off the destabilized wall move across and impact the stabilized wall, creating spots. The spots are now in "a stabilizing environment" and they have some of the properties you are looking for and those movies exist.

Van Atta:

How do the spots decrease? Do they decrease?

Kline:

In some of the movies, they appear to decrease. The runs are relatively short so that they run out at the end of the apparatus. However, there is definite evidence in some of the scenes that the spots are dying rather than growing. These are in the movies of Halleen and Lezius who were students of Jim Johnston's.

Landahl:

Are the spots dying in size or in amplitude?

Kline:

Size. Amplitude was not measured. These were water flows.

Hussain:

As a non-wall researcher, I'm still confused by the relevance of the spot that Wygnanski and others doing similar work find which seems to be independent of the initial condition of the method by which they are triggered. I would very much appreciate if someone could show some connection between these spots and the eddies or the horseshoe vortices that the visualization pictures seem to show.

Willmarth:

I don't think anybody's got any convincing experiment proposed to prove that the spots are really important until they can show that they cause turbulence production and Reynolds stress. No one indicates that they're measuring that or that anybody is planning to measure it. Everybody is just looking at things and talking. I think they should measure uv.

Brodky:

I would like to suggest just another experiment that is important in biological fluid flow and that's the oscillatory flow which is sometimes associated with the aortic flow. Of particular interest is the straight oscillation in a pipe or a boundary layer that even under normal conditions would be turbulent. After you pass peak velocity, you have a very rapid transition and generation of turbulence as you begin to decelerate. What happens in this case has a great deal of similarity, at least visually, to the sort of things that have been observed in more steady flow. It's another type of experiment that is very controlled because you can just oscillate back and forth and look at that one segment over and over.

COMMITTEE 3

Question: WHAT IS THE RELATION BETWEEN VORTICAL STRUCTURES IN THE INNER AND OUTER LAYERS, IF ANY?

Spokesman: JIM WALLACE

Our group met twice; once Monday night and again yesterday afternoon. We had quite a large group that appeared Monday night, so I don't really feel that it is necessary to go through and identify all the protoganists, antoganists, and people who are more concillatory. But let me go into the items on which we agreed and where there was strong disagreement. We did this primarily the first time we met and then yesterday we spent most of the time discussing what particular kinds of experiments might help to resolve the disagreements.

We didn't universally agree on very much. What was agreed upon was that there exists thin shear layers throughout the boundary layer. There was no agreement as to where and at what point in the dynamics of the boundary layer growth and development these thin shear layers are important. Secondly, there exists visually observed and probe measured flow structural elements which when pieced together give a picture which is not inconsistent with an inclined and stretched horseshoe vortex model. You can see that's a highly qualified statement, because there was considerable disagreement as to whether these are regularly reoccuring individual structures or simply an average picture. There was also considerable disagreement on whether these structures exist over the entire boundary layer or primarily exist only in the region near the wall. In addition, there was general agreement that important coherent eddy-like motions have been recognized in the outer region of the flow from visual studies and that some of these are Reynolds number dependent and can be directly associated with large Reynolds stress contributions for Re_θ less

5,000. These eddies appear to be laminar-like vortex loops or perhaps vortex rings.

The third statement that everyone assented to was that everyone agrees that the mean features of the flow scale with u_τ and δ in the outer flow region and with u_τ and ν near the wall, just from the universal laws. There was considerable disagreement about what this implies for coherent motions, particularly those near the wall, where there seems to have developed over the last 8 or 9 years the idea that these scale with the outer flow parameters. A number of people in our discussion felt that this hasn't really been firmly established, and that we haven't even established to everyone's satisfaction and agreement what a burst is and what the bursting frequency is. So, we have considerable disagreement as to what the implication of the universal scaling laws on frequency and periods of coherent motions near the wall are. As you can see, it was a difficult job to put together something that wasn't overly bland and yet that most people in the group could agree to.

Let me go on to some suggested experiments which we discussed in our second meeting. I felt that no truly critical experiments, were suggested (i.e. experiments that in a unequivocal way, would resolve these disagreements). There were a number of useful suggestions and I'll just go through the list. First, in order to help us try to sort out the scaling problem, experiments should be done in the boundary layer region where flow parameters (particularly streamwise velocities), seem to scale equally well with inner and with outer flow parameters.

The second experiment, suggested by Prof. Kovaszny, would utilize an array of hot wire probes - either probes that are sensitive only to the streamwise velocity or even preferably multi-component probes. Perhaps an 8 by 8 array would suffice to probe the area about y/δ of about 0.1. Such velocity information could be integrated using Poisson's equation to study the effect of the velocity field on the pressure field at the wall. Using some conditional analysis techniques one could sort out which parts of the velocity field or what parts in the phase of the velocity field are the primary contributors to the pressure field at the wall. This data could subsequently be tied to the coherent structure motion near the wall.

The third suggestion was really a cautionary note and not so much an experiment. The experimenter should be careful to make sure that the phenomena they investigate or the coherent structures that they look at are Reynolds stress contributors. If they aren't, the person who suggested this felt like they may not be terribly significant to the dynamics of the flow.

Fourth, experiments to determine how a turbulent spot regenerates itself in a turbulent environment should be done. We all agreed this would be a difficult experiment to do, but one that certainly is necessary if the relationship of turbulent spots to turbulent boundary layers is ever to be firmly established.

The fifth suggestion was that all experiments should be done at higher Reynolds numbers to enable us to sort out the scales. At high Reynolds numbers we get a wider range of scales and thus we can more easily sort out the importance of scale and how we should be properly scaling the phenomena.

The sixth suggestion is that two point vorticity component correlation measurements should be made with the hope that these would throw some light on the existence or non-existence of the horsehoe type vortex structures that many people feel simply have to exist in the boundary layer.

The last suggested experiment I have here is that visual studies or visual techniques should, if possible, be automated, so that the data obtained from the visual studies can be quantified to a much greater degree than presently is done by tedious manual data reduction from pictures. If they're automated than we can get some quantitative information related in a clearer and better defined way to traditional probe measurements.

Discussion

Kline:

I'd like to refer to the remarks I made in my paper about the stages of bursting, where I use the word bursting to mean all of the events or stages which comprise the bursting process. I think there is a serious danger of confusion if we look for a frequency of "bursting" because there are at least a number of different frequencies which relate to "events" which occur in a turbulent boundary layer - some which are related to the "bursting"process, but a number which are not or are only indirectly related. This is distinctly tied to a question which your committee has posed regarding how do spots form the total turbulent environment. I do think that if we're going to clarify these issues, and perhaps I'm repeating myself because I feel very strongly about this, we've got to determine the frequency of occurrence of the overall burst process, which means we have to identify the stage in which the lifted low speed streak oscillates in both the side view and the plan view. We have got to find the duration of the transition from oscillation to break-up of the lifted streak, we've got to find the frequencies in the uv content occurring during break-up, and we've got to find the overturning moment of the fluid during break-up. Those are things which are askable and perhaps answerable questions. To say "the frequency of bursting", I think will confuse us.

Wallace:

I thoroughly agree with you Steve (Kline) that what is needed is precisely what your committee seems to have been working on. That is, to clearly identify what phenomena it is you're attaching a frequency to so that it can be compared to what other people are attaching a frequency to.

COMMITTEE 4

Question: WHAT ARE THE MAIN DISTINQUISHING FEATURES BETWEEN DIFFERENT BREAKDOWN MODELS AND TO WHAT EXTENT ARE THESE FEATURES MEASUREABLE?

Spokesman: STEPHEN KLINE

[Editors Note: The above question was addressed originally during the workshop, with the subsequent committee report evolving into a floor discussion moderated by Professor Mark Morkovin. Since the issues raised during this discussion were many, none of which were resolved to any substantial degree, the discussion of the question was continued at a later, informal meeting in July 1978. At this latter meeting, the transcript of the original workshop discussion was reviewed and discussed. The general consensus was that the original discussion offered little in terms of resolved issues and might even prove to be misleading. A decision was made to not publish the original workshop discussion, but to publish a document summarizing the consensus of the informal July discussions at which it was attempted to clarify the original issues raised at the workshop. The following is that document as prepared by Professor Stephen Kline, host for the July discussions.]

A number of workers at the workshop were concerned particularly with three questions:

1. On what points do the major data sets on quasi-coherent structures in boundary layers agree?

2. On what points are these data sets ambiguous or in apparent disagreement, and how can these questions be sharpened so that experiments can be performed to clarify the nature of turbulence structure further?

3. What data might particularly assist workers trying to form analytic or computer models of turbulence, and conversely what can available theory suggest in the form of critical experiments?

The meeting at Lehigh began to clarify some of these questions. However they are sufficiently complex that much was left still undone.

Accordingly, a much smaller group of workers who have been particularly active in taking data or creating models of turbulence structure met at Stanford University for three days in late July, 1978, to continue the discussions. Considerable further progress was achieved on questions 1,2,3 above, but the work still is not finished. It is intended to continue these informal meetings from time to time in an attempt to complete a picture of what is known in the sense of 1 above, and what might be useful experiments in the sense of 2 and 3 above.

Because the results are unfinished and because consultation with a number of workers who have made important contributions has not yet occurred, these results are not being published at this time. As consensus is reached on various points and clear positions recorded on remaining questions, the results will hopefully be published in a suitable proceedings or journal. In the meantime, two pieces of preliminary work from the Stanford discussions are attached for general circulation. The first, Appendix A, is a set of nomenclature which may have some general value as a starting point for further improvements. The intention of this semantic exercise is to reduce, insofar as possible, certain ambiguities that have become troublesome; for example, several apparently disparate uses of the word "bursting". The second result, Appendix B, is a recording of what seems to be implied by the phrases: large-scale, small-scale, and medium-scale in shear layers. It is believed that this set of scalings clarifies these ubiquitous terms considerably and also relates various scalings in the literature to each other. It seemed to the workers at the Stanford discussions that this set of scalings, worked out on the second day, in fact answered several questions that had arisen earlier in the meeting but had then had no answers. Hence, these scalings may be of some general utility.

The remaining results are intended, for the present, to be open but informal, that is, not published but accessible to active researchers who are willing to seriously review and comment. Such individuals should write to S.J. Kline, who will make materials available as they come into appropriate form. It will be some months, at best, before materials other than the two attachments reach such a form.

Appendix A

DEFINITIONS

I. Lagrangian Terminology

A. Streak: A high- or low-speed (relative to the mean) region in the linear sublayer, highly extended (aspect ratio greater than 10:1) in the flow direction.

B. Low-Speed Streak Lifting: Outward movement of fluid in the low-speed streak to a point outside the linear sublayer.

C. Linear Sublayer: y^+ less than 7-10.

D. Streak Oscillation: Apparent amplifying three-dimensional oscillation in side and plan view of a lifted low-speed streak.

E. Wall Scales: $\nu/u_\tau, u_\tau$.

F. Mixing Region: Region after a breakdown in which chaotic motions affect a large propagating region.

G. Breakdown: An abrupt event in which the streak oscillations terminate in the formation of a large region containing a wide range of small scales.

H. Bursting: The set of processes beginning with the lifting of low-speed streaks and terminating at the end of the mixing region.

I. Quiescent Period: Period between bursting processes.

J. Visual Ejection (after Brodkey & Corino): Rapid motion away from the wall of fluid that came from a decelerated region and penetrates into the log region. NOTE: The Stanford group uses "ejection" to denote motion from linear sublayer into the outer layers.

K. Visual Sweep (after Brodkey & Corino): Large-scale inward motion of faster moving fluid, producing local acceleration in the flow field.

L. Log Region: y^+ greater than 30-40 but less than wake matching point.

M. Compact Vortical Flow Structure: A compact, coherent, three-dimensional, ring-like structure observed in the outer region of the turbulent boundary layer having a characteristic core diameter of about $L^+ \sim 100$.

NOTE: This is called "typical eddy" by Falco, but the name seemed to lack specificity for several attendants.

N. Bulge: A large-scale, three-dimensional structure which dominates the visual appearance of the outer layer, with scales of the order of the boundary layer thickness.

O. Valley: Region between bulges in which outer fluid penetrates the (average) boundary layer thickness.

II. Eulerian Terminology

A. Scale: Characteristic dimension of a recognizable flow structure.

B. Coherent Structure: A confined region in space and time in which definite phase relationships exist among flow variables.

Appendix B

SCALES

The following is the result of discussion on interpretation of the usually undefined terms small, medium, and large scales.

In a turbulent boundary layer, we can use the following associations:

Scale Size	Math Expression	Other Names
Large	δ (or size of apparatus, whichever is smaller)	Integral Scale
Medium	$50 < \ell u_\tau/\nu < 300$	$\sim$ Taylor Microscale
Small	$1 < \ell u_\tau/\nu < 10$	Kolmogorov Scale

(Note: Motion of scale $\ell u_\tau/\nu < 1$ dies rapidly, owing to viscosity.)

ℓ = characteristic size of coherent motion, $u_\tau = \tau_w/\rho$.

SESSION V(B)

PANEL DISCUSSION

Session Chairman:

Mark V. Morkovin

Panel Members:

Brian Quinn

Donald Coles

Peter Bradshaw

Dennis Bushnell

AMO Smith

PANEL: QUINN

PANEL DISUCSSION

Panel Member: DR. BRIAN QUINN, AFOSR

I'm going to start off with some things that have absolutely nothing to do with this conference technically, but which attempt to put this conference in the perspective of a much larger national effort (figure 1). This figure shows what is about an 8 1/2 million dollar investment on the part of the Federal Government in turbulence. This is a very conservative figure. This is an annual investment and it's an investment only in basic research, which in the Department of Defense we call 6.1 research. These are figures that are not easy to come by. It takes a lot of work on the part of several people to determine for example what these figures ought to be, and I'll indicate just how conservative they are. When we asked Dennis Bushnell what the figure for Langley ought to be, he said about 1.5 million dollars. The 1.3 million figure that you see up there reflects a figure that I got from Carl Scrank, at NASA Headquarters, who also provided me with the NASA-AMES figure. Both Dennis and Carl pointed out that there are other activities at AMES and Langley, and even at Lewis, that you could relate to turbulence, but which are not reflected in these figures. For example, both Air Force and the Navy support other activities under what's called 6.2 or exploratory development funds that relate to turbulence and which are not indicated in figure 1. I repeat that these figures primarily reflect basic research, the type of thing which we have been talking about for the last two days. The Navy figure came from Mort and Ralph Cooper, George Lee provided the NSF figure, and my good friend and former colleague, Jergen Birkland gave me the DOE figure.

Let's examine the Air Force contribution, that three million dollars that you see up there. Figure 2 indicates how the Air Force 6.1 program in turbulence is broken out. There are essentially two players: AFOSR and the laboratories. Now, there are four columns of figures. The first on the left is the AFOSR figures in those areas which I've indicated. The second column is the amount of money that the laboratories, primarily the flight dynamics laboratory, are spending on contracts. The third column is the amount of money in FY 78 that the flight dynamics laboratory is spending on in-house activities. Some of this is Will Henke's research on modeling and computation and some of it includes the work being done in the high Reynolds number facilities on aspects of turbulent boundary layers. These four numbers then add up to the figure on the far right.

ESTIMATED
NATIONAL FY 78 INVESTMENT IN
BASIC TURBULENCE RESEARCH

-NASA	
Langley	1.3
Ames	0.7
-DOD	
Air Force	3.3
Navy	1.0
-NSF	1.2
-DOD	1.0
	$8.5 M

FIGURE 1.

AIR FORCE FY 78 RESEARCH (6.1) INVESTMENT
IN TURBULENCE

	AFOSR	LABS CONTRACTS	IN-HOUSE	TOTALS
Modeling & Theory	460	45	-	505
Experiments	1217	-	-	1217
Instrumentation and Diagnostics	284	67	-	351
Transition	319	45	68	432
Correlation and Engineering Computation	439	22	316	777
TOTALS	$ 2719K	$179K	$384K	$3282K

FIGURE 2.

Let's focus first on the left-hand column, the AFOSR contribution. You notice we have a lot more money invested in experiments than we have in modeling and theory. That's no accident; we planned it that way. That might change around in five years if good results come from the experiments and we feel that modeling can be improved as a consequence of those experiments. However, right now we're focusing on and encouraging experiments, but trying to keep some theoretical balance. We're trying to also keep some balance in what it takes to do those experiments, i.e. instrumentation and diagnostics. We're advancing that area not so much in the area of basic turbulence, but in the area of turbulence of combusting mixtures, where there's reacting flows and heat addition.

This should give you a feel for our program of basic research in turbulence. Now why is the Air Force investing 3 million or more dollars a year on turbulence? In his opening remarks, Hans Mark indicated that all you have to do to understand why is live through one compressor stall in a fighter aircraft. I doubt if more than two or three people in this room have ever had that experience and it's more an emotional experience than anything else - it can be terminal (laughter). However, most of us in this room have made calculations of drag and you're all probably aware that between 50% and 60% of the drag on a large air transport comes from skin friction. Thus, understanding turbulence in a way such that we can control skin friction represents a considerable saving, as well as advancement of technology to the Air Force. With respect to drag, we want to get rid of turbulence, but in another respect, we want to augment turbulence. We need more turbulence, for example, in combustors. We've got to mix fuel and air, but we've got to be careful how we do that. That is an example in which we want to increase turbulence. In each case above, we want to control turbulence.

We also want to do a number of practical things with turbulent flows, like diffuse them with compact short diffusers. You may or may not be aware that the thrust to weight ratio of turbo jet engines continues to climb very quickly. One way that's happening is by increasing the mass flow through the engine. What that's doing is increasing the Reynolds number and flow velocity upstream of the combustor, so that diffusion of that very mixed up, messy turbulent flow in a short distance is becoming a severe problem.

We also would like to improve the loading or the performance of compressors, whose blades are being bathed by the vortices and the wakes of upstream rotors. Stage pressure ratios are rising. They seem to be assymptoting. We don't know how to handle the full calculations of the blade geometries or how to make even realistic representation for that matter. The Air Force would also like to use advantageously, the structure that exists in the deflected and highly energetic wakes or jets which result from V/STOL devices. These entrain a lot of momentum, they are representative of circulation, and we would like to use that induced flow field.

So many of the things the Air Force would like to do with turbulence it cannot do because it does not know how to control turbulence. We don't know how to control turbulence because we don't have sufficient knowledge of turbulence and of the large scale structures which we've been discussing these past two days. But a good engineer doesn't wait for knowledge. When Dr. Bevilaqua wanted to improve the performance of thrust augmenting ejectors--compact, short ejectors--he didn't wait for a symposium such as this to discuss ways of enhancing mixing. He just went ahead with a team of others and discussed and worked with hypermixing jets. He found ways to augment and amplify the streamwise vortices in a free shear layer by improving the entrainment and promoting mixing. He didn't wait for knowledge, he went out and did the job based on intuition, feeling, and some analysis.

The Air Force is concerned with very real turbulent flows. The point is that none of the things that the Air Force needs to do with turbulent flows relates in any real, practical sense with flat plates. Yet, in the last two days, I have seen nothing but flat plates. Where are the pressure gradients, where is the roughness, where is the strain? Are you aware for example, that the performance of a simple two-dimensional, subsonic, straight wall diffuser is critically sensitive to the orientation of the large scale structures of the shear flow passing through it? I don't mean in the boundary layer, I mean going right down the middle of the damn thing. It is.

There was a time, not too long ago when I worked for a living, that I was less naive of turbulence than I am right now. That experience certainly lends appreciation for your desire to study flat plates and understand a geometry which attempts to unify a rather complex situation. But everybody? Are all students of turbulence so adverse to risk? Are you younger men forever going to follow the ways of the older fellows? Could it be, that the flat plate, the two-dimensional constraint that we've been talking about, in some way inhibits our ability to understand a process which is essentially three-dimensional and time-dependent? What about other experiments such as corner flows or certain diffusers? Where have the risk takers been the last few days? For that matter, where have the risk takers been for the last two years that we've been putting together this program?

Let me change horses for a moment and talk about some personal things. This conference has been mighty refreshing. It's been interesting and it's been a very educational interlude. Since I have not worked in an area of turbulence for several years, you can appreciate what I've just learned in two simple days. Professor Blackwelder, if my notes are correct, for example, mentioned the strong analogy between what we've been discussing and transition. So bear with me while I use that analogy to organize some of the messages that I have received in the past several days. Professor Falco is one of a growing number of investigators who see large scale vortex-like structures in turbulent boundary layers. He has sketched this in one of his articles.

PANEL: QUINN

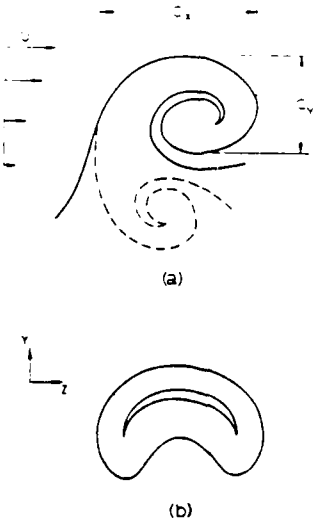

Figure 3.

Figure 3a is a transverse view of the flow which is going from left to right. When one is downstream such that the flow is toward you, Professor Falco sees a structure indicated by figure 3b. These structures are most pronounced, I understand, in the outer layers of the turbulent boundary layer and, in fact, scale with outer variables. Leading down toward the wall from these transverse vortices, are streamwise vortices. Some people refuse to call them vortices, some people don't accept them, some people call them instabilities, but there's something there that goes down below the transverse eddy or vortex. These extend very far down into the boundary layer to very small values of y+. However, these streamwise vortices are not universally accepted.

Everyone agrees on the other hand, that some place in this process, there is low momentum fluid which is expelled from deep within the reaches of the boundary layer near the wall out into the outer reaches of the boundary layer. I think the verb to describe this was ejected and that sounds like jet, so if you'll excuse me in terms of my transition analogy, I'll think of a low momentum jet expelled normal to an approaching stream, which is what we see in figure 4. This is an isometric view with the flow from your right to left. The jet is expelled in the far righthand lower corner normal to this flow. The fluid is water and the jet is water colored with a Meriam fluid oil. The jet, when not in a cross-flow (we did that experiment, too), exhibits a peristaltic instability which grows into ring-like vortices. But when placed in a cross flow as shown here, it is not only kicked over as you see, but developes a different structure. You can see the loops of vorticity, if I can call them that, but the lower part of the loops coalesce into stream-wise vortices. That's much more apparent in the top view which is a projection down onto the wall. The streamwise

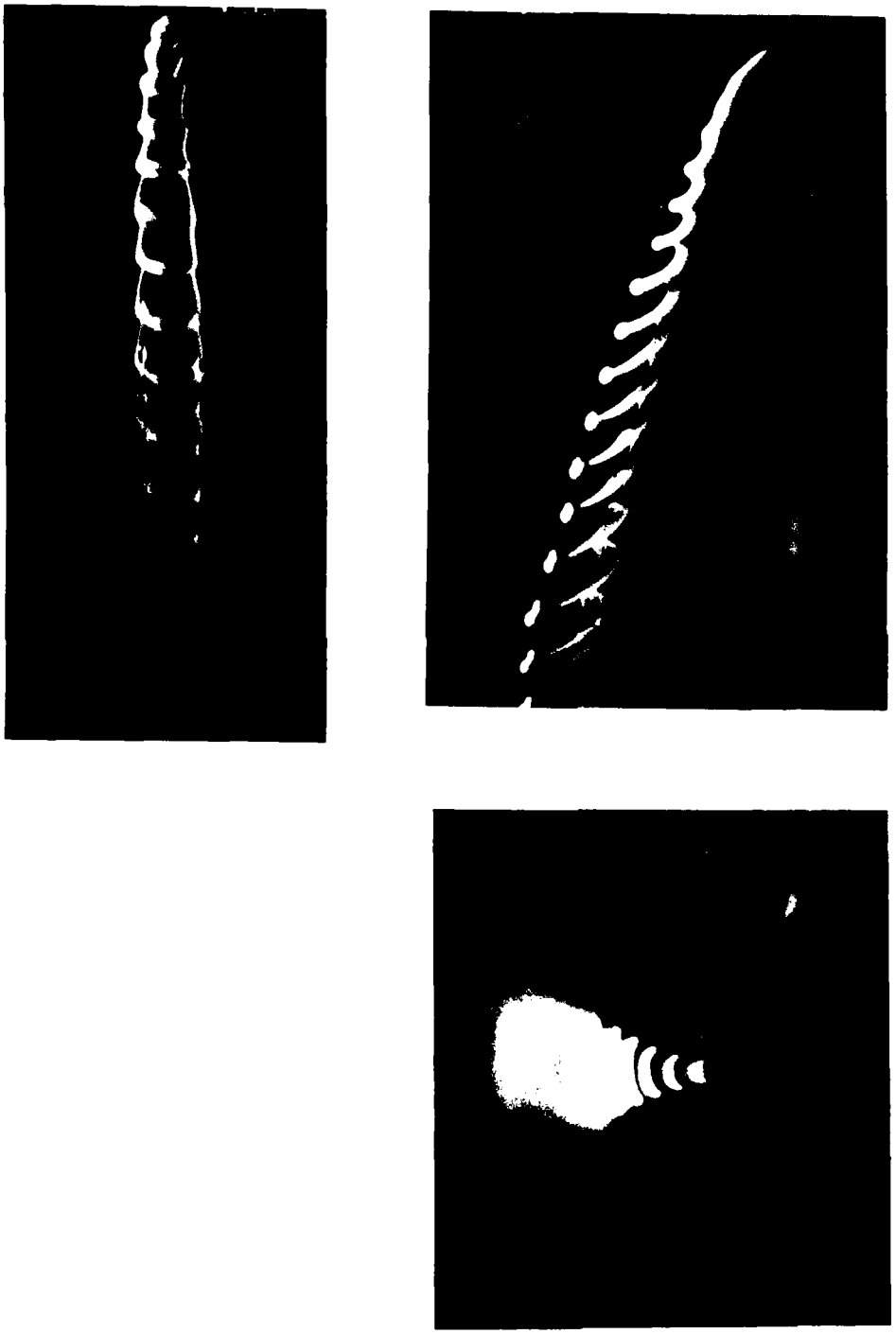

FIGURE 4.

view Professor Falco had in his article which appears in figure 3 exhibited a typical kidney shape, which is what you observe in the flow here as the water is coming out of the screen and toward you. This is typical of jets in cross-flow. These patterns exist in all jets in cross-flows. Figure 5 is one with which you are probably very familiar. You can see the organization of these ring-like vortex loops into streamwise vortices down near their base. I bring to your attention the fact that here is another example of transverse vortices above streamwise vortices. In fact, they are probably one and the same. The picture remains the same of a very turbulent and large scale flow.

Now you can understand that the Air Force would be expressly interested in this previous phenomenon, if you were to stand on your head, so that down would be up and recognize that this would also represent the jet from a deflected engine exhaust. In figure 6 you see the structure I alluded to earlier and you can understand how the entrainment effect and the circulation which is bound in this thing would be very important to V/STOL flight.

Let me pass on to something else that I learned in the last two days. Professor Wygnanski in his paper, proposed that we re-examine concepts which suggest that the flows forget quickly. That's probably a good idea. In figure 7 we see the wake of a flat plate and the generation of streamwise vortices in that wake at three different Reynolds numbers. These are based on plate Reynolds numbers and in terms of Re_θ, they are from around 200 to around 400. These become important to the Air Force because each of those things might be containing fuel in a combustor. If you had to burn that stuff or their really fully turbulent counterparts, you might become concerned with whether or not you were burning the fuel inside the elephant or only on the edges of the elephant, and whether or not you were going to completely burn that fuel by the time it reached the end of a very compact or short combustor. Now to demonstrate how hardy these eddies are, we performed a subsequent experiment in which we placed a plate into the wake of the first flat plate(figure 8). This second plate was intended to destruct those eddies, to cut them to ribbons, and so we raised the second plate very slightly above the center line of the second and tilted it somewhat to provide a favorable pressure gradient on the top and an adverse pressure gradient on the bottom. If you look at the photographs, you can actually watch the boundary layer on the second plate grow by observing the space between these vortex globs.

I have one final thing that I would like to talk about. At one point during the discussion of Professor Smith's paper, Professor Brodky alerted us to the effect of the experimental technique used on the interpretation of the experiments, and Professor Nagib underscored this concern with the photographs taken using his smoke wire. I'm going to add my emphasis with a particular example shown in figure 9. At one time we took a look at the development of a wall jet in transition.

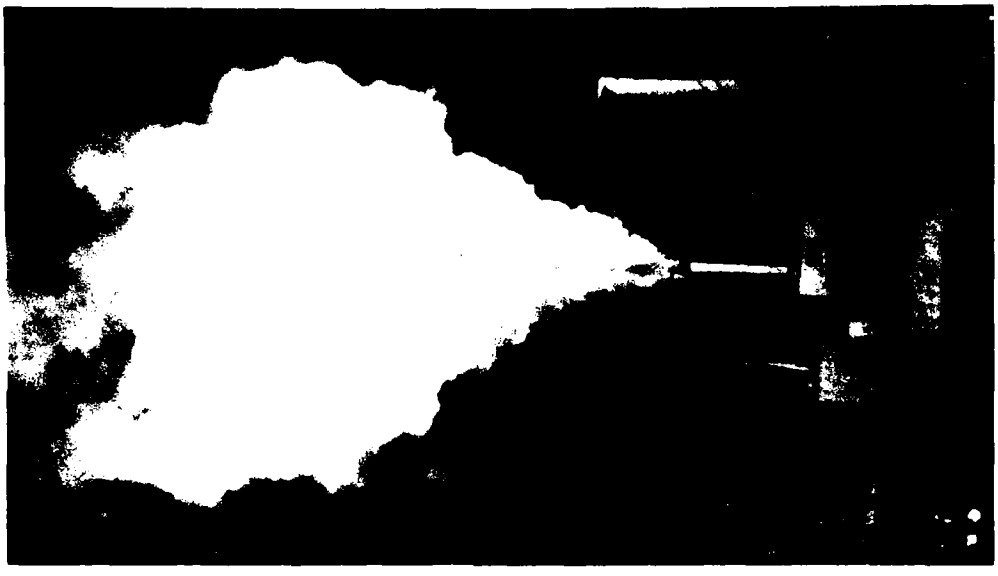

FIGURE 6.

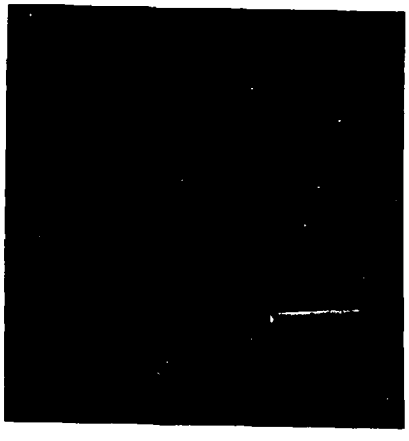

FIGURE 5.

$R = 7.77 \times 10^4$

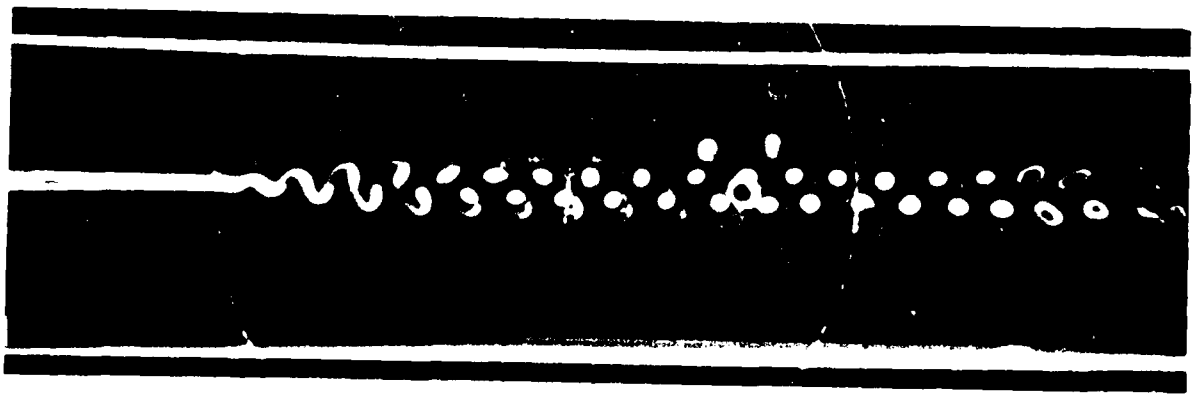

$R = 12.8 \times 10^4$

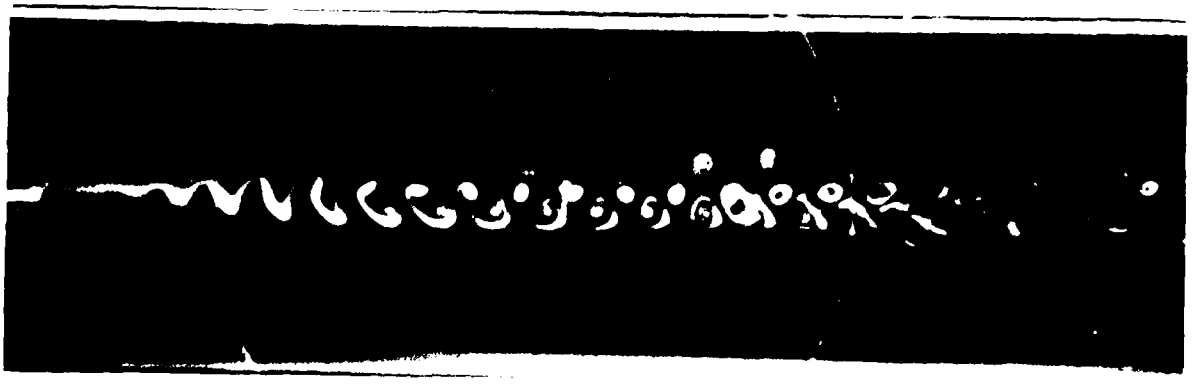

$R = 14.5 \times 10^4$

FIGURE 7.

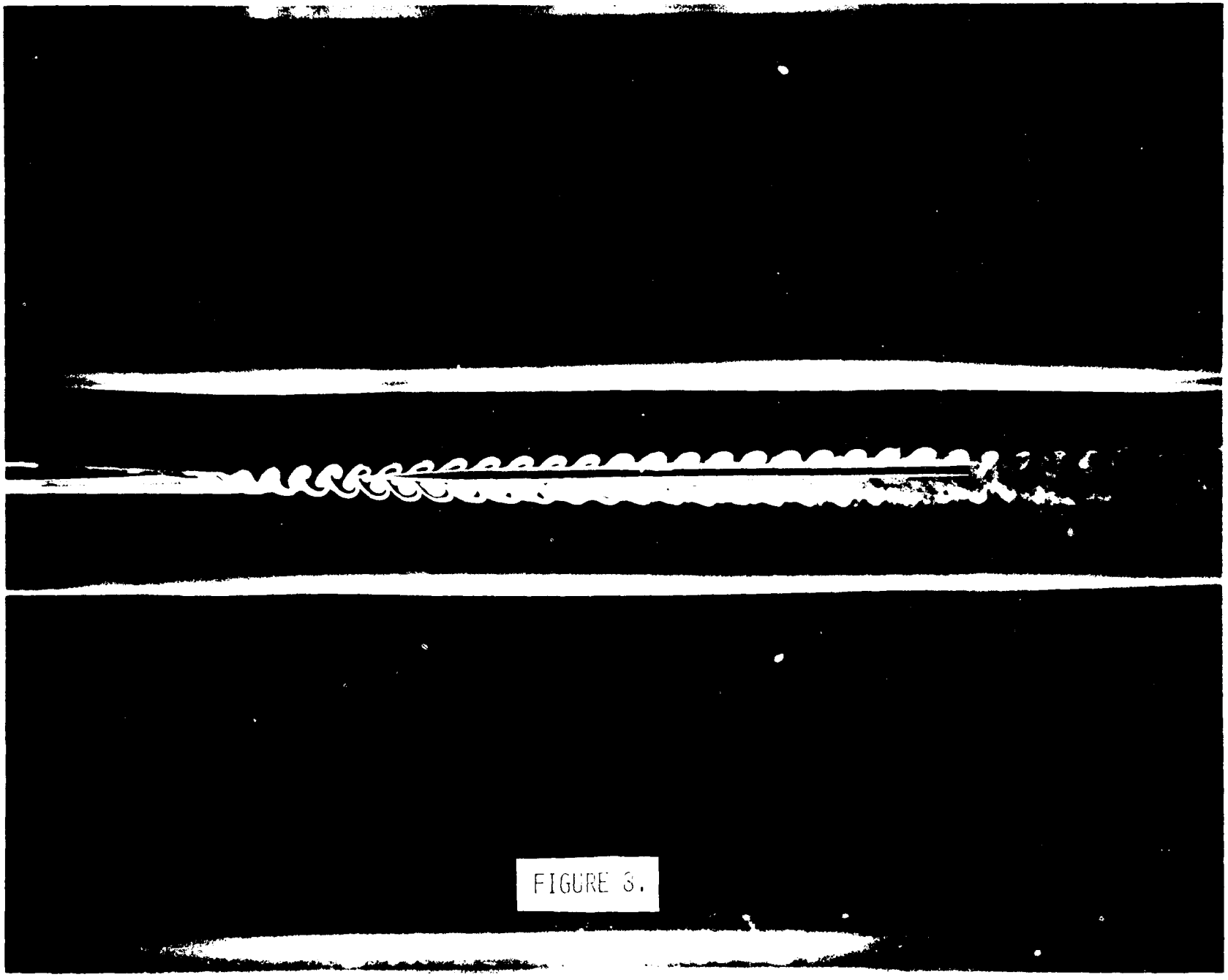

FIGURE 3.

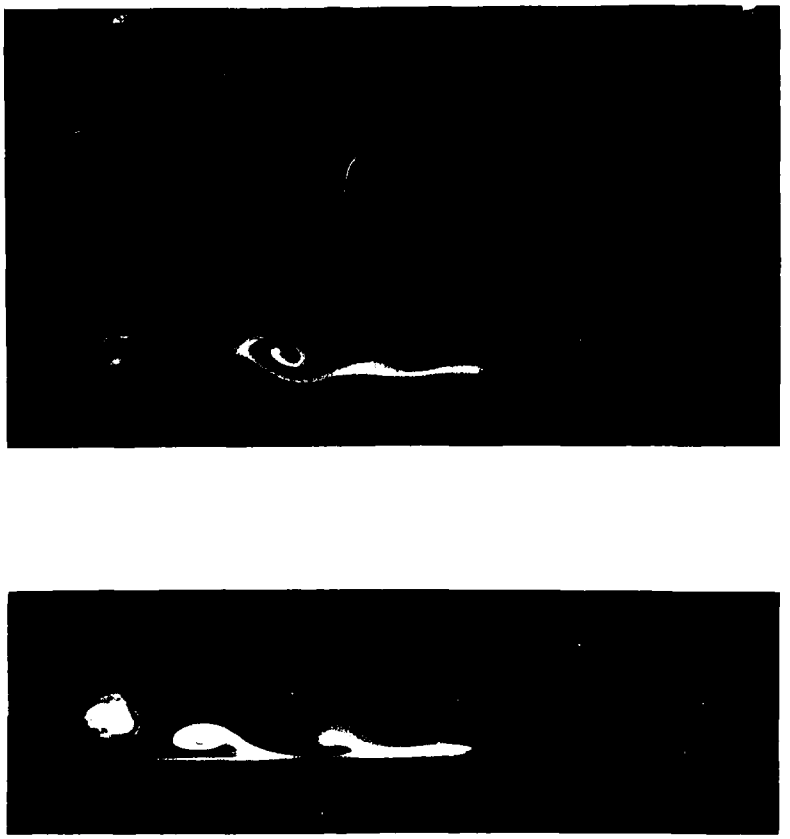

FIGURE 9.

The wall jet issued right to left with the boundary wall below it. The jet slot was about two inches high and we had two positions at which we could inject smoke. In the top photograph the smoke is injected well above the wall and in the lower photograph, the smoke has been injected right on the wall. Notice that you see apparently two different structures. In the top photo, you'd swear that the vortex was going backwards, and in the bottom one, you'd swear it was going forwards. In fact, there are two vortices there. There's one above and one below because of the nature of the wall jet velocity profile. However, had the experiment been done in such a way that one only saw one smoke line, this would not have come to light.

I appreciate your indulgence in letting me explain why I'm here, and why the Air Force is interested in turbulence and in turbulent structures. I hope that it is clear that Colonel Ormand's turbulence program is aggressively pursuing the questions of turbulence,and that it is equally clear that AFOSR is not afraid of risk and, in fact, encourages risk. I hope that in my naive understanding of turbulence, I have not confounded myself, and if that's the case, I request that you write me and clarify my interpretations.

PANEL: COLES

Panel Member: PROFESSOR DONALD COLES, Cal Tech

I first woke up to the existence of a crisis in the turbulent shear flow business in 1971 at an AGARD meeting in London on Turbulent Shear Flows, where there were clearly two types of researchers present. There were the eddy chasers and there were the supersonic boundary layer people, and they had almost nothing in common. In particular, the eddy chasers had nothing in common with any of the analytical work being presented there or most of it since.

Now crises can shake you up a little bit and make you rethink the premises on which you work. One interesting exercise is to try to define the crisis while you are in the middle of it. I think you can classify yourself as a forward or rearward member of the Army carrying on the assault against turbulence by simply answering the question of whether you are willing to stop thinking of mean flow as real. Most of us old timers are highly predictable and I'm certain Peter Bradshaw will take a different view on this question from the one I take. I think the prospect is good--frightening, but good--that the concept of averaging can be moved one level down in the turbulent shear flows in an attempt to describe what we all refer to as coherent structures. You have noticed that these words coherent structure and big eddy and hairpin vortex and so on are being used in two different and incompatible ways by two different groups of people. One to refer to what's going on in the sub-layer and the other to refer to what's going on in the outer flow; but as long as we understand that that's happening it doesn't cause much trouble. It's possible for the pendulum to swing too far, however, and I'm nervous about that. Instead of measuring simply mean quantities and thinking in terms of Reynolds averaging, it is possible, I think, to move too far in the direction of observing individual and perhaps not characteristic events which occur in turbulent flows. The risk is highest in the flow visualization business. The risk is very high that you accumulate great quantities of numbers in which there is very little information unless you are clever about extracting the essence of it. Now I speak as a man who has been there. I think I probably hold the record at the moment for the largest quantity of computer words generated in any one single experiment. That number is 600 million words, and believe me, that's a lot of words.

There's a possibility that we're not really doing what we think we're doing. I'm reminded of the children's fairy tale about the Emperor's new clothes. Here we are all standing around admiring the Emperor's new clothes, and in the back a childish voice says "but the Emperor has no clothes". It's quite possible that this study of structure won't payout. The payout is on hard numbers or on formulas capable of generating hard numbers. In the material presented here so far, there's a singular lack of hard numbers or formulas capable of generating hard numbers. I think the attempt to predict what turbulence research might look like in 15 or 20 years, is something I undertake only with some trepidation. I already

said my notion is that we're stuck with Reynolds averaging, even if we could move it down one level and describe a watermelon or whatever in terms of stresses that determine its structure and operational transport mixing properties, and so on. We haven't really solved any problems until we can somehow put those things together in a simple way, not into large eddy simulations and things that take incredible and unreasonable amounts of computer time. They have to be extracted to the point where they're useful almost at the slide rule level, I think, before we can consider that we've succeeded in anything. That's the success that I think is very problematic.

The whole effort of resolving this crisis is going to have to be very ambitious. Even if I knew that a turbulent spot was a prototype eddy for a boundary layer, I agree completely that I am not serving society if all I talk about is boundary layers at constant pressure. I have to know what happens to the characteristic eddy under the influence of all of the practical conditions that come up such as pressure gradients, three-dimensionality, roughness, mass transfer, and so on. That's such an ambitious program, I'm sure I won't contribute that much to it. I vascilate between the position that things are moving much faster in this business than I expected and then I notice the lack of hard numbers and decide that they are in fact moving slower than I hoped. I will be interested in watching future events.

One of the disturbing elements of this revolution is that I see no effort on the analytical side which is compatible with, and comparable to, the effort on the experimental side. As far as I can tell, nobody is thinking about how to describe a big eddy in a way that anybody can use for anything. When I talk to people like Philip Saffman and ask why he isn't thinking about this, his answer is that I first have to prove to him that this is better than the old stuff, and I can't prove that. So I sympathize with his position.

I'd like to make one more remark. We are all the victims at any given moment of the state-of-the-art in instrumentation. I consider that what is happening in the turbulence business now is the first significant advance in development of ideas since roughly 1935, when the original eddy viscosity approaches rescued people from log log paper and power laws. That was a significant advance, I think, and I'm sure they were excited about it. I think we're in the middle of another one, and although I certainly can't describe it, I know I'm excited about it. However, the instrumentation problem is severe. If you remember in the 40's and 50's the contribution people made was with hot wires and the measurement of spectra. There are thousands of spectra published in the world's journals, and several dozen more ambitious results refer to energy balances--that's the evaluation of all the terms in the turbulent energy equation, i.e., the production, the dissipation, the diffusion. Some of us had a part in some of those and they were also singularly unproductive, because they just showed that you could not separate out any small number of these processes in any given flow and keep them in isolation. I think the computer is leading us into the same kind of trap again. That now the problem will be masses of data which are not necessarily productive enough, and I've said already that I'm helping in that effort.

I really hope that young people are coming along rapidly who don't pay quite so much attention to people like me. Crises are created by the established people because the old methods aren't good enough, but they are resolved by new people. This has happened over and over in Physics and Medicine and so on. Therefore, I hope you won't pay all that much attention to what we tell you are the important problems or the definitive experiments. If we're really right about that, then all we have to do is go away and do our own definitive experiments. Furthermore, the old timers are too predictable. I think all of us who know each other well, would agree. I'll pick Peter Bradshaw as an example. If I ran into Peter Bradshaw at a meeting and he failed to call my attention to the importance of the pressure-strain correlation, I think I would inquire about his health (laughter). The rest of us are all the same way. You've noticed that. If you haven't, why just ask somebody and he'll tell you what the predictable thing is.

Panel Member: PROFESSOR PETER BRADSHAW, Imperial College

I would like to reassure Don that I am still in good health and I'm still interested in the pressure-strain correlation or at least I'm still interested in the Reynolds stress transport equations. I'm still interested in Reynolds averaging, because I find it difficult to believe that we're going to be able to cook up calculation methods for engineering use which use anything which is much more sophisticated than Reynolds averaging. As far as I can see, it's going to be very difficult to find any level of averaging between straight Reynolds averaging and the sort of averaging which the large eddy simulators like Bill Reynolds are using in which they simply model the small scale structure and leave the large scale structure time-dependent. Now we all know that it takes a lot of hours of computer time, and although computational power may increase, and computational efficiency may increase, I think we are going to be stuck with selling or trying to sell calculation methods which actually use Reynolds averaging.

Well, I am not of course saying that the whole of this meeting talking about instantaneous structures, conditional sampling and so on has been a waste of time. I'm much too far from the exit to make such an incautious remark as that. I do believe in conditional sampling and it's usefulness, but I think that it's usefulness is in the medium term, say the order of 10 years at least, is going to be in helping us to formulate Reynolds Average models. That is, to get a better handle on the physical processes which determine what goes on in the Reynolds stress transport equations. For instance,we've already had a mention this morning of the possibility of determining how the pressure fluctuations and the pressure strain term behave by using conditional sampling to find out what the eddies are doing.

I think the next stage and the question we ought to address ourselves to as we sit waiting at the airport to get home is how we are going to use the conditional sampling information to tell us more about the simple things like turbulent transport of Reynolds stress, the pressure-strain term, the energy cascade, and so on. I think there are going to be cases in which higher order, or as Don (Coles) called it, lower level averaging--averaging of more complication than Reynolds averaging--is going to be useful. Combustion is one obvious example. Paul Libby's work on the introduction of intermittency into shear layer calculations has been mentioned already. Paul, of course, is at least partly motivated by combustion. In general, I would say that trying to plug in intermittency as a variable is going about it the wrong way, because intermittence--I'm talking about the outer layer interface intermittency--is a consequence of the large eddy structure, the orderly structure or whatever, rather than a variable in its own right. So if you understand large eddy modeling such that you could model the turbulent transport terms and the pressure-strain term, you could also model what the intermittency was going to do.

PANEL: BRADSHAW

The thing that I see as being perhaps most useful in modeling in the next few years, and I've said this many times before, is the numerical simulations which Bill Reynolds and friends are doing, because they can measure things that the rest of us can't. They can, in effect, do a quantitative flow visualization experiment to deduce whatever statistics they want. I have an example of the usefulness of this. Yesterday I asked Bill Reynolds for his pressure-strain correlation evaluations and he showed them to me and they started me thinking rather seriously what is going on in the viscous sublayer, and my thoughts might conceivably lead to something. I'm not going to bore you with my thoughts, I'm merely indicating that Bills' results triggered some thoughts and that the feed-back from modeling such as he has done may set other people thinking as well.

I feel that the basic message that I'd like to put forward is that we need a bit more motivation of the conditional sampling work towards use in calculation methods. This, of course, is something that Don (Coles) mentioned.

To address Brian Quinn's point that we're perhaps concentrating too much on flat plates, I think we have to try and decide which of the features that we're looking at are likely to be universal and, therefore, worth studying in a universal basis. I'm going to upset several people, I guess, by saying that I'm not convinced that it is going to do much good in the practical world to worry about what happens in the viscous sublayer, because in most calculations methods, the viscous sublayer is probably going to have to be represented by a Van Driest constant or something like that. God forbid that we should try to do a complete turbulence model of the viscous sublayer, because if there's anything harder than turbulence, it's turbulence that's being messed around by viscosity. So, purely from a pragmatic point of view--I'm being deliberately provacative--it may be that scubbling around in the sublayer is one of the lowest priorities of all (laughter), either in the geometric sense or otherwise, for actually doing some good in calculation methods.

I don't think it will be helpful to get into arguments about the different types of calculation methods which Maury Rubesin discussed two days ago. I think it's a pity perhaps that there aren't more turbulence calculators here. They could have been kept under sedation until this final session and then asked to give their views. I think perhaps the next time that we run a meeting like this we ought to invite some calculators along and get them to say what things they would like the eddy chasers to look at. I've tried in my limited way, to indicate that myself. It's very easy to get interested in what you're doing--to look at the eddies--and we've spent a lot of time looking at Chuck Smith's film for instance which I find absolutely fascinating. We get interested in what we are doing and we forget the 8 million bucks that's being contributed.

I have a sort of private view of what the day of judgment is going to be. I'm going to be confronted by all the tax payers who paid all the money that I have spent and they're going to say "what have you been doing for us". It's a sobering thought with which I think I will leave you.

DISCUSSION

Morkovin:

If I heard you correctly, you feel that the present Reynolds averaged equations are not in as good a shape as you would like them to be?

Bradshaw:

You heard me correctly. I believe in the exact equations, and they come from a Navier-Stokes equations in which I believe. What I do not believe is that there is any set of equations with constant coefficients in front of all of the terms, which describe turbulent flow, except for the Navier-Stokes equations themselves. The Good Lord has given us one set of such exact equations and there's not going to be another. So the most that we can hope from any calculation method, short of a complete time-dependent solution of the Navier-Stokes equations, is that it will cover at least some of the flows that we're interested in. If I may pick on poor Morrie (Rubesin), who was very wisely set-up by the predictors to take all the flack. Morrie mentioned the improvements to Brian Launder's calculation method which will enable him to predict a couple more flows. I think it's unlikely, and I believe that Brian also thinks that it is unlikely, that we will be able to use a model such as his with universal constants to predict jets from VTOL aircraft, flow in combustors, and the other really practical problems. I think we are going to be stuck with flow dependent coefficients in our models and I would like to make a plea for some sort of classification of the flows that we're interested in, and a classification by phenomena rather than hardware. I think that our coefficients are going to have to be changed according to which phenomena we believe dominate the flows that we're trying to calculate. This is a gloomy sort of council, but I think that we ought to recognize that the last ten years of turbulence transport modeling have not led us to a universal method with constant coefficients and that we are unlikely to ever achieve such.

Panel Member: DR. DENNIS BUSHNELL, Langley Research Center

When I was asked to serve on the panel, it was requested that since I had been trying to utilize coherent structure concepts, I might comment on the usefulness of such information to either understanding the data or in modeling. I put down three possible uses (Fig. 1). Peter (Bradshaw) has already discussed some of this (first item (item (a), Fig. 1). Most of my comments will be on item (b), Fig. 1 which Wygnanski just touched on this morning. Most of the last two days, of course, has been on the last item (item (c), Fig. 1).

What is the use of these coherent structures as far as prediction is concerned? (Fig. 2). I think that one of the realizations ($\bar{v}$ ($\bar{x}$,t) from a coherent structure experiment provides a very stringent check upon the stuff Bill Reynolds is trying to do. It provides guidelines, in particular for the subgrid scale modeling. In other words, if Reynolds subgrid scale modeling doesn't look like some of these thin shear layers, then we're in trouble (laughter). The three-dimensional, interactive and multi-scale nature of these structures is very pronounced. When I look at Chuck Smith's movies, it looks to me like there's not that much coherence there. If you do ensemble averages, they do start to look coherent. Maybe if we can come up with some simplified models, such as Jim Danberg and many others have started, and if we can prove that these simple models do indeed yield data consistent with experimental results, then we may be able to use these simple coherent structure models in prediction techniques.

Now what I am going to do essentially is to add, I think, two other things to the 14 ways that Kline suggested you can do to fold, spindle and mutliate the turbulent boundary layer. What we're trying to do now is to make some money with the coherent structures. We're trying to produce something technologically significant by modifying the structures (Fig. 3). If you have as little information as a knowledge of the structure's dimensions or as much information as a deterministic model of a structure, then you can hopefully dream-up or invent or concoct some way to interfere with the structure in a favorable way. Note that the definition of favorable depends on whether you want to increase or decrease shear. The two examples I am going to discuss happen to be ways to decrease shear. But you can hopefully interfere with any one of these feedback mechanisms, and possibly end up doing something technologically significant. The first modification scheme is the use of essentially large eddy break-up devices (Fig. 4). This was touched on in Nagib's talk yesterday. It was also mentioned by Wygnanski this morning when he suggested putting a lid on the flow. This is a lid which is very small in the streamwise extent. The idea is to put something somewhere across the flow only up to boundary layer height with the intent of disintegrating the large scale structures. The problem then is to determine how long it takes the structures to heal. In the healing process it is observed, as I will show you in a minute, that the skin friction is lower. The question is: can you design an interference device which has a low enough element drag such that its

USES FOR TURBULENT BOUNDARY LAYER COHERENT STRUCTURE DATA/MODELING

(A) o IMPROVE TURBULENCE MODELING IN CFD CODES

(B) o TURBULENCE TRANSPORT ENHANCEMENT/REDUCTION

(C) o INCREASED UNDERSTANDING OF TURBULENCE/CHECK ON OTHER INFORMATION

FIGURE 1.

POSSIBLE IMPACT OF TURBULENT BOUNDARY LAYER COHERENT STRUCTURE INFORMATION ON CFD TURBULENCE MODELING

- PROVIDES STRINGENT REQUIREMENTS/EXCELLENT CHECK UPON NUMERICAL TURBULENCE SIMULATIONS FOR WALL FLOWS
  - ALSO GUIDELINES FOR SUBGRID MODELING
- THREE-DIMENSIONAL, INTERACTIVE AND MULTI-SCALE NATURE OF THESE "STRUCTURES" PROBABLY PRECLUDES DIRECT NEAR TERM USE AS MODULES IN A GENERAL CLOSURE TECHNIQUE
- COULD SUGGEST POSSIBLE FORMS FOR PRESSURE FLUCTUATION/DIFFUSION TERMS IN SECOND ORDER CLOSURES

FIGURE 2.

PAGE: SUSTAINED

TURBULENCE TRANSPORT ENHANCEMENT/REDUCTION VIA "COHERENT STRUCTURES"

PHILOSOPHY:

I. CONCOCT HEURISTIC MODELS FOR PORTIONS OF THE CYCLE

- PREBURST
- BURST
- SWEEP
- LARGE STRUCTURES

II. FOR THIS PORTION, COMPUTE/OR EMPIRICALLY DETERMINE INFLUENCE OF VARIOUS PARAMETRIC MODIFICATIONS ("TURBULENCE CONTROL")

RATIONALE— TO DETERMINE RANGE OF PARAMETERS FOR FAVORABLE EFFECTS (INCREASED OR DECREASED SHEAR/TRANSPORT)

FIGURE 3.

HONEYCOMBS/SCREENS FOR TURBULENT VISCOUS DRAG REDUCTION

OBJECTIVE: DEVELOP A TURBULENCE "BREAK-UP" DEVICE WITH A MINIMUM NUMBER OF LOW DRAG VERTICAL/HORIZONTAL MEMBERS SUCH THAT THE DEVICE DRAG PLUS SKIN FRICTION REDUCTION DOWNSTREAM PRODUCES A NET REDUCTION IN VEHICLE DRAG

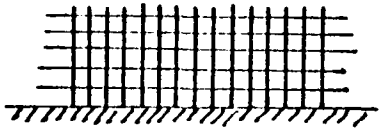

SCREENS
$C_D \sim O(1)$
(YAJNIK)

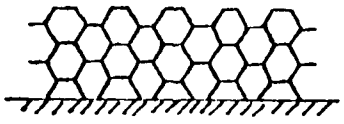

HONEYCOMBS
$C_D \sim O(.1)$
(CURRENT LaRC)

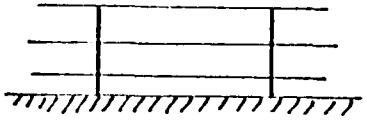

OPTIMIZED BREAK-UP
DEVICE
(PRESENT CONFIGURATION
SUGGESTED BY NAGIB)

FIGURE 4. HONEYCOMB/SCREENS FOR TURBULENT VISCOUS DRAG REDUCTION

drag is less than the integrated skin friction drag reduction downstream? The original work on interference devices was done by Yagnik in India; we've done some honeycomb work that I'll show, and yesterday Nagib showed some flow visualization results. If Nagib's device works, there is a possibility of some sort of a net benefit. The Yagnik work (Fig. 5) shows that these devices create a relaxation length which is the order of 60 to 80 boundary layer thicknesses with a very low initial skin friction. The indication is that the devices are, as Nagib's flow visualization shows, changing the outer structures, which then take a very long distance to restore themselves. Now what we've done at Langley is to just put a honeycomb in the flow at about boundary layer height (Figs. 6 and 7). The parasite drag on the honeycomb is about an order of magnitude less than on the screen, yet we can achieve skin friction reduction levels of the order that Yagnik measured. The question then is can this process be further optimized to yield a net drag reduction? This sort of research also contributes to the knowledge of the feedback mechanism, because it indicated that evidently if you do disintegrate the outer stuff, you are also interfering with the bursting at the wall because that presumably is where the skin friction is determined.

Now I'm going to discuss a possible item 16 on Kline's list. This is something that Stanford looked at back in the late 60's (Fig. 8). We call them riblets, which are very small longitudinal striations on a surface. The basic idea is straightforward. What you do is attempt to skrunch the bursting process down inside a region of very small transverse extent. In terms of what Martin Landahl discussed, this would alter the spanwise pressure gradient. An alternate mechanism involves increasing the wall streak spacing. These things obviously increase the wetted surface area, so the trick is to see whether you can get enough decrease in the turbulence production to offset the area increase and thus end up with a net skin friction reduction. In the early Stanford measurements on this type of a surface, I believe that they did measure a reduction in the burst frequency. These are the sorts of surfaces that one can look at (Fig. 9). The slots are milled out using a numerically controlled milling machine with a special milling cutter which is made for each surface. If the skin friction increased directly as the wetted area (for the same plan form area) you would have a monotonically increasing curve (Fig. 10). However, the data fall far below that curve, and we can effectively increase the wetted area by about a factor of four with essentially no drag increase. These results have been checked. There is a point which has not been checked (and thus not shown) which indicates about a 5 per cent drag reduction, and there is an area in parameter space where you may, in fact, be able to get even more drag reduction. Other possibilities include destroying the periodicity and symmetry of the surface waves. Again, I must point out that this riblet plate was designed by attempting to constrain the dimensions of the bursting process in the spanwise direction. Perhaps of even more technological interest is the sort of Reynolds analogy factor one measures on these surfaces. When we determine both heat transfer and drag on the riblet surface and compare it to the flat plate, we obtain the order of a 10 to 20 per cent increase in the

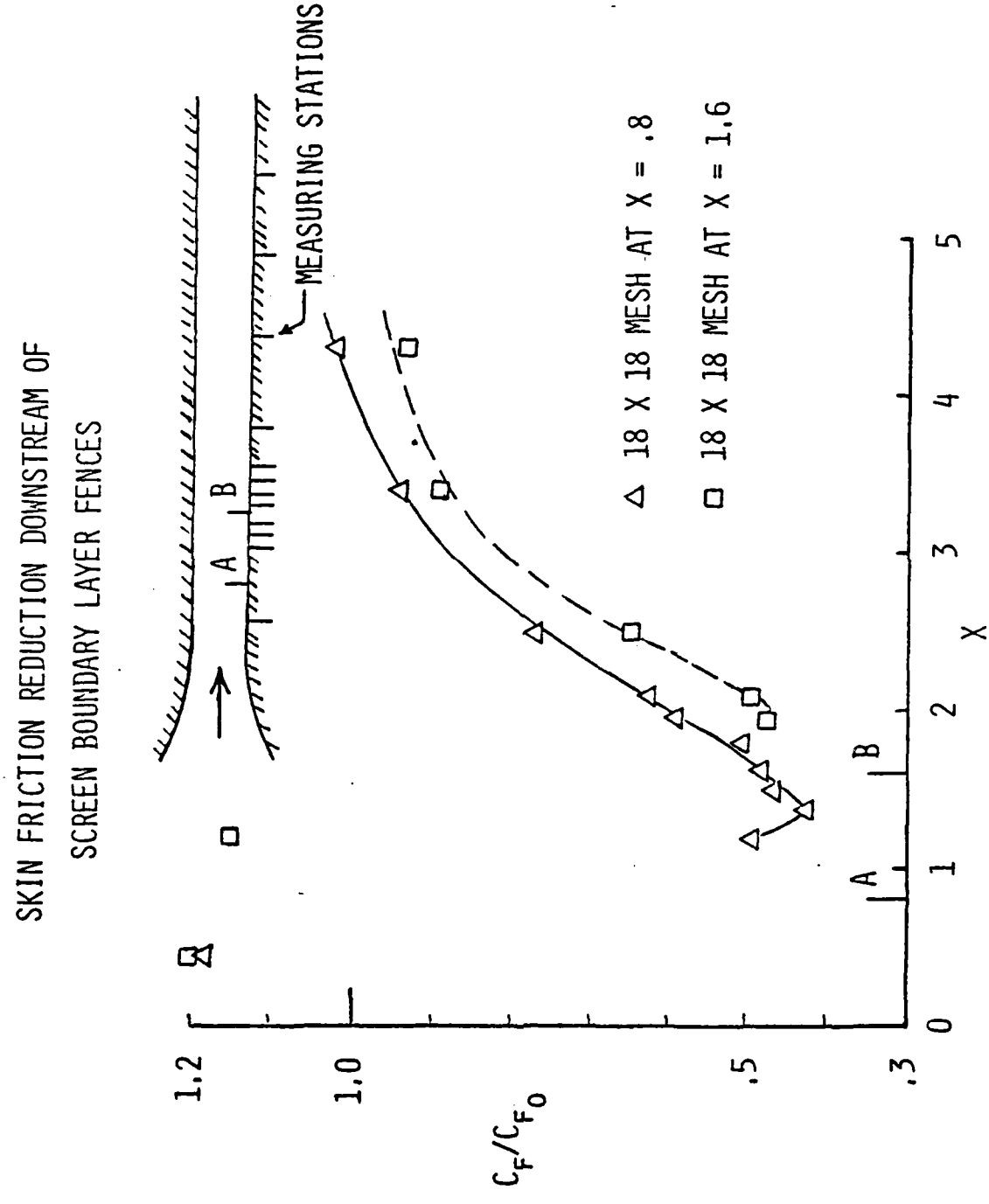

FIGURE 5. DATA FROM YAJNIK AND ACHARYA.

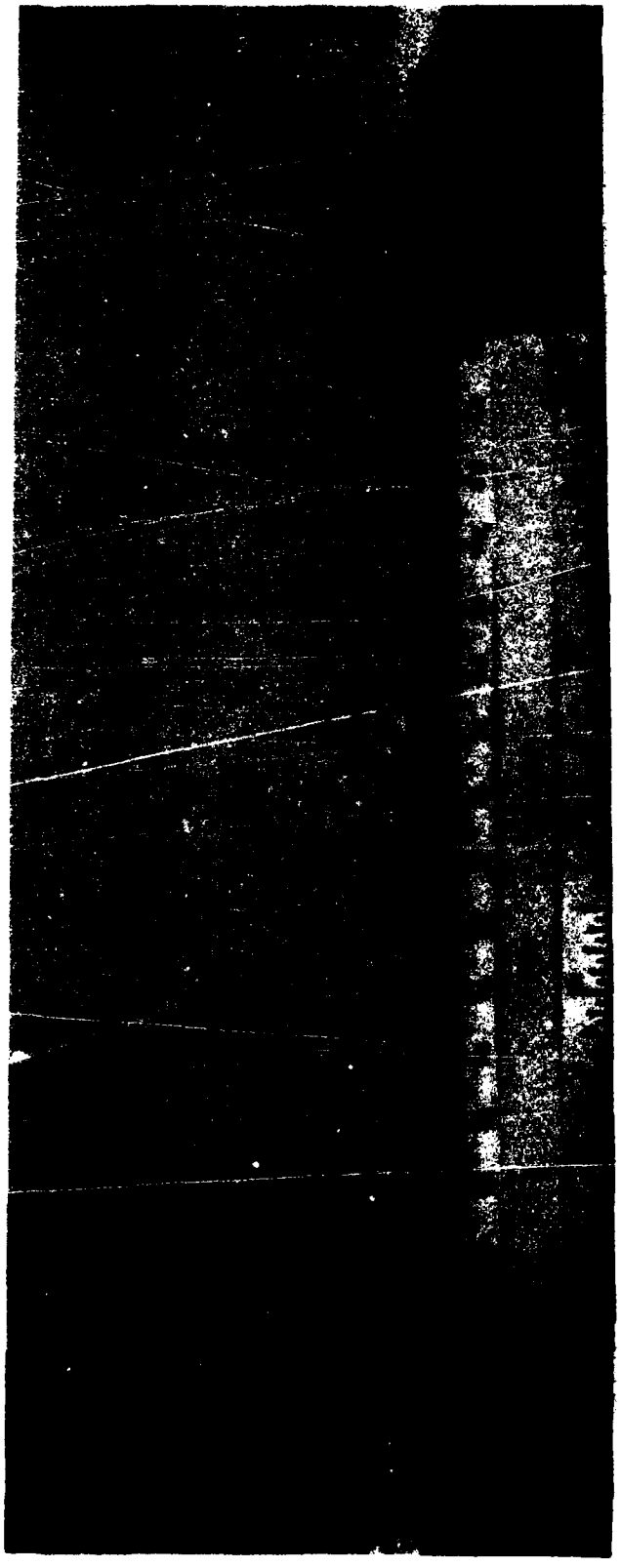

FIGURE 6

PRELIMINARY RESULTS OF DIRECT DRAG MEASUREMENTS WITH HONEYCOMB FENCES

$H/\delta \approx 1$

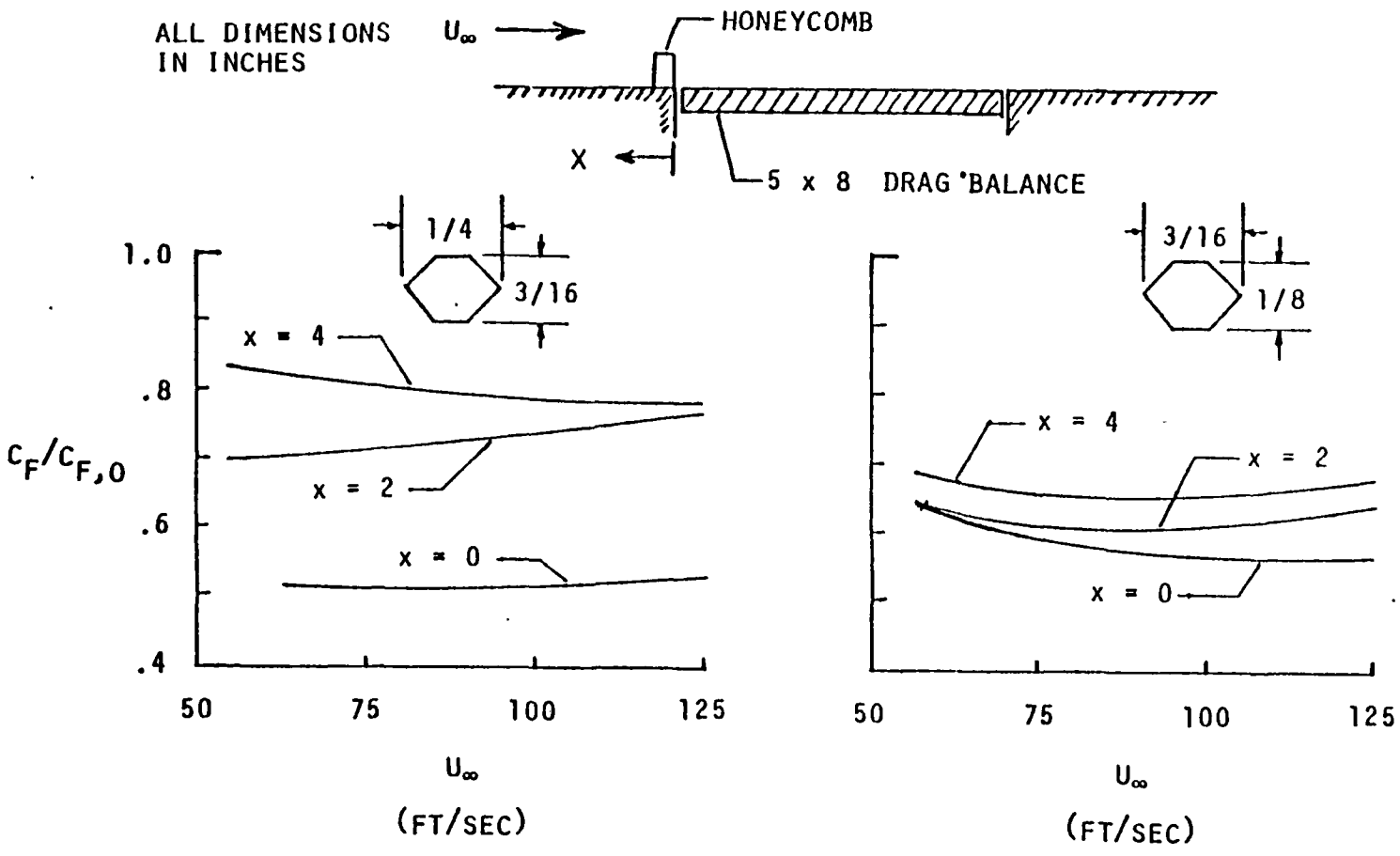

FIGURE 7.

SMALL LONGITUDINAL SURFACE STRIATIONS ("RIBLETS")

BACKGROUND

≈ 1956 RESEARCH BY ECKERT/IRVINE ON NON-CIRCULAR DUCTS

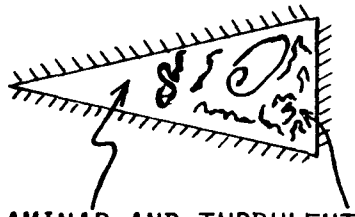

COEXISTENCE OF LAMINAR AND TURBULENT FLOW

- PRESUMABLY DUE TO SMALLER LOCAL TRANSVERSE SCALE

APPROACH

ATTEMPT TO REDUCE/ELIMINATE WALL BURSTS BY CONFINEMENT IN REGION OF SMALL TRANSVERSE EXTENT

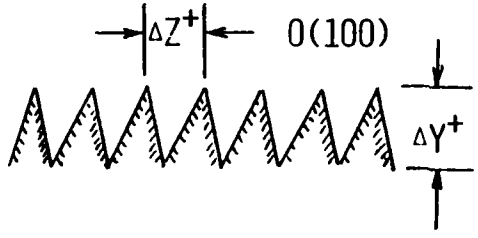

I.E., O(50), FLOW INTO PLANE OF SKETCH

FIGURE 8.

FIGURE 9.

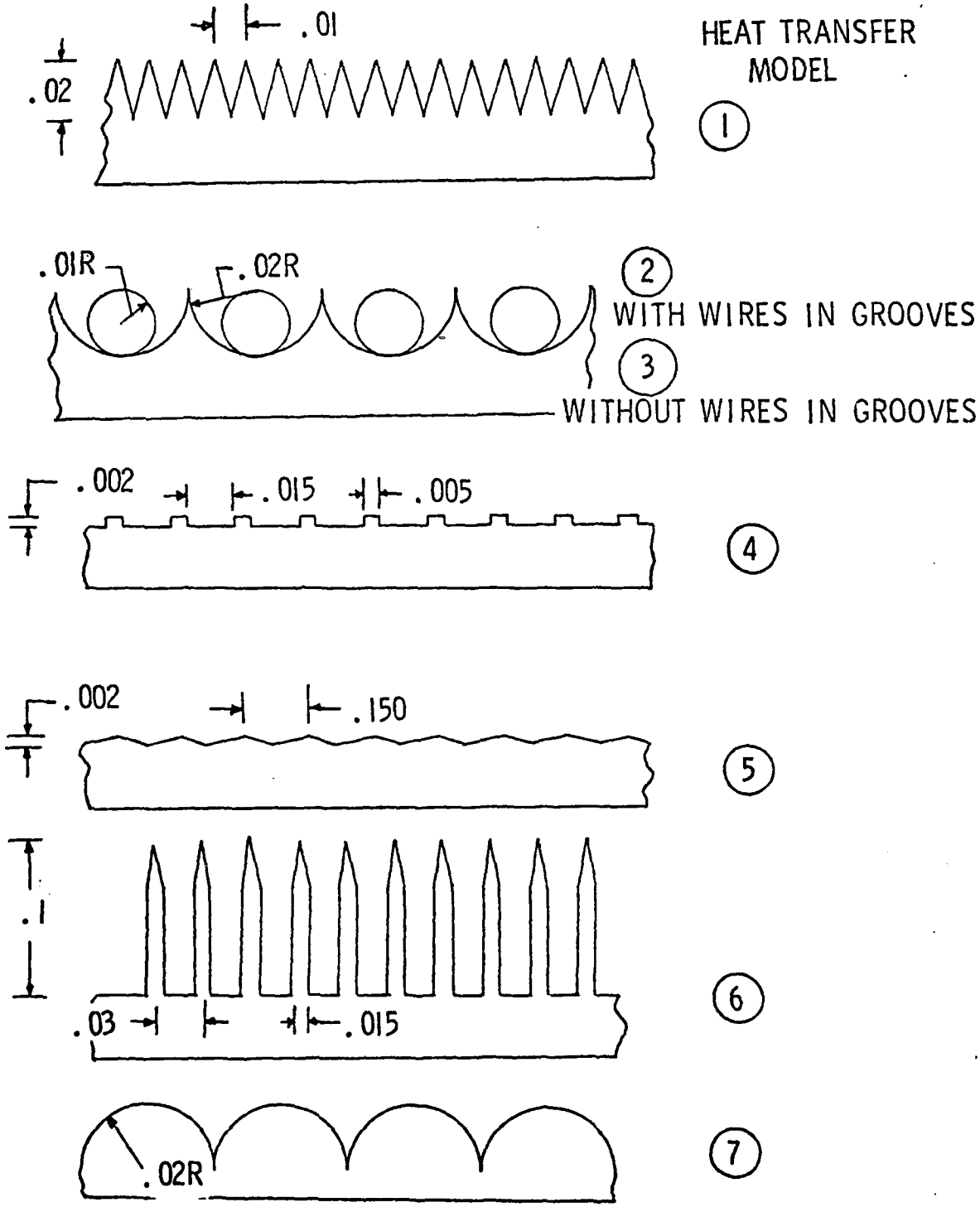

FIGURE 10A. RIBLET MODELS TESTED FY 77

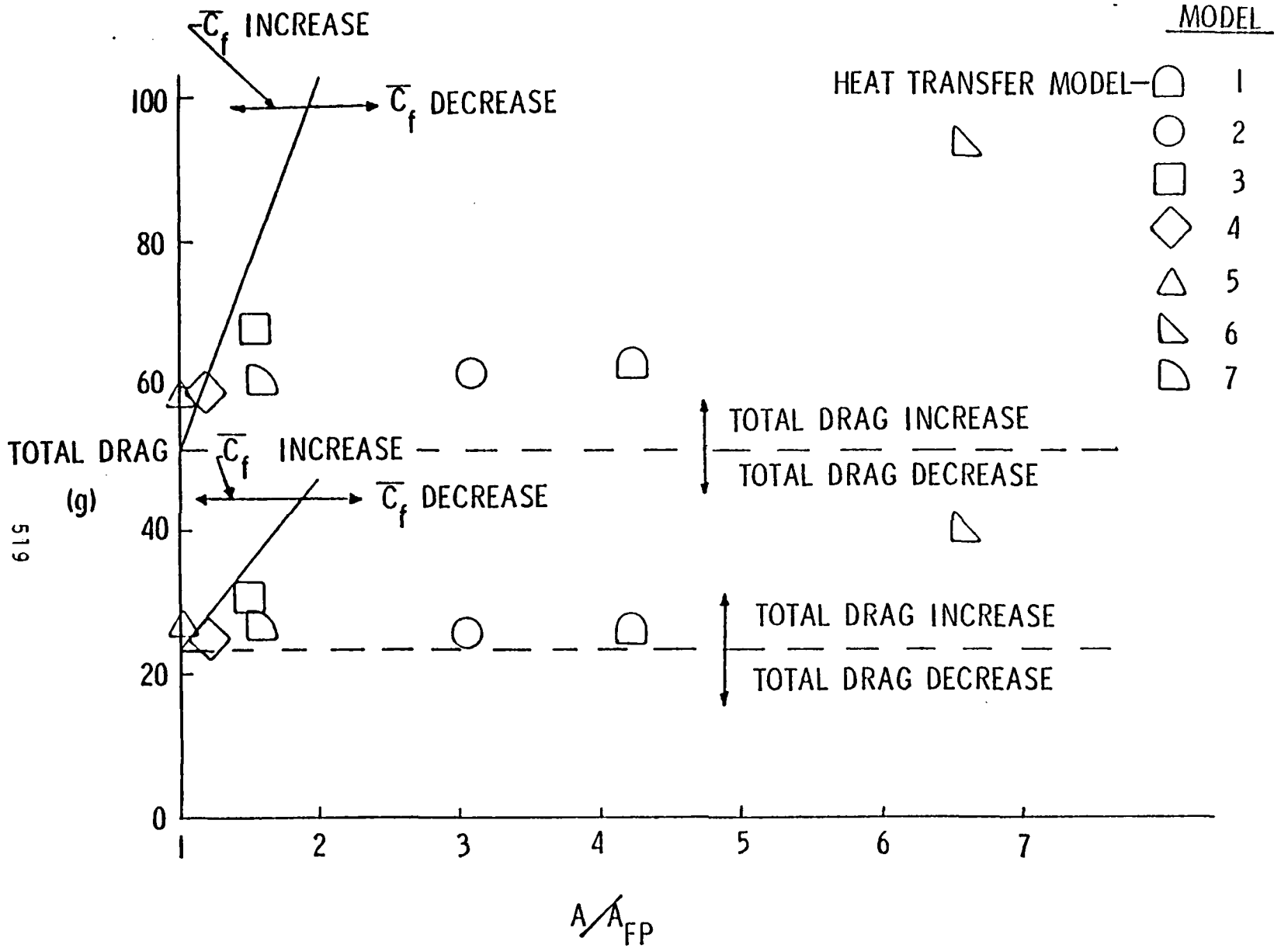

FIGURE 10B. RIBLET C_F EFFECTS

Reynolds analogy factor (Fig. 11). Now this is one of the few surfaces which will give you heat transfer augmentation without an increase in pumping power. Most of the roughnesses and so forth give you an increase in heat transfer, but the drag increases more. Internal flows people have actually used something like this wrapped around the inside of a pipe and they do get more heat transfer than drag increase.

I have some final comments (Fig. 12). There's a possible experiment that I haven't heard mentioned except in a derrogatory fashion. That is because of the amount of the data one might have to handle. It is essentially the use of holographic microphotography to measure a single realization of the three-dimensional velocity field by looking at the motion of seeded particles. There is a suggestion of a three-layer structure; in particular a flow module coming up from the wall and serving as an intermediate layer between the outer and wall structures. That needs to be looked at. The question of birth and death versus eternal life with the large structures I think needs to be looked at also. Other areas for research are the feedback mechanism, the role of the spanwise structure, and the high Reynolds number effect. I'd like to also add my two cents for looking at some of the non-simple cases and the applications thereof, which may be the most important near term use of the coherent structure information and research.

INFLUENCE OF "RIBLETS" ON HEAT TRANSFER

$\delta \approx .5"$

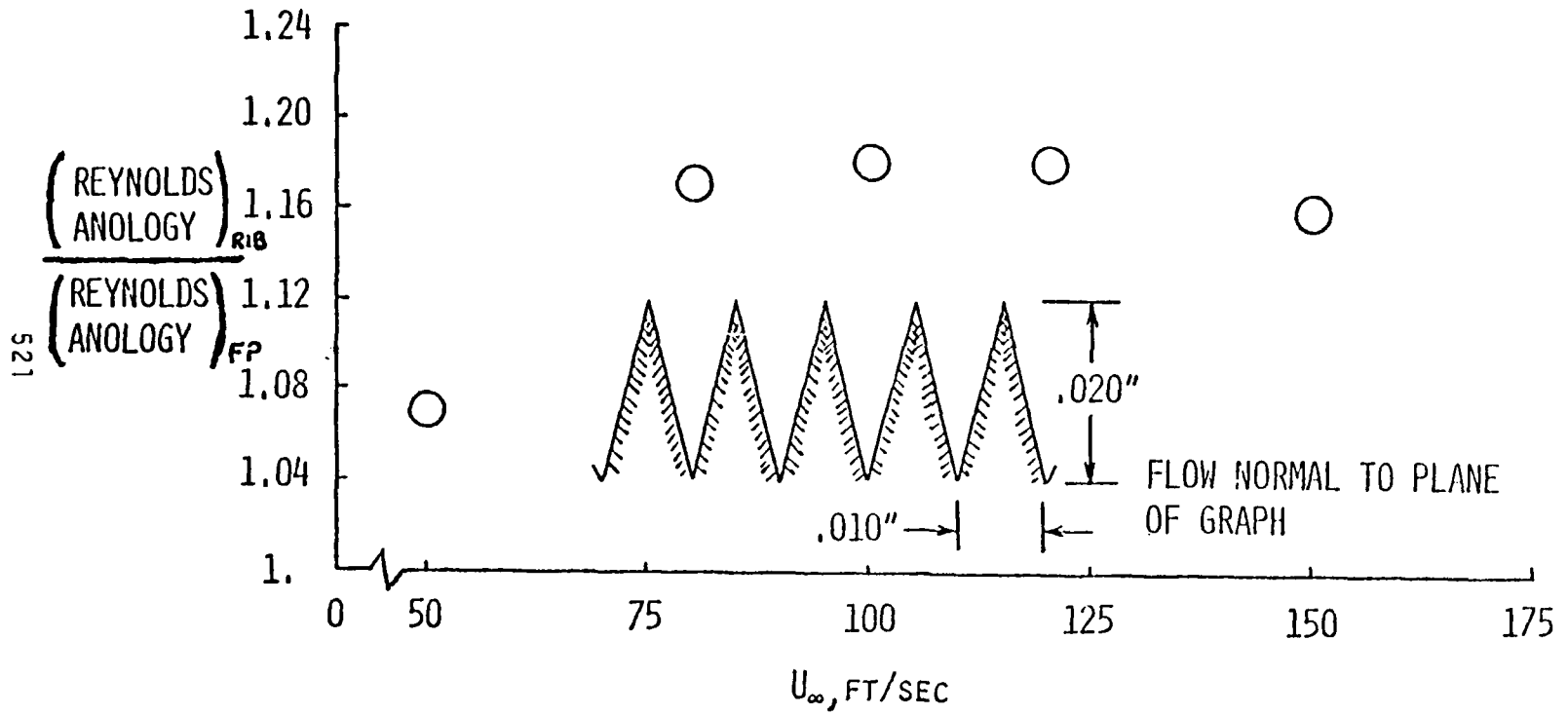

FIGURE 11.

SUGGESTIONS - WHERE DO WE GO FROM HERE?

(A) o MORE DETAILED DATA REQUIRED

- (V,W) AS F(X,Y,Z,T) IN PREBURST/BURST NEAR WALL (AS WELL AS U)

  COULD BE OBTAINED FROM REAL TIME PARTICLE TRACKING,
  AS IN LINDGREN'S WORK AT UNIVERSITY OF FLORIDA

- TO ALLOW DETAILED CHECKS ON NEAR WALL MODELING

(B) o MORE RESEARCH (DATA/ANALYSIS) NEEDED TO SORT OUT

(A) TWO LAYER vs. THREE LAYER STRUCTURE
(B) BIRTH/DEATH vs. ETERNAL LIFE FOR LARGE STRUCTURES
(C) FEED BACK/COMMUNICATION BETWEEN OUTER AND NEAR WALL PHENOMENA
(D) ROLE OF THREE-DIMENSIONAL (SPANWISE) NATURE OF OUTER STRUCTURES ON NEAR WALL BREAKDOWN

(C) o FURTHER EXAMINATION OF STRUCTURES

(A) AT HIGH REYNOLDS NUMBER
(B) FOR OTHER THAN SIMPLE ($DP/DX \sim 0$, CURVATURE = 0) CASES

(D) o APPLICATIONS - SUGGEST MORE ATTEMPTS TO INTERFERE WITH STRUCTURE DEVELOPMENT/FEEDBACK TO ENHANCE/RETARD MOMENTUM TRANSPORT

FIGURE 12.

Panel Member: DR. A.M.O. SMITH, Dynamics Technology, Inc.

I guess from the standpoint of the general gradation in this committee, I've been more of an end user of information on turbulence than anybody else. So, my comments will be as a user and I will point out some problems that researchers in turbulence should keep in mind. First, I might say that it seems to me that there are two basic categories of research: pure research and applied research. I think broadly speaking that the whole effort in turbulence research is applied research because our aim is to solve real flow problems that arise in technical applications. For that reason, people should keep in mind the end applications of turbulence research.

To clarify, I will list and discuss a number of problems, mostly external aerodynamics, since that has mainly been my field. However, the problems of internal aerodynamics are every bit as bad. Compressor stall is an example and it is a very spectacular thing. Closer prediction and analysis of it is an end problem. Pitchup of an airplane, a phenomenon where the nose goes up when stalling instead of down and diving out, may be about as bad, but at least it is a bit more gradual. Hence, here is a second end problem.

Another end application is the viscous drag problem, both 2D and 3D. Presently, if we have completely attached flow, we can calculate the drag of a simple 2D airfoil to within approximately 3%. One problem which requires further improvement even for 2D flows is the effect of curvature, both concave and convex. The most exasperating problem is the last 2 or 3% of an airfoil at the very trailing edge. This is a full blown problem of turbulent flow and interaction. Here the top and bottom boundary layers merge together, the pressure distribution is changed drastically from its inviscid value, and conventional boundary layer theory does not apply. At the trailing edge for most airfoils the C_p would be +1 if the flow were inviscid, but the strong interaction changes it to -0.1 or so, a large, not small , perturbation. As you see, this trailing edge region is a mess and is certainly an end problem of great importance.

So far, the only practical way of calculating drag of a body is to calculate the growth of the momentum defect along the body to the trailing edge and then continue it somehow to infinity to get out of the local pressure field of the body. Squire-Young's method is the usual, but it is quite approximate. What is really needed is an accurate solution of the turbulent wake in an arbitrary pressure field. This brings up a more complicated airfoil problem - a multi-element airfoil with slots and slotted flaps. The drag of these are calculated so poorly that it is hardly worth bothering. The wake momentum defect of all the several elements must each be corrected to infinity. Consider a slat, for instance. It has its own trailing edge problem, but in addition, one must calculate its wake history through the strong pressure field of the rest of the airfoil all the way to infinity or at least several chords downstream. This is another aspect of the drag end problem and no one has a good solution as far as I know. This multi-element problem often gets worse because the several wakes may merge.

PANEL: SMITH

I feel separation points can be predicted fairly well. However, as far as I know the momentum thickness and boundary layer profile shape are not predicted well. So improvement of predictions very near separation is another end problem. The calculation of $C_{L_{max}}$ is a worse problem. We now cannot handle this problem because it involves separated, interactive flow. $C_{L_{max}}$ usually occurs after a considerable amount of separation has developed that substantially modifies the pressure distribution. So here is another end problem. It is certainly an important problem to the airplane designer.

Then, of course, there are other end problems, like the growth of a boundary layer across a shock, separation bubbles, transition, and reattachment as well as extra thick boundary layers as at the tail of a body of revolution.

There are more exotic categories. For example, looking into the future there might be a liquid hydrogen fueled airplane where the hydrogen is used to cool the surface. We once did some calculations to see if there was a drag reduction due to the low μ. Mechanically, the problem was simple, we just loaded the necessary information into our turbulent computer program and pressed the button. But is it that simple; do we know enough about the transport processes so far outside the explored domain? Interestingly enough, no improvement was found. As μ at the wall was reduced, du/dy is increased so that $\tau_w = \mu(du/dy)_w$ the shear at the wall remained essentially unchanged. There are plenty of other more or less exotic problems, such as jet flap flows, and flow corners, such as wing-fuselage junctions. Also, in a different category is the noise problem.

Mostly, I have been talking about 2D problems which are hard enough. For 3D boundary layer flows some kind of mixing length or eddy viscosity approach seems to handle the problem well, but it is a frightful mess to get the geometry and everything else needed for a 3D boundary layer program loaded into the machine. So, here is a practical computing problem. The 3D problem is like the 2D, only worse. Consider predicting stall patterns, moment coefficients for pitchup problems and, of course, $C_{L_{max}}$ for a real 3D wing. So you see, the end problems are multiplied manifold over the 2D. It seems to me that about all the problems I have mentioned are special problems not covered by conventional boundary layer theory.

Like Peter Bradshaw said, I can't imagine all these problems being solved by one grand computer program because there are just too many different conditions and inputs. But I hope I have outlined some of the classes of problems we face. I think Brian (Quinn), Peter (Bradshaw) and Dennis (Bushnell) have already indicated a good deal

of what industry wants to have quantitative answers for. If improvements are made in the art of calculation of turbulent flows they can be in the differential equations of transport or in some kind of improved turbulent transport laws like Bradshaw's method of correlating against turbulent kinetic energy or our own eddy viscosity method, or things like that. Anyway, if you want a quantitative answer there has to be a definite input. It must be something that can be written down in some kind of equation form. Most of what I have seen at this meeting is still far from getting down into equation form. Most is still in some kind of descriptive or qualitative stage and still subject to a lot of argument.

Possibly some kind of elementary process will be discovered one of these days like Danberg tried with his horseshoe vortex. Such types of things are what I really would like to see. Until then, I concur that Reynolds averaged equations are still going to be here for a long time. I've always had an instinctive feeling that we're not going to make any significant progress until we can get some kind of true physical process incorporated into the turbulent prediction methods.

I think I'll end up with a comment in regard to direction of efforts. It's something that has guided me for a long time and it's in the form of an old joke. There's a drunk out on an empty street late at night looking along a gutter under a streetlight, when a policeman walks by and sees him. The policeman stops and asks him what he had lost. The drunk replies that he had lost some money. So the policeman offers to help him search for it and asks exactly where he thought he lost it. "Oh, down the street a ways," replies the drunk. "Well, why are you looking here?", asks the policeman. The drunk's reply is, "The light is better here." I have seen a lot of tests that followed the drunks thinking. An easy test was done instead of facing up to the situation and going after the answers really needed. I think I have seen some of that situation prevailing in some of the work presented at this workshop. A lot of times we shouldn't do some research just because a result is easy to get, but do what the problem really needs.

FLOOR DISCUSSION FOLLOWING PANEL

Morkovin:

I think what Amo has discussed regarding applications has been pointed out several times by the other panel members. I think we should emphasize the point that no matter how small a part of the total problem we are studying, we must always ask if there is an eventual practical application of the experiment or model under study. One should always ask if there is a promise of sufficient universality in our research so that somebody else can use the information generated. Now, having made my comment, I would like to call on several people, who were mentioned in passing, for their comments. One person whose name has been mentioned is Bill Reynolds.

Reynolds:

Let me just say that I've been very struck by some of the flow visualization pictures we've seen in this Workshop. I seem to observe a lot of small structures sticking out from the wall which appear to be the constituents of some sort of larger structure. I'm reminded of cars responding to a traffic light. The cars all stop for the light and then they move off together in a very coherent structure. They are all very individualized small structures that initially travel along behind the slowest ones, but after awhile they spread out, diffuse if you will, and no longer appear coherent. I'm wondering whether or not these large, apparently coherent structures we observe in turbulence really might be just a bunch of small structures that are just locked together in some way?

Morkovin:

So, they may be coagulating in some sort of an anti-cascade fashion? That is a possibility. Another gentleman whose name has been mentioned is Morrie Rubesin.

Rubesin:

I think I agree with the modelers here who feel that the Reynolds stress equations are going to be the mainstay of prediction methods for the next few years. However, I don't see a long term future for those methods, especially slide rule methods. I think back to the times of Prandtl and Nikuradse. Then it was a matter of mean measurements and mean theory. Now we've seen 10 years of dynamic measurements and dynamic observations, and I think it is time for the analyst and the predictor to start thinking about how to solve

Rubesin: (Cont'd)

the equations dynamically. I think the large scale structure approach is a very powerful tool that we really have to explore as much as possible. Another comment, I'd like to make in terms of the Reynolds stress modeling and the complexity of these models. We started with zero equation models and we're up now to maybe 10 equation models. This has not been done just for the sake of complexity. There's an underlying hope that generality grows with complexity, and indeed there seems to be indications that a two-equation model can be extended beyond a one-equation model. We find for example that we can fudge the factors in the old mixing length models to make them fit many different cases. But if you examine cases where you have adverse pressure gradients followed by favorable pressure gradients, the coefficients take on hysteresis loops within the data, whereas we're representing them with single lines in our models. So I think that we learn by our mistakes and I'm going to close by saying we have to be active in many, many fields because we don't know today where the answer lies.

Morkovin:

Thank you Morrie. Bob Falco.

Falco:

It's just a very brief comment, on a possible new and important experimental technique which we're just going to try in conjunction with Gary Cloud. We plan to use laser speckle photography to get a two-dimensional velocity map in a turbulent flow field. It's one step less complicated than holography, both in terms of economics and procedure, and it has been demonstrated at Bell Labs in a very, very slow fluid flow. We're going to try it, using a Fourier reduction technique to make it semi-automated. It has a lot of potential in terms of understanding the turbulence bursting and production process, because we will be able to measure at any instant the velocity field at any chosen y+. Thus, we will be able to determine the velocity field in any given plane.

Morkovin:

Bill George please.

George:

One thing that really has not been addressed at this conference is the Lumley orthogonal decomposition. I swore several years ago that I wouldn't mention it again until I had hard data, but I think that the solution to the problem Don Coles referenced, namely, how do you accumulate data and interpret it, can be

George: (Cont'd)

handled by the Lumley approach. I'm happy to say that at present there are three experiments underway to apply the full blown Lumley decomposition, which has never been done before. One is an experiment which I initiated at Penn State which utilized a pipe with large time lags and large space lags to try to reproduce the Kline eddies and all of their dynamics. That experiment is being continued by others and is nearing completion. The second experiment is a low Reynolds number jet mixing layer study that is just being initiated, and the third experiment is a high Reynolds number jet mixing layer study. The advantage of these experiments is that you get deterministic information, you can reconstruct the random velocity field with all the same statistics, and then you can perform numerical experiments looking for intermittency, calculating radiated noise, streak line behavior, and hopefully sorting out what is coherent and what is random. The next few years should indicate whether LOD is a viable technique and what the implications of it are.

Morkovin:

Thanks, Bill George. I think it was quite clear at this symposium we still have a conceptually unclear picture of the type and degree of coherency that occurs in turbulent boundary layers and we have plenty of work to do. I would like to now have us all stand up and give a real sense of appreciation to the home team. They have done a tremendous job. (Standing Ovation).